Orogenic architecture of the Mediterranean region and kinematic reconstruction of its tectonic evolution since the Triassic

van Hinsbergen, Douwe; Torsvik, Trond; Schmid, Stefan; Matenco, Liviu; Maffione, Marco; Vissers, Reinoud L.M.; Gürer, Derya; Spakman, Wim

DOI:
10.1016/j.gr.2019.07.009

Gondwana Research 81 (2020) 79–229

Contents lists available at ScienceDirect

Gondwana Research

journal homepage: www.elsevier.com/locate/gr

Orogenic architecture of the Mediterranean region and kinematic reconstruction of its tectonic evolution since the Triassic

Douwe J.J. van Hinsbergen [a, *], Trond H. Torsvik [b, c], Stefan M. Schmid [d], Liviu C. Maţenco [a], Marco Maffione [a, e], Reinoud L.M. Vissers [a], Derya Gürer [a, f], Wim Spakman [a, b]

[a] Department of Earth Sciences, Utrecht University, Budapestlaan 4, 3584 CD, Utrecht, the Netherlands
[b] Centre for Earth Evolution and Dynamics (CEED), University of Oslo, Sem Sælands vei 24, NO-0316, Oslo, Norway
[c] School of Geosciences, University of the Witwatersrand, WITS 2050, Johannesburg, South Africa
[d] Institut für Geophysik ETH, NO D 65, Sonneggstrasse 5, 8092, Zürich, Switzerland
[e] School of Geography, Earth and Environmental Sciences, University of Birmingham, B15 2TT, UK
[f] School of Earth and Environmental Sciences, University of Queensland, St. Lucia, QLD4072, Australia

ARTICLE INFO

Article history:
Received 3 April 2019
Received in revised form
29 June 2019
Accepted 21 July 2019
Available online 3 September 2019

Keywords:
GPLates
Plate tectonics
Mediterranean
Mesozoic
Cenozoic
Reconstruction

ABSTRACT

The basins and orogens of the Mediterranean region ultimately result from the opening of oceans during the early break-up of Pangea since the Triassic, and their subsequent destruction by subduction accommodating convergence between the African and Eurasian Plates since the Jurassic. The region has been the cradle for the development of geodynamic concepts that link crustal evolution to continental break-up, oceanic and continental subduction, and mantle dynamics in general. The development of such concepts requires a first-order understanding of the kinematic evolution of the region for which a multitude of reconstructions have previously been proposed. In this paper, we use advances made in kinematic restoration software in the last decade with a systematic reconstruction protocol for developing a more quantitative restoration of the Mediterranean region for the last 240 million years. This restoration is constructed for the first time with the GPlates plate reconstruction software and uses a systematic reconstruction protocol that limits input data to marine magnetic anomaly reconstructions of ocean basins, structural geological constraints quantifying timing, direction, and magnitude of tectonic motion, and tests and iterations against paleomagnetic data. This approach leads to a reconstruction that is reproducible, and updatable with future constraints. We first review constraints on the opening history of the Atlantic (and Red Sea) oceans and the Bay of Biscay. We then provide a comprehensive overview of the architecture of the Mediterranean orogens, from the Pyrenees and Betic-Rif orogen in the west to the Caucasus in the east and identify structural geological constraints on tectonic motions. We subsequently analyze a newly constructed database of some 2300 published paleomagnetic sites from the Mediterranean region and test the reconstruction against these constraints. We provide the reconstruction in the form of 12 maps being snapshots from 240 to 0 Ma, outline the main features in each time-slice, and identify differences from previous reconstructions, which are discussed in the final section.

1. Introduction

1.1. Rationale

The intensely deformed Mediterranean region forms the plate boundary zone between the African and Eurasian plates and has been instrumental for the development of numerous fundamental geological principles and geodynamic concepts on mountain building and collapse and their relationship with subduction evolution. An area as tectonically complex as the Mediterranean region invites attempts to geological reconstruction, and various views are available (e.g., Argand, 1924; Barrier and Vrielynck, 2008; Csontos and Vörös, 2004; Dercourt et al., 1986, 2000; Faccenna et al., 2014; Frisch, 1979; Gealey, 1988; Golonka, 2004; Handy et al., 2010; Jolivet et al., 2009; Meulenkamp and Sissingh, 2003; Moix et al., 2008; Rosenbaum et al., 2002b, 2005; Royden and Faccenna, 2018; Schettino and Turco, 2010; Şengör and Yılmaz, 1981; Stampfli et al., 1991; Stampfli and Hochard, 2009; Stampfli

* Corresponding author.
E-mail address: d.j.j.vanhinsbergen@uu.nl (D.J.J. van Hinsbergen).

https://doi.org/10.1016/j.gr.2019.07.009
1342-937X/

and Kozur, 2006). Such reconstructions are not only a translation of – frequently qualitative – geological data into a semi-quantitative description of surface evolution. With the advent of three-dimensional numerical modelling tools reconstructions also constitute critical input in attempts of integrating regional tectonic evolution with mantle dynamics (e.g., Chertova et al., 2014; Faccenna and Becker, 2010). A now widely used computer platform for plate kinematic reconstructions is the freely available GPlates software (Boyden et al., 2011) (http://www.gplates.org). In this paper, we provide the first fully quantitatively described GPlates-based kinematic reconstruction of the Mediterranean region, establishing a restoration back to the Triassic opening of Neotethys-related oceanic basins. We include all shape (digitized terrane units) and rotation files of this reconstruction, which can be used as a platform for further improvement when new constraints demand so, or when the reader wishes to implement and/or test alternative or more detailed tectonic scenarios.

1.2. How to read this paper?

This paper presents a restoration that uses individual nappes, basins, core complexes, and faults as input and restores these back into time. Because there are many of these in the Mediterranean region, this paper is inevitably long. To navigate through this work, here follows a brief outline of its structure.

Key data used for the restoration are summarized in Table 1. Stratigraphies, emplacement histories, and metamorphic histories of nappes, and major structures cutting them, are shown in schematic cross sections coined 'orogenic architecture diagrams'. Modern nappe outlines and major structures are displayed on the large tectonic map of Supplementary Information 1 – map 1, and in detailed cuts of this map given in the paper. These summaries, in combination with the reconstruction approach outlined in Section 3, give all the information that was used for the reconstructions shown in this paper.

Justifications and explanations for our selection of input data are given for the plate kinematic constraints from the Atlantic Ocean in Section 4, for orogenic architecture in Section 5, and paleomagnetic tests and modifications in Section 6. Sections 5 and 6 are organized generally from west to east through the region and subdivided in headings per orogen. Section 7 gives the sec description of our paleotectonic maps, from young to old, and in this section, we simply note key differences with a set of previous reconstructions. We will not repeat all evidence in this section again, for which the reader is referred to the constraints summarized in tables and figures. Finally, Section 8 discusses the key differences between our and previous reconstructions identified in Section 7 and explains our choices and arguments.

2. General outline of Mediterranean tectonic history

Reconstructions invariably infer that during the main Pangea break-up in early-middle Jurassic time, the Mediterranean region had a complex paleogeography with ribbon continents and narrow, elongated basin systems that in places became oceanic (Csontos and Vörös, 2004; Dercourt et al., 1986; Frisch, 1979; Gaina et al., 2013; Golonka, 2004; Handy et al., 2010; Rosenbaum and Lister, 2005; Schettino and Turco, 2006; Schmid et al., 2004b, 2008; Stampfli and Borel, 2002). A northwestern ocean basin system was genetically related to the Atlantic Ocean, opened in Middle to Late Jurassic time, and is known as the Alpine Tethys Ocean, which include multiple branches, such as the Piemonte-Liguria Ocean between Greater Adria (i.e. modern Adria and the its restored portions now folded and thrusted in circum-Adriatic orogens), Iberia, and the Briançonnais continental fragment, and the Valais Ocean between the Briançonnais fragment and Europe (Frisch, 1979; Gaina et al., 2013; Rosenbaum et al., 2002b; Schmid et al., 2004b, 2008; Vissers et al., 2013). A southern and eastern basin system was genetically related to the opening of the Neotethys Ocean between Gondwana and Eurasia, opening in the Mediterranean realm from at least Triassic to Jurassic times (Catalano et al., 2001; Frizon de Lamotte et al., 2011; Hosseinpour et al., 2016; Rosenbaum et al., 2004; Schettino and Turco, 2010; Schmid et al., 2004b, 2008; Speranza et al., 2012). Upon opening of these ocean basins continental fragments rifted and drifted off Eurasia, Iberia, and Africa (Gondwana), and became internally deformed into platforms and basins (Dercourt et al., 1986, 2000). The resulting mosaic of continental and oceanic lithosphere became subsequently consumed by a complex configuration of subduction zones that accommodated convergence between Africa and Eurasia since middle Jurassic times (e.g., Gaina et al., 2013; Handy et al., 2010, 2015; Schmid et al., 2008).

Subduction of oceanic and, especially, continental lithosphere became widely associated with stacking of upper crust at subduction plate boundaries, forming regional nappe stacks of, for instance, the Apennines, Alps, Carpathians, Dinarides, and Hellenides, whereas their original lower crustal and mantle underpinnings subducted (Faccenna et al., 2001b, 2003; Handy et al., 2010; Jolivet and Brun, 2010; Maţenco et al., 2010, 2016; Schmid et al., 2004b, 2008; van Hinsbergen et al., 2005a, 2010c). In several of these fold-and-thrust belts, e.g. in the Dinarides, and the Tisza and Dacia blocks underlying the Pannonian Basin, strain associated with Africa-Europe convergence became partitioned between the subduction zone and the overriding plate, adding complexity to the structural history by out-of-sequence thrusting, transitions from thin- to thick-skinned thrusting, and reactivation of older parts of the nappe stacks (e.g., Capella et al., 2017; Maţenco et al., 2007; Picotti and Pazzaglia, 2008; Schmid et al., 2004a, 2004b,; 2017). Finally, throughout the subduction history, extensional back-arc basins formed in overriding plates above subduction zones throughout the Mediterranean region, locally leading to the formation of highly extended continental crust or to the formation of new ocean floor, a process generally interpreted as a result of roll-back of subducted slab segments (Balázs et al., 2017, 2018; Edwards and Grasemann, 2009; Faccenna et al., 2001b, 2004, 2014; Handy et al., 2010; Horváth et al., 2006, 2015; Jolivet et al., 2009; Malinverno and Ryan, 1986; Rosenbaum et al., 2008; Rosenbaum and Lister, 2004a; Royden and Burchfiel, 1989; Ustaszewski et al., 2008; van Hinsbergen and Schmid, 2012; van Hinsbergen et al., 2014a), culminating in today's complex and strongly curved configuration of mountain ranges and subduction zones (Spakman and Wortel, 2004; Wortel and Spakman, 2000) (Fig. 1). The kinematic reconstruction in this paper starts with the final, modern configuration of the Mediterranean geology, and restores it back in time to the original configuration at the beginning of the opening of the northwesterly Neotethyan basins in mid-Triassic time.

3. Approach: reconstruction protocol

Relative plate kinematic reconstructions back to the Jurassic are based on reconstructions of modern ocean basins, using marine magnetic anomalies to constrain paleo-spreading rates, and fracture zones and transform faults to constrain paleo-spreading directions (e.g., McKenzie and Parker, 1967; Cox and Hart, 1986; Müller et al., 2008; Seton et al., 2012; Torsvik and Cocks, 2017). The elegance of such reconstructions is that scientists who study the history of an ocean basin uses the same types of data and the same reconstruction philosophy. As a result reconstructions of ocean basins can be directly compared and compiled into a global plate circuit (e.g., Besse and Courtillot, 2002; Doubrovine et al., 2012; Patriat and Achache, 1984; Seton et al., 2012; Torsvik et al.,

Table 1
Summary of kinematic constraints used as input for the reconstruction.

Region/structure	sense	amount	Age	reference
Iberia; Pyrenees				
North Pyrenean Fault	sinistral transpression	unknown	83–55	Choukroune (1976) and Vissers and Meijer (2012a)
Pyrenees on Iberia	shortening	>80 km		Beaumont et al. (2000) and Roure et al. (1989)
Extensional exhumation Cap de Creus	extension	unknown	170-150 Ma	Vissers et al. (2017)
Ansó-Arzacq section, West Pyrenees	shortening	>75–80 km	80-19 Ma	Teixell (1996, 1998)
Ansó-Arzacq section, North Pyrenean Zone	shortening	23–30 km	80-19 Ma	Teixell (1996, 1998)
ECORS-Pyrenees, Central Pyrenees	shortening	100–165 km	80-19 Ma	Muñoz (1992), Beaumont et al. (2000) and Roure et al. (1989)
ECORS-Pyrenees, North Pyrenean Zone	shortening	37 km	80-19 Ma	Muñoz (1992), Beaumont et al. (2000) and Roure et al. (1989)
East Pyrenees	shortening	125 km	80-19 Ma	Vergés et al. (1995)
East Pyrenees, North Pyrenean Zone	shortening	32 km	80-19 Ma	Vergés et al. (1995)
Central Iberian Ranges	shortening	20 km	35-20 Ma	de Vicente et al. (2007)
Timing Iberia rotation	paleomagnetic rotation	unknown	126-112 Ma	Gong et al. (2008) and Vissers et al. (2016)
Adria; Ionian Basin; Sicily Straights				
Ionian Basin	extension	unknown	Triassic (227-219 Ma?)	Speranza et al. (2012)
Herodotus Basin	extension	unknown	~360-316 Ma	Granot (2016)
Northern Adria	extension	unknown	Jurassic	Santantonio and Carminati (2010)
Strait of Sicily	extension	50–60 km	10-0 Ma	Civile et al. (2008) and Argnani (2009)
Adria rotation	paleomagnetic rotation	10°ccw	20-0 Ma	van Hinsbergen et al. (2014b)
Gulf of Valencia; Baleares; Algerian Basin; Kabylides; Alboran; Atlas				
Golf of Valencia	extension	80 km	25-16 Ma	Vergés and Sàbat (1999) and Séranne (1999)
High Atlas	shortening	30 km	50-35 Ma; 2-0 Ma	Beauchamp et al. (1999), Brede (1992), Teixell et al. (2003), Frizon de Lamotte et al. (2008)
Malaguide/Ghomaride/Upper Kabulides on Alpujarride/Sebtide/Lower Kabylides	shortening	unknown	>45-25 Ma	Chalouan et al. (2001), Goffé et al. (1989), Mahdjoub et al. (1997), Michard et al. (2006), Monié et al. (1994), Platt et al. (2005) and Vissers et al. (1995)
Alpujarride/Sebtide on Nevado-Filabride/ Temsamane	shortening	unknown	20-12 Ma	Booth-Rea et al. (2012), Gómez-Pugnaire et al. (2012), Negro et al. (2007) and Platt et al. (2006)
External Betics/External Rif on Iberia/Meseta	shortening	unknown	12-8 Ma	Chalouan et al. (2006), Meijninger and Vissers (2007) and Platt et al. (2003, 2013)
Kabylides on Tell belt on Meseta	shortening	unknown	25-16 Ma	Benaouali-Mebarek et al. (2006), Coulon et al. (2002), Maury et al. (2000) and Michard et al. (2006)
Mallorca	shortening	85 km	26-16 Ma	Gelabert et al. (1992) and Sàbat et al. (2011)
Alboran Basin	extension	220 km	25-10 Ma	Faccenna et al. (2004), Michard et al. (2006), Platzman and Platt (2004) and Vissers et al. (1995)
Provence; Gulf of Lion; Corsica, Sardinia; Tyrrhenian Sea				
Gulf of Lion	extension	100 km	30-21 Ma	Bache et al. (2010) and Séranne (1999)
Gulf of Lion	extension	up to 200 km	21-16 Ma	Burrus (1984), Gorini et al. (1993) and Séranne (1999)
Provence	shortening	>30 km	75-30 Ma	Andreani et al. (2010), Espurt et al. (2012a) and Lacombe and Jolivet (2005)
Corsica-Sardinia rotation	paleomagnetic rotation	45° ccw	75-30 Ma	Advokaat et al. (2014b)
Sicily; Calabria; Apennines				
Sicily				
Stilo unit off Aspromonte unit	NE-SW detachment faulting	unknown	30-20 Ma	Heymes et al. (2008, 2010)
Aspromonte unit on Africo-Polsi unit	shortening	unknown	46-30 Ma	Heymes et al. (2008, 2010)
Africo-Polsi unit on Sicilide units (Sicily)	shortening	unknown	25-20 Ma	Catalano et al. (1996), Ogniben (1960) and Pepe et al. (2005)
Sicilide units on Outer Carbonate unit	shortening	unknown	20-14 Ma	Catalano et al. (1993)
Outer Carbonate on Inner Carbonate unit	shortening	unknown	14-4 Ma	Catalano et al. (1993)
Outer Carbonate unit	paleomagnetic rotation	90°cw	14-0 Ma	Fig. 20
Inner Carbonate unit on Hyblean Plateau/Gela Nappe	shortening	unknown	4-0 Ma	Butler et al. (1992) and Ogniben (1969)
Inner Carbonate unit	paleomagnetic rotation	40°cw	4-0 Ma	Fig. 20 and Speranza et al. (2003)

(*continued on next page*)

Table 1 (*continued*)

Region/structure	sense	amount	Age	reference
Calabria				
Stilo unit off Aspromonte unit	NE-SW detachment faulting	unknown	30-20 Ma	Heymes et al. (2008, 2010)
Aspromonte unit on Africo-Polsi unit	shortening	unknown	46-30 Ma	Heymes et al. (2008, 2010)
Calabro-Peloritan block on Ligurian accretionary complex	shortening	unknown	38-20 Ma	Rossetti et al. (2004) and Iannace et al. (2007)
Extensional exhumation Ligurian accretionary complex	NW-SE extension	unknown	15-11 Ma	Mattei et al. (1996) and Argentieri et al. (1998)
Ligurian accretionary complex on Calabrian Accretionary prism	shortening	unknown	20-0 Ma	Cavazza and Barone (2010) and Minelli and Faccenna (2010)
North Pollino Fault Zone	left-lateral strike-slip	unknown	6-0 Ma	Catalano et al. (1993), Knott and Turco (1991) and Monaco et al. (2001)
Calabria rotation	paleomagnetic rotation	40°ccw	13-10 Ma	Duermeijer et al. (1998b)
Calabria rotation	paleomagnetic rotation	20°cw	10-0 Ma	Duermeijer et al. (1998b) and Fig. 20
Southern Apennines				
Liguride and Sicilide over Apenninic Platform	shortening	unknown	20-14 Ma	e.g., Patacca and Scandone (2007)
Apenninic Platform over Lago Negro Basin	shortening	unknown	14-11 Ma	e.g., Pescatore et al. (1999)
Lago Negro over Apulian Platform	shortening	unknown	11-6 Ma	Mostardini and Merlini (1986) and Ricchetti et al. (1988)
Duplexing within Apulian Platform	shortening	>100 km	6-0 Ma	Cello et al. (1989)
normal faulting affecting internal Southern Apennines	NE-SW extension	unknown	15-0 Ma	Cello and Mazzoli (1998) and Patacca et al. (1990)
Apenninic Platform rotation	paleomagnetic rotation	60°ccw	14-0 Ma	Gattacceca and Speranza (2002)
Central Apennines				
Sicilide over Latium-Abruzzo Platform	shortening	unknown	25-16 Ma	Vitale and Ciarcia (2013)
Shortening within Latium-Abruzzo Platform	shortening	unknown	11-7 Ma	Cavinato and DeCelles (1999) and Cosentino et al. (2010)
Latium-Abruzzo over Molise Basin	shortening	unknown	7-4 Ma	Cosentino et al. (2010) and Patacca et al. (1990)
shortening of Umbria-Marche over Latium Abruzzo from NW	shortening	unknown	4-3 Ma	Satolli et al. (2005) and Speranza (2003)
normal faulting affecting internal Central Apennines	NE-SW extension	unknown	6-0 Ma	Calamita et al. (1994), Cavinato and DeCelles (1999) and D'Agostino et al. (2001)
minimum total shortening since ~25 Ma	NE-SW shortening	116–175 km	25-0 Ma	Ghisetti et al. (1993)
Northern Apennines				
Westward shortening within Internal Ligurides	shortening	unknown	60-50 Ma	Marroni and Pandolfi (1996) and Pertusati and Horrenberger (1975)
Internal and Tuscan Ligurian ophiolites on External Ligurides	shortening	unknown	30-25 Ma	Marroni et al. (1988), Marroni et al. (2001) and Molli (2008)
Extremal Ligurides on Sub-Ligurides	shortening	unknown	21-16 Ma	Cerrina Feroni et al. (2002) and Molli et al. (2010)
Sub-Ligurides on Tuscan Nappes	shortening	unknown	25-16 Ma	Brunet et al. (2000) and Kligfield et al. (1986)
normal faulting exhuming metamorphosed Tuscan Nappes	NE-SW extension	unknown	13-10 Ma	Fellin et al. (2007)
Tuscan Nappes on Umbria-Marche basin	shortening	unknown	16-7 Ma	Barchi et al. (2012) and Speranza et al. (1997)
Umbria-Marche nappes on external foredeep	shortening	unknown	7-0 Ma	Calamita et al. (1994)
Shortening Northern Apennines	shortening	unknown	75–150 km	Calamita et al. (1994), Ghisetti et al. (1993) and Finetti et al. (2001)
Rotation Tuscan units northern limb North Apennine orocline	paleomagnetic rotation	30° ccw	16-0 Ma	Fig. 22
Alps; AlCaPa				
Corsica				
Nappes Supérieures on Schistes Lustrés Corsica	shortening	unknown	84 Ma	Lahondère and Guerrot (1997)
Schistes Lustrés on Tenda/Lower External Continental Units	shortening	unknown	54-35 Ma	Maggi et al. (2012), Ferrandini et al. (2010) and Bezert and Caby (1988)
Extensional exhumation	E-W extension	unknown	32-21 Ma	Brunet et al. (2000), Rossetti et al. (2015), Zarki-Jakni et al. (2004) and Cavazza et al. (2001)
Ligurian Alps				
Sestri-Voltaggio Line	top-E extension	unknown	>34 Ma	Gelati et al. (1992) and Hoogerduijn Strating (1994)
Piedmont basin covering Ligurian Alps	seal	unknown	35 Ma	Piana (2000)
Northward shortening of Ligurian Alps over Piedmont basin	shortening	unknown	10-3 Ma	Piana (2000)
Western Alps; Jura				
Burial and metamorphism of Sesia fragment	shortening	unknown	85-70 Ma	Manzotti et al. (2014)
Burial and metamorphism of Piemonte-Ligurian units	shortening	unknown	80-55 Ma	Lagabrielle et al. (2015) and Weber and Bucher (2015)
Piemonte Ligurian on Briançonnais mega-unit	shortening	unknown	55-45 Ma	Lanari et al. (2014) and Villa et al. (2014)
Briançonnais on Valais	shortening	unknown	45-40 Ma	Wiederkehr et al. (2009)

Table 1 (*continued*)

Region/structure	sense	amount	Age	reference
Valais on European foreland (Helvetic; Molasse basin)	shortening	unknown	40-20 Ma	Herwartz et al. (2011), Kempf and Pfiffner (2004) and Schmid et al. (1996)
Shortening within Helvetic Nappes	shortening	55 km	40-20 Ma	Schmid et al. (2004b)
Shortening in Molasse Basin	shortening	20 km	20-7 Ma	Kempf and Pfiffner (2004)
Shortening in Jura Mountains	shortening	30 km	20-7 Ma	Affolter (2004) and Affolter et al. (2008)
Northern limb Jura orocline; Molasse basin	paleomagnetic rotation	10°cw	20-7 Ma	Kempf et al. (1998)
Western Alps extension	E-W extension	>10 km	34-30 Ma	Beltrando et al. (2010)
Insubric Line	sinistral strike-slip	>100 km	35-20 Ma	Schmid et al. (2017)
Simplon detachment faulting	NE-SW extension	20 km	20-7 Ma	Mancktelow (1992)
Insubric back-thrust	shortening	15 km	20-7 Ma	Schmid et al. (2004b) and Simon-Labric et al. (2009)
External Massifs	paleomagnetic rotation	0°		Crouzet et al. (1996)
Briançonnais SW Alps	paleomagnetic rotation	40° ccw	28-0 Ma	Sonnette et al. (2014)
Briançonnais western Ligurian Alps	paleomagnetic rotation	110°ccw	28-0 Ma	Collombet et al. (2002)
Eastern Alps; AlCaPa				
Meliaticum (West Vardar ophiolites) on Upper Austroalpine	shortening	unknown	145 Ma	Schmid et al. (2008)
Onset shortening and nappe stacking upper Austroalipine	shortening	unknown	135 Ma	Schmid et al. (2008)
Upper Austro-Alpine on Eo-Alpine metamorphics	shortening	unknown	95-90 Ma	Janák et al. (2004), Janák et al. (2015) and Thön et al. (2008)
Extensional exhumation Eo-Alpine metamorphics	shortening	NW-SE extension	90-85 Ma	Froitzheim et al. (1997)
Eo-Alpine metamorphics on Lower Austroalpine	shortening	unknown	90-80 Ma	Handy et al. (2010) and Schuster (2015)
Lower Austroalpine over Valais/ Rhenodanubian/Magura	shortening	unknown	80-40 Ma	Handy et al. (2010) and Schuster (2015)
Valais on European foreland (Helvetic; Molasse basin)	shortening	unknown	40-20 Ma	Herwartz et al. (2011), Kempf and Pfiffner (2004) and Schmid et al. (1996)
Shortening in Molasse Basin	shortening	20 km	20-9 Ma	Kempf and Pfiffner (2004)
Pannonian basin extension	SW-NE	300 km	20-9 Ma	Ustaszewski et al. (2008)
AlCaPa rotation Pannonian basin	paleomagnetic rotation	70°ccw	20-9 Ma	Fig. 24
Giudicarie Fault	sinistral strike-slip	80 km	20-10 Ma	Scharf et al. (2013)
Out-of-sequence shortening eastern Alps	shortening	113 km	20-10 Ma	Frisch et al. (1998)
Southern Alps on Adria	shortening	45–70 km	10-0 Ma	Schönborn (1999) and Scharf et al. (2013)
Shortening in Outer West Carpathians; increasing eastward	N-S shortening	38–105 km	55-15 Ma	Beidinger and Decker (2014), Nemčok et al. (2000) and Castelluccio et al. (2015)
Shortening in northern Eastern Carpathians	E-W shortening	183–250 km	20-9 Ma	Behrmann et al. (2000), Nemčok et al. (2006) and Gągała et al. (2012)
Shortening in northern Eastern Carpathians	E-W shortening	250 km	35-20 Ma	Gągała et al. (2012)
Shortening in SE Carpathians, Vrancea area	shortening	40 km	12-8 Ma	Bocin et al. (2009), Leever et al. (2006), Merten et al. (2011) and Tărăpoancă et al. (2003)
Shortening in SE Carpathians, Vrancea area	shortening	5 km	5-0 Ma	Bocin et al. (2009), Leever et al. (2006), Merten et al. (2011) and Tărăpoancă et al. (2003)
Moesian Platform; Dobrogea				
North Dobrogea rifting	extension; no oceanization		280-220 Ma	Saccani et al. (2004)
Triassic-Jurassic inversion North Dobrogea rift	shortening	50 km	220-180 Ma	Săndulescu (1984) and this paper
Central Dobrogea on North Dobrogrea	shortening	10 km	150-120 Ma	Hippolyte (2002), Rădulescu et al. (1976), Săndulescu (1984), Seghedi (2001), Grădinaru (1995) and this paper
North Dobrogea on Scythian Platform	shortening	10 km	150-120 km	Espurt et al. (2012b), Seghedi (2001) and this paper
Tisza; Dacia; Severin-Ceahlau; Danubian; Pannonian Basin; Carpathians				
Tisza-Dacia on Dinarides	shortening	unknown	70-60 Ma	Gallhofer et al. (2015, 2017), Schmid et al. (2008) and Toljić et al. (2018)
Codru on Bihor, Bihor on Mecsek (Tisza)	shortening	50 km	95-85 (extended to 110-85 Ma)	Kounov and Schmid (2012) and Reiser et al. (2017)
Biharia (Dacia) on Codru	shortening	70 km	95-85 (extended to 110-85 Ma)	Schmid et al. (2008), Kounov and Schmid (2012) and Reiser et al. (2017)
East Vardar ophiolites on Biharia (Dacia)	shortening	10's of km	155-145 Ma	Schmid et al. (2008)
East Vardar ophiolites on Bucovinian-Getic system (Dacia)	shortening	>170 km	110-100 (extended to 120-100 Ma)	Schmid et al. (2008)
Biharia (Dacia) and East Vardar over Transylvanian Basin	shortening	20 km	80-40 Ma	De Broucker et al. (1998), Krézsek and Bally (2006) and Schmid et al. (2008)
Supragetic on Getic	shortening	60–70 km	110-100 (extended to 135-95 Ma)	Săndulescu (1984), Schmid et al. (2008) and geological maps
Bucovinian nappe stack	shortening	60–150 km	110-100 (extended to 135-95 Ma)	Kräutner and Bindea (2002) and geological maps

(*continued on next page*)

Table 1 (*continued*)

Region/structure	sense	amount	Age	reference
Getic (Dacia) on Severin (Ceahlau-Severin) in S Carpathians	shortening	>25	110-100 (extended to 110-95 Ma)	Săndulescu (1984, 1994) and Iancu et al. (2005a, 2005b).
Bucovinian (Dacia) over Ceahlau (Ceahlau-Severin) in E Carpathians	shortening	unknown	110-60 Ma	Badescu (1997), Merten (2011), Săndulescu (1984) and Stefanescu (1983)
Severin (Ceahlau-Severin) over Danubian	shortening	85 km	80-70 Ma	Berza et al. (1983), Berza and Iancu (1994), Schmid et al. (1998) and Merten (2011)
Ceahlau (Ceahlau-Severin) over Outer Carpathians	shortening	unknown	80-70 Ma	Badescu (1997) and Săndulescu (1984, 1988)
Extension in Danubian window	NE-SW extension	30 km	35-25 Ma	Fügenschuh and Schmid (2005), Schmid et al. (1998) and Maţenco and Schmid (1999)
East and SE Carpathians over European foreland	shortening	117–150 km	33-9 Ma	Roure et al. (1993), Ellouz et al. (1994) and Maţenco (2017)
South Carpathians over Moesian Platform	transpression and shortening	0 (W) to 35 (E) km	14-9 Ma	Matenco et al. (1997), Maţenco (2017) and Răbăgia and Tărăpoancă (1999)
Tisza-Dacia (Pannonian Basin) extension next to the Mid Hungarian Shear Zone	E-W extension	250 km	20-9 Ma	Balázs et al. (2016)
Tisza-Dacia extension in South Pannonian Basin	E-W extension	80 km	20-9 Ma	Ustaszewski et al. (2008)
Tisza-Dacia extension in SE-most Pannonian Basin	E-W extension	50 km	29-8 Ma	Erak et al. (2017), Maţenco and Radivojević (2012) and Toljić et al. (2013)
Cerna Fault	dextral strike-slip	35 km	33-23 Ma	Berza and Drăgănescu (1988), Fügenschuh and Schmid (2005) and Kräutner and Krstić (2002)
Timok Fault	dextral strike-slip	65 km	20-9 Ma	Fügenschuh and Schmid (2005) and Kräutner and Krstić (2002)
Tisza-Dacia rotation Pannonian basin	paleomagnetic rotation	75°cw	20-9 Ma	Fig. 24
Balkanides; Rhodope; Circum-Rhodope				
East Vardar ophiolites on Circum-Rhodope	shortening	unknown	155-150 Ma	Ferriere and Stais (1995), Michard et al. (1994) and Kockel (1986)
Circum-Rhodope on Serbomacedonian	shortening	unknown	150-130 Ma	Schmid et al. (2019)
Serbomacedonian on Sredna Gora	shortening	>70 km	130-120 Ma	Schmid et al. (2019)
Circum-Rhodope (Strandja) on Sredna Gora	shortening	>50 km	110-100 Ma	Gerdjikov (2005)
Sredna Gora on Balkanide nappes	shortening	>120 km	120-95 Ma	Bergerat et al. (2010) and Kounov et al. (2010)
Balkanide nappes on Moesian Platform	shortening	75 km	80-65 Ma	Burchfiel et al. (2008), Ivanov (1988) and Sinclair et al. (1998)
Eastern Balkanide nappes on Moesian Platform	shortening	30 km	50-40 Ma	Burchfiel et al. (2008), Ivanov (1988) and Sinclair et al. (1998)
Nestos Thrust	shortening	70 km	55-42 Ma	Jahn-Awe et al. (2010) and Kounov et al. (2015)
Rhodope Uppermost Unit on Rhodope Upper Unit	shortening	unknown	Jurassic-Cretaceous	Schmid et al. (2019)
Rhodope Upper Unit on Rhodope Middle Unit (Nestor Suture)	shortening	unknown	Jurassic-Cretaceous	Schmid et al. (2019)
Closure Nestos Suture	shortening	unknown	Triassic-Middle Jurassic	Turpaud and Reischmann (2010)
Rhodope Middle Unit on Rhodope Lower Unit	shortening	unknown	Jurassic-Cretaceous	Schmid et al. (2019)
Dinarides; Albanides; Hellenides; Aegean basin				
Tisza-Datca and Sava suture zone on Jadar Kopaonik	shortening	50 km	80-65 Ma	Erak et al. (2017), Marovic et al. (2007) and Schmid et al. (2008)
West-Vardar ophiolites on Adriatic margin	shortening	>180 km	150-130 Ma	Baumgartner (1985), Mikes et al. (2008), Bortolotti et al. (2005) and Scherreiks et al. (2014)
Upper on Lower Pelagonian (Greece)	shortening	>120 km	150-95 Ma	Kilias et al. (2010) and Most (2003)
Jadar Kopaonik on Drina-Ivanjica/Upper Pelagonian	oblique shortening	30 km	85-60 Ma	Schmid et al. (2008) and this paper
Drina-Ivanjica on East Bosnian Durmitor	shortening	25 km	150-100 Ma	Schmid et al. (2008), Porkoláb et al. (2019) and this paper
East Bosnian Durmutor on pre-Karst	shortening	100 km	150-60 Ma	Schmid et al. (2008, 2019), this paper
Reactivation East Bosnian Durmutor on pre-Karst	extension	25 km	18-14 Ma (reconstructed as 20-10 Ma)	van Unen et al. (2019)
Pre-Karst on High Karst	shortening	30 km	85-65 Ma	Hrvatović (2006) and Tari (2002)
High Karst/Pelagonian on Budva/Pindos	shortening	<5 (NW) to >130 (SE) km	60-35 Ma	van Hinsbergen et al. (2005a), Tari (2002), Schmid et al. (2008) and this paper
Shortening within Pindos	shortening	>120 km	60-35 Ma	Skourlis and Doutsos (2003)
High Karst on Budva	shortening	30 km	5-0 Ma	this paper
Budva on Dalmatian	shortening	>60 km	35–23	this paper
Dalmatian on Adria	shortening	10–30 km	23-0 Ma	Bega (2015), Cazzini et al. (2015), Glavatovic (2007) and Tari (2002)
High Karst vs Adria	paleomagnetic rotation	20°cw	120-100 Ma	Fig. 25
Dalmatian vs Adria	paleomagnetic rotation	0°	100-0 Ma	Fig. 25
Medvenica Mountains	paleomagnetic rotation	130°cw	60-20 Ma	Tomljenović et al. (2008) and Fig. 25

Table 1 (*continued*)

Region/structure	sense	amount	Age	reference
Medvenica Mountains	paleomagnetic rotation	50°ccw	20-0 Ma	Tomljenović et al. (2008) and Fig. 25
Tripolitza on Ionian	shortening	>75 km	35-15 Ma	IGRS-IFP (1966), Kamberis et al. (2000), Sotiropoulos et al. (2003) and van Hinsbergen et al. (2005a)
Shortening within Ionian	shortening	100 km	35-15 Ma	Roure et al. (2004)
Ionian on Pre-Apulian	shortening	unknown	15-4 Ma	van Hinsbergen et al. (2006) and van Hinsbergen and Schmid (2012)
Ionian on Mediterranean Ridge	shortening	unknown	13-0 Ma	Finetti (1982), Kastens (1991) and Underhill (1989)
Upper Pelagonian Attica	paleomagnetic rotation	50°cw	70-60 Ma	Morris (1995) and Fig. 26
Zakynthos	paleomagnetic rotation	20°cw	1-0 Ma	Duermeijer et al. (1998a, 1998b)
Rhodos	paleomagnetic rotation	25°ccw	4-0 Ma	van Hinsbergen et al. (2007)
Anatolia; Black Sea; Eastern Mediterranean Basin; Cyprus; Caucasus; South Armenia; Arabian collision zone				
Scythian Platform on Tauric Flysch (Crimea)	shortening		Triassic-Early Jurassic	Muratov et al. (1984), Nikishin et al. (2015c), Oszczypko et al. (2017) and Sheremet et al. (2016a)
Western Black Sea	extension; transform	160 km	130-80 Ma	Nikishin et al. (2015a, 2015b)
Black Sea inversion	shortening	30	40-20 Ma	Khriachtchevskaia et al. (2010), Munteanu et al. (2011) and Gobarenko et al. (2017)
Sakarya on Karakaya	shortening	unknown	<203 Ma	Okay and Monié (1997) and Okay et al. (2002)
Opening Intra-Pontide Ocean	extension	unknown	180-170 Ma	Göncüoğlu et al. (2014), Robertson and Ustaömer (2004) and Alparslan and Dilek (2017)
Closure of Intra-Pontide Suture	shortening	unknown	158-110 Ma	Akbayram et al. (2013)
Oldest cherts in Ankara Mélange			240 Ma	Tekin and Göncüoğlu (2007) and Tekin et al. (2002)
Sakarya on Cretaceous ophiolites and underlying orogen	shortening	unknown	65-60 Ma	Gökten and Floyd (2007)
Formation Cretaceous Eastern Mediterranean Ophiolites	extension	unknown	95-89 Ma	van Hinsbergen et al. (2016) and references therein
Onset metamorphic sole formation Cretaceous Ophiolites	shortening	unknown	~104 Ma	Peters et al. (2018) and Pourteau et al. (2019)
Cretaceous Ophiolites on Tavşanlı	shortening	unknown	91-83 Ma	Mulcahy et al. (2014) and Pourteau et al. (2019)
Tavşanlı on Afyon/Ören	shortening	unknown	70-65 Ma	Göncüoğlu et al. (1992) and Pourteau et al. (2013)
Kırşehir on Afyon	shortening	unknown	70-65 Ma	Göncüoğlu et al. (1992) and Pourteau et al. (2013)
Akdağ-Yozgat block of Kırşehir Block	paleomagnetic rotation	15°cw	45-25 Ma	Lefebvre et al. (2013a) and Fig. 30
Kırıkkale-Kırşehir block of Kırşehir Block	paleomagnetic rotation	10°ccw	45-25 Ma	Lefebvre et al. (2013a) and Fig. 30
Ağacören-Avanos block of Kırşehir Block	paleomagnetic rotation	30°ccw	45-25 Ma	Lefebvre et al. (2013a) and Fig. 30
Afyon/Bolkardağı on Aladağ	shortening	unknown	65 Ma	Özgül (1984) and Mackintosh and Robertson (2013)
Afyon/Ören on Dilek	shortening	unknown	60-45 Ma	this paper
Aladağ on Dilek	shortening	unknown	65-45 Ma	McPhee et al. (2018a)
Dilek on Menderes	shortening	unknown	45-35 Ma	Lips et al. (2001) and Schmidt et al. (2015)
Aladağ/Dilek on Geyikdağı	shortening	>75 km; >154 km	45-35 Ma	McPhee et al. (2018a, 2018b)
Lycian Nappes on Bey Daglari	shortening	>75 km	23–15	Hayward (1984) and van Hinsbergen et al. (2010b)
Alanya Nappes on Antalya Nappes	shortening	unknown	91-83 Ma	Çetinkaplan et al. (2016) and Okay and Özgül (1984)
Antalya Nappes on Bey Daglari	shortening	unknown	83-70 Ma	Okay and Özgül (1984)
Heart of Isparta Angle	shortening	25 km	20-5 Ma	McPhee et al. (2018b)
Central Tauride Intramontane Basins	extension	25 km	20-0 Ma	Koç et al. (2017, 2018)
Northern limb Antalya Basin orocline	paleomagnetic rotation	20°cw	20-5 Ma	Koç et al. (2016)
Southern limb Antalya Basin orocline	paleomagnetic rotation	20°cw	20-5 Ma	Koç et al. (2016)
Geyikdagi rotation	paleomagnetic rotation	~40°cw	45-40 Ma	McPhee et al. (2018a)
Kyrenia Range	shortening	17.5 km	9-6 Ma	McPhee and van Hinsbergen (2019)
Cyprus rotation	paleomagnetic rotation	30°ccw	6-0 Ma	Fig. 32
Cyprus rotation	paleomagnetic rotation	45°ccw	90-70 Ma	Clube (1985) and Fig. 32
Uludağ-Eskisehir Fault	dextral strike-slip	100 ± 20 km	38-27 Ma	Okay et al. (2008a, 2008b)
North Anatolian Fault Zone	dextral strike-slip	≤85 km	11-0 Ma	Akbayram et al. (2016), Hubert-Ferrari et al. (2002) and Şengör et al. (2005)
Forearc to foreland basin transition Cankiri Basin	shortening	unknown	65-60 Ma	Kaymakcı et al. (2009)
Central Pontide shortening	shortening	30 km	45-25 Ma	Espurt et al. (2014)
Western limb Central Pontide orocline	paleomagnetic rotation	40°ccw	65-45 Ma	Meijers et al. (2010a, 2010b, 2010c) and Fig. 29
Eastern limb Central Pontide orocline	paleomagnetic rotation	40°cw	65-45 Ma	Meijers et al. (2010a, 2010b, 2010c) and Fig. 29

(*continued on next page*)

Table 1 (*continued*)

Region/structure	sense	amount	Age	reference
Exhumation of Kırşehir Block	E-W extension	unknown	85-55 Ma	Lefebvre et al. (2013a), 2015, van Hinsbergen et al. (2016) and references therein
Ivriz Detachment	extension	unknown	65-50 Ma	Gürer et al. (2018a) and Seyitoğlu et al. (2017)
Savcılı-Mucur Fault zone	shortening	>27 km	40-23 Ma	Isik et al. (2014) and Advokaat et al. (2014a)
Ecemiş Fault	sinistral strike-slip	60 km	35-20 Ma	Jaffey and Robertson (2005) and Gürer et al. (2016)
Eastern Taurides	paleomagnetic rotation	30°ccw	25-15 Ma	Gürer et al. (2018b) and Fig. 31
Ophiolite emplacement on Malatya, Binboğa, Geyikdağı	shortening	unknown	90-85 Ma	Perincek and Kozlu (1984), Robertson et al. (2013a), Boztuğ et al. (2005) and Kuşcu et al. (2010)
Malatya on Binboğa	shortening	unknown	85-80 Ma	Karaoğlan et al. (2013a), Parlak et al. (2004, 2013b), Rızaoğlu et al. (2009) and Yıldırım (2015)
Binboğa on Geyikdağı	shortening	unknown	45-35 Ma	Perincek and Kozlu (1984) and Robertson et al. (2013a)
Malatya/Binboğa on Misis	shortening	unknown	35-16 Ma	Robertson et al. (2004a)
Malatya on Kahramanmaraş Basin/Arabia	shortening	unknown	13-11 Ma	Hüsing et al. (2009a, 2009b)
Levant Basin	extension	B factor ≈ 2	Triassic-Early Jurassic	Gardosh et al. (2010), Schattner and Ben-Avraham (2007) and Erduran et al. (2008)
East Anatolian Fault Zone	sinistral strike-slip	unknown	6 Ma	Karaoğlu et al. (2017)
Sürgü Fault	sinistral strike-slip	unknown	6 Ma	Koç and Kaymakcı (2013)
Malatya-Ovacık Fault Zone	sinistral strike-slip	29 km	5-3 Ma	Westaway and Arger (2001)
Göksun Fault	sinistral strike-slip	unknown	11-6 Ma	Kaymakcı et al. (2010) and this paper
Greater Caucasus shortening	shortening	130–300 km	35-0 Ma	Ershov et al. (2003) and Cowgill et al. (2016)
Greater Caucasus Basin	extension	unknown	180-170 Ma	Adamia et al. (2011a, 2011b), McCann et al. (2010), Saintot et al. (2006a) and Topchishvili (1996)
Transcaucasus and Jurassic ophiolites on South Armenian Block	shortening	unknown	80-75 Ma	Rolland et al. (2012)
South Armenian block intrusion by arc plutons			157 Ma	Hässig et al. (2015)
South Armenian Block rotation	paleomagnetic rotation	45°cw	80-75 Ma	Fig. 29
Cretaceous ophiolites on easternmost Taurides	shortening	unknown	83-78 Ma	Topuz et al. (2017)
Cretaceous ophiolites on Bitlis-Pütürge metamorphics	shortening	unknown	83-78 Ma	Oberhänsli et al. (2010a, 2012, 2014)
Exhumation Keban metamorphics	extension (?)	unknown	80-50 Ma	Kuşcu et al. (2010, 2013) and Beyarslan and Bingöl (2000)
Maden arc on Pütürge massif	deposition/ intrusion	unknown	55-50 Ma	Aktaş and Robertson (1984a)
Bitlis-Püturge on Maden-Hakkari	shortening	unknown	50-40 Ma	Huvaz (2009) and Oberhänsli et al. (2010b)
Hakkari and Bitlis on Guvan ophiolite (Arabia)	shortening	40 km	18-11 Ma	Oberhänsli et al. (2010b) and Yılmaz et al. (1981)
Hakkari-Maden on Arabia	shortening	unknown	18-11 Ma	Cavazza et al. (2018), Okay et al. (2010), Hüsing et al. (2009a, 2009b) and Huvaz (2009)

2012). Uncertainties in such reconstructions are then limited to different interpretations on the exact location of a specific magnetic anomaly, or the use of different timescales, and typically stay within tens of kilometers (DeMets et al., 2015a; Doubrovine and Tarduno, 2008). The relative positions of tectonic plates determined from ocean-floor magnetic anomalies and fracture-zone geometries are only applicably back to the Jurassic. In addition, many ocean basins underwent substantial continental stretching (commonly referred to as pre-drift extension) before break-up and seafloor spreading, which must be accounted for, in order to reconstruct Pangea back to Late Palaeozoic-Early Mesozoic times. Estimates of pre-drift extension can be rather subjective but possible to quantify through a detailed analysis of continent–ocean boundaries, and comparison of paleomagnetic poles from conjugate margins (which needs high-quality data) in concert with seismics and gravity data to determine the amount of crustal extension (thinning) before break-up.

Reconstructing the world's oceans also quantifies the area consumed through subduction, particularly around the Pacific Ocean and its predecessor the Panthalassa Ocean, and in the Tethyan Realm. The areas lost were dominantly underlain by oceanic lithosphere but also contained continental lithosphere, as testified by rock-records preserved at (former) subduction plate boundary zones. The restored area of subducted lithosphere becomes larger farther back in time (termed 'world uncertainty' by Torsvik et al., 2010), for example, 60% of the Earth's lithosphere has been subducted since the Late Jurassic. Reconstructing the paleogeography of such areas, and even more so, plate configurations that existed within such areas relies on indirect geological evidence for plate motion. The Mediterranean region is one of such areas and contains an incomplete, highly deformed rock record that was for a large part off-scraped from now-subducted lower crust and/or lithospheric mantle. Indirect evidence that is widely used for restoring the paleogeography and tectonic plates of this subducted lithosphere comes from a variety of geological, geochemical, and geophysical observations, such as tectonic structure, paleomagnetism, biogeography (i.e. reconstructions based on fossil flora and fauna), clastic sediment composition and inferred provenance, geochemistry of magmatic rocks, seismic tomographic images of modern mantle structure, lithostratigraphic correlations, or timing or conditions of regional metamorphism. Reconstructions of consumed plates and their paleogeography tend to integrate all or part of such data types (Barrier and Vrielynck, 2008; Csontos and Vörös, 2004; Dercourt et al., 1986, 2000; Golonka, 2004; Handy et al., 2010; Meulenkamp and Sissingh, 2003; Moix et al., 2008; Schettino and Turco, 2010; Scotese, 2001; Stampfli and Borel, 2002; Stampfli and Hochard, 2009). Although it seems logical to use as much information as possible to build reconstructions, integrating all types of often qualitative data sets has some drawbacks.

First, using so many different data and types and assigning them equal weight offers many degrees of freedom to infer a variety of reconstructions. This may be illustrated by the fact that reconstructions portrayed in the references cited above display variable plate configurations and paleogeographies, the more so the farther back in time. Second, using different types of qualitative data, e.g., magmatic geochemistry, adds a level of subjectivity to

Fig. 1. Map of the Mediterranean region with the main geographic features discussed in the text. Key to abbreviations: Aeg = Aegean Sea; Alb = Albania; Alb. = Albanides; Als = Alboran Sea; ana = Anaximander Seamount; apu = Apuseni Mountains; Arm = Armenia; att = Attica; Aze = Azerbaidjan; bal = Baleares; BET = Betic Cordillera; big = Biga Peninsula; BoH = Bosnia and Herzegovina; cal = Calabria; cha = Chalkidiki Peninsula; CIR = Central Iberian Ranges; cor = Corsica; cri = Crimea; Cro = Croatia; cyp = Cyprus; EAHP = East Anatolian High Plateau; E-Carp = East Carpathians; era = Eratosthenes Seamount; evv = Evvia; flo = Florence Rise; GdL = Gulf de Lion; GoV = Gulf of Valencia; gar = Gargano Peninsula; goc = Gulf of Corinth; gs = Gran Sasso Mountains; ibi = Ibiza; isa = Isparta Angle; Kos = Kosovo; Kyr = Kyrenia Range; Leb = Lebanon; lig = Ligurian Alps; LV = Lake Van; Mac = North Macedonia; mal = Mallorca; me = Malta Escarpment; Mol = Moldova; Mon = Montenegro; myk = Mykonos; nax = Naxos; pro = Provence; par = Paros; Pan = Pannonian Basin; pel = Peloponnesos; po = Po Plain; pug = Puglia; PYR = Pyrenees; rho = Rhodos; sam = Samothraki Island; sar = Sardinia; S-Carp = South Carpathians; sic = Sicily; Slo = Slovenia; sma = Sea of Marmara; SoG = Strait of Gibraltar; SoS = Strait of Sicily; Swi = Switzerland; tat = Tatra Mountains; tin = Tinos; tra = Tracia; UK = United Kingdom; vra = Vrancea area; W-Carp = West-Carpathians.

reconstructions, which become dependent on the conceptual connection of the data ascribed to a tectonic process. Third, reconstructions of different areas by different authors are not based on the same philosophies, reconstruction approaches, or weighting of the importance of a particular data type and cannot be directly compared and compiled. Finally, it is difficult to judge where a different interpretation is permitted within the available constraints, since it is not always clear which data sets inspired the choice for a particular reconstruction.

We therefore limit the types of input data that we use for our reconstruction to as few data types as possible. We also try to refrain from using any geodynamic interpretation of a cause-consequence relationship, e.g. between the rock and deformation record and subduction or collision. We therefore selected only those data that provide quantitative kinematic evidence, i.e. evidence that shows the direction, amount, and/or timing of relative motion between geological units. Additionally, we apply a strict reconstruction hierarchy of data types that defines the order in which data were used to build and fine-tune the reconstruction. This hierarchy has been applied earlier to reconstructions of the India-Arabia-Asia Plate boundary zones (van Hinsbergen et al., 2011, 2012, 2019), the Arabia-Asia collision zone (McQuarrie and van Hinsbergen, 2013), the Caribbean region (Boschman et al., 2014), and circum-Pacific orogens (Schepers et al., 2017; van de Lagemaat et al., 2018; Vaes et al., 2019) and can be directly compared to, and integrated with these reconstructions. We restrict ourselves to the following data types, in the following reconstruction hierarchy (Table 2):

(1) *Ocean basin reconstructions.* Almost all reconstructions of the Mediterranean region use reconstructions of the Central and North Atlantic ocean and Bay of Biscay, based on marine magnetic anomalies and fracture zones, as first and foremost boundary constraint on the area gained and lost in the Mediterranean region through time (Capitanio and Goes, 2006; Dewey et al., 1989; Handy et al., 2010; Hosseinpour et al., 2016; Rosenbaum et al., 2002b; Stampfli and Hochard, 2009). We will discuss the reconstructions of the Atlantic Ocean in the next section.

(2) *Continental extension reconstructions.* As a second constraint, we apply reconstructions of continental extensional regions, such as back-arc basins. The maximum geological record is obtained at the end of an extensional event, whereas a contractional event leaves a minimum geological record. The amount of extension in e.g. the Gulf of Lion, Tyrrhenian, Pannonian, or Aegean back-arc basins may be estimated from modern crustal thickness, and detachment fault displacements, but are less accurate than ocean basin reconstructions.

(3) *Transfer fault and strike-slip fault displacements.* Strike-slip faults are useful in that these constrain in high precision the relative motion direction of the adjacent blocks. If present, displaced markers may constrain offsets, and cross-cutting relationships with stratigraphy or plutons may constrain the timing of activity. Transfer faults (with or without transpressional or transtensional components) may accurately constrain extension or contraction directions in tandem with normal or thrust faults, similar to oceanic transform faults.

(4) *Shortening records.* Detailed balanced cross-sections of fold-and-thrust belts are relatively rare in the Mediterranean region, but where available, e.g., for the southern Alps (Schönborn, 1999), outer Carpathians (Ellouz et al., 1994; Gągała et al., 2012; Morley, 1996; Roure et al., 1993), or Pyrenees (Beaumont et al., 2000; Roure et al., 1989) constrain the minimum amount of area loss accommodated in these belts. It is more common that fold-and-thrust belts have been subdivided in major nappe systems, without detailed constraints on intra-nappe shortening. In those cases, we reside to the approach detailed in van Hinsbergen and Schmid (2012) and estimate the timing and duration of underthrusting of a nappe. Timing of accretion of a nappe is bracketed between the youngest stratigraphic ages of rocks involved, and the oldest cooling or crystallization ages from metamorphic rocks in that nappe. We note that ages from HP-LT metamorphic rocks may be cooling ages and may post-date peak temperature and – importantly – peak pressure. In addition, after the transfer of rocks from the downgoing plate to the overriding fold-and-thrust belt, slower burial and prograde metamorphism of the latter, recorded by the geochronometers, may continue. We thus regard these ages as minimum ages for the moment of accretion only. We infer the original paleogeographic extent of a nappe prior to thrusting by the amount of shortening that corresponds to the amount of Africa-Europe convergence that occurred during the underthrusting of the nappe(s), whereby the presently stacked nappes restore adjacent to each other.

(5) *Geometrical consistency.* The final reconstruction should not contain overlaps between geological units without geological evidence for extension or contain major 'gaps' without evidence for shortening. We tune the reconstruction to remain geometrically consistent along areas or structures where no kinematic constraints are available, as long as the final reconstruction remains consistent with constraints provided in steps 1–4. These reconstruction steps should be considered model predictions, and we will clearly identify where we made reconstruction choices.

(6) *Paleomagnetism.* The resulting geometry is then tested against paleomagnetic data. Paleomagnetic data quantitatively place geological units relative to the paleomagnetic pole and constrain the net vertical axis rotation and paleolatitudinal change since rock formation and can be directly compared to the reconstruction by placing the plate circuit in a paleomagnetic reference frame (whereby we use the Global Apparent Polar Wander Path (GAPWaP) of Torsvik et al. (2012)). We chose to place paleomagnetic constraints low in the reconstruction hierarchy, however, for three reasons. Firstly, in the context of the Mediterranean region, paleolatitudinal study of rocks is not meaningful, since typical error bars are on the order of ±5°, i.e. ±>550 km. The constraints listed above provide a much higher precision. Secondly, for tectonic reconstructions as performed here, vertical axis rotations constrained by paleomagnetism are useful, but the Euler pole around which a block rotated cannot be constrained from paleomagnetic data alone, but has to come from structural geological observations, which are constrained or estimated in steps 1–5. Thirdly, where

Table 2
Seven-step reconstruction systematic for plate boundary zone deformation restoration.

1	*Net area change between Africa, Iberia, Arabia, and Eurasia constrained by Atlantic-Red Sea marine magnetic anomaly-based reconstructions*
2–4	*Structural geological constraints on timing, direction, and magnitude of 2) continental extension; 3) transform or strike-slip motion; and 4) continental shortening*
5	*Develop smoothed, geometrically consistent reconstruction.*
6	*Test against paleomagnetic data using the* www.paleomagnetism.org *integrated tool set*
7	*Basic rules of plate tectonics: plates are surrounded by plate boundaries or PBZs that end in triple junctions*

possible, we use paleomagnetic data as an independent test on a reconstruction based on structural geological data. Only where structural geological information cannot constrain a total amount of rotation, we use paleomagnetic data as a primary source of information.

In addition, because the Central Atlantic Ocean reconstruction of Labails (2007) and Labails et al. (2010), included in Torsvik et al. (2012), predicted Early Jurassic convergence in the western and central Mediterranean region which is not evident from the geological record – there are no indication for shortening or subduction there, we revisited the constraints for the early opening history (see Section 3). As detailed below, we made a few minor adjustments to this early opening history. In addition, we used for our reconstruction the latest rendition of the timescale (Gradstein et al., 2012), which slightly deviates from the timescale used in Torsvik et al. (2012) – only for the ~126 Ma age of M0 given by Gradstein et al. (2012), which in the marine magnetic anomaly community is more commonly assigned a ~121–122 Ma age (e.g., Midtkandal et al., 2016). We note that these small adjustments, on the order of 1° in relative Eurasia-Africa positions, mean that our plate model deviates slightly from that of Torsvik et al. (2012) that was used to calculate the GAPWaP. Because we use the GAPWaP to predict and test our reconstructions against paleomagnetic data (see Section 6), our updates on the plate model introduces a minor error of ~1° in paleomagnetic directions that we predict for especially the Mesozoic, which, as will be shown in Section 6, is too small to affect our conclusions.

(7) *Basic rules of plate tectonics.* As a final test, the reconstruction should comply with the basic rules of plate tectonics: all plates should be surrounded by plate boundaries that end in stable triple junctions (Cox and Hart, 1986). These basic rules assume plate rigidity and motion along discrete fault zones, whereas instead in the strongly deformed Mediterranean regions such boundaries are diffuse and distributed over larger regions. Rather than discrete plate boundaries, we may have to infer plate boundary zones instead distributing deformation, but the basic rules remain valid.

Other types of geological data, e.g. paleontological, sedimentological, or geochemical data, are only used to identify regionally correlative rock units, such as carbonate platforms, deep-marine basins, or ophiolite belts. Today, these define a pattern that is displayed on geological maps, and this is the pattern that we restore to its original, Triassic configuration. In some cases, we have tested the final configuration in our reconstruction against pre-Alpine basement characteristics, e.g. for the position of Calabria versus Sardinia. We will discuss these isolated cases in the text, but we did not perform a systematic, Mediterranean-wide analysis of the pre-Alpine basement configurations, which is subject for future studies.

4. Atlantic Ocean reconstruction

Atlantic Ocean reconstructions lie at the basis of the reconstruction of the Mediterranean Region and dictate area gain and loss since the Triassic. Below, we summarize the constraints we used in this paper, and re-analyzed and slightly modified the Early Jurassic Africa-North America rotations. Following the pioneering kinematic study of Klitgord and Schouten (1986), recent work by Sahabi et al. (2004), Labails (2007), and Labails et al. (2010) have accumulated kinematic data that form a basis to describe the early rifting history between Africa and North America. We apply the most recent constraints on the opening of the Atlantic using the plate circuit recently summarized in Torsvik et al. (2012), which is based on Gaina et al. (2002) for the north Atlantic, and on Labails et al. (2010) and Müller et al. (1999) for the Central Atlantic Ocean between Africa and North America. For the Central and Northern Atlantic Ocean the Triassic reconstructions include Euler poles for Europe with respect to North America (Torsvik et al., 2012). We updated the reconstruction of Torsvik et al. (2012) for the Neogene opening of the Atlantic Ocean with recent high-resolution poles of DeMets et al. (2015b). We further apply reconstructions of Vissers and Meijer (2012a, 2012b) and Vissers et al. (2013). For Arabia-Africa rotations we use the reconstruction poles for the Red Sea opening of Joffe and Garfunkel (1987).

We revisit three aspects of the early opening history of the Central Atlantic Ocean. First, Labails (2007) and Labails et al. (2010) used the Blake Spur Magnetic Anomaly (BSMA, ~170 Ma) to assess the early oceanic geometry of the Central Atlantic Ocean, but careful inspection leads us to slightly adjust the pertinent Euler pole as shown below. Secondly, prior to the BSMA, a magnetic anomaly developed named the E anomaly, which was first recognized on the American side by Rabinowitz (1974) and documented by Labails (2007) on the African side, but so far no attempt has been made to calculate a reconstruction pole for this anomaly. Thirdly, as first suggested by Sahabi et al. (2004), it became clear that the Moroccan Meseta north of the Atlas belt represents a microplate, but Labails (2007) and Labails et al. (2010) suggest continuous deformation in the Atlas range during the Jurassic and early Cretaceous while the geology of the Atlas provides no evidence for such Mesozoic deformation. Below we address these three aspects of the rifting and opening of the Central Atlantic Ocean.

To quantitatively study the kinematics of the Central Atlantic Ocean, we used the magnetic dataset in Labails (2007), her Figs. II-13, 14, 22 and 23 for the Jurassic and early Cretaceous. Using the pole for the BSMA published by Labails (2007) and Labails et al. (2010), we have inspected the pertinent anomaly match at BSMA times (Fig. 2a). The fit of the corresponding anomaly on the African side (ABSMA) with the BSMA is certainly acceptable but predicts up to several hundreds of kilometers of convergence in Mediterranean region in the Early Jurassic. In the Eastern Mediterranean, there is widespread evidence for Early Jurassic subduction, but in the western and central part, there is no evidence at all for shortening – instead, the geology suggests extension until the Cretaceous. Because the prediction of convergence hinges entirely on the BSMA pole of Labails (2007) and Labails et al. (2010), we have studied the data to assess whether this prediction is robust.

The BSMA has two branches, a long NNE trending one and a shorter ENE trending branch. Labails (2007) reconstruction pole leads to a fit in which the African picks plot slightly east of the BSMA, whilst in the ENE trending branch the African picks are somewhat too southerly. Inspired by Stock and Molnar (1983) we use the following procedure to find an adjusted total reconstruction pole for the BSMA yielding an improved fit (Fig. 2a and b). We estimate a center of the data, labelled R1, and define three mutually perpendicular rotation axes R1, R2, and R3, where R1 is the center of the data, R2 the pole to the great circle through R1 and the current reconstruction pole, whilst R3 is located on the great circle 90° away from R1. We apply a small rotation about R2 of −0.5° and add that rotation to the current reconstruction pole. This causes the African ABSMA to be anticlockwise rotated with respect to the BSMA (not shown here). A second small rotation about R1 of −2.0° added to the first rotation serves to counterbalance this mismatch and optimize the fit. The resulting adjusted pole (65.87°N-15.08°W, −71.929) differs, albeit not considerably, from the pole of Labails (2007) and Labails et al. (2010). The resulting reconstruction pole lies about halfway the poles for the 195 Ma closure proposed by Sahabi et al. (2004) and the M25 calculated by Labails et al. (2010), as shown in Fig. 3e.

Both on the North American and African side, anomaly E documented by Labails (2007) has a shape similar to that of the (A)

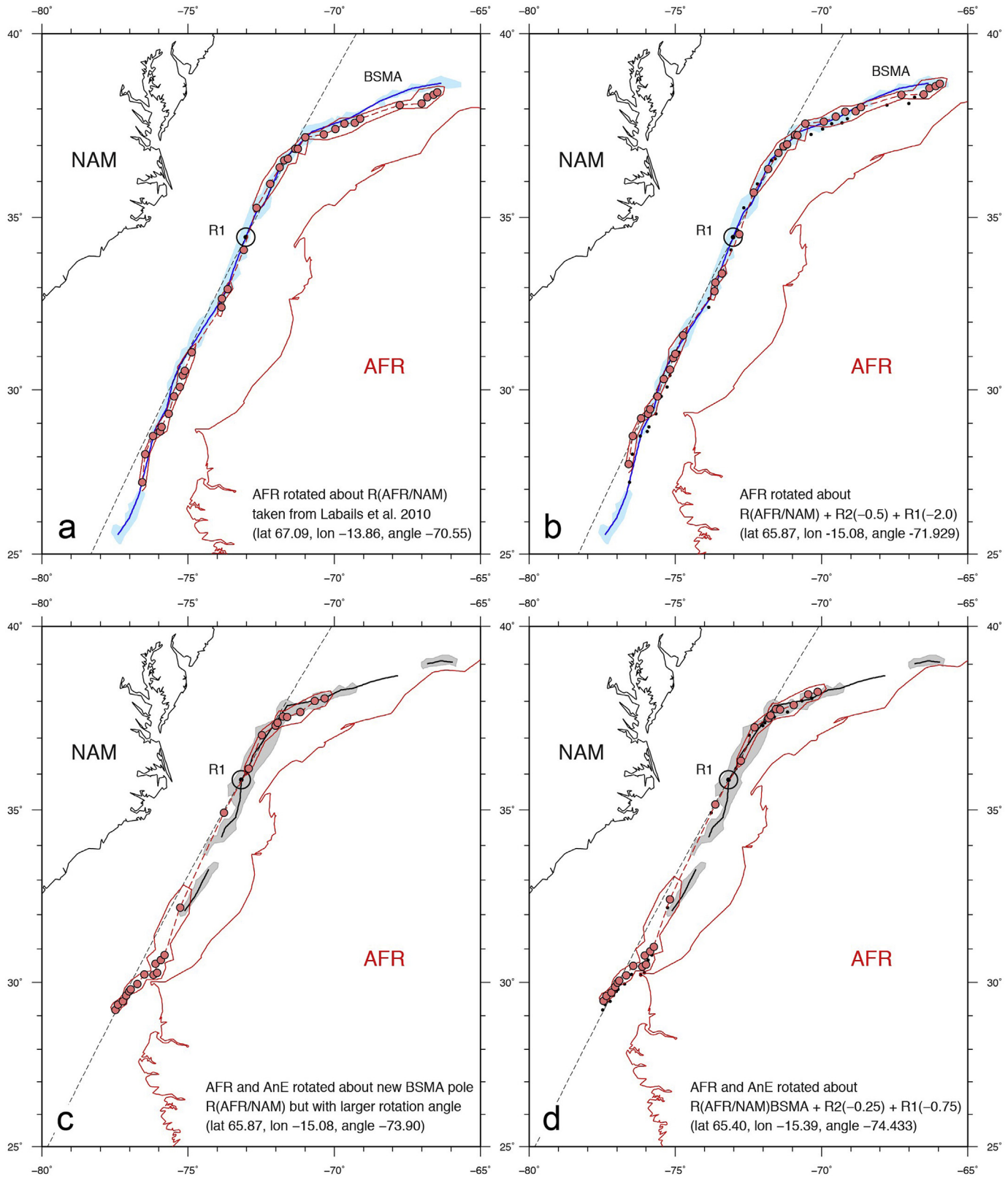

Fig. 2. (a, b). Detailed magnetic anomaly map showing fits of the BSMA with the corresponding anomaly on the African Plate, after westward rotation using the AFR/NAM reconstruction pole of Labails et al. (2010). African magnetic anomaly data indicated in red. R1 denotes arbitrarily chosen center of the data, dashed line the greatcircle through R1 and the current Euler pole. (a) Fit obtained with the current reconstruction pole without any correction. (b) Fit obtained after a small correction rotation of −0.5° about the pole R2 to the great circle (dashed line) through the data (R1) and the current Euler pole, followed by an additional rotation of −2.0° about R1. Small dots in b indicate initial rotatd positions of African picks shown in a. (c, d) Magnetic anomaly map showing fits of anomaly E with the corresponding African anomaly, after rotation about a guessed AFR/NAM reconstruction pole based on the BSMA pole. African magnetic anomaly data again indicated in red. (c) Fit without any further correction, R1 and dashed line defined as in a and b. (d) Fit after a small correction rotation of −0.25°about the pole R2 to the great circle (dashed line) through the data (R1) and the guessed reconstruction pole, followed by an additional rotation of −0.75° about R1. Small dots in b indicate initial rotated positions of African picks shown in a. For further explanation see text.

BSMA (Fig. 2c and d), with a NNE trending and an ENE trending branch, whilst the two counterparts seem more or less symmetrically disposed with respect to the BSMA (see also Fig. 3). We therefore try a provisional reconstruction pole for anomaly E with a same latitude and longitude as the BSMA pole but with a larger rotation angle (−73.9°). This results in a moderately reasonable match (Fig. 2c). We improve the fit along the ENE trending branch using the same approach as for our recalculation of the BSMA pole, estimating a center of the data R1 of the anomaly on the American side, and calculating R2 and R3 as defined above. A clockwise rotation about R2 of −0.25° serves to cause a better coincidence of the African data along the ENE trending branch, whilst a subsequent clockwise rotation of −0.75° optimizes the fit (Fig. 2d). The resulting pole (65.4°N, 15.39°W, rotation angle −74.433°) clearly differs from that of the BSMA, albeit that the difference is not considerable (Table 2). The calculated pole lies approximately between the pole for the 195 Ma closure of Sahabi et al. (2004) and Labails (2007) and Labails et al. (2010), and the Euler pole for the BSMA calculated above (see Fig. 3e). The rather simple northward track described by the subsequent reconstruction poles for 195 Ma, anomaly E, BSMA and M25 lends support to the belief that they form a coherent set of reconstruction poles.

The northwestern part of Africa comprises the Moroccan Meseta separated from the continental African mainland by the Atlas range, a Cenozoic fold-and-thrust belt inverting a Triassic to Mid–Jurassic rift with Jurassic–Cretaceous post-rift sedimentation (Beauchamp et al., 1999; Frizon de Lamotte et al., 2008). The Moroccan Meseta (MES) needs special attention because it separates Iberia to the north from the main African Plate (AFR). According to Labails (2007) and Labails et al. (2010) there is a component of convergence, albeit small, between MES and AFR, but the kinematic evidence for motion of the Meseta relative to Africa during the Jurassic and Early Cretaceous seems at variance with the lack of geological evidence from the Atlas range for Mesozoic convergence. Vissers et al. (2013) therefore suggested that the motion of the Moroccan Meseta relative to Africa during the development of the Atlas rift could be described by one single correction pole P (MES/AFR) (27.3°N, 13.73°W, rotation angle 1.91°), and that changes of the MES/AFR poles reported by Labails (2007) and Labails et al. (2010) could well be within the errors involved in the MES/NAM and AFR/NAM poles, hence within errors in the MES/AFR poles (see also Ruiz-Martínez et al., 2012).

A balanced cross-section study in the high Atlas by Beauchamp et al. (1999) points to a Cenozoic convergence of ~37 km. The predicted shortening of Sahabi et al. (2004)'s MES/NAM and MES/AFR poles for 195 Ma is significantly larger, i.e. ~55 km. The P (MES/AFR) correction pole proposed by Vissers et al. (2013) yields a Cenozoic shortening along the section studied by Beauchamp et al. (1999) of ~30 km, which reasonably concurs with the shortening inferred from the balanced section.

With the published reconstruction poles of Sahabi et al. (2004), Labails (2007) and Labails et al. (2010), our poles for Anomaly E and the BSMA, and a correction pole to describe the displacement of the Moroccan Meseta relative to Africa, we may now describe the rifting and drifting history of the Central Atlantic Ocean. The reconstruction poles used are summarized in Table 3. Fig. 2a–d shows four stages of the opening of the Central Atlantic Ocean. We take the 195 Ma fit proposed by Sahabi et al. (2004) as a starting point (Fig. 3a). This reconstruction juxtaposes the ECMA and WACMA, with the notion that in the region of the Meseta microplate the fit is slightly less ideal because our correction pole for the Meseta relative to Africa differs from the reconstruction pole proposed by Sahabi et al. (2004) as discussed above. The motion between 195 Ma and anomaly E times was roughly southward (Fig. 3b). The stage pole for the subsequent motion toward BSMA times (~170 Ma), however, indicates southeast-directed flow (Fig. 3c) which continues well during further oceanization and formation of the M25 anomaly (Fig. 3d). This change in flow direction, previously inferred to have occurred at BSMA times (Labails, 2007), apparently occurred earlier, at anomaly E times. As the stage poles R (AFR/NAM) for anomaly E to BSMA and for BSMA to M25 are close to each other, we estimate the age of anomaly E on the basis of the presumption that the spreading velocity was essentially the same for these two stages. This yields an age of 174.7 Ma which is an approximate age only, first because the age of the BSMA is approximate, and secondly because we assume constant spreading velocity between anomaly E and M25 times. There are, unfortunately, no independent data to verify our age estimate.

A notable aspect of the early rifting stage concerns the asymmetry of the crustal dimensions between the ECMA and anomaly E on the American side and between the WACMA and anomaly E on the African side, where the crust between the ECMA and anomaly E on the American side is about four times as wide as that of the corresponding crust on the African side (Fig. 2b). This strongly suggests that the early stages of Oceanization were accommodated by an asymmetric extensional shear zone system dominated by shearzones dipping towards Africa. In contrast, spreading since anomaly E was in general more symmetric (Fig. 2c and d).

The motion of Africa with respect to North America since the initial Triassic fit is illustrated in Fig. 3e showing the locations of the reconstruction poles, whilst Fig. 3f the motion of AFR with respect to fixed EUR. This motion defines the net area gain and loss that forms the boundary condition for our reconstruction of the Mediterranean region.

5. Orogenic architecture

We reconstruct the present-day pattern of major tectonic units of the Mediterranean region, whereby we characterize their first-order paleogeographic appearance (platforms and basins) based on sedimentary facies, or on crystalline oceanic or continental basement. In this section, we describe the modern tectonic architecture of the Mediterranean orogens: we identify the major nappes whose paleogeographic origin and tectonic evolution we restore, and identify their timing of emplacement based on structural, stratigraphic and geochronological constraints, using the philosophy explained in Section 3. We also identify major extensional windows and review the quantitative constraints on extension, strike-slip displacement, and shortening. The descriptive sections below provide the documentation of the constraints used for our reconstruction and cites the relevant literature. We summarize these constraints in Table 1 and display these in orogenic architecture diagrams that show schematic cross-sections through the main orogenic belts with first-order kinematic relationships and timing of displacement. Finally, the modern distribution of tectonic units and bounding faults are displayed on tectonic maps that are detailed versions of the overview map of Fig. 4. A larger version of Fig. 4 is provided in the Supplementary Information 1. A key to the tectonic units is given in Fig. 5. Finally, all tectonic units below have abbreviations used on the maps and in the orogenic architecture diagrams. These are listed in Table 4 and given in between brackets behind every tectonic unit the first time it is mentioned in the text.

Schmid et al. (2008) used the term 'mega-units' to identify certain groups of fault-bounded tectonic units that consist of large-scale rock assemblies with a common geological history and that have a similar paleogeographic origin. Here we use this term also for other groups of tectonic elements that are frequently bounded from each other either by suture zones or by first-order fault zones. These mega-units may for instance represent rocks deposited on former carbonate platforms, on slopes, in deep basins, or on Ocean floor, and they are frequently interpreted to represent suture zones

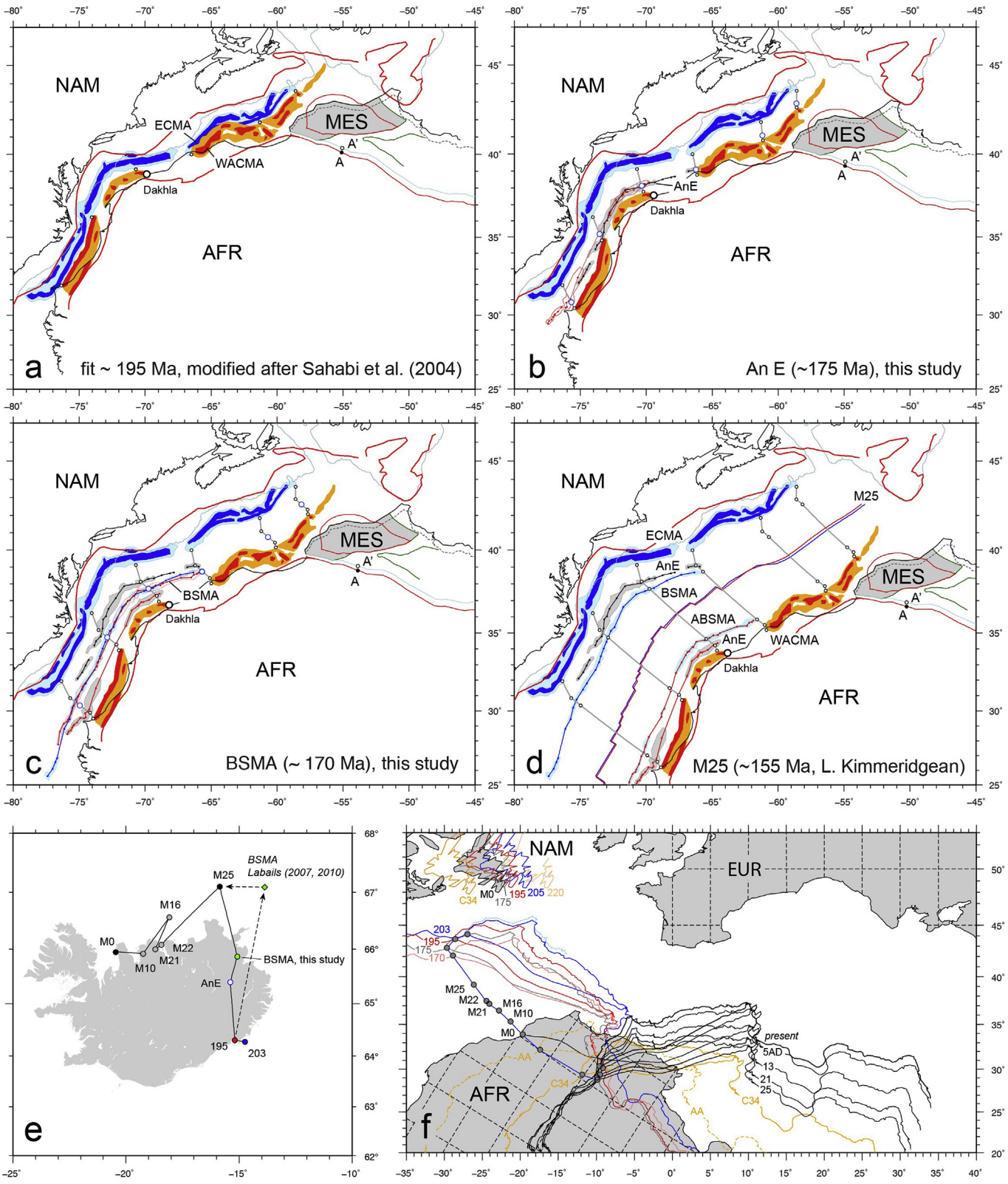

Fig. 3. (a–d). Rifting and onset of spreading in the central Atlantic Ocean, relative to N America fixed. NAM: North America; AFR: Africa; MES: Moroccan Meseta; A, A': markerpoints at the High Atlas cross-section studied by Beauchamp et al. (1999). (a) Reconstruction for the 195 Ma fit, modified after Sahabi et al. (2004). (b) Reconstruction for anomaly E times (~175 Ma). Small-circle segments denote flow direction. Note strong asymmetry of the basin floor on either side of anomaly E suggesting asymmetric stretching. (c) Reconstruction for BSMA times (~170 Ma). Note change in flow direction since anomaly E. (d) Reconstruction for anomaly M25 (~154 Ma), flow direction remains roughly the same as in c. (e) Projections of total reconstruction poles for Africa with respect to North America, showing migration of these poles with time. Green diamond and dashed arrows represents BSMA reconstruction pole of Labails et al. (2010). For further details see text. (f) Motion history of AFR with respect to EUR from the Tiassic fit, estimated at 203 Ma, until the present. Contours of Africa during early stages of rifting are shown in different colours to improve readability. Motion history is accentuated by the motion of a markerpoint representing the city of Agadir. The southern boundary of the Atlas range is indicated for each stage shown; note that it also forms the northern boundary of the African pre-Triassic basement. Intermediate stages between the BSMA and M0 are omitted for clarity, except for pertinent marker points. Lightblue dashed coastline of Meseta illustrates displacement of Meseta Block relative to AFR as explained in text. Tertiary stages of north directed motion are shown in black for anomalies 25 (57.4 Ma), 21 (46.5 Ma), 13 (33.4 Ma) and 5AD (14.7 Ma), where the finite rotation poles are after Vissers and Meijer (2012a) and ages according to Gradstein et al. (2012). Anomaly 5AD taken from DeMets et al. (2015a).

Table 3
Euler poles for North America with respect to Northwest Africa. Lat = pole latitude, lon = pole longitude.

anom	age[a]	lat	lon	angle	reference
(fit)	203	64.28	−14.74	−78.05	Labails et al. (2010)
(ECMA)	195[b]	64.31	−15.19	−77.09	Sahabi et al. (2004)
(ECMA)	190[b]	64.31	−15.19	−77.09	Labails et al. (2010)
AnE	174.7	65.40	−15.39	−74.433	This study
BSMA	170	65.87	−15.08	−71.929	This study
M25	155.69	67.10	−15.86	−64.23	Labails et al. (2010)
M22	150.56	66.08	−18.44	−62.80	Labails et al. (2010)
M21	148.89	66.00	−18.70	−62.29	Labails et al. (2010)
M16	141.03	66.57	−18.08	−59.34	Labails et al. (2010)
M10	133.63	65.92	−19.24	−57.55	Labails et al. (2010)
M0	126.11	65.95	−20.46	−54.56	Labails et al. (2010)
A34	83.64	76.81	−20.59	−29.506	AFR/NAM Müller et al., 1999

[a] Ages of M series according to Gradstein et al. (2012).
[b] Note that poles for 195 (Sahabi et al., 2004) and for 190 (Labails et al., 2010) are identical.

or continental blocks. We do not a priori define suture zones or continental fragments but will instead interpret those from their reconstructed patterns. The pattern of mega-units is shown in Fig. 4, and they will be defined in the sections below, roughly from west to east. For the Alps, we follow the mega-units defined by Handy et al. (2010) and Schmid et al. (2004b), for the Carpathians, Pannonian region, and Dinarides we follow the definitions of numerous previous works systematized and summarized in Schmid et al. (2008) and Schmid et al. (2019), and for the Albanides-Aegean-west Anatolian region those of van Hinsbergen and Schmid (2012) and Schmid et al. (2019). For the western Mediterranean region, we define mega-units based on references specified in Section 5.

The mega-units are subdivided in polygons in the GPlates reconstruction (see Supplementary Information 3, and Fig. 4) bounded by faults for times that they behave as coherent units. In times that the rocks contained in these polygons underwent internal deformation, we represent the mega-units by polylines that move relative to each other and redefine the new shape of the mega-unit's polygon when the deformation event ends.

Below, we review the orogenic architecture of the Mediterranean region at first order, illustrated with maps and orogenic architecture charts that show the juxtapositions of the main tectonic units of the orogen, and the timing of their emplacement, and detail the kinematic constraints on Mediterranean deformation used in our restoration. The key for the abbreviations for tectonic and geographic elements shown on the tectonic maps and orogenic architecture charts is provided in Table 4. We first review the constraints on the major tectonic blocks from the forelands of the various fold-and-thrust belts that were not (always) part of Eurasia or Africa since the Triassic. These include Iberia, Adria, and the Moesian Platform. Then, we review the constraints on the Mediterranean fold-and-thrust belts from west to east.

5.1. Iberia; Pyrenees

The Iberian continent bounds the Mediterranean region in the west and is separated from North America and western Eurasia by active or former mid-Ocean ridges, from Africa by the transpressional Azores-Gibraltar transform system and a convergent margin, and from southwestern Eurasia by the Pyrenean fold-and-thrust belt. Below, we provide an overview of kinematic constraints on Iberian motion relative to the surrounding plates using marine magnetic anomaly data, transforms, and geological constraints from the Pyrenees.

Convergence in the Pyrenean domain was primarily controlled by the motion history of Iberia in between the Eurasian, North American and African Plates, and the progressive northward opening of the central and northern Atlantic Ocean since the early Mesozoic (Srivastava et al., 1990a). The position of Iberia relative to North America and Eurasia back to M20 (~148 Ma) is constrained by marine magnetic anomalies (see below). During and before that time, Iberia was bounded to the Central Atlantic Ocean, which already started spreading in the Early Jurassic, by the Azores-Gibraltar Fracture Zone. The precise fit of the Iberian Plate during the Triassic and Early Jurassic requires assessment of pre-Late Jurassic predrift extension between Iberia, North America and Europe. Srivastava and Verhoef (1992) applied a de-stretching technique to estimate the pre-extensional position of Iberia relative to North America and Eurasia, and proposed Euler poles for Iberia for this fit at 175 Ma, and for M25 (~156 Ma). However, Vissers et al. (2013) noticed that these poles predict a considerable Jurassic shortening, essentially subduction, across the Azores-Gibraltar Fracture Zone for which there is no evidence. They therefore hypothesized that the continental fit of Srivastava and Verhoef (1992) might in fact apply to the latest Triassic, and that during the early stages of rifting and drifting in the Central Atlantic, between 205 and 170 Ma, Iberia moved with Africa, which considerably reduced the predicted shortening across the Azores-Gibraltar Fracture Zone. Aside this aspect, however, we also note that Srivastava and Verhoef (1992) did not account for any motion between Europe and North America prior to and during the inferred fit as proposed by Torsvik et al. (2012) to account for Triassic rifting between Norway and Greenland.

Since the early work of Srivastava and Verhoef (1992), two kinematic studies have quantitatively addressed the Triassic position of Iberia. Sibuet et al. (2012) strictly adhere to the role of the Newfoundland-(Azores)-Gibraltar Fracture Zone as a main structure controlling the kinematics of plate motion. They infer a continental fit of Iberia for the Late Triassic (~203 Ma), followed by small motions of continental Iberia in response to early rifting which places Iberia farther south than Srivastava and Verhoef (1992). In a recent study, Fernandez (2019) presents a different position of Iberia for the continental fit, based on geometric reconstructions of a series of seismic sections west and south of Iberia, but adopts the Sibuet et al. (2012) reconstruction poles for anomalies M22 (~150 Ma) and M0 (126 Ma). The main difference with the Sibuet et al. (2012) reconstruction is that there is no clear response in terms of Iberian motion to the progressive stretching of the thinning continental crust. This leads to a quasi stationary position of Iberia between the Late Triassic and M22, which we feel is an artifact of the method chosen. Bearing in mind the problems

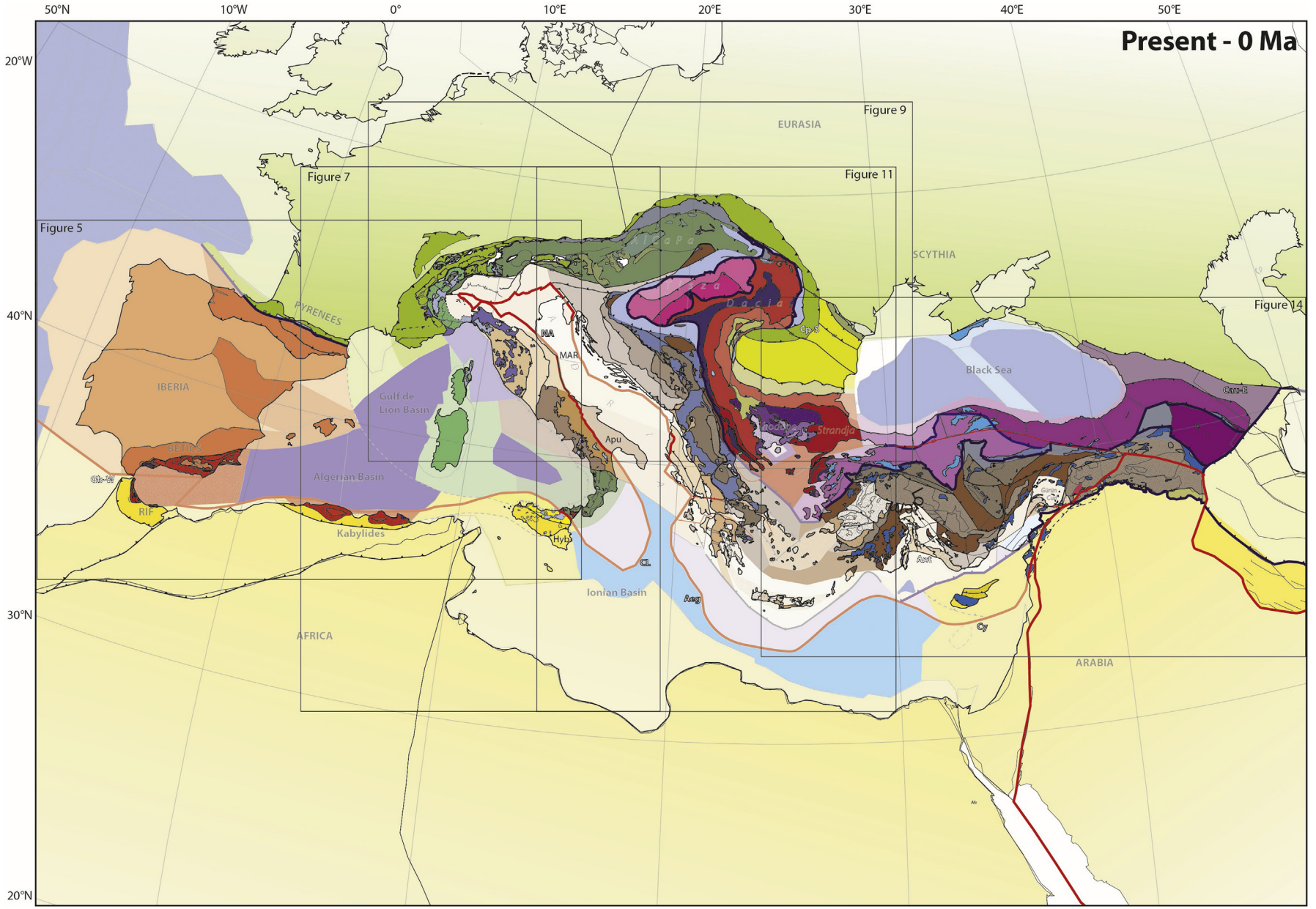

Fig. 4. Tectonic map of the Mediterranean region outlining the locations of detailed maps per sub-area. For key to abbreviations, see Table 4. A larger (A2) version of this map with indications of all tectonic units and elements is provided in Supplementary Information 1. Outlines of these tectonic units correspond to the polygons and polylines in the GPlates reconstruction files of Supplementary Information 2.

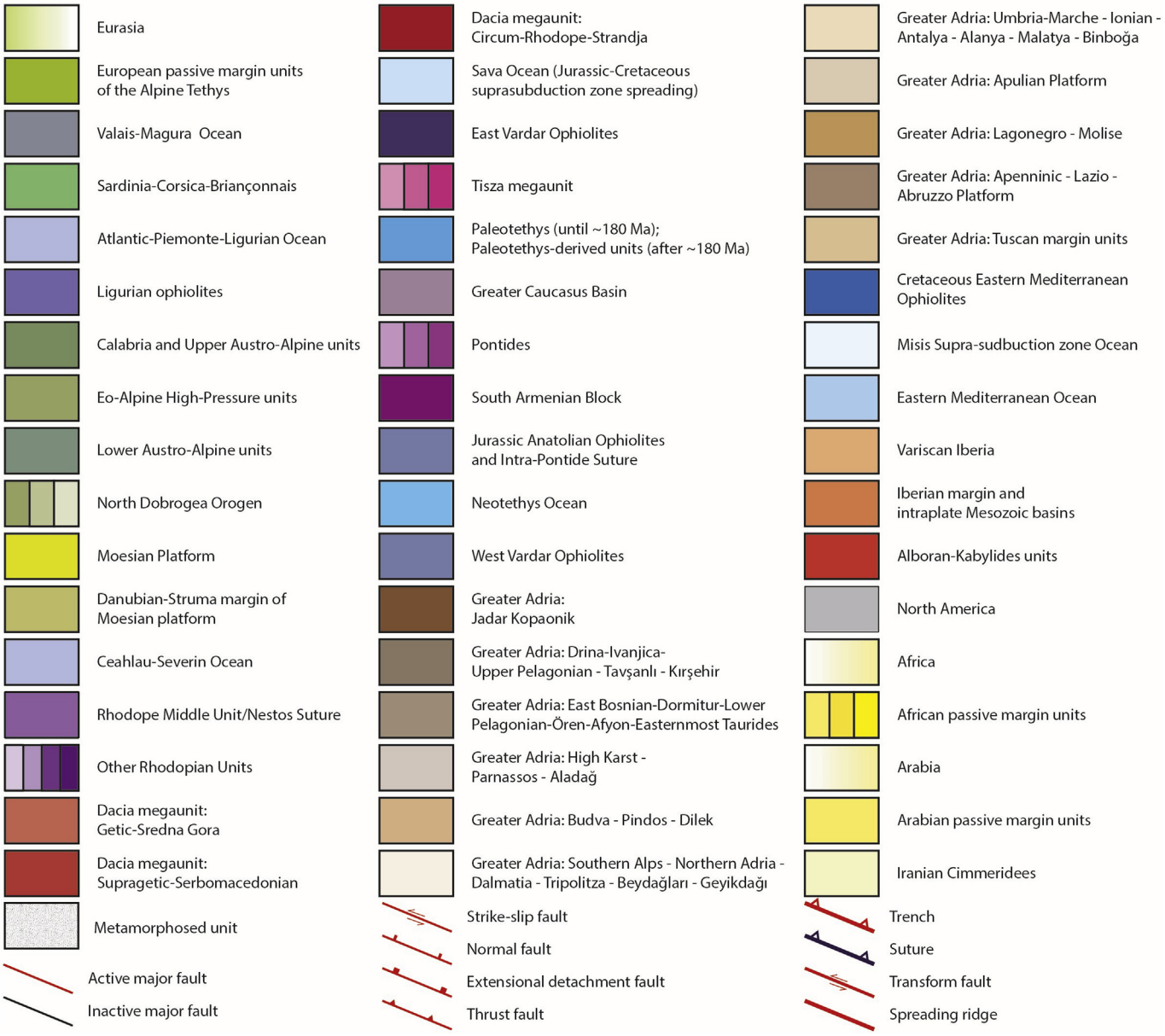

Fig. 5. Key to the maps and orogenic architecture diagrams.

involved in the Srivastava and Verhoef (1992) analysis, we follow Sibuet et al. (2012) for our reconstruction.

The opening history of the central Atlantic Ocean south of the Azores-Gibraltar Fracture Zone until the Aptian (M0, ~126 Ma) has most recently been studied by Labails (2007) and Labails et al. (2010), showing that from 170 Ma onward Africa moved east-southeastward with respect to North America. Oceanization between Iberia and North America started around M20 (~148 Ma) times. Differential motion between Iberia and Africa was accommodated in the western Mediterranean region east of Iberia through opening of the Alpine Tethys Basin between 170 Ma and M21 (~149 Ma) (Vissers et al., 2013) followed by essentially joint motion of Iberia and Africa until the Aptian (M0, 126 Ma). Euler poles for M0 (126 Ma) place Iberia rotated 42° clockwise (cw) with respect to its present orientation, prior to about 35° counterclockwise (ccw) rotation during the Cretaceous Normal Superchron (Vissers and Meijer, 2012b).

From M0 (126 Ma) times onward, the reconstruction of the motion history of Iberia was complicated by the existence of the Porcupine Microplate, first postulated by Srivastava and Tapscott (1986) and discussed in detail by Srivastava and Roest (1996). This microplate existed in the northern part of the Bay of Biscay and was separated from Eurasia by a strike slip zone (see Vissers and Meijer, 2012b, and references therein). In addition, Srivastava and Roest (1996) differentiated the Porcupine Microplate from another plate fragment, termed by these authors the King's Trough plate fragment and referred to by Vissers and Meijer (2012a) as the Southern Biscay Microplate, bounded to the north by the Bay of Biscay spreading axis, and separated from Iberia by the King's Trough – Bay of Biscay – Pyrenees fault system. In addition to the concept of the Porcupine Microplate, Srivastava et al. (1990a, 1990b) and Roest and Srivastava (1991) showed that the motion history of Iberia could in essence be described with the assumption that Iberia moved with Africa for a significant part of the Cenozoic. They formulated a jumping plate boundary hypothesis, in which the Eurasia-Africa boundary was first located along the Bay of

Table 4
List of abbreviations of tectonic units displayed in on the maps and in the orogenic architecture diagrams in the paper, and the Supplementary Information.

Achara-Trialet region	at
Adriatic Basin	ABa
Aegean	Aeg
Aegean-west Anatolia	Aeg-WA
Africa	Afr
Africo-Polsi Nappe	APo
Afyon Zone (metamorphic Bolkardağı Zone)	Afy
Ağacören–Avanos Block	AAB
Ağvanis Massif	ağm
Akdağ-Yozgat Block	AYB
Al Jawf	AJ
Aladağ Nappe	Ala
Alanya Nappes	Aly
Alboran Basin	Abo
Algeria	Ag
Algerian Basin	AlB
Alps	Alp
Alpuarride Nappe	Alp
Amasia Ophiolite	AmO
Anaximander Seamount	Ana
Ankara Mélange	AnM
Ano Garefi Ophiolite	AgO
Antalya	Ant
Antalya Nappes	Ant
Apenninic Platform Nappe	App
Apulian Escarpment	AEs
Apulian Platform	Apu
Aquitanian Basins	Aqu
Arabia	Ara
Arabia	Ar
Arax Fault	ArF
Armorican Margin	AmM
Axial Zone	AxZ
Azores-Gibraltar Fracture Zone	AGFZ
Baer Bassit Ophiolite	BBO
Baleares Block	Bls
Balkanide Nappes	Bal
Ballaton Fault	BaF
Basal Unit	bu
Bay of Biscay Axis	BBA
Bay of Biscay Basin	Bis
Beni Boussera Peridotite	BBP
Beydağları Platform	Bey
Beyşehir-Hoyran Ophiolite	BHO
Bihor Nappes	Bih
Binboğa Metamorphics	Bin
Bitlis	Bi
Bitlis Massif	Bit
Bitlis Suture	BS
Bogdan Dragos Voda Fault	BDVF
Bolkardağı Nappe	Bol
Bornova Flysch	Bfl
Bozkır Nappe	Boz
Briançonnais Nappe	Bri
Budva-Cukali Nappe	Bud
Bükk mountains	bü
Calabria slab	Cl
Calabrian Accretionary Prism	CAP
Çankırı Basin	Çan
Capidava-Ovidiu Fault	COF
Carpathians-North	Cp-N
Carpathians-South	Cp-S
Caucasus-East	Cau-E
Ceahlau-Severin Units	CSe
Central Dobrogea	CDo
Central Tauride Intramontane Basins	CTIB
Cerna Fault	CeF
Chaînes Sub-Alpines	CSa
Chenaillet Ophiolite	ChO
Çiçekdağı Ophiolite	ÇiO
Cilicia Basin	Cil
Cilicia Suture	CS
Circum-Rhodope	CRh
Codru Nappes	Cod
Corsica	cor
Corsica-Sardinia Block	CSB

Table 4 (*continued*)

Cretaceous Eastern Mediterranean Ophiolites	CEO
Crnook-Osogovo-Lisets core complex	CCC
Cycladic Blueschist Unit	cbs
Cyprus	cy
Cyprus	Cy
Dalmatian Nappe	Dal
Danubian Nappes	Dan
Deliler-Tecer Fault	DTF
Dilek Nappe	Dil
Divriği Ophiolite	DiO
Doğanşehir meta-Ophiolite	DoO
Dorsale Calcaire	DoC
Drina-Ivanjica Nappe	DIv
East Anatolian Fault Zone	EAFZ
East Bosnian Durmitor Nappe	EBD
East Vardar Ophiolites	EVO
Eastern Black Sea Basin	EBS
Eastern Pontides	EPo
Easternmost Taurides	EmT
Ebro Basin	Ebr
Ecemiş Fault	EcF
Egypt (Mediterranean part of Arabia slab)	Eg
Elaziğ magmatic suite	Ela
Eldivan Ophiolite	ElO
Emile Baudot Transform	EmB
Emporios	Emp
Engadine Window	EW
Eo-Alpine high-pressure units	EoA
Eurasia	Eur
External Betics	ExB
External Foredeep (Northern Apennines)	EFd
External Massifs	EMa
External Rif	ExR
Getic Nappes	Get
Geyikdağı Nappe	Gey
Ghomaride Nappe	Gho
Gibraltar-Betic	Gb-B
Gibraltar-West	Gb-W
Giudicarie Fault	GiF
Göksun Fault	GöF
Göksun Ophiolite	GöO
Greater Caucasus	GCA
Greater Caucasus Basin	GCB
Guevgueli Ophiolite	GO
Guleman Ophiolite	GuO
Gulf of Corinth Graben	GoC
Gulf of Lion Basin	GdL
Gulf of Valencia Basin	GoV
Güre Ophiolite	GüO
Guvan Ophiolite	GvO
Hakkari Basin Nappe	Hak
Halilbağı Ophiolite	HbO
Hatay Ophiolite	HaO
Haymana Basin	Hay
Helvetic Nappes	Hel
Herodotus	He
Herodotus Basin	HeB
High Karst Nappe	HKa
Hyblean Plateau	HyP
Iberia	Ibe
Ibiza	ibi
Inner Carbonate Unit (Sicily)	Icu
Insubric Line	IL
Intra-Moesian Fault	IMF
Intra-Pontide Suture	IPS
Ionian Basin	IoB
Ionian Nappe	Ion
Iranian Cimmerides	ICi
Iranian Paleotethys Suture Zone	IPSZ
Ispendere Ophiolite	IsO
Istanbul Zone	Ist
Ivrea Zone	Ivr
Ivriz Detachment	IvD
Izmir-Ankara-Erzincan Suture Zone	IAESZ
Jadar-Kopaonik Nappe	JKo
Jura fold-thrust belt	Jur
Jurassic Anatolian Ophiolites	JAO
Kabylides	Kb

Table 4 (*continued*)

Kağızman-Khoy suture	KKS
Kağızman-Tuzluca Basin	KTB
Kahramanmaraş Basin	Kah
Karakaya Complex	Kar
Karlıova Triple Junction	KTJ
Keban Metamorphics	Keb
Kefallonia Fault Zone	KFZ
Khost Ophiolite	KhO
King's Trough – Bay of Biscay – Pyrenees fault system	KTBIS
Kırşehir Block	Kır
Kırşehir-Kırrıkkale block	KKB
Koçali Ophiolite	KoO
Kömürhan Ophiolite	KöO
Korab Nappe	Kor
Krasta-Cukali Nappe	Kra
Kruja Nappe	Kru
Kura Fold Belt	KFB
Küre Accretionary Prism	KAP
Lago Negro Nappe	LNe
Latio-Abruzzi Platform	LAp
Lesser Caucasus	lc
Levant Basin	LeB
Ligurian-Sicilide Units	LSi
Ligurides	Lig
Lower Kabylides Unit	LKU
Lower Pelagonian Zone	LPe
Lycian Nappes	LNa
Lycian Ophiolites	LyO
Macin Nappe	Mac
Maden arc/basin	Mad
Magura Flysch	Mag
Main Caucasus Thrust	MCT
Malaguide Nappe	Mlg
Malatya Metamorphics	Mal
Malatya-Ovacık Fault	MOF
Mallorca	mal
Malta Escarpment	MEs
Mammonia Complex	Mam
Maritsa Shear Zone	MSz
Mecsek Nappes	Mec
Mediterranean Ridge	MeR
Medvenica mountains	me
Meliaticum ophiolites	Mel
Menderes Nappes	Men
Mersin Ophiolite	MeO
Meseta	Mes
Mesopotamia	Me
Meydan Ophiolite	MyO
Mid-Adriatic Ridge	MAR
Mid-Adriatic Ridge	MAR
Mid-Black Sea High	MBSH
Mid-Cycladic Lineament	MCL
Mid-Hungarian Shear Zone	MHSZ
Mirdita Ophiolite	MiO
Misis Mélange	MiM
Moesian Platform	Moe
Molise Basin Nappe	Mol
Munzur mountains	mu
Munzur Zone	Mun
Muş-Hınıs Basin	MHı
Nappes Supérieures	NSu
Nestos Thrust	NeT
Nevado-Filabride Unit	NeF
Niculitel Nappe	Nic
North African Transform	NAf
North America	NAM
North Anatolian Fault Zone	NAFZ
North Apennines	NA
North Baleares Transform Zone	NBTZ
North Pollino Fault Zone	NPFZ
North Pyrenean Fault	NPF
North Pyrenean Zone	NPZ
Northern Adria	nAd
Olevano-Antrodoco-Sibillini Thrust	OAS
Olympos-Ossa Window	OOW
Ören Unit (metamorphic Bolkardağı Zone)	Öre
Organyà Basin	Org
Outer Carbonate Unit (Sicily)	Ocu
Outer Carpathians	OCa
Pangaion-Pirin Unit	PaP
Paranassos Nappe	Par
Parentis Basin	Par
Paros	pa
Peceneaga-Camena Fault	PCF
Pelion Window	PW
Periadriatic Fault	PeF
Phyllite-Quartzite Unit	pq
Piedmont Basin	Pie
Pindos Nappe	Pin
Pınarbaşı Ophiolite	PıO
Plattenkalk-Tripali Unit (metamorphosed Ionian Zone)	Pla
Pliny and Strabo Trenches	PST
Pontides	Po
Porcupine Microplate	Por
Pozantı-Karsantı Ophiolite	PKO
Pre-Apulian Nappe	PrA
Pre-Dobrogea	PDo
Pre-Karst Nappe	PKa
Provence	pro
Püturge Massif	Püt
Pyrenean Peridotites	PPe
Racha–Lechkhumy Fault	RLF
Raggane	Re
Rechnitz Window	RW
Refahiye Ophiolite	ReO
Rhenodanubian Flysch	RdF
Rhodope Lower Unit	RhL
Rhodope Middle Unit	RhM
Rhodope Upper Unit	RhU
Rhodope Uppermost Unit	RUm
Ronda Peridotite	RoP
Sakarya Zone	Sak
Sardinia	sar
Sarıkaraman Ophiolite	SaO
Sava Suture	SS
Schistes Lustrés Corsica	Slc
Scutari-Pec Fault	SPe
Scythian Platform	Scy
Serbo-Macedonian units	SeM
Sesia Fragment	Ses
Sestri-Voltaggio Line	svl
Sevan-Akera Mélange	SAM
Sevan-Akera Suture	SAS
Simplon Detachment	SD
Sirte Basin	SiB
Sivas Basin	Siv
South Armenian Block	SAB
South Caspian Sea Basin	SCS
South Dobrogea	SDo
South Pyrenean Zone	SPZ
Southern Alps	Sal
Southern Biscay Microplate	SBi
Sredna-Gora Unit	SGo
Stilo-Aspromonte-Peloritan Block	SAP
Strait of Sicily Basin	SSB
Strimon Detachment	StD
Struma Unit	Str
Subpenninic Units	Spe
Supragetic Nappes	Sge
Talysz	ta
Tauern Window	TW
Tauric Flysch	Taf
Tavşanlı Nappe	Tav
Tell Belt	Tel
Temsamane Unit	Tsm
Tenda unit and Lower External Continental Units	Ten
Timok Fault	TiF
Tisza-Dacia Suture	TDS
Tornqvist-Tesseyre Line	TTL
Transcaucasus Zone	TCa
Transylvanian Basin	Tsv
Tripolitza Nappe	Tri
Trojan Flysch	Tro
Troodos Ophiolite	TrO
Trotus Fault	TrF

(*continued on next page*)

Table 4 (*continued*)

Trypa Group	Try
Tulcea Nappe	Tul
Tuscan Nappes	Tus
Tuzgölü Basin	Tuz
Tuzgölü Fault	TuF
Tyrrhenian Basin	Tyr
Uludağ-Eskisehir Fault	UEF
Ulukışla Basin	Ulu
Umbria-Marche Nappe	Uma
Upper Kabylides Unit	UKU
Upper Pelagonian Nappe	UPe
Upper West Alpine Nappe	UWA
Val Marecchia Ophiolite	VMO
West Black Sea Transform	WBT
West Vardar Ophiolites	WVO
Western Black Sea Basin	WBS
Zagros	Za
Zagros fold-thrust belt	Zag
Zagros Suture	ZS

Biscay axis, then jumped at around chron 17 (38 Ma) to the King's Trough – Bay of Biscay – Pyrenees fault system and eventually, since anomaly 6c (23 Ma), to the Azores-Gibraltar Fracture Zone.

A few plate-kinematic studies of recent date address the Iberia motion history with special attention to shortening in the Pyrenees (Rosenbaum et al., 2002b; Vissers and Meijer, 2012a, 2012b; Macchiavelli et al., 2017). Vissers and Meijer (2012a) analyzed the late Cretaceous and Cenozoic motion history of Iberia in a six-plate circuit including Europe, Porcupine, North America, Africa, Iberia and Southern Biscay. In addition, these authors included recent sampling of magnetic anomalies in the Bay of Biscay by Sibuet et al. (2004), and the Euler poles for the Mesozoic and Cenozoic used here are adopted from Vissers and Meijer (2012a, 2012b).

Rifting in the Bay of Biscay has been constrained in marine studies on the Armorican margin (Montadert et al., 1979) and in seismic sections (MARCONI) across the Parentis Basin (Ferrer et al., 2008) (one of the Aquitanian Basins, Fig. 6). According to Montadert et al. (1979), rifting on the Armorican margin was submarine and reactivated a pre-existing Mesozoic basin developed during Triassic times. The onset of rifting is not well established, but comparison with Aquitanian basins suggests it may have started in the Late Jurassic and continued during the Early Cretaceous. The end of rifting and onset of spreading is suggested to be intra-Aptian. From the MARCONI-3 profile and available well data, Ferrer et al. (2008) infer Late Jurassic (?)–Early Albian rifting related to the opening of Bay of Biscay. This is consistent with data from South Pyrenean Mesozoic basins, such as the Organyà Basin, which suggests that rifting did not start before the Late Jurassic (see e.g. Vergés and García-Senz, 2001). Regional data and quantitative subsidence analyses indicate that the Parentis Basin was previously affected by rifting during the Late Permian and during the latest Triassic–Early Liassic (e.g. Brunet, 1997; Ziegler, 1990).

The Azores-Gibraltar Fracture Zone separates Iberia from Africa and clearly accommodates differential motions between 170 Ma and M21 (149 Ma). During progressive oceanization in the Central and North Atlantic the Azores-Gibraltar Fracture Zone continues to act as a major transform fault. A second major structure that accommodated strike-slip components is the North Pyrenean Fault, although the magnitude of this strike-slip motion as constrained from the geology, is debated (e.g., Vissers and Meijer, 2012a, and references therein) (Fig. 6). Kinematic data on fault planes associated with the North Pyrenean Fault, though scarcely documented, are consistent with transcurrent and presumably sinistral motions. This includes the presence, in high-grade Mesozoic rocks, of subhorizontal synmetamorphic stretching lineations, and near-vertical fold axes of small-scale folds immediately adjacent to the North Pyrenean Fault (Choukroune, 1976). Sinistral motion is consistent with the kinematics inferred from Central Atlantic spreading records across the belt during the Late Cretaceous and Paleocene (Vissers and Meijer, 2012a), but the magnitude of the associated displacements are not constrained by geological data.

The Pyrenees are an ~E-W trending mountain belt, about 450 km long and 125 km wide (Fig. 1). Structural and deep seismic studies show that the orogen is an asymmetric, doubly-vergent wedge, with Iberian continental lithosphere underthrust at least about 80 km beneath Europe (Beaumont et al., 2000; Roure et al., 1989). At shallow crustal levels, the European continental margin preserved in the North Pyrenean Zone (Fig. 6) was backthrust onto the Aquitaine foreland basin to the north, while Variscan basement units of the Axial Zone in the central Pyrenees and their sedimentary cover of the Iberian margin exposed in the South Pyrenean Zone were thrust southward onto the Ebro foreland basin (Fig. 7). The North Pyrenean Zone and Axial Zone of the central Pyrenees are separated by the North Pyrenean Fault (Fig. 6).

The Variscan basement of the Axial Zone comprises a several km thick psammitic-pelitic sequence of latest pre-Cambrian, Cambrian and Ordovician age and, in the eastern part of the belt, granitic gneisses, overlain by Silurian to Carboniferous pelites, carbonates, and siliciclastic rocks (Zwart, 1979). The total thickness of this sequence is about 12 km. All of these rocks may show variable degrees of Variscan LP-HT metamorphism and were intruded by late Variscan granodioritic and gabbroic plutons (Zwart, 1979) with ages around 310-290 Ma (Aguilar et al., 2014; Druguet et al., 2014; Kilzi et al., 2016). These Paleozoic rocks are unconformably overlain by Triassic redbeds and evaporites, Jurassic carbonates and shales, and a highly variable Cretaceous sequence dominated by carbonates and mass flow deposits. These are overlain by both terrestrial and marine sediments of Cenozoic age deposited in syntectonic piggy-back basins, unconformably overlain by Oligocene coarse-clastic fan systems. The Mesozoic and Cenozoic sequence is mainly found in the South Pyrenean Zone, whereby Triassic evaporites form the main decollement horizon. The thicknesses of the restored Mesozoic and Cenozoic units varies, and may be up to ~8 km (Muñoz, 1992).

Aside the Variscan basement rocks and their Mesozoic-Tertiary cover, upper mantle peridotites and lower crustal granulites occur as up to km-scale fragments along the North Pyrenean Fault amidst Mesozoic sediments deposits in small extensional basins, showing Albian-Cenomanian LP-HT metamorphism and coevally emplaced alkaline magmatic rocks (Clerc et al., 2015; Ubide et al., 2014). A widely held view is that these peridotites were extensionally exhumed in Cretaceous time and caused the ~105-100 Ma HT metamorphism (Clerc et al., 2015; De Saint Blanquat et al., 2016; Lagabrielle et al., 2010). Recent low-temperature thermochronological data showed that both in the North and South Pyrenees, there was heating, uplift and (erosional) exhumation in this time (Rat et al., 2019; Ternois et al., 2019) These, and other authors (e.g., Jammes et al., 2009) therefore inferred 105-100 Ma Iberia-Eurasia transtension to explain these geological observations. Such transtension is inconsistent with marine magnetic anomaly interpretations, particularly of the M0 anomaly, which was consequently speculated to be unreliable (Bronner et al., 2011; Jammes et al., 2009). Because also paleomagnetic constraints are inconsistent with the transtensional scenario (see section 6.2.1), which is therefore left with no independent support, and because also seismic tomography is consistent with Mesozoic subduction in the Pyrenees, Vissers et al. (2016) suggested instead that mantle exhumation occurred during Late Jurassic rifting in the Bay of Biscay (if these rocks were derived from the North Iberian Margin) or from the Alpine Tethys (if they exhumed at the Aquitane margin), and minor extension in the Pyrenees and the HT metamorphism in the Cretaceous of the Pyrenees were related to the break-off of a slab that subducted below the Pyrenees during Early Cretaceous

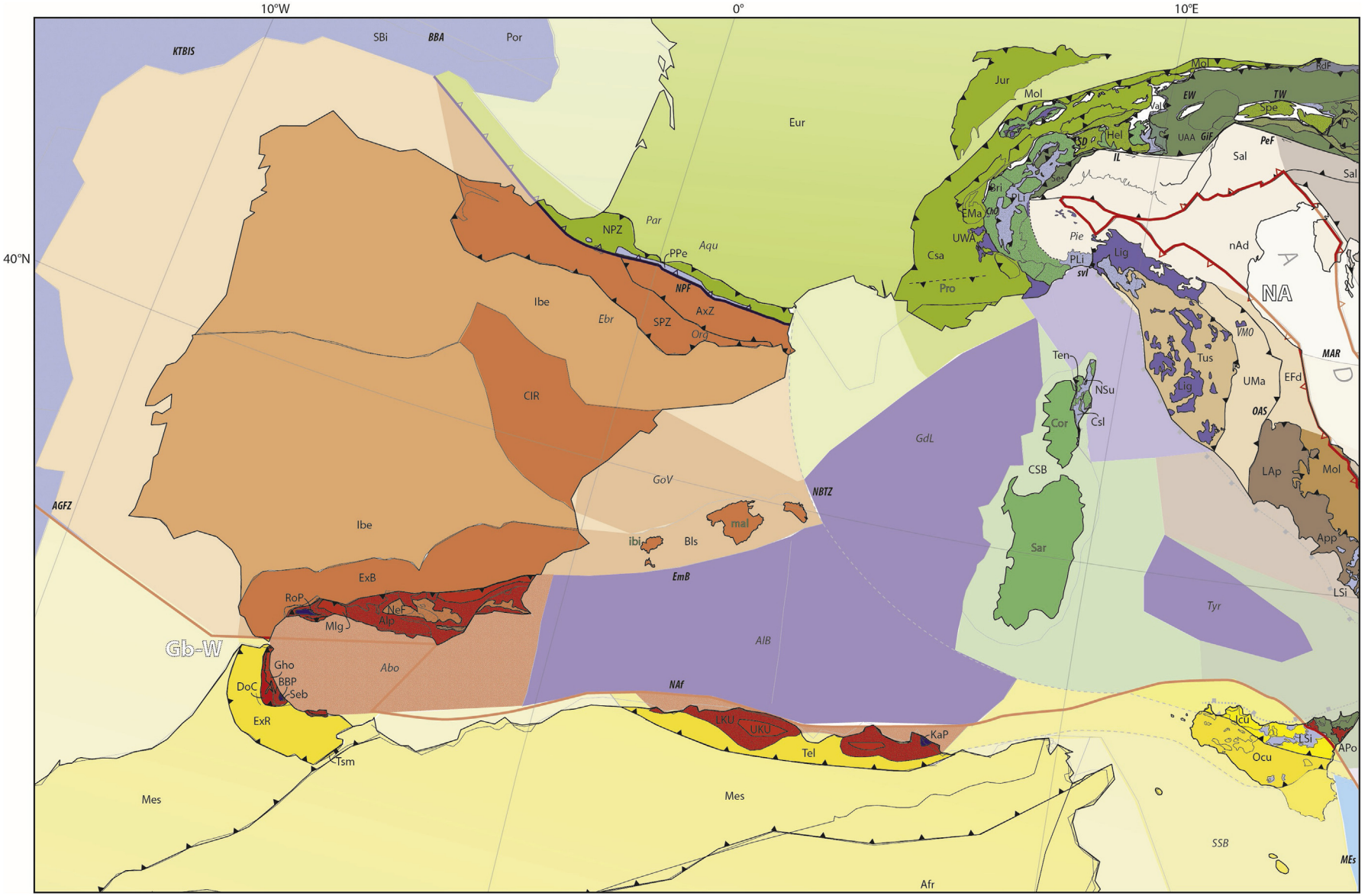

Fig. 6. Tectonic map of the western Mediterranean region. For key to abbreviations, see Table 4, for key to tectonic units, see Fig. 5. For location of the map within the Mediterranean region, see Fig. 4.

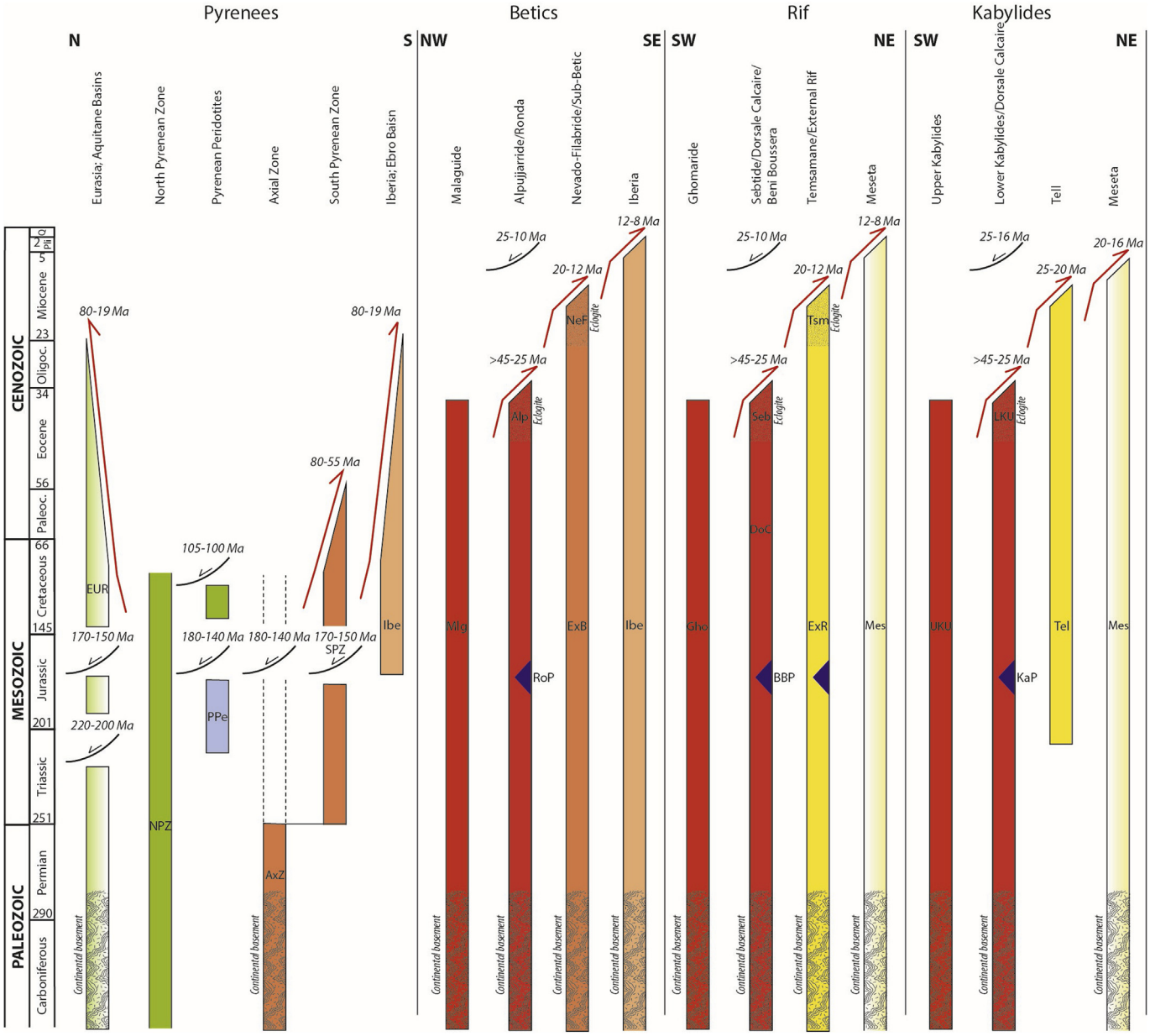

Fig. 7. Orogenic architecture charts for the Pyrenees, Betic Cordilleras, Rif, and Kabylides Mountains. For Key to abbreviations, see Table 4, for key to tectonic units, see Fig. 5. For regional distribution of tectonic units, see Fig. 6. See Table 1 for summery of kinematic constraints corresponding to this chart. Periods of metamorphism are indicated with dotted hatching and formation of pre-Alpine crystalline basement with curved hatching.

rotation of Iberia. Such Jurassic exhumation is consistent with 177–138 Ma Sm/Nd ages derived from these peridotite bodies, previously suggested to reflect Nd loss to explain the difference with the $^{40}Ar/^{39}Ar$ ages (Henry et al., 1998). Finally, recent $^{40}Ar/^{39}Ar$ dating revealed that greenschist-facies ductile shear zones in the easternmost Pyrenees, on Cap de Creus, have 170-160 Ma ages, and were likely low-angle extensional shear zones that formed along the east Iberian margin during the opening of the Piemonte-Ligurian Ocean (Vissers et al., 2017).

The North Pyrenean Fault separates the Eurasian margin rocks thrust northward and Iberian margin rocks thrust southwards and can therefore be interpreted as the surface expression of a suture zone. The structure of the North Pyrenean Zone is in essence an imbricate stack. South of the North Pyrenean Fault the structure is more complex and includes an antiformal stack of Variscan basement units in the Axial Zone presumably detached along the underlying lower crust, whilst the Triassic evaporites allowed the development of cover units now exposed in the South Pyrenean Zone (e.g., Beaumont et al., 2000).

Shortening across the Pyrenees has been estimated in three crustal-scale cross sections across the Pyrenees. The western section (Ansó-Arzacq section), a minimum shortening of 75–80 km was calculated, of which 23–30 km was accommodated in the North Pyrenean Zone (Teixell, 1996, 1998). The central (ECORS-Pyrenees) section yielded minimum shortening estimates of 100–165 km, of which 37 km was accommodated in the North Pyrenean Zone (Beaumont et al., 2000; Muñoz, 1992; Roure et al., 1989). The eastern, E-Pyrenees section gave a minimum shortening of 125 km, of which 32 km in the North Pyrenean Zone (Vergés et al., 1995). Shortening in the ECORS and E Pyrenees sections is thought to have started in Campanian times (~80 Ma), i.e. close to chron A33o, and ended around 19 Ma (Vissers and Meijer,

2012a). The onset of shortening in the Ansó-Arzacq section was presumably Late Cretaceous (Teixell, 1998). Plate kinematic reconstruction for chron A33o suggests that the amount of total convergence between Iberia and Eurasia since chron A33o increases from west to east due to a ccw rotation of ~8° (Vissers and Meijer, 2012a). Their modeled convergence values normal to the trend of the Pyrenees since A33o, adopted in our reconstruction, is 138 km for the Ansó-Arzacq section, 159 km for the ECORS section and 167 km for the Eastern Pyrenees. Except for the ECORS section, in which the modeled convergence of 159 km (Vissers and Meijer, 2012a) is roughly equal to the 165 km shortening estimated by Beaumont et al. (2000), the modeled convergence is several tens of km higher than the minimum crustal shortening values inferred from section restoration. Uncertainties both in the anomaly-based plate kinematic reconstruction and in the published restorations of the crustal-scale balanced sections may have contributed to these differences.

In Central Iberia, Jurassic to earliest Cretaceous extension led to the formation of shallow marine sedimentary basins which inverted in Cenozoic time, between 35 and 20 Ma (de Vicente et al., 2007). We adopt the reconstruction of van Hinsbergen et al. (2014a) and reconstruct 20 km of shortening across the Central Iberian ranges estimated by de Vicente et al. (2007).

5.2. Adria; Ionian Basin; Strait of Sicily

The continental part of the Adria Microplate, in short **Adria**, occupies the Central Mediterranean region and is for its largest part covered by the Adriatic Sea (Figs. 1 and 6). Adria is connected to the oceanic Ionian Basin by a passive margin – the Apulian Escarpment. The Ionian Basin also shares an originally Mesozoic or even older, but in places reactivated passive margin with Northern Africa – the Malta Escarpment (Fig. 6). For time periods after the spreading in the Ionian Basin, Adria is widely viewed as an African Plate promontory that reaches all the way to the Alps, although structural, paleomagnetic, and GPS evidence shows that it has undergone and still undergoes motion relative to stable Africa in the Cenozoic. Because Adria is overthrust by the Apennines in the west, the Southern Alps in the north, and the Dinarides and Albanides-Hellenides in the east (Figs. 1, 4 and 6), resolving its kinematic history is important for restoring these fold-and-thrust belts.

The **Ionian Basin** is underlain by a 7–9 km thick crust (Chamot-Rooke et al., 2005) associated with a low heat flow (Pasquale et al., 2005), and is therefore interpreted as old ocean floor of the Neotethys Ocean (e.g., Gallais et al., 2011; Granot, 2016; Speranza et al., 2012). The age of the Ionian Basin has been estimated to range from late Paleozoic to Cretaceous (Dercourt et al., 1986; Frizon de Lamotte et al., 2011; Gallais et al., 2011; Golonka, 2004; Granot, 2016; Le Pichon et al., 2019; Robertson et al., 1991; Schettino and Turco, 2010; Şengör et al., 1984; Stampfli and Borel, 2002). Speranza et al. (2012) showed that the Ionian Ocean floor is characterized by a reversed polarity and argued it may fit with a Triassic (227-219 Ma) reversed chron. Recently, Granot (2016) showed marine magnetic anomalies with two polarity reversals in the Herodotus Basin, to the west of Cyprus (Fig. 4), and used the skewness of the anomalies as measure for the paleolatitude of formation. Compared with the GAPWaP of the African Plate (Torsvik et al., 2012), this study showed a possible age range of 360–255 Ma. Because the Herodotus Basin contains a 200 km wide normal time interval, which with reasonable spreading rates of ~5 cm/yr would require a minimum of 4 Myr to form, he argued that the Herodotus crust must have formed prior to the onset of the Kiaman Superchron at 316 Ma, leaving a ~340 ± 25 Ma age for this crust, i.e. Carboniferous.

The Malta Escarpment is a passive margin that links the Ionian Basin to the Hyblean Platform of Sicily (Fig. 4), which is underlain by African continental crust. The Hyblean Platform, however, underwent some 50–60 km late Miocene and younger NE-ward motion relative to Africa, accommodated by extension in the **Strait of Sicily Basin** (Argnani, 2009; Civile et al., 2008), and to the southeast in the Sirte Basin of Libya (Capitanio et al., 2011). The Ionian Basin shows no evidence for significant Cenozoic deformation, other than some minor late Miocene and younger inversion (Gallais et al., 2011; Hieke et al., 2006).

North of the Apulian Escarpment lies the Apulian carbonate platform that forms the southern part of Adria (Finetti, 1985) (Fig. 4). Rocks of the Apulian Platform are exposed on the Puglia Peninsula of southern Italy (Fig. 1) and contain an up to 6 km thick stratigraphy with disconformities spanning the Lower Cretaceous to Messinian (Bosellini, 2006; Ricchetti et al., 1988; Spalluto and Caffau, 2010; Spalluto and Pieri, 2008; Tropeano et al., 2004). The Apulian Platform is bounded in the north by a NW-SE running hemipelagic Adriatic Basin connecting the Ionian Zone of the Hellenides with the Umbria-Marche Zone of the Apennines (see sections 5.5.5 and 5.11, Fig. 4), with the transition to deeper water sedimentation exposed on the Gargano Peninsula (Bosellini et al., 1999; Graziano, 2013; Santantonio et al., 2013) (Fig. 1). Towards the north, the Adriatic Basin gives way to northern Adria, a complex horst-graben structure that developed in Jurassic time (Santantonio and Carminati, 2010).

Although Adria is sometimes regarded as having been rigidly connected with Africa since the end of opening of the Ionian Basin (e.g., Muttoni et al., 2013; Rosenbaum et al., 2004), GPS measurements show that it is currently moving at a 2–5 mm/yr to the north relative to Africa (D'Agostino et al., 2008; Grenerczy et al., 2005; Métois et al., 2015). In the central Adriatic Sea, where the thrust fronts of the Apennines and Dinarides are closest, Adria is cut by the Mid-Adriatic Ridge (Fig. 4) that consists of Neogene NW–SE striking oblique thrusts (Grandic et al., 2001; Kastelic et al., 2013; Scisciani and Calamita, 2009; Scrocca, 2006). South of the Mid-Adriatic Ridge there are a few E–W to NE–SW striking, probably dextral strike-slip structures (Argnani et al., 1993; Favali et al., 1993; Finetti, 1982) that are not restored in detail here. Hence, in addition to the deformation in the Strait of Sicily Basin, probably dextral transpressional faults cut central Adria, although no detailed estimates of associated displacements are known.

5.3. Gulf of Valencia; Baleares; Algerian Basin; Kabylides; Alboran; Atlas

The southwestern Mediterranean region contains two, partly oceanic extensional basins. The intra-continental **Gulf of Valencia Basin** opened due to up to 80 km of extension between ~25 and 16 Ma and separated the Baleares blocks from Iberia (Figs. 1 and 6) (Maillard et al., 1992; Séranne, 1999; Vergés and Sàbat, 1999). We have used this number for our reconstruction, as in van Hinsbergen et al. (2014a, 2014b), but we note that this should be regarded a maximum number: recent work suggested that a large part of this extension may result from Late Jurassic-Early Cretaceous extension related to the opening of the Piemonte-Ligurian ocean (Etheve et al., 2016). The Gulf of Valencia is bounded in the northeast from the partly oceanic Gulf of Lion along the North Baleares Transform Zone (Séranne, 1999) (Fig. 6, see Section 5.4).

Between the Baleares and the North African margin lies the **Algerian Basin**, which contains oceanic crust. The northern and southern margins of this basin consist of Middle to upper Miocene transform faults (the Emile Baudot and North African transforms) and the western and eastern margins are ocean-continent transitions (Acosta et al., 2001; Booth-Rea et al., 2007; Mauffret et al., 1992) (Fig. 6). We here follow the reconstruction of Mauffret et al. (2004) in which the Algerian Basin formed due to 560 km of E-W extension between 16 and 8 Ma, for reasons discussed in Chertova

et al. (2014) and van Hinsbergen et al. (2014a), but see also Faccenna et al. (2004) and Schettino and Turco (2006) for alternative hypotheses. The North African transform system has been shortened by Plio-Pleistocene northward thrusting (Stich et al., 2006), which may reflect the inception of southward subduction of the Algerian Ocean floor below Northern Africa (Baes et al., 2011; Hamai et al., 2018).

In the southwest, south, and east, the Algerian and Valencia Basins are bordered by the thin-skinned Betic-Rif fold-and-thrust belt of SW Iberia and northern Morocco surrounding the **Alboran Basin**, and by the Kabylides of northern Algeria (Fig. 1). The eastward continuation of this thrust belt is the Sicilian Maghrebide-Calabria-Apennine system (see Section 5.5).

Across northwestern Africa are the Atlas Mountains (Fig. 1). These separate the Meseta region in the north, underlain by a late Paleozoic crystalline basement resulting from Variscan Orogeny during the formation of Pangea, from Pan-African and older crystalline basement to the south (Michard et al., 2010). This Paleozoic thrust front was reactivated as a rift in late Triassic to earliest Jurassic time associated with earliest break-up of the Atlantic Ocean (Frizon de Lamotte et al., 2008, 2011). We follow the reconstruction of van Hinsbergen et al. (2014a) and adopt 30 km N-S shortening between 50 and 35 Ma (Beauchamp et al., 1999; Brede, 1992; Teixell et al., 2003).

The highest structural units in these fold-and-thrust belts are continental nappes that contain Variscan metamorphic basement and a Permian to Jurassic sedimentary cover: the Malaguide nappe in the Betics, the Ghomaride nappe in the Rif and the Upper Unit of the Kabylides (Chalouan and Michard, 1990; Lonergan, 1993; Zaghloul et al., 2010) (Fig. 6). The Ghomaride and Malaguide units underwent no regional Alpine metamorphism (Chalouan and Michard, 1990) but reach greenschist-facies metamorphic conditions at their base, in the Malaguide unit dated around 18 Ma (El Kadiri et al., 2006; Lonergan, 1993; Negro et al., 2006; Platzman et al., 2000). These upper units are unconformably overlain by an Eo-Oligocene carbonate to clastic sedimentary unit (Lonergan and Mange-Rajetzky, 1994) that is interpreted as a relict of a basin originally contiguous with equivalent units in the Kabylides, and perhaps as far-east as Calabria (Bonardi, 2003; Weltje, 1992), likely representing forearc basin deposits (van Hinsbergen et al., 2014a).

Structurally below these upper units, Paleozoic to Mesozoic metasediments occur, in places including Variscan basement rocks. These include the Alpujarride unit of the Betics, the Sebtide unit of the Rif, and the Lower Kabylides unit (Fig. 7). These were thrust onto imbricated non-metamorphosed Mesozoic to Paleogene carbonate-dominated rocks known as the Dorsale Calcaire, which may have been cover units of the now-metamorphosed Alpujarride, Sebtide, and Lower Kabylides units (Chalouan et al., 2008; El Kadiri et al., 2006; Frizon de Lamotte et al., 2000; Michard et al., 2006; Sanz de Galdeano et al., 2001). The upper contacts of these metamorphic units with the overlying Malaguide, Ghomaride, and Upper Kabylides units, respectively, are latest Oligocene to Miocene extensional detachments, which accommodated up to 220 km of E-W extension between 25 and 10 Ma (Faccenna et al., 2004; Michard et al., 2006; Platzman and Platt, 2004; Saadallah and Caby, 1996; Vissers, 2012; Vissers et al., 1995). The Alpujarride, Sebtide, and Lower Kabilides units were incorporated in the lower AlKaPeCa unit, defined by Boullin et al. (1986) in van Hinsbergen et al. (2014a), together with units with similar ages and burial history in the Peloritani-Calabria Mountains of Sicily and southern Italy. Within the Alpujarride, Sebtide, and Lower Kabilides units, bodies of subcontinental lithospheric mantle rocks were tectonically incorporated, such as the Ronda peridotite of the Betics, the Beni Boussera peridotite of the Rif, and the Lower Kabylides peridotites (El Atrassi et al., 2011; Michard et al., 2006; Pearson et al., 1989), which include pyroxenite dykes with zircons that yielded ~180-130 Ma U/Pb core ages (Sánchez-Rodrıguez and Gebauer, 2000). The lower Alboran-Kabylides units were subjected to Eo-Oligocene eclogite or blueschist-facies metamorphism (Chalouan et al., 2001; Goffé et al., 1989; Mahdjoub et al., 1997; Michard et al., 2006; Monié et al., 1994; Platt et al., 2005; Vissers et al., 1995) and were overprinted by 25–19 Ma High-Temperature (HT) metamorphism and intruded by granitic dykes (Esteban et al., 2011; Kelley and Platt, 1999; Michard et al., 2006; Platt and Whitehouse, 1999; Sánchez Rodríguez, 1998; Sánchez-Rodrıguez and Gebauer, 2000). In many places, the HT metamorphism occurred at considerably lower pressures than those associated with eclogite-blueschist facies metamorphism, interpreted to reflect a pre-Miocene exhumation stage in a subduction channel setting (Avigad et al., 1997; Jolivet et al., 2003). The Miocene high-temperature metamorphism also affected the Ronda peridotite at ~16 kbar (Lenoir et al., 2001), and the juxtaposed Alpujarride metasediments at ~15 kbar (Argles et al., 1999). Because the pressure difference between the peridotites and metasedimentary envelope was minimal, van Hinsbergen et al. (2014a) concluded that the excision of the lower crust that juxtaposed the peridotites to the metasedimentary units must have predated the HT event rather than have caused it (as widely perceived, e.g., Platt et al., 2013; Platt and Vissers, 1989; Précigout et al., 2013), and was likely the result of Jurassic-Early Cretaceous (hyper)extension of the southern Iberian margin, simultaneously with slow break-up of the Piemonte-Ligurian Ocean (Vissers et al., 2013). Such a hyperextension phase is consistent with the intrusion of gabbroic dykes into the Alpujarride sedimentary units that occurred around ~180 Ma (Martin-Rojas et al., 2009; Tubía et al., 2009).

In Algeria, the upper and lower **Kabylides** and Dorsale Calcaire units lie thrust on intensely deformed deep-marine turbidite units of the Maghrebian flysch and African passive margin rocks of the Tell Belt (both included in the Tell Belt on Fig. 6), and the contact is pierced by post-emplacement 16-15 Myr old granitoids (Benaouali-Mebarek et al., 2006; Coulon et al., 2002; Maury et al., 2000; Michard et al., 2006). Thrusting of the Upper and Lower Alboran and Calcaire Dorsale units over the SE Iberian and NW African margins led to 20-12 Ma metamorphism in the Nevado-Filabride and Tamsamane units, respectively (Behr and Platt, 2012; Booth-Rea et al., 2012; Gómez-Pugnaire et al., 2012; Kirchner et al., 2016; Negro et al., 2007; Platt et al., 2006). Mesozoic to Miocene carbonate-dominated units that likely formed the original sedimentary cover of the Nevado-Filabride and Temsamane units are now found as the non-metamorphosed, thin-skinned Sub-Betic and Rif fold-and-thrust belts that accommodated at least several hundred kilometers of shortening (Chalouan et al., 2006; Crespo-Blanc, 2007; Di Staso et al., 2010; Meijninger and Vissers, 2007; Platt et al., 2003, 2013). The large-scale thrusting of the Alboran units over the African and Iberian margins and over the intervening flysch basin that formed in the oceanic corridor in between, largely ceased around 8–9 Ma (Fig. 7). Lower offset, thick-skinned thrusting and transpressive deformation continues today in northwest Morocco (Capella et al., 2017; Chalouan et al., 2006; Comas et al., 1999; Crespo-Blanc and Campos, 2001; Do Couto et al., 2016; Iribarren et al., 2007; Martínez-García et al., 2013; Medialdea et al., 2004; Sani et al., 2007) and was explained by resistance of the Gibraltar Slab against African absolute plate motion (slab dragging) (Spakman et al., 2018).

Between the Alpujarride and Nevado-Filabride units, HP-LT mafic and ultramafic rocks and associated metasediments are found with ~185 Ma magmatic ages (Bodinier et al., 1987; Puga et al., 1989, 2011), and ultramafic rocks and ~166 Myr old gabbroic intrusions are also found in the non-metamorphic nappes of the external Rif, where they are overlain by and reworked in Jurassic sediments (Benzaggagh et al., 2014; Michard et al., 1992) (Fig. 7). Finally, between the Rif and Betic chains, the Alboran units

overlie a thick Jurassic to Miocene flysch sequence which contains Jurassic mafic lavas (Durand-Delga et al., 2000). These Jurassic mafic and ultramafic rocks are generally interpreted to be derived from now-subducted ocean floor that once separated Iberia, Africa, and the Alboran-Kabylides units (Durand-Delga et al., 2000; Michard et al., 1992; Puga et al., 2011; van Hinsbergen et al., 2014a).

Towards the east, the Balearic islands contain a thin-skinned fold-and-thrust belt of carbonate units that is correlated to the Iberian passive margin stratigraphy exposed in the External Betic thrust sheets (Díaz de Neira and Gil-Gil, 2013). On the island of Mallorca, this stratigraphy became shortened by ~85 km along top-to-the-northwest thrusts with ages of shortening estimated between 26 and 16 Ma (Gelabert et al., 1992; Sàbat et al., 2011), i.e. simultaneously with the opening of the Gulf of Valencia. The island of Ibiza, on the other hand, was in extension during this time period, and underwent a brief period of ~N-S shortening in the middle Miocene, when the Kabylides collided with North Africa. This was followed by renewed extension during the E-W opening of the Algerian Basin (Etheve et al., 2016).

More detailed kinematic constraints on the evolution of the SW Mediterranean region were reviewed and reconstructed in van Hinsbergen et al. (2014a). We use their reconstruction as a basis for this study, although we will critically re-evaluate some of the paleogeographic interpretations in that study in the light of the pre-Cretaceous history reconstructed here.

5.4. Provence; Gulf of Lion; Corsica, Sardinia; Tyrrhenian Sea

The northwestern and central Mediterranean region host two major Cenozoic extensional basins. The Gulf of Lion Basin separated the Corsica-Sardinia Block from the Provence margin of southern France, and the Tyrrhenian Basin formed between Sardinia and the Calabrian Block in the south, and Corsica and the Apennine fold-and-thrust belt in the north where extension overprints pre-Miocene parts of the Alpine and Apennine thrust stack (Fig. 1).

The **Gulf of Lion** Basin opened between 30 and 16 Ma. In a first stage, this happened cylindrically, accommodating ~100 km of extension between 30 and 21 Ma (Bache et al., 2010; Séranne, 1999), including the exhumation of an 80 km wide core complex along the Provence margin (Jolivet et al., 2015a). At ~21 Ma, extension in the Gulf of Lion became accommodated by oceanic spreading, which formed up to 200 km of oceanic crust (Burrus, 1984; Gorini et al., 1993; Séranne, 1999) (Fig. 6). There are no unequivocal marine magnetic anomalies reported, but based on paleomagnetic data from Corsica and Sardinia (see section 6.2.4), extension must have continued until ~16 Ma (Gattacceca et al., 2007) and the magnitude of NW-SE to E-W extension increased southeastward to become maximum along the North Baleares Transform Zone (Séranne, 1999; van Hinsbergen et al., 2014a).

To the north, the Gulf of Lion is bordered by the Eurasian continental margin of the **Provence** (Fig. 1). The geology of the Provence shows evidence for Paleogene (~60-30 Ma) top-to-the-north directed thrusting accommodating a minimum of 15–30 km of N-S to NW-SE shortening (Andreani et al., 2010; Arthaud and Laurent, 1995; Espurt et al., 2012a; Lacombe and Jolivet, 2005; Tempier, 1987). This shortening, which must have occurred between Corsica and Eurasia prior to opening of the Gulf of Lion, may have been considerably larger, but was overprinted by the Gulf of Lion extension, which hampers further shortening estimation (Advokaat et al., 2014b; Lacombe and Jolivet, 2005).

The conjugate, eastern margin of the Gulf of Lion is formed by the **Corsica-Sardinia Block** (Fig. 6). The geology of Corsica and Sardinia is dominated by Variscan basement overlain by a discontinuous Permian to Cenozoic sedimentary cover including Neogene volcanic rocks. The Variscan basement comprises metamorphic rocks that experienced HP metamorphism between 420 and 350 Ma overprinted by late Variscan extension and HT metamorphism between 350 and 345 Ma. These were intruded by large granitoid plutons in multiple stages between 340 and 280 Ma (e.g., Casini et al. (2012) and references therein). Corsica and northern Sardinia expose metasedimentary and meta-igneous rocks, which reach high-grade, up to migmatite, in the north with ~345 Ma ages (Carmignani et al., 1994; Faure et al., 2014; Giacomini et al., 2006). Central Sardinia contains a low-grade Variscan nappe stack, while South Sardinia is part of the non-metamorphosed Variscan foreland (Casini et al., 2010; Funedda et al., 2015). Cenozoic deformation on Sardinia is limited to relatively small-scale Eo-Oligocene, top-to-the-southwest thrusting, with an estimated (but debated: Berra et al. (2017)) magnitude of ~15 km, overprinted by post-Oligocene strike-slip faults (Arragoni et al., 2016). Northeastern, 'Alpine' Corsica in addition contains a west-verging 'Alpine' nappe pile thrust over the Variscan autochthon that constitutes most of the Corsica-Sardinia Block. We will review the constraints on this history in section 5.6, where we describe the architecture of the Alps.

Sardinia and Corsica are bordered in the east by the extensional **Tyrrhenian Basin**. Extension in the South Tyrrhenian Basin between Sardinia and Calabria started in the Serravallian (~13-11 Ma) as shown in supra-detachment basin sediments of the northwest Calabrian Amantea Basin that is conjugate to the east Sardinia margin (Mattei et al., 2002; Milia and Torrente, 2014). To the south, the Tyrrhenian Sea is bounded by the right-lateral North Sicily Fault (Rosenbaum and Lister, 2004b). Tyrrhenian Basin extension took place in Plio-Pleistocene times and was accommodated along two fast-spreading, but small (Vavilov and Marsili) ridges (Nicolosi et al., 2006) not detailed on our tectonic maps. We follow the reconstruction of Faccenna et al. (2001b) and Rosenbaum and Lister (2004b) and restore ~550 km of 13–0 Ma extension, ~300 km of which occurred in the last 3 Ma during the opening of the oceanic basins.

The amount of extension in the North Tyrrhenian Sea is poorly constrained but may have been on the order of ~150 km, decreasing northward (Faccenna et al., 2001b, 2004; Rosenbaum and Lister, 2004b). On northeastern Corsica, western Tuscany, as well as on islands such as Elba within the North Tyrrhenian Sea, major top-to-the-East directed Miocene extensional detachments exhumed metamorphosed parts of previously thickened crust (Bianco et al., 2015; Brunet et al., 2000; Jolivet et al., 1990). Rb/Sr and $^{40}Ar/^{39}Ar$ geochronology on mica yield extension-related cooling ages from at least 21 Ma or even as old as 32 Ma and younger (Brunet et al., 2000; Rossetti et al., 2015; Zarki-Jakni et al., 2004), consistent with fission track ages showing rapid unroofing since early Miocene (Cavazza et al., 2001). Extension from Corsica to Tuscany thus appears to have started at least 8 Ma earlier than extension between Sardinia and Calabria in the Tyrrhenian Sea Basin.

5.5. Sicily; Calabria; Apennines

The Apennines are a NW-SE striking, NE verging fold-and-thrust belt, comprising ocean and continent-derived sedimentary and in places crystalline rock units thrust upon Adriatic continental crust (e.g., Bernoulli, 2001; Calamita et al., 2011; Dewey et al., 1989; Scrocca, 2006). The Apennines run through most of the Italian Peninsula, forming two curved belts interpreted as oroclines (e.g., Cifelli et al., 2007, 2008a; Speranza et al., 1997). The northern orocline (Northern Apennines) developed between the Alps-Apennines junction are in northwestern Italy (Fig. 1) (Molli et al., 2010) and the Pliocene Olevano-Antrodoco-Sibillini curved thrust system in central Italy (Calamita et al., 2012) (Fig. 8). The current front of the Northern Apennines is buried below sediments of the Po plain or lies below the Adriatic Sea. The southern orocline, known as Calabrian Arc (e.g., Cifelli et al., 2007, 2008a; Maffione et al., 2013b; Vitale and Ciarcia, 2013) comprises the Southern

Apennines, the crystalline rocks of the Calabro-Peloritan Nappes and the underlying accretionary prism, and the Sicilian Maghrebides. The orogenic front of the Central and Southern Apennines is exposed on the Puglia Peninsula (Figs. 1 and 8), where the orogenic wedge is thrust over carbonate units of the Apulian Platform (Figs. 8 and 9, see section 5.5.3). From here towards the south, the thrust front forms a tight curvature changing from a NW-SE to an E-W direction in Sicily. There, the Maghrebides are thrust over the Hyblean Platform that represents the African foreland (Figs. 8 and 9). The northern and southern oroclines meet in the Central Apennines, where their interference leads to a complex deformation pattern with folds and thrusts at high angles in the Gran Sasso area (Satolli et al., 2005; Speranza, 2003) (Figs. 1 and 8).

Growth of the Apenninic-Maghrebian orogenic system by thrusting was for much of the Neogene accompanied by extension and crustal attenuation in the Tyrrhenian Sea in the hinterland, with both compressive and extensional fronts migrating towards the foreland over time (Casero et al., 1988; Cello and Mazzoli, 1998; Faccenna et al., 1997, 2001b; Malinverno and Ryan, 1986; Nicolosi et al., 2006; Patacca et al., 1990; Rosenbaum and Lister, 2004b). Below, we describe the structure and evolution of the different segments of the Apennines orogenic system, from the Sicilian Maghrebides to the Calabro-Peloritan Block, the Southern, Central, and Northern Apennines and the Ligurian Alps.

5.5.1. Sicily

The Sicilian Maghrebides form an ~E-W trending, south-verging fold-and-thrust belt (Figs. 1, 8 and 9) (e.g., Catalano et al., 1996; Ogniben, 1960). The highest structural units of the Maghrebides are the basement nappes of the Calabro-Peloritan Block (see Section 5.5.2), which is either considered part of Sardinia, or as an isolated ribbon continent within the Alpine Tethys for part of its pre-Neogene history (see e.g. Handy et al., 2010; Michard et al., 2006; van Hinsbergen et al., 2014a). These basement units thrust in late Oligocene-early Miocene time upon deep marine Upper Jurassic-lower Miocene basinal carbonates, sandy mudstones, and turbiditic sandstones known as the Sicilide Units, which are interpreted to be derived from an oceanic or ocean-continent transition domain (Catalano et al., 1996; Ogniben, 1960; Pepe et al., 2005). In the early Miocene, (~20 Ma), the Sicilide Units overthrust the Inner Carbonate Unit, which is currently represented by an imbricated fan of Mesozoic platform and basinal pelagic and turbiditic carbonate and siliceous sediments, and Upper Triassic to Lower Jurassic shelf and Jurassic to Paleogene deep-water carbonate rocks (Panormide Platform, pre-Panormide slope, and Imerese Basin units, respectively). The Inner Carbonate unit is thrust in Langhian to Pliocene time (~14-4 Ma) onto the Outer Carbonate units, including the Trapanese and Saccense platforms and intervening Sicanian Basin units, which currently consist of internally imbricated shallow and deep-water Mesozoic-Cenozoic carbonates (Catalano et al., 1993). In the middle Plio-Pleistocene, the Outer Carbonate units were thrust over Hyblean Platform which is the stable foreland, and its duplexed and deformed equivalent, the Gela Nappe (Butler et al., 1992; Ogniben, 1969), a thin-skinned duplex containing Cretaceous-Eocene clays, upper Oligocene-lower Miocene 'Numidian' flysch, and lower Miocene to Pleistocene clastic sediments and evaporites (Argnani, 1987; Butler et al., 1992; Catalano et al., 1996). From the middle Pleistocene until today, the Gela Nappe has been thrusting over the Hyblean carbonate platform in the southeast of Sicily, which is the present-day stable foreland of the Sicilian Maghrebides (Figs. 8 and 9) (Butler et al., 1992; Ogniben, 1969).

The northern nappes of the Sicilian Maghrebides became extended along the southern margin of the Tyrrhenian Basin simultaneously with the advancement of the thrust fronts in the south (e.g., Doglioni, 1991; Doglioni et al., 1999; Malinverno and Ryan, 1986; Pepe et al., 2005). A Tortonian to Messinian top-to-the-north low-angle detachment fault system, cut by high-angle normal faults (e.g., Catalano et al., 2013), was identified in the internal domains of the belt along the northern coast of Sicily (Giunta et al., 2000; Pepe et al., 2005).

5.5.2. Calabria

The geology of **Calabria** and NE Sicily is dominated by units of the Calabro-Peloritan Block exposed in the Aspromonte-Peloritani, Serre, and Sila Massifs. This block contains the Stilo and Aspromonte-Peloritani basement units and overlies the Africo-Polsi metasedimentary thrust slices. Together, these form the highest structural units of the Southern Apennines and Sicilian Maghrebides (Figs. 8 and 9).

The Stilo unit consists of non-, to anchimetamorphic, up to 7 km thick Upper Jurassic-Lower Cretaceous neritic carbonates. These carbonates were unconformably deposited on Variscan, Upper Devonian low-grade phyllites. The Variscan grade of metamorphism increases down-section from a chlorite to garnet to staurolite-andalusite zone (Cirrincione et al., 2013; Fazio et al., 2015) and is devoid of a noticeable Alpine metamorphic overprint (Heymes et al., 2010). The Aspromonte unit is separated from the overlying Stilo unit by an Alpine extensional detachment (Heymes et al., 2008, 2010), which is associated with the Oligocene-lower Miocene Stilo-Capo d'Orlando supra-detachment basin (Cavazza, 1989; Weltje, 1992). The Aspromonte-Peloritan unit consists of high-grade Variscan and older continental basement rocks (gneisses and schists) that experienced HT-LP (650–675 °C at 4–5 kbar) metamorphism around 305-290 Ma (U/Pb monazite ages), and subsequent granitoids were emplaced around 300-290 Ma (U/Pb zircon ages) (Graessner et al., 2000; Micheletti et al., 2009; Ortolano et al., 2005). An Alpine metamorphic overprint at 5–8 kbar was reported from the lower (northern) part of the Aspromonte Unit (Bonardi et al., 1984; Platt and Compagnoni, 1990). The Variscan HT-LP metamorphism was coeval with an even higher grade metamorphism observed in the lower crustal basement of the Aspromonte Unit (690–800 °C at 5.5–7.5 kbar (Graessner et al., 2000)). In the Serre and the northerly adjacent Sila Massif, the Aspromonte unit exposes a section across lower continental crust that is remarkably similar to that exposed in the Ivrea Zone of the Alps, both in terms of age and metamorphic grade (Handy et al., 1999; Schenk, 1990) (see section 5.6). Sm/Nd dating of garnets in the Aspromonte unit in the Serre Massif yielded Triassic ages down to ~215 Ma age interpreted as cooling during the precursory stages of rifting of the Piemonte-Ligurian Ocean (Del Moro et al., 2000; Micheletti et al., 2008).

The Calabro-Peloritan Block was thrust over the Africo-Polsi unit, which is composed of Paleozoic metasedimentary and metavolcanic amphibolites and micaschists. Alpine metamorphism reached 9.5–13.5 kbar at 400°-600 °C (Heymes et al., 2008, 2010; Ortolano et al., 2005). Slivers of Mesozoic carbonates at the base of the Apromonte-Peloritani unit in the Peloritani Mountains show that thrusting was an Alpine event. In present-day coordinates this thrusting was top-to-the-S to -SE in Sicily and top-to-the-SE in Calabria (Cirrincione et al., 2012; Heymes et al., 2008; Langone et al., 2006; Messina et al., 2004; Somma et al., 2005). The age of thrusting is poorly dated, but must predate the ~30 Ma onset of crustal thinning operated by the two top-to-the-NE extensional detachments (i.e. orthogonal to the thrust motion direction) that cut and exhume the Aspromonte, Stilo, and Africo-Polsi units (Heymes et al., 2008, 2010; Ortolano et al., 2005; Platt and Compagnoni, 1990). The Africo-Polsi unit experienced an Alpine metamorphic overprint reaching 11–12 kbar and 540–570 °C (Cirrincione et al., 2008; Heymes et al., 2010; Ortolano et al., 2005; Platt and Compagnoni, 1990). $^{40}Ar/^{39}Ar$ ages from the Africo-Polsi unit give Alpine as well as Variscan ages and it is hence difficult

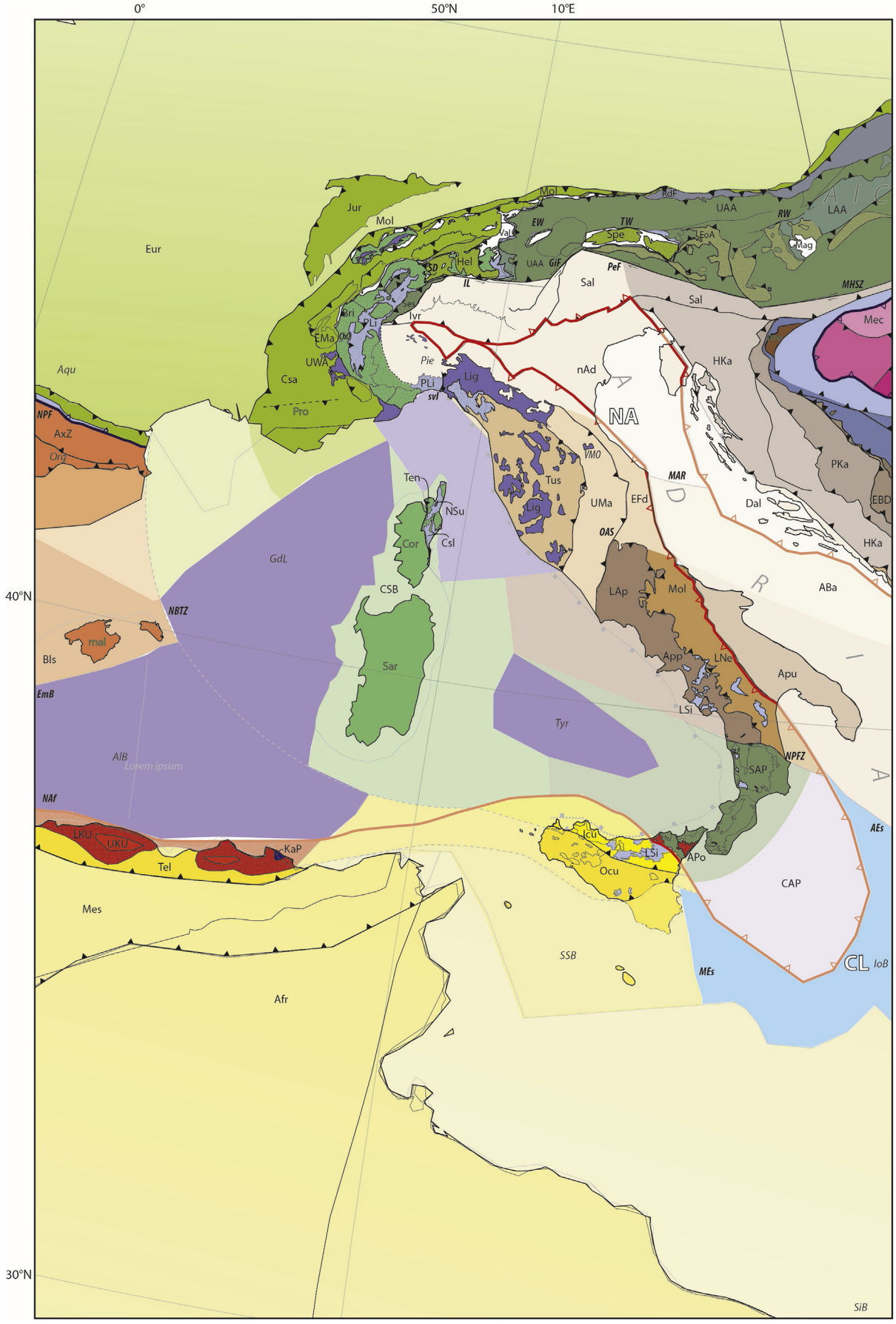

Fig. 8. Tectonic map of the central Mediterranean region. For key to abbreviations, see Table 4, for key to tectonic units, see Fig. 5. For location of the map within the Mediterranean region, see Fig. 4.

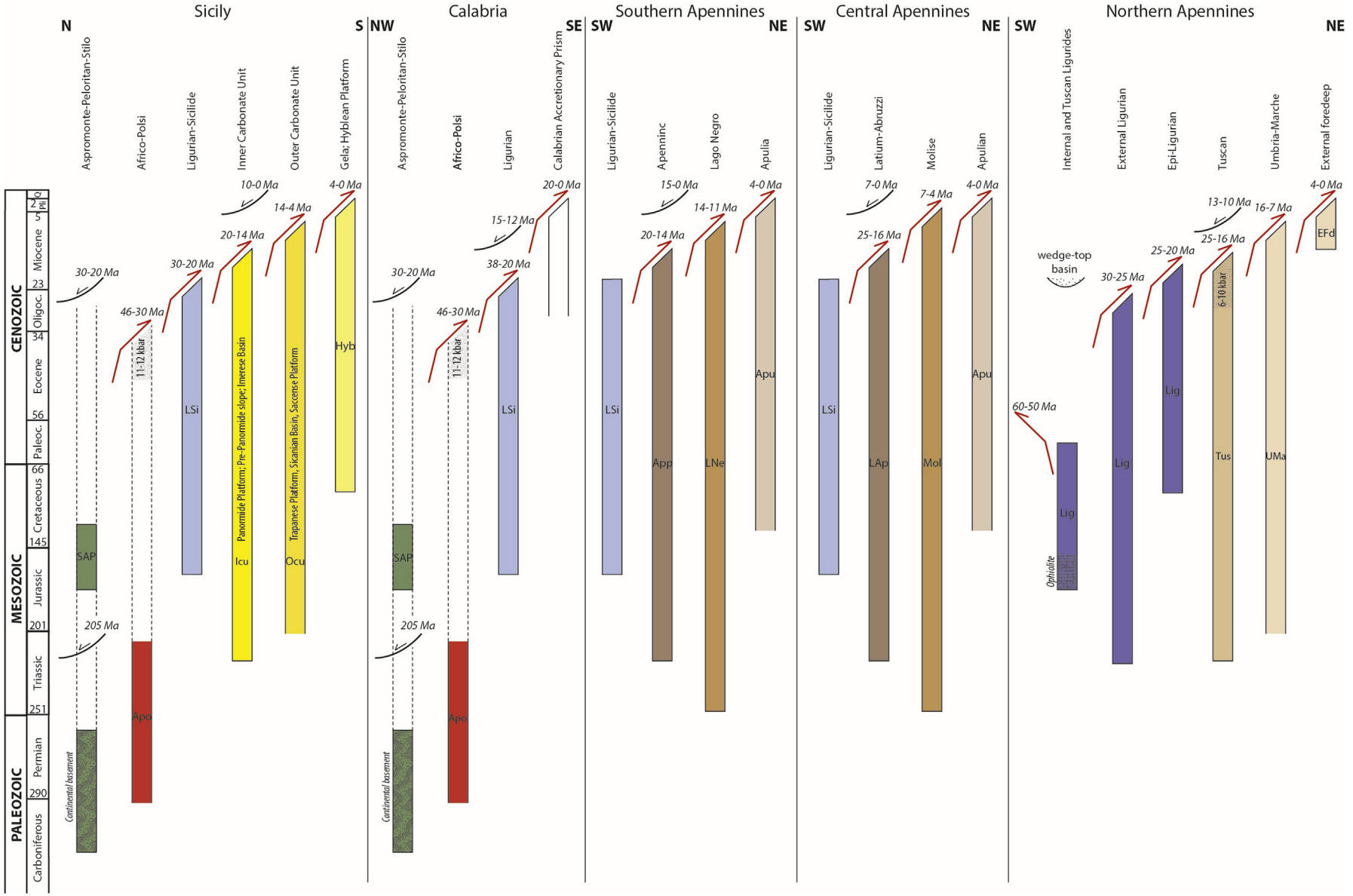

Fig. 9. Orogenic architecture charts for the Sicilian Maghrebides, Calabria, and the Apennines. For key to abbreviations, see Table 4, for key to tectonic units, see Fig. 5. For regional distribution of tectonic units, see Fig. 8. See Table 1 for summery of kinematic constraints corresponding to this chart. Periods of metamorphism are indicated with dotted hatching, formation of oceanic basement (ophiolites) with vertical hatching, and formation of pre-Alpine crystalline basement with curved hatching.

to date the age of Alpine thrusting there, although a maximum age limit for the Alpine overprint is probably around 46 Ma (Heymes et al., 2010) (Fig. 9).

Below the Africo-Polsi unit lies an accretionary complex, often referred to as Ligurian accretionary complex, containing deep-marine sediments and mafic rocks derived from oceanic crust (e.g. Vitale and Ciarcia, 2013; Vitale et al., 2013). On our maps, these are included in the Ligurian-Sicilide composite unit (Fig. 8), whereby the Ligurides are ocean-derived units, and the Sicilide units are the distal passive margin sediments. A non- to slightly metamorphosed 'Upper Ophiolitic Unit' (Rossetti et al., 2001) underlies the Calabro-Peloritan Block and consists of pelagic limestones, pelites and turbiditic sandstones, with lenticular serpentinite and pillow basalt bodies at the base, roughly dated between the Upper Jurassic and Upper Cretaceous (Amodio Morelli et al., 1976). The lower green-schist metamorphism (chlorite-albite paragenesis) characterizing the basaltic rocks of this unit has been ascribed to seafloor metamorphism (Rossetti et al., 2001). The Lower Ophiolitic Unit consists of basal mafic and ultramafic rocks grading into Mg carpholite-bearing quartz-mica schists, marbles and calcschists that underwent HP/LT metamorphism (10–12 kbar/330–380 °C) (Rossetti et al., 2001). $^{40}Ar/^{39}Ar$ dating on the high-pressure phyllites yielded 38-33 Ma ages, while the syn-exhumation greenschist retrogression may have occurred until ~17 Ma (Rossetti et al., 2001). Plastically deformed, carpholite-bearing rock slices of the Lungro-Verbicario unit found deep in the Ligurian accretionary complex (Vitale and Ciarcia, 2013) comprises Triassic (Anisian) to lower Miocene (Aquitanian) phyllites, quartzites, marbles, metapelites, dolomites, red siliceous slates, radiolarite beds, and evaporites and represents the distal-most continental margin of Adria or Tethyan oceanic crust (Iannace et al., 2007). The Aquitanian fossils in this unit are considerably younger than the late Eocene to Oligocene $^{40}Ar/^{39}Ar$ ages reported by Rossetti et al. (2001, 2004) from the Ligurian accretionary complex. This may indicate that the Ligurian accretionary prism formed throughout the late Eocene to early Miocene, although a 35.5 + 0.1 Ma $^{40}Ar/^{39}Ar$ age obtained by Rossetti et al. (2004) (their sample CLB8) appears to come from the same Lungro-Verbicario unit and, therefore, is likely in conflict with the biostratigraphic constraints.

Parts of the Ligurian accretionary complex were exhumed along top-to-the-west extensional detachments, antiparallel to the overall thrust direction, and orthogonal to the detachments cutting the higher Calabro-Peloritan units. Clasts of ophiolitic rocks are not found in the Oligocene Stilo-Capo d'Orlando Basin, but are first found reworked in the middle Miocene of the Amantea Basin (Argentieri et al., 1998) that forms a supra-detachment basin above a top-to-the-west extensional detachment (Mattei et al., 1996).

The Ligurian accretionary complex and overlying Calabro-Peloritan units lie thrust upon the Sicilian nappes in Sicily, as described above, on the Apenninic carbonate platform of the Southern Apennines to the north, and on an Oligocene to Quaternary accretionary wedg, likely derived from now-subducted oceanic Ionian lithosphere that once intervened Adria and Sicily (Cavazza and Barone, 2010; Minelli and Faccenna, 2010). In the last 6-5 Ma, the left-lateral North Pollino Fault Zone formed, which now marks the boundary between the Southern Apennines and the Calabro-Peloritan Block (Catalano et al., 1993; Knott and Turco, 1991; Monaco et al., 2001). Rosenbaum and Lister (2004a, 2004b) proposed that this fault accommodates ongoing southeastward motion of Calabria relative to Adria associated with the young and rapid extension in the South Tyrrhenian Sea.

5.5.3. Southern Apennines

The nappes of the Southern Apennines comprise an assemblage of sedimentary units of continental and oceanic origin (e.g., Cello and Mazzoli, 1998; Patacca and Scandone, 2007). The Southern Apennines contain a nappe stack that accommodated at least 300 km of shortening, and is currently arranged into a NE-verging, dominantly thin-skinned fold-and-thrust belt. Thick-skinned thrusting affected the deepest structural unit (i.e. the Apulia Platform), which is still attached to downgoing Adria (Butler et al., 2000; Cello and Mazzoli, 1998; Lentini et al., 2002; Monaco et al., 1998; Noguera and Rea, 2000; Scrocca et al., 2005).

Here, we follow the first-order unit subdivision proposed by Mostardini and Merlini (1986) and describe the units from structurally high to low and from internal to external. In the Southern Apennines the Upper Jurassic to Oligocene ophiolite-bearing Ligurian units and Upper Cretaceous to lower Miocene non-metamorphic pelagic Sicilide Units form the highest nappe, and are structurally equivalent to the Ligurian accretionary complex of Calabria (Monaco and Tortorici, 1995; Ogniben, 1969; Vitale and Ciarcia, 2013). These units were initially thrust over the Apenninic Platform in Burdigalian-Langhian time (20-14 Ma), and then were thrust again during an out-of-sequence stage in the Tortonian (Argnani, 2000; Maffione et al., 2013b; Mazzoli et al., 2001b; Morley, 1988; Mostardini and Merlini, 1986; Patacca and Scandone, 2007). The Apenninic Platform nappe comprises Upper Triassic-lower Miocene platform carbonates (Argnani, 2000; Mazzoli et al., 2001a; Mostardini and Merlini, 1986; Patacca and Scandone, 2007), which were thrust in Serravallian time (14-11 Ma) over rocks of the Lagonegro Basin comprising Middle Triassic-Cenozoic pelagic rocks of the Lagonegro basin (Boiano, 1993, 1997; Mazzoli et al., 2008; Ogniben, 1969; Pescatore et al., 1999). In the meantime, the internal parts of the Southern Apennines became affected by NW-SE striking, SW-dipping normal faults associated with the opening of the Tyrrhenian basin (Cello and Mazzoli, 1998; Patacca et al., 1990). Since late Tortonian-early Messinian time (11-6 Ma), the Lagonegro Basin rocks were emplaced above the Apulia Platform, which comprises Mesozoic-upper Miocene platform carbonates (Mostardini and Merlini, 1986; Ricchetti et al., 1988). Between the Messinian and the early Pleistocene, the Southern Apenninic wedge thrust the Apulia Platform over more than 100 km. In the early Pleistocene The Apulia Platform was then thrust forming a large-scale antiformal stack known as "buried Apulian belt" (Cello et al., 1989).

5.5.4. Central Apennines

The Central Apennines comprise a complexly deformed nappe stack that exposes rocks from four adjacent paleogeographic domains that are in part equivalent to those exposed in the Southern Apennines. From structurally high to low, and internal to external, these domains there are: (i) the Sicilide Units, (ii) the Latium-Abruzzi Platform, equivalent to the Apenninic Platform, (iii) the Molise Basin, forming the northward extension of the Lagonegro Basin, and (iv) the Apulia Platform (Cosentino et al., 2010; Patacca et al., 1990; Vezzani et al., 2010). The attribution of the Sannio Unit to either the Molise Basin (Vezzani et al., 2010) or a more internal unit (Cosentino et al., 2010) remains controversial.

The central-western sectors of the Central Apennines are dominated by an overall NW-SE structural trend, which connects with structures in the Southern Apennines. Approximately N-S striking thrusts dominate instead in the eastern sector of the Central Apennines (i.e. Latium-Abruzzi unit in the eastern Gran Sasso Mountain) (Fig. 1). As for the Southern Apennines, the Central Apennines formed upon E- to NE-ward (forelandward) propagation of thrusts (Fig. 9), which is reflected in the eastward younging of foredeep basins and thrust-top basins (e.g., Cipollari and Cosentino, 1995; Patacca et al., 2008).

The tectonic units forming the Central Apennines are described according to Vezzani et al. (2010) and Cosentino et al. (2010). The highest structural domain is represented by the Sicilide Units (Elter

et al., 2012), equivalent to those exposed in the Southern Apennines, which were emplaced over the western edge of the Latium-Abruzzi Platform (Mt. Caccume Klippe and Carpineto Romano area (Angelucci and Devoto, 1966)) between the late Oligocene and the Burdigalian (25-16 Ma) (Vitale and Ciarcia, 2013). Eastward propagating thrusting within the Latium-Abruzzi Platform started in the Tortonian and continued throughout the Messinian (11-7 Ma) (Cavinato and DeCelles, 1999; Cosentino et al., 2010). The eastern part of the Latium-Abruzzi Platform was thrust in the Messinian-early Pliocene (7-4 Ma), above the adjacent Molise Basin (Figs. 8 and 9) (e.g., Cosentino et al., 2010; Patacca et al., 1990; Vezzani et al., 2010). Shortly after, the Umbria-Marche basinal units of the Northern Apennines to the north of the Latium-Abruzzi Platform were obliquely thrust eastward over the carbonate units of the Central Apennines along the N-S–striking Olevano-Antrodoco-Sibillini out-of-sequence thrust (see Section 5.5.5). At the end of the Pliocene (~4-3 Ma) the Gran Sasso massif was emplaced to the north upon a local, out-of-sequence event (Satolli et al., 2005; Speranza, 2003). Finally, the eastern edge of the Latium-Abruzzi Platform was incorporated into the orogenic wedge in the middle Pliocene, forming an east-facing macro-anticline. The deformation of the eastern sector of the Central Apennines is structurally complex due to the interference of younger, ~E-W trending out-of-sequence thrusts (e.g. the frontal Gran Sasso thrust) and older ~N-S trending thrusts. After the Pliocene, approximately N-S trending, predominantly right-lateral strike-slip faults (although also left-lateral strike-slip faults like the Rovereto Fault formed (e.g., Sirna, 1988)) dismembered and reactivated pre-existing contractional structures (e.g., Corrado et al., 1997). We do not explicitly restore this motion in our reconstruction but ascribe it to complex Central Apennine tectonics at the junction of the Calabrian and North Apennine oroclines.

Extensional tectonics, producing mainly NW-SE striking normal faults, affected the Central Apennines from the late Messinian until Recent (e.g., Calamita et al., 1994; Cavinato and DeCelles, 1999; D'Agostino et al., 2001). Section balancing along a SW-NE oriented profile crossing the Central Apennines indicates minimum total shortening of 116 km, 82 km of which occurred during Messinian to Pleistocene out-of-sequence thrusting, while a total of 175 km shortening is calculated when assuming an in-sequence thrusting (Ghisetti et al., 1993).

5.5.5. Northern Apennines

The transition from the Central Apennines to the Northern Apennines is abrupt and follows the left lateral and N-S striking Olevano-Androcco lateral ramp that curves around in the north into the NNW-SSE-striking Sibillini top-ENE thrust (Calamita et al., 2012). This curved fault formed late and out-of-sequence and obliquely thrusts the Triassic to Miocene Umbria-Marche-Sabine Tectonic Unit, characterized by Meso-Cenozoic shelf-to-basin and deeper-water limestones of the Umbria-Marche and Sabine domains, over uppermost Miocene to lowermost Pleistocene deposits of the Periadriatic foothills, with a similar sedimentary succession, in front of the Sibillini thrust (Calamita et al., 1994). The Olevano-Androcco lateral tramp obliquely thrusts the Umbria-Marche-Sabine Tectonic Unit over the Apenninic Platform units of the Central Apennines.

The Northern Apennines is a curved fold-and-thrust belt with an overall NE-ward vergence, towards the Adriatic foreland (e.g., Argnani, 2012; Molli et al., 2010; Picotti and Pazzaglia, 2008). The main trend ranges from WNW-ESE in the northern limb of the salient, to ~N-S in the southern limb (Fig. 8). The transition between the Northern Apennines and western Alps is gradual because the late stages of the Apennines orogeny also affected the Ligurian Alps that became a part of the Apennines. The often-quoted Sestri-Voltaggio Line (Fig. 8), claimed to represent the boundary between the two orogens (Miletto and Polino, 1992) is best interpreted as a top-to-the-east extensional fault within the Alpine system (Hoogerduijn Strating, 1994) exhuming the HP-LT ultramafic Voltri Massif (Vignaroli et al., 2010), overprinted by minor strike-slip faulting (Crispini and Capponi, 2001). This normal fault predates the Eocene-Oligocene boundary deduced from overlying sediments of the Cenozoic Piedmont Basin (Gelati et al., 1992). The Voltri Massif was buried below the ophiolites of the Internal Ligurian units (see below) at or before 65 Ma, during 'Alpine', i.e. west-vergent thrusting, and was then extensionally exhumed since ~35-30 Ma as part of the top-west orogeny that also affected northern Corsica (Vignaroli et al., 2010) (see section 5.6.1). For the Apennines, the Voltri Massif and similar metamorphic massifs to the east were passive riders that are part of the Internal Ligurian units.

From the eastward younging of foreland basin deposits in the Northern Apennines, a first-order eastward migration of the orogenic fronts since the late Oligocene is inferred (e.g., Argnani and Lucchi, 2001), with minor out-of-sequence thrusting also being documented (Picotti and Pazzaglia (2008) and references therein). The so-called Internal Ligurian units (Elter et al., 1966), together with the Tuscan Ligurides are the most internal and highest structural units of the Northern Apennines and are today exposed along the Tyrrhenian coast (Fig. 8) as well as on the Giglio and Gorgona islands. The Internal Ligurian and Tuscan Ligurides consist of dismembered ophiolites exposing mantle and oceanic crustal rocks with 170–168 Ma ages, Upper Jurassic to Lower Cretaceous cherts, limestones and shales and an Upper Cretaceous–Paleocene turbiditic sequences (Balestro et al., 2019; Marroni and Pandolfi, 1996) that represent the pelagic cover of the Alpine Tethys Ocean (Decandia, 1972; Marroni et al., 2010; Marroni and Treves, 1998). The Tuscan Ligurides (Figs. 8 and 9) have similar characteristics but lack the earlier Alpine deformation that is present in the Internal Ligurides. In the Paleocene to early Eocene these units were part of the European foreland-verging (W to NW) Alpine orogen (e.g. Marroni and Pandolfi, 1996; Pertusati and Horrenberger, 1975), and only subsequently during the main Oligocene Apenninic tectonics they were retro-thrust towards Adria (Molli, 2008; Molli et al., 2010). The most internal parts of the Internal Ligurian units (exposed today in the Gorgona Island) exhibit high-pressure metamorphism dated at ~25 Ma (Brunet et al., 2000) and interpreted as related to the earliest, east-verging Apenninic phase (Faccenna et al., 2001a; Jolivet et al., 1998; Brunet et al., 2000; Rossetti et al., 2002).

The External Ligurian units are derived from an ocean-continent transition domain, lack coherent slices of oceanic crust and mantle rock and include a mélange-type basal complex with both oceanic and continental units and Triassic-Jurassic sedimentary sequences derived from the thinned continental margin of Adria. These are overlain by Upper Cretaceous to Paleogene flysch and upper Oligocene and younger wedge-top 'Epiligurian' basins (Marroni et al., 1988, 2001; Molli, 2008). The Val Marechhia Ophiolite (Fig. 8) is the easternmost remnant of the Internal and Tuscan Ligurides and overlies the External Ligurides (Plesi et al., 2002). The Internal, External, and Epi-Ligurian units were thrust onto the Sub-Ligurian units during the Early Miocene (Molli et al., 2010). The Sub-Ligurian units are characterized by strong thickness variability locally reducing to zero, and are represented by Upper Cretaceous–Eocene shales and carbonates, and younger sandstones and shaly-calcareous deposits, followed by an Oligocene–lower Miocene (Aquitanian) flysch sequence (Cerrina Feroni et al. (2002) and references therein). They were accreted to the Ligurides during the early Miocene (Molli et al., 2010). The first deformation phase recognized in the Sub-Ligurian units has been dated to the early Oligocene (c. 30 Ma) (e.g., Cerrina Feroni et al., 2002). The paleogeographic origin and structural position

of the Sub-Ligurian units is comparable to that of the Sicilides of the Central and Southern Apennines (Elter et al., 2003). The Sub-Ligurian units are not specifically identified on our tectonic map, but are included in the Ligurides, collectively representing upper plate rocks (Tuscan Ligurian, ophiolites), overlying ocean-derived mélange (External Ligurian) and distal passive margin (Sub-Ligurian).

The Tuscan tectonic units are mostly exposed in extensional windows and form the more internal parts amongst all the units that are structurally below Ligurian and Sub-Ligurian units. The Tuscan units are composed of Triassic to lowermost Jurassic platform carbonates overlain by pelagic sediments formed during continental margin subsidence of Adria (Bernoulli, 2001). Oligocene to Early Miocene turbidite sequences (Pseudomacigno and Macigno Units) are also present in the Tuscan units and have been interpreted as syn-contractional clastic wedges of the Apennine foredeep and wedge top basins. The Tuscan nappes were deformed at shallow structural levels while their original underpinnings the Tuscan metamorphic units, were deeply buried into the accretionary wedge and became metamorphosed (Tuscan metamorphic units) in the late Oligocene-early Miocene (~25-16 Ma) (Brunet et al., 2000; Kligfield et al., 1986) under medium to high-pressure greenschist facies conditions (up to 6–8 kbar and 450 °C in the Alpi Apuane, and 10 kbar and 350 °C farther south in the Montagnola Senese and Argentario areas (Molli et al., 2001). A record of Cretaceous to Eocene minor contraction of this domain is recorded within the Scaglia Formation and reflected in several internal unconformities (Fazzuoli et al., 1994). Internal shortening within the Tuscan unit progressed throughout the Miocene producing an overthickened orogenic wedge which returned to a more stable configuration in the late Miocene by developing syn-collisional core-complex-type low angle normal faults, which exhumed the Tuscan metamorphic units between 13 and 10 Ma ago (Fellin et al., 2007), just before other high-angle normal faults related to the opening of the Tyrrhenian Sea developed (Carmignani and Kligfield, 1990).

The current configuration of the Northern Apennines has the Tuscan units thrust over the Umbria- Marche units, with both units covered by the more external Ligurian units. Paleogeographically the Umbria-Marche units represent the eastern and more proximal part of the Tuscan passive margin (Bernoulli, 2001) characterized from bottom to top by Upper Triassic evaporates below platform carbonates and Middle Jurassic to Palaeogene pelagic sediments. These are overlain by Oligocene to lower Miocene clastics and Serravallian to Tortonian foreland basin clastics (Barchi et al., 2012; Calamita et al., 1994). Thrusting of the Umbria-Marche units occurred throughout the middle to late Miocene (ca. 16-7 Ma) (e.g., Barchi et al., 2012; Speranza et al., 1997). In the southern limb of the northern Apennines Arc, the Umbria-Marche units started to thrust at 7 Ma towards the ENE over the Messinian to Pleistocene terrigenious clastic deposits of the external foredeep (Calamita et al., 2012; Casati et al., 1976). Post-7 Ma thrusting in the external foredeep units culminated in ~100 km of shortening (Calamita et al., 1994). Ghisetti et al. (1993) obtained a total of 74–133 km of shortening (depending on the assumed decollement horizons) along an E-W section along a profile that also includes shortening within the Umbria Marche units west of the Sibilini frontal thrust, depending on assumptions regarding the choice of the decollement horizons. Finetti et al. (2001) interpreted the SW-NE oriented CROP-03 seismic reflection line across the Northern Apennines and estimated 71 km and 85 km shortening for the late Oligocene to early Miocene and the late Miocene to present stages, respectively.

Finally, towards the junction with the Alps, the WNW-ESE striking northern limb of the northern Apennine Arc comprises the External Ligurides that are traced all the way to the Monferrato Hills west of Torino, located north of the Tertiary Piedmont Basin, and the E-W-striking segment of the Ligurian Alps (Elter and Pertusati, 1973; Hoogerduijn Strating et al., 1991; Mosca et al., 2009) (Fig. 8). The Oligo-Miocene Piedmont Basin is essential for restoring the deformation in the Alps-Apennines transition zone (the 'Ligurian Knot') since it seals the south-facing Alpine nappe stack of the Ligurian Alps but is transported piggy-back towards the north during the Apenninic thrusting of both Ligurian Alps and External Ligurides in the late Miocene to Pliocene (Piana, 2000).

From the eastward younging of foreland basin deposits in the Northern Apennines, a first-order eastward migration of the orogenic front since the late Oligocene is inferred, (e.g., Argnani and Lucchi, 2001), similar to the southern sectors of the Apennines, although also out-of-sequence thrusting has been documented (Picotti and Pazzaglia, 2008 and references therein). The early tectonic history of the Internal Ligurides was characterized by top-to-the-West to NW Alpine thrusting (e.g. Marroni and Pandolfi, 1996; Pertusati and Horrenberger, 1975) during the Paleocene to early Eocene, when the Internal Ligurides formed the highest structural unit during Alpine thrusting. The most internal and metamorphic parts of the most internal Tuscan Ligurian units (Gorgona Island) exhibit high-pressure metamorphism dated at ~25 Ma (Brunet et al., 2000) and is related to the Apenninic, east-vergent thrusting that must have been underway by late Oligocene time (Faccenna et al., 2001a; Jolivet et al., 1998; Rossetti et al., 2002) and was followed by the Northern Apennine nappe stacking described above.

5.6. Alps; AlCaPa

The Eastern Alps form an E-W trending fold-and-thrust belt in the north of the Mediterranean region that continue eastwards as the Western Carpathians. The Western Alps define a large-scale arch, progressively bending the E-W trend of the Eastern Alps into a N-S and finally into an E-W trend in Liguria, and N-S again on northeastern Corsica (Figs. 1 and 10). Together with the Western Carpathians the Alps were thrust towards and onto the European foreland (Figs. 10 and 11). The Alps accretionary wedge consists of continent and ocean-derived units that were thrust in Late Cretaceous to Cenozoic times. A prominent along-strike change is marked by the nature of the highest structural units above this wedge: In the Eastern Alps this 'orogenic lid' consists of a continent-derived Lower Cretaceous nappe pile (Austroalpine nappes) while in the Western Alps the highest structural units are dominantly non-metamorphic ophiolitic units derived from those parts of the Piemonte-Ligurian Ocean that escaped subduction (Handy et al., 2010). The Southern Alps (Fig. 10) represent a retro-wedge characterized by mainly Neogene-age top-to-the-S thrusting of Adria-derived rocks, with Adria as the foreland. To the east, this retro-wedge gradually changes or transfer its offsets to the dominantly dextral shearing displacement of the Peri-Adriatic lineament that mark the transition to the Pannonian Basin and the Dinarides (Frisch et al., 2000; Tomljenović and Csontos, 2001; Vrabec and Fodor, 2006; Wölfler et al., 2011; Zibret and Vrabec, 2016). In our reconstruction, we adopt the mega-unit subdivision of the Alps of Schmid et al. (2004a, 2004b) (Fig. 10).

Below, we first describe the nappe structure of Alpine Corsica and the western Alps from structurally high to low, then indicate changes towards the east, and finally describe how Oligocene and younger deformation that re-deformed the nappe stack.

5.6.1. Alpine Corsica

The highest structural units of **'Alpine Corsica'** (Nappe Superieure) contain non-metamorphic Jurassic ophiolites (the Balagne nappe) and continental basement (the Nebbio klippe and Santa Lucia unit, not specified on our tectonic map). These are underlain by HP meta-ophiolites associated with the Schistes Lustrés, forming

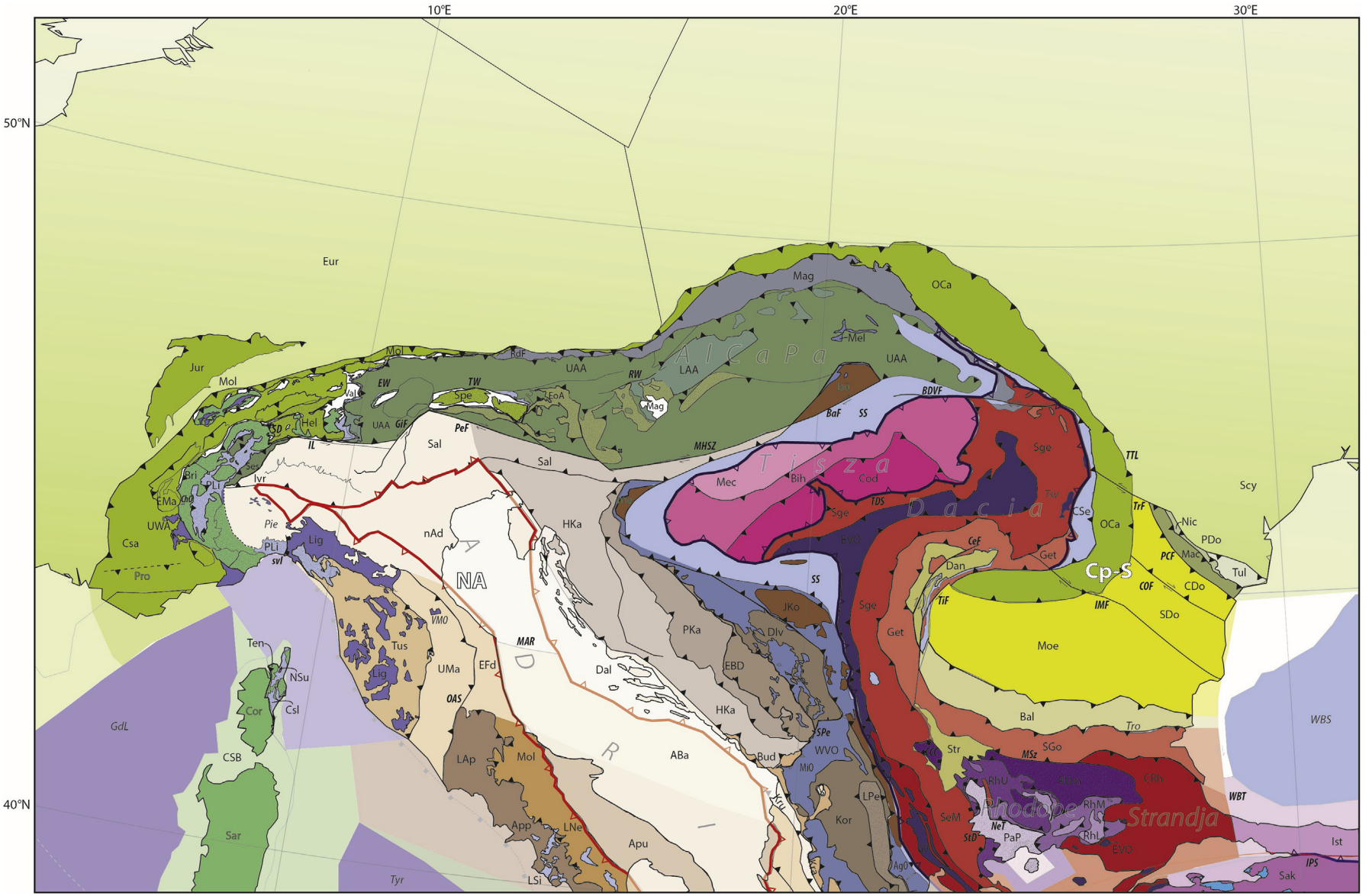

Fig. 10. Tectonic map of the northern Mediterranean region. For key to abbreviations, see Table 4, for key to tectonic units, see Fig. 5. For location of the map within the Mediterranean region, see Fig. 4.

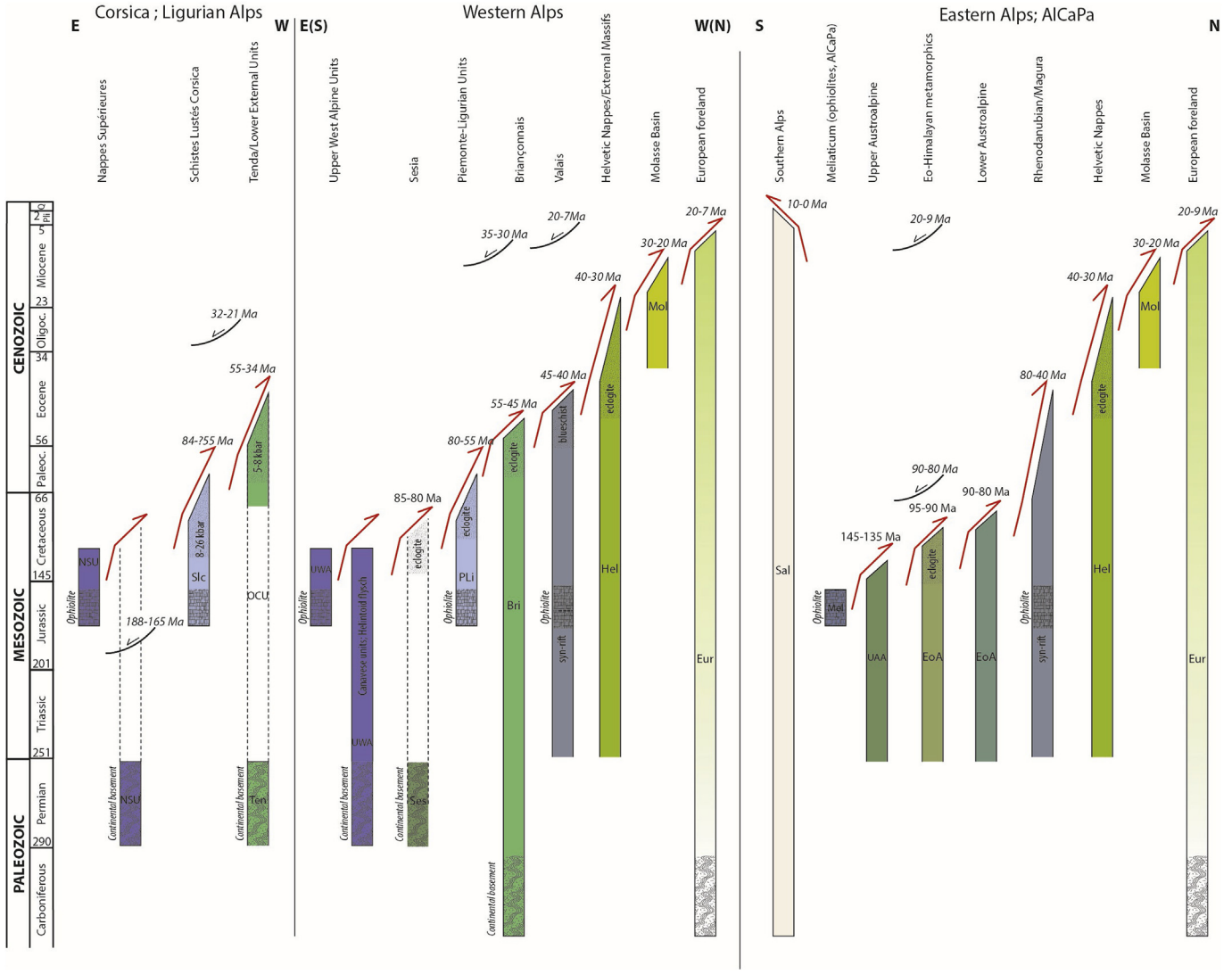

Fig. 11. Orogenic architecture charts for Alpine Corsica, the Alps, and the AlCaPa Block. For key to abbreviations, see Table 4, for key to tectonic units, see Fig. 5. For regional distribution of tectonic units, see Fig. 10. See Table 1 for summery of kinematic constraints corresponding to this chart. Periods of metamorphism are indicated with dotted hatching, formation of oceanic basement (ophiolites) with vertical hatching, and formation of pre-Alpine crystalline basement with curved hatching.

the southern continuation of the Piemonte-Ligurian metamorphic units of the Alps. Variscan basement and sedimentary cover units with an Alpine metamorphic overprint form the deepest units (i.e. the Tenda Unit) (Figs. 10 and 11).

The weakly deformed and extensionally dismembered Jurassic ophiolites and an Upper Jurassic to Upper Cretaceous volcano-sedimentary cover of the Nappes Supérieures in places overlies thrust slices derived from Variscan basement and sedimentary cover units that underwent no more than sub-greenschist facies metamorphism (Marroni and Pandolfi, 2003; Vitale Brovarone et al., 2013 and references therein). The ophiolites, interpreted to have formed at a slow-spreading mid-ocean ridge (Sanfilippo and Tribuzio, 2012), are overlain by Lower Cretaceous (Barremian to Aptian) continental clastic sediments (Marroni et al., 2004), and they are interpreted to have formed close to an ocean-continent transition (Vitale Brovarone et al., 2013). Below the ophiolites lie the Upper External Continental Units (Vitale Brovarone et al., 2013) that largely escaped Alpine metamorphism and contain pre-Alpine basement with Permian HT metamorphism and Jurassic (188-165 Ma) exhumation ages, the latter interpreted to relate to the rifting stages of the Alpine Tethys (Beltrando et al., 2013; Rossi et al., 2006). The mixed association of ocean and continent-derived units has in recent years been interpreted as derived from a hyper-extended ocean-continent transition zone, whereby the internal continental units represent klippen of Variscan continental basement overlying exhumed mantle portions (e.g., Beltrando et al., 2013; Marroni and Pandolfi, 2007; Vitale Brovarone et al., 2011).

The Corsican Schistes Lustrés are a composite series of thrust slices of metamorphosed sedimentary, mafic, and ultramafic rocks interpreted to be derived from ocean floor (Vitale Brovarone et al., 2013). Protolith ages of the mafic rocks range from 162 to 155 Ma (e.g., Rampone et al., 2009) and are associated with N-MORB geochemical signatures (Saccani et al., 2008b). These rocks preserved structural and stratigraphic evidence for the presence of former oceanic core complexes, indicating formation in a slow-spreading ridge environment (Lagabrielle et al., 2015). The Schistes Lustrés is metamorphosed to blueschist to eclogite facies, although the peak metamorphic conditions vary between tectonic slivers, from 8 to 26 kbar and 300 to >500 °C (Vitale Brovarone et al., 2013 and references therein). Garnet and lawsonite Lu/Hf ages obtained from the highest-grade lawsonite-eclogites of the Schistes Lustrés interpreted to date peak metamorphism yield ages

ranging from 37.5 ± 1.3 Ma to 34.2 ± 1.6 Ma (Vitale Brovarone and Herwartz, 2013). Consequently, these authors interpreted late Eocene $^{40}Ar/^{39}Ar$ ages on phengite to reflect the age of HP metamorphism rather than exhumation-related cooling as originally proposed (Brunet et al., 2000). Lahondère and Guerrot (1997), however, provided a Sm/Nd age of an eclogite of the Schistes Lustrés of 83.8 ± 4.9 Ma and suggested that subduction-related metamorphism already occurred in Cretaceous time. The much younger Eocene ages obtained from U/Pb, Lu/Hf, and $^{40}Ar/^{39}Ar$ would then reflect late-stage retrogression and metasomatism (e.g. Brunet et al., 2000; Molli and Malavieille, 2010). The latter interpretation is consistent with the pre-late Eocene ages of metamorphism of the deepest, Tenda and Lower External Continental units that derived from Corsican continental basement.

The Tenda Unit was deeply buried, metamorphosed, and exhumed (Molli, 2008; Molli et al., 2006; Vitale Brovarone et al., 2013) and underwent blueschist-facies metamorphism (8–11 kbar/300–500 °C, e.g. Molli et al. (2006)) estimated by U/Pb dating to occur at 54 ± 8 to 48 ± 18 Ma (Maggi et al., 2012) and by $^{40}Ar/^{39}Ar$ on phengite at >45-32 Ma (Brunet et al., 2000). Above the Tenda Massif lie the 'Lower External Continental Units' (Vitale Brovarone et al., 2013), also derived from the Variscan Corsican basement, metamorphosed at blueschist facies (5–8 kbar, 300–370 °C (Malasoma et al., 2006)). Metamorphosed sediments in these most external units are of Priabonian (38-34 Ma) (Ferrandini et al., 2010) and Bartonian (41-38 Ma) (Bezert and Caby, 1988) age, requiring a HP metamorphic age of late Eocene at the oldest. U/Pb dating from rims of an inherited zircon yielded an age of 292 ± 3.3 Ma, reflecting Permian HT metamorphism of the Variscan basement, of the external continental units, and an outermost rim gave 34.4 ± 0.8 Ma interpreted as the age of Alpine HP metamorphism (Martin et al., 2011). On the other hand, non-metamorphosed Eocene sediments have been reported to straddle the contact between the Schistes Lustrés and Variscan Corsica (Egal, 1992) and HP minerals were reported from anchimetamorphosed Eocene sediments (Amaudric du Chaffaut and Saliot, 1979). The metamorphic units of Alpine Corsica were exhumed starting in Oligocene time associated with the opening of the Tyrrhenian Basin (Brunet et al., 2000; Rossetti et al., 2015; Zarki-Jakni et al., 2004) (see section 5.4).

5.6.2. Western Alps

The highest structural units of the western Alps are ophiolite-bearing klippen that preserve part of the ophiolite pseudostratigraphy and that escaped metamorphism beyond prehnite-pumpellyite facies. These are thought to belong to the original upper plate of the subduction system, which in the western Alps consisted of Piemonte-Ligurian oceanic lithosphere (Schmid et al., 2017). The most prominent amongst these klippen is the Chenaillet Ophiolite (Li et al., 2013). This ophiolite, with gabbros and dolerites with Mid-Ocean Ridge Basalt (MORB) geochemical compositions and crystallization ages around 165 Ma, preserves detachment faults and oceanic core complexes suggesting they formed at a slow-spreading ridge (Li et al., 2013; Manatschal et al., 2011). These rocks were interpreted to derive from the Piemonte-Ligurian Ocean, where slow spreading between 170 and 145 Ma was inferred from reconstruction of Atlantic magnetic anomalies (Vissers et al., 2013). Other upper plate units in the Western Alps include the Canavese unit, which contains Permian high-temperature metamorphic basement, Triassic platform carbonates and Jurassic-Cretaceous deep-marine rocks interpreted to be deposited close to an ocean-continent transition, likely of Adria (Beltrando et al., 2014; Ferrando et al., 2004), and various Helmintoid flysch bearing units (Schmid et al., 2017; their Fig. 6). The latter are located at the front of the Western Alps, occasionally carry an ophiolitic mélange at their base and are considered to be derived from the Piemonte-Ligurian Ocean, close to a continental margin, likely Adria (Molli et al., 2010). These highest structural units, here collectively referred to as **Upper West-Alpine nappes**, as well as the Nappes Supérieures of Corsica, were thus likely part of a piece of Piemonte-Ligurian oceanic lithosphere originally attached to the west and northwest of the Adria continental fragment, and part of the same tectonic plate (Handy et al., 2010).

The non-metamorphosed Chenaillet ophiolitic klippe rests with a tectonic contact on meta-ophiolites, also with relict oceanic core complexes, and associated calcschists, here referred to as **Piemonte-Ligurian units**. These were deeply underthrust and metamorphosed at blueschist or eclogite facies conditions, of which geochronological results are in the 80-55 Ma age range (e.g., Queyras and Monviso Ophiolites (Festa et al., 2015; Lagabrielle et al., 2015; Weber and Bucher, 2015). The most internal and structurally highest nappe, however, incorporated into the western Alps nappe stack between meta-ophiolite rocks like those mentioned above, is the high-pressure **Sesia Unit**. This unit was interpreted to be part of a 'Margna-Sesia' continental fragment consisting of lower and upper crustal Permian basement that resembles the basement of Adria exposed in the Ivrea Zone NW of the Po Plain (see below) (Handy et al., 2010; Schmid et al., 2004b, 2017). It is therefore interpreted as a block, or an extensional klippe, broken off Adria during opening of, and since then paleogeographically surrounded by the Piemonte-Ligurian Ocean (Froitzheim et al., 1996; Schmid et al., 2004b). Its eclogite-facies rocks yielded ages between ~85 and ~70 Ma (Manzotti et al., 2014) and demonstrate that during this time interval, the Sesia fragment was carried into the subduction zone together with the downgoing European lithosphere.

The Piemonte-Ligurian meta-ophiolites of the Western Alps thrust upon continental rocks of the **Briançonnais** mega-unit (Figs. 10 and 11). This mega-unit consists of a pre-Alpine basement, a Carboniferous to Mesozoic sedimentary cover including platform carbonates that is now frequently found decoupled from and displaced relative to their pre-Alpine basement underpinnings (Schmid et al., 2004b). Eclogite and blueschist-facies rocks of the basement of the most internal Briançonnais unit ("internal massifs") yield ages up to 50 Ma (Lanari et al., 2014; Villa et al., 2014). These ages are in apparent conflict with stratigraphic ages in the external parts of the Briançonnais (e.g. Préalpes Médianes), where fossils of Lutetian age (49-41 Ma) are found (Jaillard, 1999). We model the moment of accretion of the Briançonnais mega-unit from the downgoing plate to the Alps fold-and-thrust belt at 55 Ma, to account for the ages of metamorphism, and thus interpret that the sedimentation in the external part of the Briançonnais nappe continued for at least 6 Myr after nappe accretion.

The Briançonnais mega-unit overlies Cretaceous-age calcareous shales and sandstones with in places ophiolitic rocks and serpentinites of the **Valais** mega-unit (Frisch, 1979; Loprieno et al., 2010; Schmid et al., 2004b; Stampfli, 1993). These Valais rock units derived from a narrow oceanic basin (internal Valais units) and the distal European margin (external Valais units). On the distal European margin, pre-rift stratigraphy continues into the Liassic (i.e. not younger than ~175 Ma), syn-rift deposits include Upper Jurassic to Lower Cretaceous rocks, and post-rift units are Barremian-Aptian to probably Cenozoic in age (Loprieno et al., 2010). Metabasic rocks ascribed to the Valais mega-unit yielded Late Jurassic U/Pb zircon ages, interpreted to date their magmatic protolith ages of 163–155 Ma (Liati et al., 2005). While these constraints would suggest an opening of the Valais Basin (including the extension of the margins) sometime after ~175 Ma, and until ~125 Ma, the opening is generally assumed to occur in the Early Cretaceous, although it should be noted that this interpretation is based on the assumption that the Valais Ocean was connected to the Bay of Biscay, and using interpretations of the age of extension and mantle rock exhumation in the Pyrenees (e.g., Handy et al., 2010; Loprieno

et al., 2010; Stampfli, 1993), the kinematic validity of which we will address in the reconstruction section. An age of 42–40 Ma for high-pressure metamorphism of the Valais units is constrained by radiometric data from the Valais Bündnerschiefer in Eastern Switzerland ($^{40}Ar/^{39}$ Ar dating of white mica; Wiederkehr et al., 2009). An age of around 40 Ma was obtained by Villa et al. (2014) for a phase of nappe stacking in the basement of the most external parts of the Briançonnais (Ruitor area of the upper Aosta Valley) that post-dates high-pressure metamorphism in this area, which is parallelized with early isoclinal folding in the Valais units of the Valais units of Savoy (Bucher et al., 2004; Loprieno, 2001). Hence, we model the moment of transfer of Valais rocks to the Alps fold-and-thrust belt at 45 Ma.

The Valais mega-unit is the most external Oceanic unit, thrust on top of a series of nappes that were derived from and thrust onto the **European foreland**. In the western Alps, these are thick-skinned thrusts that form the External Massifs and the Chaînes Subalpines of France (Guellec et al., 1990; Mugnier et al., 1990; Bellahsen et al., 2012; Schmid et al., 2017). The amount of shortening increases towards Switzerland where the so-called Helvetic cover nappes, extending into Austria and detached from their pre-Triassic basement lie in front of the External Massifs. Helvetic nappes and External Massifs are thrust over an Oligo-Miocene foreland 'Molasse' Basin. In the Swiss and Austrian Alps (Lepontine dome and Tauern window), large volumes of pre-Triassic basement were deeply underthrust, metamorphosed and decoupled from their lower crustal and lithospheric mantle underpinnings (Subpenninic units of Schmid et al. (2004b)). The HP-LT Adula nappe and the Eclogite Zone of the Tauern Window (Fig. 10) also belong to these units derived from the distal European passive margin. Ages of HP-LT metamorphism in these two units are ~35–38 Ma (Herwartz et al., 2011) and ~40 Ma (Kurz et al., 2008), respectively. We adopt an age of around 40 Ma for decoupling of these units from Eurasia.

Thrusting of the Helvetic, Subpenninic European margin and higher mega-units over the Molasse Basin occurred until about 20 Ma ago after which shortening migrated into the Molasse Basin (Kempf and Pfiffner, 2004; Pfiffner, 1986; Schmid et al., 1996). A minimum amount of some 55 km of shortening within the Helvetic nappes is inferred from a section by Schmid et al. (2004b), which is here reconstructed between 35 and 20 Ma. Only ~25 km of total shortening occurred after 20 Ma in the Swiss Alps (Kempf and Pfiffner, 2004). Part of the shortening in the distal foreland led to the formation of the Jura Mountains (Figs. 1 and 10) between 20 and 7 Ma, exhibiting a maximum of 30 km in the center of the Jura Mountains (Affolter, 2004; Affolter et al., 2008), decreasing to zero km at the tips.

The kinematic evolution of the arcuate shape of the Western Alps is subdivided into three steps (Schmid and Kissling, 2000; Schmid et al., 2017). A first step (pre-35 Ma) of the West-Alpine orogenic evolution is characterized by top-NNW thrusting in sinistral transpression causing at least some 260 km differential displacement of internal Western Alps and E-W-striking Alps farther east, together with Adria, towards N to NNW with respect to stable Europe. The second step (35–20 Ma) accentuated the arc; it is associated with top-WNW thrusting in the external zones of the central portion of the arc and is related to the lateral indentation of the Ivrea mantle slice towards WNW by some 100 km. This leads to dextral strike slip along the Insubric line (Schmid et al., 1989; Schmid and Kissling, 2000) during which the front of the Western Alps together with the Ivrea mantle slice, both being located south of the E-W-running Insubric line, moved to the west in respect to stable Europe. At the same time the southernmost Western Alps hosted a diffuse sinistral strike slip zone later overprinted during step 3 (Argentera-Cuneo line of Schmid et al., 2017). This last step 3 of arc formation (20–0 Ma) is associated with orogeny in the Apennines leading to oroclinal bending in the southernmost Western Alps in connection with the 50° counterclockwise rotation of the Corsica-Sardinia block and the Ligurian Alps block (Gattacceca et al., 2007; Maffione et al., 2008; see Sections 6.2.4 and 6.2.5).

5.6.3. Eastern Alps; AlCaPa

The Eastern Alps display several first-order differences with the Western Alps. At the western margin of the Eastern Alps, westwards of the Engadine window, rocks of the Briançonnais mega-unit are still present but disappear farther east (Fig. 10). In the Eastern Alps a series of continent-derived thrust slices known as the 'Austro-Alpine nappes' (Neubauer et al. (1999) and references therein) lie thrust above ocean-derived sediments interpreted to be derived from the Piemonte-Ligurian and/or Valais oceans, exposed in the Tauern and Rechnitz Windows (Fig. 10). These Austro-Alpine nappes, internally imbricated during the Cretaceous, can be traced into the Western Carpathians and are bounded in the south by the Mid-Hungarian Shear Zone (Fig. 10) (Csontos and Nagymarosy, 1998; Csontos and Vörös, 2004; Horváth et al., 2015; Jeřábek et al., 2012; Plašienka, 1997, 2018; Schmid et al., 2004b, 2008). The Austro-Alpine nappes together with the Central and parts of the Inner West Carpathian units are known as the AlCaPa (Alps, Carpathians, Pannonian) mega-unit that forms the hangingwall in respect to accretion in the Eastern Alps and Western Carpathians during Late Cretaceous and Cenozoic thrusting (e.g., Csontos, 1995; Oszczypko, 2006; Schmid et al., 2008). In the North, the AlCaPa mega-unit thrust onto the Rhenodanubian and Magura flysch units that are correlated to the Valais mega-unit (e.g., Plašienka, 2003; Schmid et al., 2004b). Farther south, e.g. in the Tauern Window, the ALCAPA mega-unit thrust onto Piemonte-Ligurian and underlying Valais oceanic units (Schmid et al., 2013). However, since east of the Engadine window no Briançonnais mega-unit has been recognized no strict division can be made between the Piemonte-Ligurian and Valais mega-units although differences may still be seen between higher and lower oceanic thrust slices based on sedimentary facies and paleontological content (Schmid et al., 2004b, 2008).

Given the top-to-the-north Cenozoic thrusting onto the remnants of the Alpine Tethys, the AlCaPa mega-unit is generally interpreted to be derived from continental rocks that were paleogeographically to the south of the Alpine Tethys, i.e. part of the Greater Adriatic microcontinental domain. Internally the AlCaPa mega-unit consists of a Cretaceous-age top-to-the-NE nappe stack (Faryad and Henjes-Kunst, 1997; Plašienka, 1997; Putiš et al., 2007; Schmid et al., 2004b; Schuster, 2015; Vojtko et al., 2016). This comprises from top to bottom (i) rare slices of ophiolitic mélange, correlated to the 'West-Vardar Ophiolites', often referred to as "**Meliaticum**" after a locality around Kosice in the eastern part of the AlCaPa unit; (ii) the Upper Austro-Alpine nappes that include an '**Eo-Alpine**' high-pressure metamorphic unit, and (iii), the lower **Austro-Alpine nappes**. Apart from the ophiolitic Meliaticum mélanges, which were emplaced around the Jurassic-Cretaceous transition (~145 Ma) (Schmid et al., 2008), all of these units are derived from continental crust. The upper Austro-Alpine units consist of the Northern Calcareous Alps, detached from their crystalline substrate, and three nappe systems consisting of upper crustal basement-cover nappes, the middle of them consisting of Eo-Alpine high-pressure metamorphic rocks (Frisch et al., 1998; Neubauer et al., 1999; Ratschbacher et al., 2004). These nappes started to be thrust and removed from their original lower crustal and lithospheric underpinnings in Early Cretaceous time, at around 135 Ma (Schmid et al., 2008). Eo-Alpine high-pressure metamorphism, associated with peak P-T conditions that typically reach eclogite facies and locally even ultra-high pressure conditions (ca. 790 °C and 30 kbar) culminated at around 95-90 Ma (Janák et al., 2004, 2015; Thön et al., 2008). These ages coincide with the onset

of deposition of the 'Gosau' sedimentary group on the Austro-Alpine nappes in the Turonian (93-89 Ma), the oldest sediments of which become younger to the west (~84 Ma) (Krohe, 1987; Ortner and Stingl, 2001; Wagreich and Decker, 2001; Wagreich and Faupl, 1994). These sediments seal the Austro-Alpine thrusts and are frequently associated with normal faulting-related basin formation and extensional detachments (Fügenschuh et al., 2000; Handy et al., 2010; Willingshofer et al., 1999). This shows that the Austro-Alpine nappes were extended, in a ~NW-SE orientation in modern coordinates, during exhumation of the Eo-Alpine HP units (Froitzheim et al., 1997). This extension affected rocks as far south as the Medvednica Mountains on the Dinarides-Alps junction (van Gelder et al., 2015).

The modern overlap between that part of the upper Austro-Alpine nappes overlying the Eo-Alpine HP units and those underlying it is at least 125 km in a N-S direction. The Eo-Alpine HP rocks were thrust over the downgoing lower Austro-Alpine nappes until ~80 Ma, probably during their exhumation, with a minimum modern N-S overlap of 100 km, after which the combined Austro-Alpine nappe stack was thrust onto Piemonte-Ligurian oceanic units (Handy et al., 2010; Schuster, 2015).

In the Western Carpathians a narrow, subvertical structural unit known as the Pienniny Klippen Belt (not specified on our maps but included in the Magura unit) marks the northern edge of the ALCAPA mega-unit. This belt contains large, non-metamorphosed blocks of Mesozoic sediments of different facies embedded in an Upper Cretaceous and Paleogene deep-marine marlstone and turbidite matrix (Birkenmajer, 1985; Plašienka, 1997, 2012). This belt is interpreted to reflect deep-marine trench deposits partly formed on oceanic crust of the Alpine Tethys domain that was overthrust by the Austro-Alpine nappe stack since the Turonian. The post-80 Ma thrusting of the AlCaPa mega-unit the Magura units and its equivalent in the Eastern Alps, the Rhenodanubian Flysch, culminated in an overlap of 130 km. Finally, a minimum modern overlap between the Magura and equivalent units in the west over the Helvetic units of the Tauern window amounts to some 120 km (Fig. 11).

The nappe stack of the eastern Alps was overprinted by younger, and out-of sequence deformation. The Eastern Alps were overprinted by a substantial orogen-parallel stretching in the Neogene referred to as lateral extrusion by Ratschbacher et al. (1991) that affects the entire AlCaPa mega-unit (Decker and Peresson, 1996; Fodor et al., 1998; Frisch et al., 2000; Scharf et al., 2013; Wölfler et al., 2011) and amounts to total a E-W stretching of 290 km (Ustaszewski et al., 2008) (see section 5.9). The western Alps were extended during Oligocene and Miocene times. Oligocene (34–30) E-W extension in the internal parts of the western Alps along top-to-the-east extensional detachments at the eastern margin of the Lepontine dome juxtapose non-metamorphic ophiolites against blueschist and amphibolite facies metamorphic units at the rim of this dome (Beltrando et al., 2010; Nievergelt et al., 1996). The amount of extension can only be estimated roughly to be in the order of 10 km. The prominent top-to-the-SW Simplon extensional fault at the western margin of the Lepontine dome (Mancktelow, 1992) accommodated approximately 20 km arc-parallel extension between ~20 and ~7 Ma at the western margin of the Lepontine dome in the western Alps.

Cenozoic strike-slip deformation was dominated by two major faults. At least 100 km of dextral displacement of Adria relative to the Europe-verging fold-and-thrust belt of the Alps was accommodated along the E-W striking Periadriatic Fault System between 35 and 20 Ma. A similar amount of E-W shortening was accommodated along the western (Roselend, or Penninic) frontal thrust (Affolter et al., 2008; Schmid et al., 2017) and along the strike-slip segment that starts north of the Argentera (Fig. 11). We trace the latter north of the Voltri Massif so as to align the HP units of the western Alps with those of the Voltri Massif. In addition, we restore 15 km of backthrusting of the western Alps over the Insubric line, following (Schmid et al., 2004b; Simon-Labric et al., 2009).

A second prominent strike-slip fault is the Neogene Giudicarie Fault, which accommodated ~80 km of left-lateral strike-slip displacement between 20 and 10 Ma (Fig. 11). This strike slip motion is contemporaneous with orogen-parallel lateral extrusion and distributed N-S out-of-sequence shortening in the eastern Alps, particularly north of the Tauern window (Scharf et al., 2013). Frisch et al. (1998) estimated 113 km of N-S out-of-sequence shortening of the Periadriatic line in the eastern Alps. This is consistent with the ~25 km post-20 Ma N-S shortening accommodated in the western Alps (Kempf and Pfiffner, 2004) added to the displacement of the Giudicarie Fault.

After some 22 Ma, shortening also localized south of the Peri-Adriatic line and was accommodated by top-to-the-south thrusting in the Southern Alps. Schönborn (1999) constructed and balanced N-S cross-sections across the southern Alps and estimated ~ 45–70 km of shortening accommodated between 22 and 7 Ma west of the Giudicarie Fault. Similar amounts of shortening (ca. 50 km) affected the eastern part of the Southern Alps between ~10 Ma and the Present (Scharf et al., 2013). Hence, to the west of the Giudicarie Fault, Messinian sediments cover the frontal thrust of the southern Alps (Schmid et al., 1996), whereas thrusting continues to the east of the Giudicarie Fault today.

5.7. Moesian Platform; Dobrogea

The **Moesian Platform** (or Moesia), west of the Black Sea, is in the northeast separated by the North Dobrogea orogen from the Scythian Platform (Figs. 1 and 13), which is generally considered a margin of the East-European craton that underwent only minor deformation after the Paleozoic (Saintot et al., 2006b; Stephenson et al., 2006). The Moesian Platform forms the foreland of the highly curved South Carpathian and Balkanide fold-and-thrust belts, and its margins were deformed and incorporated in these deformed belts (see sections 5.8 and 5.10) (Fig. 13). Outside the orogen, the Moesian Platform contains two crustal scale faults – the Intramoesian and Capidava-Ovidiu Faults – that separate the South Dobrogea and Central Dobrogea units from the main Moesian (or Valachian) Platform (Visarion et al., 1988) (Fig. 13). The Moesian Platform has an uppermost Precambrian - lowermost Paleozoic basement exposed in Central Doborgea and contains parts of a Neoproterozoic and Cadomian volcanic arc, foreland basin sediments, and ophiolites (e.g., Măruntiu et al., 1997; Oaie et al., 2005; Săndulescu, 1988; Seghedi et al., 2005a).

In the main Moesian Platform and neighbouring Western Balkans, these basement units are overlain by up to 4 km of Upper Cambrian - Upper Carboniferous clastic and carbonate sediments with fossils suggesting a northern Gondwana affinity. Thick Devonian turbidites and a Middle - Upper Carboniferous regressive sequences to a continental facies are interpreted to relate to the Variscan orogen, which in the neighbouring Sredna Gora and Balkans units (see section 5.10) led to high-grade metamorphism (Boncheva et al., 2010; Carrigan et al., 2003, 2005; Tari et al., 1998; Vaida et al., 2005; Yanev, 2000).

The Moesian Platform has been affected by a Permo-Triassic episode of rifting and volcanism distributed in a number of (half-)grabens throughout the entire main Moesian and pre-Balkans unit, where the syn-kinematic thickness may reach 3–4 km (Georgiev et al., 2001; Paraschiv, 1979; Răbăgia and Tărăpoancă, 1999; Tari et al., 1998). The significance of this extensional event is poorly understood, but similar rifting episodes were documented in the Strandja Unit, North Dobrogea as well as in Crimea (Figs. 1 and 13), and has been proposed to relate to the tectonic evolution of the Paleotethys (Nikishin et al., 2001; Okay et al., 1996, 2001a, 2001b;

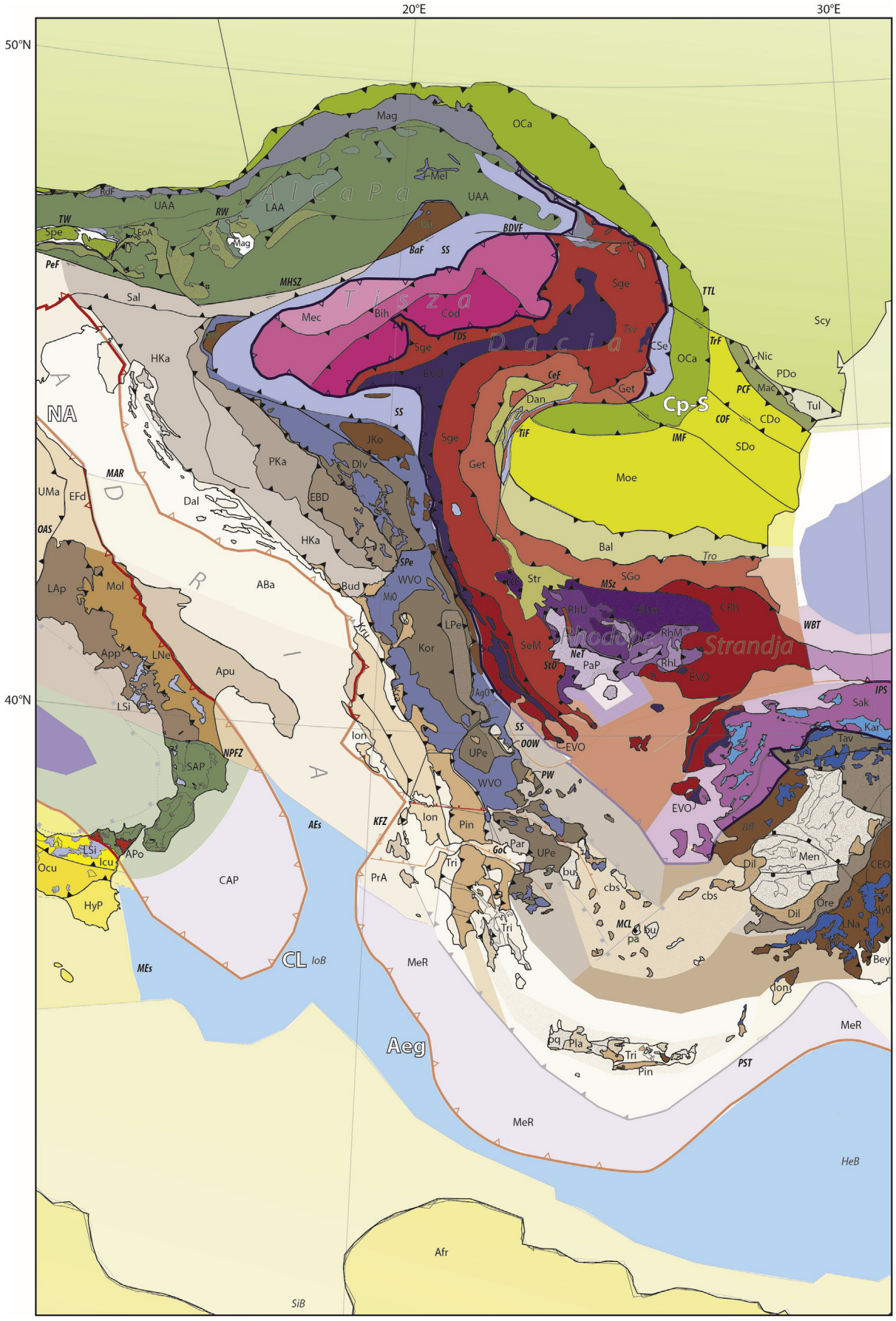

Fig. 12. Tectonic map of the wider Balkan region. For key to abbreviations, see Table 4, for key to tectonic units, see Fig. 5. For location of the map within the Mediterranean region, see Fig. 4.

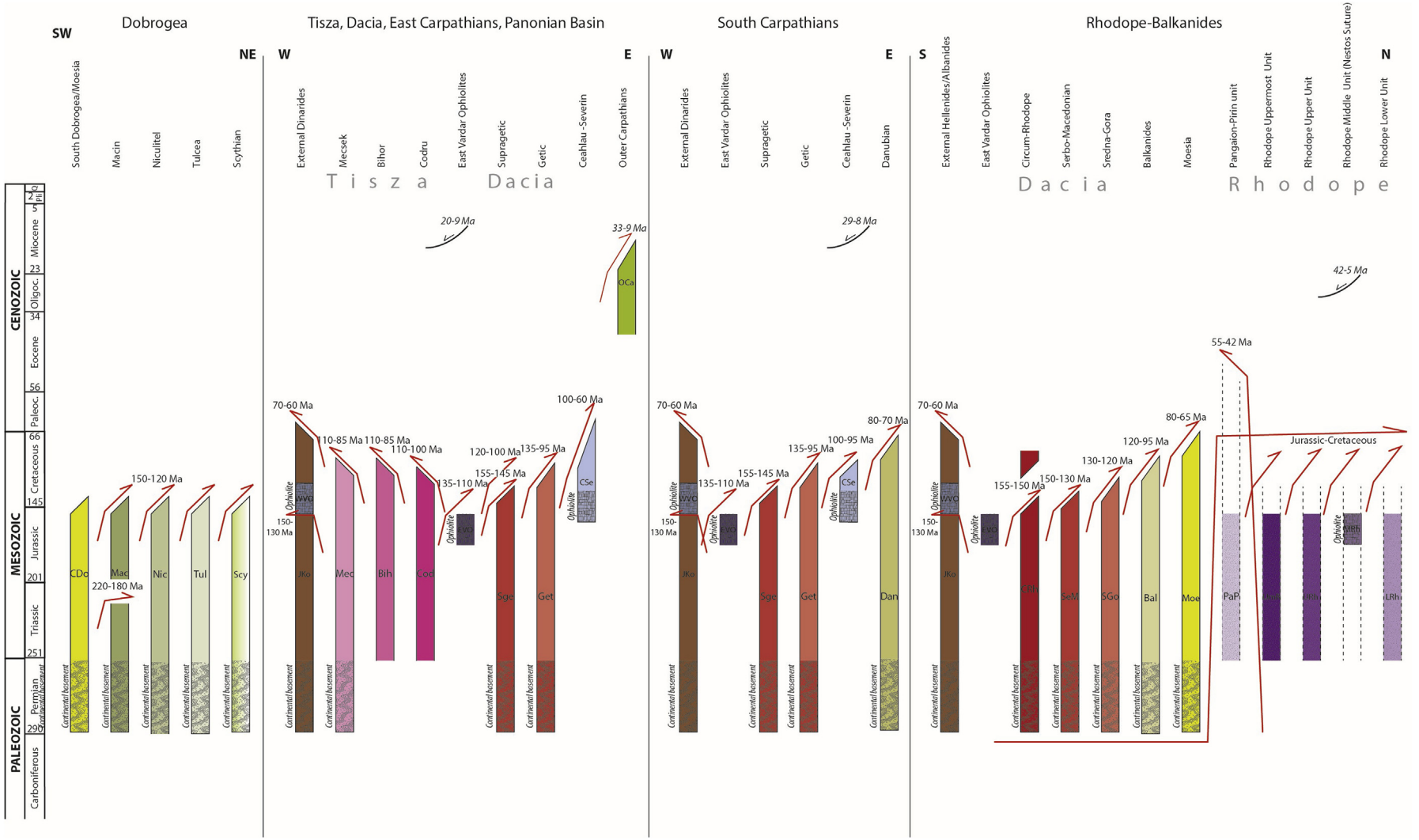

Fig. 13. Orogenic architecture charts for the Dobrogea, Tisza, Dacia, Carpathian, and Rhodope mega-units. For key to abbreviations, see Table 4, for key to tectonic units, see Fig. 5. For regional distribution of tectonic units, see Fig. 12. See Table 1 for summery of kinematic constraints corresponding to this chart. Periods of metamorphism are indicated with dotted hatching, formation of oceanic basement (ophiolites) with vertical hatching, and formation of pre-Alpine crystalline basement with curved hatching.

Okay and Nikishin, 2015). The Moesian Platform was affected during the Late Triassic to Jurassic by significant shortening (Georgiev et al., 2001; Tari et al., 1998) and formation of abundant NW-SE oriented strike-slip faults that offset the Permo-Triassic grabens in the Moesian Platform (Răbăgia and Tărăpoancă, 1999). The kinematic evolution of this system is poorly constrained, but may be in part contemporaneous with opening of the Ceahlau-Severin Ocean to the west and north of the Moesian Platform (see section 5.8) (Săndulescu, 1984; Tari, 2005). The Moesian Platform has been subsequently affected by Cretaceous - Miocene deformation associated with the foreland propagating Carpatho-Balkanide fold-and-thrust belts. Only strike-slip reactivations occurred in Miocene-Quaternary times (Maţenco et al., 2007; Paraschiv, 1983, 1997; Tărăpoancă et al., 2003; Tari et al., 1998; see also Section 5.9) primarily along the Intramoesian, Peceneaga-Camena fault and Trotuș faults. These offsets reach 35–40 km beneath the Carpathians orogen, but transfer rapidly their offsets to orogenic structures at farther distances (Maţenco et al., 2007) and have been, therefore, reconstructed together with the Carpathians nappe system.

The North **Dobrogea** orogen (Figs. 13 and 14) separates the Moesian and Scythian Platforms and is an area that has undergone repeated deformation episodes throughout Mesozoic times and before (Săndulescu, 1984; Seghedi, 2001). A variety of interpretations are available, but these generally agree that North Dobrogea is separated into three units by two NE-verging Mesozoic thrusts, from structurally high to low, and from SW to NE, comprising the Macin, Niculitel, and Tulcea units (Figs. 13 and 14) (Rădulescu et al., 1976; Săndulescu, 1984; Seghedi, 2001). The Macin unit is a composite nappe of uppermost Precambrian amphibolite-facies metamorphic basement (Săndulescu, 1984; Seghedi, 2001). This North Dobrogea basement is overlain by a dominantly shallow-water Lower Paleozoic cover and a Carboniferous - Lower Permian clastic and volcanoclastic series that is in places metamorphosed in (sub-) greenschist-facies conditions during the Variscan orogeny, and intruded by likely Middle Carboniferous – Lower Permian plutons (Seghedi, 2001, 2012, and references therein). Similar to the Moesian Platform, this composite basement was subsequently overprinted by extension and dextral strike-slip deformation during Late-Permian – Middle Triassic times, resulting in well-observed syn-rift deposition, intrusions, acid volcanism, dykes and extrusions of basalts, the latter well developed in the intermediate Niculitel unit (Mirăuță, 1982; Saccani et al., 2004; Săndulescu, 1980; Seghedi, 2001). This rifting probably did not result in the formation of oceanic crust (Saccani and Photiades, 2004). The Triassic - Jurassic series are well developed in the Tulcea unit, in a laterally variable but deeper marine facies than on the neighbouring Moesian Platform (e.g., Grădinaru, 1995; Seghedi, 2001). Rift inversion started in the Late Triassic and ceased by mid-Jurassic times. A second event of shortening occurred in latest Jurassic to Early Cretaceous times, sealed by Cenomanian deposits. Both events resulted in the present-day three-nappe structure of the North Dobrogea orogen (Săndulescu, 1980, 1984). Although the displacement along the nappe-bounding thrusts is unknown, and appear to be associated with en-echelon folds well observed in the Tulcea unit (e.g., Grădinaru, 1988), their map contours and associated tectonic klippen suggest a minimum shortening on the order of 30 km for the emplacement of the Macin over the Niculitel unit and some ~20 km offset of thrusting of the Niculitel over the Tulcea unit. These displacements include the sub-divisions of the main units (Consul and Sarica digitations of Săndulescu (1984)). We implemented these offsets in our reconstruction during Tithonian – Aptian times (~150-120 Ma) following the age of the main deformation episode inferred by Espurt et al. (2012b) and Seghedi (2001). The North Dobrogea orogen is bordered along the Peceneaga-Camena Fault from Central Dobrogea (Fig. 13). This crustal fault has a reverse displacement of at least some 10 km that is of likely Middle Jurassic to Early Cretaceous age (Hippolyte, 2002; Rădulescu et al., 1976; Săndulescu and Visarion, 1988), although the verticalization of Late Jurassic strata suggest much higher offsets of up to 50 km (see Grădinaru, 1988). Strike-slip deformation has also been inferred for the Peceneaga-Camena Fault and the faults in the North Dobrogea orogen and the basement underlying the Carpathian foredeep, and both sinistral and dextral displacement has been argued for, but total displacements remain unquantified (Hippolyte, 2002; Rădulescu et al., 1976; Seghedi, 2001; Tărăpoancă et al., 2003; Tari, 2005). The Mesozoic structures of the North Dobrogea orogen and the Peceneaga - Camena Fault are unconformably covered by Albian and Upper Cretaceous sediments (Mirăuță and Mirăuță, 1964; Grădinaru, 1988) and by Mesozoic - Eocene sequences of the western Black Sea, which also provide little evidence for significant strike-slip or contractional deformation (Dinu et al., 2005; Munteanu et al., 2011) and references therein). From late Early Cretaceous time onwards the Moesian Platform and North Dobrogea orogen can thus be considered as a promontory of the Eurasian continent.

5.8. Tisza; Dacia; Severin-Ceahlau; Danubian

The southern and eastern parts of the Pannonian Basin and the highest structural units of the adjacent Carpathians are occupied by a collage of two internally deformed major tectonic mega-units, Tisza and Dacia, which evolved as independent continental units that were separated from Europe via the opening of the eastern-most extensions of Alpine Tethys in Mid-Jurassic to Early Cretaceous times (Piemonte-Ligurian, Valais-Magura and Ceahlau-Severin oceans (Săndulescu, 1984; Schmid et al., 2004b, 2008). To the South and West, they were adjacent to the Neotethys Ocean (Gallhofer et al., 2015), whose ophiolitic remnants are found in the East and West Vardar Ophiolite belts (*sensu* Schmid et al., 2008) (Fig. 13). The East Vardar Ophiolite belt thrust in Late Jurassic to Early Cretaceous times eastward (in present day coordinates) onto the Dacia mega-unit; the West Vardar belt was obducted over Adria during Late Jurassic - earliest Cretaceous times. The remainder of the Neotethys branch (Sava Ocean) progressively closed until collision with Europe in Latest-Cretaceous to Early Paleocene times, forming the **Sava Suture** (Fig. 13) (Pamić et al., 2002; Ustaszewski et al., 2009). The Late Cretaceous subduction of the Neotethys Ocean is in agreement with the observation of genetically related accretionary deposits, the evolution of a fore-arc basin and the emplacement of typical subduction-related magmatism in the European-derived upper plate (Gallhofer et al., 2015, 2017; Schmid et al., 2008; Toljić et al., 2018) (see section 5.11).

The **Tisza** continental unit is made up by a medium to high-grade Late Paleozoic (Variscan) metamorphic basement. At least a part of this basement (Mecsek Mountains) is thought to have been attached to the Bohemian Massif or other parts of the European foreland presently north of the Western Carpathians, and is consequently interpreted as having separated from Europe during opening of the Alpine Tethys (Ebner et al., 2007; Klötzli et al., 2004; Vozárová et al., 2009). In the Mecsek nappe system this basement is overlain by a Permian – Triassic 'Germanic' facies and continental Liassic deposits (Gresten facies); rapid deepening of the basin started in mid-Jurassic times, as the Alpine Tethys opened (Haas and Péró, 2004) also suggesting its derivation from continental Europe. The southern parts of Tisza show significant lateral variations in the facies of the Triassic sediments, including deeper water sediments (so-called Hallstatt) facies sediments in parts of the Codru nappe system, suggesting increasing influence of the Neotethys passive margin from WNW towards ESE in present-day coordinates over the Tisza Block (Balintoni, 1996; Burchfiel and Bleahu, 1976; Haas and Péró, 2004).

The Tisza mega-unit is separated from the AlCaPa mega-unit to the north (section 5.6.3) along the Mid-Hungarian shear zone (Csontos and Nagymarosy, 1998; Csontos and Vörös, 2004; Schmid et al., 2008). Along this shear zone, ophiolite relics are rarely found at the surface (Bükk Mountains) and mostly suspected in the subsurface of the Pannonian Basin, linking Alpine Tethys to Western Vardar Ophiolites of the Dinarides (Fig. 13) (Schmid et al., 2008, and references therein) (see section 5.11). Whilst klippen of Neotethys ophiolitic mélange are found as highest structural units of the AlCaPa Block north of the Mid-Hungarian Shear Zone (see section 5.9), there are no Neotethyan, or other, ophiolites found obducted onto the Tisza Block. The West Vardar Ophiolites root thus in the Sava Suture Zone, below the Tisza mega-unit (Schmid et al., 2008, and references therein) (Figs. 12 and 13). There are also no East Vardar Ophiolites on the Tisza Block, suggesting that these likely root in a suture between the Tisza and Dacia units.

Large-scale contractional deformation is recorded in the Tisza unit by, in present day coordinates, top NW nappe stacking between ~in any case between 95 and 85 Ma (extended to 110 to 85 Ma in our reconstruction to reconcile shortening rates with convergence rates), with minor reactivations during Late Cretaceous - Oligocene times (Csontos and Vörös, 2004; Kounov and Schmid, 2012; Merten et al., 2011; Reiser et al., 2017). The top-to-the-NW shortening that affected the Tisza mega-unit formated, from northwest to southeast, and from structurally lower to higher, the Mecsek, Bihor, and Codru nappes. This was associated with at least ~50 km of shortening (Kounov and Schmid, 2012; Reiser et al., 2017). Additionally, the Dacia mega-unit and overlying East Vardar Ophiolites were back-thrust towards the northwest over the Tisza unit with a minimum displacement of 70 km between 95 and 85 Ma (extended to 110 to 85 in our reconstruction) (Schmid et al., 2008). This top NW thrusting represents an out-of-sequence backthrust in respect to earlier top E to NE thrusting that characterizes nappe stacking in the adjacent Dacia mega-unit and affected also the Tisza unit at its contact (Kounov and Schmid, 2012; Reiser et al., 2017) (see below). More specifically, the eastern parts of the Bihor nappe were affected by pre-110 Ma top E to NE deformation (Reiser et al., 2017). Combined with the absence of East Vardar Ophiolites on Tisza, the top-to-the-NW backthrust of Dacia over Tisza is thought to offset and obscure a Tisza-Dacia suture (Schmid et al., 2008; their profile 3 in plate 3). In any case, Tisza and Dacia formed a coherent block after 85 Ma and invaded the Carpathian embayment together during the Miocene.

The **Dacia** continental mega-unit of Romania separated from the European and Moesian platforms by the Severin-Ceahlau ophiolitic mélange and is consequently considered a former microcontinental domain (Csontos and Vörös, 2004; Maţenco et al., 2010; Săndulescu) (Fig. 13). The Dacia mega-unit consists of two main nappe systems, the Supra-Getic and Getic nappes (also known as Bucovinian and Getic nappe systems, whereby Infrabucovinian equals the Getic nappe and the Sub-Bucovinian and Bucovinian are the Supragetic nappes), with a type locality in the South Carpathians. Recently, also the Biharia nappe system of in the Apuseni Mountains was assigned to the Dacia megaunit (Figs. 12 and 13) (Iancu et al., 2005a; Kräutner and Krstić, 2002; Schmid et al., 2008; Kounov and Schmid, 2012; Reiser et al., 2017) and correlated with part of the basement and Mesozoic cover buried beneath the East Vardar Ophiolites and Miocene sediments of the Transylvanian Basin (Ionescu et al., 2009; Krézsek and Bally, 2006; Săndulescu and Visarion, 1978; Schmid et al., 2008; Tiliţă et al., 2013).

In the East and South Carpathians the Bucovinian and Getic nappe systems contain a Precambrian to lowermost Paleozoic crystalline basement (Balintoni and Balica, 2013; Balintoni et al., 2011, and references therein) locally affected by Variscan metamorphism and magmatism (e.g., Duchesne et al., 2008; Iancu et al., 2005a, 2005b, 1998; Medaris et al., 2003; Stoica et al., 2015). This basement is overlain by a Permian to Lower Cretaceous sedimentary series, partly metamorphosed under low-grade conditions during the Alpine cycle in deeper parts of the nappe stack (Culshaw et al., 2011; Gröger et al., 2013; Iancu et al., 2005a). The Bucovinian and Getic nappes stack was emplaced until late Early Cretaceous times over the East and South Carpathians (Iancu et al., 1998; Kounov and Schmid, 2012; Kräutner and Bindea, 2002; Reiser et al., 2017; Săndulescu, 1984; Schmid et al., 2008). Given the variability of deformation combined with kinematic and timing constraints, we have assumed a larger 130-95 Ma time interval for this deformation.

The Getic nappe stack of the South Carpathians is traced farther southward into the Carpatho-Balkan orogen of eastern Serbia (e.g., Kräutner and Krstić, 2002) from where it bifurcates around the Rhodope extensional province into an E-W branch that follows the Balkan Mountains to the Black Sea, and a N-S branch that is followed all the way down to Greece (see section 5.10) (e.g., Kounov et al., 2010; Schmid et al., 2011) (Fig. 13).

The **East Vardar Ophiolites** are found as a highest structural unit in the Apuseni Mountains, in the subsurface of the Transylvanian Basin, in the East Carpathians, and in eastern Serbia, and into Greek Macedonia and western Turkey as part of the Circum-Rhodope belt (Fig. 13) (Csontos and Vörös, 2004; Gallhofer et al., 2017; Haas and Péró, 2004; Kounov and Schmid, 2012; Săndulescu, 1975; Săndulescu and Visarion, 1978; Schmid et al., 2008, 2019; Vörös, 1977). These ophiolites consist of MORB-type oceanic crust, intruded and overlain by calcalkaline magmatic rocks (e.g., Božović et al., 2013; Gallhofer et al., 2017; Nicolae and Saccani, 2003). The ophiolites have crustal ages around 170 Ma (Bajocian) and were first emplaced onto Dacia over a distance of several tens of kilometers between 155 Ma (Kimmeridgian) and the end of the Jurassic (145 Ma) as can be observed in eastern Serbia (Figs. 1 and 13). Underlying olistostromes and tectonic mélanges contain sedimentary formations partly in deep-water facies of Middle-Late Triassic ages, as well as ophiolitic olistoliths (Hoeck et al., 2009; Ionescu et al., 2009; Kukoč et al., 2015; Resimić-Šarić et al., 2005; Schmid et al., 2008). Following latest Jurassic-earliest Cretaceous emplacement of the East Vardar Ophiolites (referred as the Transylvanides by Săndulescu (1994) continued by E-ward thrusting, in present-day coordinates, during the Early Cretaceous in the highest structural position overlying the Bucovinian nappes, as observed beneath the Paleogene-Miocene sediments of the Transylvanian Basin and in the East Carpathians (Săndulescu and Visarion, 1978; De Broucker et al., 1998; Schmid et al., 2008; Tiliţă et al., 2013). In the Apuseni Mountains - East Carpathians transect, we have reconstructed the thrusting of the East Vardar Ophiolites over a minimum distance of ~170 km over the Dacia mega-unit in Early Cretaceous times (reconstructed as ~120-100 Ma), following initial obduction at the end of the Jurassic.

We have considered a broader time interval of the nappe stacking of the Bucovinian nappes, the thrusting of the Supragetic over Getic nappes and the initial thrusting of Tisza over the Biharia nappe to have occurred during the a broader 135-95 Ma time interval, as shown by the age of the sub-greenschist facies maximum degree of metamorphism, geometry of the thrusting system and existing restorations of tectonic units (e.g., Ciulavu et al., 2008; Iancu et al., 2005a; Kounov and Schmid, 2012; Kräutner and Krstić, 2002; Maţenco and Schmid, 1999; Reiser et al., 2017; Schmid et al., 1998). More specifically, the present-day configuration shows a minimum internal Bucovinian shortening top- E to NE in the order of 60 km in the East Carpathians (following the principles of Kräutner and Bindea (2002)). The geometry of the Supragetic over Getic thrusting in the South Carpathians shows a minimum of 70 km top- S to SSE displacement (see also Iancu et al., 2005a). We have added around 20 km out-of-sequence shortening observed by thrusting of the Dacia mega-unit and overlying ophiolites in the

Apuseni Mountains over the sediments of the Transylvanian Basin between 80 and 40 Ma (De Broucker et al., 1998; Krézsek and Bally, 2006).

The Bucovinian and Getic nappe system in turn thrust over the ocean-derived Severin-Ceahlau units. These represent relics of an ocean basin that opened in the Middle Jurassic and was closed and accreted to the base of the Bucovinian and Getic nappes of the East and South Carpathians in at the same time with their internal stacking during the late Early Cretaceous (Badescu, 1997; Săndulescu, 1994; Stefanescu, 1983; Schmid et al., 2008) (reconstructed at 110-95 Ma). A present-day overlap of 25 km between the Dacia and Severin-Ceahlau units provides a minimum amount of shortening that does not account for the formation of the internal Danubian stack (see below), but the amount of accommodated convergence must have been much higher, estimated to around 100 km by previous studies (Iancu et al., 2005a, 2005b).

The Severin-Ceahlau units including the overlying Dacia mega-unit and East-Vardar Ophiolites became thrust NE-, E to SSE-ward over the East-European, Scythian, and Moesian platforms during the latest Cretaceous ("Laramian") orogeny, and towards the south, over the Rhodopes and external Balkanides (see section 5.10). The underthrust parts of the Moesian Platform that became exhumed during the subsequent Cenozoic orogen parallel- extension, strike-slip and shortening from beneath this nappe stack in the south-western Carpathians, eastern Serbia and western Bulgaria are known as the Danubian nappes (Figs. 13 and 14) (Berza et al., 1983; Ciulavu et al., 2008; Fügenschuh and Schmid, 2005; Kräutner and Krstić, 2002; Schmid et al., 1998). The Danubian nappes were derived from the Precambrian basement and sedimentary cover of the Moesian Platform. These are deformed into a system of basement and cover nappes with the overall geometry of an antiformal stack that is as a whole thrust onto the Moesian foreland (Berza and Drăgănescu, 1988; Berza et al., 1983; Ciulavu et al., 2008; Iancu et al., 2005a; Krézsek et al., 2013; Săndulescu, 1984; Seghedi et al., 2005b). These studies showed that in the South Carpathians, the thrusting of the Getic over the Severin nappe and the underlying Danubian antiformal stack took place during the late Campanian - early Maastrichtian (~80-70 Ma), with a top SSE sense of shear (Schmid et al., 1998; Maţenco and Schmid, 1999). The overall minimum displacement given the geometry of the nappe pile, latest Cretaceous burial and subsequent exhumation is estimated to ~85 km (Merten, 2011; Merten et al., 2010). This thrusting was followed by the late Eocene - early Oligocene formation of the Danubian detachment during orogen-paralel extension in the South Carpathians, the adjacent foredeep, and the Transylvanian Basin (Fügenschuh and Schmid, 2005; Krézsek et al., 2010; Maţenco and Schmid, 1999; Schmid et al., 1998). This extensional deformation is estimated to amount ~30 km from the associated tectonic omission and geometry of normal faults. These deformations were subsequently followed by the 100 km cumulative dextral offset of the curved late Oligocene Cerna-Jiu and early Miocene Timok faults systems (Berza and Drăgănescu, 1988; Kräutner and Krstić, 2002) described below.

In the easternmost south Carpathians and adjacent East Carpathians, thrusting of the Dacia mega-unit over the Ceahlau oceanic units likely lasted longer, into the Paleocene (Merten, 2011; Săndulescu, 1988; Stefanescu, 1983), after which accretion of the more external thin-skinned Carpathian units started, as described below.

5.9. Pannonian Basin; Outer Carpathians

Together with the central-western Mediterranean (sections 5.3 and 5.4) and Aegean (section 5.11) back-arc basins, the Pannonian Basin is one of the three major extensional back-arc basins of the Mediterranean region (e.g., Royden, 1993; Horváth et al., 2006, 2015). The Pannonian Basin is underlain by thin continental lithosphere, with a crustal thickness of 21–35 km, within the basin mostly ~25 km (Horváth et al., 2006), and its mostly 2–5 (up to 6.5) km thick Miocene cover (Balázs et al., 2017) overlies a collage of thrust and subsequently extended units that formed during Cretaceous to Paleogene orogeny that were subsequently affected by the Miocene extension (e.g., Horváth et al., 2006; Schmid et al., 2008; Tari, 2002). The Pannonian Basin is surrounded by the Carpathian curved orogen in the north, east, and south, and by the Eastern Alps and the Dinarides in the west. Contemporaneous with the extension in the Pannonian Basin the Carpathians thrust over Variscan and older Eurasian basement in the north and east, and over the Moesian Platform in the S and SE (e.g., Golonka, 2004; Schmid et al., 2008 and references therein) (Fig. 13). The Pannonian basin formed during the Miocene and overlies large parts of the AlCaPa and Tisza-Dacia megaunits' nappes of the Carpathians and Alps, as well as the eastern Dinarides (Balla, 1986; Csontos, 1995; Horváth et al., 2006, 2015; Ustaszewski et al., 2008). Pannonian Basin extension is, in modern coordinates, dominantly ENE-WSW directed, and is thought to have started during early Miocene times at ~20 Ma and lasted until ~8–9 Ma (Balázs et al., 2016, 2017; Hámor, 1985; Horváth et al., 2006; Pálfy et al., 2007). Extension of the basin occurred at peak rates around 15-11 Ma, leading to the formation of large offset normal faults, detachments and locally metamorphic core complexes that are exposed in the eastern Alps and the northern parts of the Dinarides and their contact with the Carpathians, as well as buried below the Miocene sediments of the basin (Cao et al., 2013; Ratschbacher et al., 1991; Stojadinovic et al., 2013; Tari et al., 1992, 1999; Ustaszewski et al., 2010; van Gelder et al., 2015). In the southwest, the Pannonian Basin extension reactivated structures of the Dinarides, as well as the uppermost Cretaceous Sava Suture Zone between the Dinarides and the Tisza-Dacia mega-units, whose geometry facilitated the exhumation of metamorphic core complexes along extensional detachments (Ustaszewski et al., 2010; van Gelder et al., 2015). Balázs et al. (2016) demonstrated that the main Great Hungarian Plain depocenters show a gradual progression of deformation along low-angle normal faults and detachments throughout the Miocene between ~20 and 8–9 Ma, while earlier moments of Oligocene - early Miocene extension seem to be localized close to the Dinarides-Carpathians contact (Erak et al., 2017; Maţenco and Radivojević, 2012; Toljić et al., 2013; Stojadinovic et al., 2017).

The E-W Miocene extension of the Pannonian Basin was largely coeval with shortening recorded in the outer Carpathians surrounding the basin in the north, east, and south (e.g., Horváth et al., 2015). The Eastern Alps, which to the east connect to the Western Carpathians, underwent coeval E-W Miocene extension and N-S shortening (Frisch et al., 1998; Scharf et al., 2013; Schmid et al., 2013). The shortening accommodated by the East Carpathians in the Miocene is fairly similar to the coeval amounts of Pannonian Basin extension (Lenkey, 1999; Maţenco et al., 2010; Merten et al., 2010) suggesting that there is little net convergence between Adria and Europe accommodated within the Carpathian-Pannonian system during the 20-8 Ma interval (Kreemer et al., 2003; Maţenco et al., 2016; Maţenco, 2017).

Our restoration of extension in the Pannonian Basin and eastern Alps starts from the compilation of Ustaszewski et al. (2008). The amount of extension in the northern Pannonian Basin and eastern Alps is approximately 300 km, comprising 100 km of E-W extension in the Tauern window, 15 km of lengthening due to strike-slip along the Levanttal Fault, and 50 km between the Levanttal Fault and the Rechnitz window (Frisch et al., 1998) (Fig. 13). Following Ustaszewski et al. (2008), we restored an additional 90 km of extension in the Rechnitz window, and 55 km in the Hungarian plains. The amount of extension accommodated in the southern Pannonian Basin overlying the Tisza-Dacia unit is less and gradually

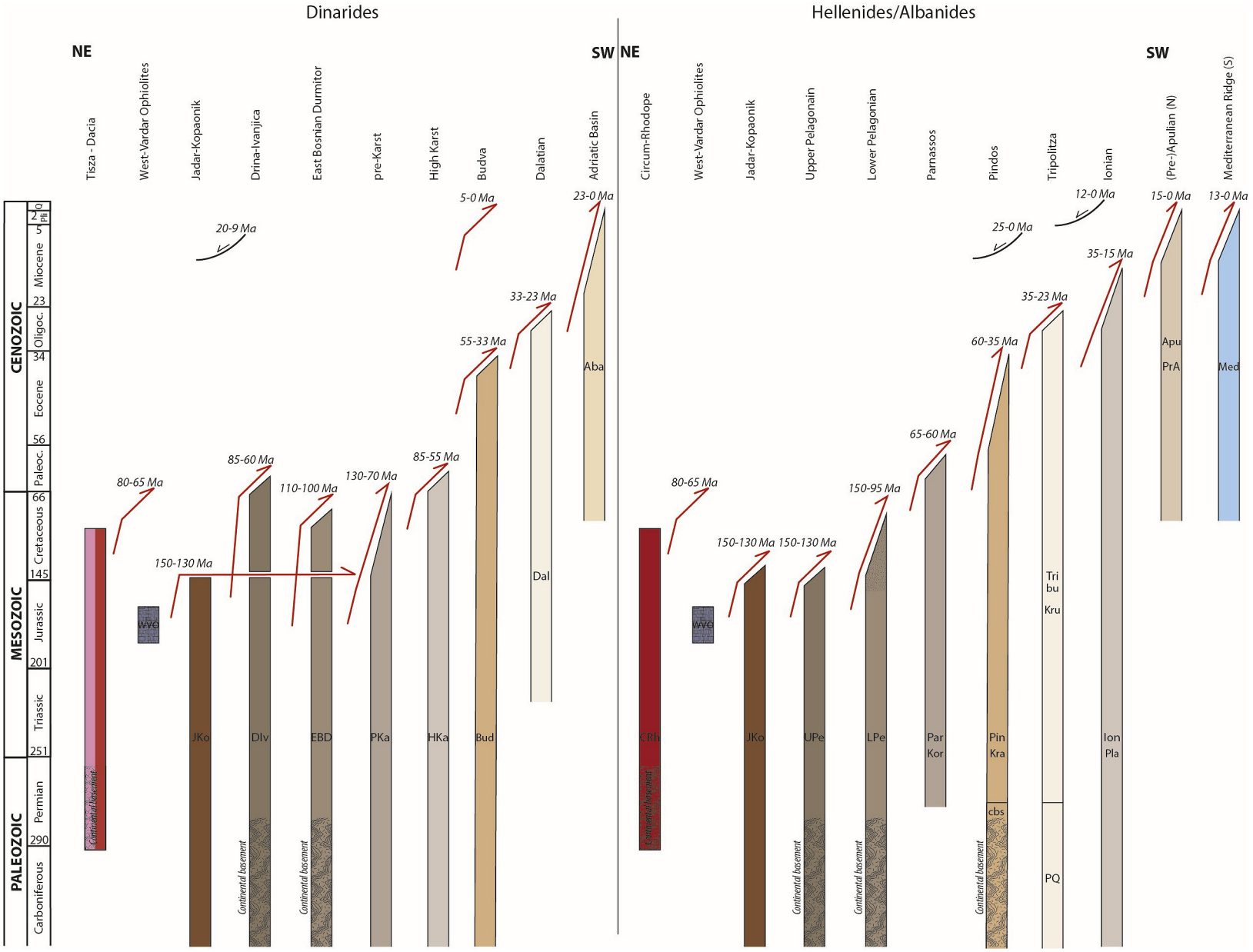

Fig. 14. Orogenic architecture charts for the Dinarides and Albanides-Hellenides. For key to abbreviations, see Table 4, for key to tectonic units, see Fig. 5. For regional distribution of tectonic units, see Fig. 12. See Table 1 for summery of kinematic constraints corresponding to this chart. Periods of metamorphism are indicated with dotted hatching, formation of oceanic basement (ophiolites) with vertical hatching, and formation of pre-Alpine crystalline basement with curved hatching.

decreases in a SE-ward direction (Csontos, 1995; Lenkey, 1999; Matenco and Radivojević, 2012). The difference is accommodated along the major right-lateral Ballaton Fault that connects eastwards to the Mid-Hungarian Shear Zone and the Bogdan Dragos Voda Fault (Fig. 13) (Csontos and Nagymarosy, 1998; Fodor et al., 2005; Tischler et al., 2006). This fault zone reactivates the Sava Suture Zone between the AlCaPa and Tisza-Dacia mega-units (Schmid et al., 2008) (see section 5.6.2), which functioned as a transfer zone between the AlCaPa and Tisza-Dacia mega-units during the Miocene extension (Balázs et al., 2018). Ustaszewski et al. (2008) estimated extension south of the Balaton Fault along three ~E-W segments, whereby the amount of extension decreases SE-ward from ~180 km near the Mid-Hungarian Shear Zone to ~80 km in the area of Belgrade city. Balázs et al. (2016) estimated up to 250 km of extension just south of the Ballaton Fault by accounting also for large offset of extensional detachments found near the border with the Dinarides (e.g., Ustaszewski et al., 2010; Stojadinovic et al., 2017 and references therein). We use this larger number in our reconstruction and test the predictions for rotation in section 6.2.6.

In the southwest of the basin near the contact between the Dinarides and Carpathians, some 50 km of 29–8 Ma E-W extension occurred between the Dinarides and the Moesian Platform, whilst no evidence exists for significant coeval E-W shortening in the South Carpathians. The magnitude of extension here decreases southeastwards and ends somewhere in southernmost Serbia northermost North Macedonia (Erak et al., 2017; Matenco and Radivojević, 2012; Toljić et al., 2013). This extension hence predicts westward, and ccw rotational motion of the northwestern Dinarides relative to the Moesian Platform (Matenco and Radivojević, 2012; Stojadinovic et al., 2013).

In the northwest, the Moesian Platform is separated from the Dacia mega-unit of the South and Serbian Carpathians by the curved Late Oligocene Cerna and Early Miocene Timok right-lateral strike-slip faults that connect more eastwards with the thin-skinned units of the external South and Southeastern Carpathains foredeep (Berza and Drăgănescu, 1988; Fügenschuh and Schmid, 2005; Kräutner and Krstić, 2002; Krézsek et al., 2013) (Fig. 13). Following these studies, we have reconstructed the Cerna Fault with 35 km of strike-slip between 33 and 23 Ma. The Timok fault accommodated 65 km of strike-slip displacement between 20 and 14 Ma assuming the middle Miocene covering of the fault and its poorly constrained post-middle Eocene onset of deformation (see discussion in Krézsek et al., 2013).

The arcuate orogenic belt of the Carpathian Mountains can be followed from the Eastern Alps along the perimeter of the Pannonian Basin and following a 180° loop around the western Moesian Platform. From there to the South and East, the Carpathians continue into the Balkanides orogen (Burchfiel and Nakov, 2015; Ivanov, 1988; Săndulescu, 1988). The AlCaPa and Tisza-Dacia continental mega-units are the highest structural units of the Carpathian fold-and-thrust belt and form a 20–110 km wide thin-skinned fold-and-thrust belt (Figs. 1 and 13). The Outer Carpathian fold-and-thrust belt largely consisting of Cretaceous-Cenozoic flysch underlies rocks that are associated with sutures. These are the Pienniny klippen belt and the Magura units, widely interpreted as the eastward continuation of the Alpine Tethys Suture Zone (Fig. 13) (Oszczypko, 2006; Plašienka, 1997; Schmid et al., 2008), and the Ceahlau-Severin units along the Tisza-Dacia mega-unit (Fig. 13) (Săndulescu, 1988; Schmid et al., 2008) (see section 5.8). The Cenozoic sediments of the Outer Carpathians thus were sheared off a paleogeographic region located between remnants of the Alpine Tethys ocean basin preserved in the sutures, and the Eurasian and Moesian foreland (i.e. the Carpathian embayment of Balla (1986) and Ustaszewski et al. (2008), and references therein). Most of the Outer Carpathian thrust slices consist of Cretaceous - Paleogene pelagic sediments and syn-contractional trench turbidites (i.e. flysch deposits) that were deposited in the now-subducted Carpathian embayment between the Moesian Platform and Eurasia to the north of the Carpathians (the Bohemian Massif) (Fig. 13). These deposits are dominantly deep marine and some of them, such as the Magura flysch, have probably been deposited on oceanic crust, but intercalations of conglomerates with continental basement pebbles show that certainly not all crust was oceanic: continental realms must have existed within the Carpathian embayment (e.g., Silesian ridges: Gągała et al., 2012; Kováč et al., 2016). Upward, these deep-water deposits grade into an upper Miocene regressive sequence (i.e. molasse) interpreted as deposited during the latest stages of Carpathian thrusting onto the foreland (Matenco et al., 2010; Schmid et al., 2008). This foreland comprises the southern margin of the Eastern European continent, to the north of the Black Sea and to the east of the Carpathians, and contains upper Proterozoic and younger sediments of the East European and Scythian platforms (e.g. Robinson et al., 1996; Saintot et al., 2006b; Şengör, 1987; Stephenson, 2004).

The thin-skinned thrusting of the Outer Carpathian nappes towards the Eurasian and Moesian foreland started in the Oligocene and continued during 20–9 Ma extension of the Pannonian Basin in a foreland-propagating fashion (Fig. 14). Contraction and thickening drove erosional exhumation that gradually affected more external units peaking during the ~13-9 Ma time interval during which the frontal part of the fold-and-thrust belt was emplaced over the undeformed foreland in the East Carpathians (e.g., Krzywiec, 2001; Matenco et al., 2010; Merten et al., 2010; Oszczypko, 2006). In addition, fission track ages showed that cooling in the West Carpathians was progressively older from west to east, ~25-10 Ma in the west to 15-5 Ma in the east (Andreucci et al., 2013). Contraction dominated in the West and East Carpathians whilst in the external South Carpathians, right-lateral strike-slip displacement was accommodated along the Cerna-Timok faults system (e.g., Fügenschuh and Schmid, 2005; Ratschbacher et al., 1993). In the external part of the South Carpathians, late Oligocene to early Miocene transtension was followed by middle Miocene dextral transpression and oblique thrusting over the Moesian Platform (e.g., Krézsek et al., 2013; Răbăgia et al., 2011). The SE Carpathians moved farther towards the foreland than the East and South Carpathians, which was accommodated along the Intramoesian right-lateral, and Trotus left-lateral strike-slip faults, 35–40 km between 12 and 8 Ma, and an additional 5 km since the Pliocene (Fig. 13, e.g., Bocin et al., 2009; Leever et al., 2006; Merten et al., 2011; Tărăpoancă et al., 2003). This young and local motion coincides with the only region of the Carpathians with still active and deep seismicity in the Vrancea area (see Fig. 1) associated with a subducted slab well imaged by teleseismic tomography (e.g., Ismail-Zadeh et al., 2012; Martin and Wenzel, 2006).

A series of balanced cross-sections have provided minimum shortening estimates along the Carpathian fold-and-thrust belt. Beidinger and Decker (2014) quantified N-S shortening at the Alps-Northern Carpathian transition region along 6 sections. They show an eastward-increasing N-S minimum shortening of 38 km in the west and 51 km in the east between 26 and 16 Ma. Sinistral oblique convergence along the West Carpathians was associated with N-S shortening components that were quantified in a series of N-S trending cross sections. Nemčok et al. (2000) showed that 20–42 km of shortening was accommodated in the Magura flysch belt during the Eocene-Oligocene (~55-23 Ma) and 80 km of Early-middle Miocene shortening occurred in the more external Silesian foreland basin units. Castelluccio et al. (2015) balanced a N-S section in the same area and constrained a minimum amount of N-S shortening of 105 km, of which 15 km occurred between 55 and 28 Ma and 90 km between 28 and 15 Ma. Nemčok et al. (2006) added three NE-SW balanced sections in the northeastern corner of the Carpathians where they reported rapidly increasing amounts

of Miocene shortening from 74, to 183, to 222 km from north to south around the bend. Eo-Oligocene Magura shortening numbers are fairly constant (18, 35, and 41 km, respectively). This trend continues southward where Behrmann et al. (2000) showed at least 260 km of NE-SW shortening between the AlCaPa Block and the Eurasian foreland, of which 80 km occurred in the Magura flysch belt. Gągała et al. (2012) showed a section in the same area as Behrmann et al. (2000) but concluded that in addition to ~250 km of post-20 Ma shortening, as much as 250 km of shortening occurred between 35 and 20 Ma. The major discrepancy is explained by the thinner stratigraphies that were assumed in the cross-section of Gągała et al. (2012) as compared to Behrmann et al. (2000) and Nemčok et al. (2006). Roure et al. (1993) and Ellouz et al. (1994), finally, balanced shortening in three sections across the eastern Carpathians accommodated in the Silesian units east of the Magura flysch belt. These show minimum Miocene shortening of 130 km, 117 km, and 130 km from north to south, respectively. These authors noted, however, that these numbers should be regarded as minimum estimates since shortening in the Magura flysch belt in the northeast, and the Ceahlau flysch belt in the south, as well as out-of-sequence deformation in the AlCaPa and Tisza-Dacia mega-units were not accounted for. Such discrepancies have become evident by inclusion of low-temperature thermochronometry data in such regional restorations, which led to higher Miocene shortening estimates (~150 km) for the East Carpathians, comparable to the amount of extension in the Pannonian Basin to the west (Maţenco et al., 2016; Maţenco, 2017, and references therein).

5.10. Balkanides; Rhodope; Circum-Rhodope

The Rhodope mega-unit is exposed in a large extensional core complex (see e.g., Brun and Sokoutis, 2018 for a recent overview) that comprises five, and partly highly metamorphosed Jurassic-Cretaceous Alpine nappe systems. These are overlain, mostly along extensional detachments, by time-equivalent nappes of the Dacia mega-unit. In the north Aegean region, these comprise of the Struma units (Bulgarian equivalents of the Danubian nappes) in the NW, the Serbomacedonian (equivalent to Supragetic; Fig. 12) as well as the Circum-Rhodope units (unknown from the Carpathian realm) in the SW, S, E and NE, and finally the Sredna Gora units (equivalent of the Getic nappes) and Balkanide nappes in the N (Schmid et al., 2019). The main part of the Cenozoic Rhodopian core complex started to form in mid- to late Eocene times, no later than 42 Ma ago according to fission track data (Brun and Sokoutis, 2007; Dinter and Royden, 1993; Kounov et al., 2015; Sokoutis et al., 1993).

The kinematics of deformation related to shortening within the Alpine Rhodope orogen are still largely unknown and controversely discussed in the literature due to the strong extensional overprint and a long tectonometamorphic history reaching back to Jurassic or even older events, associated with high-pressure metamorphism (Burg, 2012; Froitzheim et al., 2014; Liati et al., 2016; Miladinova et al., 2018). What is clear, however, is that the Rhodope nappe stack underlies the Dacia nappe stack, and both formed simultaneously, likely recording the same shortening accommodated at different structural levels (i.e., at two decollements) during overall top-to-the-north thrusting (Schmid et al., 2019). Below, we first describe the Dacia megaunit around the Rhodope region, and subsequently the structure of the Rhodope nappe pile.

The highest structural units of the Dacia megaunit are **East Vardar Ophiolites** that overlie the **Circum-Rhodope** unit, exposed in Kosovo and farther south (Figs. 1 and 12). In the west, the Circum-Rhodope belt originally overthrust the Serbomacedonian Massif, equivalent to the Supragetic nappes farther north (Fig. 12) (see section 5.8) although the contact was later cut by Cenozoic top-W thrusts (see below). In the SE (Chalkidiki Peninsula) and in Thracia (Fig. 1), the Circum-Rhodope Belt is in direct contact with the Rhodopian core along a thrust contact, or extensional detachments (Kydonakis et al., 2014). The Circum-Rhodope unit is formed by an imbrication of East Vardar Ophiolites of middle to late Jurassic age with pieces of the distal parts of the European continental margin facing Neotethys (Brown and Robertson, 2004; Ferrière et al., 2001; Ferriere and Stais, 1995; Gallhofer et al., 2017; Koglin et al., 2009). Ophiolites, such as the Guevgueli Ophiolite (Fig. 12), are equivalent to those found farther to the north in the East Vardar Zone rooting in the Sava suture. In contrast to the East Vardar Ophiolites north of Kosovo, the ophiolites of the Circum-Rhodope Belt are thought to represent an “ensialic” back-arc ophiolite complex, which opened within Circum-Rhodope passive margin continental lithosphere (Brown and Robertson, 2003; Saccani et al., 2008a). The best profile across the Circum-Rhodope Belt and adjacent units is exposed at the Greece-North Macedonia border. Adjacent to the West Vardar Ophiolites and the Sava suture one finds, from west to east: the Paikon volcanic arc built onto crust of the Circum-Rhodope distal margin, thrust by the Guevgeli Ophiolites along a west-verging thrust and followed by other W-verging slices of continental crust referred to as Peonia in the French literature and finally by the Serbomacedonian Zone thrust to the west. According to Ferriere and Stais (1995) and our own observations all these W-verging thrusts formed in the Cenozoic and post-date earlier E-directed thrusting of Late Jurassic age. In the Late Jurassic the Guevgeli Ophiolites were thrust over and imbricated with underlying continental units constituting the Circum-Rhodope belt that also contains latest Triassic to Jurassic flysch-type sediments (e.g. the Melissochori or Svoula sediments of Bonev et al. (2015) and Kockel (1986), respectively). This Late Jurassic event is associated with a pressure dominated metamorphic overprint (Michard et al., 1994) and transgressed by uppermost Jurassic to lowermost Cretaceous non-metamorphic overstep sediments (“oberjurassische Diskordanz” of Kockel (1986)).

The composite Circum-Rhodope Unit bends into an E-W orientation at the southeastern tip of Chalkidiki (Kockel, 1977; Kydonakis et al., 2016) where it is separated by an extensional detachment from the Upper Unit of the Rhodopes (see below) (Fig. 12). The Circum-Rhodope Unit is found again in Thrace, on Samothraki island and the easternmost Biga Peninsula of Turkey (e.g., Meinhold and Kostopoulos, 2013) (see section 5.12). We also correlate the **Strandja** orogen to the east of the Rhodope core to the Circum-Rhodope belt following (Schmid et al., 2019), as it was also metamorphosed in Late Jurassic time associated with top-N East Vardar Ophiolite emplacement (Bonev et al., 2011, 2013; Jahn-Awe et al., 2010; Okay et al., 2001a; Schmid et al., 2008; Sunal et al., 2011) (Figs. 12 and 13). Natal'in et al. (2016) showed a prolonged magmatic history from the Paleozoic to the Triassic in the Strandja Massif and interpreted this as a long-lived arc above a Paleotethys subduction zone, which they as well as Şengör et al. (1984), interpreted to have had a northward polarity.

The Circum-Rhodopes and Strandja orogen were thrust in Early Cretaceous time, starting prior to 130 Ma, in the west over the **Serbomacedonian** nappe and over the **Sredna Gora**-East Balkan units. The Sredna Gora unit is equivalent to the Getic unit of the Carpathians (Ivanov, 1988; Schmid et al., 2008, 2019), and hosts a Late Cretaceous volcanic arc that belongs to the ~92-67 Ma Apuseni–Banat–Timok–Sredna Gora magmatic arc and associated sedimentary basins (Gallhofer et al., 2015; von Quadt et al., 2005; Zimmerman et al., 2007). This arc and associated intra-arc sediments probably connected to the western Black Sea Basin and the Pontides. There was some extension in the arc, but the amount is minimal. Also in the Serbomacedonian unit, post-late Early Cretaceous extension has been inferred in units adjacent to the Sava Suture Zone (e.g., Antić et al., 2016; Erak et al., 2017), but the

magnitude of this deformation is poorly constrained and not reconstructed here. In the west, a minimum overlap of Circum Rhodope and Serbomacedonian units over Sredna Goa is ~70 km, as observed by the minimum extent in map view in areas where the subsequence Cenozoic extension is minimal. In the east, the Sredna Gora Unit was overthrust with a minimum displacement of 50 km by 110 to 100 Ma by the Strandja units, as estimated from the geometry of the nappe contact and differences in the degree of metamorphism (Gerdjikov, 2005).

Thrusting of the Sredna Gora over the **Balkanide nappes** was associated with at least 120 km of displacement mainly between ~120 and 95 Ma, although displacement may have been considerably higher depending on the interpretation of the Rhodope units (see below). These estimates come from the offset over and the structural geometry observed in the Kraishte window and the Balkan Mountains (e.g., Bergerat et al., 2010; Kounov et al., 2010). The Balkanide units are thought to be derived from the southern margin of the Moesian Platform, but contain the deep-marine, Upper Jurassic to Lower Cretaceous **Trojan flysch**, thought to have been deposited in deep rift basins within the Moesian shelf (Burchfiel and Nakov, 2015). The Balkanides thrust toward Moesia again over a distance of ~75 km between ~80 and 65 Ma, and accommodated another Eocene (50-40 Ma) phase of N-S shortening north of the Strandja Massif (Burchfiel et al., 2008; Ivanov, 1988; Sinclair et al., 1998) of ~30 km.

The **Rhodope mega-unit** represents the tectonically deepest mega-unit of the Balkan Peninsula but its structural and metamorphic history, even the sense of nappe stacking (top-S versus top-N) and the timing of nappe formation are highly controversial (e.g. Burg, 2012; Froitzheim et al., 2014). The formation of the metamorphic nappe stack is assumed to be south-verging by most authors in analogy to the rest of the Hellenides (e.g., Ricou et al., 1998). Undoubtedly, numerous but not all sense of shear criteria indicate top south to southwestward shearing (Burg, 2012) but many of these shear senses are associated with subsequent extension rather than nappe imbrication. Hence, it is often unclear which of the shear senses relate to nappe stacking, and which relate to subsequent Cenozoic extension. Moreover, (1) thrust-related top-N senses of shear are also found, particularly in the highest tectonic units of the Rhodopes, (2) there is disagreement on the way the nappe stack should be subdivided, (3) there is disagreement where its northern and western boundary has to be looked for and (4) there is disagreement on the age(s) of high-pressure metamorphism and nappe stacking.

The only undisputed case of top S-SW thrusting is well documented for the case of the Nestos thrust with a minimum transport estimate of some 70 km that formed after 55 Ma ago (Jahn-Awe et al., 2010) and before the onset of extension in the Rhodopes at some 42 Ma ago (Kounov et al., 2015), or a few million years later (Gautier et al., 2017). This Nestos thrust fault, not to be confused with the terms “Nestos suture” (Turpaud and Reischmann, 2010) or “Nestos Shear Zone” (Krenn et al., 2008, 2010; Gautier et al., 2017) thrusts high-grade rocks, amongst them ultrahigh pressure (UHP) rocks dated at ca. 180 Ma (Bauer et al., 2007) and even older, 200 Ma (Miladinova et al., 2018) that are part of the Jurassic Nestos Suture (Rhodope Middle Unit, see below), over the lower pressure (greenschist to amphibolite facies) **Pangaion-Pirin complex**, also known as Drama continental element (Nagel et al., 2011; Ricou et al., 1998). Some authors (e.g. Jahn-Awe et al., 2010) consider the Pangaion-Pirin Unit, characterized by a prominent and thick sequence of presumably Mesozoic marbles (Benderev et al., 2015; Ivanov, 1981), as a window exposing rocks of the Pelagonian Zone of the external Hellendides (section 5.11) thrust by the rest of the Rhodopes. The Nestos Suture would then be equivalent to the Sava Suture, but this scenario would require Cenozoic thrusting over a distance of some 500 km. Alternatively, the Pangaion-Pirin complex may paleogeographically belong north of the Neotethys, as part of a separate microcontinent that was separated from Gondwana and docked with Europe in the Jurassic, explaining the 180 Ma UHP rocks in the Nestos Suture (e.g. Turpaud and Reischmann, 2010). Given their Early-Mid Mesozoic age, the Nestos suture oceanic rocks are the only candidate for a Paleotethys suture in the Aegean and Balkan region that we know of. We will discuss this further in section 7.10.

In the hangingwall of the Eocene, out-of-sequence Nestos thrust, Schmid et al. (2019) identified four main structural units which we use in our reconstruction. The deepest, partly migmatitic, high-grade metamorphic **Rhodope Lower unit** is dominated by quartzo-feldspatic gneisses. It forms Cenozoic core complexes exposed in windows below the overlying ophiolite-bearing eclogitic Rhodope Middle Unit (‘Nestos’ suture Zone) that rims these domes. The Rhodope Lower Unit exposed in windows north of the Nestos thrust has been parallelized with the marble-rich Pangaion-Pirin Complex by most authors (e.g. the Lower Terrane of Burg (2012), or Lower Allochton of Froitzheim et al. (2014)) in spite of the large differences between these domes and the marble-rich Pangaion-Pirin complex both in terms of lithology and metamorphic grade. We prefer to parallelize the Pangaion-Prin complex with a marble-bearing unit, which overlies the Nestos suture: the Rhodopes Uppermost Unit (see below). This would imply that the Pangaion-Pirin Complex originally represented a high structural level of the Rhodopes that only became the deepest tectonic unit due to Paleogene out-of-sequence thrusting along the Nestos thrust.

The **Rhodope Middle Unit** (Nestos Suture Zone) rimming the domes of the Rhodope Lower Unit consists of a high-grade variable series that contains, amongst many other lithologies, ultramafic rocks and eclogites (occasionally indicating ultra-high pressure), interpreted as a mélange zone by Turpaud and Reischmann (2010). Reported ages of metamorphism are often Latest Triassic to Jurassic (e.g. Krenn et al., 2010; Petrík et al., 2016) but Cretaceous and Cenozoic ages were reported as well (see reviews by Liati et al. (2011, 2016)), which is not surprising since these rocks remained under high-grade metamorphic conditions until exhumation in Cenozoic times. Reported protolith ages of the ophiolites are Latest Permian and Triassic (Bauer et al., 2007; Liati et al., 2011) but also Oxfordian (Froitzheim et al., 2014). Derivatives of quartzo-feldspatic meta-granitoids from the Rhodope middle Unit yielded Jurassic zircon ages (Turpaud and Reischmann, 2010) which led these authors to postulate the presence of a Jurassic magmatic arc in the Rhodopes. In view of all the data available we interpret that the Rhodope Middle Unit represents a suture zone that formed during Triassic to Jurassic subduction, perhaps followed by renewed oceanization to account for the Oxfordian oceanic crustal ages reported by Froitzheim et al. (2014).

The **Rhodope Upper Unit** (Kerdillion-Madan) is dominated by quartzo-feldspatic, pre-Alpine gneisses intruded by large volumes of Late Cretaceous to Cenozoic granitic intrusions. It suffered amphibolite grade conditions locally reaching anatexis near the base of the unit (Burg, 2012). High-pressure rocks occasionally occur near the contact with the Rhodope Middle Unit but the boundary with the underlying Netsos suture is not a sharp one.

The **Rhodope Uppermost Unit** (Asenitsa-Thrace) is of particular interest since it is characterized by a lower grade of metamorphism (upper greenschist to lower amphibolite grade) and is often characterized by top-N senses of shear (Burg, 2012; Schmid et al., 2019). We also regard the small Crnook-Osogovo-Lisets core complex, underlying the Struma Unit in Western Bulgaria and North Macedonia (Kounov et al., 2004, 2010) that was exhumed 48-39 Ma ago (Antić et al., 2016) as an isolated window exposing the Rhodope Uppermost Unit. It includes the Thrace Lithotectonic Unit of Naydenov et al. (2013) rimming the northern slopes of the

Rhodopes. Both the Asenica Unit and Thrace Lithotectonic Unit are rich in thick marble sequences. This, together with the relatively low metamorphic grade, makes the Rhodope Uppermost Unit comparable to the Pangaion-Pirin Unit, supporting the idea that the Pangaion-Pirin Unit originally, i.e. prior to the Nestos out-of-sequence thrust, occupied a high tectonic position. The Thrace Lithotectonic Unit is in direct contact with the northerly adjacent Sredna Gora Unit along a ductile dextral shear zone (Iskar-Yavoritsa Shear Zone) that is a part of the wider Maritsa Shear Zone (Georgiev et al., 2009; Naydenov et al., 2013) of Late Cretaeous age.

The frequent top-N senses of shear observed in the Rhodope Uppermost Unit and the fact that the Rhodopes are overlain by the Sredna-Gora and Circum-Rhodope units, also characterized by top-N senses of shear (Bonev and Stampfli, 2008; Kounov et al., 2010; Okay et al., 2001b), make top-N imbrication within the Rhopian nappe stack in Jurassic and Cretaeous times likely. Hence, in contrast to Turpaud and Reischmann (2010), and following Bonev et al. (2011), we envisage north-directed thrusting of the ophiolites preserved in the Nestos suture in Jurassic times. This implies a Balkan Peninsula-wide Late Jurassic-Early Cretaceous Moesia-verging nappe stack, whereby the Rhodope nappe stack formed at depth by duplexing the underpinnings of the stratigraphically higher Circum Rhodope-Balkanides trajectory. North-directed thrusting continued until the Late Cretaceous, followed by dominantly southward nappe stacking in the Hellenides since (see section 5.11). Northward subduction that led to Hellenide thrusting must have started before the ~90 Ma onset of the Sredna Gora magmatic arc (Gallhofer et al., 2015; von Quadt et al., 2005).

Extension in the northern Aegean region, that eventually exhumed the Rhodope mega-unit from underneath the Dacia mega-unit, started in Mid-late Eocene time (~42 Ma) with the formation of the Thrace and Mesta basins (Brun and Sokoutis, 2010; Burchfiel et al., 2008; Georgiev et al., 2010; Kounov et al., 2015). Subsequently, top-to-the-north and northeast and top-to-the-southwest extensional detachments (Miocene Strimon detachment) exhumed a triangular metamorphic core complex that opened as a result of cw rotation of the Chalkidiki Peninsula relative to the Moesian Platform (Brun and Sokoutis, 2007, 2010, 2018; Georgiev et al., 2010). Our reconstruction adopts the restoration of the Eocene and younger extensional history of the Aegean region as explained in van Hinsbergen and Schmid (2012), and we refer the reader to that work for further details.

5.11. Dinarides; Albanides; Hellenides; Aegean Basin

The Dinarides, Albanides, and Hellenides (Fig. 1) comprise a largely thin-skinned, (W)NW-(E)SE trending and (S)SW verging fold-and-thrust belt that thrust upon the autochtonous Adriatic continental or Ionian oceanic crust in the foreland. This belt is separated from the Tisza and Dacia mega-units in the northeast by the Sava Suture (Pamić et al., 2002; Prelević et al., 2017; Toljić et al., 2018; Ustaszewski et al., 2009, 2010) (Fig. 12). Upon closure of the Sava suture at around 66 Ma, the Tisza-Dacia units (including the Serbo-Macedonian Massif, the Circum-Rhodope unit, the East Vardar Ophiolites and the Paikon unit, see section 5.8) were thrust westwards over the easternmost composite nappes of the Dinarides-Albanides-Hellenides over a distance of at least 50 km, as deduced from their presence in the Jastrebac window (Fig. 12) (e.g., Erak et al., 2017; Marovic et al., 2007; Schmid et al., 2008). The final closure of the Sava Ocean occurred towards the end of the Maastrichtian, while continuing convergence until the Eocene along the Sava Zone was fairly minor (Stojadinovic et al., 2017; Toljić et al., 2013, 2018; Ustaszewski et al., 2009, 2010; van Gelder et al., 2015). The Cretaceous subduction was also associated with the evolution of a forearc basin developed over the European-derived margin (Serbomacedonian and overlying Eastern Vardar ophiolites) that changed deformation from compressional during the Early Cretaceous - Cenomanian, extensional during Turonian - Early Campanian to ultimately compressional during the late Campanian - early Paleocene (Toljić et al., 2018). Although the evolution of this forearc is an important element completing the justification of the Cretaceous subuction of the Neotethys Ocean in the Dinarides, its internal deformation is rather minor at the scale of our restoration. In northernmost Greece the end of convergence accommodated along the Sava Suture Zone post-dates the deposition of Campanian-Maastrichtian flysch (Fidopetra flysch) that marks the Sava suture between the Circum-Rhodope unit and the ophiolites of the Jadar-Kopaonik composite nappe (Ano Garefi Ophiolite of Brown and Robertson (2004)) as further explained below.

To the northwest, the Dinarides are bounded by the Southern Alps (Fig. 12). The Southern Alps thrust southward during the Miocene onto the undeformed Adriatic foreland in the west, and onto the Dinarides in the east (see section 5.6), structurally overprinting pre-existing Dinaridic thrust sheets (e.g., Castellarin et al., 1992; Placer, 1998; Tomljenović et al., 2008; van Gelder et al., 2015). To the southeast, the Dinarides are separated from the Albanides-Hellenides by the Scutari-Pec Fault Zone (Fig. 12). Across the Scutari-Pec Fault Zone, the strike abruptly changes from WNW-ESE in the Dinarides to NW-SE in the Albanides-Hellenides. We here follow the subdivision of the Dinaridic thrust sheets of Schmid et al. (2008, 2019) and refer to those authors for a detailed account of the regional correlations. We use the same scheme of thrust sheets in the Albanides-Hellenides where applicable. The Dinaridic-Hellenidic thrust belt is complex in that it is not characterized by a strict foreland basin propagation of thrusts. Many thrusts were simultaneously active, and cases of out-of-sequence thrusting have been documented, as detailed below.

The Dinarides recorded the onset of the Middle Triassic opening of the Neotethys Ocean by widespread magmatism, mostly consisting of intermediate to mafic volcanics, and by local or regional, coeval or subsequent deepening of the Adriatic margin carbonate facies (Čadjenović et al., 2008; Gawlick et al., 2017; Pamić, 1984; Schefer et al., 2010; Vlahović et al., 2005). The highest structural unit of the Dinarides, Albanides, and Hellenides are ophiolites and ophiolitic mélange that are referred to as the **West-Vardar Ophiolites** (Schmid et al., 2008). These root in the Sava suture and became obducted W- to WNW- wards (in modern coordinates and highly oblique to the strike of the Dinarides) over the carbonate platforms preserved in the internal nappes of the Dinarides, Albanides, and Hellenides that were at that time still part of the undeformed continental margin of Adria (Pamić et al., 2002; Scherreiks et al., 2014; Schmid et al., 2008; Tremblay et al., 2015). $^{40}Ar/^{39}Ar$ dating of hornblende and micas in metamorphic soles below these ophiolites yielded ~171-157 Ma ages (Borojević Šoštarić et al., 2014; Dimo-Lahitte et al., 2001; Liati et al., 2004; Spray et al., 1984; Spray and Roddick, 1980), and a ~170 Ma age is generally interpreted as the age of onset of intra-oceanic subduction below them (e.g., Maffione et al., 2015). The West Vardar Ophiolites show MORB geochemistries in the west, overprinted by supra-subduction zone geochemical signatures in the east (e.g., Bortolotti et al., 2002, 2005; Dilek et al., 2008). Both are overlain by Bajocian (170-168 Ma) radiolarian cherts (Chiari et al., 2002, 2003, 2004; Marcucci et al., 1994; Marcucci, 1996). Intra-oceanic subduction below the West-Vardar Ophiolites likely started adacent to the N-S striking mid-Neotethys ridge (Maffione et al., 2015). The ophiolites were obducted onto the Adriatic margin over a minimum distance of ~180 km at around the Jurassic-Cretaceous boundary, as shown by the age of foreland basin clastics in front of the ophiolites (Baumgartner, 1985; Mikes et al., 2008; Thiébault et al., 1994) and by continental to shallow water sediments deposited on top of the obducted ophiolites (Bortolotti et al., 2005; Scherreiks et al., 2014).

Detritus shed from the internal Adriatic-Hellenic margin and overlying obducted ophiolites are found across the Pelagonian Platform below the ophiolites, and also reach the Pindos Basin in Greece to the west of the Pelagonian Platform in the mid-Cretaceous sediments (Faupl et al., 2006; Fleury, 1975). The mélanges below the ophiolites contain radiolarites interpreted to be derived from the Neotethyan oceanic crust that subducted below these ophiolites. These span an age range of Triassic (Ladinian, ~240 Ma) to Late Jurassic, which marks the age of initial obduction onto the platforms of Adria (Bragin et al., 2011; Gawlick et al., 2009, 2017; Vishnevskaya et al., 2009).

After obduction, the ophiolitic zones became parts of individual nappes, referred to as composite nappes since they consist of Adriatic margin sequences and previously obducted ophiolites (Schmid et al., 2008). Thereby, the nappe-bounding thrusts cut up section across the previously emplaced ophiolites.

The most internal nappe of the entire sequence is the **Jadar-Kopaonik** composite nappe of the Dinarides of Serbia and North Macedonia and its equivalents in the Medvednica Mountains of Croatia and the Bükk unit of Hungary (Fig. 12). The latter was displaced during Miocene extension of the Pannonian Basin along the Mid-Hungarian Shear Zone (Filipović et al., 2003; Karamata, 2006; Schmid et al., 2008; Toljić et al., 2013; van Gelder et al., 2015). The Jadar-Kopaonik unit is composed of Variscan deformed Devonian-Carboniferous sediments overlained by a gradually deepening Permian - Kimmeridgian cover, which is locally metamorphosed where exhumed by the Miocene extension in the footwall of detachments, that are tectonically overlain by the Western Vardar ophiolites and their ophiolitic mélange (Dimitrijević and Mijović-Pilić, 1997; Gawlick et al., 2017; Schefer et al., 2010, 2011; Stojadinovic et al., 2013, 2017; Toljić et al., 2013). Separated by a long belt of highly deformed uppermost Cretaceous syn-contractional turbidites (the Kosovska Mitrovica Flysch of Dimitrijević and Mijović-Pilić (1997)), the Jadar Kopaonik nappe is thrust over the **Drina-Ivanjica** composite nappe of the Dinarides that is equivalent to the Korab unit of Albania and the **Upper Pelagonian** nappe of the Hellenides, all overlain by West Vardar Ophiolites (Figs. 12 and 14) (Kilias et al., 2010; Schmid et al., 2019).

The Pelagonian nappes of the Hellenides comprise Paleozoic and older metamorphic basement intruded by Upper Paleozoic granitoids, overlain by Permo-Triassic low-grade metamorphic volcanics and sediments and Triassic-Jurassic carbonates and marbles interpreted as passive margin sediments (Kilias et al., 2010; Schenker et al., 2014). The Upper Pelagonian nappe was thrust over a Lower Pelagonian nappe that is characterized by a high degree of Alpine metamorphism, locally reaching amphibolite facies conditions (Kilias et al., 2010; Most, 2003). Most (2003) documented a Latest Jurassic (ca. 150 Ma) blueschist facies metamorphic event associated with a top-to-the-W thrusting of the Upper over the Lower Pelagonian nappe, extending into the Lower Cretaceous (150-130 Ma). This thrusting between the Pelagonian nappes is partly synchronous with and partly follows W-directed West Vardar Ophiolite obduction (Tremblay et al., 2015). In the lower Pelagonian unit contractional tectonics with the same top-to-the-West kinematics continued until Mid-Cretaceous time (110-95 Ma) under retrograde conditions, and fission track data documented cooling below 240° between 85 and 65 Ma (Kilias et al., 2010; Most, 2003). In a transect through North Macedonia and Albania we model the pre-95 Ma amount of thrusting of the Upper over the Lower Pelagonian unit to at least 120 km.

The composite nappes of the internal Dinarides and Hellenides were largely piled up by (S)SW directed out-of sequence thrusting between ~85 and 60 Ma. The contact between the Jadar-Kopanik and Drina Ivanjica units is a Late Cretaceous -Paleocene dextral transpressive fault system affecting the northern prolongation of the Kosovska Mitrovica Flysch, well observed in the Dinarides of western Serbia as a zone with various branches (the Zvornik suture of Karamata et al. (1994) and Gerzina and Csontos (2003)). Our own field observations at this contact in one of the classical exposed areas (Ovcar Kablarska gorge in Central-Eastern Serbia) show a high-angle fault, where stratigraphic markers allow the reconstruction of ~30 km of shortening associated with ~30 km of right-lateral strike-slip displacement in Campanian-Paleocene times (~85-60 Ma).

The Drina-Ivanjica composite nappe contains low-grade metamorphic Paleozoic basement overlain by deep-marine Triassic and Jurassic carbonates and siliceous limestones similar as in the Jadar-Kopaonik nappe and interpreted as the distal passive margin of the Greater Adriatic Platform (Dimitrijević and Mijović-Pilić, 1997; Djoković, 1985; Schefer et al., 2010; Schmid et al., 2008). The Drina-Ivanjica composite nappe overthrust the East Bosnian-Durmitor composite nappe by ramping into and duplicating the overlying ophiolitic mélange (Profile 5 in plate 3 of Schmid et al. (2008) with a displacement of at least 25 km. A recent detailed structural and geochronological study along a transect across the Drina Ivanjica thrust sheet (Porkoláb et al., 2019) revealed a top-WNW deformation under anchizonal metamorphic conditions, dated to have taken place during the 150-135 Ma time interval, i.e. in Tithonian to Valanginian times. Since this is synchronous with and kinematically compatible with the W-directed obduction of the West Vardar ophiolites, this event likely demonstrates also the thrusting of the entire Drina-Ivanjica composite unit over the East Bosnian-Durmitor composite unit. This thrusting should have ended by the pre-Turonian erosional surface affecting the hanging-wall Drina-Ivanjica thrust sheet, cutting down into Paleozoic strata and unconformably overlain by the Upper Cretaceous Kosovska Mitrovica Flysch (Schmid et al., 2008) and references therein).

The non-ophiolitic part of the **East Bosnian-Durmitor** composite nappe consists of distal Paleozoic clastic sedimentary rocks affected by low-grade Variscan metamorphism, overlain by Permian - Lower Triassic clastics and volcanoclastics and a Triassic to Lower Jurassic carbonate platform that drowned gradually in its internal parts to radiolaritic deposition in Middle Jurassic times, after which it was thrust by the West Vardar Ophiolites during obduction (Chiari et al., 2011; Dimitrijević and Mijović-Pilić, 1997; Ilić and Neubauer, 2005; Ilić et al., 2005; Schmid et al., 2008). The age of thrusting of the East Bosnian-Durmitor sheet over the nappe is constrained by a turbidite sequence deposited in their footwall. The Bosnian Flysch is a long belt of turbidites stretching from western Slovenia to western Albania, which is composed of an older higher Upper Jurassic-Cenomanian Vranduk Flysch and a younger Late Albian - Maastrichtian (possibly also Paleocene) Ugar-Durmitor Flysch (or Vermoshi flysch in Albania) that are locally separated by unconformities (Aubouin et al., 1970; Cadet, 1970; Goričan et al., 2012; Hrvatović, 2006; Mikes et al., 2008; Schmid et al., 2008). Our reconstruction relates the earlier Late Jurassic - Early Cretaceous deposition of the Vranduk flysch to the obduction of the Western Vardar Ophiolites (Mikes et al., 2008), followed by ~100 km shortening at the contact between the East Bosnian - Durmitor and the pre-Karst unit (~Barremian - Maastrichtian, 130-70 Ma), derived from the geometry of the former unit and the amount of subsequent Miocene exhumation recorded at this contact. This exhumation is related to the early - middle Miocene (~17-14 Ma) extensional reactivation of the thrust at the base of the East Bosnian-Durmitor in Montenegro and the coeval extensional reactivation of the deformed Bosnian Flysch beneath the Miocene Sarajevo-Zenica Basin in Bosnia and Herzegovina, as shown by Andrić et al. (2017), Sant et al. (2018a, 2018b) and van Unen et al. (2019). We have modeled this extension as ~25 km in the longer time interval between 20 and 10 Ma, accounting also for lower amounts of extension that these authors have observed in other smaller Miocene basins in the Dinarides.

The Vranduk part of the Bosnian Flysch unconformably overlies the more external **Pre-Karst nappe** basement and its sedimentary cover, originally located in front of the obducted West Vardar Ophiolites. The basement of the Pre-Karst nappe is widely exposed in the Bosnian Schist Mountains in the form of Paleozoic sediments, volcanics, and intrusions affected by various degrees of Paleozoic and Cretaceous metamorphism (Hrvatović, 2006; Hrvatović and Pamić, 2005; Pamić et al., 2004). These are overlain by Permian - Lower Triassic clastics and Middle Triassic-Cretaceous shallow-water platform and slope carbonates of the pre-Karst nappe. The next external nappe, the **High Karst nappe**, is characterized by shallow water Triassic-Paleogene sediments, interrupted by a short episode of Middle Triassic deepening and rifting-related volcanism, all typical for the larger Adriatic carbonate platform (Aubouin et al., 1970; Korbar, 2009; Pamić, 1984; Vlahović et al., 2005). The separation between the pre-Karst and the underlying High Karst is a laterally discontinuous thrust that was interpreted to accommodate at least 30 km shortening during Late Cretaceous to Paleocene time (~85-55 Ma) (Hrvatović, 2006; Tari, 2002). However, this estimate is approximate, as the thrust is largely overprinted by post-Eocene deformation in most of Bosnia and Herzegovina.

The still more external Budva nappe of Montenegro is part of a longer belt of Mesozoic deep-water deposits. It recorded continuous deep water deposition from the Middle Triassic to the Upper Cretaceous in its center, while shallower carbonatic facies was gradually recorded towards its margins, and is separated in several laterally discontinuous thrust sheets (Čadjenović et al., 2008; Črne et al., 2011; Goričan, 1994; Korbar, 2009; Robertson and Shallo, 2000). The Budva unit as tectonic and paleogeographic domain wedges out NW of the Kotor Bay, while to the SE it is laterally continuous with the Krasta-Cukali nappe of Albania and the Pindos nappe in Greece, collectively termed the **Pindos** mega-unit (Fig. 12, see below). Given the exposure of this unit in the Peshkopia tectonic window (e.g., Muceku et al. (2008) and the Cukali half-window combined with the deformation taking place along the Scutari-Pec Fault (Fig. 12), we estimated at least ~130 km of thrusting of the overlying High-Karst nappe in the Dinarides between 55 and 33 Ma, and an additional minimum 30 km in the last 5 Ma. The thrust is probably still active (Bennett et al., 2008; Schmid et al., 2008). Tecent field kinematic investigations have shown that the onshore Bosnia and Herzegovina contains a large number of post- middle Miocene dextral strike-slip and reverse faults (van Unen et al., 2019) that may cumulate 60–70 km of movement towards S to SSE. Therefore, the 30 km of recent High Karst thrusting is a conservative estimate.

To the SE of the Skutari-Pec Fault, the Pelagonian composite nappe directly overlies the Pindos mega-unit, and equivalents of the East Bosnian Durmitor, the Pre-Karst, and the High Karst units are not present. A small re-appearance of a carbonate platform between the Pelagonian and Pindos nappes in central Greece, around the Gulf of Corinth known as the Paranassos Zone (e.g., Robertson et al., 1991) is correlated to the Pre-Karst unit (Fig. 12). The Pindos mega-unit contains occasional middle Triassic basalts with back-arc basin geochemical signatures (Pe-Piper, 1982; Pe-Piper and Piper, 1991) overlain by Triassic to Upper Cretaceous hemipelagic sediments and radiolarites, and a Paleocene to upper Eocene flysch (~60-35 Ma; Degnan and Robertson (1998)). The deeply underthrust, metamorphosed and exhumed portion of a probable equivalent of the Pindos nappe in the Aegean Basin is known as the Cycladic Blueschist unit, showing ~55-40 Ma high-pressure metamorphism, overprinted by retrograde greenschist-facies metamorphic parageneses between ~30 and 25 Ma (see reviews in van Hinsbergen et al. (2005c) and Jolivet et al. (2015b)). Based on the ages of the Pindos flysch and Cycladic Blueschist HP metamorphism a first-order estimate for the time-span of subduction of the Pindos mega-unit is estimated at ~60-35 Ma (van Hinsbergen et al., 2005c). The Cycladic blueschist unit contains a Permo-Carboniferous metamorphic basement (Keay and Lister, 2002; Tomaschek et al., 2008), covered by a metasedimentary carbonate-rich sequence that is comparable to the Pindos mega-unit contains mafic Triassic volcanics (Bröcker and Pidgeon, 2007) and a stratigraphy that extends into the Upper Cretaceous (Löwen et al., 2014). The deep-marine sedimentary facies and associated volcanics of the Pindos Basin are often interpreted to suggest an oceanic nature of the basin (Pe-Piper and Piper, 1991). If true, this oceanic basin was narrow: apart from thin ophiolitic slices of uncertain origin on Syros island (e.g., Philippon et al., 2011), most of the Cycladic Blueschist unit is associated with continental crust (e.g., Keay and Lister, 2002; Zlatkin et al., 2018).

Windows in the eastern part of the Pelagonian composite nappe (mt. Olympos, mt. Ossa and mt. Pelion) show that this nappe is underlain by the Cycladic-Pindos Blueschist unit, yielding a minimum displacement of Pelagonian over Pindos of ~130 km in mainland Greece (van Hinsbergen et al., 2005a). In addition, Skourlis and Doutsos (2003) estimated an additional ~120 km of shortening within the Pindos mega unit in Eocene time based on cross-section restoration.

In the Hellenides and Albanides, the Pindos mega-unit was thrust over the so-called **Tripolitza** mega unit (equivalent of the Kruja unit of Albania and the Dalmatian unit of the Dinarides, Figs. 12 and 14). The Tripolitza mega-unit consists of mid-Triassic mafic volcanics overlain by platform carbonates of Late Triassic to Eocene age (Jacobshagen, 1987), and an Oligocene flysch (~33-23 Ma) (Peeters et al., 1998). In the Aegean Basin, the Cycladic Blueschist unit is underlain by the so-called 'Basal Unit', a metamorphosed platform carbonate succession with up to Eocene sedimentary ages and Oligocene meta-flysch, metamorphosed at HP-LT metamorphic conditions with peak-metamorphic ages around 24-21 Ma (Ring et al., 2001). The Basal Unit is therefore interpreted as the underthrust and metamorphosed equivalent of the Tripolitza unit. It is also found as the deepest structural unit in the windows of mt. Olympos and mt. Ossa in Greece (Fleury and Godfriaux, 1974; Kisch, 1981) (Fig. 12) from which a minimum overlap between the Pindos and Tripolitza units of 130 km was concluded (van Hinsbergen et al., 2005a). On Crete and the Peloponnesos, anchimetamorphic Tripolitza rocks are separated by an extensional fault from the HP-LT metamorphic Phyllite-Quartzite unit, which has similar peak metamorphic ages as the Basal unit: ~24-20 Ma (Jolivet et al., 1996). This fault has long been considered a major extensional detachment (Jolivet et al., 1996; Ring et al., 2001), but more recently it was shown that much of the exhumation of the Phyllite-Quartzite unit was accommodated by distributed thinning of the Tripolitza, Pindos, and Uppermost Unit (in part equivalent to the West Vardar Ophiolites, in part to the Bozkir unit of the Taurides) (Rahl et al., 2005). Moreover, in places the modern contact between the Phyllite-Quartzite unit and overlying Tripolitza unit on Crete may be an out-of-sequence thrust (Chatzaras et al., 2006; Ring and Yngwe, 2018), suggesting that exhumation occurred under compression, by extrusion rather than extension (Ring and Yngwe, 2018). The first unequivocal evidence for crustal extension comes from extensional sedimentary basins on Crete that started forming shortly after 11 Ma (Zachariasse et al., 2011) after the majority of exhumation of the Phyllite Quartzite as suggested by $^{40}Ar/^{39}Ar$ phengite ages of ~20 Ma thought to date HP metamorphism (e.g, Jolivet et al., 1996), and low-temperature fission track data that give 15-11 Ma ages (Marsellos et al., 2010; Thomson et al., 1998).

The Phyllite-Quartzite unit consists of a metamorphosed alternating marine series of mudstones, turbiditic sandstones and debris flow conglomerates of Carboniferous to Triassic age (Krahl et al., 1983, 1986) overlying a Paleozoic metamorphic basement (Romano et al., 2004; Xypolias et al., 2006). The Phyllite-Quartzite

unit probably formed the original stratigraphic underpinnings of the Tripolitza unit (van Hinsbergen et al., 2005c) and were derived from erosion of a Permian volcanic arc interpreted to represent a Paleotethys subduction zone (Kock et al., 2007; Marsellos et al., 2012; Zulauf et al., 2015, 2016). Based on ages of the flysch and HP metamorphism, the Tripolitza unit is interpreted to have been underthrust between 35 and 23 Ma.

In the Dinarides, the Dalmatian Zone (equivalent to the Tripolitza mega unit) directly thrust over the undeformed Adriatic foreland offshore northern Dalmatia in Miocene to recent times, with a displacement of no more than ~10 km (Tari, 2002). Towards the south, offshore Montenegro, the Oligocene to recent thrusting of the Dalmatian nappe over Adria along the South Adriatic Fault increases to a maximum of 30 km (Bega, 2015; Cazzini et al., 2015; Glavatovic, 2007). The amount of Miocene shortening suddenly increases across the Skutari-Pec Fault Zone, south of which the Kruja Zone is underlain by the **Ionian** mega-unit, implying a component of dextral strike slip motion on the Skutari-Pec Fault. The Ionian mega-unit consists of Triassic evaporites and Jurassic to Eocene well-bedded hemipelagic limestones with radiolarite intervals (Durmishi, 2014; IGRS-IFP, 1966; Underhill, 1988). The Ionian facies zone (basin) leaves the Dinarides-Hellenides offshore northern Albania into the Adriatic Basin, joining with the Apennines in the Umbria area where it is known as the Umbria-Marche Basin (Figs. 4 and 8). In the Albanides, Miocene-age shortening is mostly absorbed within the Ionian and Kruja Zones and amounts to an estimated 100 km based on available cross sections (Roure et al., 2004).

In western Greece thrusts divide the Ionian Zone into an external, central and internal part. All parts are covered by a flysch unit that becomes thicker and coarser grained from external to internal, and is indistinguishable in facies and age from the Tripolitza flysch (IGRS-IFP, 1966). Thrusting of the Pindos mega-unit over the Tripolitza mega-unit, and of the Tripolitza mega-unit over the Ionian mega-unit occurred simultaneously throughout the early Miocene, as shown by growth structures in seismic lines across western Greece and the Peloponnesos (Kamberis et al., 2000; Sotiropoulos et al., 2003). In the middle and internal Ionian Zone, flysch deposition in a foreland basin setting ceased around 23 Ma followed by uplift. In the central Ionian Zone, an extensional half-graben (Klematia-Paramythia Basin) developed between ~23 and 17 Ma, which became subsequently inverted (van Hinsbergen et al., 2005c). In the external Ionian Zone, including the parts on the Ionian islands, deep marine clastic turbidite series continued to develop until the middle Miocene, ~15 Ma (Bizon, 1967; de Mulder, 1975), after which they became uplifted, suggesting that thrusting of the middle Ionian Zone over the external Ionian Zone continued until this time. On the Peloponnesos and Crete, the so-called Phyllite-Quartzite unit is underlain by Paleozoic meta-pelites and quartzites, well-bedded Mesozoic to Eocene 'Plattenkalk' marbles, and Oligocene meta-flysch, which are interpreted as the metamorphic equivalent of the Ionian Zone (Kowalczyk and Zügel, 1997; Thiébault, 1979) (Figs. 12 and 14). This shows a minimum overlap of the Tripolitza over the Ionian Zone of ~75 km (van Hinsbergen et al., 2005a).

On the Ionian Islands and in western Albania, the Ionian Zone is underlain by the pre-Apulian Zone representing the deformed slope of the Apulian Platform to the North of the Apulian escarpment, offset from Apulia along the Kefallonia Fault Zone (Fig. 12). The Pre-Apulian Zone comprises a Cretaceous to Miocene sequence of platform slope carbonates (Bornovas et al., 1980; Dermitzakis, 1978; Underhill, 1989) overlain by clastic foreland basin deposits that started forming in the Burdigalian-Langhian (~20-15 Ma) on Kefallonia and Levkas, and Serravallian to Tortonian time (~12-10 Ma) on Corfu and Zakynthos (Dermitzakis, 1978; Drinia and Antonarakou, 2012; Duermeijer et al., 1999; Underhill, 1989; van Hinsbergen et al., 2006). The Pre-Apulian Zone was folded and uplifted in Pliocene time (~4 Ma) interpreted as the moment of accretion of the Pre-Apulian Zone to the Hellenides and initiation of the Kefallonia Fault Zone, and its decoupling from the Adriatic foreland (Apulian Platform) (van Hinsbergen et al., 2006). The end of thrusting of the middle over the external Ionian Zone around 15 Ma is assumed to represent the onset of thrusting of the external Ionian Zone over the Pre-Apulian Zone (van Hinsbergen and Schmid, 2012). The Apulian escarpment likely enters the Hellenic thrust stack to the South of the island of Zakynthos, south of which oceanic subduction of the modern Ionian oceanic basin (not to be confused with the Ionian Zone which was likely underlain by continental crust) has been continuous since at least ~13 Ma, forming the Mediterranean ridge (Finetti, 1982; Kastens, 1991; Underhill, 1989).

The internal parts of the Dinarides fold-and-thrust belt has been overprinted an Oligocene-Miocene extension that overlaps in time and has been estimated together with the one observed in the neighbouring Pannonian Basin (see section 5.9). Older, late Cretaceous extensional deformation has been identified in the Medvednica Mountains in the northern Dinarides, which was genetically linked to the extensional exhumation of the Eo-Alpine HP rocks in the Eastern Alps (van Gelder et al., 2015) and in the vicinity of the Sava Zone in Serbia and North Macedonia (Antić et al., 2017; Toljić et al., 2018) (see section 5.6.3). Cenozoic extension is much more pronounced in the Hellenides, particularly in the Aegean Basin, where it started in Mid-Eocene times in the Rhodope in the north, and affected the Hellenides nappe stack since the latest Oligocene or early Miocene (Brun et al., 2016; Jolivet and Brun, 2010; Jolivet et al., 2015b; Menant et al., 2016; Ring et al., 2010; van Hinsbergen and Schmid, 2012). This extension led to the exhumation of widespread metamorphic core complexes (see e.g., Brun and Sokoutis, 2010; Edwards and Grasemann, 2009; Gautier et al., 1999; Jolivet and Brun, 2010; Ring et al., 2010). We adopt here the kinematic restoration of Aegean extension of van Hinsbergen and Schmid (2012), who followed the same reconstruction hierarchy and who reconstructed the Aegean region by closing the triangular extensional complexes in the back-arc, in combination with restoring nappe stacking during upper plate extension. A debated element is the role of trench-parallel extension in the Aegean region during oroclinal bending: van Hinsbergen and Schmid (2012) inferred that this is important, accommodated e.g. by regional extreme thinning of the nappe stack in the forearc on Crete, and along the Mid-Cycladic Lineament, which they infer is a detachment (later documented by Malandri et al., 2017), whilst e.g. Jolivet et al. (2010), Philippon et al., 2012; Brun et al. (2016), and Menant et al. (2016) assume that there is no significant trench-parallel extension in the Cycladic segment. We will return to this debate in the reconstruction and discussion sections (Sections 7.1.3 and 8.5).

5.12. Anatolia; Black Sea; Eastern Mediterranean Basin; Cyprus; Caucasus; Arabian collision zone

The Anatolian segment has a similar overall architecture as the Balkan region in that it contains Adria-derived continental units to the south of a Neotethys suture (locally termed Izmir-Ankara-Erzincan suture, the continuation of the Sava Suture), and units that were part of Eurasia since middle Mesozoic time to the north of this suture. The units to the north of the Izmir-Ankara-Erzincan suture, however, differ considerably from those in the Balkans. Moreover, the Adriatic units are overlain by widespread Cretaceous ophiolites unknown from the Balkans. We describe this region in three broad transects, from west to east and summarize for each the tectonic history from north to south (Figs. 15–17).

5.12.1. Western Anatolia

The undeformed Southern Eurasian margin is the Scythian Platform to the north of the Black Sea (Fig. 15). Well data, as well as detrital zircon studies in Mesozoic clastic sedimentary rocks of Crimea and the Pontides, suggests that a wide Triassic volcanic arc is buried below the Cenozoic sedimentary cover of the Scythian Platform, from northern Crimea to north of the Caucasus (Alexandre et al., 2004; Okay and Nikishin, 2015; Tikhomirov et al., 2004). This arc is interpreted to result from northward Triassic subduction below Eurasia (Okay and Nikishin, 2015).

Such northward subduction is consistent with the geology of the Crimean Peninsula in the northern Black Sea (Figs. 1 and 15). There, an intensely deformed, kilometers-thick, deep-marine unit of shales and turbiditic sandstones known as the Tauric flysch is found, with a Triassic to Early Jurassic age (Muratov et al., 1984; Nikishin et al., 2015c; Oszczypko et al., 2017; Robinson, 1997; Sheremet et al., 2016a). This unit contains large olistoliths consisting of limestones with Carboniferous to Early Triassic ages (Kotlyar et al., 1999). The Tauric flysch is interpreted as a trench fill unit. It is overlain by a Middle Jurassic (Bajocian to Callovian) shallow marine to terrestrial clastic and volcaniclastic succession overlain by Middle to Upper Jurassic conglomerates (Lalomov, 2007; Muratov et al., 1984; Robinson, 1997). This shows that by Middle to Upper Jurassic time, the deep foreland basin unit was uplifted above sea level. Volcanic rocks on Crimea have ages from the Middle Jurassic to earliest Cretaceous (~170-140 Ma) and have geochemistries consistent with arc volcanism (Meijers et al., 2010c). Dredge samples of arc volcanic rocks offshore southern Crimea gave K-Ar ages to ~100 Ma, or even as young as 70 Ma (Shnyukov et al. (1997), cited in Kazmin et al. (2000)) The clastic sequence of Crimea is overlain by only weakly deformed shallow marine platform carbonates of Upper Jurassic to Lower Cretaceous age, and subsequently a deepening marine sequence that is thought to be related to the opening of the Black Sea (Lalomov, 2007; Muratov et al., 1984; Robinson, 1997). In Cenozoic time, Crimea was uplifted again during inversion in the Black Sea Basin (Robinson, 1997; Saintot et al., 2006b).

To the southwest of the Black Sea lies the Rhodope-Pontide fragment (Şengör and Yılmaz, 1981). The Rhodope-Pontide fragment consists of the **Istanbul Zone**, separated from the **Sakarya Zone** by the relics of a Jurassic ocean basin found in the **Intra-Pontide Suture**. Towards the east, the Istanbul and Sakarya zones are separated by the Mesozoic Küre accretionary prism and Intra-Pontide suture from the **Eastern Pontides** and **Transcaucasus zones** (Şengör and Yılmaz, 1981) (Fig. 15).

The Istanbul Zone was displaced southward relative to the Moesian Platform along the West Black Sea transform upon opening of the western Black Sea (Okay et al., 1994) (see below). It is in its sedimentary facies and age often correlated to the Moesian Platform: the Moesian Platform and Istanbul Zone contain fauna and Precambrian basement that suggest they were part of Gondwana in Ordovician to Silurian time (Bozkurt et al., 2008; Chen et al., 2002; Okay et al., 2008a; Okay and Nikishin, 2015; Yiğitbaş et al., 2004). Sediment provenance studies, however, place the Istanbul Zone as contiguous with, and located south of, the Strandja Massif rather than the Moesian Platform in Triassic time (Ülgen et al., 2018). This correlation is consistent with the ~160 km of N-S extension that was associated with the opening of the Black Sea (Dinu et al., 2005; Hippolyte et al., 2010; Munteanu et al., 2011; Okay et al., 1994), which places the Istanbul Zone adjacent to Strandja in the Early Cretaceous.

The **Black Sea** Basin overlies crust of the East European Platform, the Istanbul Zone, and the eastern Pontides and the intervening sutures (Fig. 15). During Black Sea opening, the Pontides hosted a volcanic arc thought to relate to northward subduction of the Neotethys (Adamia et al., 1981; Letouzey et al., 1977; Okay et al., 1994; Yılmaz et al., 1998; Zonenshain and Le Pichon, 1986). The Black Sea Basin is hence interpreted as a back-arc basin (Okay et al., 1994; Stephenson and Schellart, 2010). The Black Sea hosts two, more or less trianglular extensional basins, the western and eastern Black Sea Basins, separated by the Mid-Black Sea high, or Andrusov Ridge (e.g., Nikishin et al., 2015a, 2015b). The Western Black Sea Basin opened with a phase of continental extension from late Barremian – Aptian time, followed by Cenomanian-Santonian time oceanic crust formation or mantle exhumation. The 160 km of Black Sea extension was accommodated between ~130 and 80 Ma (Nikishin et al., 2015a, 2015b; Akdoğan et al., 2019). Nikishin et al. (2015a, 2015b) interpreted that both Black Sea Basins opened during this time. Others, (e.g., Banks and Robinson, 1998; Robinson et al., 1995; Saintot and Angelier, 2002; Vincent et al., 2016) suggested that the eastern Black Sea is younger, and opened in Santonian to Danian time, based on ~5 km thick Paleocene-Eocene series exposed in e.g. the Achara-Trialet region on the eastern Black Sea coast (Saintot and Angelier, 2002; Vincent et al., 2016; Yılmaz et al., 2014), although these may also have formed in a retro-foreland basin above north-thrusting Pontides (Sheremet et al., 2016b). Magnetic anomalies have been suggested to be consistent with a ~71-68 Ma opening history (Shreider, 2005), but until biostratigraphic well data are available to confirm this, the age of the opening of the eastern Black Sea remains enigmatic (Vincent et al., 2016). In our reconstruction, we tentatively follow (Nikishin et al., 2015a, 2015b), among others because a diachronous opening requires major faults to crosscut the Pontides to the south of the Black Sea, for which there is no evidence to date. Future identification of such major structures may require us to revisit this part of the reconstruction. Between late Eocene to late Miocene the western and eastern Black Sea became inverted (Khriachtchevskaia et al., 2010) accommodating ~30 km N-S shortening in the western Black Sea (Munteanu et al., 2011) and similar or larger magnitudes of shortening are likely for the eastern Black Sea (Gobarenko et al., 2017; Sheremet et al., 2016b).

The basement of the Sakarya, Eastern Pontide, and Transcaucasus zones exposed to the south and southeast of the Black Sea, is heterogeneous and comprises Variscan basement and post-Variscan volcano-sedimentary cover (Dokuz et al., 2017; Okay et al., 2006a; Topuz et al., 2006; Yılmaz et al., 2000). The Variscan continental basement is represented by a high-grade metamorphic sequence of Paleozoic gneiss, amphibolites and marbles. Metamorphism is in amphibolite to granulite facies and is dated at Carboniferous (330-310 Ma). It became intruded by Carboniferous and Permian granitoids (Kaygusuz et al., 2012; Okay and Whitney, 2010; Şengün and Koralay, 2016; Topuz, 2004; Topuz et al., 2006, 2010). Within or structurally below the Sakarya Zone, and perhaps extending into the Eastern Pontides, is the **Karakaya complex** (e.g., Okay and Göncüoğlu, 2004). The Karakaya complex includes pelagic sedimentary and mafic magmatic rocks thought to be off-scraped at a subduction interface from the downgoing oceanic crust. These include Devonian to Triassic radiolarian cherts and show that Paleozoic oceanic crust (Paleotethys) was consumed in Early Mesozoic time (Okay et al., 2011; Sayit et al., 2011). Furthermore, the complex includes greywackes and shales interpreted as trench infill, and blueschists and eclogites knockers thought to have exhumed in a subduction channel. $^{40}Ar/^{39}Ar$ ages of eclogite blocks of 215–203 Ma (Okay and Monié, 1997; Okay et al., 2002) show that deep oceanic underthrusting below the Sakarya Zone, either northward (Okay and Nikishin, 2015) or southward (Şengör and Yılmaz, 1981), was active until at least the latest Triassic below Sakarya. We note that there is debate on whether the Karakaya complex marks an accretionary prism derived from the Paleotethys Ocean, as suggested by the presence of Devonian cherts (Okay et al., 2011), or whether it was a back-arc basin (Şengör and Yılmaz, 1981; Eyuboglu et al., 2018). In our reconstruction, we assume southward

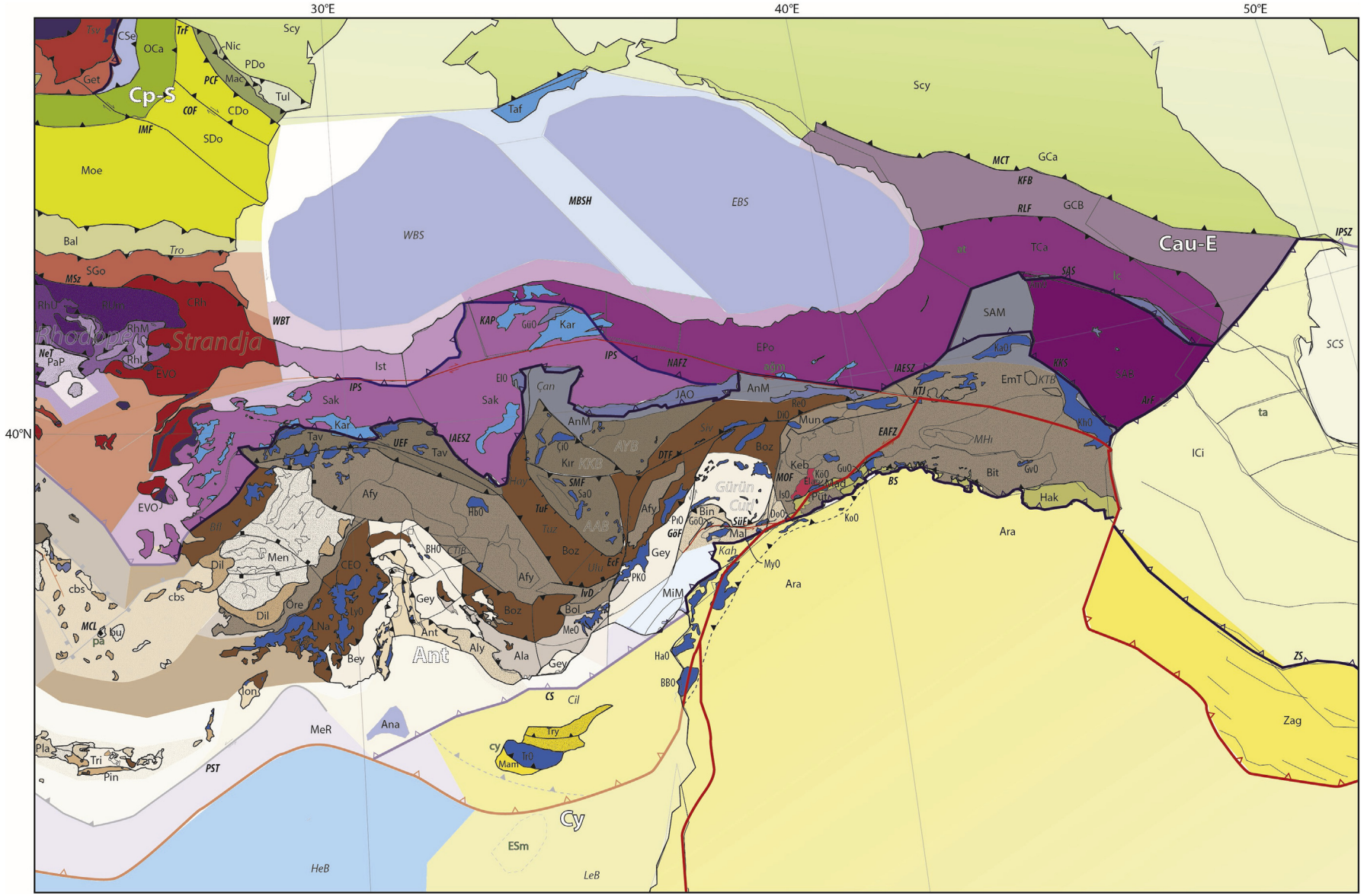

Fig. 15. Tectonic map of the eastern Mediterranean region. For key to abbreviations, see Table 4, for key to tectonic units, see Fig. 5. For location of the map within the Mediterranean region, see Fig. 4.

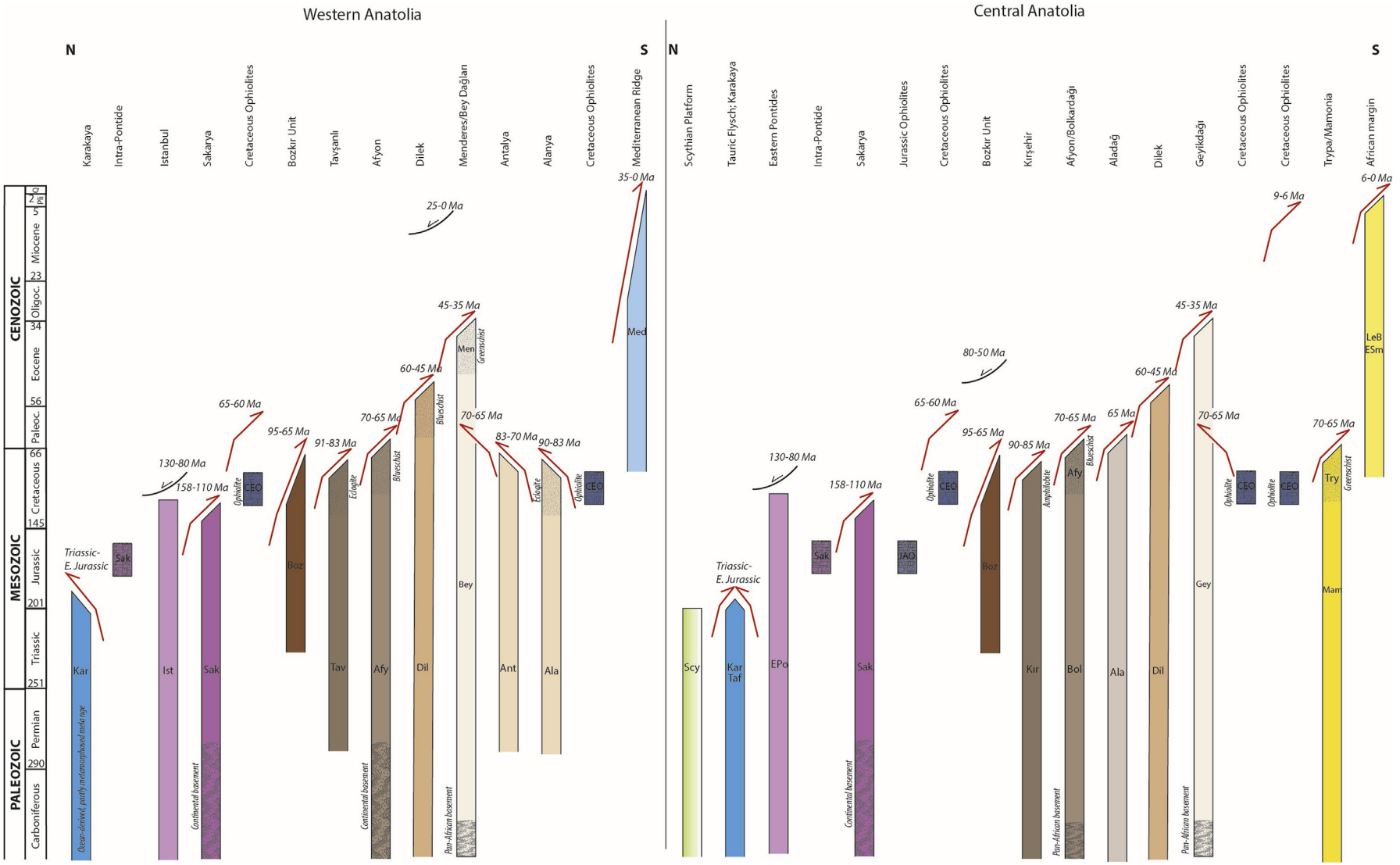

Fig. 16. Orogenic architecture charts for western and central Anatolia. For key to abbreviations, see Table 4, for key to tectonic units, see Fig. 5. For regional distribution of tectonic units, see Fig. 15. See Table 1 for summery of kinematic constraints corresponding to this chart. Periods of metamorphism are indicated with dotted hatching, formation of oceanic basement (ophiolites) with vertical hatching, and formation of pre-Alpine crystalline basement with curved hatching.

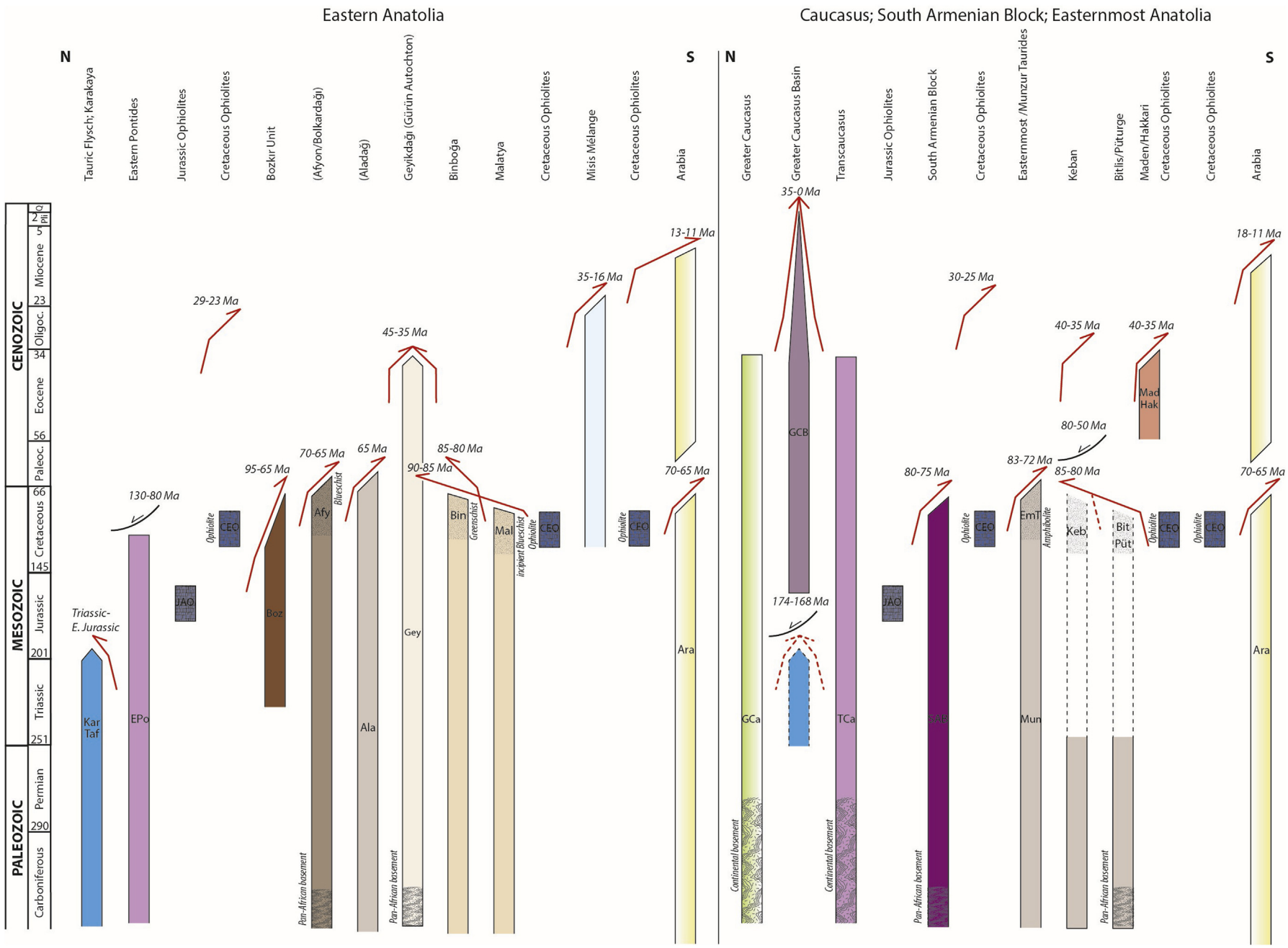

Fig. 17. Orogenic architecture charts for eastern Anatolia and the Caucasus. For key to abbreviations, see Table 4, for key to tectonic units, see Fig. 5. For regional distribution of tectonic units, see Fig. 15. See Table 1 for summery of kinematic constraints corresponding to this chart. Periods of metamorphism are indicated with dotted hatching, formation of oceanic basement (ophiolites) with vertical hatching, and formation of pre-Alpine crystalline basement with curved hatching.

underthrusting of the Karakaya complex along a paleo-trench to the north of the Istanbul and Eastern Pontide zones (Figs. 16 and 17), and we will discuss the reasons and alternatives in the Discussion section. The above-mentioned Paleozoic basement and accretionary complexes are both unconformably overlain by Upper Jurassic and younger clastic sediments, mafic volcanics and limestones (Dokuz et al., 2017; Sayıt and Göncüoğlu, 2013), and references therein).

The **Intra-Pontide suture**, running from the Sea of Marmara to the central part of the Pontides separates the Sakarya from the Istanbul Zone (Figs. 1 and 15). It contains metamorphosed mafic magmatic rocks with overall supra-subduction zone geochemical signatures associated with Middle and Upper Jurassic radiolarian cherts (Göncüoğlu et al., 2014; Robertson and Ustaömer, 2004; Ustaömer and Robertson, 2000; Sayit et al., 2015b). Immediately east of the Istanbul Zone, in the Küre region, the Küre SSZ ophiolite between Sakarya and the Eastern Pontides is also Jurassic (169 ± 2 Ma) in age (Alparslan and Dilek, 2017). The formation of the Küre Ophiolite follows directly upon high-temperature, low-pressure metamorphism affecting arc magmatic rocks in the same region, which was interpreted to reflect extension during opening of the Intra-Pontide Ocean (Okay et al., 2014) within an active volcanic arc. Closure of the Jurassic intra-Pontide ocean basin occurred in Early Cretaceous time, and was associated with, or followed by, 158-110 Ma metamorphism constrained by cooling ages in the associated accretionary prism and unconformably overlying sediments (Akbayram et al., 2013).

The paleogeographic position of the Pontide blocks relative to the Paleotethys suture has been a major debate or decades and remains disputed. Şengör and Yılmaz (1981) and Şengör et al. (1984) were the first to offer a modern plate tectonic interpretation, which remains popular today (e.g., Candan et al., 2016a; Dokuz et al., 2017), and suggested that a south-dipping Paleotethys subduction zone existed north of the Istanbul Zone and Eastern Pontides, cropping out in the upper Paleozoic to middle Jurassic Küre accretionary prism of the north-central Pontides (Okay et al., 2006a; Şengör et al., 1980) (Fig. 15). Towards the east, in the Eastern Pontides, several massifs were interpreted as related to syn-southward subduction of Paleotethys lithosphere by Şengör et al. (1980). This includes e.g., the Ağvanis Massif, an accretionary wedge made of phyllite, marble, metabasalts, and cherts that contain evidence for Triassic (~209 Ma or somewhat older) metamorphism (Topuz et al., 2014b) (Fig. 15). Şengör and Yılmaz (1981) and Şengör et al. (1984), however, interpreted the Karakaya complex, however, to represent a Permian back-arc basin that formed within the Rhodope-Pontide fragment and that closed by Triassic time, although the more recent findings of Devonian chert may make a Paleotethys derivation more likely (Okay et al., 2011; Sayit et al., 2011). Alternative views propose instead that the Pontides have been part of Eurasia since at least the Variscan orogeny in the Late Paleozoic, and all subduction was northward since that time (Golonka, 2004; Moix et al., 2008; Okay and Nikishin, 2015; Robertson et al., 2004b; Rolland et al., 2016; Stampfli and Kozur, 2006; Topuz et al., 2013; Ustaömer and Robertson, 2010), for instance based on correlations from the Caucasus region (see section 5.12.4). The Karakaya complex in this context is viewed as a Paleotethys-derived accretionary prism underthrust below Sakarya and exposed in windows (Okay and Nikishin, 2015; Okay et al., 2011). There are arguments for both views, and we will return to this debate in our reconstruction for Jurassic and Triassic time, and in the discussion (see section 7.10).

A prominent tectonic feature in northern Anatolia is the major dextral **North Anatolian Fault** (Ketin, 1948) that spans 1200 km between the northern Aegean region to the Karlıova Triple Junction in eastern Turkey. It is though to have formed in the Middle-late Miocene (13-11 Ma ago) in the east (Şengör et al., 2005) or younger, ~5 Ma (e.g., Armijo et al., 1999), and propagated westward. Its cumulative offset remains debated, with at least ~50, and perhaps as much as ~70–85 km (Akbayram et al., 2016; Hubert-Ferrari et al., 2002) – see Şengör et al. (2005) for a detailed discussion. In the western Turkey transect, the North Anatolian Fault runs along the Intra-Pontide Suture Zone.

The Sakarya Zone is bordered to the south by the **Izmir-Ankara-Erzincan Suture Zone** (Fig. 15), which is traced from western Turkey to Armenia, and from there southward through western Iran, spanning ~2000 km (Şengör and Yılmaz, 1981). In the west, this suture connects with the Sava suture in Greece and the Balkans (Schmid et al., 2008, 2019). In the east it merges in a triple junction with the Zagros and Bitlis sutures (Fig. 15).

In western Anatolia, the Izmir-Ankara-Erzincan Suture Zone hosts a mélange (the Ankara Mélange, Fig. 15) made of ocean floor volcanics, oceanic sediments with Middle Triassic (Ladinian-Carnian) and younger ages, as well foreland basin clastic rocks with ages up to the Maastrichtian (Gökten and Floyd, 2007; Tekin and Göncüoğlu, 2007; Tekin et al., 2002). Within the suture zone, from the Çankırı Basin eastward, the **Jurassic Anatolian Ophiolites** are found, in places associated with metamorphic soles, both with ages ranging from Middle to Late Jurassic, ~180-140 Ma (Çelik et al., 2011, 2016; Çörtük et al., 2016; Topuz et al., 2014a; Eyuboglu et al., 2016). These are interpreted to be relict oceanic basement that formed to the south of the Pontide forearc in the upper plate of a subduction zone (Okay et al., 2013; Topuz et al., 2013, 2014a; Eyuboglu et al., 2016). These forearc ophiolites are of the same age as the Intra-Pontide Ocean rocks and thus likely formed as part of the same upper plate extensional system (Fig. 15).

To the south of the IAESZ, **Cretaceous Eastern Mediterranean Ophiolites** are widespread, forming the highest structural unit overlying thrust continent-derived nappes of Greater Adria, in Turkey often referred to as the Anatolide-Taurides. All these ophiolites and their associated metamorphic soles are invariably Late Cretaceous in age, ~95-89 Ma (Çelik et al., 2006; Parlak and Delaloye, 1999; see reviews in van Hinsbergen et al., 2016; Parlak, 2016). The westernmost ophiolites that are attributed to the Cretaceous ophiolite belt are found on Crete and Rhodos (Koepke et al., 2002), which kinematically restores adjacent to the SW Anatolian Lycian Ophiolites in Paleogene time (van Hinsbergen and Schmid, 2012). The presence of these Cretaceous ophiolites, exclusively with a supra-subduction zone signature (e.g., Dilek and Furnes, 2011; Parlak, 2016) from westernmost Turkey eastwards is widely interpreted as evidence that an intra-oceanic subduction zone formed within the Neotethyan Ocean before ~95 Ma (Çelik et al., 2006; Maffione et al., 2017; Menant et al., 2016; Parlak et al., 2006; Plunder et al., 2013, 2016; Robertson et al., 2012; van Hinsbergen et al., 2015, 2016). Recent Lu/Hf dating of garnet in metamorphic soles yielded ages of ~104 Ma for the and Halilbağı (Pourteau et al., 2019) and Pınarbaşı (Peters et al., 2018) Ophiolites (Fig. 15), and similar ages were reported from the sole of the Cretaceous Semai'l Ophiolite of Oman (Guilmette et al., 2018), suggesting that subduction started slowly around 105 Ma, followed by inception of upper plate spreading some 10–15 Myr later. This intra-oceanic subduction zone is thought to have ended in a trench-trench-trench triple junction (Lefebvre, 2011) at the longitude of westernmost Anatolia to the west of which the Cretaceous ophiolites disappear (e.g., Maffione et al., 2017; van Hinsbergen et al., 2016).

The Cretaceous ophiolites overlie a sub-ophiolitic, non-metamorphic mélange that contain Middle Triassic to Maastrichtian radiolarian cherts, e.g. below the Lycian and Beysehir Ophiolites (Ricou et al., 1984, and references therein). This subophiolitic mélange is not to be confused with the Ankara mélange, which lies structurally above the Cretaceous ophiolites. In Central Turkey, the subophiolitic mélange also contains kilometer-scale blocks and

thrust slices of Triassic to Upper Cretaceous limestones accreted from the underthrust Tavşanlı and Kırşehir platforms (see below and section 5.12.2), or from isolated seamounts (Okay et al., 2008b). The ophiolites, underlying mélange, and included thrust slices are collectively known as the **Bozkır unit** (Andrew and Robertson, 2002; Özgül, 1976), but on our tectonic map, we separate the ophiolites from the rest of the Bozkır Unit. In Northwestern Turkey, a Maastrichtian to Paleocene flysch unit with major, up to 10 km wide blocks of Adria-derived limestones and cherts is known as the Bornova Flysch (Moix and Goričan, 2014; Okay and Altıner, 2007; Okay et al., 2012). We tentatively include this flysch in the Bozkır Unit (Fig. 15).

Below the Bozkır Unit in western Turkey, a series of nappes are exposed that form an overall southward propagating fold-and-thrust belt that developed in Late Cretaceous to Paleogene time (Fig. 16). This fold-and-thrust belt is exposed in a major extensional window exhumed along extensional detachments. The highest structural unit is the composite **Tavşanlı Zone**, which consists of HP-LT metamorphic rocks with oceanic, sedimentary, and magmatic protoliths (Plunder et al., 2013, 2015, and references therein) which likely correlate to the Bozkır unit, overlying the Tavşanlı Zone *sensu stricto*. The Tavşanlı Zone *s.s.* consists of Permo-Triassic metapelitic schists, Mesozoic marbles, metabasite, metachert, and phyllite, interpreted to have detached from a subducted distal passive continental margin (Okay, 1984; Okay et al., 2008a). These rocks underwent eclogite-facies metamorphism (Davis and Whitney, 2006; Okay, 1981; Okay and Whitney, 2010), and yielded Lu/Hf lawsonite and garnet ages of 91–83 Ma (Mulcahy et al., 2014; Pourteau et al., 2019), and $^{40}Ar/^{39}Ar$ ages of 88–78 Ma (e.g., Seaton et al., 2014; Sherlock et al., 1999; see review in van Hinsbergen et al., 2016) interpreted as reflecting peak metamorphism, and cooling upon exhumation, respectively.

The Tavşanlı zone is cut by the enigmatic, ductile, right-lateral Uludağ-Eskişehir strike-slip fault that was active between at least 38 Ma, until ~27 Ma at which time the zone was intruded by a pluton. The fault has an estimated displacement of 100 ± 20 km (Okay et al., 2008b). Based on low-temperature thermochronology, Zattin et al. (2010) suggested that this fault may have continued towards the western Sea of Marmaris, to be later reactivated by the North Anatolian Fault Zone, but from there on it remains unclear how this motion was accommodated.

The **Afyon Zone** is located south of and likely structurally below the Tavşanlı Zone and also represents a continent-derived sedimentary sequence with Paleozoic basement slivers and a stratigraphy up to the Maastrichtian (Göncüoğlu et al., 1992). It was metamorphosed under blueschist facies conditions (Candan et al., 2005; Pourteau et al., 2014). Retrograde white mica $^{40}Ar/^{39}Ar$ ages of ~67-62 Ma are interpreted as cooling ages during exhumation (Özdamar et al., 2012, 2013; Pourteau et al., 2013). The metamorphic rocks of the Afyon Zone are in western Turkey unconformably overlain by Upper Paleocene–lower Eocene shallow marine sedimentary rocks (Candan et al., 2005).

In western Turkey, the Afyon Zone is underlain by the Menderes Massif and the contact is the major Simav extensional detachment (Isik et al., 2004; Ring et al., 2003). This detachment cuts out part of the tectonostratigraphy that must have existed between the Afyon Zone and the Menderes nappes. This tectonostratigraphy is identified along the southern margins of the Menderes nappes instead (Fig. 5). There, the **Ören unit** has a similar sedimentary and metamorphic facies and age as the Afyon Zone, and the Ören unit and Afyon Zone are interpreted as equivalents (Güngör and Erdoğan, 2002; Pourteau et al., 2010, 2013; Rimmelé et al., 2003a, 2005). The Ören unit is underlain by a belt of Eocene HP-LT metamorphic rocks (Rimmelé et al., 2003b; Whitney and Bozkurt, 2002) of the **Dilek nappe** that correlate well in terms of tectonic position and metamorphic grade with the Cycladic Blueschist unit (Ring et al., 2007). White mica $^{40}Ar/^{39}Ar$ yielded 42-32 Ma ages from the Dilek nappe (Ring et al., 2007) and likely represent cooling ages. We model the onset of emplacement of the Dilek nappe simultaneously with the Pindos-Cycladic Blueschist unit of Greece (see section 5.11), starting 60 Ma, until ~45 Ma when the Menderes nappes start underthrusting.

Below the Dilek Nappe and separated from the Afyon/Ören Zone with the aforementioned Simav detachment are the **Menderes nappes**. These consist of a series of low to high-grade, Pan-African basement-bearing nappes (Gessner et al., 2013; Oberhänsli et al., 2010b, and references therein) intruded by Carboniferous (330-315 Ma) as well as Triassic (250-225 Ma) arc-related granitoids (e.g., Candan et al., 2016a; Gessner et al., 2001a). Although there is evidence for earlier Pan-African metamorphism and magmatism in the highest of these nappes (Çine nappe) (Candan et al., 2016b; Oberhänsli et al., 2010b), garnet Lu/Hf ages of 43–25 Ma (Schmidt et al., 2015) and Rb/Sr muscovite ages in this nappe indicate cooling below 500 ± 50 °C at ~46 Ma (Bozkurt et al., 2011), indicating that high-grade metamorphic conditions were also reached during the Alpine cycle. The Çine nappe is underlain by the Bozdağ nappe, and the lowermost Menderes nappe is the Bayındır nappe. The latter nappe is the deepest exposed structural unit of the Menderes Massif, experienced greenschist-facies metamorphism (Gessner et al., 2001b) contains uppermost Cretaceous carbonates (Özer, 1998; Özer and Sözbilir, 2003), and yielded a $^{40}Ar/^{39}Ar$ age of 36 ± 2 Ma (Lips et al., 2001).

Cooling ages of the Dilek, Çine, and Bayindir nappes all overlap in the ~45-35 Ma age range and can therefore not all represent moments of nappe accretion from the downgoing to the overriding plate. First-order estimates of the amount of overlap between these nappes were made by the restoration of Miocene extension in the Menderes Massif of van Hinsbergen (2010) and van Hinsbergen and Schmid (2012). Following that analysis, we assume that the ~35 Ma age of the lowermost, Bayındır nappe represents the moment of accretion of the nappe to the overriding plate and restore the accretion of these nappes by restoring the overlaps assuming in-sequence thrusting driven by Africa-Europe convergence.

Overlying the Ören unit to the south are the **Lycian nappes**, which are in turn overlain by Cretaceous ophiolites (e.g., de Graciansky, 1972; Okay, 1989; Plunder et al., 2016), Fig. 15). In many places in the Lycian Nappes, Upper Cretaceous to upper Eocene foreland basin clastics overstep non-metamorphic Paleozoic to Lower Cenozoic carbonate-dominated sediments (Bernoulli et al., 1974; Collins and Robertson, 1999; de Graciansky, 1972; Okay, 1989; Poisson, 1977). Sayit et al. (2015a) reported lower Upper Triassic (Carnian) arc lavas intercalating with pelagic limestones and radiolarian cherts from the Lycian nappes. Because the ages of the foreland basin clastics in the Lycian Nappes appear to cover the entire time span of metamorphism of the Tavşanlı and Afyon-Ören units as well as that of the higher nappes of the Menderes Massif, they may represent offscraped upper crustal portions of the west-Anatolian metamorphic units that decoupled from their now-metamorphic underpinnings and remained in a forearc position, thus escaping metamorphism. We do not restore the internal structure of the Lycian nappes in any detail, but instead focus our restoration on the major metamorphosed nappes. Our tectonic map simplifies the Lycian Nappes by placing them entirely in the Bozkır unit, although more detailed structural analysis will likely require recognizing elements of also deeper structural units of the Tauride tectonostratigraphy, such as the Geyikdağı nappe (see section 5.12.2).

The Lycian nappes and overlying ophiolites overthrust the 'autochtonous' **Beydağları** Platform to the SE (Figs. 15 and 16). The Beydağları Platform exposes Lower Cretaceous to Oligocene platform carbonates (Farinacci and Köylüoğlu, 1982; Poisson, 1967; Sari, 2002), overlain by a lower Miocene (~23-16 Ma) foreland basin

series in front of and below the Lycian Nappes. These foreland basin clastic rocks constrain the timing of thrusting of the Lycian Nappes towards Beydağları (Hayward, 1984; van Hinsbergen et al., 2010b). Langhian (~16-13 Ma) sediments seal the thrust (Flecker et al., 2005; Poisson et al., 2003). A window near Göçek exposes Burdigalian sediments of similar foreland basin facies (Hayward, 1984) demonstrating at least 75 km of SE-ward displacement of the west-Anatolian Taurides relative to Beydağları between ~23 and 16 Ma simultaneous with extensional unroofing and exhumation of the Menderes Massif to the northwest (van Hinsbergen, 2010, and references therein). The Beydağları Platform is generally considered to have formerly been physically connected to the Menderes Massif and to have formed the southern part of a contiguous Menderes-Beydağları Platform (Collins and Robertson, 1997). van Hinsbergen (2010), as well as earlier workers (Collins and Robertson, 2003; Hayward, 1984) reconstructed the Lycian Nappes back on top of the Menderes Massif at 25 Ma, and suggested that SE-ward translation between ~25 and ~15 Ma was gravity-driven and only affected a few km thick tectonostratigraphy. We adopt this reconstruction here, and refer to van Hinsbergen (2010) and van Hinsbergen and Schmid (2012) for a detailed discussion.

Finally, the Beydağları and Geyikdağı Platform is overlain in the east by the **Antalya-Alanya Nappes** (Fig. 15). These consist of a Paleozoic-Paleocene folded and thrust series dominated by carbonate and uppermost Cretaceous foreland basin deposits (Angiolini et al., 2007; Robertson and Woodcock, 1981), overlain by ophiolites and mélanges that contain ~95-90 Myr old metamorphic sole fragments, comparable in age with other Anatolian ophiolites (Çelik et al., 2006). The Antalya-Alanya nappes are part of a thrust belt that was emplaced from south to north over the Beydağları foreland, and the Geyikdağı unit of the Central Taurides to the east, until Maastrichtian times (e.g., Okay and Özgül (1984). The Alanya nappes overlie the Antalya nappes and are structurally below the ophiolites, and comprise a HP-LT metamorphic complex (~85–82 Ma) of continental origin (Çetinkaplan et al., 2016; Okay and Özgül, 1984). This complex has been interpreted to relate to a subduction system that evolved from southeastern Anatolia and radially rolled back westwards, leading to ophiolite emplacement around the eastern Mediterranean oceanic basin, i.e. onto Arabia, blocks off Northern Africa (e.g., Kyrenia, Cyprus) and the southern Taurides (Beydağları, Geyikdağı) (Maffione et al., 2017).

Offshore Beydağları to the south, the submerged **Anaximander Seamount Complex** is located at the junction of the Hellenic and Cyprus Arcs. The complex comprises three submarine highs, from west to east the Anaximander, Anaximenes, and Anaxigoras Seamounts (e.g., ten Veen, 2004; Zitter et al., 2003). These features are composed of variably deformed Cretaceous to Miocene successions and are interpreted to be the submarine continuation of the Beydağları Platform and the overlying Antalya nappes (ten Veen et al., 2004). The Anaximander Mountains are separated to the south by the Mediterranean Ridge, which is the accretionary prism associated with Oligocene and younger subduction (ten Veen et al., 2004; Zitter et al., 2003) and that hosts today's Africa-Europe plate boundary. South of this plate boundary, on the African Plate, the **Herodotus Basin** is floored by the oldest ocean crust still on the sea floor today, with a Carboniferous age (Granot, 2016) that is connected to the North African passive margin. To the east of the Herodotus Basin, from Cyprus to Africa and from Cyprus to Arabia, there is no oceanic lithosphere left, and all appears to be thinned continental crust (Erduran et al., 2008) (see next section).

5.12.2. Central Anatolia

The tectonic architecture of Central Anatolia (Fig. 15) contains similarities as well as major differences with Western Anatolia. The northern part of the section is the Crimea Peninsula exposing the Scythian Platform overthrusting the Tauric Flysch (Figs. 15 and 16), bounded to the south by the Black Sea Basin. In the Pontides to the South, the Istanbul Zone disappears and across the Intra-Pontide suture lie the **Eastern Pontides**.

The eastern Pontides comprise abundant upper Paleozoic metamorphic basement ascribed to the Variscan orogeny (e.g., Rolland et al., 2016; Topuz, 2004). In NE Turkey, it is underlain by the Ağvanis Massif, a Triassic greenschist to epidote-amphibolite facies metamorphic complex with metabasites, phyllites, marbles, calcschists, metacherts, metagabbros and serpentinites, interpreted as a metamorphosed oceanic accretionary complex (Topuz et al., 2014a) equivalent to the Karakaya Complex to the west (Fig. 15). These units are overlain by a Jurassic to Eocene carbonate and continental clastic stratigraphy with abundant volcanic intervals (Dokuz et al., 2017). Volcanism was active from Jurassic onwards, and remained episodically active until the early Miocene, with lulls in the Late Cretaceous to Paleocene, and late Eocene to late Oligocene (Eyuboğlu et al., 2012, 2013; Schleiffarth et al., 2018). Okay et al. (2014) reported Jurassic HT/LP metamorphic rocks from the northern Central Pontides and ascribed these to extension in an arc setting.

The Sakarya Zone in the Central Pontides is dominated by metamorphic belts of ages including the Triassic accretionary Karakaya Complex, overlain by Jurassic and younger carbonate, volcanic, and clastic sediments, whereas deeper structural units include accretionary complexes of Late Jurassic, Early, and Middle Cretaceous age (Okay et al., 2006b, 2013).

To the south of the Sakarya accretionary prism the previously described Jurassic ophiolites (e.g. Eldivan Ophiolite, Fig. 15) are found along the southern margin of the Pontides, in the Izmir-Ankara-Erzincan Suture Zone. These have ~180-170 Ma (in places perhaps as young as 140 Ma) oceanic crust, and metamorphic sole rocks of ~180-170 Ma (Çelik et al., 2011, 2013), interpreted to have formed in the Sakarya forearc during (nascent) northward subduction (Topuz et al., 2014a). These lie structurally above the Ankara mélange to the south, which in turn overlies the Cretaceous Eastern Mediterranean Ophiolites and associated Bozkır mélange units (Fig. 15) (Gökten and Floyd, 2007; Rojay, 1995). The Cretaceous ophiolites and underlying mélange in Central Anatolia overlie the HT-LP metamorphic Kırşehir Block instead of the Tavşanlı Zone of western Turkey (see below) (Fig. 15).

Straddling the IAESZ in the Central Pontides is the Çankırı Basin, which covers the Jurassic Eldivan Ophiolites, and the Pontides in the northwest, and Upper Cretaceous ophiolites and ophiolitic mélange as well as Kırşehir Block in the south (Fig. 15). The basin has an up to 3 km thick stratigraphy from Upper Cretaceous to lower Miocene, of which the Cretaceous part is interpreted as a forearc basin above an oceanic subduction zone, and the Paleocene and younger part a foreland basin related to collision with the Kırşehir Block (Kaymakcı et al., 2009). Contractional deformation in the basin continued until the early Miocene, and was in Eocene-Miocene time associated with oroclinal bending (Çinku et al., 2011; Kaymakcı et al., 2003; Lucifora et al., 2013) thought to be related to indentation of the central Kırşehir Massif (Kırşehir–Kırıkkale Block of Lefebvre et al. (2013a), see below; Fig. 15). Since Eocene time, and likely related to this same phase of deformation, the Pontides to the north of the Cankırı Basin underwent ~30 km N-S shortening accommodated along inverted normal faults that formed during Black Sea opening (Espurt et al., 2014).

The largest portion of the Central Anatolian transect is occupied by the **Kırşehir** Block and the overlying **Central Anatolian Ophiolites**, which are part of the Cretaceous Eastern Mediterranean Ophiolites. These ophiolites are strongly dismembered and form isolated klippen scattered on the high-grade metamorphic, Adria-derived continental Kırşehir Block. The two most complete and best studied ophiolite occurrences are the Sarıkaraman and

Çiçekdağı supra-subduction zone ophiolites of Late Cretaceous age (Floyd et al., 2000; Göncüoğlu and Türeli, 1993; Radwany et al., 2017; van Hinsbergen et al., 2016; Yaliniz et al., 1996, 2000).

Below these ophiolites lies the **Kırşehir Block** (Görür et al., 1984), a continent-derived series of Paleozoic to Mesozoic metasedimentary rocks with peak HT/LP metamorphic conditions of up to 800 °C/8 kbar (Lefebvre et al., 2015; Whitney et al., 2001) at ~85–90 Ma (U/Pb on metamorphic zircon and monazite (Whitney and Hamilton, 2004; Whitney et al., 2003). The Kırşehir Block is characterized by a regionally pervasive, flat-lying foliation with an overall top-to-the-southwest sense of shear (Lefebvre, 2011). This foliation is intruded by mostly undeformed granitoids with ages of 85–70 Ma (van Hinsbergen et al., 2016, and references therein). Intrusion occurred at lower pressures than prevailing at regional climax metamorphism, at 3–4 kbar, causing syn-decompressional heating in the surrounding Kırşehir metamorphic rocks (Kocak and Leake, 1994; Lefebvre et al., 2015; Whitney and Dilek, 1998; Whitney et al., 2001). The metamorphism of the Kırşehir Block is explained by underthrusting below the Central Anatolian Ophiolites (Boztuğ et al., 2009) and occurred simultaneously with the burial and accretion of the Tavşanlı continental rocks to the west, which thus likely formed a lateral paleogeographic continuation of the Kırşehir Block (van Hinsbergen et al., 2016). It is also interesting to note that the ages of climax metamorphism in the Kırşehir Block overlap with the ages of plagiogranites in the overlying ophiolites, which may suggest that the Kırşehir Block underthrust the supra-subduction zone ophiolites while the latter were still spreading (van Hinsbergen et al., 2016).

Decompression of the Kırşehir Block must have started immediately after climax metamorphism and the end of regional shearing as shown by the decompression from up to 8, to 3–4 kbar between ~90 Ma peak pressure metamorphism and 85-70 Ma granitoid intrusion. Some of these granites are affected by discrete ductile shear zones which suggest syntectonic emplacement during extension (Isik, 2009; Isik et al., 2008). Extensional detachments were found in the Kırşehir Block, particularly the Niğde, Kaman, and Hırkadağ detachments (Gautier et al., 2002, 2008; Lefebvre et al., 2011, 2015). When corrected for Cenozoic vertical axis rotations (Lefebvre et al., 2013a) (see section 6.2.10), kinematic indicators in the detachment faults show that exhumation occurred under ~E-W-directed extension since at least ~80-75 Ma. ^{40}Ar-^{39}Ar cooling ages cluster between ~75 and 65 Ma (see review and data in van Hinsbergen et al., 2016) and apatite fission track ages from the granites indicate cooling below ~100 °C in early to middle Paleocene time (~62-57 Ma; Boztuğ et al. (2009)). Lutetian and younger rocks regionally unconformably cover the Kırşehir metamorphics as well as associated supra-detachment basins (Advokaat et al., 2014a; Göncüoğlu et al., 1993; Gülyüz et al., 2013).

Paleomagnetic analysis of the granite intrusions shows that after its exhumation, the Kırşehir Block broke into three blocks (Akdağ-Yozgat, Kırşehir-Kırrıkkale, Ağacören–Avanos) that underwent differential block rotations (Lefebvre et al., 2013a). These rotations were accommodated by transpression and thrusting along fault zones (Isik et al., 2014; Lefebvre et al., 2013a; Oktay, 1981; Seymen, 1984) and led to at least 17–27 km of syn-sedimentary shortening in uppermost Eocene to Oligocene stratigraphy of associated basins (Advokaat et al., 2014a; Gülyüz et al., 2013). ^{40}Ar-^{39}Ar dating of fault gouges of the Savcılı-Mucur Fault Zone between the Kırşehir-Kırrıkkale and Ağacören–Avanos blocks showed faulting between ~40 and 23 Ma (Isik et al., 2014).

The Kırşehir Block is surrounded by the Central Anatolian basins (Görür et al., 1998; Nairn et al., 2013). These include from north to south the already described Çankırı Basin (Kaymakcı et al., 2009; Tüysüz et al., 1995), the Haymana Basin (e.g., (Görür et al., 1984; Koçyiğit, 1991; Nairn et al., 2013), the Tuzgölü Basin, which is bounded from the Kırşehir Block by the Tuzgölü normal fault (e.g., (Cemen et al., 1999; Fernández-Blanco et al., 2013; Görür et al., 1984) and the Ulukışla Basin (e.g., (Clark and Robertson, 2005; Gürer et al., 2016). All of these basins have in common that they contain an Upper Cretaceous to Cenozoic marine to terrestrial stratigraphy that rests on ophiolites or ophiolitic mélanges, and from the Eocene onwards also on Afyon Zone metamorphics (e.g., (Gautier et al., 2008; Gürer et al., 2018a; Gürer et al., 2016). The basal stratigraphy of the Tuzgölü and Ulukışla basins recorded syn-sedimentary extension in Late Cretaceous to Paleocene time (Görür et al., 1998; Gürer et al., 2016; Nairn et al., 2013). The Haymana Basin (Fig. 15) is floored by sub-ophiolitic mélange and for Eocene and younger rocks, also the underlying Kırşehir Block (Görür et al., 1984; Koçyiğit, 1991). Its stratigraphy comprises Upper Cretaceous (Late Campanian) to Eocene clastic sediments of roughly 4–5 km thickness. Below the Upper Neogene cover, the Haymana Basin is probably connected to the Tuzgölü and the Ulukışla Basins to the southeast. Both the Tuzgölü and Ulukışla basins comprise an Upper Cretaceous to Eocene sequence. The lithostratigraphy in the Tuzgölü Basin is similar to the Haymana Basin (Cemen et al., 1999). The Ulukışla Basin's stratigraphy differs in that it comprises a thick sequence of Paleocene basalts and basaltic andesites, and Paleocene to Eocene granitic intrusions (Clark and Robertson, 2002; Gürer et al., 2016). The Ulukışla Basin and Kırşehir Block are bounded in the east by the Ecemiş Fault Zone, a left-lateral strike-slip fault with a displacement of ~60 km (Jaffey and Robertson, 2005). This fault was active as a strike-slip fault between the late Eocene and early Miocene and that seems to follow the eastern margin of the Kırşehir Block, offsetting the Ulukışla Basin from the Sivas Basin in the east (Gürer et al., 2016) (see next section).

The Upper Cretaceous to Paleocene stratigraphy of the Ulukışla Basin recorded syn-sedimentary extension (Gürer et al., 2016), that was shown by Gürer et al. (2018a) to relate to the exhumation of the underlying **Afyon Zone** from underneath the southern margin of the basin along the top-to-the-NE Ivriz detachment (which restores to top-to-the-northeast when corrected for post-Eocene vertical axis rotations (Gürer et al., 2018b). In the Bolkar Mountains the HP-metamorphic rocks of the Afyon Zone consist of marbles and glaucophane-epidote-bearing metabasic rocks (Gürer et al., 2018a; van der Kaaden, 1966). The timing of extensional exhumation along the Ivriz detachment is bracketed between the ~67-62 Ma ^{40}Ar/^{39}Ar retrograde mineral growth ages of the Afyon Zone metamorphic rocks (Pourteau et al., 2013; Özdamar et al., 2013), a ~50 Ma syntectonic granite intrusion in the footwall (Horoz granite), and an unconformable Lower to middle Eocene onlapping cover on the detachment surface (Gürer et al., 2018a).

The **Central Taurides** (Blumenthal, 1947) formed a thin-skinned fold-and-thrust belt below the Bozkır Nappe in latest Cretaceous to Eocene time (Demirtaşlı et al., 1984; Gutnic, 1979; McPhee et al., 2018a; Özgül, 1984). Below the Bozkır unit, there are three major nappes (Özgül, 1984). The highest is the Bolkardağı nappe that comprises platform-margin sediments, which where subject to HP-LT metamorphism corresponds to the Afyon Zone (Candan et al., 2005; Pourteau et al., 2010, 2014), which accreted ~70-65 Ma. The Aladağ nappe is a rootless nappe with a Paleozoic to Maastrichtian platform carbonates that is restricted to south central Turkey, adjacent to, and backthrust over, the Bolkardağı nappe, and accreted in the latest Cretaceous (~65 Ma) (Mackintosh and Robertson, 2013; Özgül, 1984). The Aladağ nappe, and where absent the Bolkardağı nappe, thrust onto the Geyikdağı nappe that is traced along most of the Taurides and accreted and duplexed in Lutetian time, ~45-40 Ma (Demirtaşlı et al., 1984; Gutnic, 1979; McPhee et al., 2018a; Özgül, 1984). Thin slivers of deep-marine carbonates with ages up to Campanian-Maastrichtian found as thrust slices between the Aladağ and Geyikdağı nappes (Mackintosh and Robertson, 2013; Özgül, 1984) were correlated by McPhee et al. (2018b) to the Dilek nappe of the Menderes Massif.

These occurrences are too small to appear on our tectonic map but are included in the orogenic architecture chart of Fig. 16.

The Central Tauride fold-and-thrust belt formed by large-displacement, regional nappe-bounding thrusts from Late Cretaceous to Eocene, followed by duplexing of the Geyikdağı nappe in late Eocene time, in turn followed by slow erosion and exhumation throughout the late Eocene to earliest Miocene (McPhee et al., 2018a, 2018b, 2019). The Eocene shortening phase accommodated ~75 km of Eocene NE-SW shortening in the Central Taurides in a section over the heart of the Isparta Angle (Figs. 1 and 15), followed by another ~25 km shortening in middle Miocene to early Pliocene time (McPhee et al., 2018a). A second section from the Alanya nappes to the east benefited from windows exposing the Geyikdağı below the Bozkır nappes and allowed demonstrating that the Eocene thrusting phase was associated with at least 154 km of shortening (McPhee et al., 2018b). The Miocene phase of shortening is likely rather local, was associated with westward convex oroclinal bending (Koç et al., 2016), and was accommodated by NE-SW extension of equal magnitude in the Miocene Central Tauride Intra-montane Basins (Koç et al., 2017, 2018). Low-temperature thermochronology results give scattered ages in the 40-20 Ma time range suggesting gradual erosion and low tectonic activity in the interval between the two main shortening events (McPhee et al., 2019).

The emplacement direction of the Cretaceous SSZ ophiolites of Central Turkey, including Beyşehir-Hoyran and Pozantı-Karsantı Ophiolites (Fig. 15) is generally thought to be top S to SW (e.g., Polat and Casey, 1995; Robertson, 2002). No detailed structural analyses of the south-Central Taurides are available and discerning between multiple deformation with opposite vergence, as shown for the Alanya-Antalya nappes (McPhee et al., 2018a, 2018b) farther west, is not possible. Parlak et al. (1996) suggested based on kinematic indicators in the metamorphic sole of the Mersin Ophiolite that the obduction direction may have been top-to-the-NW, which would make Mersin Ophiolite equivalent to those in the Antalya Nappes. Later, Parlak and Delaloye (1999) questioned this interpretation and suggested top-to-the-south emplacement instead. It is interesting to note that contrary to the Lycian and Beyşehir-Hoyran Ophiolites (Fig. 15), which derive from the northern margin of the wider Tauride Platform (Collins and Robertson, 1997; McPhee et al., 2018a; Plunder et al., 2016), the Mersin Ophiolite (in Transect II) is underlain by a mélange that contains two thrust slices of radiolarian cherts. An upper one also includes slope deposits and is as old as the Carboniferous to Permian (Moix et al., 2011; Okuyucu et al., 2018), a lower one has cherts not older than the Middle Triassic (Moix et al., 2011; Tekin et al., 2016) overlying basalts with a back-arc basin geochemical signature (Sayit et al., 2017). This suggests that Carboniferous as well as Triassic (back-arc basin) crust was subducted below the Mersin Ophiolites. Moix et al. (2011) correlated the Mersin ophiolitic mélange to the Antalya and Troodos Ophiolites, hence derived from subduction in the Eastern Mediterranean Ocean, although paradoxically interpreted some of the mélange units derived from the northern margin of the Taurides. Okay and Nikishin (2015) assumed a northern derivation of the Mersin Ophiolite and used the results of Moix et al. (2011) to argue that the northern passive margin of the Anatolide-Tauride part of Greater Adria was Paleozoic in age, facing a Paleotethys Ocean. We here note that the two ages of ocean floor recorded in the Mersin cherts are both reported from the Eastern Mediterranean Basin to the south of the Taurides: a Triassic age was estimated from the crust underlying the Ionian Basin (Speranza et al., 2012), whilst a Carboniferous age was estimated for the Herodotus Basin (Granot, 2016). A derivation of the Mersin Ophiolites from the Eastern Mediterranean Ocean between the Taurides and Africa may thus straightforwardly explain the ages of radiolarian cherts in the mélange below Mersin. Also paleomagnetic analyses of net tectonic rotations are consistent with a southward derivation of the Mersin Ophiolite (Morris et al., 2017) (see section 6.2.11).

The sedimentary cover of Central Taurides is dominated by the marine sediments of the Lower to upper Miocene **Mut Basin**, which were uplifted by >2 km since ~7–8 Ma without strong deformation of the stratigraphy (Bassant et al., 2005; Schildgen et al., 2012), and form a gradual monocline from such >2 km elevations in the north to the coast in the south (Fernández-Blanco, 2014; Fernández-Blanco et al., 2019).

The Tauride Mountains of southern Turkey are separated from Cyprus by the **Cilicia-Adana Basin** (Fig. 15). This marine basin was cut by top-to-the-south and –north thrust faults that were active until at least Pliocene time (Fernández-Blanco, 2014). Towards the east, the onshore Adana Basin contains a shallow to deep-marine stratigraphy of lower Miocene to Pliocene limestones and continental clastics (Derman and Gürbüz, 2007; Gül, 2007; Radeff et al., 2017) unconformably overlying Oligocene terrestrial sediments and continental clastic sediments (Ünlügenç and Akıncı, 2015). Offshore to the south, the eastern part of the Cilicia Basin was deformed by Plio-Pleistocene NE-SW extension between left-lateral strike-slip faults that link eastwards to the East Anatolian Fault Zone that together with the North Anatolian Fault Zone accommodate westward Anatolian extrusion (Aksu et al., 2014).

To the south of the Cilicia Basin lies the island of **Cyprus**. On the northern part of the island lies the Kyrenia range (Figs. 1 and 15), a fold-and-thrust belt comprising greenschist-facies metacarbonates of Triassic to Cretaceous stratigraphic age (Trypa Group) (Fig. 16). In the eastern Kyrenia range is also a 1.5 km wide body of serpentinite mélange with gabbro pockets, fragments of oceanic crust, and oceanic crust-derived conglomerates (Aldanmaz et al., 2019). Metamorphism is Late Cretaceous in age and was followed by latest Cretaceous extensional exhumation (e.g., Robertson et al., 2011). The exhumed Trypa group is unconformably overlain by marine uppermost Cretaceous to Paleocene marls and volcanics, Eocene conglomerates, and an Oligocene to upper Miocene deep-marine turbidite sequence (McCay and Robertson, 2012; Robertson et al., 2011). Late Miocene thrusting, between ~9 and 6 Ma accommodated at least 17 km of shortening (McPhee and van Hinsbergen, 2019). Robertson et al. (2013b) and Robertson and Kinnaird (2015) argued that thrusting also occurred in Eocene time, but McPhee and van Hinsbergen (2019) showed that all deformation is straightforwardly explained by late Miocene shortening alone. To the south of the Kyrenia ranges lies the **Troodos Ophiolite** and the underlying Mammonia mélange complex (Fig. 15). The age of the Troodos Ophiolite and of high-grade rocks in the Mammonia mélange interpreted to be metamorphic sole-derived, has an ^{40}Ar-^{39}Ar age of 92–90 Ma (Chan et al., 2007; Mukasa and Ludden., 1987), and the ophiolite has a supra-subduction zone signature (Pearce and Robinson, 2010) similar to the ophiolites of Anatolia. The Mammonia Complex is an accretionary prism and contains oceanic and continental rocks of Triassic to Early Cretaceous age (Bailey et al., 2000). The thrust between the Troodos Ophiolite and the Mammonia Complex is unconformably covered by uppermost Maastrichtian mass flow deposits (Swarbrick and Naylor, 1980). Because of similarities in the ophiolite structure and as well as a shared Late Cretaceous major counterclockwise rotation phase demonstrated paleomagnetically (e.g., Clube et al., 1985; Clube and Robertson, 1986) (see section 6.2.11), the Troodos Ophiolite is widely considered to have been part of a microPlate together with the Baer-Bassit and Hatay Ophiolites that were thrust over the NW Arabian margin in the latest Cretaceous (Inwood et al., 2009b; Maffione et al., 2017; Morris and Anderson, 2002; Morris et al., 2006) (Fig. 15). In contrast to the Hatay and Baer-Bassit Ophiolites, however, Cyprus has in latest Miocene (~6 Ma) times accreted to the overriding Anatolian orogen (Barrier et al., 2008; McPhee and van Hinsbergen, 2019), and is presently located in the forearc of the

eastern Mediterranean subduction zone south of Cyprus (Fig. 15).

Finally, the leading edge of the African Plate is represented by the **Eratosthenes Seamount** that is part of the stretched African passive margin (Kempler, 1998; Robertson, 1998; Robertson et al., 1995). Underthrusting of the Eratosthenes Seamount is thought to be responsible for major uplift that affected Cyprus since the Early to Middle Pleistocene (Harrison et al., 2013; Kinnaird et al., 2011; Palamakumbura et al., 2016; Robertson, 1998; Schattner, 2010). The Eratosthenes Seamount is thought to have moved to the (N)NW during the Triassic-early Jurassic, obliquely opening of the Levant Basin (Gardosh et al., 2010; Schattner and Ben-Avraham, 2007). This basin with thinned continental crust has a lithospheric thickness of 60–80 km (Erduran et al., 2008), suggesting stretching by a factor of ~2.

McPhee and van Hinsbergen (2019) suggested that the Trypa group of the Kyrenia range may either reflect a continental block on the stretched African passive margin, similar to the modern Eratosthenes Seamount, onto which in Late Cretaceous time the Troodos Ophiolite was emplaced in Late Cretaceous time, or a far-traveled block similar to the Alanya nappes. Post-obduction slab break-off was associated with extension and exhumation of the obducted Kyrenia range rocks to the sea floor, where open marine chalks and volcanics with a geochemistry consistent with slab break-off were deposited (Robertson et al., 2011). Eocene uplift documented in the Kyrenia stratigraphy marks the passage of Cyprus over a forebulge associated with the Anatolian subduction zone, after which Cyprus entered the foredeep and upward thickening foreland basin clastics were deposited. These became deformed by ~17.5 km of shortening accommodated by thrusting and erosional exhumation in the Tortonian (~9-6 Ma) marking collision of Cyprus with the Anatolian collage. Subsequently, the subduction thrust jumped south, thereby accreting the Troodos Ophiolite and underlying mélange to the Anatolian orogen (Fig. 16). Tilted and eroded Tortonian strata are unconformably overlain by Messinian gypsum and deep marine lower Pliocene rocks showing a rapid phase of subsidence (McPhee and van Hinsbergen, 2019), followed by latest Pliocene and Pleistocene uplift and emergence (Kinnaird et al., 2011; Palamakumbura et al., 2015).

5.12.3. Eastern Anatolia

The tectonic architecture of Eastern Anatolia is similar to Central and Western Anatolia in that the Pontides and Taurides are contiguous. The main differences are two-fold. First, there appears to be no unit that is equivalent to the Kırşehir Block or Tavşanlı Zone, and the Afyon Zone is only mapped in a small strip along the southwestern Sivas Basin. Second, much of the eastern and southeastern Taurides were metamorphosed in Late Cretaceous time following ophiolite obduction. Third, the eastern Taurides have collided with Arabia along the Bitlis Suture Zone.

The eastern **Pontides** are separated from the Scythian Platform by the Eastern Black Sea Basin, which is a separate basin from the western Black Sea Basin, and opened in Cretaceous or perhaps Paleocene time (Nikishin et al., 2015b). Similar to Central Anatolian, the Izmir-Ankara-Erzincan Suture Zone contains a narrow belt of Jurassic supra-subduction zone ophiolites. This includes the well-studied Lower to Middle Jurassic Refahiye Ophiolite (e.g., Topuz et al., 2013, 2014a) (Fig. 15). As mentioned before, these Jurassic ophiolites were interpreted to have formed in the Pontide forearc (Topuz et al., 2014a). The Refahiye Ophiolite backthrust northward onto the Sakarya Zone (Dilek, 2006) and together with the Ankara Mélange thrust southward over Cretaceous Eastern Mediterranean Ophiolites (Fig. 17).

These Cretaceous ophiolites overthrust southward the Lower Triassic-Campanian Munzur limestones (Yılmaz, 1985, 1994) which belong to the easternmost Taurides (see below). There are no intervening continental slivers equivalent to the Kırşehir Block or Tavşanlı Zone in this region (Topuz et al., 2013). To the east of the Ecemiş Fault, Cretaceous ophiolites and associated Bozkır Mélange are widespread (Kavak et al., 2017; Legeay et al., 2018; Parlak et al., 2013a). The most complete tectonostratigraphy of the Taurides including the Afyon (Bolkardağı) Zone Aladağ and Geyikdağı nappes is only present in the west of the Eastern Taurides, just east of the Ecemiş Fault. The Afyon unit in the eastern Taurides was also metamorphosed around 65 Ma (Pourteau et al., 2013), and there is no record of continental accretion between the formation of the supra-subduction ophiolites (e.g., for the Divriği Ophiolite at 88.8 ± 2.5 Ma based U-Pb zircon dating on gabbros (Parlak et al., 2013a)) and the latest Cretaceous (Parlak et al., 2013a; Robertson et al., 2013c). This suggests that pre-obduction oceanic subduction continued longer in eastern Turkey than in central and western Turkey.

The Afyon Zone and Aladağ nappes disappear eastwards, where only the Bozkır and Geyikdağı units are present. There is no equivalent of a Dilek nappe known from the eastern Taurides. Similar to the Central Taurides, the youngest sediments in the Geyikdağı unit are middle Eocene in age, and apatite fission track cooling ages of ~40-25 Ma (Darin et al., 2018) from the eastern Taurides are consistent with thrusting and slow erosion since the late Eocene, comparable to the Central Taurides (McPhee et al., 2019).

The contact between the Taurides and the eastern Kırşehir Block, as well as the Izmir-Ankara-Erzincan Suture Zone in eastern Anatolia is covered by the **Sivas Basin** (**Fig.**). This basin has two parts with different stratigraphies, separated by the Deliler-Tecer Fault, an Oligocene and older thrust fault in the central part of the basin that in its most recent motions was transpressional (Legeay et al., 2018) (Fig. 15). The southern Sivas Basin has a basement of Cretaceous ophiolites and ophiolitic mélange underlain by rocks of the (eastern) Taurides, and a Maastrichtian to Eocene marine sedimentary sequence (e.g., Dirik et al., 1999; Legeay et al., 2018; Poisson et al., 1996) overlain by middle Oligocene to lower Miocene (~29-23 Ma) continental clastics (Krijgsman et al., 1996). The northern part of the basin, thrust over the Oligo-Miocene continental clastics along the Deliler-Tecer Fault, is floored by ophiolites and covered by occasional upper Cretaceous shallow marine limestones, and has an extensive shallow marine to terrestrial, Eocene to Pliocene stratigraphy with abundant Oligocene and Miocene evaporite deposits (e.g., Legeay et al., 2018; Şenel, 2002). This part developed a regional unconformity between ~40 and 34 Ma, also reflected in apatite-fission track cooling ages, suggesting uplift and erosion (Darin et al., 2018). Towards the west, the Deliler-Tecer Fault connects to the Ecemiş Fault Zone through a series of NE-SW striking sinistral strike-slip faults (Higgins et al., 2015), and to the Savcılı-Mucur Thrust Zone (Gürer et al., 2018b) (Fig. 15). Collision between the Taurides and Pontides across the Sivas Basin is often assumed to be synchronous with the ~65-60 Ma collision between the Kırşehir and Tavşanlı blocks and the Pontides farther west but is not straightforwardly interpreted from the geology of the Sivas Basin. It seems plausible that there was no deep-marine basin between the Taurides and Pontides from the Oligocene (~29 Ma) onwards, but prior to that time, the stratigraphic and vertical motion evolution on both sides of the Deliler-Tecer Fault is markedly different, sediments in the south are marine, and the separation between the Taurides and Pontides is hard to constrain from the geology directly. Gürer and van Hinsbergen (2019) argued, based on a paleomagnetic and kinematic analysis (Gürer et al., 2018a), which is incorporated in our reconstruction (see section 6.2.10 for paleomagnetic constraints), that the Deliler-Tecer Fault is the best candidate to mark the final suture between the Taurides and Pontides in the Sivas Basin, and is of Oligocene or even younger age.

The non-metamorphic Taurides and overlying nappes of Eastern

Turkey end towards the east in a peculiar structure coined the '**Gürün Curl**' by Lefebvre et al. (2013b). There, strikes of the Tauride folds and thrusts change from ENE-WSW to N-S, and then end with thrust faults against the Malatya metamorphic massif (see below). In the core of the curl lie the Binboğa metamorphics, separated from the similar Malatya metamorphics by the Sürgü Fault, a branch of the East Anatolian Fault (Kaymakcı et al., 2010; Koç and Kaymakcı, 2013). Similar to the Taurides farther to the west, the youngest rocks incorporated in contiguous Geyikdağı stratigraphy within the Gürün Curl are Eocene, and contrary to the easternmost Taurides to the east of the Gürün Curl, there are no Cretaceous or Paleogene magmatic intrusions or volcanoes (Kuşcu et al., 2010; Şenel, 2002).

The Geyikdağı unit in the core of the Gürün Curl (the 'Gürün autochton' of Perincek and Kozlu (1984)) is overthrust from the north by the Bozkır unit (Figs. 15 and 16), but also from the south, by the Southern Allochton (Perincek and Kozlu, 1984). This nappe comprises an ophiolitic mélange thrust northward onto Mesozoic carbonates of the Geyikdağı unit. The latest thrust motion is post-middle Eocene, but the stratigraphy of the Tauride units reveal that ophiolite emplacement occurred in the Late Cretaceous (90-80 Ma), with a Turonian unconformity followed by Campanian marine pelagic limestones, redeposited limestones, and ophiolite debris (Perincek and Kozlu, 1984; Robertson et al., 2013a). These ophiolites and mélanges are traced around the Curl to the east and are bounded by the Malatya-Ovacık Fault (Fig. 15). The easternmost Taurides, to the east of the Gürün Curl were metamorphosed and extensionally exhumed prior to and during thrusting of the Geyikdağı unit (see next section). The latest tightening of thrusting in the Gürün Curl younger than Miocene sediments involved in thrusting in the center of the structure.

The **Malatya and Binboğa metamorphics** are greenschist-facies (and for the Malatya metamorphics, incipient blueschist-facies (Oberhänsli et al., 2012)) metamorphic massifs comprising carbonate-dominated Paleozoic to Triassic sedimentary sequences of the Tauride carbonate platform (Özgül et al., 1981; Perincek and Kozlu, 1984; Yılmaz, 1993). Their metamorphism was caused by Cretaceous ophiolite obduction (Boztuğ et al., 2005; Kuşcu et al., 2010). Post-obduction out-of-sequence thrusting brought Malatya metamorphics on Binboğa and overlying ophiolites and Binboğa metamorphics on the Southern Allochton, and on the Göksun Ophiolite (Figs. 15 and 17). Out-of-sequence thrusting started shortly after ophiolite emplacement as shown by 85–80 Ma granitoids, with a geochemistry revealing subduction influence (e.g., the Esence granitoid intruding the thrust between the Göksun Ophiolite and the Binboğa metamorphics, the Baskil granite intruding the Ispendere Ophiolite-Malatya metamorphics thrust) (Karaoğlan et al., 2013a; Parlak, 2006; Parlak et al., 2004, 2013b; Rızaoğlu et al., 2009; Robertson et al., 2007; Yıldırım, 2015; Yılmaz et al., 1998). In the Meydan Ophiolite, also underlying the Malatya metamorphics, a volcanic arc lava unit is sandwiched between the ophiolite and ophiolitic mélange, and the thrust between lavas and ophiolite is cut by granitoid dykes with 87 ± 5 Ma U/Pb ages (Nurlu et al., 2016).

Collectively, this suggests that the Malatya metamorphics represent the distal, deeply underthrust Tauride margin, and the Southern Allochton is the proximal, shallowly underthrust margin. The age of metamorphism is similar to that of the eclogite-facies Alanya metamorphics farther west (see section 5.12.1), which is thought to represent a far-traveled part of this SE Anatolian metamorphic belt (Çetinkaplan et al., 2016).

Interestingly, the Ispendere Ophiolite, and the nearby Kömürhan Ophiolite, yielded U/Pb zircon ages slightly younger than most Cretaceous ophiolites, of 87–85 Ma (Karaoğlan et al., 2012), only slightly older than the granitoids that pierce the contact with the overlying metamorphic rocks. This shows that the above sequence of events must have occurred in a time span of only a few Myr, and that, paradoxically, ophiolite spreading and arc volcanism were essentially active during emplacement and out-of-sequence thrusting, an observation made earlier for the Kırşehir Block and overlying SSZ ophiolites (van Hinsbergen et al., 2016).

The above-described metamorphic massifs, as well as the non-metamorphic Taurides of the Gürün Curl underwent further thrusting after the Eocene. Tectonic maps and sections in Kuşcu et al. (2010), Michard et al. (1984), and Perincek and Kozlu (1984) suggest that in the southeast of the Gürün Curl, the Geyikdağı unit lies thrust southward over the Malatya metamorphics. This thrusting may have obscured, or reactivated, earlier Cretaceous thrusts or extensional faults.

Finally, the Malatya metamorphics lie thrust southward over a sequence of **Arabian Ophiolites** and overlying Maastrichtian to Miocene sediments (Beyarslan, 2017; Boulton and Robertson, 2007; Boulton et al., 2007; Hüsing et al., 2009b). These structurally lowermost ophiolites, once again Late Cretaceous in age (~92 Ma) were thrust directly onto the **Arabian foreland**, with a southward emplacement direction (Al-Riyami and Robertson, 2002; Al-Riyami et al., 2002; Bağcı, 2013; Chan et al., 2007; Inwood et al., 2009a, 2009b; Robertson, 2002, 2004). The frontal thrust of the Arabian Ophiolites is sealed by Maastrichtian platform carbonates showing that these ophiolites have been part of the Arabian Platform since late Cretaceous time (Al-Riyami and Robertson, 2002; Beyarslan, 2017; Kaymakcı et al., 2010; Robertson et al., 2016). The Cretaceous Koçali Ophiolite, emplaced onto Arabia south of the Püturge Massif (Fig. 15), was overthrust by Triassic (Carnian to Rhaetian) radiolarian cherts and MORB-basalts interpreted to be derived from the ocean once bordering the Arabian continent, and also this thrust sequence was sealed by Upper Maastrichtian to lower Miocene limestones (Beyarslan, 2017; Varol et al., 2011), showing that similar to the southern Gürün Curl, Cretaceous obduction along the Arabian margin was associated with complex imbrication of the ophiolite and underlying Arabia-derived nappes.

In the northwestern corner of the Arabian continent, the suture between the Binboğa-Malatya metamorphics and NW Arabia contains the Misis Mélange. This mélange consists of an oceanic crust-derived lower part, comprising Upper Cretaceous volcanic rocks with arc signature, and associated Paleogene pelagic sediments, and Tauride passive margin-derived mass-deposited sediments. The youngest rocks in the mélange are early Miocene in age (Robertson et al., 2004a) (Figs. 15 and 17). Cenozoic foreland basin sedimentation on the Arabian foreland is generally dated at Early to middle Miocene (Akıncı et al., 2016; Robertson et al., 2016). A detailed section through the Kahramanmaraş Basin that overlies Arabia and is overthrust by the Malatya metamorphics (Figs. 15 and 17), however, revealed an up to 6 km thick turbidite sequence that unconformably overlies Eocene limestones covering the Arabian foreland and overlying ophiolites (Hüsing et al., 2009b) – an Eo-Oligocene hiatus is regional on northernmost Arabia (Robertson et al., 2016) – and that is overthrust by the Malatya metamorphics. This section spans the middle Miocene, ~13-11 Ma (Hüsing et al., 2009b) showing that thrusting onto the NW Arabian foreland continued until at least 11 Ma.

Finally, the SE Anatolian orogen was since the late Miocene cut by a series of strike-slip dominated fault zones and associated transtensional basins (e.g., Kaymakcı et al., 2010). The most prominent of this is the left-lateral **East Anatolian Fault Zone** that currently accommodates the westward extrusion of Anatolia, together with the North Anatolian Fault (Fig. 15) (e.g., Lyberis et al., 1992). The East Anatolian Fault branches towards the southwest into two strands, the northern of which is known as the Sürgü Fault (e.g., Koç and Kaymakcı, 2013), whereby the latter appears to accommodate one third of the total deformation of the East Anatolian Fault Zone (Duman and Emre, 2013). The total

displacement of the East Anatolian Fault is not well constrained, but the fault must accommodate the westward displacement of Anatolia constrained along the North Anatolian Fault Zone as up to 85 km (see section 5.12.1).

Whilst the North Anatolian Fault Zone is thought to have initiated around 11 Ma (Şengör et al., 2005), the East Anatolian Fault Zone appears to have started later, at ~6-3 Ma (e.g., Karaoğlu et al., 2017; Kaymakcı et al., 2010). Earlier deformation may have been accommodated along a series of left-lateral strike-slip faults that cut through the Taurides, to the west of the East Anatolian Fault (Kaymakcı et al., 2010; Koç and Kaymakcı, 2013), of which the Malatya-Ovacik Fault Zone is the most prominent and accommodated ~29 km of left-lateral displacement between 5 and 3 Ma (Westaway and Arger, 2001), but it may already have started earlier as the part of the Malatya Basin stratigraphy controlled by this fault started already in Early to middle Miocene time (Kaymakcı et al., 2010; Önal and Kaya, 2007). No displacements are known for the faults farther west within the eastern Taurides (Kaymakcı et al., 2010), but the mapped units of the Eastern Taurides across the Göksun Fault (Fig. 15) appear to have been offset by some 20 km. We therefore treat the Göksun Fault as the conjugate of the North Anatolian Fault in the 11-6 Ma interval in our reconstruction.

5.12.4. Caucasus; South Armenian block; easternmost Taurides; Bitlis-Pütürge

The Caucasus to Arabia transect is the easternmost transect that belongs to the Mediterranean/Greater Adriatic tectonic province. To the east are the Cimmerian blocks of Iran, which were separated from the Mediterranean realm by a long-lived transform fault (e.g., Barrier et al., 2008; Stampfli and Borel, 2002). The Iranian Cimmerides rifted off Gondwana already in Permian times and collided with Eurasia in the Triassic (e.g., Muttoni et al., 2009), and were part of tectonic Plates that did not extend into the Mediterranean region (e.g., Stampfli and Borel, 2002), and are therefore not included in our reconstruction.

In this easternmost transect, the Scythian Platform of Eurasia is bounded to the south by the WNW-ESE trending Greater Caucasus orogen, which spans 1200 km and reaches peaks of >5500 m, from the Cretaceous Black Sea Basin in the west, to the South Caspian Sea Basin in the east, which is thought to be a Middle-Late Jurassic back-arc basin probably floored by oceanic crust (Brunet et al., 2003). The long-lived transform Plate boundary that separates the Iranian and Anatolian systems is located to the south of the Caucasus, with the eastern one third of the orogen located north of the Iranian Cimmerides (Fig. 15).

The **Greater Caucasus** exposes a series of thick-skinned thrust nappes that comprise a pre-Mesozoic, crystalline basement and a Paleozoic to Cenozoic sedimentary cover. The basement-cored Greater Caucasus was emplaced onto sediments of the Greater Caucasus Basin along the Main Caucasus Thrust (Figs. 15 and 17). The orientation of this thrust has long been debated, with one school of thought suggesting a steep structure at depth, particularly in Russian literature (see Saintot et al. (2006a) and references therein) suggesting only relatively minor shortening (~80 km, Nikishin et al. (2010)) was involved in the major Cenozoic uplift of the range to modern elevations. Alternatively, recent literature portrayed the Main Caucasus Thrust as a flat-lying structure at depth, forming a roof thrust of a dominantly south-vergent thick- to thin-skinned thrust wedge (Cowgill et al., 2016; Gamkrelidze, 1986; Mikhailov et al., 1999; Saintot et al., 2006a). This model allows for much larger shortening values across the Caucasus, of at least 130 km of N-S shortening (Cowgill et al., 2016) to as much as 200–300 km (Ershov et al., 2003).

The Greater Caucasus basement consists of a mainly Variscan crystalline basement separated from the Scythian Platform by a zone of ophiolites and 330-310 Ma eclogite-blueschist assemblages interpreted as a Late Paleozoic suture between the Scythian Platform and peri-Gondwana terranes to the South (Perchuk and Philippot, 1997; Şengör, 1984; Somin, 2011; Yılmaz et al., 2014). The metamorphic core is overlain by an upper Paleozoic sedimentary cover that was shortened and deformed in the Late Triassic, likely associated with the collision of the Iranian Cimmerides (e.g., Saintot et al., 2006a; Şengör, 1984). Renewed extension and subsidence culminated in the deposition of a >15 km thick sequence Jurassic to Cenzoic sediments in the western strand of the Greater Caucasus Basin connecting eastwards to the South Caspian Basin (Adamia et al., 2011b; Golonka, 2004; Saintot et al., 2006a; Zonenshain and Le Pichon, 1986). The onset of sedimentation in the Sinemurian to Pliensbachian (199-183 Ma), and the main phase of rifting occurred in the Aalenian to Bajocian (~174-168 Ma), during which time deep-marine clastic rocks and marls, and Jurassic and mid-Cretaceous volcanic rocks were deposited (Adamia et al., 2011b; McCann et al., 2010; Robinson et al., 1996; Saintot et al., 2006a; Topchishvili, 1996). Aalenian (~174-170 Ma) basalts have MORB-like compositions (Saintot et al., 2006a), suggesting that extension reached a point of near-continental breakup, although there is no unequivocal evidence for oceanization in the Greater Caucasus Basin, which had been underlain by hyperextended crust (e.g., McCann et al., 2010)). Absolute extension estimates are absent, but local oceanization or hyperextension in the Black Sea Basin followed upon an estimated 160 km of extension (Hippolyte et al., 2010; Munteanu et al., 2011; Okay et al., 1994), which may provide an analogue for the extension in the Greater Caucasus Basin. A second phase of subsidence in the Late Cretaceous to Paleocene was proposed to be related to extension in the eastern Black Sea Basin (Mikhailov et al., 1999; Vincent et al., 2016), but the amount of extension remains unquantified.

Contraction in the Caucasus is dated as latest Eocene (~35 Ma) through the onset of foredeep sedimentation in the Fore-Caucasus region overlying the Scythian Platform, in growth strata seen on seismic lines across the eastern Black Sea, and recorded in the southern foreland basins of the Greater Caucasus (e.g., Ershov et al., 2003; Gamkrelidze, 1986; Mikhailov et al., 1999; Robinson et al., 1996; Vincent et al., 2016). This was followed by erosional exhumation of the Greater Causasus reflected in Oligocene (~30 Ma) low-temperature thermochronological data (Vincent et al., 2007, 2011). The bulk of Caucasus uplift occurred since early Pliocene time, ~5 Ma, during which time thrusting propagated into the Kura foldbelt (Avdeev and Niemi, 2011; Cowgill et al., 2016; Forte et al., 2013; Mosar et al., 2010) where convergence is still accommodated today at several mm/yr (Sokhadze et al., 2018).

The Great Caucasus Basin is traced southward to the Racha–Lechkhumy Fault, which appears to have formed the Mesozoic basin-bounding normal fault (Saintot et al., 2006a; Yakovlev, 2005) (Fig. 15), reactivated as or cut by a thrust during Cenozoic Caucasus orogenesis. To the south of the Racha-Lechkhumy Fault lie the **Transcaucasus** Massifs, which comprises a Variscan basement and which form the northern margin of the north-verging **Lesser Caucasus** fold-and-thrust belt that thrust over the relics of the Greater Caucasus Basin (Banks et al., 1998; Robinson, 1997; Vincent et al., 2005) (Fig. 15). The Transcaucasus range exposed in the Dzirula-Khrami-Loki Massifs, contain a polyphase, Proterozoic to Carboniferous crystalline basement with ~329–337 Ma high-pressure metamorphism (Rolland et al., 2011) and widespread, 330-280 Ma granite intrusion and HT-LP metamorphism (Rolland et al., 2016).

The pre-Alpine basement of the Transcaucasus range is overlain by the Lesser Caucasus volcanic arc with ages ranging from ~185 Ma – 110 Ma (Adamia et al., 1981; Mederer et al., 2013; Rolland et al., 2011). Younger, voluminous magmatism of ~50 Ma also cut the Sevan-Akera suture (Fig. 15) between the Transcaucasus and the South Armenian Block (Rolland et al., 2009a; Sokół et al., 2018), and

widespread late Miocene-recent volcanism affecting the entire East Anatolian High Plateau extended into the South Armenian and Transcaucasus blocks (Dilek et al., 2010; Karapetian et al., 2001; Keskin et al., 1998; Neill et al., 2013, 2015; Yılmaz et al., 1987). The Lesser Caucasus volcanic arc is interpreted as contiguous with the Pontide Arc to the west (Yılmaz et al., 2000), and is thought to have formed above a north-dipping subduction zone above which the Greater Caucasus Basin formed as a back-arc basin (Rolland et al., 2011, 2016). To the west, in the Achara-Trialet region (Figs. 1 and 15), the oldest exposed rocks are Aptian to Turonian volcaniclastics, Maastrichtian to Paleocene limestones, and a ~5 km thick Paleocene to lower Eocene turbiditic clastic series topped by Middle-upper Eocene arc volcanic and volcaniclastic series (Adamia et al., 2017; Lordkipanidze et al., 1989), deposited either during eastern Black Sea extension (e.g., Saintot and Angelier, 2002; Vincent et al., 2016; Yılmaz et al., 2014), or inversion (e.g., Sheremet et al., 2016b) (see section 5.12.1).

The Transcaucasus metamorphic and post-Carboniferous sedimentary history is widely correlated based on its metamorphic facies and age, and post-metamorphic Paleozoic sedimentary cover to the Variscan basement of the crystalline core of the Greater Caucasus, which would suggest that the Transcaucasus range has been part of Eurasia since the Variscan orogeny in Carboniferous time (e.g., Rolland et al., 2016). On the other hand, the Transcaucasus also correlates well to the eastern Pontides in metamorphic facies and (Yılmaz et al., 2000), therefore suggesting that these are the same tectonic blocks. From this, it would follow that the eastern Pontides, and by inference also Sakarya and the Istanbul Zone, have been part of Eurasia since the Paleozoic, whilst the logic from the western Pontides and particularly Crimea suggests that the Pontides may have been Cimmerian blocks separated by a late Triassic-Jurassic Paleotethys suture from Eurasia (e.g., Dokuz et al., 2017; Şengör and Yılmaz, 1981; Şengör et al., 1980). We will return to this debate in section 7.10, but we here note that the Caucasus region has a conspicuous absence of a record of Permian to Lower Jurassic subduction – no arc, no accretionary prism, no metamorphic record is present. During this time interval, only occasional heating caused resetting of $^{40}Ar/^{39}Ar$ ages in the eastern Pontides and Transcaucasus Massifs (Rolland et al., 2011). Because such records are present to the west (e.g., in the Karakaya complex) and in the east in Iran (Triassic Paleotethys suture), it is quite unlikely that there was no subduction in the early Paleozoic in the Caucasus segment, and the record must be quite incomplete. Scholars who studied the Caucasus place the Paleotethys subduction zone between the Transcaucasus ranges and the South Armenian Block (Adamia et al., 1981; Rolland et al., 2011, 2016; Yılmaz et al., 2014). Alternatively, Şengör (1987) and Natal'in and Şengör (2005) suggested that the Paleotethys suture is located between the Transcaucasus range and the Scythian Platform, but was somehow obscured by suture-parallel strike-slip duplexing. We note that if shortening has indeed been as much as 300 km, as suggested structurally as well as from paleomagnetic restoration of the conspicuous northward bend formed by the eastern Pontides – Lesser Caucasus – Talysz region that formed after the middle Eocene (Meijers et al., 2017; van der Boon et al., 2018), a Mesozoic record of accretion and subduction between the Transcaucasus range and the Greater Caucasus may have first been obliterated by Greater Caucasus Basin extension, and subsequently buried below the Greater Caucasus.

South of the Transcaucasus and the Lesser Caucasus Arc is a belt of **Jurassic ophiolites** that demarcates the Sevan-Akera suture and lies thrust upon the South Armenian Block (Knipper and Khain, 1980) (Figs. 15 and 17). This belt of ophiolites is thought to be the eastern continuation of the south Pontide ophiolites in northern Turkey (Hässig et al., 2013b). They contain ~180-170 Myr old oceanic crust with a MORB to arc geochemical signature interpreted to have formed in an upper Plate above a Jurassic subduction zone (Galoyan et al., 2007, 2009; Hässig et al., 2013a; Rolland et al., 2010), whereby all elements of the ophiolite sequence are found overlain by pillow lavas or Middle to Upper Jurassic radiolarian cherts (Danelian et al., 2006, 2010, 2015). Hässig et al. (2017) interpreted this as evidence for sea floor spreading dominated by detachment faulting rather than magmatic accretion. The Jurassic ophiolites are overlain by Lower Cretaceous lavas with an OIB signature that are interbedded with pelagic limestones (Rolland et al., 2009b). The youngest of these are found on the Amasia Ophiolite (Fig. 15), bracketed between ~113 and 92 Ma by radiolarian cherts (Asatryan et al., 2012; Danelian et al., 2014). This extended magmatism is not related to SSZ spreading, but was interpreted as either plume-related, or sub-slab mantle melting, e.g. facilitated through slab break-off, or slab edges (Hässig et al. (2017); see Nikogosian et al. (2018) for recent examples of such lavas in Turkey).

Below the Amasia and associated ophiolites lies a mélange that contains blueschist-grade metabasites, which yielded $^{40}Ar/^{39}Ar$ phengite ages of 95–90 Ma, whist epidote-amphibolite retrogression was dated at 73.5–71 Ma (Rolland et al., 2009a). The latter ages are interpreted as post-collisional exhumation ages. Hässig et al. (2019) recently also found amphibolites (~600 °C, 6–7 kbar) in the mélange below the Amasia Ophiolite with 90 ± 2 Ma $^{40}Ar/^{39}Ar$ ages of amphibole and mica and rutile U/Pb ages and interpreted these rocks as derived from a dismembered metamorphic sole.

The **South Armenian Block** consists of a Proterozoic basement with ages consistent with a peri-Gondwana origin, an incomplete section of Paleozoic to Upper Cretaceous (volcano-)sedimentary rocks, and an ophiolite-derived, Coniacian to Santonian (~90-84 Ma) flysch (Sosson et al., 2010, and references therein). This flysch appears to also overlie the ophiolites, as a forearc basin deposit, and connects to the Lesser Caucasus Arc (Rolland et al., 2012). This shows that the Jurassic ophiolites formed the forearc of the Lesser Caucasus Arc, and ophiolite obduction essentially dates South Armenian Block-Transcaucasus collision, as in the eastern Pontides (Topuz et al., 2014a). The final collision between the South Armenian Block and the Transcaucasus range is bracketed between ~80 and 75 Ma (Rolland et al., 2012).

Hässig et al. (2015) showed that the South Armenian Block was intruded by a 157 Ma granodiorite that cooled, assumedly by extension, around ~120 Ma. They interpreted this granodiorite to be subduction-related. The South Armenian Block was intruded by large arc-related, porphyry copper-bearing plutons in Eocene to early Miocene time (~50-20 Ma) (Moritz et al., 2016; Rezeau et al., 2016, 2017).

Most authors assume that the South Armenian Block was a contiguous part of the Taurides, given the similarities in basement and stratigraphy, and especially the age of obduction of the Jurassic Armenian ophiolites, in the late Cretaceous (e.g., (Barrier et al., 2008; Hässig et al., 2013a, 2017; Meijers et al., 2015a; Menant et al., 2016; Rolland et al., 2012). Continent-derived rock units to the south of the South Armenian Block, comprising the Taurides units east of the Gürün Curl, as well as the Bitlis and Püturge Massifs (see below), are all overlain by Cretaceous SSZ ophiolites (Fig. 15). Towards the west, in the Sivas Basin area, these Cretaceous ophiolites are found overthrust in Cenozoic time by the Jurassic ophiolites of the southern Pontide margin (Topuz et al., 2014a, 2014b; see section 5.12.1), suggesting that the Taurides were in the downgoing Plate relative to two subduction zones that contained oceanic lithosphere in their upper Plate – a southern with Cretaceous and a northern with Jurassic crust, whereas the South Armenian Block was in a downgoing Plate position relative to only the northern one. Upper Cretaceous SSZ ophiolites only found backthrust northward onto the South Armenian Block. The ~83-78 Ma metamorphism in the easternmost Taurides to the south of

the South Armenian Block (Topuz et al., 2017) shows that obduction of the Cretaceous ophiolites onto the eastern Taurides occurred more or less simultaneously with the emplacement of Jurassic ophiolites onto the South Armenian Block at two different subduction zones. The South Armenian Block is thus separated by a suture (Yılmaz et al., 2014), here coined **Kağızman-Khoy suture** from the easternmost Taurides. This suture is demarcated by a belt of ophiolites from the Kağızman Ophiolite close to the Pontides to the Khoy Ophiolite in easternmost Turkey and westernmost Iran (Fig. 15) (Yılmaz et al., 2014). Along the northern margin of this suture, on the South Armenian Block in NE Turkey, there is Eocene to Miocene sedimentation in the Kağızman-Tuzluca Basin (Fig. 15), which in Oligocene is briefly marine, and evaporites formed (Varol et al., 2016). This basin may be a lateral continuation of the Sivas Basin and may indicate that convergence between the easternmost Taurides and the South Armenian Block continued into the Oligo-Miocene.

The Kağızman-Khoy suture must have witnessed the history of two subduction systems: the first one was intra-oceanic and emplaced Cretaceous SSZ ophiolites onto the easternmost Taurides causing ~83-78 Ma metamorphism (Topuz et al., 2017). The second one closed the ocean basin and led to juxtaposition of the easternmost Taurides and the South Armenian Block. This latter closure likely occurred after ~80-75 Ma, when the South Armenian Block collided with and accreted to the Transcaucasus (Rolland et al., 2012) and subduction moved south, either re-initiating, or (more likely) after accreting the crust of the South Armenian Block to the Transcaucasus Block in the upper Plate.

The Khoy Ophiolite complex is the best studied of the suture between the South Armenian Block and the easternmost Taurides. The Khoy complex is juxtaposed against the Iranian Cimmerian blocks to the east, the South Armenian Block to the North and the easternmost Taurides to the west (Fig. 15). Detailed mapping has led to the interpretation that this complex consists of a long-lived, Jurassic to Upper Cretaceous (180-65 Ma), ocean-derived, and metamorphosed accretionary prism in the east and a non-metamorphosed, Upper Cretaceous, 'Penrose'-type ophiolite in the west (Khalatbari-Jafari et al., 2003, 2004). The accretionary prism is interpreted to have formed below the Iranian Cimmerides after their suturing against Eurasia in the late Triassic (Khalatbari-Jafari et al., 2003). An alternative view correlates this pre-Cretaceous part of the Khoy Ophiolite to the Sanandaj-Sirjan Zone of Iran based on finding of much older, up to Ediacaran zircons in the 'Jurassic' belt (Moghadam et al., 2019). Either way, the Cretaceous Khoy Ophiolite is of supra-subduction zone nature (Monsef et al., 2010) and thrusted onto the easternmost Taurides or Bitlis Massif (Khalatbari-Jafari et al., 2003). Below the Khoy Ophiolites lie Campanian olistostromes, equivalent to the Bozkır ununit, but on our map included in the ophiolite complex (Fig. 15). These likely date the obduction, of similar age as the metamorphism documented in the easternmost Taurides identified by Topuz et al. (2017) (see below). The Khoy prism and ophiolite also lie backthrust northward onto the South Armenian Block (Avagyan et al., 2017). To the southeast of Khoy, the easternmost Taurides disappear, and a single belt of ophiolites is found fringing the suture zone between the Cimmerian blocks of Iran and the Arabian foreland (e.g., Rezaii and Moazzen, 2014).

The Taurides to the south of the South Armenian Block, and to the east of the Gürün Curl (Fig. 15) are mostly low to high-grade metamorphic. The degree of metamorphism increases both eastward and southward. In the Munzur Mountains, Tauride Platform rocks mostly escaped metamorphism despite being obducted by ophiolites (e.g. the Divriği Ophiolite, Fig. 15) in Campanian time (Yılmaz, 1985, 1994). From there southward, the Munzur Mountains are bounded (in its latest configuration along an Eocene top-to-the-south thrust (Kuşcu et al., 2010; Michard et al., 1984; Perincek and Kozlu, 1984) by the low-grade Keban metamorphics, which are bounded in the south by the up to eclogite-facies Bitlis-Pütürge metamorphics (e.g., Oberhänsli et al., 2012). Towards the east, metamorphic grades in the easternmost Taurides increase to amphibolite facies (Topuz et al., 2017). All these east Anatolian Tauride units lack a contiguous Cenozoic stratigraphy, but instead, uppermost Cretaceous and Cenozoic sedimentary and volcanic rocks unconformably overlie metamorphosed and exhumed Tauride units and overlying ophiolites (Kuşcu et al., 2010; Topuz et al., 2017; Yılmaz et al., 2010). These ophiolites are also Cretaceous SSZ ophiolites (e.g., near Divriği (Kavak et al., 2017; Kuşcu et al., 2010). The metamorphosed easternmost Taurides and Keban metamorphics and overlying ophiolites were subsequently intruded by syenitic granitoids, with 74–68 Ma ages (Kuşcu et al., 2010).

South of the Keban metamorphics and easternmost Taurides lie the **Bitlis and Püturge** metamorphic massifs, along the northwestern perimeter of the Arabian Platform, over an E-W distance of 500 km (Erdem and Bingöl, 1995; Göncüoğlu and Turhan, 1984) (Figs. 1 and 15). The Bitlis-Püturge Massifs are overthrust by Cretaceous SSZ ophiolites (e.g., the Guleman Ophiolite (Rizeli et al., 2016)) (Fig. 15), overthrust Cretaceous ophiolites, experienced Late Cretaceous metamorphism, and have stratigraphies not younger than Triassic. In addition, the Bitlis and Püturge Massifs expose a Pan-African and older, Neoproterozoic basement (Beyarslan et al., 2016; Ustaömer et al., 2012) overlain by a Devonian section intruded by granitoids. Overlying Upper Permian limestones seal the granitoids, constraining a pre-Late Paleozoic intrusion age (Göncüoğlu and Turhan, 1984). Second, the Bitlis Massif underwent eclogite and blueschist metamorphism, i.e. much higher pressure than the Keban metamorphics. U/Pb zircon ages of 85–82 Ma, and $^{40}Ar/^{39}Ar$ phengite cooling ages of 78–65 Ma (Oberhänsli et al., 2010a, 2012, 2014), are similar to K/Ar and Rb/Sr ages from the Püturge Massif (Helvaci and Griffin, 1984; Hempton, 1985) and reveal similar timing of metamorphism as to the metamorphics to the north and west. The 85-82 Ma metamorphism is interpreted to result from the obduction of the Guleman and other ophiolites onto the Bitlis Massif (Göncüoğlu and Turhan, 1984; Şengör and Yılmaz, 1981).

The Bitlis-Püturge, as well as the Keban metamorphics, exhumed between 80 and ~70 Ma. The Keban memamorphic rocks were exhumed by Late Cretaceous time and were are overlain by Upper Cretaceous to Eocene volcanic and sedimentary rocks (Kuşcu et al., 2010; Perincek and Kozlu, 1984). The Bitlis-Püturge metamorphics were first covered by Maden volcano-sediments in Eocene time (~55 Ma) showing that (extensional) unroofing may have continued somewhat longer in the southernmost massifs. There is no evidence for significant unroofing after the Eocene, until the latest phase of Miocene exhumation ascribed to uplift and erosion, based on low-temperature thermochronology constraints (Cavazza et al., 2018) (see below).

Collectively, these data suggest that the Bitlis and Püturge Massifs represent more distal, deeper underthrust equivalents of the southern Tauride Platform than the Keban metamorphics. Otherwise, these massifs seem to share a similar Cretaceous history of obduction, out-of-sequence thrusting, and exhumation. This exhumation in Late Cretaceous to early Eocene time was presumably extensional, but major detachments have not been identified – but detailed structural analysis has not been widely performed and future field analyses are required.

During and after exhumation, the Keban and Bitlis-Pütürge Massifs were overlain by prominent arc complexes. The ~83-70 Ma **Elazığ magmatic suite** (or Baskil Arc, and eastwards, Yüksekova complex) is a complex of intermediate to felsic intrusive and extrusive rocks (Beyarslan and Bingöl, 2000; Çolakoğlu et al., 2014; Karaoğlan et al., 2013a; Kuşcu et al., 2013; Tekin et al., 2015). It

intrudes and overlies the Kömürhan Ophiolite and is overthrust northward by the Püturge metamorphics (Aktaş and Robertson, 1990; Beyarslan and Bingöl, 2000). The Keban metamorphics, Kömürhan Ophiolite, and Elazığ magmatic suite are thought to have extensionally exhumed in the Late Cretaceous to Paleogene and are unconformably covered by the middle Eocene-Oligocene clastic sediments and limestones (Kırkgeçit Group) (Beyarslan and Bingöl, 2000; Kuşcu et al., 2013).

To the south of the Elazığ magmatic suite, as part of a volcanic belt that runs from Kahramanmaraş in the west to Lake Van in the east (Elmas and Yılmaz, 2003; Nurlu et al., 2016; Yıldırım, 2015), lies the still younger, Late Paleocene to early Eocene **Maden complex**, a series of marine sediments and arc volcanic rocks (Aktaş and Robertson, 1984; Yıldırım, 2015; Yılmaz, 1993). Towards the east, a time-equivalent unit without abundant arc magmatic rocks is known as the **Hakkari complex** and consists of a mélange unit that includes Eocene limestone blocks, and a tectonically underlying low-grade metasedimentary unit known as the Urse formation of Early to middle Eocene age (Oberhänsli et al., 2010b; Yılmaz, 1993) and references therein). The Maden complex has shallow marine middle Eocene limestones at the base, but then rapidly deepens towards middle Eocene radiolarian cherts. Because of the deepening sequence within the Maden stratigraphy, the complex is interpreted to have formed in an extensional upper Plate setting (Aktaş and Robertson, 1984; Önal and Kaya, 2007; Robertson et al., 2006, 2007; Yiğitbaş and Yılmaz, 1996). Across the easternmost Taurides to the north of the Maden Arc, Eocene magmatism and associated mineralizations are widespread, with 50–43 Ma ages for magmatism and associated mineralizations, interpreted to have formed in the back-arc of the Maden Arc (İmer et al., 2013; Kuşcu et al., 2013).

In the west, the complex unconformably covers and intrudes the Püturge Massif and overlying ophiolites (Aktaş and Robertson, 1984; Erdem and Bingöl, 1995; Göncüoğlu and Turhan, 1984; Oberhänsli et al., 2010b; Yılmaz, 1993). The complex is also overthrust by the Pöturge and Bitlis Massifs in the west and east, and the Kömürhan Ophiolite and overlying Elazığ magmatic complex to the north. To the west of the Püturge Massif, rocks of the Maden group are overthrust by the granulite-facies (800 ± 100 °C, 13–15 kbar) Doğanşehir meta-ophiolite and overlying Malatya metamorphics (Awalt and Whitney, 2018). The metaophiolite yielded Sm/Nd ages of 52–50 Ma for metamorphism, and is intruded by 51–45 Ma granitoids, suggesting that the high temperatures occurred in the root of the Maden Arc (Karaoğlan et al., 2013b). This shows that the Maden Arc also formed within the Malatya metamorphic complex and underlying ophiolites. The exhumation of the Dogansehir Ophiolite likely occurred due to Maden intra-arc extension (Karaoğlan et al., 2013b). The thrust contact between the Bitlis Massif and overlying ophiolites, and the Hakkari complexes is the region south and west of Van unconformably covered by the uppermost Eocene to lower Miocene Kırkgeçit Formation of the Muş-Hınıs Basin (Hüsing et al., 2009b; Huvaz, 2009) showing late Eocene thrusting.

The Bitlis lies thrust on the intensely deformed Gevan Ophiolite, which is also overlain by deformed with Maastrichtian limestones with rudists similar to those from Arabia (Özer, 2005) and is thus likely one of the Arabian ophiolites (Oberhänsli et al., 2010b; Yılmaz et al., 1981). This constraints Miocene thrusting of the Eocene Hakkari and Maden complexes and overlying Bitlis-Püturge nappe stack onto Arabia by at least 40 km.

We note that Eocene sediments that unconformably overlie the metamorphics, are involved in all major thrust zones that currently define the SE Anatolian orogen, and the modern architecture of the orogen is thus Eocene or younger in age. The structures associated with Turonian-Cenomanian obduction, and subsequent late Cretaceous exhumation, are obscured or reactivated, and remain unidentified.

Apatite fission track and zircon U-Th-He ages of the Bitlis and Püturge Massifs have revealed a cluster of ages between ~18 ands 13 Ma, and also the underlying Hakkari-Maden complexes (18 ± 2 and 25 ± 7 Ma) and overlying Oligocene (Hüsing et al., 2009b) Muş Basin (13.7 ± 0.2 Ma) yielded Miocene ages (Cavazza et al., 2018; Okay et al., 2010). Finally, the subsidence modelling in the Muş Basin revealed a distinct phase of middle Miocene uplift (Huvaz, 2009). Collectively, these data demonstrate that the onset of thrusting of the Bitlis-Püturge-Hakkari-Maden nappe stack onto the Arabian continental foreland likely started around 18 Ma and lasted until at least ~13 Ma, and given ongoing foreland basin sedimentation in the Kahramanmaraş Basin (Hüsing et al., 2009b), likely until at least 11 Ma (Fig. 17).

6. Kinematic restorations tested against paleomagnetic data

6.1. Paleomagnetic database of the Mediterranean region

As explained in the method section, vertical axis rotations of our reconstruction are tested against, and in cases where structural constraints are lacking, based on paleomagnetic constraints (included in Table 1). We compiled a database of 2300 paleomagnetic sites from the orogens and tectonic blocks of the Mediterranean region published in the last 50 years, from several hundred publications. This database is too large to comprehensively display in figures or tables. We have instead developed a paleomagnetic database, provided in Supplementary Information 2, both in the form of Supplementary Tables, and as files for the online tool www.paleomagnetism.org (Koymans et al., 2016). Each site entry in the database contains a reference to the published source, which is listed in the reference list of this paper. All sites are given in tectonic coordinates (i.e., corrected for bedding tilt) unless in rare cases where rotations were concluded by the original authors based on remagnetized sites, or in cases of sites from plutonic rocks where no paleohorizontal was available. Reversed paleomagnetic directions were converted to normal polarity.

The database was built according to the following selection criteria: Paleomagnetic data from rocks older than the Triassic, as well as archeomagnetic data from the Holocene, were not included in the compilation. We applied and expanded on quality criteria as detailed in Lippert et al. (2014): Data were excluded from sites that (1) are not used by the original authors if reason for exclusion is provided; (2) are characterized by fewer than four samples; (3) were not analyzed using principle component analysis (Kirschvink, 1980); (4) have site k or K-values below 7. We normally prefer to apply the $A95_{min/max}$ reliability envelope of Deenen et al. (2011), but A95 values are often not provided and estimating these from the parametrically sampled datasets adds uncertainty. Hence, we include all data interpreted to be primary by the original authors, whereby we use $k/K = 7$ as the bare minimum. Typical paleomagnetic scatters as a result of paleosecular variation have K-values of 12.5–50 (Deenen et al., 2011) and we thus include a maximum amount of data. The resulting dataset is so large that we consider outliers as a result of inclusion of undersampled PSV records, or enhanced scatters due to added sources of error to be averaged out; and (5) contain magnetizations of primary origin, or in rare cases of well-dated secondary origin, as interpreted by the original authors. In addition, lava sites were discarded if these (6) contained directions of mixed polarity, as lava sites should be spot readings that cannot record a reversal; (7) have k-values (Fisher (1953) precision parameter) <50; or (8) are beyond a 45° angular threshold (following Johnson et al. (2008)). To ensure that the paleomagnetic database only contains paleomagnetic directions that average (at least to some extent) paleosecular variation of the paleomagnetic field (PSV), we only include data from lava sites where at least 4

sites could be averaged from a small area. Whenever fewer lava sites were reported, these were not included in the database.

Paleomagnetic data from sedimentary sites were included on a per-site level as reported by the original authors where possible. The paleomagnetic community does normally not publish their original data, but only statistical descriptions of the data set. Regional rotations are then obtained by averaging site averages, whereby the definition of a site changes from author to author. Some consider a site a spot reading of the magnetic field. This is correct for lava sites, whereby acquisition of the natural remanent magnetization occurs geologically instantaneous upon lava cooling and the recorded direction is a spot reading of the paleomagnetic field. For sedimentary sites or plutonic rocks, however, each sample can be at first order considered a spot reading (although for sediments with low sedimentation rates some averaging of PSV may occur within one sample). As pointed out by Deenen et al. (2011), a better approach is then to always perform statistics on paleomagnetic directions instead of site averages, also to weigh larger over smaller datasets. Except for the few sites where we had the original directions at our disposal, we have therefore created parametrically sampled data sets for each site, a default procedure in Paleomagnetism.org. The average directions in the database are based on these parametrically sampled data sets and may differ somewhat from the published average directions. Given the large number of sites (2300), these deviations are insignificant. In almost all cases, however, we have followed the site definition of the original authors, although at times we have combined paleomagnetic sites from the same study at the same location in the same formation by combining (parametrically sampled) directions.

Most papers do not provide GPS coordinates of sampling sites but indicate approximate locations on sketch maps. In cases that no accurate information was provided, we have attempted to determine sampling locations with the provided information, using Google Earth. Where many sites were sampled within a few kilometers, and no individual sampling locations could be determined for each site, we have grouped these into new sites based on parametrically sampled directions.

From this extensive database (see Supplementary Information), we show maps with measured declinations for the areas reviewed below. The tool set on www.paleomagnetism.org (Koymans et al., 2016) allows to predict the APWP for any element in the reconstruction, by providing their Euler poles in 10 Myr intervals relative to South Africa (Plate ID 701) (for methodology see Li et al. (2017)). The program will then calculate the Global APWP (where we chose Torsvik et al. (2012) as our paleomagnetic frame of reference) in the coordinates of the reconstructed element. Where datasets from blocks in our reconstruction were sufficiently large, we used these to calculate independent APWPs, e.g., for Iberia, Adria, and several nappe systems in the Mediterranean orogens (Table 1). To this end, we followed the same approach as Torsvik et al. (2012), applying a 20 Myr sliding window and 10 Myr intervals. We primarily use these paleomagnetic datasets to test vertical axis rotations, which often happen on a shorter time scale than the 20 Myr sliding window, and rotations in both the calculated and predicted APWPs thus tend to be smeared out over longer time intervals than the actual rotation interval. Where this may be the case, this will be discussed.

6.2. Paleomagnetic tests and constraints on reconstruction

Based on the Atlantic Plate circuit and the constraints on deformation in the Mediterranean region as explained in the previous section, we developed a geometrically and kinematically consistent restoration using the GPlates reconstruction software (Supplementary Information 3). Here, we test the reconstruction against the paleomagnetic database for the Mediterranean region. As explained in the reconstruction hierarchy (section 3), we use paleomagnetic data as test, and only modified the reconstruction in case of clear inconsistencies with the paleomagnetic database. Because the paleolatitudinal motion of Africa relative to Eurasia in western and central Anatolia is within 1000 km, tests of our reconstruction against paleolatitudes are mostly inconclusive. Those tests we only apply to the eastern Mediterranean region (Pontides, South Armenian Block) and focus mostly on vertical axis rotation histories. Where our reconstruction is modified based on paleomagnetic data – without violating Plate circuit or structural constraints – this is indicated in Table 1. The motion of AFR with respect to EUR fixed.

6.2.1. Iberia

A paleomagnetic database for stable Iberia for rocks of 200 Ma and younger was recently compiled by Vissers et al. (2016). To this database, we added a few recently published poles, and added data from the Triassic, as well as from the Pyrenees and the Pyrenean foreland.

Data from stable Iberia cluster well around the Iberian APWP predicted by the marine magnetic anomaly-based reconstruction (Fig. 18) (van Hinsbergen et al., 2017; Vissers et al., 2016). Moreover, Ruiz-Martínez et al. (2012) showed that reconstructing Iberia according to marine magnetic anomalies leads to an optimal clustering of Iberian, African and North American paleomagnertic poles of the latest Triassic. We follow Gong et al. (2008) and Vissers et al. (2016) in using these paleomagnetic data to finetune the timing of Iberian rotation relative to Eurasia, which occurred during the Cretaceous Superchron, to Aptian (126-112 Ma) (Table 1). Both the timing and amount of the Cretaceous Iberian rotation phase are controversial, as the paleomagnetic and marine magnetic anomaly data argue against the interpretation that high temperature metamorphism and peridotite exhumation in the Pyrenees are contemporaneous, and causally related. We refer to Vissers et al. (2016) and van Hinsbergen et al. (2017) for a detailed discussion, and here follow the marine magnetic anomaly and paleomagnetic constraints, which are both inconsistent with Iberia-Eurasia divergence in the Early Cretaceous.

In addition, an extensive set of paleomagnetic poles from the Permo-Triassic of the axial zone of the North Pyrenean Zone in the western Pyrenees shows scattered, often large rotations deviating consistently clockwise, but with rotations of 0–90° relative to the Iberian APWP (Fig. 18). We interpret these as local rotations associated with strike-slip components of Iberia-Europe motion accommodated along the North Pyrenean Fault zone (Vissers and Meijer, 2012a) and have not reconstructed these in detail. Further inspection shows that data from the Pyrenees and Pyrenean foreland show more scattered declinations than those from stable Iberia, suggesting local thrust-related rotations of up to ~30°, which we have not restored in detail. Finally, two localities from the Balearic islands show declinations that suggest ~30–40° cw rotation relative to Iberia, more than the ~20° cw Oligocene-early Miocene rotation suggested by restoring extension in the Gulf of Valencia (Séranne, 1999). We interpret this to result from local rotations during thrusting (Gelabert et al., 1992).

6.2.2. Adria

Paleomagnetic data from Adria are available from rocks of ~185 Ma and younger in the southern Alps foreland, the Istria Peninsula of Croatia, and the Gargano and Puglia Peninsulas of Italy (Fig. 19). For pre-Miocene time, these are systematically offset relative to the APWP of Africa, suggesting that Adria rotated relative to Africa, estimated in van Hinsbergen et al. (2014b) at ~10° counterclockwise between 20 and 0 Ma. We adopt this rotation, which leads to a good match between the predicted GAPWaP of Torsvik et al. (2012) in coordinates of Adria, and the APWP

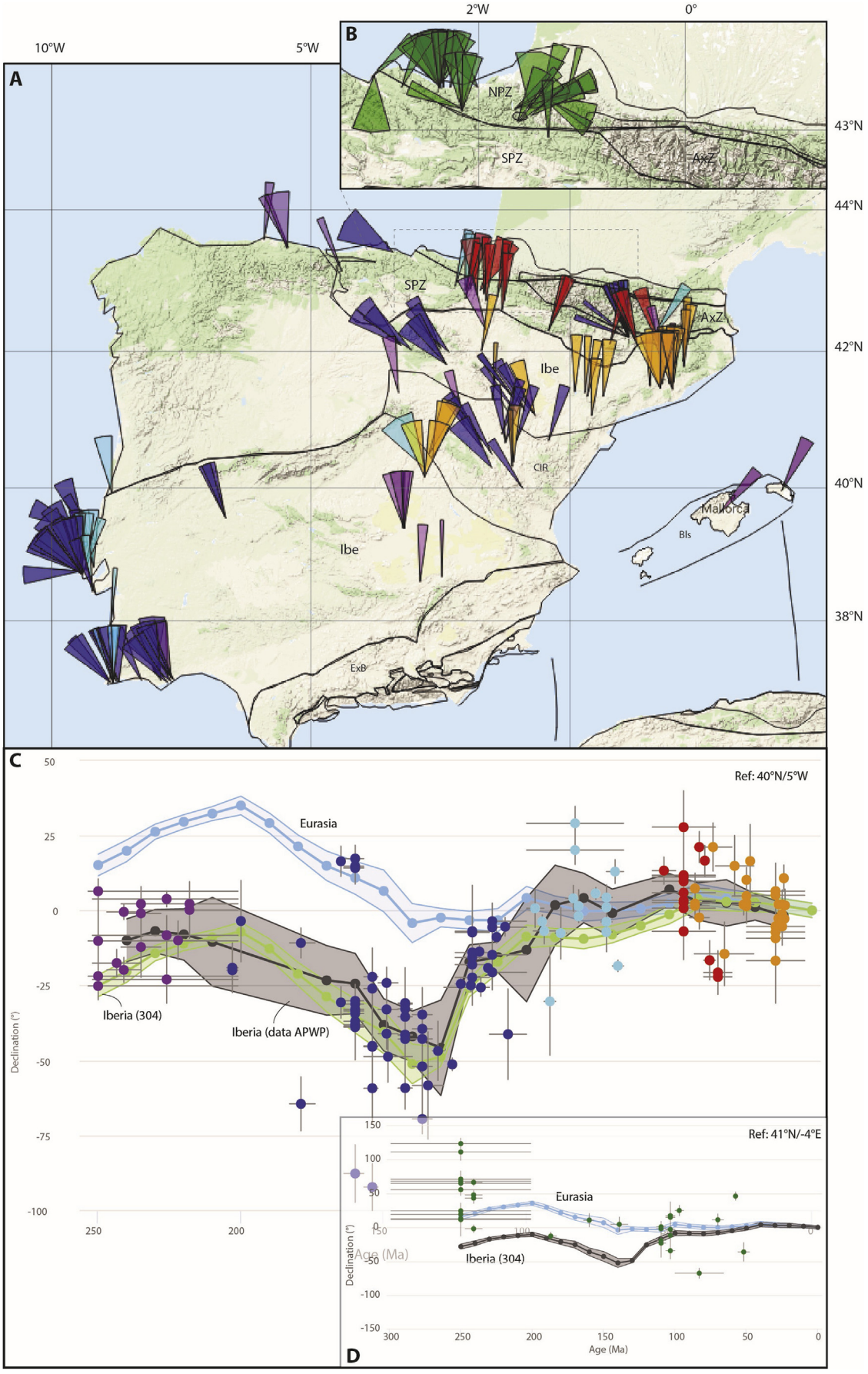
A
B
C
D
10°W
5°W
2°W
0°
43°N
44°N
42°N
40°N
38°N
NPZ
SPZ
AxZ
Ibe
CIR
Mallorca
Bls
ExB
Ref: 40°N/5°W
Eurasia
Iberia (304)
Iberia (data APWP)
Declination (°)
Age (Ma)
Ref: 41°N/-4°E

calculated based on Adria paleomagnetic data (Fig. 19; Table 1). The paleomagnetic data allow for a somewhat smaller rotation of ~5°ccw proposed by Le Breton et al. (2017), which was in part based on interpretations of seismic tomography, which is outside of our reconstruction hierarchy. For consistency with the rest of the reconstruction, we therefore adopt the reconstruction of van Hinsbergen et al. (2014b). The consistently higher Adria-Africa rotation of up to 20°ccw proposed by e.g., Márton et al. (2011b, 2017) appear to not be representative for the data, and requires major Neogene extension between Adria and Africa, for which there is no evidence. Some scattering of the declinations occurs on the Istria Peninsula of Croatia, which we interpret as local rotations resulting from young deformation.

6.2.3. Alboran domain

Paleomagnetic constraints of the Alboran domain in the Betic Cordillera of Southern Iberia come from Jurassic and Upper Cretaceous and Mio-Pliocene sediments from the External Betic chain, from Neogene sedimentary basins overlying the Alboran domain (Malaguide, Alpujarride and Nevado-Filabride units), from Oligocene mafic dykes in the Alpujarride and Malaguide units, and from the Ronda peridotite (Fig. 20). In the Rif belt, paleomagnetic directions were obtained from Eocene to Miocene sediments overlying the Ghomaride nappes, from the Beni Boussera and Ceuta peridotite bodies, and from Cenozoic rocks of the African margin-derived External Rif fold-and-thrust belt (Fig. 20).

Data from Jurassic and Cretaceous rocks in the External Betics, comprising nappes decoupled from the Iberian foreland below the advancing Alboran Platelet, reveal a pattern of consistently clockwise rotations. There are, however, major variations in the amount of rotation particularly in the northeastern Betic cordillera, reaching 90° or more (Fig. 20), and no systematic relationship has been detected between declination and orogen strike. These rotations are interpreted to result from thrust sheet rotations within the Sub-Betic thrust belt resulting from highly oblique convergence between the westward advancing Alboran Platelet and southern Iberian continental margin (Platt et al., 1995, 2003, 2013; Platzman, 1994). The absence of correlation between paleomagnetic declination and orogen strike indicates that the Sub-Betic chain is not an orocline — an originally straight fold-and-thrust belt that was subsequently bent (Carey, 1955). We have not specifically included the detailed rotations of the various thrust nappes of the Sub-Betic chain in our reconstruction, which follows that of van Hinsbergen et al. (2014a), but the general highly oblique thrusting that is thought to cause these rotations is clearly present.

Paleomagnetic data from the External Rif show a similar pattern, but with consistently counterclockwise rotations that continued into the Miocene (Fig. 20). Also in this case, there is no systematic relationship between declination and strike, and rotations are interpreted as thrust-sheet rotations during oblique convergence (Cifelli et al., 2008b). Mesozoic rocks from the Dorsale Calcaire sampled by (Platzman and Lowrie, 1992; Platzman et al., 1994) yielded major clockwise as well as counterclockwise rotations. These are difficult to interpret as the Dorsale Calcaire accreted to the Alboran Platelet in Eo-Oligocene time, subsequently moved westwards as part of the Alboran forearc, and subsequently thrust onto the African margin. We therefore do not specifically restore the individual thrust sheets of the Calcaire Dorsale but note that the overall left-lateral shear between this unit and the African margin proposed to explain these rotations (Platzman and Lowrie, 1992; Platzman et al., 1994) is consistent with our restoration.

Our reconstruction of the Alboran region, which follows van Hinsbergen et al. (2014a), is similar to that of Lonergan and White (1997) and Rosenbaum et al. (2002a) in inferring that the Gibraltar subduction zone and the Betic thrust front originated as a ENE-WSW striking, NNW-dipping subduction zone below the Baleares islands. This trench rolled back since mid-Oligocene times first to the south, and subsequently towards the west, during which time the pre-mid-Oligocene forearc and accretionary prism (i.e., the Malaguide and Alpujarride units of the Betic Cordillera, respectively) rotated up to as much as 200° cw. Paleomagnetic data from Oligocene (26 ± 4 Ma) mafic dykes in the Alpujarride and Malaguide units are consistent with this reconstruction (Fig. 20). Paleomagnetic declinations from the Ronda peridotite in the Betic Cordillera, and in the Ceuta and Beni Boussera peridotites of the Rif, are believed to record rotations following cooling of the peridotite after a 20-17 Ma regional high-temperature overprint. We combined all individual paleomagnetic directions of Ronda, yielding a data scatter consistent with paleosecular variation ($A95 = 2.6$, $A95_{min} = 1.4$, $A95_{min} = 2.9$, $n = 203$, *sensu* Deenen et al. (2011)), yielding a declination of ~$44 \pm 3°$, consistent with our reconstruction (Fig. 20). The Ceuta peridotite recorded no rotation, whereas the Beni Boussera peridotites give *in situ* declinations suggesting ~80° ccw rotation (Berndt et al., 2015; Saddiqi et al., 1995). No tilt correction was applied to these in absence of a paleohorizontal control (e.g., Feinberg et al., 1996), but for Ronda, the *in situ* paleomagnetic inclination is within a few degrees similar to the predicted inclination for Iberia, suggesting no major tilting occurred after the recording of the magnetization. The Moroccan peridotites give inclinations that deviate some 20° from the expected inclination, and some tilting may just have occurred. Nevertheless, assuming that the *in situ* declinations are reliable recorder of post-Burdigalian vertical axis rotation of the Alboran units, these suggest that the now strongly curved thrust front of the Alboran units over the Iberian and African margin-derived thrust slices around the Ronda, Ceuta, and Beni Boussera peridotites was a ~N-S striking thrust front (i.e. trench) around 18 Ma, as we reconstructed (Fig. 20) (see section 7.2.1).

6.2.4. Corsica-Sardinia

Paleomagnetic data from the Corsica-Sardinia Block come mainly from Sardinia. There is no evidence for a major tectonic disconnection between the two islands, however, and paleomagnetic data from Upper Paleozoic dykes in North Sardinia and South Corsica gave similar results (Vigliotti et al., 1990), such that the data shown in Fig. 21 are considered representative for a joint Corsica-Sardinia Block.

Restoring the motion of the Corsica-Sardinia Block relative to Eurasia from the extensional history of the Gulf of Lion (Séranne, 1999) predicts a ~50° ccw early Miocene rotation, which has long been recognized in paleomagnetic data (Gattacceca et al., 2007). In Fig. 21, there is a minor misfit between the APWP of Corsica-Sardinia calculated based on our reconstruction, which results from the calculation of this APWP in 10 Myr intervals: the Miocene rotation ended by ~16 Ma, which is restored as such in the GPlates restoration (Supplementary Information 3; see section 7.1.1).

Prior to the Oligocene onset of opening of the Gulf of Lion, there are no quantitative constraints from structural geology on the

Fig. 18. A) Paleomagnetic data from stable Iberia and the Central Iberian Ranges. Color coding according to age, see graph of Fig. 18C. For key to abbreviations, see Table 4. B) Paleomagnetic data from the North Pyrenean Zone. C) Declination versus age graph for stable Iberia, including data from the Organyà Basin and the Central Iberian Ranges. Green curve corresponds to the apparent polar wander path of Iberia calculated from the data (20 Myr sliding window, 10 Myr intervals), see Table 5. The GAPWaP of Torsvik et al. (2012) is shown in coordinates of Iberia (code 304 in reconstruction files, see Supplementary Information 3) and Eurasia. D) Declination versus age graph of paleomagnetic data from the North Pyrenean Zone, showing enhanced scatter interpreted as local rotations. Ref = Reference location for which graph was calculated. See Supplementary Information 2 for data files. See text for further explanation.

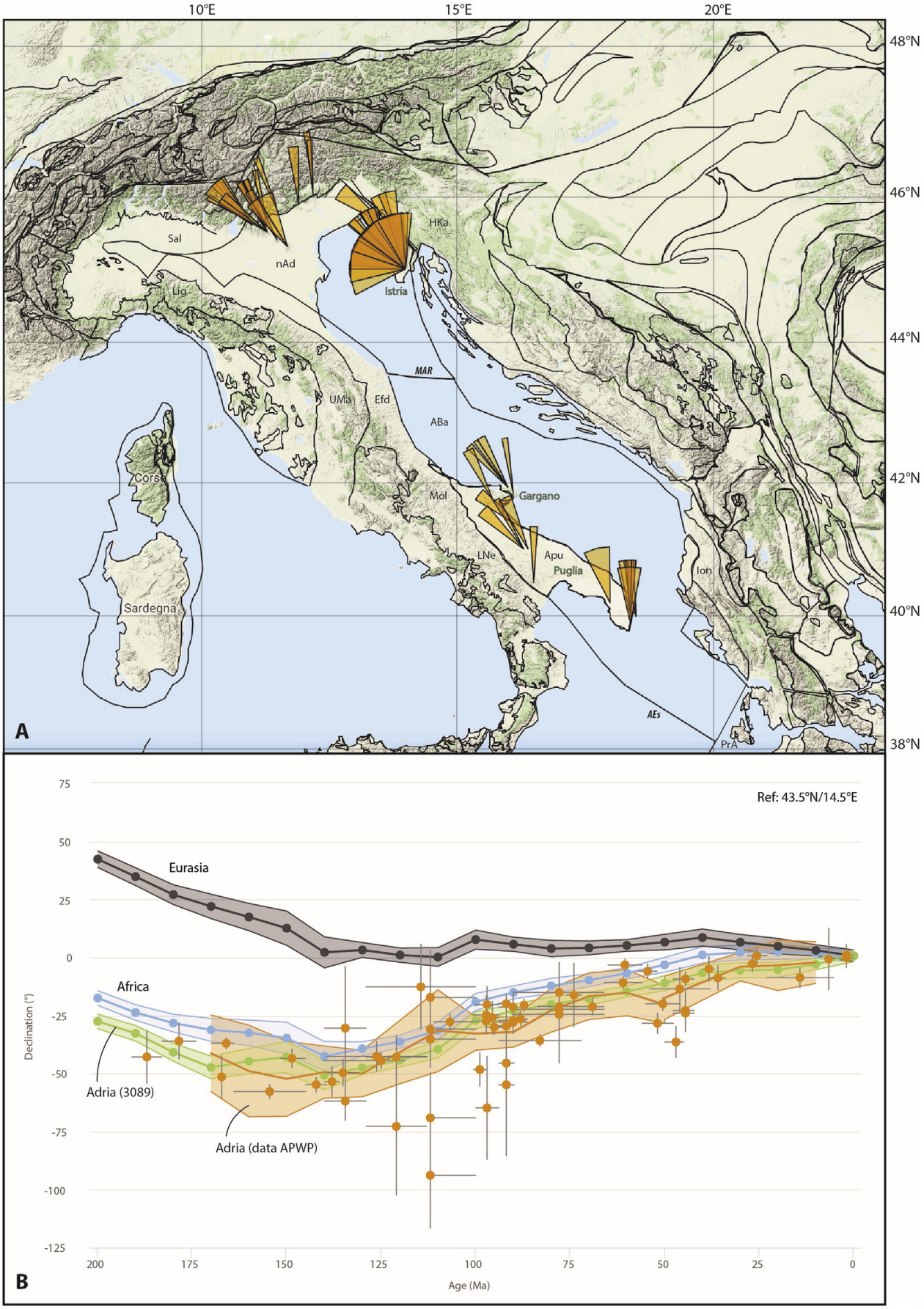
10°E
15°E
20°E
48°N
46°N
44°N
42°N
40°N
38°N
Sal
nAd
HKa
Istria
Lig
MAR
UMa
Efd
ABa
Corse
Mol
Gargano
LNe
Apu
Puglia
Ion
Sardegna
AEs
PrA
A
Ref: 43.5°N/14.5°E
Eurasia
Africa
Adria (3089)
Adria (data APWP)
Declination (°)
Age (Ma)
B

motion of the Corsica-Sardinia Block relative to Eurasia, other than the widespread evidence for uppermost Cretaceous to Eocene shortening in the Provence (e.g., Espurt et al., 2012a). Paleomagnetic data from Upper Cretaceous and Eocene rocks show that in Eocene time, an additional ~45° ccw rotation relative to Eurasia affected the Corsica-Sardinia Block (Advokaat et al., 2014b) (Fig. 21). We restore this additional rotation more gradually, since the Late Cretaceous, consistent with the time constraints on shortening in the Provence, as restoring the rotation entirely since 50 Ma is unlikely in the light of Africa-Eurasia convergence rates in this time interval.Finally, the predicted declinations for Triassic and Jurassic times deviate by some 25–35° from the measured declinations (Fig. 21). Reconstructing Corsica-Sardinia in the strike as suggested by these data would require restoring a major counterclockwise rotation phase in the Jurassic that would place Corsica-Sardinia in an unrealistic position relative to the modern Provence margin – almost orthogonally. If the Triassic and Jurassic directions are primary, this reconstruction is inconsistent with paleomagnetic evidence (Fig. 21). Particularly the Triassic sites may be remagnetized during Valais Ocean opening as suggested by the anomalously high inclination in the Triassic rocks (Advokaat et al., 2014b). In addition, the Jurassic pole is based on a large set of sites that show evidence for internal rotations (Advokaat et al., 2014b).

6.2.5. Sicily and the Apennines

A large set of paleomagnetic sites from ***Sicily*** was collected from Mesozoic and Cenozoic rocks of the Inner Carbonate units (Panormide and Pre-Panormide Platforms, and Imerese Basin) and Outer Carbonate units (Trapanese, and Saccense platforms, and Sicanian Basin) that were first stacked below Ligurian ocean units and subsequently thrust onto the Hyblean foreland (Fig. 8). Data from upper Miocene and Plio-Pleistocene sedimentary rocks of these units reveal a rapid, late Neogene ~40° cw rotation relative to Africa (Fig. 22) (Speranza et al., 2003). Data from the Inner Carbonate units (green dots in Fig. 22) are sparse, but consistently show that a large, ~90° cw rotation relative to Africa occurred sometime after the Eocene. These rotations are interpreted to result from the southeastward advance of the Calabrian-Peloritan Block during the late Miocene-Pliocene opening of the Tyrrhenian Sea (Speranza et al., 2018). Based on these paleomagnetic constraints, we have reconstructed a ~90° cw rotation of the Outer Carbonate Units since their ~14 Ma onset of thrusting over the Inner Carbonate Units (Catalano et al., 1993), assuming a constant rotation rate from 14 to 0 Ma. To reconstruct the paleoposition of the Outer Carbonate units, we assumed they were rigidly attached to the Inner Carbonate units after the 4 Ma onset of thrusting of the Outer Carbonate units over the Gela Nappe and Hyblean Plateau. This satisfies the ~40° cw rotation of the Outer Carbonate Units relative to Africa that follow from paleomagnetic measurements. Data from the pre-Neogene of the Outer Carbonate units reveal a highly scattered pattern with rotations up to the 90° of the Outer Carbonate Units (Fig. 22). We tentatively explain this scatter as the result of thrust sheet rotations between the Outer and Inner Carbonate units, whereby early accreted units experienced larger rotations than later accreted units.

Paleomagnetic data from ***Calabria*** show a gradual rotation of ~20° cw relative to Africa since ~10 Ma (Fig. 22). The closure of the Tyrrhenian Sea rather requires that Calabria underwent a net ~20°ccw rotation relative to Africa since middle Miocene time. To fit the paleomagnetic constraints, we have therefore assumed an initial counterclockwise rotation of Calabria versus Sardinia between ~13 and 10 Ma during the initial opening of the Tyrrhenian Basin, followed by the paleomagnetically constrained clockwise rotation. Such an initial early Tortonian counterclockwise rotation preceding a younger clockwise rotation was previously argued for by Duermeijer et al. (1998b). Fig. 22 cannot accurately display the detailed rotations since they are much faster than the 10 Myr interval resolution of the global APWP that we use to predict declinations (Torsvik et al., 2012).

Paleomagnetic data from the ***Southern Apennines*** mainly come from rocks of the Apenninic Platform (Green datapoints in Fig. 23). This is the highest, most internal structural unit underlying the Ligurian oceanic units, and shows a ~60° ccw rotation (Gattacceca and Speranza, 2002). Constraints from young sedimentary basins overlying the Southern Apenninic nappes (Pink datapoints in Fig. 23) show a major (~40°) counterclockwise rotation in late Miocene time, since ~6 Ma (Fig. 23). We modeled the maximum rotation that the Apenninic Platform could have undergone since 6 Ma by placing the southwestern limit of the Apenninic Platform against Calabria while keeping the northern part of the platform close to its modern position relative to Eurasia. This generates a ~45° ccw rotation of the Apenninic Platform relative to Adria. Between 6 Ma and the 14 Ma onset of thrusting of the Apenninic Platform over the Lagonegro Basin (e.g., Pescatore et al., 1999), we rigidly attached the Apenninic Platform to Calabria, and assumed rigid connection of the Apenninic Platform to Adria before that time. The resulting predicted declinations fit well with most paleomagnetic constraints from the Apenninic Platform (Fig. 23), with the exception of four localities that are located close to the left-lateral North Pollino Fault Zone between the Southern Apennines and the Calabrian Block (Cyan datapoints in Fig. 23). We explain the excess counterclockwise rotations of these four localities by local rotations induced by this major fault zone.

In addition, we reconstructed a ~40° cw rotation of the Apenninic Platform in Triassic time to open the triangle-shaped Lagonegro Basin (see section 7.10). This rotation optimizes the Triassic fit of the Adria with the north African passive margin and is consistent with the sparse paleomagnetic data available from the Triassic of the Apenninic Platform (Jackson, 1990).

Paleomagnetic studies in the ***Central Apennines*** have mainly focused on deformation associated with folding, thrusting, and strong but local oroclinal bending around the Gran Sasso range front during the northward Pliocene indentation of the Lazio-Abruzzi Platform (Satolli and Calamita, 2008). We modeled this indentation by assuming that the Lazio-Abruzzi Platform was rigidly attached to the Adria back to 3 Ma, and to the counterclockwise rotating Apenninic Platform before that time. Such counterclockwise rotations have been reported, but declinations are too scattered owing to local deformation to quantitatively constrain.

Paleomagnetic data from the curved fold-and-thrust belt of the ***Northern Apennines*** were derived from the Tuscan units (green datapoints in Fig. 24) that form the highest structural unit below the Ligurian ophiolites, thrust slices of Umbria-Marche Basin sediments (orange datapoints in Fig. 24), and young foredeep sediments of the Adriatic foreland (pink datapoints in Fig. 24). Consistent with our approach for Sicily, and the Southern and Central Apennines, we used data from the highest structural unit below the Ligurian ophiolites – the Tuscan nappes – to infer the total amount of rotation associated with the formation of the orocline. Such data are only available for the northern limb of the orocline, where a ~30° ccw rotation since the 16 Ma onset of

Fig. 19. A) Paleomagnetic data from stable Adria. For key to abbreviations, see Table 4. B) Declination versus age graph for stable Adria. Orange curve corresponds to the apparent polar wander path of Adria calculated from the data (20 Myr sliding window, 10 Myr intervals), see Table 5. The GAPWaP of Torsvik et al. (2012) is shown coordinates of Adria (code 3089 in reconstruction files, see Supplementary Information 3), Africa, and Eurasia. Ref = Reference location for which graph was calculated. See Supplementary Information 2 for data files. See text for further explanation.

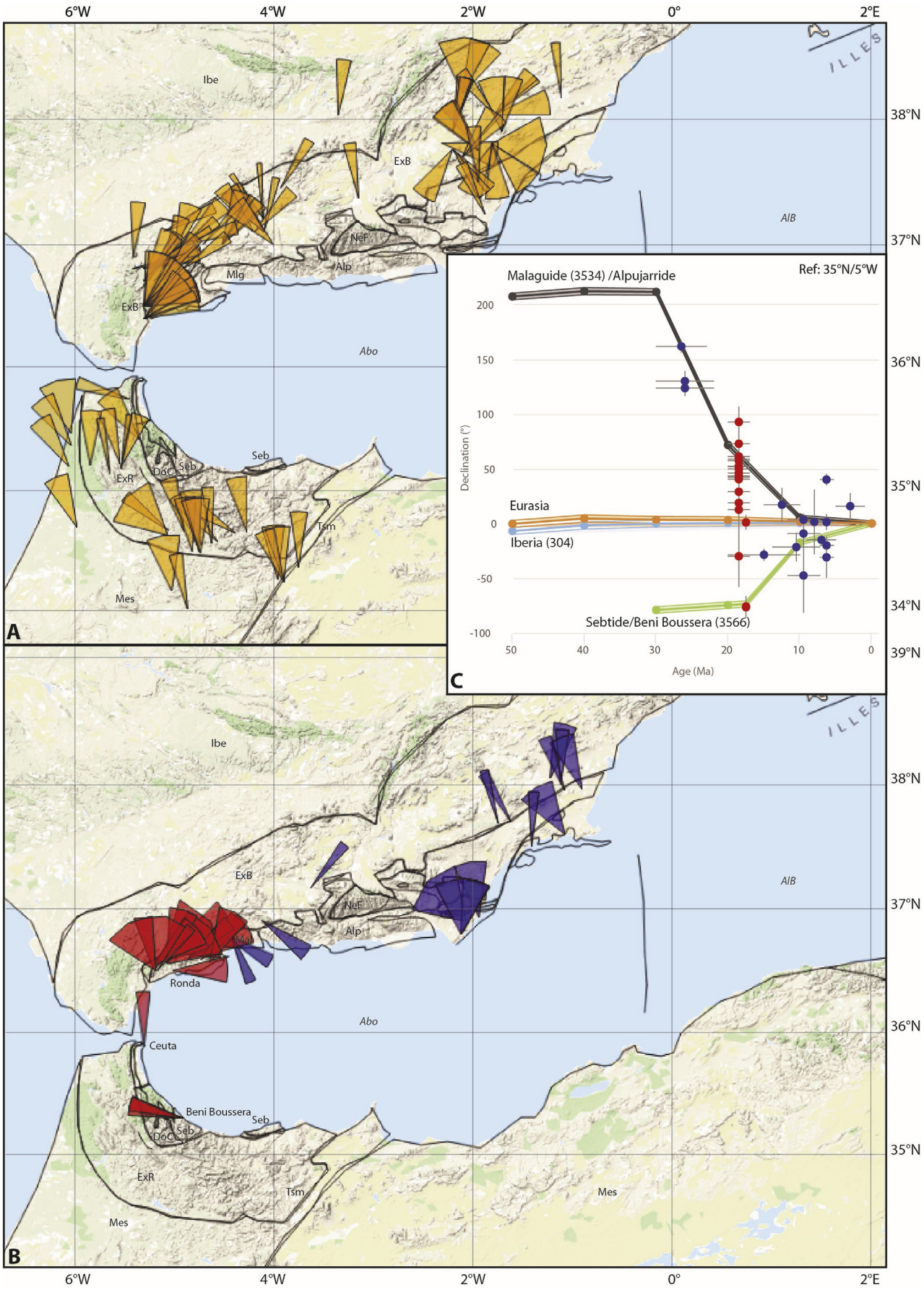
6°W
4°W
2°W
0°
2°E
38°N
37°N
36°N
35°N
34°N
39°N
Ibe
ExB
NeF
Alp
Mlg
Abo
Seb
DoC
ExR
Tsm
Mes
AlB
ILLES
A
Malaguide (3534) /Alpujarride
Ref: 35°N/5°W
Declination (°)
200
150
100
50
0
-50
-100
Eurasia
Iberia (304)
Sebtide/Beni Boussera (3566)
50
40
30
20
10
0
Age (Ma)
C
Ronda
Ceuta
Beni Boussera
B

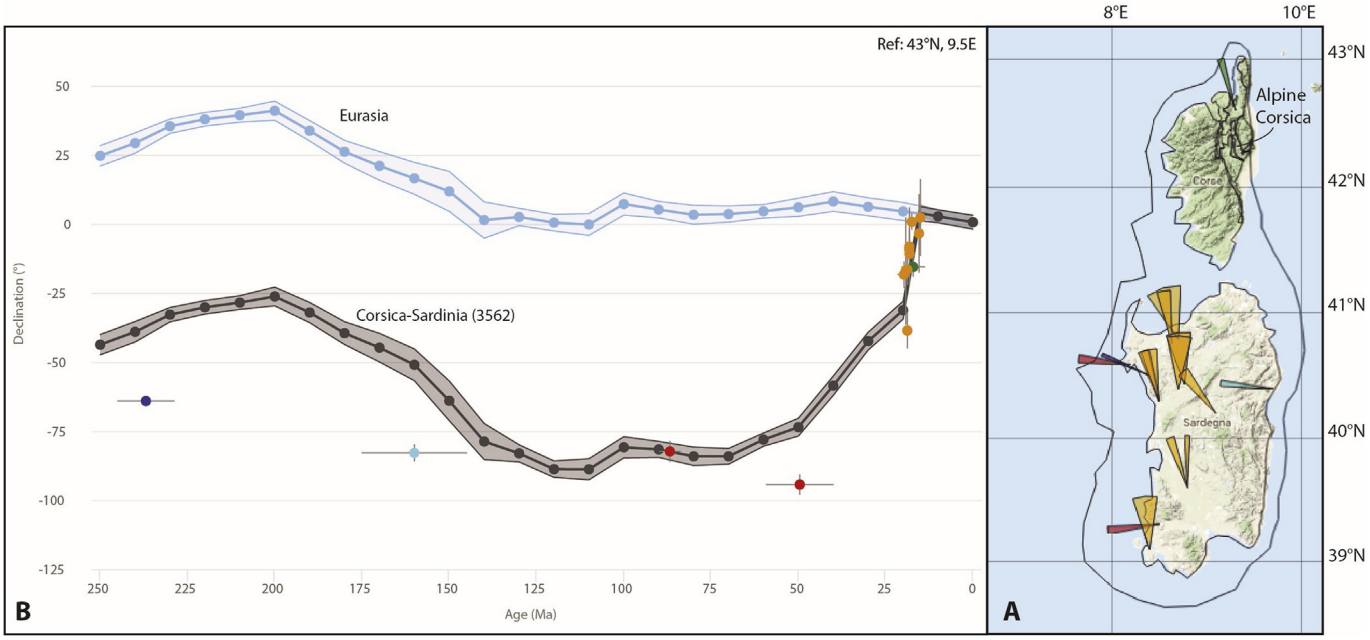

Fig. 21. A) Paleomagnetic data from Corsica and Sardinia. For key to abbreviations, see Table 4. B) Declination versus age graph for Corsica-Sardinia. The GAPWaP of Torsvik et al. (2012) is shown in coordinates of Corsica-Sardinia (code 3562 in reconstruction files, see Supplementary Information 3), and Eurasia. Ref = Reference location for which graph was calculated. See Supplementary Information 2 for data files. See text for further explanation.

thrusting of the Tuscan units over the Umbria-Marche Basin sediments fits the paleomagnetic data best (Fig. 24). The southern limb of the orocline was reconstructed by assuming a Euler pole relative to the Central Apennines at their junction at the Olevano-Antrodoco Fault, while keeping the Tuscan units of the northern and southern limbs connected, and choosing the rotation of the Tuscan nappes by fitting the enveloping surface of maximum rotations (Fig. 24).

The Umbria-Marche Units display rather scattered declinations that, with the exception of some Cenozoic sites in the Northern Apennines, generally indicate as high as, or lower than the Tuscan nappe rotation. Like for Sicily, we interpret this scatter to result from either individual thrust sheet rotations, or the different times at which thrust sheets were incorporated into the rotating oroclinal thrust belt during progressive foreland-ward thrusting. We did not incorporate these individual thrust sheets in our reconstruction.

Finally, in the center of the Umbria-Marche orocline, some Tuscan units display rotations as high as 90° ccw, which were interpreted by Caricchi et al. (2014) as resulting from a combination of Corsica-Sardinia rotation and oroclinal bending of the Northern Apennines. Rocks from the Tuscan units to the north, however, do not display such high rotations (Fig. 24). Moreover, the age of thrusting of the Tuscan units over the Umbria-Marche units (16-7 Ma) (Barchi et al., 2012; Speranza et al., 1997) post-dates the Corsica-Sardinia rotation (21-16 Ma) (Gattacceca et al., 2007) (Fig. 21). We therefore rather interpret these as local rotations within the heart of the orocline.

Finally, paleomagnetic data from Oligocene and Miocene sediments of the Piedmont Basin overlying the ***Ligurian Alps*** around the Voltri Massif have demonstrated a counterclockwise rotation of this region in Miocene time, in the same time window as the Corsica-Sardinia rotation. Maffione et al. (2008) therefore suggested a causal relationship between these events and argued that the location of the Ligurian Alps at the junction between the east-dipping Western Alps subduction zone and the west-dipping Northern Apennines subduction zone may have aided this rotation. Reconstructing Voltri as rigidly attached to Corsica yielded an unrealistic rapid westward motion of Voltri during the Miocene that would require major shortening to its west and major extension to its east, neither of which are observed in the Miocene geology of the region. We have therefore modeled that the Ligurian oceanic thrust sheets, to which Voltri had accreted in Eocene time and that were thrusting over the Tuscan units in the early Miocene (Brunet et al., 2000; Kligfield et al., 1986), experienced a northward translation driven by the Corsica-Sardinia rotation relative to the Briançonnais units to the west of the Voltri Massif. The Voltri Massif and Piedmont Basin at its northwestern part were then thought to have been caught in distributed left-lateral wrenching that kinematically allows for its counterclockwise rotation (see section 7.2.1) (see also Peral et al. (2018)). The predicted declinations of our reconstruction fit the paleomagnetic constraints (Fig. 24).

6.2.6. Alps, Jura Mountains, AlCaPa

Paleomagnetic data from ***the Jura Mountains*** come largely from a study of Gehring et al. (1991), and from an extensive study of Oligo-Miocene sediments of the Molasse Basin of Kempf et al. (1998). Vertical axis rotations are expected in the Jura Mountains based on structural geological estimates of a maximum of ~30 km of shortening in the center of the Jura Mountains between 20 and 7 Ma, decreasing to 0 on the tips of the fold-and-thrust belt (Table 1; Fig. 10) (Affolter, 2004; Affolter et al., 2008). This predicts ~10°cw rotation of the eastern part of the north Jura Mountains relative to Eurasia, and ~10°ccw rotation for the south Jura Mountains. Paleomagnetic data from the Molasse Basin immediately to the east of the northern Jura fold-and-thrust belt (Kempf et al., 1998) (blue dots in Fig. 25) validates this reconstruction. Data

Fig. 20. Paleomagnetic data from A) the External Betics and External Rif and B) the Alboran domain (in blue) and peridotite massifs within the Alboran units (in red). For key to abbreviations, see Table 4. B) Declination versus age graph for the Alboran units of the Betics and Rif. The GAPWaP of Torsvik et al. (2012) is shown in coordinates of Malaguide (code 3534 in reconstruction files, see Supplementary Information 3) and for the last 40 Ma, also the Alpujarride of the Betics, the Sebtide/Beni Boussera (code 3566 in reconstruction files), Iberia, and Africa. Ref = Reference location for which graph was calculated. See Supplementary Information 2 for data files. See text for further explanation.

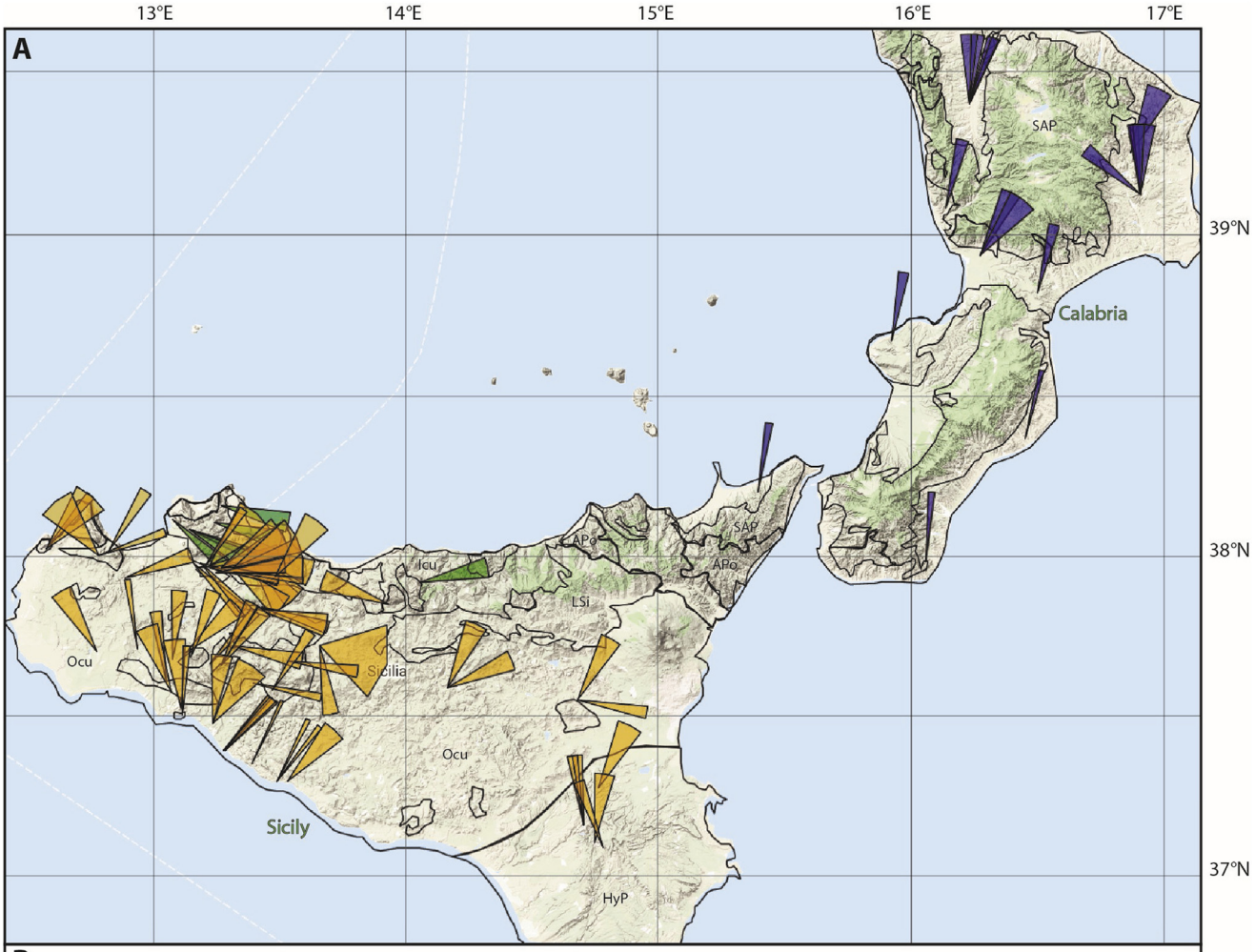
A
13°E
14°E
15°E
16°E
17°E
39°N
38°N
37°N
SAP
Calabria
APo
Icu
LSi
Ocu
Sicilia
Sicily
HyP

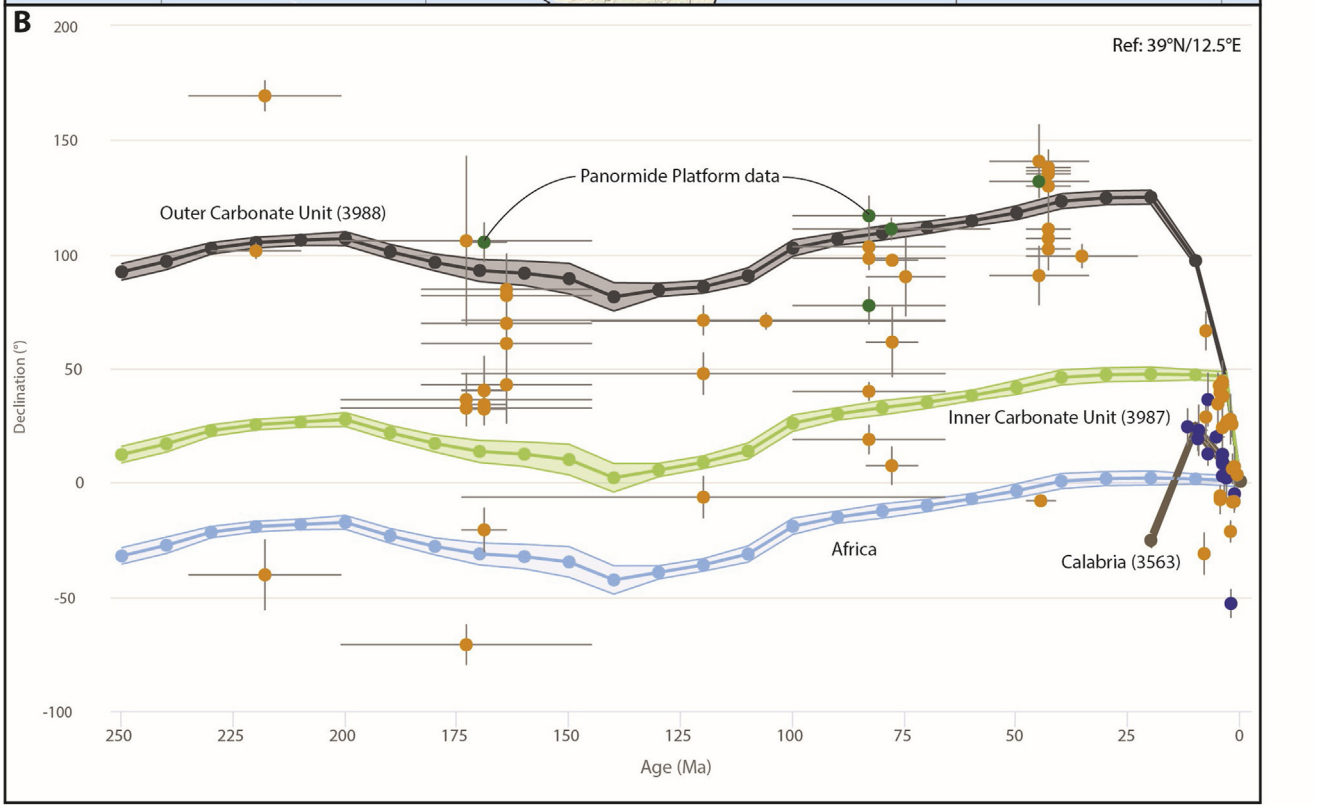
B
Ref: 39°N/12.5°E
Panormide Platform data
Outer Carbonate Unit (3988)
Inner Carbonate Unit (3987)
Africa
Calabria (3563)
Declination (°)
Age (Ma)
200
150
100
50
0
-50
-100
250
225
200
175
150
125
100
75
50
25
0

from the Jura fold-and-thrust belt itself are more scattered. Most data from the Jura Mountains show rotations between ~10 and 0° relative to Eurasia, whereby the more external sites show less rotation (Fig. 25), as expected in a foreland propagating oroclinal fold-and-thrust belt (see also e.g. Sicily and the Northern Apennines, Figs. 22 and 24, Section 5.5.1).

Paleomagnetic data from the ***Western Alps*** comprise a series of isolated sites in Mesozoic rocks of the External Massifs (light green datapoints in Fig. 25) and the Briançonnais in the southwestern Alps (pink datapoints in 22). In addition, there are sites with Oligocene and early Miocene (re)magnetizations from the External Massifs of the Western Alps (dark green datapoints in Fig. 25 (Crouzet et al., 1996)), and the Briançonnais of the southwestern Alps (orange datapoints in Fig. 25 (Sonnette et al., 2014)) and from the Briançonnais in the Ligurian Alps (red datapoints in Fig. 25 (Collombet et al., 2002)). When averaged, these data demonstrate that the External Massifs of the western Alps, that became incorporated in thrusting in the Miocene (e.g., Schmid et al., 2017) and references therein), did not significantly rotate. The Briançonnais of the southwestern Alps, however, underwent approximately 40° counterclockwise rotation since the Oligocene. We have used these paleomagnetic data as input to infer such a rotation to occur during the westward motion of the western Alps along the Insubric Line between 30 and 20 Ma (Fig. 25), because after this time, the amount of shortening in the western Alps is limited (e.g., Schmid et al., 2017)). Reconstructing this paleomagnetically constrained 40° counterclockwise rotation means that we reconstruct a southward decreasing amount of E-W convergence in the western Alps between 30 and 20 Ma, from ~100 km, constrained by the motion along the Insubric line, to only some tens of kilometers in the southwesternmost Alps. In addition, major rotations in excess of 90°ccw were found in the Briançonnais units of the Ligurian Alps, likely as a result of left-lateral shearing between Corsica and the western Alps in the same 30-20 Ma time window. We have modeled this rotation, which may well be the result of distributed wrench faulting between the westward moving western Alps and the southeastward moving Corsica-Sardinia Block (Peral et al., 2018), by rotation of a small Ligurian Briançonnais Block (Figs. 10 and 25).

Paleomagnetic data from the ***Southern Alps*** come from Mesozoic rocks spanning the Triassic to Cretaceous. The Southern Alps form the Adria-derived nappe stack that is bounded by the Peri-Adriatic Fault from the European Plate-derived units that constitute most of the Alps (Figs. 10 and 11). Reconstructing the Miocene shortening in the Alps predicts ~15 and ~20°cw rotation of the Peri-Adriatic Fault relative to stable Adria west (purple datapoints) and east (green datapoints) of the Giudicarie Fault, respectively (Fig. 25), which should be considered the maximum rotation of the thrust slices in the Southern Alps, as they were progressively incorporated in the orogen during rotation. Paleomagnetic data from the Jurassic and Cretaceous thrust slices of the western Alps show rotations scattered between the declinations of Adria and the Peri-Adriatic Fault, consistent with this prediction. Data obtained from Triassic rocks show a large scatter with a ~60° spread in the data, generally clockwise from the predicted declinations. Given the large spread in directions, we interpret these as local block rotations, perhaps associated with Alpine thrusting, or with the break-up of Adria from Eurasia in the Early Jurassic.

Nearly 300 paleomagnetic sites are available from the AlCaPa units of the ***eastern Alps***, the ***northern Pannonian Basin***, and the ***Carpathians*** (Fig. 26). These come from Triassic to Neogene, mostly sedimentary rocks. We subdivided these data into two areas: those from the Upper Austro-Alpine nappes of the eastern Alps, and from the Upper Austro-Alpine nappes of the Pannonian Basin and Carpathians. In addition, there are some data from the Dinaridic affinity Jadar-Kopaonik Zone of the Bükk Mountains, in the heart of the Pannonian Basin, and from the Lower Austro-Alpine units of the Tatra Mountains of Poland and Slovakia (Figs. 1 and 26).

The most striking feature of the paleomagnetic data from the northern Pannonian Basin, both derived from the Upper and Lower Austro-Alpine Nappes, is a strong, counterclockwise rotation of on average ~70° relative to Eurasia measured from rocks across the northern basin of Oligocene to early Miocene age. Middle Miocene rocks give much smaller rotations, consistent with the rotation occurring during Pannonian Basin extension between ~20 and 10 Ma (e.g., Márton and Márton, 1996; Márton et al., 1992). The southern margin of stable Eurasia shows a ~20° bend along the northern Carpathians (Figs. 10 and 26), and 20 of the 70° counterclockwise rotation is thus straightforwardly reconstructed associated with the eastward invasion/extrusion of the AlCaPa block into the Carpathian embayment (Ustaszewski et al., 2008). The excess ~50° rotation that follows from paleomagnetic data is unlikely to represent a regional rigid block rotation, since such a rotation would require 100s of km of N-S extension or contraction along the western or eastern margins of the AlCaPa Block, respectively, for which there is no evidence. Instead, we infer that this excess rotation results from regionally distributed simple shear of the AlCaPa Block owing to northward decreasing Miocene extension in the northern Pannonian Basin. If the amount of E-W extension was 180 km more along the Mid-Hungarian shearzone than along the northern Carpathians, the excess rotation is straightforwardly reconstructed (see section 7.1.1). Ustaszewski et al. (2008) estimated a total of 290 km of E-W extension from the Tauern window to eastern AlCaPa along a transect close to the Mid-Hungarian Shear Zone, and we thus infer that the amount of extension decreases to ~110 km in northern AlCaPa close to the contact with the Magura belt and the Outer Carpathians.

Our reconstruction infers that between ~55 and 30 Ma the AlCaPa units underwent a clockwise rotation of ~25°. This rotation is inferred based on a major overlap between AlCaPa and Tisza units that would arize if we assume that the Austro-Alpine units were fixed relative to Adria in the Paleogene. Paleomagnetic data from the Upper Austro-Alpine units of the northern Pannonian Basin and northern Carpathians are consistent with this clockwise rotation, as shown by the APWP for the Upper Austro-Alpine units (Fig. 26). Finally, the Lower Austro-Alpine Units exposed in windows in the Tatra Mountains appear to have undergone little net rotation relative to Eurasia since the Jurassic. Because these units were part of the AlCaPa unit during the Cenozoic, we interpret that these units underwent a ~60° clockwise rotation relative to the Upper Austro-Alpine units, either during the 145–125 opening of the Valais-Magura Ocean, or during the incorporation of the Tatra Lower Austro-Alpine in the fold-and-thrust belt in the Early Cretaceous. We do not explicitly restore this local rotation in our reconstruction.

6.2.7. *Tisza-Dacia, Carpathians*

Paleomagnetic data from the Tisza-Dacia Block come mainly from the Transylvanian Basin, the southern Carpathians, and the Apuseni Mountains in the eastern part of the Tisza-Dacia Block, and were measured in from Upper Cretaceous to Quaternary volcanics and sediments (Fig. 26). These demonstrate a major, ~60° clockwise

Fig. 22. A) Paleomagnetic data from Sicily and Calabria. For key to abbreviations, see Table 4. B) Declination versus age graph for Sicily and Calabria. The GAPWaP of Torsvik et al. (2012) is shown in coordinates of the Outer Carbonate Unit (code 3988 in reconstruction files, see Supplementary Information 3), the Inner Carbonate Unit (code 3987), Calabria (code 3563) and Africa. Ref = Reference location for which graph was calculated. See Supplementary Information 2 for data files. See text for further explanation.

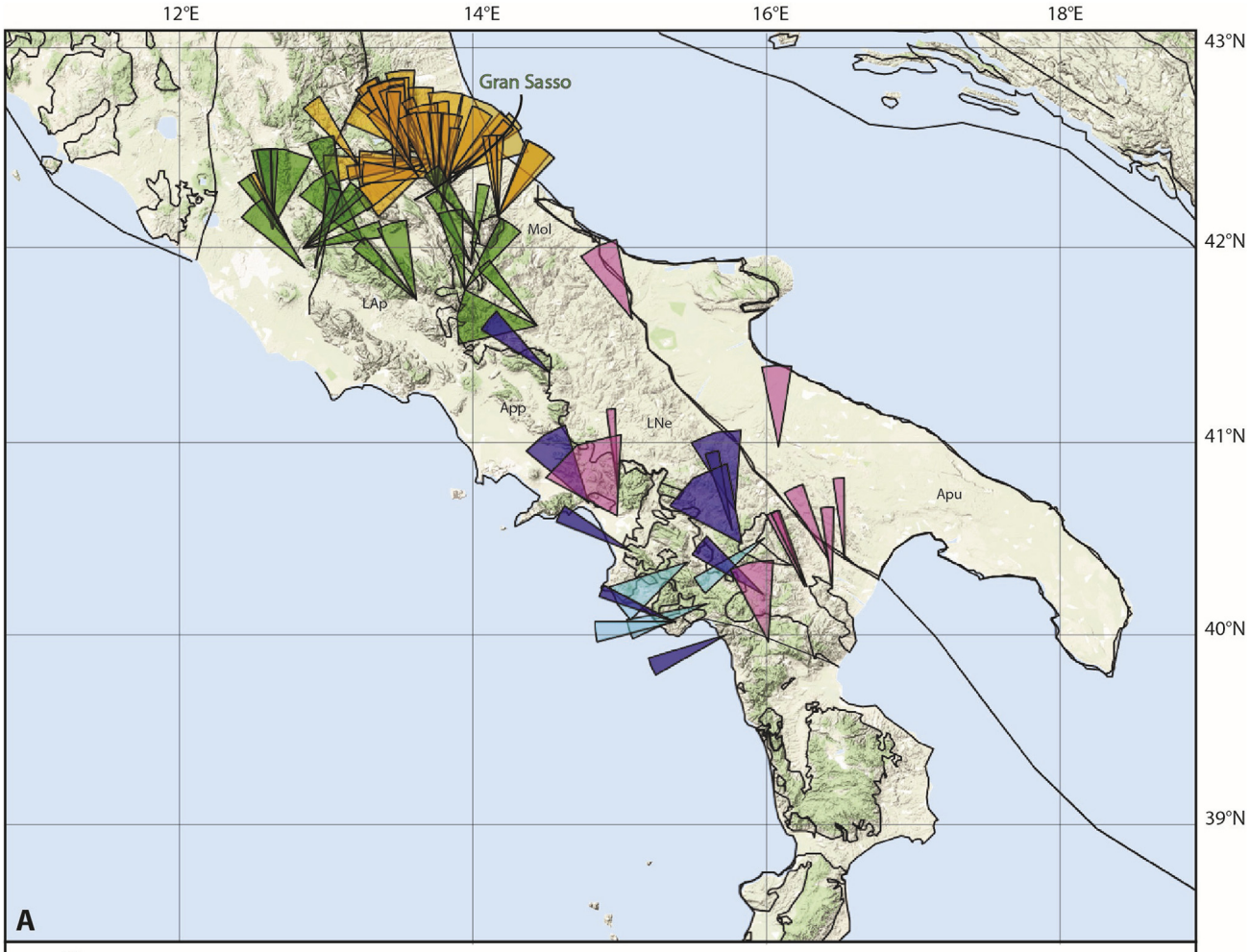
12°E
14°E
16°E
18°E
43°N
42°N
41°N
40°N
39°N
Gran Sasso
Mol
LAp
App
LNe
Apu
A

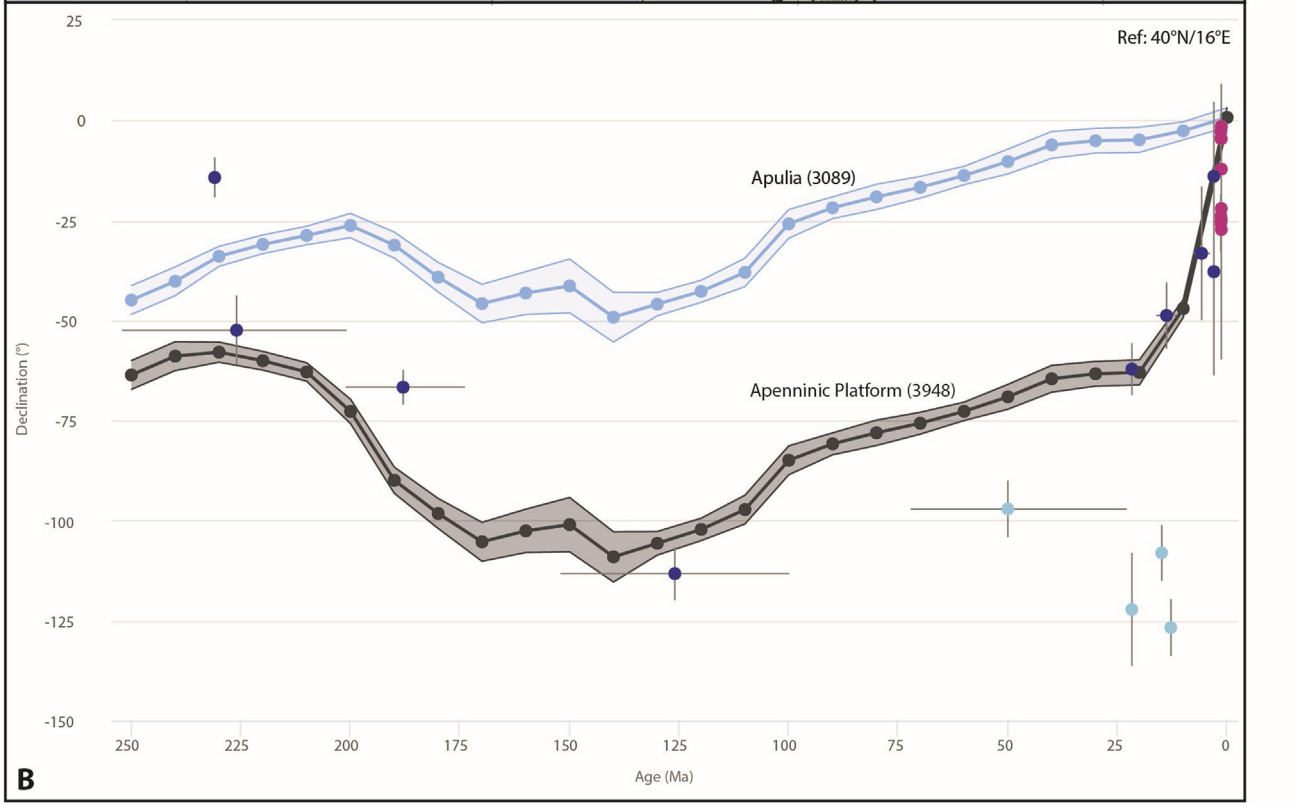
Ref: 40°N/16°E
Apulia (3089)
Apenninic Platform (3948)
Declination (°)
25
0
-25
-50
-75
-100
-125
-150
250
225
200
175
150
125
100
75
50
25
0
Age (Ma)
B

rotation relative to Eurasia between ~30 and 10 Ma (Fig. 26) associated with its eastward invasion into the Carpathian embayment (e.g., Panaiotu and Panaiotu, 2010; Pătraşcu et al., 1994). Approximately 35° cw rotation of this rotation follows from the Oligo-Miocene motion along the Timok and Cerna Faults (Fig. 10). In addition, the northward increasing amount of E-W extension in the south Pannonian Basin adds to the rotation of the eastern Tisza-Dacia Block. We restore 250 km of extension in the northern part of the Tisza Block along the Mid-Hungarian Shear Zone following (Balázs et al., 2016), which allows for ~10° more clockwise rotation of the Apuseni Mountains and Transylvanian Basin yielding a good fit with paleomagnetic data (Fig. 26). Sparse data from the westernmost Tisza Block close to the Sava Suture give scattered, counterclockwise rotations (Fig. 26) which we strongly deviate from the regional pattern and are here interpreted as resulting from local deformation. There are no paleomagnetic data from the Tisza-Dacia Block from rocks older than Upper Cretaceous, and the Early Cretaceous history of strong deformation and nappe stacking of the Tisza-Dacia terrane is thus not further be constrained by paleomagnetic data.

Extensive paleomagnetic datasets have been collected from Oligocene rocks of the northern Carpathian foredeep (e.g., Márton et al., 2009b), and Miocene rocks of the Southern Carpathian foredeep (e.g., Dupont-Nivet et al., 2005) (Fig. 26). These show variable rotations, but consistently counterclockwise in the north and clockwise in the south, in line with the overall sinistral shear between the AlCaPa Block and Eurasia in the north, and between the Dacia Block and the Moesian Platform in the south. These are thus best explained by local thrust sheet rotations during oblique convergence along the Carpathian margins. We did not restore these individual thrust sheet rotations in detail but consider the rotations consistent with the overall reconstructed motions.

6.2.8. Dinarides

A large paleomagnetic dataset of more than 150 sites is available from the Dinarides. These were obtained from Cretaceous to Miocene rocks of the Dalmatian Nappe (red datapoints) and High Karst Nappe (blue datapoints) (e.g., Kissel et al., 1995; Márton et al., 2014), from Miocene sedimentary basins overlying the more internal nappes (brown datapoints) (e.g., de Leeuw et al., 2012), and from the Medvednica Mountains around the city of Zagreb (cyan datapoints) (Tomljenović et al., 2008) (Fig. 27). The Dalmatian Zone accreted in late Miocene time to the Dinarides nappe stack and only underwent minor thrusting over Adria. The APWP predicted by our reconstruction for the Dalmatian Zone thus almost coincides with Adria. The data from the Dalmatian Zone are consistent with our path for Adria, including the Miocene ~10° counterclockwise rotation (Fig. 27).

From the High Karst Zone, some 65 paleomagnetic poles cover the Lower Jurassic to Miocene, sufficient to calculate an independent APWP (Table 5). This APWP shows that the High Karst Zone did not undergo major vertical axis rotations relative to Eurasia in the last ~100 Ma. Between 120 and 100 Ma, during which time much of the thrusting of the Dinarides nappe stack has not occurred yet (including the High Karst and pre-Karst units), but postdates the Late Jurassic-earliest Cretaceous deformation of the Vranduk Flysch and emplacement of the Western Vardar ophiolites, the paleomagnetic data suggest that the High Karst Zone underwent a ~20° clockwise rotation relative to Adria. We have adopted this rotation in our reconstruction and tentatively applied this to the entire deforming Dinaric nappe stack. The resulting predicted APWP from our kinematic reconstruction fits the APWP based on paleomagnetic data from the High Karst Zone well (Fig. 27).

Finally, Tomljenović et al. (2008) reported paleomagnetic data from Upper Cretaceous and Miocene rocks from the Medvednica Mountains (Fig. 27) that are located at the intersection of three megaunits: the AlCaPa megaunit to the north, the Tisza megaunit to the east, and the Dinarides megaunit to the west. These paleomagnetic data suggest ~130° clockwise rotation in the Paleogene and ~50° counterclockwise rotations since the early Miocene (Fig. 28). van Gelder et al. (2015) recently showed that restoring these rotations leads to a structural history of the Medvednica Mountains that is compatible with the overall Dinaridic orogeny and restores Cretaceous extension directions that compare well with those from the Eo-Alpine metamorphics to the north. We model the first, clockwise rotation phase to occur largely simultaneously with the Paleogene clockwise AlCaPa rotation, whereas the second, counterclockwise rotation phase occurred during opposite Tisza-AlCaPa rotations in the Miocene, and associated transpression between these. The resulting predictions for the declination fit the data well (Fig. 28).

6.2.9. Aegean and West Anatolia

The evolution of the Aegean and west-Anatolian region is characterized by accretionary orogenesis of African Plate derived crustal units since the Cretaceous, which since Eocene time became associated with overriding plate extension and orocline formation (e.g., Kissel and Laj, 1988; van Hinsbergen and Schmid, 2012). The relationship between extension and oroclinal bending follows straightforwardly from the decreasing width of extensional windows exposing metamorphosed portions of the fold-and-thrust belt to the NW and east (Brun and Sokoutis, 2007; van Hinsbergen et al., 2010a). For the Aegean region, van Hinsbergen and Schmid (2012) restored three such extensional windows pincing out to the northwest: the Rhodope window, the Cyclades-eastern Mainland Greece window, and the Peloponnesos window. Opening these windows led to clockwise rotations, the total magnitude of which increases over each window. Here, we test whether the predicted rotations satisfy paleomagnetic constraints.

Paleomagnetic data from the Chalkidiki Peninsula in the northern Aegean region (Figs. 1 and 28) allow testing the restored rotations associated with opening of the Rhodope window. Data come from Eocene granitoids of the Chaldiki Peninsula (e.g., Kondopoulou and Westphal, 1986), from volcanic rocks in the Rhodope Mountains that bound the main window to the northeast, and few sites from the Moesian Platform proper (e.g., Kissel et al., 1986b; van Hinsbergen et al., 2008). Sites from the Moesian Platform north of the Rhodope, not shown in Fig. 28, yielded no significant rotation, consistent with the presumed fixed position of Moesia relative to Eurasia in Cenozoic time (van Hinsbergen et al., 2008). Averaging all sites from the Chalkidiki granitoids yields a declination of ~30°, which fits well with the predicted declination for Chalkidiki in the reconstruction (Fig. 28). Sites from volcanic rocks to the northeast of the Rhodope metamorphic window scatter between the non-rotated Moesia position and the rotated Chalkidiki position (Fig. 28).

A total of 65 paleomagnetic sites are available from the Triassic to Pleistocene of the Upper Pelagonian Zone of eastern mainland Greece. We restored the rotation history associated with the central Aegean extension following (van Hinsbergen and Schmid, 2012), and connected the Pelagonian Zone to Adria prior to 60 Ma collision. As mentioned before, the Upper Pelagonian thrust nappes

Fig. 23. A) Paleomagnetic data from the Southern and Central Apennines. For key to abbreviations, see Table 4. B) Declination versus age graph for the Southern Apennines. The GAPWaP of Torsvik et al. (2012) is shown in coordinates of the Apenninic Platform (code 3948 in reconstruction files, see Supplementary Information 3), and the Apulian Platform of Adria (code 3089). Ref = Reference location for which graph was calculated. See Supplementary Information 2 for data files. See text for further explanation.

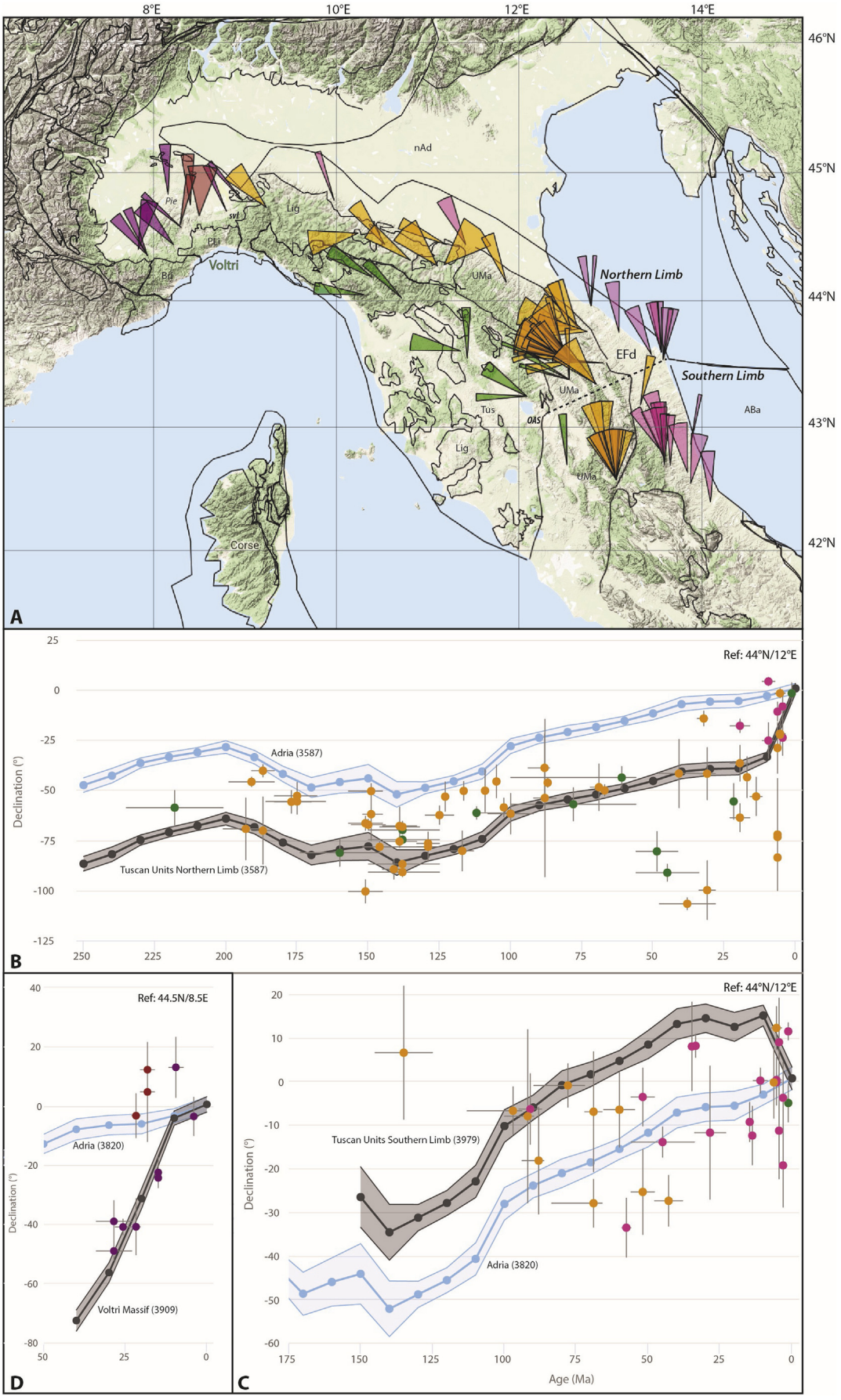
8°E
10°E
12°E
14°E
46°N
45°N
44°N
43°N
42°N
nAd
Pie
Lig
Voltri
UMa
Northern Limb
EFd
Southern Limb
Tus
ABa
Corse
A
Ref: 44°N/12°E
Declination (°)
Adria (3587)
Tuscan Units Northern Limb (3587)
B
Ref: 44.5N/8.5E
Adria (3820)
Voltri Massif (3909)
D
Ref: 44°N/12°E
Tuscan Units Southern Limb (3979)
Adria (3820)
Age (Ma)
C

were emplaced over the Lower Pelagonian nappes in the Early Cretaceous, ~130-110 Ma, following West Vardar Ophiolite obduction. Our reconstruction assumes that this was not associated with vertical axis rotations. Comparison of the predicted APWP for the Upper Pelagonian Zone based on this reconstruction shows a close match with the (averaged) declination for Oligocene and younger rocks. The declinations derived from Triassic and Jurassic rocks, however show a major mismatch with the predicted APWP and suggests an additional, ~50° clockwise rotation of the Upper Pelagonian units occurred sometime between the Late Jurassic and the Oligocene. These Triassic and Upper Jurassic sites were collected from the Argolis Peninsula of the Peloponnesos, the Attica Peninsula, and from Evvia island (Aiello et al., 2008; Morris, 1995) (Figs. 1 and 28), all towards the southernmost occurrences of the Upper Pelagonian nappe. These regions may have experienced a few degrees additional clockwise rotation relative to mainland Greece during the opening of the Sperchios and Gulf of Corinth grabens since the Pliocene, but the overall continuity of the main trends of Cenozoic folds, thrusts, and normal fault systems across the Pelagonian Zone make it unlikely that the excess ~50° clockwise rotation resulted from Cenozoic tectonics. This is further confirmed by the Miocene declinations derived all across the Pelagonian Zone that follow the same rotation trend through time and provide no argument for a much faster and larger rotation in the southern part of the zone than in the northern part.

There are two feasible periods in time for this larger clockwise rotation to have occurred: either during collision of Greater Adria with Europe following the closure of the Neotethys (Sava) Ocean and accretion of the Pelagonian nappe to the orogen, around 70-60 Ma, as suggested by Morris (1995), or during the Early Cretaceous thrusting that followed upon West Vardar Ophiolite obduction. Of these two, we consider the former more likely, as our restoration suggests that collision of the Pelagonian Zone may have occurred slightly earlier in the south(east) than in the north(west) due to an irregular overriding plate margin owing to the westward disappearance of the Sakarya Zone (see Section 7.4.2). We tentatively restored a 50° clockwise rotation of the Pelagonian units of Evvia, Attica, and Argolis between 70 and 60 Ma relative to the belt of mainland Greece to satisfy the paleomagnetic constraints (Fig. 28). There are no paleomagnetic data from pre-Oligocene time from the upper Pelagonian nappe north of Evvia and Attica but inferring that the whole nappe underwent a 50° clockwise rotation in this time interval would restore a sharply kinked Neotethyan margin, which we consider unrealistic – we thus restrict the 70-60 Ma rotation to Attica-Evvia.

Paleomagnetic data from the Pindos Zone are scarce and restricted to the western margin of the Mesohellenic Basin where they show major clockwise to non-rotated declinations, likely reflecting local structural architecture (Fig. 28). From the Ionian and Tripolitza zones of western Greece and Albania, however, an extensive paleomagnetic dataset of nearly 250 sites is available (e.g., Broadley et al., 2006; Horner and Freeman, 1983; Kissel and Laj, 1988; Speranza et al., 1995; van Hinsbergen et al., 2005b). The Tripolitza nappe underthrust the Pindos nappe, and the Ionian nappe underthrust the Tripolitza nappe along two simultaneously active thrusts between ~35 and 23 Ma (Kamberis et al., 2000; Sotiropoulos et al., 2003) (Fig. 14) and their paleomagnetic datasets are here combined into an APWP from Triassic to recent times. The reconstruction of van Hinsbergen and Schmid (2012) predicted ~45° clockwise rotation of the Ionian and Tripolitza zones. In addition, Broadley et al. (2006) suggested that the external Ionian Zone of NW Greece, separated from more internal parts of the zone by a thrust, underwent a smaller, ~30° clockwise rotation. To accommodate this difference, van Hinsbergen and Schmid (2012) inferred that the accretion of the external Ionian Zone occurred later, in the middle Miocene, after part of the clockwise rotation of mainland Greece had already taken place.

We revisit this reconstruction in the light of the paleomagnetic dataset. First, we note that whilst data from Oligocene rocks of the external Ionian Zone indeed suggest only ~30° clockwise rotation, Triassic to Eocene rocks yield declinations consistently showing a much larger rotation that is not well predicted by the reconstruction of van Hinsbergen and Schmid (2012). Close inspection of the sites in the Oligocene show that the small clockwise declinations mainly come from two localities of van Hinsbergen et al. (2005b). As noted by van Hinsbergen et al. (2005b), the folds and thrusts of the Ionian Zone, although overall striking NNW-SSE, show local curvature, likely owing to along-strike complexities in structural architecture (e.g., sidewall ramps in the underlying thrust configuration), and strike is proportional to declination. The two sites that decrease the apparent rotation estimate for the external Ionian Zone are located on a fold flank with a NW-SE strike, likely reflecting such a local deviation from the overall trend. If we assume that the external Ionian Zone was already accreted to the orogen in the early Miocene, together with the rest of the Ionian Zone, we predict an APWP that fits the Triassic to Eocene data well and we thus modified the reconstruction of van Hinsbergen and Schmid (2012) accordingly.

We computed an APWP for the Ionian-Tripolitza zones (Fig. 28, Table 5). The predicted APWP based on the reconstruction of van Hinsbergen and Schmid (2012) fits well with the APWP computed based on the data (Fig. 28), although an optimal fit would arise with a ~5–10° larger clockwise rotation of the Ionian and Tripolitza zones in the last ~25 Ma. Because the predicted and computed APWP for the Pelagonian nappes are a close match, such an additional rotation is unlikely to be explained by a larger amount of extension in the Aegean Basin. This small mismatch may thus better be explained by a small component of rotation accommodated along the nappe-bounding thrusts, local rotations associated with non-cylindrical thrusting, as argued for above in the external Ionian Zone, and bending of the Ionian nappes in and out of shear zones that in places cut through the Ionian Zone (e.g., Jordan et al., 2005; van Hinsbergen et al., 2005b, 2006; see also Jenkins, 1972). We have not restored this small excess rotation in detail.

From the Pre-Apulian Zone of Zakynthos and Kefallonia, finally, only data from upper Miocene and younger rocks are available, preventing testing long-term reconstructions. van Hinsbergen and Schmid (2012) restored a ~20° clockwise rotation of Zakynthos in the last 1 Ma following Duermeijer et al. (1999), which we adopt here.

An extensive set of paleomagnetic data is also available from the eastern limb of the Aegean orocline in western Turkey. This limb is separated from non-metamorphic nappes of northwestern Turkey by the Menderes extensional metamorphic complex, which kinematically accommodated the rotation in the middle Miocene (van Hinsbergen, 2010; van Hinsbergen et al., 2010a). During this opening, the Beydağları and Lycian Nappes rotated ~25° ccw relative to the northern Menderes Massif, and opposite to the clockwise

Fig. 24. A) Paleomagnetic data from the Northern Apennines. For key to abbreviations, see Table 4. B) Declination versus age graph for the northern limb of the Northern Apennine orocline. The GAPWaP of Torsvik et al. (2012) is shown in coordinates of the Tuscan units of the northern limb (code 3587 in reconstruction files, see Supplementary Information 3), and northern Adria (code 3820). C) Declination versus age graph for the southern limb of the Northern Apennine orocline. The GAPWaP of Torsvik et al. (2012) is shown in coordinates of the Tuscan units of the southern limb (code 3979), and northern Adria (code 3820). D) Declination versus age graph for the Voltri Massif and Piemonte Basin of the Ligurian Alps. The GAPWaP of Torsvik et al. (2012) is shown in coordinates of the Voltri Massif (code 3909), and northern Adria (code 3820). Ref = Reference location for which graph was calculated. See Supplementary Information 2 for data files. See text for further explanation.

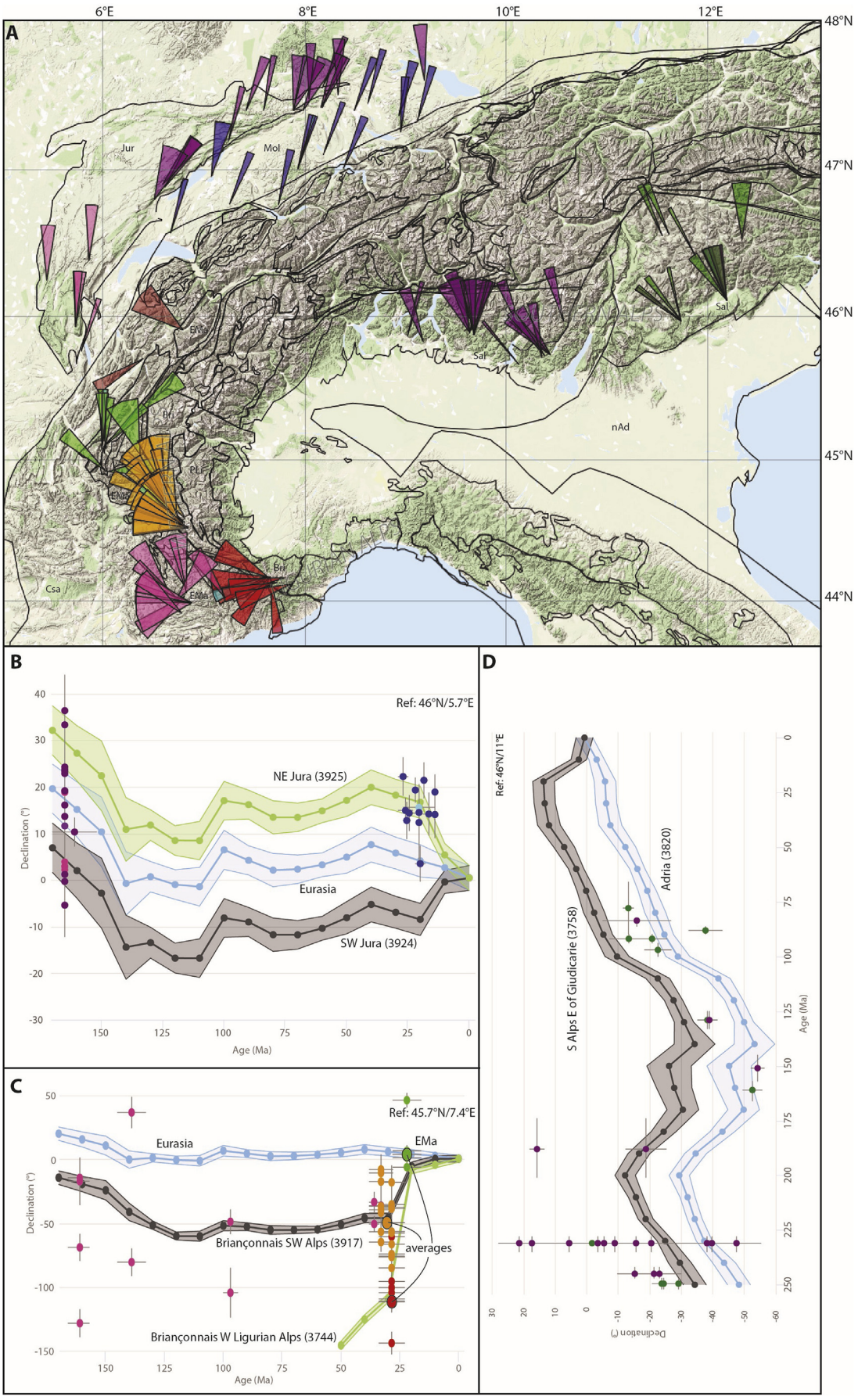
A
6°E
8°E
10°E
12°E
48°N
47°N
46°N
45°N
44°N
Jur
Mol
Sal
nAd
Csa
B
Ref: 46°N/5.7°E
NE Jura (3925)
Eurasia
SW Jura (3924)
Declination (°)
Age (Ma)
C
Ref: 45.7°N/7.4°E
Eurasia
EMa
Briançonnais SW Alps (3917)
averages
Briançonnais W Ligurian Alps (3744)
Declination (°)
Age (Ma)
D
Ref: 46°N/11°E
Adria (3820)
S Alps E of Giudicarie (3758)
Declination (°)
Age (Ma)

rotations in the western Aegean region, a long-recognized pattern (Kissel and Laj, 1988). Recently, a large paleomagnetic dataset was reported from the Lycian Nappes (Kaymakcı et al., 2018), which is consistent with the previously inferred ccw rotation. Our predicted APWPs for the blocks on both sides of the Central Menderes Massif are consistent with the poles based on paleomagnetic data (Fig. 29). Üzel et al. (2015, 2017) published extensive studies for the western Menderes region, close to the Aegean coast, and showed that this region underwent local, but systematic, rotations in a strike-slip dominated corridor (much of the cyan datapoints in Fig. 29). We interpret this corridor to reflect a transfer zone between the detachment systems of the Central Aegean and west Anatolian regions, following van Hinsbergen and Schmid (2012).

The difference between the oppositely rotating limbs of the Aegean orocline was proposed to be accommodated by the enigmatic Mid-Cycladic Lineament (Walcott and White, 1998) (Figs. 12 and 29). This lineament forms the boundary between ~N-S and ~NE-SW trending stretching lineations in the exhumed metamorphic complexes of the Central Aegean region (Walcott and White, 1998), and their azimuth is proportional to the magnetic declination, showing that the lineations are a good marker to map the dimensions and boundaries of the regionally rotating Aegean and west-Anatolian domains (Pastor-Galán et al., 2017; van Hinsbergen and Schmid, 2012). Although often assumed to be a strike-slip dominated feature (e.g. Philippon et al., 2014; Walcott and White, 1998), restoring the opposite rotations predicts that the Mid-Cycladic Lineament is an extensional fault that accommodates trench-parallel extension (van Hinsbergen and Schmid, 2012). Structural and paleomagnetic work showed that on the island of Paros, the only location where the Mid-Cycladic Lineament is exposed, showed that it is a top-to-the-southeast extensional detachment across which the opposite rotations were accommodated (Malandri et al., 2017) (Fig. 29).

The southern Aegean region consistently underwent counterclockwise rotations that average around ~20°, consistent with this inference (Fig. 29), but strong extensional and transtensional deformation (ten Veen and Kleinspehn, 2002, 2003) likely locally affected the declinations (Duermeijer et al., 1998a; van Hinsbergen et al., 2007) making a grand average not conclusive evidence to date the regional rotation (e.g., Rhodos appears to rotate later, and more, than Crete, ~25° since 4 Ma (van Hinsbergen et al., 2007). We follow van Hinsbergen and Schmid (2012) and connect the deforming south Aegean region to the SW Anatolian, counterclockwise rotating limb of the Aegean orocline and refer to that paper for further discussion.

6.2.10. Central and East Anatolia, Caucasus

Central Anatolia hosts a series of partly superimposed oroclines, which have received extensive paleomagnetic attention in recent years (Çinku et al., 2016; Gürer et al., 2018b; Kaymakcı et al., 2018; Koç et al., 2016; Lefebvre et al., 2013a; McPhee et al., 2018b; Meijers et al., 2010a). The Rhodope-Pontide fragment and the Transcaucasus/Lesser Caucasus region have been deformed into two adjacent, northward convex oroclines (Meijers et al., 2010a, 2017; van der Boon et al., 2018). The Central Pontides orocline was defined by Meijers et al. (2010a) based on paleomagnetic results from the Istanbul Zone and Eastern Pontides, north of the Intra-Pontide suture. They defined five segments of the Pontides, from Istanbul to the west to the eastern Pontides near Samsun in the east. We restored this orocline averaging paleomagnetic data from the Upper Cretaceous of the blocks of the Pontides defined by Meijers et al. (2010a) (Fig. 30), and modeled each as a rigid block in the reconstruction using the inferred timing of Paleocene to middle Eocene (60-45 Ma) for bending by Meijers et al. (2010a). Rotation and shortening in the heart of the Pontide orocline continued into the Miocene, interpreted to reflect ongoing tightening of the orocline due to Kırşehir indentation (Çinku et al., 2011; Espurt et al., 2014; Kaymakcı et al., 2003), and in late Miocene time local rotation associated with North Anatolian Fault Zone motions (Lucifora et al., 2013). We have not restored these local rotations in detail.

A large set of paleomagnetic sites is available from the region between the North Anatolian Fault Zone and Izmir-Ankara-Erzincan Suture Zone (Fig. 30). As expected, this dataset shows scattered declinations owing to smaller or larger fault block rotations within the fault zone (Avşar and İşseven, 2009; Tatar et al., 1995), which we have not systematically reconstructed in detail. Instead, we model the NAFZ and the suture as discrete fault zones.

The easternmost part of the Pontides experienced counterclockwise rotation since the Eocene, as part of the larger Caucasus orocline (Fig. 30). Our reconstruction of the Caucasus orocline follows van der Boon et al. (2018), and we refer the reader to that paper for further details and fits of APWPs predicted by the reconstruction and *in situ* paleomagnetic data.

We updated the paleomagnetic database compiled and collected by Meijers et al. (2015a) for the South Armenian Block. In our reconstruction, we restore the South Armenian Block in Triassic time as a part of the Cimmerian blocks that broke away from northern Gondwana. The South Armenian Block subsequently became an isolated microcontinent due to a Late Triassic ridge jump (see section 7.10). The predicted paleolatitude path of the South Armenian Block is consistent with paleolatitudes provided by Bazhenov et al. (1996) and Meijers et al. (2015a) (Fig. 31), although data from the key interval of the Triassic to Jurassic are sparse. In addition, paleomagnetic data suggest that the South Armenian Block underwent a ~45° clockwise rotation in the Late Cretaceous, which we reconstruct between 80 and 75 Ma during collision between the South Armenian and the Transcaucasus (Fig. 31).

The Kırşehir Block forms a westward convex orocline made by three more or less rigidly rotating blocks. We reconstructed these blocks according to the average directions of these blocks computed by Lefebvre et al. (2013a), which aligns the stretching lineations in these blocks to NNE-SSW (see also van Hinsbergen et al., 2016) (Fig. 32) (Table 1). To the west of the Kırşehir Block, counterclockwise rotations of some 20–30° were recorded from the Haymana Basin (Fig. 32). This may indicate that the Haymana Basin was part of the SE Anatolian rotating domain (see below). Because the Savcılı-Mucur Fault Zone may continue into the Haymana Basin, it is also possible that these rotations reflect local deformation induced by Kırşehir oroclinal bending (Özkaptan et al., 2016).

Gürer et al. (2018b) recently provided new and reviewed published paleomagnetic constraints on rotations in Central Anatolia, and showed that a domain from the southern Kırşehir Block (the Ağacören–Avanos block of Lefebvre et al. (2013a)) together with the Ulukışla Basin, the Central and Eastern Taurides, and the southern Sivas Basin rotated coherently counterclockwise in the Neogene. We update their APWP for the SE Anatolian rotating

Fig. 25. A) Paleomagnetic data from the Western and Southern Alps, the Molasse Basin, and Jura Mountains. For key to abbreviations, see Table 4. B) Declination versus age graph for the Molasse Basin and Jura Mountains. The GAPWaP of Torsvik et al. (2012) is shown in coordinates of the southwest and northeast Jura Mountains (codes 3924 and 3924, respectively, in reconstruction files, see Supplementary Information 3), and Eurasia. C) Declination versus age graph for the Western Alps. The GAPWaP of Torsvik et al. (2012) is shown in coordinates of the Briançonnais of the southwestern Alps (code 3917) and western Ligurian Alps (code 3744), and Eurasia. D) Declination versus age graph for the Southern Alps. The GAPWaP of Torsvik et al. (2012) is shown in coordinates of the Southern Alps (code 3758), and northern Adria (code 3820). Ref = Reference location for which graph was calculated. See Supplementary Information 2 for data files. See text for further explanation.

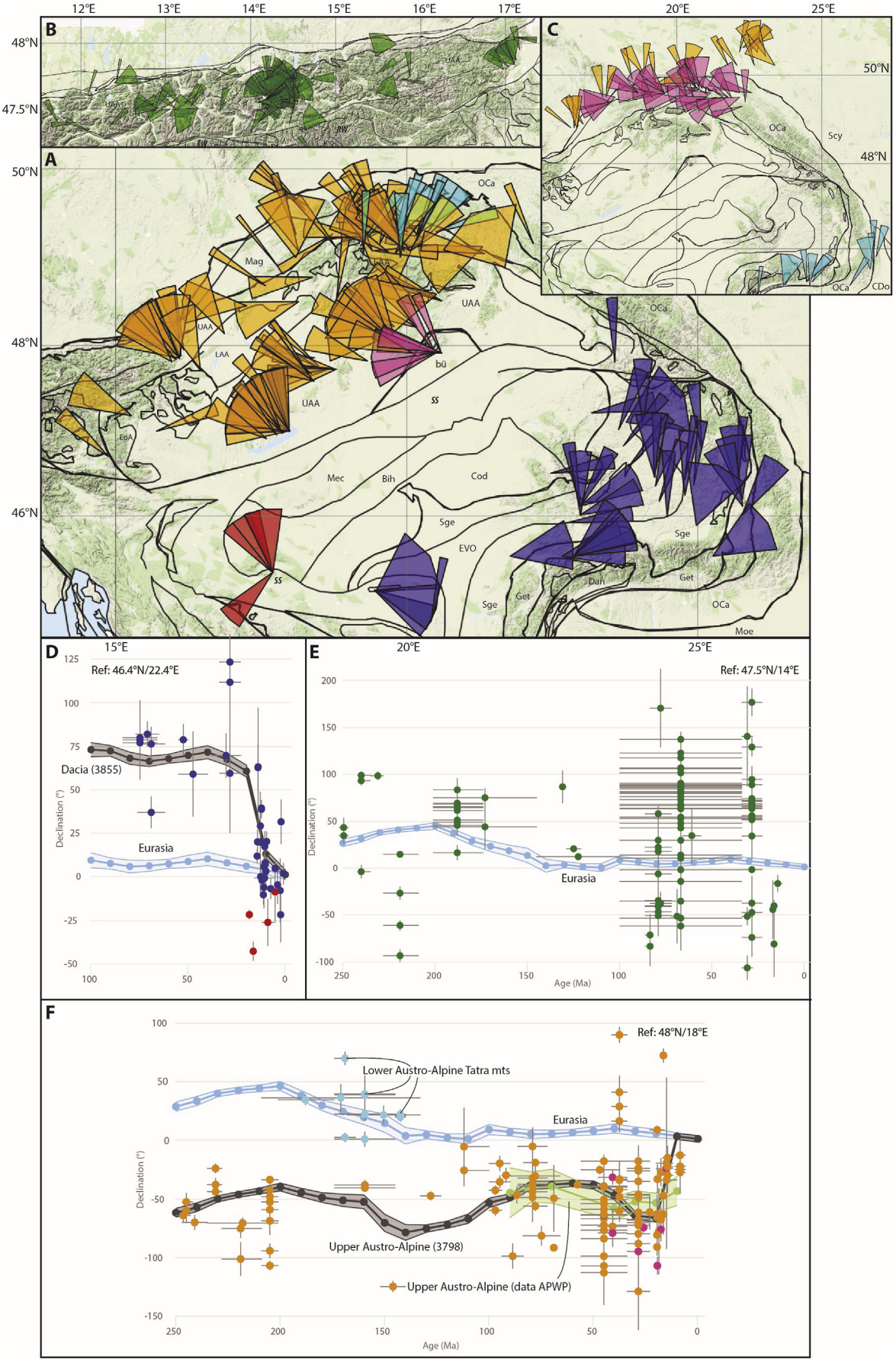
12°E
13°E
14°E
15°E
16°E
17°E
20°E
25°E
48°N
47.5°N
50°N
48°N
46°N
B
C
A
UAA
RW
50°N
48°N
OCa
Scy
CDo
Mag
LAA
bü
ss
EoA
Mec
Bih
Cod
Sge
EVO
Dan
Get
Moe
D
15°E
Ref: 46.4°N/22.4°E
Dacia (3855)
Eurasia
Declination (°)
E
20°E
25°E
Ref: 47.5°N/14°E
Age (Ma)
F
Ref: 48°N/18°E
Lower Austro-Alpine Tatra mts
Upper Austro-Alpine (3798)
Upper Austro-Alpine (data APWP)

domain with new paleomagnetic results of Çinku (2017) and Çinku et al. (2017) from the easternmost Taurides on the East Anatolian High Plateau (Fig. 33; Table 5). The results of Çinku (2017) and Çinku et al. (2017) are consistent with the counterclockwise rotations found farther west, suggesting that the SE Anatolian rotating domain (Gürer et al., 2018b) extends to the suture between the easternmost Taurides and the Iranian Cimmerides. We reconstructed the easternmost Taurides similar to Gürer and van Hinsbergen (2019) and Gürer et al. (2018b), and maximized the amount of Neogene counterclockwise rotation, which fit the kinematic and paleomagnetic data well (Fig. 33). A sharp deviation of the declination at the 30 ± 10 Ma interval is strongly influenced by several sites in the footwall of the Deliler-Tecer Fault in the Sivas Basin, that rotate ~50° ccw, which appears to not be representative for the entire block (Gürer et al., 2018b).

For the clockwise rotation of the Central Taurides (Fig. 32), adjacent to the Beydağları Platform, we follow the recent kinematic reconstruction of McPhee et al. (2018b). A secondary, Miocene orocline formed within the Central Taurides (Koç et al., 2016) (Fig. 32), which is kinematically balanced by shortening in the west (McPhee et al., 2018a) and extension in the east (Koç et al., 2018). The detailed reconstructions of McPhee et al. (2018b) and Koç et al. (2018) are incorporated in our reconstruction.

6.2.11. Eastern Mediterranean ophiolites; Cyprus

Extensive paleomagnetic work has been done on the Cretaceous ophiolites of the eastern Mediterranean region. So-called net tectonic rotation analyses consistently restore N-S to NE-SW trending paleo-spreading axes for the Troodos Ophiolite of Cyprus (Allerton and Vine, 1987; Granot et al., 2006; Hurst et al., 1992; Maffione et al., 2017; Morris et al., 1998; Morris and Maffione, 2016; Varga et al., 1999), the Baer Bassit Ophiolite of Syria (Morris et al., 2002), and for the Turkish part of Arabia, from the Hatay Ophiolite (Inwood et al., 2009b). Similar paleo-ridge orientations were obtained for the Göksun, Divriği, and Aladağ (Maffione et al., 2017) and Mersin (Morris et al., 2017) Ophiolites overlying the Taurides, and the Sarıkaraman Ophiolite on the Kırşehir Block (van Hinsbergen et al., 2016).

Because for these analyses only the net tectonic rotation axis is calculated, no specific information is available for the precise rotation around a vertical axis for these ophiolites. Nevertheless, the Troodos, Baer Bassit, and Hatay Ophiolites rotated counterclockwise, the Göksun and Mersin Ophiolites clockwise, and the Divriği and Aladağ Ophiolites again counterclockwise (Maffione et al., 2017; Morris et al., 2017). Our reconstruction is consistent with these rotations.

Only for Cyprus is there extensive paleomagnetic information from the ophiolites magmatic and sedimentary cover, from the Upper Cretaceous to the Pleistocene. These reveal a consistent counterclockwise rotation pattern, in two stages (Fig. 34). The first stage occurred sometime between the formation of the ophiolite around 92 Ma and its emplacement and uplift around 65 Ma, and accounts for ~45° counterclockwise rotation. A second stage appears to take place sometime in the late Neogene and accounts for ~30° of counterclockwise rotation (Fig. 34). We tentatively ascribe this phase to occur during the ~6 Ma accretion of Cyprus to the Anatolian orogen (McPhee and van Hinsbergen, 2019). Our reconstruction accommodates this rotation by extension, which is documented but poorly quantified, in the Cilicia Basin.

7. Step-wise reconstructions

We now present the GPlates reconstruction of the Mediterranean region in a series of paleo-tectonic maps of the Mediterranean realm in 15–40 Myr time-slices from the present back to the Early Triassic. These maps follow from integrating the plate kinematic constraints that govern relative Africa-Iberia-Europe motions (Section 4) with the tectonic architecture and evolution (Section 5) and the paleomagnetic constraints (Section 6) when reconstructed according to our reconstruction philosophy (Section 3). The key constraints are summarized in Table 1. We refer the reader to those sections for details and will in this section not repeat all lines of evidence for the events identified in the reconstruction. We describe the main events shown in the reconstruction and compare them to previous reconstructions to identify where major differences occur through time. In this section, we merely identify these differences, and discuss their origin and the validity of alternatives in Section 8.

Reconstructions are often presented as a forward tectonic evolution, starting at old and moving forward in time to the present. Although this may be the most intuitive for a general reader, we prefer a backward reconstruction description from the present to the past. This allows identifying key interpretations and reconstruction choices that propagate with the reconstruction back in time. In a way, the final reconstruction at 240 Ma is the sum of all our possible mistakes and would make for the least constrained and most speculative paleotectonic map, which we feel is best presented last instead of first.

In the paper, we provide the paleotectonic maps as full-page figures that highlight the location and configuration of megaunits and plate boundaries. Larger, A1-sized versions of these maps with detailed labels for each tectonic unit identified in the maps presented in section 7 are provided in Supplementary Information 1. These maps are presented in a Eurasia-fixed reference frame. The GPlates shape and rotation files of the reconstruction are provided in Supplementary Information 3. Finally, a movie of the reconstruction that displays the GPlates reconstruction in 500 kyr intervals between the time-slices displayed in detailed maps below is provided in Supplementary Information 4. For each time-slice, we briefly describe the main features and changes relative to the previous time-slice. At the trenches, we indicate codes of upper and lower mantle slabs in the modern mantle that we infer subducted at these trenches, and that were previously documented in the Atlas of the Underworld (van der Meer et al., 2018), and for some additional Anatolian slabs in Gürer (2017). Note that we define subduction here as lithosphere sinking into the mantle, regardless whether this lithosphere is oceanic or continental.

Supplementary video related to this article can be found at https://doi.org/10.1016/j.gr.2019.07.009.

In the descriptions below, we will compare our restoration with widely used, or recent reconstructions (Barrier et al., 2018; Brun et al., 2016; Csontos and Vörös, 2004; Darin et al., 2018; Faccenna et al., 2014; Golonka, 2004; Handy et al., 2010, 2015; Le Pichon et al., 2019; Lonergan and White, 1997; Menant et al., 2016;

Fig. 26. Paleomagnetic data from A) the AlCaPa and Tisza-Dacia megaunits; B) the AlCaPa units of the Eastern Alps; C) the Outer Carpathians and Eurasian foreland. For key to abbreviations, see Table 4. D) Declination versus age graph for the Tisza-Dacia mega-unit. The GAPWaP of Torsvik et al. (2012) is shown in coordinates of the Central Dacia megaunit (code 3855 in reconstruction files, see Supplementary Information 3), and Eurasia. Green curve corresponds to the apparent polar wander path of the Upper Austro-Alpine units of the Pannonian Basin and Carpathians calculated from the data (20 Myr sliding window, 10 Myr intervals), see Table 5. E) Declination versus age graph for the Eastern Alps. The GAPWaP of Torsvik et al. (2012) is shown in coordinates of Eurasia. F) Declination versus age graph for the AlCaPa mega-unit of the Pannonian Basin and northern Carpathians. The GAPWaP of Torsvik et al. (2012) is shown in coordinates of the eastern margin of the megaunit (code 3798), and Eurasia. In pink: data from the Jadar-Kopaonik Zone of the Bükk Mountains, in cyan: data from the Lower Austro-Alpine units of the Tatra Mountains. All other data come from the Upper Austro-Alpine Units. Ref = Reference location for which graph was calculated. See Supplementary Information 2 for data files. See text for further explanation.

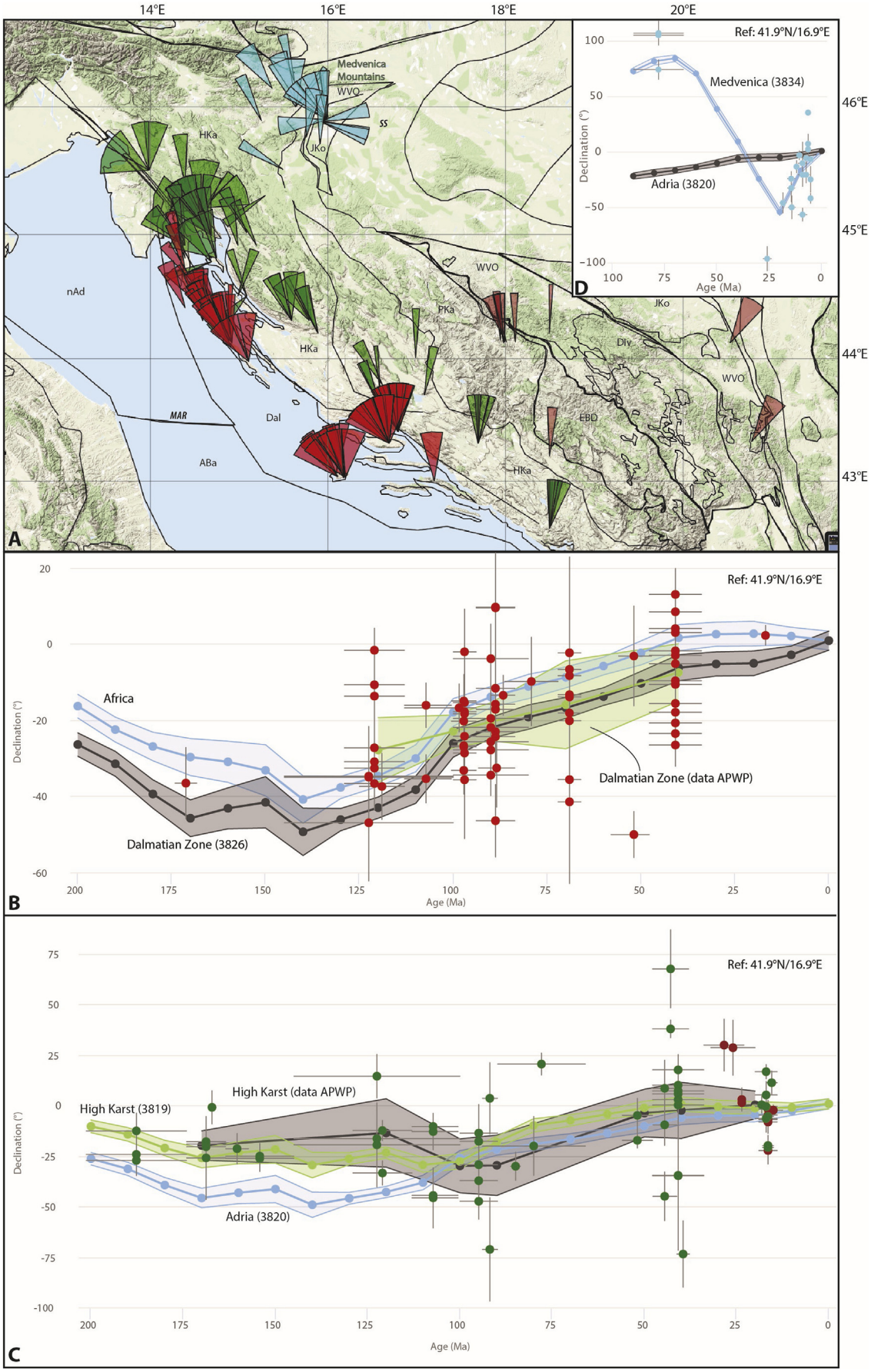
14°E
16°E
18°E
20°E
46°E
45°E
44°E
43°E
Medvenica Mountains
WVO
SS
HKa
JKo
nAd
PKa
DIv
EBD
MAR
Dal
ABa
A
Ref: 41.9°N/16.9°E
Medvenica (3834)
Adria (3820)
Declination (°)
Age (Ma)
D
Africa
Dalmatian Zone (3826)
Dalmatian Zone (data APWP)
B
High Karst (3819)
High Karst (data APWP)
Adria (3820)
C

Meulenkamp and Sissingh, 2003; Moix et al., 2008; Okay and Nikishin, 2015; Robertson et al., 2013c; Rosenbaum et al., 2002a; Royden and Faccenna, 2018; Schettino and Turco, 2010; Sosson et al., 2016; Stampfli and Hochard, 2009) to identify key differences, and establish when in the reconstructed time these differences appear and if possible, based on which reconstruction choices. We here merely illustrate where our reconstruction deviates from previous renditions, as a basis for the discussion section, where we will address (un)certainties and alternatives.

7.1. Langhian – 15 Ma

7.1.1. Western Mediterranean region

Our reconstruction of the western Mediterranean region includes E-W extensional opening of the Algerian Basin between 16 and 8 Ma following Mauffret et al. (2004), and consequently restores the Alboran domain, unstretched by up to 200 km, to the east, close to the Baleares (Fig. 35). We restore transform offset between the Kabylides and Rif blocks, and along the Emile Baudot escarpment (Fig. 1). At 15 Ma, the South Iberian and northwest African margins, together with the intervening Piemonte-Ligurian oceanic corridor are subducting at the westward retreating Gibraltar trench, leading to the accretion of the external Betic and Rif zones, the intervening flysch of the Gibraltar region, and the deep underthrusting of the Nevado-Filabride and Temsamane units (Fig. 35, Supplementary information (SI) 1-map 1). Roughly N-S Africa-Europe convergence constrained by Atlantic ocean reconstructions (Section 4) was slow, on the order of several mm/yr, insufficient to drive a N-S convergent subduction zone in the Piemonte-Ligurian corridor, although some contractional deformation must have occurred. Around 15 Ma the Kabylides nappes are emplaced onto the African margin (Section 5.3), and subduction of the Kabylides Slab is terminating.

To the east, Adria is undergoing its ~10° counterclockwise rotation relative to Eurasia (Fig. 19) accommodated by extension in the Sicilian Basin. In the Apenninic system, the Tyrrhenian Basin (Fig. 1) is closed, juxtaposing the Calabria-Peloritani Block (Stilo-Aspromonte-Peloritan and Africo-Polsi units) against the Corsica-Sardinia Block (Figs. 8 and 35, SI1-map 1). The Calabrian orocline is restored, aligning the Sicilian Inner Carbonate Unit and the Apenninic Platform as a single, NE-SW trending platform (Fig. 35, SI1-map 1), consistent with paleomagnetic constraints (Figs. 22 and 23), whose lithosphere at 15 Ma is being subducted. This platform was separated by the Lago Negro - Molisse Basin from the Apulian Platform. Restoring the dimensions of their modern relics juxtaposes between the Inner Carbonate Unit and Apenninic Platform, and we thus infer that the Ionian oceanic basin pinched out westward, to the east of the Inner Carbonate platform and Apenninic Platform (Fig. 35).

In the Northern Apennines, extension in the north Tyrrhenian Basin and much of the north Apenninic orocline is restored. At 15 Ma, the northern Apenninic subduction zone was consuming lithosphere of the Umbria-Marche Basin aligning the northern Apenninic and Calabrian trenches and by inference, slabs.

We agree with all previous reconstructions that restore a narrow oceanic corridor between Iberia and northwest Africa. Debate mainly focuses on whether the Algerian Basin, from which no unequivocal marine magnetic anomalies are known, opened from north to south or from east to west. Reconstructions adopting E-W extension (Handy et al., 2010; Lonergan and White, 1997; Rosenbaum et al., 2002a; Royden and Faccenna, 2018) are similar to our restoration, whilst those assuming N-S extension place the Alboran region much closer to its modern position (Faccenna et al., 2014; Golonka, 2004; Meulenkamp and Sissingh, 2003; Schettino and Turco, 2010; Stampfli and Hochard, 2009). A mix between these is the reconstruction of Platt et al. (2013), who documented E-W shortening from the external Betics and Rif placing the Alboran domain ~300 km eastward since the early Miocene, requiring a similar amount of E-W extension in the Algerian Basin. Conversely, restoring 800 km of E-W Alboran extension requires that the displacements on main nappe-bounding thrusts in the Betic-Rif orogen is considerably larger than the minimum overlaps documented from the geology.

Finally, most (but not all (Rosenbaum et al., 2002a; Royden and Faccenna, 2018; Schettino and Turco, 2010)) previous reconstructions suggest an oceanic connection from the Piemonte Ligurian to the Eastern Mediterranean oceanic basins (Faccenna et al., 2014; Handy et al., 2010; Meulenkamp and Sissingh, 2003). If that is correct, then the Inner Carbonate unit and Apenninic units must have undergone considerable trench-parallel extension during their rotational emplacement onto the African and Adriatic margins, which is possible but not documented, hence not restored.

7.1.2. Central Mediterranean region

Since the middle Miocene there is only minor motion in the Alps. Our 15 Ma reconstruction restores shortening and oroclinal bending in the Jura Mountains and in the external Alpine massifs, some of the western Alpine oroclinal bending, and extension on the Simplon detachment fault. In addition, shortening of the Southern Alps is restored, as well as upper plate N-S shortening of the Tauern window in the eastern Alps (Figs. 10 and 35). There is active thrusting of the Alps over the European foreland, but only slowly and likely not associated with active subduction.

Towards the east, in the Carpathians, westward subduction consumes lithosphere of the Carpathian embayment, which retreats relative to Adria causing Pannonian Basin extension. This leads to the accretion of the Outer Carpathians, whose stratigraphy suggests that the basin was underlain mostly by thinned continental crust (e.g., Gągała et al., 2012; Maţenco, 2017 and references therein). We note that in direct contradiction with these geological observations, geophysical studies that showed the Vrancea tomographic high velocity anomaly visible beneath the SE Carpathians until 250–300 km depth have always inferred that it the anomaly represents subducted oceanic lithosphere instead (Martin and Wenzel, 2006; Bokelmann and Rodler, 2014 and references therein). Finding the continental or oceanic nature of this embayment requires further studies and is beyond the scope of our restoration. The amount and rate of extension affecting the AlCaPa units in the northern Pannonian Basin, north of the mid-Hungarian Shear Zone, is considerably larger and faster than the extension affecting the Tisza-Dacia units to the south (Ustaszewski et al., 2008). As a result, we infer that the Carpathian subduction zone consisted of two segments separated by a transform fault, at which two disconnected slab subducted (see also van der Meer et al., 2018). This transform has functioned as a large-scale transfer zone during the Miocene extension, allowing the differential motions and explaining the locally contrasting senses of shear observed (Balázs et al., 2018). At the intervening shear zone, the

Fig. 27. Paleomagnetic data from the Dinarides. For key to abbreviations, see Table 4. B) Declination versus age graph for the Dalmatian Zone. The GAPWaP of Torsvik et al. (2012) is shown in coordinates of the Dalmatian Zone (code 3826 in reconstruction files, see Supplementary Information 3), and Africa. Green curve corresponds to the apparent polar wander path of the Dalmatian Zone calculated from the data (20 Myr sliding window), see Table 5. C) Declination versus age graph for the High Karst Zone. The GAPWaP of Torsvik et al. (2012) is shown in coordinates of the High Karst (code 3826). Grey curve corresponds to the apparent polar wander path of the High Karst Zone calculated from the data (20 Myr sliding window), see Table 5. D) Declination versus age graph for the Medvednica Mountains. The GAPWaP of Torsvik et al. (2012) is shown in coordinates of the Medvednica (code 3834), and Adria (code 3820). Ref = Reference location for which graph was calculated. See Supplementary Information 2 for data files. See text for further explanation.

Table 5
Apparent Polar Wander Paths calculated for selected regions in the Mediterranean region. N = number of sites used for pole calculation; λ = pole latitude, ϕ = pole longitude, A95 = 95% cone of confidence; age in Ma.

Iberia					Adria					Upper Austro-Alpine Pannonian					Dalmatian					High Karst					Ionian-Tripolitza		
n	λ	ϕ	A95	age	n	λ	ϕ	A95	age	n	λ	ϕ	A95	age	n	λ	ϕ	A95	age	n	λ	ϕ	A95	age	n	λ	ϕ
14	76.9	181.9	3.7	10	4	87.6	237.3	6.7	10	21	57.8	289.4	9.48	10											31	68.0	127.3
18	75.6	170.9	3.9	20	3	80.9	212.3	8.9	20	33	48.1	289.2	6.84	20						19	81.6	195.4	5.7	20	82	43.2	117.2
15	75.3	166.1	7.0	30	4	77.8	210.7	5.2	30	22	45.9	282.8	7.93	30											101	43.6	117.3
20	77.5	162.5	5.5	40	7	69.6	243.2	8.2	50	24	43	288.7	8.29	40	14	72.4	220.2	6.8	40	12	73.3	204.7	12.5	40	51	42.2	112.5
13	77.2	146.0	4.6	50	8	66.7	245.8	7.2	50											14	73.3	208.8	10.6	50	36	46.6	117.1
					6	66.7	231.7	9.1	60	10	50.4	264.3	13.2	70											20	53.3	128.1
7	76.7	178.5	7.2	70	8	68.1	238.2	9.0	70	11	49.4	264.4	11.9	80	11	72.9	251.2	9.92	70								
11	72.5	162.2	7.6	80	8	65.3	250.0	8.4	80	7	51.4	277.2	18.3	90											10	50.3	129.6
10	77.9	167.4	11.7	90	17	59.1	262.1	5.8	90						29	66.9	250.3	4.48	90	9	61.9	265.4	13.2	90			
6	79.5	256.4	13.6	100	15	58.8	263.3	6.4	100						22	64	251.4	3.93	100	11	62.7	268.4	11.6	100			
17	74.6	234.8	4.4	110	6	59.9	262.4	15.6	110																		
17	73.8	239.5	4.8	120	9	53.1	270.8	12.2	120						11	62.6	262.4	7.58	120	5	69.7	234.8	15.3	120			
9	54.2	274.6	12.8	130	8	44.5	274.9	9.2	130																		
18	50.9	252.5	7.8	140	6	44.8	274.2	10.3	140																		
16	52.5	246.3	8.1	150	3	41.1	273.8	15.1	150																		
19	64.6	235.9	9.2	160	3	44.2	272.2	18.3	160																		
17	65.6	235.2	10.5	170	3	49.7	265.7	15.3	170											8	68.5	251.8	6.4	170	8	77.4	168.5
																									10	64.0	135.3
5	71.4	206.5	13.5	210						11	41.1	304.3	11.3	210													
6	61.9	191.8	8.3	220																					5	60.1	168.1
7	61.8	189.4	7.1	230																							
10	55.9	192.9	7.1	240						7	43.4	275.1	11.6	240													

Bükk Block of Dinaridic origin, as well as the High Karst Zone in the southern Alps were smeared and transported eastwards. The restoration thus closes the gap between the Bükk and Medvednica blocks. Deformation in the Dinarides is restricted to Pannonian Basin-related extension. At 15 Ma, the Dalmatian Zone is restored as part of Adria, and slow underthrusting is accommodated below the High Karst and Budva zones, where we restore the plate boundary (Fig. 35) although we note that Adria was slowly moving rotating relative to Africa (Fig. 19). This difference was accommodated by the differential strike-slip and transpressional system observed in the external Dinarides (van Unen et al., 2019).

The main difference between our restoration and previous renditions lies in the widely held assumption that the Carpathian trench was one contiguous feature, rather than two trenches offset by a transform fault as in our restoration. The difference observed in our restoration is related to the significantly larger, but more precise estimates of the Miocene extension in the Tisza-Dacia block (Balázs et al., 2016, 2017 and references therein). Most previous reconstructions accommodate this by reconstructing a smaller amount of extension in the AlCaPa domain (Barrier et al., 2018; Faccenna et al., 2014; Golonka, 2004; Meulenkamp and Sissingh, 2003; Royden and Faccenna, 2018). Stampfli and Hochard (2009) restore no deformation in the Pannonian Basin after 40 Ma, whilst Schettino and Turco (2010) appear to restore much more extension in the Tisza-Dacia domain than in the AlCaPa domain. Handy et al. (2015) did not restore deformation in the Tisza Block, and consequently disconnected the northern and southern Carpathian trenches, but their AlCaPa restoration is similar in amount of extension. Not surprisingly, our reconstruction is similar to Ustaszewski et al. (2008), whose extension reconstructions we used as starting point for ours.

7.1.3. Eastern Mediterranean region

In our reconstruction at 15 Ma, the Dinaridic thrust front connected in a straight, NW-SE trending line with the Aegean trench in the middle Miocene, as a result of the restored extension in the Aegean back-arc region (see van Hinsbergen and Schmid (2012) for details), consistent with paleomagnetic constraints on west-Aegean rotations (Fig. 28). Extension at 15 Ma is accommodated in the Rhodope and Central Aegean extensional provinces (Fig. 35, SI1-map1) where the Rhodopian metamorphics, and the Cycladic Blueschist and Basal Unit, respectively, are exhuming. In western Anatolia, the Central Menderes Massif has been closed, restoring paleomagnetically documented counterclockwise rotations of SW Turkey (Fig. 29). As a result, a smooth curve in the trench is present towards ENE-WSW in the eastern Mediterranean region (Fig. 35). The opposite rotations of the Aegean region inevitably require major trench-parallel motion, either arc-parallel extension increasing southward, or arc-parallel shortening increasing northward. Taking the ~85 km of westward motion of Anatolia into account, restored in Fig. 35, we restore hundreds of kilometers of arc-parallel extension in the south Aegean forearc, and towards the north infer that arc-parallel extension was accommodated along the Mid-Cycladic lineament following van Hinsbergen and Schmid (2012), see also (Malandri et al. (2017).

In Anatolia, the Antalya Basin orocline was restored, along side the E-W shortening in the heart of the Isparta Angle, and E-W extension in the Central Tauride Intramontane Basins (Fig. 15). Post-15 Ma collision of the African margin and Anatolia in Cyprus is restored and we infer active subduction of oceanic crust that intervened Cyprus and Anatolia to be accommodated in a position occupied in the modern Cilicia Basin, following McPhee and van Hinsbergen (2019). This lithosphere was likely Late Cretaceous in age, genetically linked to the Cretaceous ophiolites that were emplaced southward onto Arabia and north Africa, and northward onto the southern Taurides. We refer to the ocean underlain by the lithosphere as the Misis Ocean – after the Misis Mélange (Robertson et al., 2004a), as opposed to the Eastern Mediterranean ocean that contains Triassic and older lithosphere. The Misis Mélange was offscraped from this lithosphere upon its subduction and contains no oceanic sediments or volcanics older than Late Cretaceous.

Motion along faults accommodating the westward motion of Anatolia (the North and East Anatolian Faults, the Sürgü Fault, and the Göksun and Malatya-Ovacik Faults (Fig. 15) is restored. Combined with the restoration of part of the bending of the Lesser Caucasus orocline, this accommodates most of the Arabia-Eurasia convergence after the middle Miocene. Remaining convergence is

Ionian-Tripolitza		Pelagonian					Bey Daglari/Lycian nappes					South Armenian Block					SE Anatolian rotating domain					Cyprus (Troodos)				
A95	age	n	λ	ϕ	A95	age	n	λ	ϕ	A95	age	n	λ	ϕ	A95	age	n	λ	ϕ	A95	age	n	λ	ϕ	A95	age
6.7	10	27	75.2	120.5	5.48	10	24	75.8	264.8	5.5	10						12	77.7	275.2	10.4	10					
3.7	20	27	50.9	118.2	7	20	18	74.1	264.0	8.2	20						12	64.3	285.2	10.3	20					
3.1	30	17	43.3	117.7	8.6	30						10	74.4	189.3	11.0	30	6	53.8	292.6	10.4	30					
4.5	40											9	71.7	182.9	8.6	40	23	63.2	280.5	8.1	40					
5.9	50						8	72.9	263.2	10.4	50	5	75.9	187.9	23.5	50	23	62.8	279.3	8.0	50					
5.7	60											4	74.9	207.7	35.6	60	11	61.2	263.6	16.2	60	11	55.6	270.4	7.1	60
												4	73.4	181.3	27.0	70	22	48.1	289.1	10.3	70	11	53.8	275.5	9.3	70
11.8	80											7	56.9	143.5	16.2	80	16	47.7	294.8	10.0	80					
												6	53.4	137.3	17.1	90						24	21.2	313.6	7.2	90
12.0	170																									
10.9	180																									
11.6	220																									

partitioned over the Sivas Basin and its eastward continuation (Kağızman-Tuzluca Basin, Fig. 15), and the Bitlis Suture Zone. This partitioning is chosen to cause maximum counterclockwise rotation of the SE Anatolian rotating domain (Gürer et al., 2018b, Fig. 33) to stay within paleomagnetic constraints. As a result, we restore a diachronous collision of the Bitlis and Püturge Massifs with Arabia, younging westwards. This is consistent with low-T thermochronology from the Bitlis Massif suggesting collision by 18 Ma (Cavazza et al., 2018), and stratigraphic constraints from the Kahramanmaraş Basin (Fig. 15) suggesting deep-marine sedimentation until 11 Ma (Hüsing et al., 2009a). To the east, collision between Arabia and Iran is well underway by 15 Ma (McQuarrie and van Hinsbergen, 2013; Mouthereau, 2011).

Previous reconstructions mainly differ on the location of the trench south of Anatolia. Whilst we agree with Stampfli and Hochard (2009) that subduction must have been accommodated to the north of the Kyrenia ranges of Cyprus – given evidence that shortening there started only in Tortonian times (McPhee and van Hinsbergen, 2019), many others infer either two subduction zones, one to the north and one to the south of Cyprus (i.e., ~100 km away from each other) in the middle Miocene (Robertson et al., 2013c), place the subduction zone south of Cyprus (Royden and Faccenna, 2018; Schettino and Turco, 2010) or already infer a wide continental collision zone in the middle Miocene with thrusting both north and south of Cyprus (Barrier et al., 2018). Our reconstruction agrees with that of Barrier et al. (2018) in that the Troodos Ophiolite of Cyprus was located on the North African margin prior to the Neogene incorporation into the Anatolian orogen. The other reconstructions do not specify Cyprus. Another key difference lies between our reconstruction and those of e.g. Menant et al. (2016) and Brun et al. (2016) for the Aegean region. The latter authors assume that the North Cycladic Detachment System (Jolivet et al., 2010), which runs along the northern margins of the Cycladic islands with a marked kink at the Mid-Cycladic Lineament (MCL). This kink has an angle that is proportional to the difference in azimuth of stretching lineations and paleomagnetic declinations on both sides (e.g., Walcott and White, 1998; Pastor-Galán et al., 2017). Menant et al. (2016) and Brun et al. (2016) consequently restore the North Cycladic Detachment System as a straight line prior to oroclinal bending, starting mostly around 25 Ma. Their restoration then restores Anatolia up to 400 km to the East and requires northward increasing E-W convergence to the north of the North Cycladic Detachment System, and southward increasing trench-parallel extension to the south.

7.2. Rupelian – 30 Ma

7.2.1. Western and Central Mediterranean region

For the Rupelian time-slice, the opening of the Gulf of Valencia and the Gulf of Lion, and the associated rotations of the Baleares and Corsica-Sardinia blocks, have been restored. The result is a NE-SW trending, northwestward dipping subduction zone along the margin of Iberia (Baleares) and the Calabria-Peloritan Block. At this subduction zone, continental rocks of the Alpujarride (Betics), Sebtide (Rif), Lower Kabylides, and Africo-Polsi unit (Calabria and Peloritani Mountains) are subducting and undergoing high-pressure, low-temperature metamorphism. These continental rocks are part of the conceptual 'AlKaPeCa' Block separated from the African margin by the Piemonte-Ligurian oceanic basin. As detailed in van Hinsbergen et al. (2014a), the peridotite massifs of the Betics, Rif, and Kabylides (e.g. Ronda, Beni Boussera) were probably already part of AlKaPeCa since the Jurassic, and were buried, metamorphosed, and exhumed along with the other AlKaPeCa units. The Malaguide (Betics), Ghomaride (Rif) and upper Kabylides unit were part of the Iberian forearc, whilst the Stilo-Aspromonte-Peloritani Block was located in the Sardinia forearc. To the west, we schematically indicate a cryptic plate boundary along the southern Iberian margin. As for the 15 Ma time-slice, the slow convergence rates and a total of only some tens of kilometers of Cenozoic convergence constrained from Atlantic Ocean reconstructions (Section 4, see also van Hinsbergen et al., 2014a, 2014b), this was not enough to drive a subduction zone, and may have been distributed over the African and/or Iberian margins.

Towards the northeast, the northwestward dipping subduction zone becomes intra-oceanic, with the Ligurian ophiolites in the upper plate below which the ocean-derived part of the Tuscan nappes is accreting. Western Greater Adria – i.e. the portion of Adria that is presently lost to subduction and of which only relics exist as nappes in circum-Adriatic orogens – and its ocean-continent transition toward the Piemonte-Ligurian Ocean, is at 30 Ma still intact. To the north, we interpret that the west-dipping Apenninic subduction zone connects through a transform system

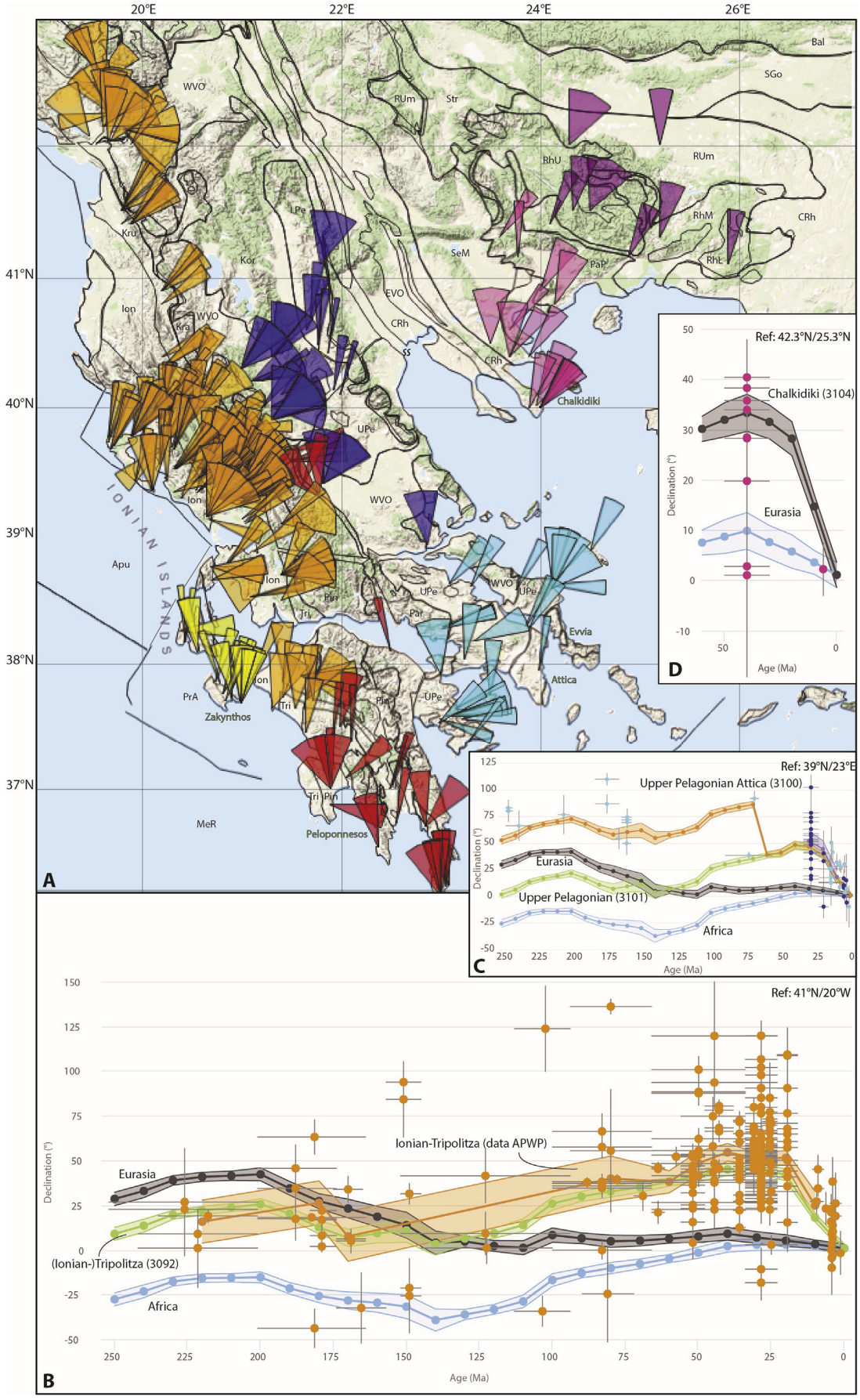
20°E
22°E
24°E
26°E
41°N
40°N
39°N
38°N
37°N
WVO
RUm
Str
Bal
SGo
RhU
RUm
RhM
CRh
RhL
PaP
SeM
LPe
Kru
Kor
Ion
Kra
EVO
CRh
SS
CRh
Chalkidiki
UPe
WVO
IONIAN ISLANDS
Ion
Apu
Ion
Pin
Tri
Par
UPe
WVO
UPe
Evvia
Attica
PrA
Ion
Zakynthos
Tri
Pin
UPe
Tri
Pin
MeR
Peloponnesos
A
Ref: 42.3°N/25.3°N
Chalkidiki (3104)
Eurasia
Declination (°)
Age (Ma)
D
Ref: 39°N/23°E
Upper Pelagonian Attica (3100)
Eurasia
Upper Pelagonian (3101)
Africa
Declination (°)
Age (Ma)
C
Ref: 41°N/20°W
Ionian-Tripolitza (data APWP)
Eurasia
(Ionian-)Tripolitza (3092)
Africa
Declination (°)
Age (Ma)
B

to the east-dipping Alpine subduction zone (Fig. 36).

The Alps are at 30 Ma thrusting northward over the Eurasian foreland that is undergoing terminal southward subduction. The westward motion of the Western Alps along the Insubric line has been restored, as well as the associated oroclinal bending. The AlCaPa unit of the eastern Alps and Pannonian Basin is fully restored for post-20 Ma extension.

As for the 15 Myr time-slice, the north and south Carpathian trenches are disconnected. The Tisza Block has been restored for clockwise rotation associated with its motion around the northwestern Moesian Platform accommodated by the Cerna and Timok Faults (Figs. 10 and 36). This restores space between the Tisza and AlCaPa units that in our reconstruction is occupied by the Bükk Block and the southern Alps portion of the High Karst unit. The Bükk and Medvednica blocks are now connected.

Deformation in the Dinarides is limited to slow underthrusting of Adria below the High Karst and Budva units. Compared to the 15 Ma time-slice, the Dinarides are restored to the SW to account for the motion of the Tisza Block. Extension between the East Bosnian-Durmitor and the Pre-Karst nappes has been restored, but the Dinaridic nappe stack otherwise did not deform between 30 and 15 Ma.

Our western and northern Mediterranean reconstruction does not differ dramatically from previous reconstructions. The different assumptions on extension direction in the Algerian Basin translate into a somewhat different distribution of the Alboran units along the southern Iberian margin, whereby our E-W extension scenarios place the Alboran units close to the Baleares (Handy et al., 2010; Lonergan and White, 1997; Rosenbaum et al., 2002a; Royden and Faccenna, 2018; and Fig. 36). N-S extension scenarios would bring the Alboran units region much closer to their modern position (Faccenna et al., 2014; Golonka, 2004; Meulenkamp and Sissingh, 2003; Schettino and Turco, 2010; Stampfli and Hochard, 2009). Platt et al. (2013) places the Alboran domain in a NE-SW orientation adjacent to the African margin above a N to NW dipping subduction zone, and do not show older reconstructions that allow evaluating how these units arrived in this position, or how they became metamorphosed. Finally, one radically different interpretation is that of Vergés and Fernàndez (2012), who proposed that subduction of the Gibraltar Slab was not northward below Iberia, but southward below Africa. They connect the plate boundary to the subduction zone below the Baleares from which they only derive the Kabylides and propose that the Gibraltar trench retreated northwestwards towards its modern position. We will address some of these alternative interpretations in the discussion section but note here that the interpretations of Algerian Basin extension are relevant for interpreting the dynamics of the Oligocene and younger subduction history, but other than placing the Alboran units somewhat differently along the Iberian (or African) margin, have little influence on preceding time-slices.

Finally, Schettino and Turco (2010, their Fig. 5B) show in their 33 Ma time-slice no subduction between Iberia and Africa, but instead suggest northward subduction to the north of a combined Iberia-Corsica-Sardinia-Adria Block, in the Pyrenees, along the Provence margin, and extending eastward along the northern edge of Adria along the Insubric line (their Fig. 5B). This is the result of their interpretation that the Corsica-Sardinia Block, in which they infer a major strike-slip fault through Sardinia and Corsica with a displacement of tens of kilometers, was part of rigid Iberia prior to 30 Ma. We are not aware of any field evidence supporting such strike slip faulting across Corsica-Sardinia. The assumption of a rigid Iberia-Sardinia-Corsica block also features in Stampfli and Hochard (2009) and Handy et al. (2010).

7.2.2. Eastern Mediterranean region

Most Aegean extension is younger than 30 Ma and is consequently restored in Fig. 36 (and SI1-map 2). This restoration juxtaposes the Adria-derived nappes of the external Hellenides against the Circum-Rhodope unit along the Sava Suture Zone, which has a conspicuous N-S striking portion in the area connecting the northern Aegean Sava suture with the western Anatolian Izmir-Ankara-Erzincan Suture Zone. Extension at 30 Myr is already active in the Rhodope region (Fig. 36 and SI1 – map 2). Africa-Europe plate boundary is reconstructed along the thrust between the Tripolitza Platform and the Ionian Zone, although the Tripolitza Platform is simultaneously underthrusting the Pindos nappe.

In western Anatolia, the Beydağları Platform and Geyikdagi nappes and the tectonically overlying Alanya and Antalya nappes were already incorporated in the Anatolian orogen by 30 Ma, and we restore the plate boundary to the south. To the East of the Troodos Ophiolite and the Anaximander and Antalya Ophiolites, Misis oceanic crust was subducting. How far west this oceanic crust, now all subducted except for the ophiolites, once reached is hard to establish and we restore a limit around the longitude of the Anaximander Mountains.

In Central Anatolia, the Kırşehir orocline is in its final stages of formation, and indentation into the Çankırı Basin (Fig. 36, SI1 – map 2). Towards the east, the eastern Taurides Block is restored southwards along the Ecemiş Fault. The separation between the eastern Taurides and Eastern Pontides becomes larger eastwards as a result of restoring the paleomagnetically documented counterclockwise rotation of the SE Anatolian rotating domain (Fig. 33). This results in a wide separation of the eastern Taurides and Pontides. There is no record of Oligocene to early Miocene significant continental shortening in the eastern Pontides or eastern Taurides – all nappes appear to have been stacked in Eocene time and before, suggesting that this convergence was accommodated by wholesale underthrusting. We follow Gürer and van Hinsbergen (2019) and map this lost lithosphere as Cretaceous oceanic crust, similar in age and nature as the Misis oceanic crust to the south of the Taurides: it must have been connected to the obducted ophiolites now found on the Kırşehir Block and the northern parts of the eastern Taurides (Fig. 36). As pointed out by Gürer and van Hinsbergen (2019), the subduction thrust accommodating the convergence between the eastern Taurides and Pontides must have been located within the Sivas Basin, along a structure that in its modern surface expression is known as the Deliler-Tecer Fault (Fig. 15).

Even by restoring the shortening associated with Lesser Caucasus-Talysz oroclinal bending, there must have been several hundreds of kilometers of convergence between the easternmost Taurides-Bitlis blocks and the South Armenian Block. We thus infer,

Fig. 28. Paleomagnetic data from the western and northern Aegean region. For key to abbreviations, see Table 4. Data from the Pre-Apulian Zone in yellow, from the Ionian and Tripolitza zones in orange, from the Pindos Zone in red, from the Upper Pelagonian Zone in blue (and the Pelagonian Zone in Attica in Cyan), from the Chalkidiki Peninsula in pink, from the Rhodope in purple. B) Declination versus age graph for the Ionian and Tripolitza zones. The GAPWaP of Torsvik et al. (2012) is shown in coordinates of the Tripolitza Zone (code 3092 in reconstruction files, see Supplementary Information 3), Eurasia, and Africa. Orange curve corresponds to the apparent polar wander path of the Ionian and Tripolitze zones calculated from the data (20 Myr sliding window), see Table 5. C) Declination versus age graph for the Upper Pelagonian Zone. The GAPWaP of Torsvik et al. (2012) is shown in coordinates of the Upper Pelagionian Zone (code 3101) and the Upper Pelagonian Zone of Attica (code 3100). Purple curve corresponds to the apparent polar wander path of the Upper Pelagonian calculated from the data (20 Myr sliding window), see Table 5. D) Declination versus age graph for the Chalkidiki Peninsula. The GAPWaP of Torsvik et al. (2012) is shown in coordinates of the Chalkidiki (code 3104), and Eurasia. Ref = Reference location for which graph was calculated. See Supplementary Information 2 for data files. See text for further explanation.

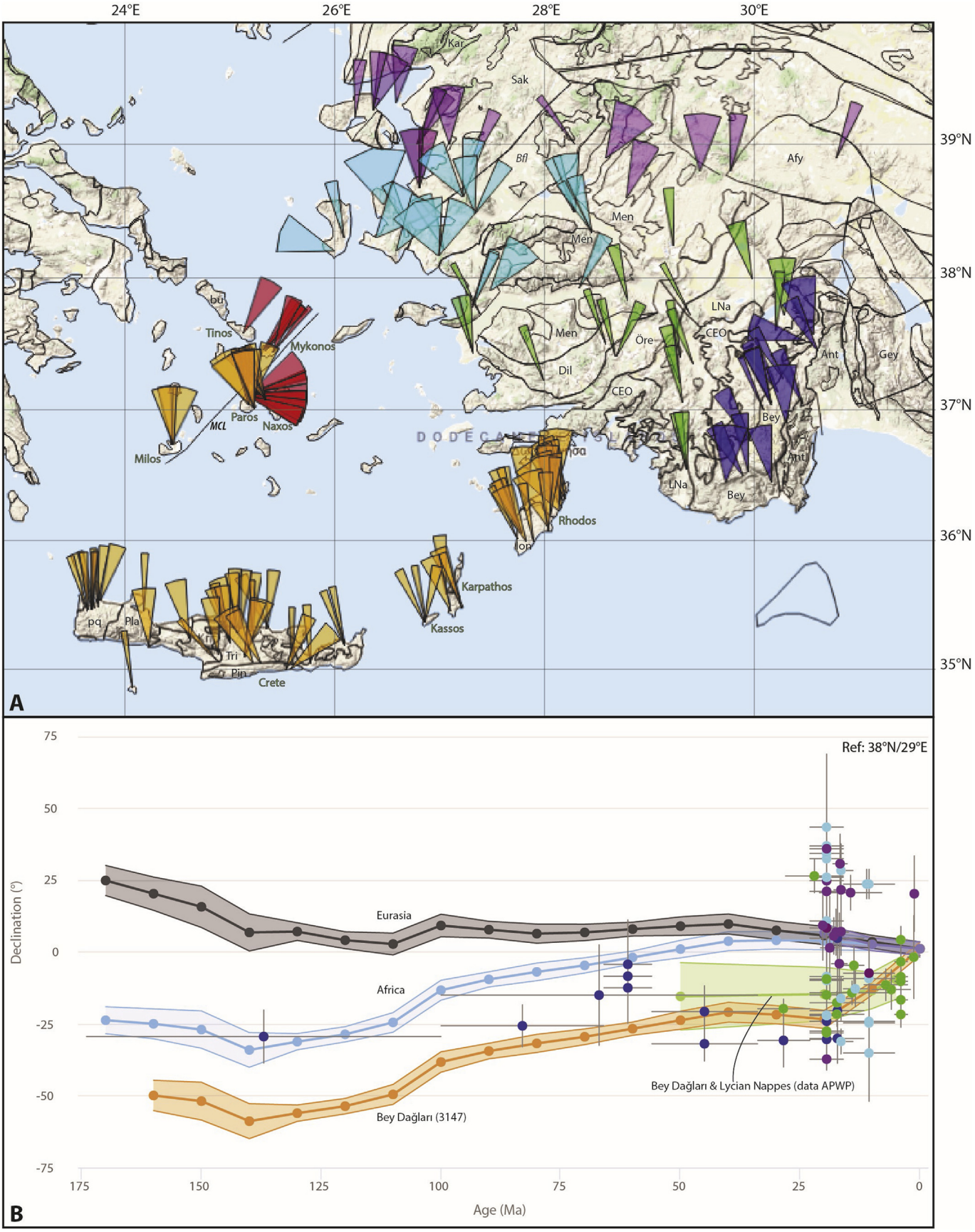

Fig. 29. Paleomagnetic data from the western Anatolia and the central, southern and eastern Aegean region. For key to abbreviations, see Table 4. B) Declination versus age graph for the Beydağları Platform, the Lycian Nappes, and Menderes Massif. The GAPWaP of Torsvik et al. (2012) is shown in coordinates of the Beydağları Platform (code 3147 in reconstruction files, see Supplementary Information 3), Eurasia, and Africa. Green curve corresponds to the apparent polar wander path of the Beydağları Platform and Lycian Nappes calculated from the data (20 Myr sliding window), see Table 5. Ref = Reference location for which graph was calculated. See Supplementary Information 2 for data files. See text for further explanation.

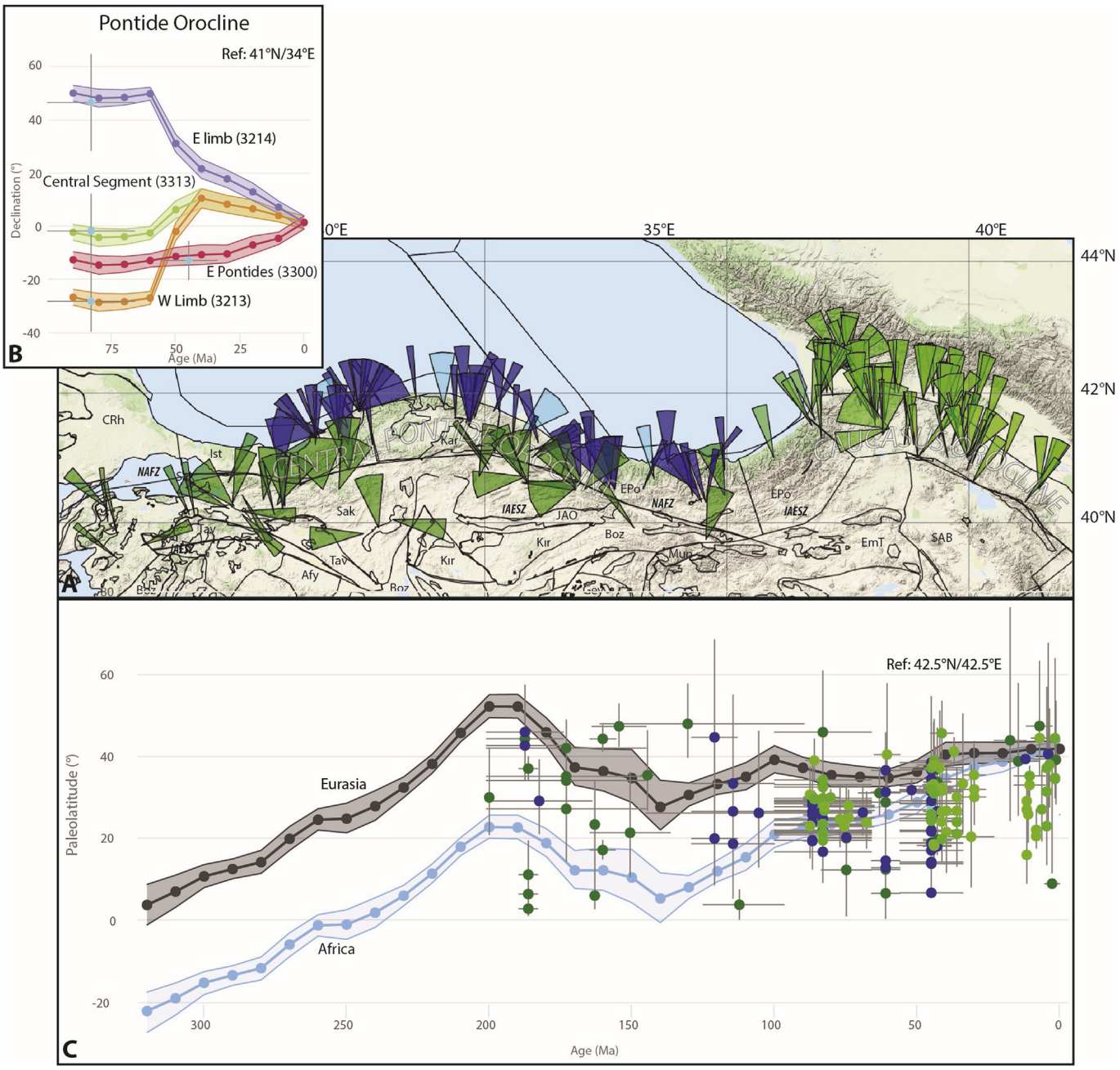

Fig. 30. Paleomagnetic data from the Pontides. For key to abbreviations, see Table 4. Data in green come from the damage zone between the Izmir-Ankara-Erzincan Suture Zone and the North Anatolian Fault Zone and are often locally rotated. Data in blue are coherent and were used to constrain the rotation history of the Central Pontide Orocline. B) Declination versus age graph for the Pontide orocline, whereby sites per limb were averaged. The GAPWaP of Torsvik et al. (2012) is shown in coordinates of the limbs of the orocline (codes 3213, 3214, 3300, and 3313 in reconstruction files, see Supplementary Information 3). C) Paleolatitude versus age graph for the Pontides. Note the large scatter of the data that make assignment to the African or Eurasian APWP paleomagnetically inconclusive. Ref = Reference location for which graph was calculated. See Supplementary Information 2 for data files. See text for further explanation.

based on similar reasoning as for the Sivas Basin, that oceanic subduction was also ongoing south between the easternmost Taurides and the South Armenian Block. There is no record of significant Oligocene shortening within the easternmost Tauride-Bitlis region, which consequently is a largely metamorphic massif occupying the same area as in the 15 Ma time-slice (Figs. 35 and 36). Restoring the paleomagnetically documented counterclockwise rotation (Fig. 33) brings the Bitlis-easternmost Taurides much farther south than at 15 Ma, but north of the north Arabian margin. We thus infer that at 30 Ma, the Misis Ocean subducted below at the Bitlis-Püturge active margin, connected to the Aegean trench to the west. Finally, the two trenches of eastern Anatolia and the Zagros trench of Iran were connected through a transform fault along the western margin of the Iranian Cimmerides (Fig. 36).

Our eastern Mediterranean reconstruction contains several first-order differences compared to previous reconstructions. First, there is disagreement in reconstructions on whether there was an oceanic corridor between the Bitlis Massif and Arabia, and second, there are different views on where convergence was accommodated in Anatolia and Greece. First, most reconstructions agree on a gradual change from a NW-SE to E-W trending trench with the bend located at the transition from the Aegean region to Anatolia

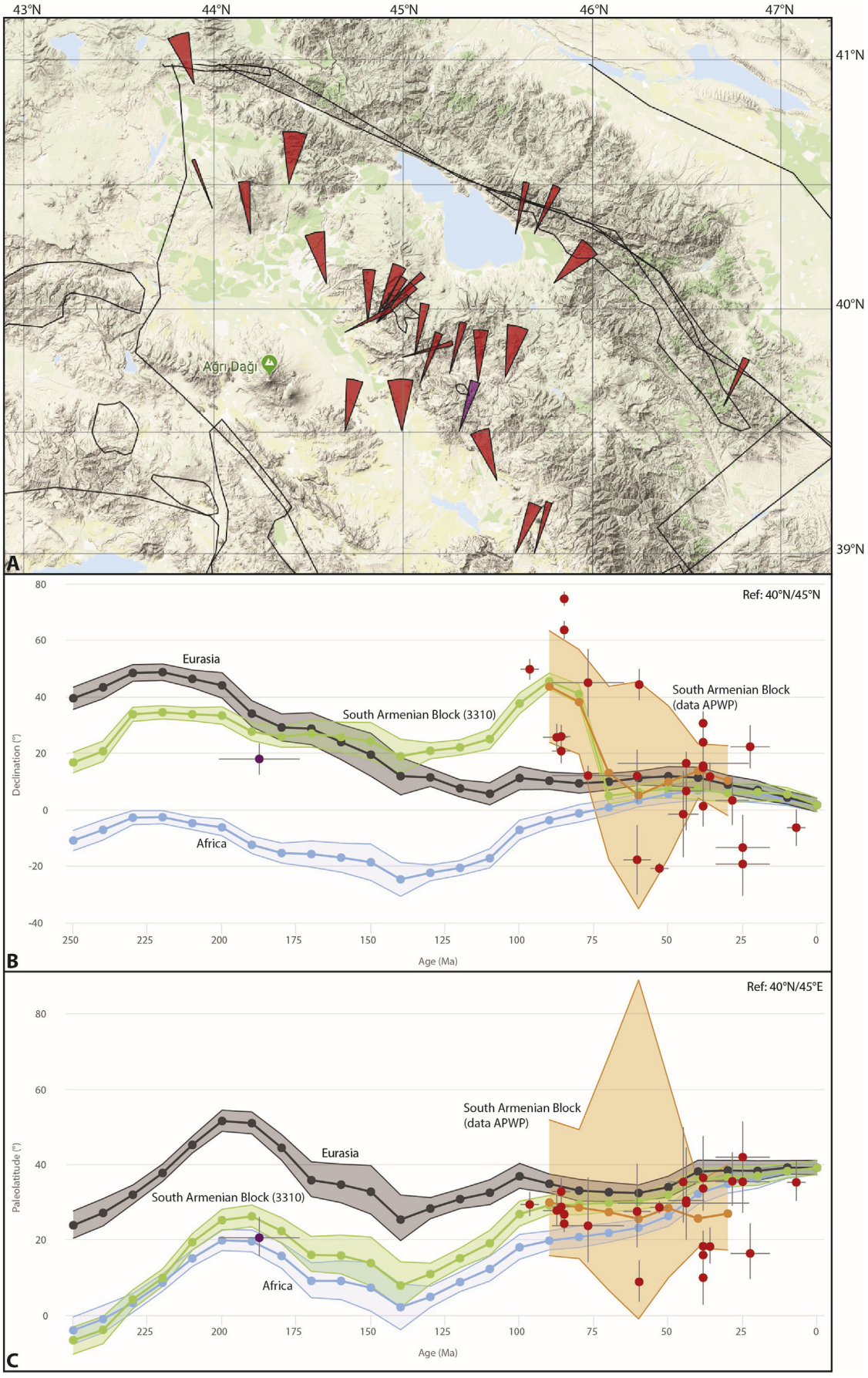
43°N
44°N
45°N
46°N
47°N
41°N
40°N
39°N
Ağrı Dağı
A
Ref: 40°N/45°N
Eurasia
South Armenian Block (3310)
South Armenian Block
(data APWP)
Africa
Declination (°)
Age (Ma)
B
Ref: 40°N/45°E
South Armenian Block
(data APWP)
Eurasia
South Armenian Block (3310)
Africa
Paleolatitude (°)
Age (Ma)
C

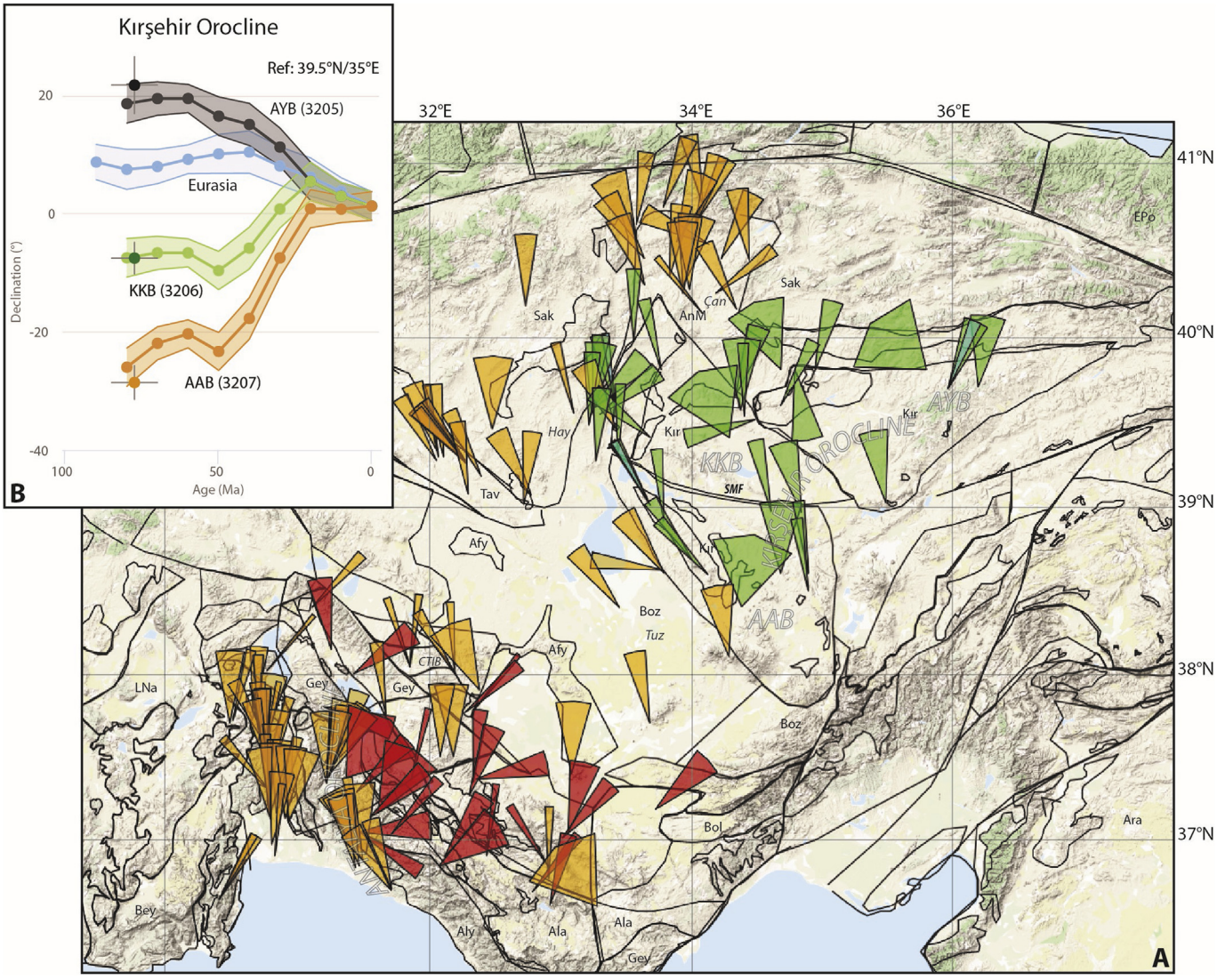

Fig. 32. Paleomagnetic data from Central Anatolia. For key to abbreviations, see Table 4. Data in lime green are from the Kırşehir Block, in red from the Tauride nappes, and in yellow from Eocene and younger sedimentary cover rocks. B) Declination versus age graph for the Kırşehir orocline, whereby sites for each block were averaged. The GAPWaP of Torsvik et al. (2012) is shown in coordinates of the Akdağ-Yozgat Block (AYB), the Kırşehir-Kırıkkale Block (KKB) and the Ağacören-Avanos Block (AAB) (codes 3205, 3206, and 3207, respectively in reconstruction files, see Supplementary Information 3), as defined by Lefebvre et al. (2013a). For discussion and detailed analyses of the Antalya Basin orocline, see (Koç et al., 2016, 2018) and the Central Taurides, see (McPhee et al., 2018b). Ref = Reference location for which graph was calculated. See Supplementary Information 2 for data files. See text for further explanation.

(Barrier et al., 2018; Brun et al., 2016; Meulenkamp and Sissingh, 2003; Stampfli and Hochard, 2009) and Faccenna et al. (2014) and Menant et al. (2016) give a more schematic WNW-ESE trend from the Dinarides to eastern Anatolia. The reconstructions of Brun et al. (2016) and Menant et al. (2016) differ significantly from ours in the reconstruction of the Aegean region. They infer that there was no trench-parallel extension in the Cycladic region and disagree on our interpretation of the Mid-Cycladic Lineament as a major extensional feature. Their reconstructions instead require up to 400 km of post-30 Ma trench-parallel convergence between western Anatolia and the Dinarides-Hellenides to account for the Hellenic oroclinal bending in the Cycladic region, but still contain several hundreds of kilometers of trench-parallel extension in the forearc region from Rhodos to Crete and the Peloponnesos.

Other differences pertain to how reconstructions distribute convergence over subduction and orogenic shortening. Stampfli and Hochard (2009) infer that most or all convergence was accommodated by the Bitlis-Aegean trench. Barrier et al. (2018) and Darin et al. (2018), who both interpret full continental collision across the Bitlis suture already at 30 Ma, instead distribute all ~700 km of post-30 Ma Arabia-Europe convergence over the Bitlis and Izmir-Ankara-Erzincan Suture and Sivas region. The reconstruction of Menant et al. (2016) is essentially similar, although they do not specify where post-30 Ma shortening is accommodated within Anatolia. Schettino and Turco (2010) reconstruct two subduction zones across all of Anatolia, whereby they infer some

Fig. 31. Paleomagnetic data from the South Armenian Block. For key to abbreviations, see Table 4. B) Declination versus age graph for the South Armenian Block. The GAPWaP of Torsvik et al. (2012) is shown in coordinates of the South Armenian Block (codes 3310 in reconstruction files, see Supplementary Information 3), Eurasia, and Africa. Orange curve corresponds to the apparent polar wander path of the South Armenian Block (20 Myr sliding window), see Table 5. C) Paleolatitude versus age graph for the South Armenian Block. The GAPWaP of Torsvik et al. (2012) is shown in coordinates of the South Armenian Block (codes 3310 in reconstruction files, see Supplementary Information 3), Eurasia, and Africa. Ref = Reference location for which graph was calculated. See Supplementary Information 2 for data files. See text for further explanation.

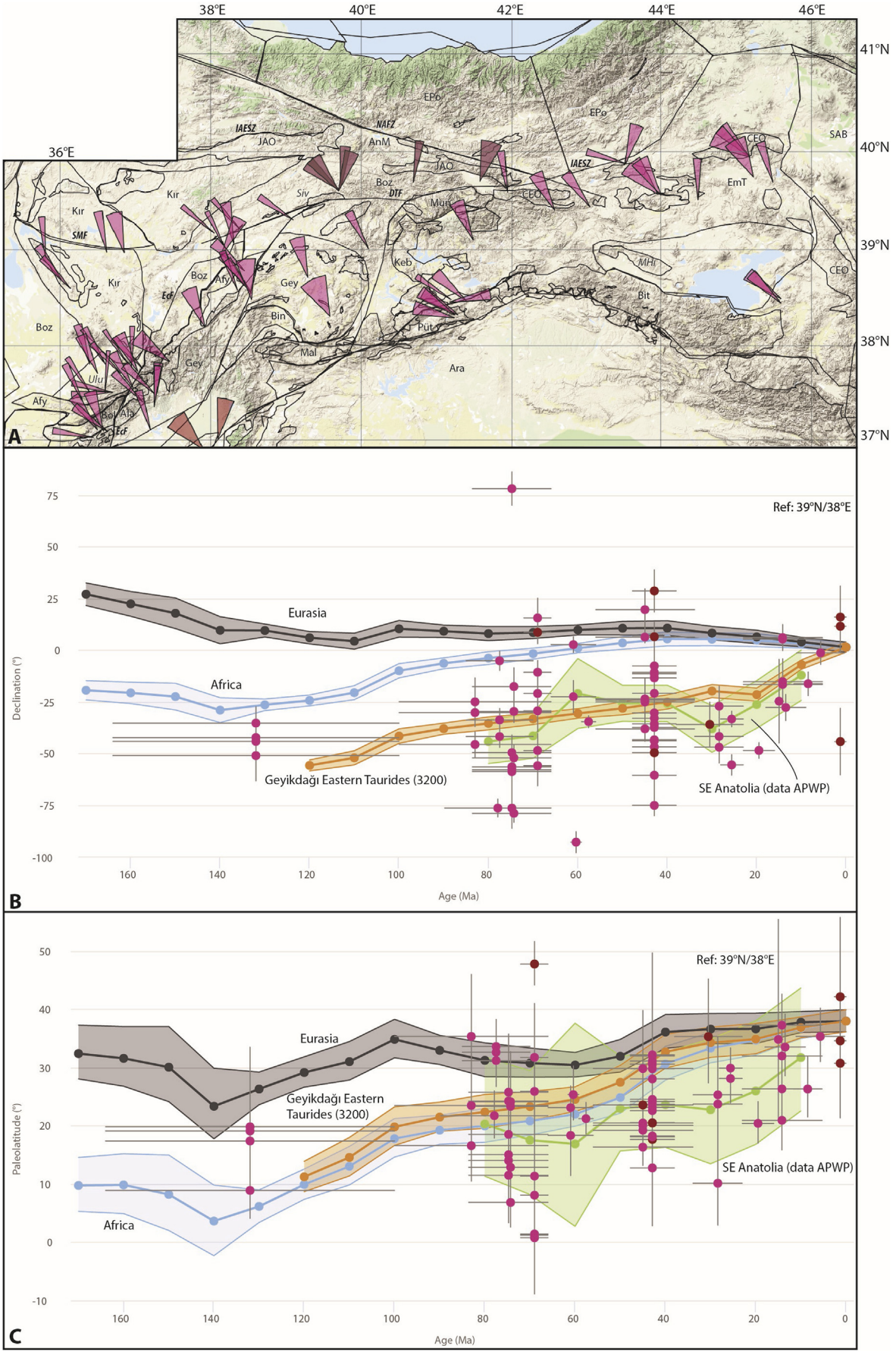
38°E
40°E
42°E
44°E
46°E
41°N
40°N
39°N
38°N
37°N
36°E
EPo
IAESZ
JAO
NAFZ
AnM
SAB
CEO
EmT
Kır
Siv
DTF
Mün
SMF
Keb
MHi
Boz
Afy
Ecf
Gey
Bit
Bin
Put
Mal
Ara
Ulu
Bol
Ala
A
Ref: 39°N/38°E
Eurasia
Africa
Geyikdağı Eastern Taurides (3200)
SE Anatolia (data APWP)
Declination (°)
Age (Ma)
B
Paleolatitude (°)
C

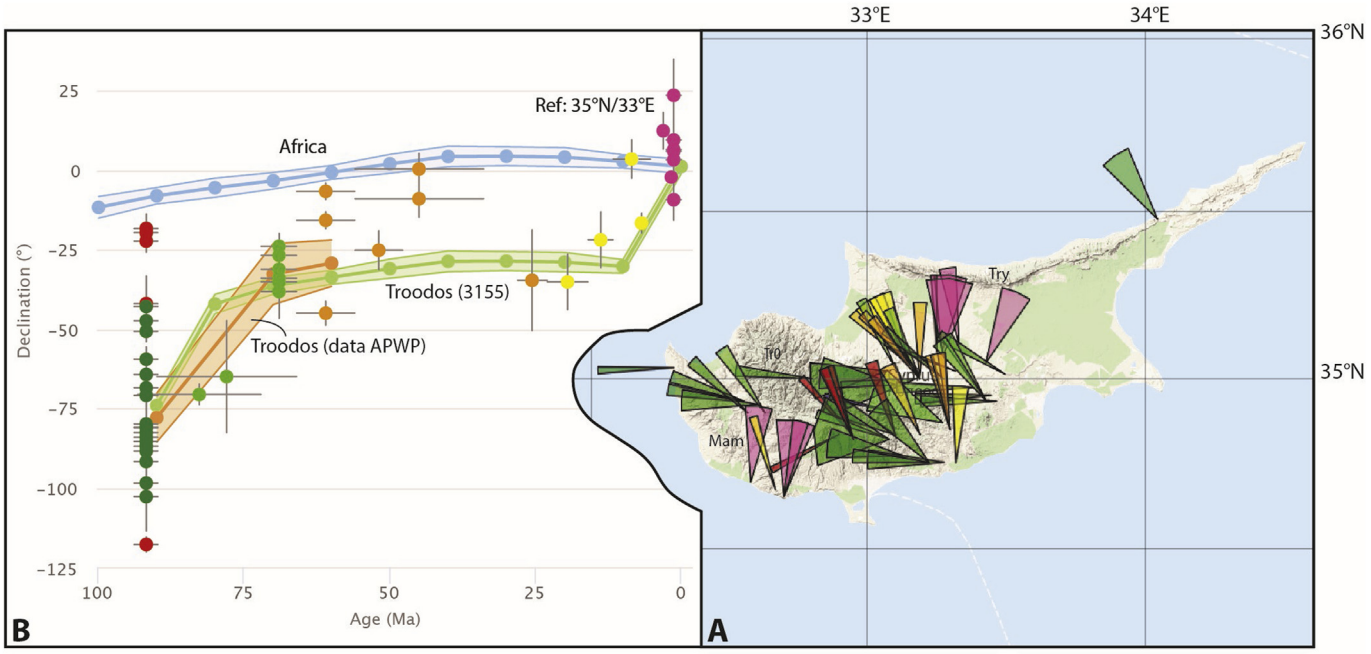

Fig. 34. Paleomagnetic data from Cyprus. For key to abbreviations, see Table 4. B) Declination versus age graph for Cyprus. The GAPWaP of Torsvik et al. (2012) is shown in coordinates of the Troodos Ophiolite (code 3155 in reconstruction files, see Supplementary Information 3) and Africa. Orange curve corresponds to the apparent polar wander path of the Troodos Massif and Cyprus calculated from the data (20 Myr sliding window), see Table 5. Ref = Reference location for which graph was calculated. See Supplementary Information 2 for data files. See text for further explanation.

300 km of post-30 Ma (continental) subduction along all of an Izmir-Ankara-Erzincan subduction zone. They infer that in Greece subduction at 30 Ma was accommodated only at the Sava suture. Royden and Faccenna (2018) also place the Aegean subduction zone far north, close to Moesia, and into the Izmir-Ankara-Erzincan Suture disappearing eastwards, jumping towards the Bitlis suture in eastern Turkey.

7.3. *Lutetian — 45 Ma*

7.3.1. *Western and Central Mediterranean region*

In Lutetian time, Africa-Europe convergence constrained from Atlantic Ocean reconstructions (Section 4) in the western Mediterranean region is slow, roughly N-S oriented, and mostly accommodated in the Pyrenees and Atlas Mountains (Fig. 37, SI1 — map 3). Towards the east, we infer slow subduction at the Baleares margin, whereby the total amount of pre-30 Ma convergence there was less than 100 km (see also van Hinsbergen et al. (2014a). To account for the Eocene burial and metamorphism of the AlKaPeCa units, we infer that subduction has always been northwestwards in this segment. Compared to a previous rendition of this reconstruction shown in van Hinsbergen et al. (2014a), we made one change in the restoration of Corsica and Sardinia, which at 45 Ma lies in a more back-rotated position to account for paleomagnetic data (Fig. 21). As a result, we cannot restore a contiguous Baleares-Sardinia trench as in van Hinsbergen et al. (2014a), but instead infer an offet along a transform fault that coincides with the later North Baleares Transform Zone (Fig. 5). As a result, post-45 Ma subduction accommodated at the Calabrian Subduction Zone was several hundred kilometers more than in the Baleares (Kabylides) segment. The polarity of pre-30 Ma subduction in the western Mediterranean region is debated, and we will address this further in the discussion section.

Subduction towards the northeast, along Corsica, however, was certainly southeastward (see also Fig. 11), dipping below oceanic lithosphere preserved in the Ligurian ophiolites. We connect the Alpine trench and the Calabrian trench along a transform fault (Fig. 37, SI1 — map 3), which later will be inherited as the transform separating the Northern Appenines and Calabria Slabs. We reconstruct the switch in subduction from southeastward Corsican to westward Northern Apenninic at 35 Ma. To account for the Eocene clockwise rotation of Corsica-Sardinia documented paleomagnetically (Fig. 21), we infer northward thrusting of Corsica towards Eurasia, consistent with structural constraints from the Provence region (e.g., Espurt et al., 2012a). Moreover, because Corsica-Sardinia did not experience the Iberian rotation, and Iberia did not undergo the rotations of Corsica-Sardinia (compare Figs. 18 and 21), we separate the two by a transform (Fig. 37, SI1 — map 3). The Eocene Corsica-Sardinia rotation requires an eastward increasing amount of shortening that is considerably larger than documented from the geology of the Provence, and we infer that much of this is accommodated along structures hidden in the basement of the Gulf of Lion.

Southeast to southward subduction continues to the northeast along the northern Alps and consumes oceanic or hyperextended lithosphere of the Valais-Magura Ocean. We infer that this oceanic basin pinched out westwards between Corsica-Sardinia and Eurasia. There is only small-scale Eocene thrusting, and no record of

Fig. 33. Paleomagnetic data from SE Anatolia. For key to abbreviations, see Table 4. Data in brown are located north of the Deliler-Tecer Fault, or within the East Anatolian Fault Zone. B) Declination versus age graph for the SE Anatolian region, which underwent a coherent, late Cenozoic, counterclockwise rotation. The GAPWaP of Torsvik et al. (2012) is shown in coordinates of the Geyikdağı unit of the Eastern Taurides (code 3200 in reconstruction files, see Supplementary Information 3), Africa, and Eurasia. Green curve corresponds to the apparent polar wander path of the SE Anatolian domain calculated from the data (20 Myr sliding window), see Table 5. C) Paleolatitude versus age graph for the SE Anatolian region. The GAPWaP of Torsvik et al. (2012) is shown in coordinates of the Geyikdağı unit of the Eastern Taurides (code 3200), Africa, and Eurasia. Ref = Reference location for which graph was calculated. See Supplementary Information 2 for data files. See text for further explanation.

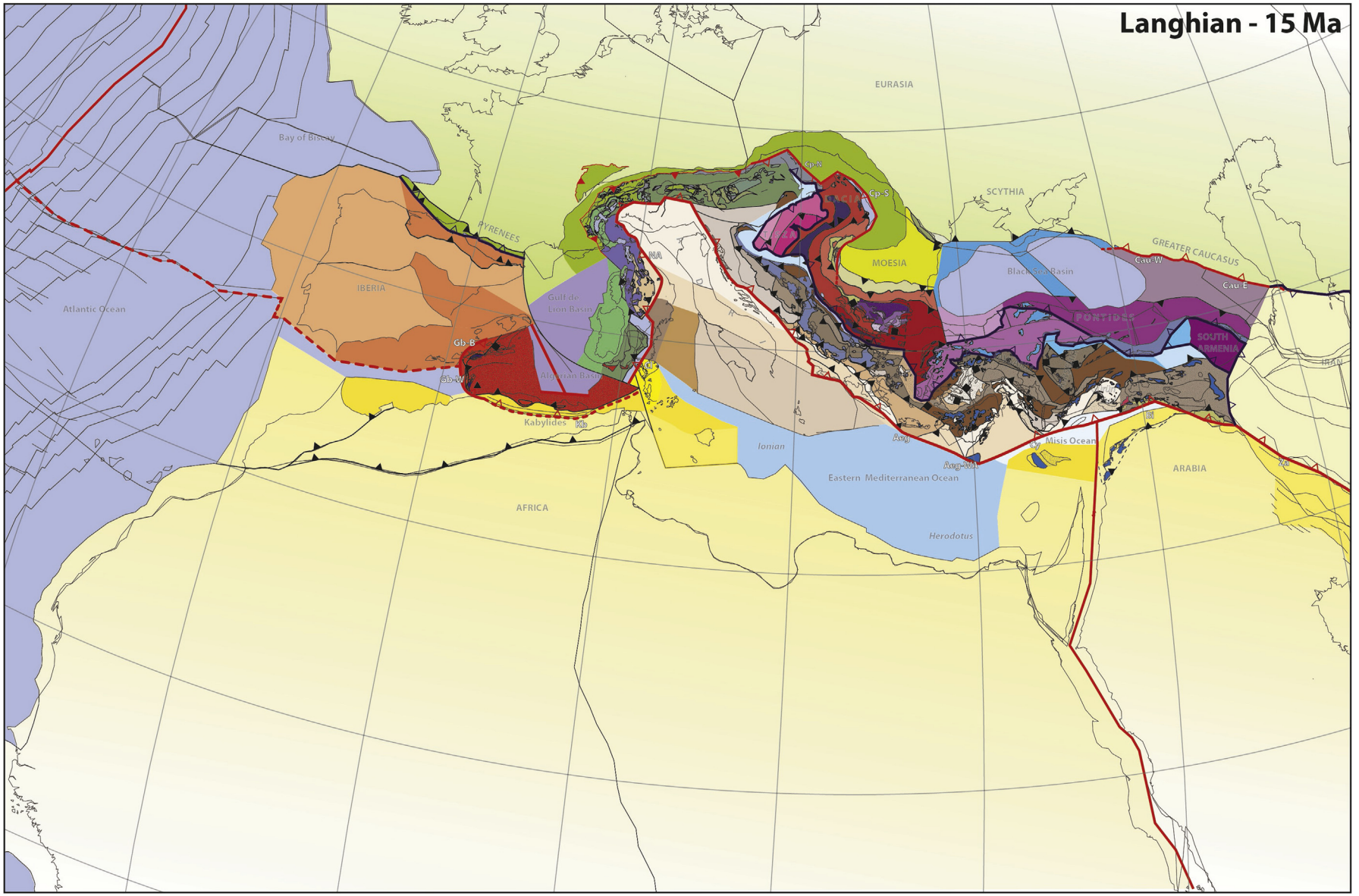

Fig. 35. Paleotectonic map of the Mediterranean region for the Langhian (15 Ma). Map is projected in a Europe-fixed reference frame. Latitudinal and longitudinal graticules in 10° intervals. See Supplementary Information 1 – map 2 for a larger version of the map that includes abbreviations of the detailed tectonic units. GPlates rotation files are provided in Supplementary Information 3. For key to tectonic units, see Fig. 5.

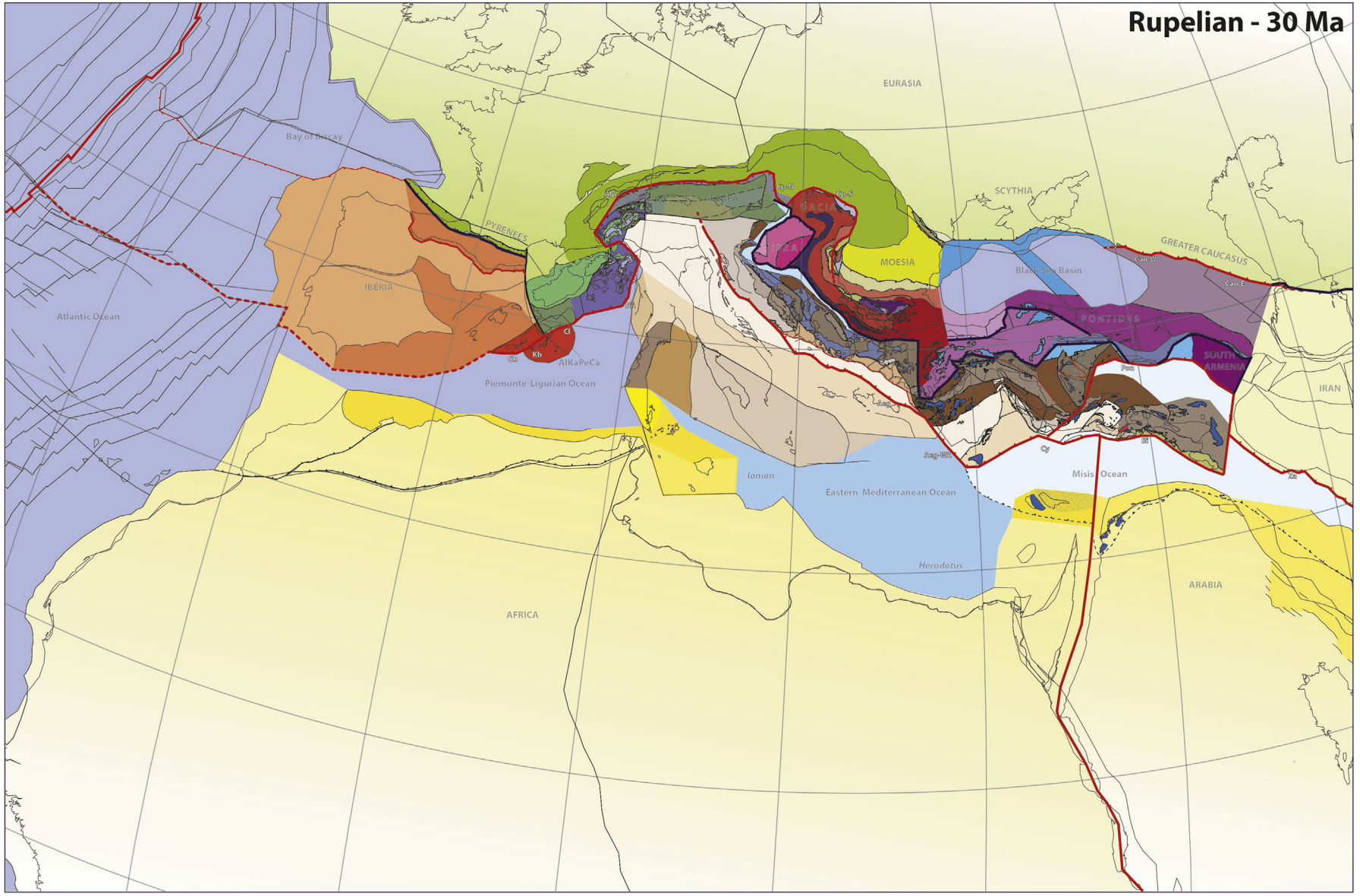

Fig. 36. Paleotectonic map of the Mediterranean region for the Rupelian (30 Ma). Map is projected in a Europe-fixed reference frame. Latitudinal and longitudinal graticules in 10° intervals. See Supplementary Information 1 – map 3 for a larger version of the map that includes abbreviations of the detailed tectonic units. GPlates rotation files are provided in Supplementary Information 3. For key to tectonic units, see Fig. 5.

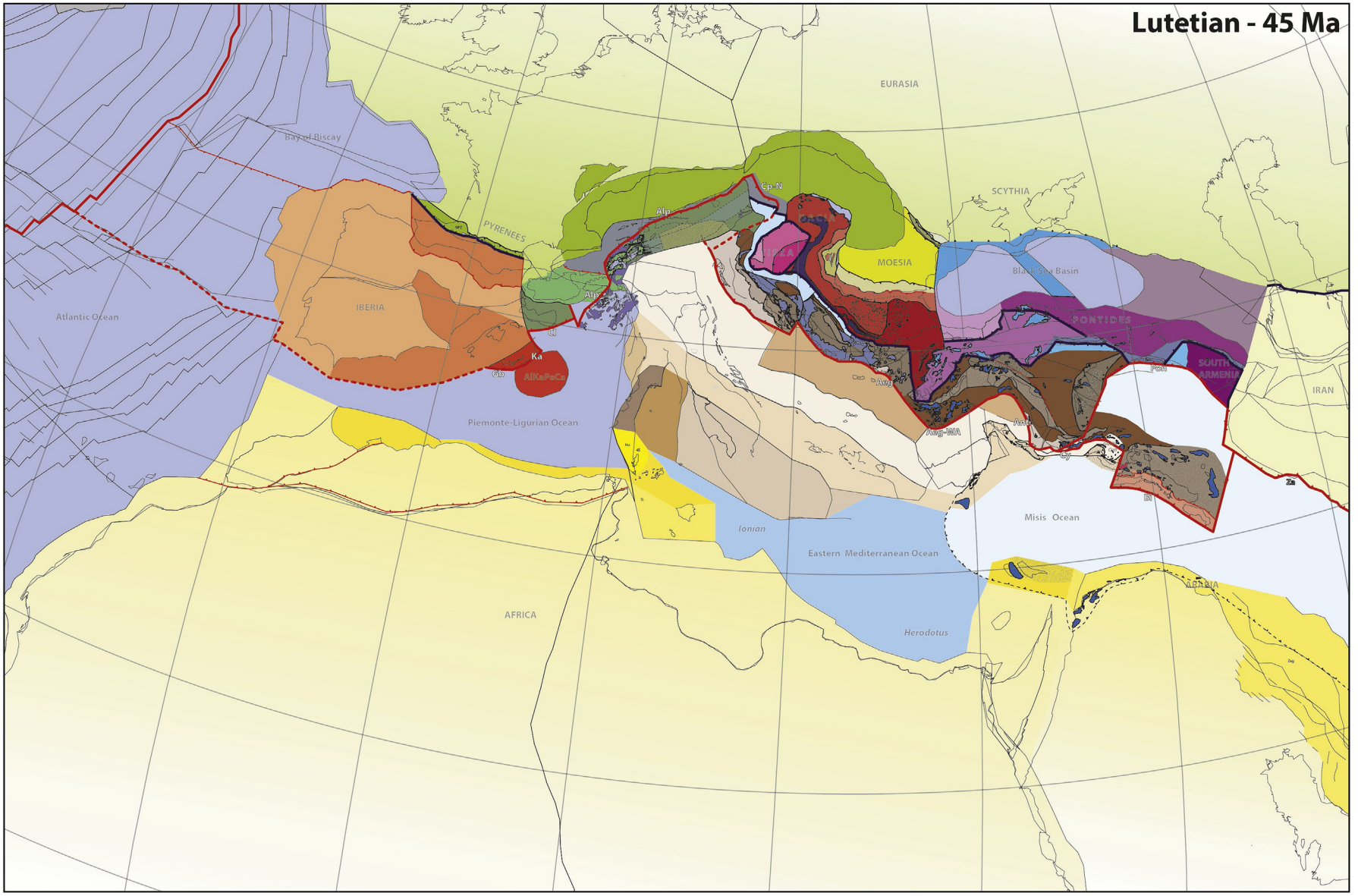

Fig. 37. Paleotectonic map of the Mediterranean region for the Lutetian (45 Ma). Map is projected in a Europe-fixed reference frame. Latitudinal and longitudinal graticules in 10° intervals. See Supplementary Information 1 – map 4 for a larger version of the map that includes abbreviations of the detailed tectonic units. GPlates rotation files are provided in Supplementary Information 3. For key to tectonic units, see Fig. 5.

Eocene accretion along the Dacia margin outside the Balkanides, nor extension in the Tisza-Dacia domain or strike-slip motion around the Moesian Platform to drive such convergence and our reconstruction infers that the Tisza-Dacia Block did not move relative to Moesia between 60 and 33 Ma. We thus infer that the north Alpine plate boundary connected to the Dinaridic thrust front along a transform system coinciding with the Sava suture in the modern Pannonian Basin (Fig. 37, SI1 – map 3). To avoid overlap between the AlCaPa nappes and the Tisza Block, we infer that this block underwent a clockwise rotation in the Paleogene. Such a rotation is consistent with paleomagnetic data (Fig. 26) but implies shortening between the AlCaPa nappes and the Southern Alps. Slow underthrusting of Adria in the Dinarides is accommodated below the High Karst nappe. From there, a trench is traced towards the southeast (see next section). Towards the northwest, the plate boundary becomes diffuse, accommodated perhaps within the AlCaPa domain, and partly transferring toward the Alpine trench (Fig. 37).

Differences between our reconstruction and previous versions at 45 Ma stem from interpretations that also featured in the 30 Ma reconstruction. Assuming Corsica-Sardinia was a part of contiguous Iberia logically suggests that the Pyrenees plate boundary – diffuse across the Pyrenean fold-and-thrust belt since the Late Cretaceous – continues along the Provence margin, and would accommodate all Africa-Europe convergence. Reconstructions for the Eocene assuming this (Schettino and Turco, 2010; Stampfli and Hochard, 2009) thus have no trench along the south Iberian margin. For the Alps-Carpathian regions, Barrier et al. (2018) and Schettino and Turco (2010) inferred a contiguous trench along Dacia and AlCaPa, instead of the separation by a transform. Csontos and Vörös (2004), however, inferred a transform plate boundary between Tisza-Dacia and AlCaPa similar to our reconstruction, although their AlCaPa Block is considerably smaller and is located west of Tisza in the Eocene. This would require ~500 km of post-Eocene extension of AlCaPa. Stampfli and Hochard (2009) restore some ocean in front of the Carpathian subduction zone, implying an end of subduction and convergence in the Carpathian realm between 45 and 30 Ma.

7.3.2. Eastern Mediterranean region

Our reconstruction of the Dinarides and Hellenides uses independent constraints from these orogens, which we assume are more or less cylindrical, non-cilindricity only being reconstructed where structural or paleomagnetic constraints require so. The constraints from the two orogens are grossly similar, but there are differences in shortening amounts and timing. In our reconstruction, these differences are accommodated along the modern Scutari-Pec Fault (Fig. 12), which acts as a transform or transfer fault for much of the last 130 Ma. To what extent this is realistic, or a reconstruction artifact will be discussed in section 8.1. At 45 Ma, our reconstruction shows an offset along this “proto-Scutari Pec Fault”. At 45 Ma, the Pindos-Kraiste Basin, and its southern Dinaridic equivalent, the Budva Zone, are subducting. To the south of the proto-Scutari-Pec Fault, the Pindos Basin is much wider than to the north in our reconstruction as a result of the differences in shortening history between the Dinarides – Tisza-Dacia orogens, and the Hellenides-Rhodope orogens (Fig. 37, SI1 – map 3).

The Pindos Basin is subducting all along the Albinides-Hellenides segment. The Aegean extensional back-arc is now fully restored, and the Rhodope nappes are buried below the Circum-Rhodope, Serbomacedonian, and Sredna Gora nappes. The Pindos Basin is traced into western Turkey where it is known as the Dilek nappe. In Western Anatolia, the Dilek Nappe underthrusted earlier and at 45 Ma the Menderes nappes, restored as part of the Tripolitza-Beydağları-Geyikdağı Platform, are underthrusting and accreting. Our reconstruction follows McPhee et al. (2018b) in the Central Taurides, where we reconstruct a pinching out Dilek Basin between the Aladağ and Geyikdağı Platforms (Fig. 37, SI1 – map 3).

At 45 Ma the Aegean trench connects to the thrust currently located below the Lycian Nappes, which we correlate to the Bozdağ nappe and overlying Cretaceous ophiolites. This trench makes a conspicuous southward turn across the Central Taurides, from where it runs eastwards. At this trench, continental subduction is ongoing all along southern Turkey, accreting the Menderes and Geyikdağı nappes, and the already existing, inactive Antalya-Alanya nappes that thrusted onto the Beydağları-Geyikdağı Platform. This Geyikdağı Platform is traced to the Gürün Curl, where stratigraphic constraints show that the Geyikdağı nappes were accreting in Lutetian times. The Geyikdağı Platform is also there overlain by a top-to-the-north thrust stack of the Malatya and Binboğa nappes and overlying and interleaved ophiolites. To the east of the Gürün Curl, however, the style of deformation was significantly different. There is no record of Eocene accretion there, but instead the Maden Arc and its non-volcanic equivalent, the Hakkari Basin, were being overthrusted by the Bitlis-Püturge Massifs. Because the Maden Arc also unconformably overlies the Püturge Massif, this shortening occurred within the upper plate of a subduction zone, and not at the subduction zone itself, which must have been located to the south. We restore this shortening and connect the trench north of the Gürün Curl with the Bitlis trench along a right-lateral transform fault (Fig. 37, SI1 – map 3). We connect the Bitlis trench with the Zagros trench along a left-lateral transform.

The subduction configuration in eastern Anatolia is similar in style as at 30 Ma. The restored distance between the eastern Taurides and eastern Pontides is larger at 45 Ma than at 30 Ma, and amounts some 400 km, taking the restoration of the Lesser Caucasus orocline into account. This larger distance is the result of the restoration of the displacement along the Ecemiş Fault and the oroclinal bending of the Kırşehir Block (see also Gürer and van Hinsbergen (2019). In western Turkey, the shortening associated with the oroclinal bending of the Kırşehir Block predicts shortening between the N-S trending Central Tauride fold-and-thrust belt and the Pontides. The magnitude of motion required coincides in timing and amount with the right-lateral strike-slip along the Uludağ-Eskişehir Fault. We thus restore the associated extrusion and restore the Tavşanlı and Afyon Zones to the south of this fault southeastward.

Our reconstruction agrees with most previous reconstructions on the location and orientation of the Hellenic and Anatolian trench, smoothly curving from NW-SE to W-E around western Anatolia, and consuming the Pindos Basin in the west (Barrier et al., 2018; Csontos and Vörös, 2004; Menant et al., 2016; Stampfli and Hochard, 2009). Stampfli and Hochard (2009), Menant et al. (2016) and Barrier et al. (2018) also restored the continental subduction of the Menderes and Geyikdağı nappes and Menant et al. (2016) and Barrier et al. (2018) also identified the Alanya and Antalya nappes as passive riders on the Beydağları- Geyikdağı margin at 45 Ma. Other reconstructions indicate northward oceanic subduction below the southern Tauride margin (Darin et al., 2018; Meulenkamp and Sissingh, 2003; Robertson et al., 2013c; Schettino and Turco, 2010). Towards the east, almost all reconstructions indicate oceanic subduction below the Bitlis Massif at 45 Ma (Barrier et al., 2018; Csontos and Vörös, 2004; Menant et al., 2016; Meulenkamp and Sissingh, 2003; Robertson et al., 2013c; Schettino and Turco, 2010; Stampfli and Hochard, 2009). Only Darin et al. (2018) infer that the >1000 km of post-45 Ma Arabia-Europe convergence was accommodated by intra-continental shortening, and map a full collision at this time at the Bitlis Suture.

Stampfli and Hochard (2009) also specifies that the crust subducting below the Bitlis Massif in the Eocene must have formed in a back-arc basin that formed during westward roll-back into the Eastern Mediterranean Ocean (also called the Mesogea Ocean) emplacing the Troodos Ophiolite. They infer that this subduction

was still active at 48 Ma, whereas our reconstruction estimates the arrest of this subduction zone at ~70-65 Ma. Moix et al. (2008) also mapped this westward roll-back, but inferred that this trench and associated upper plate ophiolites at 48 Ma was active and was still located between the eastern Taurides and NW Arabia, obducting the NW Arabian ophiolites. Robertson et al. (2013c) inferred a transform fault between the easternmost Taurides and Püturge Massif and the Gürün Curl, similar as in our reconstruction. Most of these reconstructions assume that everywhere in Anatolia, there was no active oceanic subduction below the Pontides. Menant et al. (2016), Darin et al. (2018), and Barrier et al. (2018) (who indicate terminal oceanic subduction at 45 Ma in eastern Turkey) map a continent in eastern Turkey from the South Armenian Block to thew Bitlis Massif, that is as wide as the Kırşehir Block and adjacent Tauride nappes of Central Turkey. Although the amount of restored convergence between the Taurides and Pontides is roughly similar to our reconstruction (about 200 km less because they do not restore the oroclinal bending of the Kırşehir Block), they imply that this was consumed by wholesale continental subduction, instead of oceanic as in our reconstruction. The reconstructions of Stampfli and Hochard (2009) and Moix et al. (2008) have no continental crust to the east of the Gürün Curl and thus indicate oceanic subduction in eastern Turkey and the South Armenian Block, an interpretation similar to Şengör et al. (2008).

The reconstruction of Schettino and Turco (2010) has some strong differences to the rest of reconstructions. They map a subduction zone along the southern Tauride margin which to the west connects to NW-SE trending transform faults, one from Beydağları across the Aegean nappe stack towards the Gargano Peninsula, and from there towards the Tuscan nappes and Sardinia, and one towards the Dinaridic front. Africa-Europe convergence in their reconstruction is in eastern Turkey accommodated by oceanic subduction, and in western Turkey in the intra-Pontide Suture Zone, and from there towards the Sava suture of the Dinarides.

7.4. Selandian — 60 Ma

7.4.1. Western and Central Mediterranean region

At 60 Ma, slow Africa-Europe convergence in the western Mediterranean region is almost entirely accommodated by thrusting in the Pyrenees. The AlCaPeCa continental rocks and associated peridotites are restored just south of the future Iberian forearc formed by the Malaguide, Ghomaride, and Upper Kabylides units, and are located within the northern Piemonte-Ligurian Ocean, possibly as an extensional klippe on a hyperextended margin. The transition towards Calabria is a transform fault, where convergence is still accommodated by northwestward underthrusting. As in our 45 Ma reconstruction, we map a transition to the south-dipping, intra-oceanic Alpine subduction zone along a transform fault (Fig. 38, SI1 — map 5). The Corsica-Sardinia Block is in this time window connected to Eurasia, separated by the westward pinching out Valais Basin.

The Tenda passive margin units of Corsica at 60 Ma are not underthrusted yet, and subduction here is still intra-oceanic below the Ligurian ophiolites, where the high-pressure, low-temperature metamorphic oceanic (or hyperextended margin) units of Corsica and the Ligurian Alps are being underthrusted. To the north, subduction zone at 60 Ma is consuming the Briançonnais terrane in the western Alps. Where the Briançonnais terrane disappears, around the Engadine window (Fig. 10), the Magura Ocean is subducting below the Austroalpine nappes of AlCaPa. Our reconstruction also restores clockwise rotation between 60 and 45 Ma for the Austroalpine nappes to avoid overlap between these nappes and the Tisza Block, while maintaining a connection of the Austroalpine nappes to northern Adria. This rotation is consistent with paleomagnetic constraints (Fig. 26). The transform connecting the northern Carpathian and southern Carpathian trenches is active, but contrary to the previous time-slice at 45 Ma, at 60 Ma there is active, consuming lithosphere of the Ceahlau-Severin Ocean, in agreement with previous correlations (Maţenco, 2017). Note that because the South Carpathians part of the ocean had already closed at 60 Ma (in the Severin suture, see below), this implies a NE-ward advancement of the South Carpathians into the East Carpathians part of the ocean, presently observed in the Ceahlau suture (compare Figs. 38 and 39). Therefore, the two presently observed sutures (Ceahlau and Severin) cannot be directly connected (Săndulescu, 1984). Furthermore, the overthrusting of the Getic over the Danubian antiformal stack is restored. At 60 Ma, most of the major deformation in the Dinarides had ended and most if not all Africa-Europe convergence is accommodated in the Tisza-Dacia and AlCaPa domains and by terminal subduction in the Sava Suture Zone (Fig. 38, SI1 — map 5). The Dinarides nappe stack at 60 Ma is part of downgoing Adria.

For the Pyrenees, differences between previous reconstructions and ours stem from the general assumption that Corsica-Sardinia was a contiguous part of Iberia (Csontos and Vörös, 2004; Handy et al., 2010; Schettino and Turco, 2010; Stampfli and Hochard, 2009). The Briançonnais in those, and our, reconstructions is considered to be connected to Corsica-Sardinia. Assuming these are all part of Iberia and given the constraints from the Atlantic Ocean and Pyrenees for Iberia-Europe motion, led Schettino and Turco (2010) and Stampfli and Hochard (2009) to infer a northward 'Pyrenean' subduction/thrust system all along the northern Valais margin already between 70 and 60 Ma, top-to-the-north below the Valais Ocean in Stampfli and Hochard (2009), but top-to-the-south below Europe in Schettino and Turco (2010). Csontos and Vörös (2004) already infer a contiguous ocean from the Valais to the Bay of Biscay at 60 Ma, with no deformation in either the Pyrenees or the Valais-Briançonnais domain. Handy et al. (2010), on the other hand, indicate active thrusting in the Pyrenees, but no deformation between the Briançonnais and Europe at 60 Ma, despite that the Briançonnais and Iberia are part of the same plate in their reconstruction.

There is widespread agreement that there was southward subduction below both the western and eastern Alps, but some disagreement on where the Alpine subduction zone stops. Stampfli and Hochard (2009) suggested that the Alpine subduction zone abuts against a transform fault that connects to the Pyrenean system. Csontos and Vörös (2004) accommodate all Africa-Europe convergence south of Iberia and indicate a north-dipping plate subduction zone from Sardinia towards the Baleares, with a switch to the Alpine trench along a transform close to Corsica. Our reconstruction is thus a hybrid of the above two solutions. Handy et al. (2010), on the other hand, suggested that the south-dipping Alpine subduction zone continued towards Gibraltar, with the AlKaPeCa continental rocks in the upper plate. Finally, Schettino and Turco (2010) inferred a west-dipping subduction zone below Corsica consuming the Piemonte-Ligurian Ocean, which abuts against a transform fault that cuts across Adria towards SE Greece.

Differences between our reconstruction and previous renditions for the Alps mainly concern the paleogeographic area occupied by the Briançonnais-Valais Ocean, which is widest in our reconstruction. In the western Alps, we restored the width of the Valais based on the stratigraphic and metamorphic constraints on the timing of accretion, and on the modern overlaps between nappes, which we drive with Africa-Europe convergence. Our resulting Valais Ocean and Briançonnais continent cannot have been narrower, since they would then occupy a paleogeographic area that is narrower than the modern nappe width, requiring net extension in the Alps during orogeny. As a result, there is no space for a Piemonte-Ligurian Ocean between Adria and the Briançonnais at 60 Ma, which thus at that time must already have been accreted to the orogen. Handy

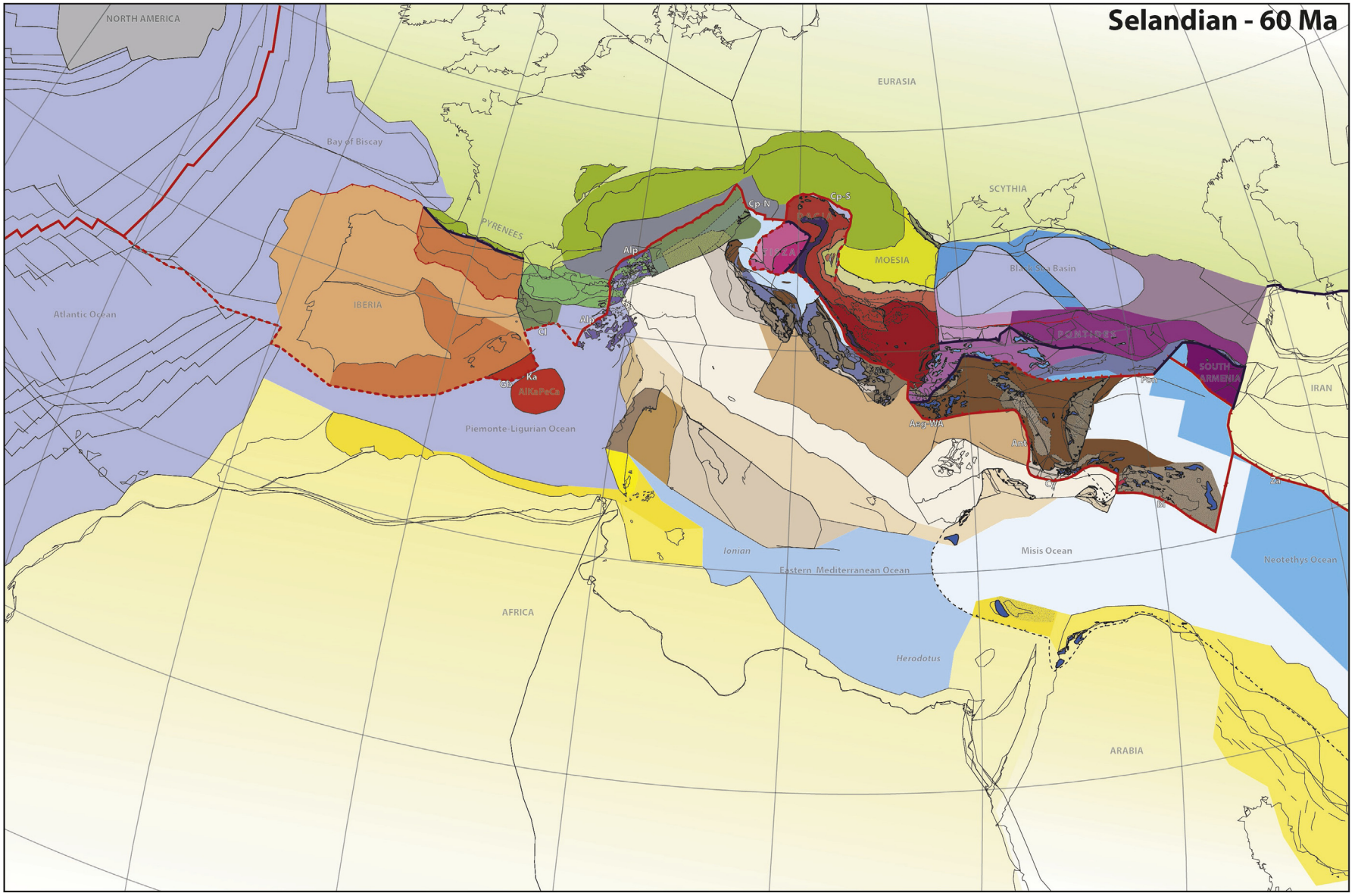

Fig. 38. Paleotectonic map of the Mediterranean region for the Selandian (60 Ma). Map is projected in a Europe-fixed reference frame. Latitudinal and longitudinal graticules in 10° intervals. See Supplementary Information 1 — map 5 for a larger version of the map that includes abbreviations of the detailed tectonic units. GPlates rotation files are provided in Supplementary Information 3. For key to tectonic units, see Fig. 5.

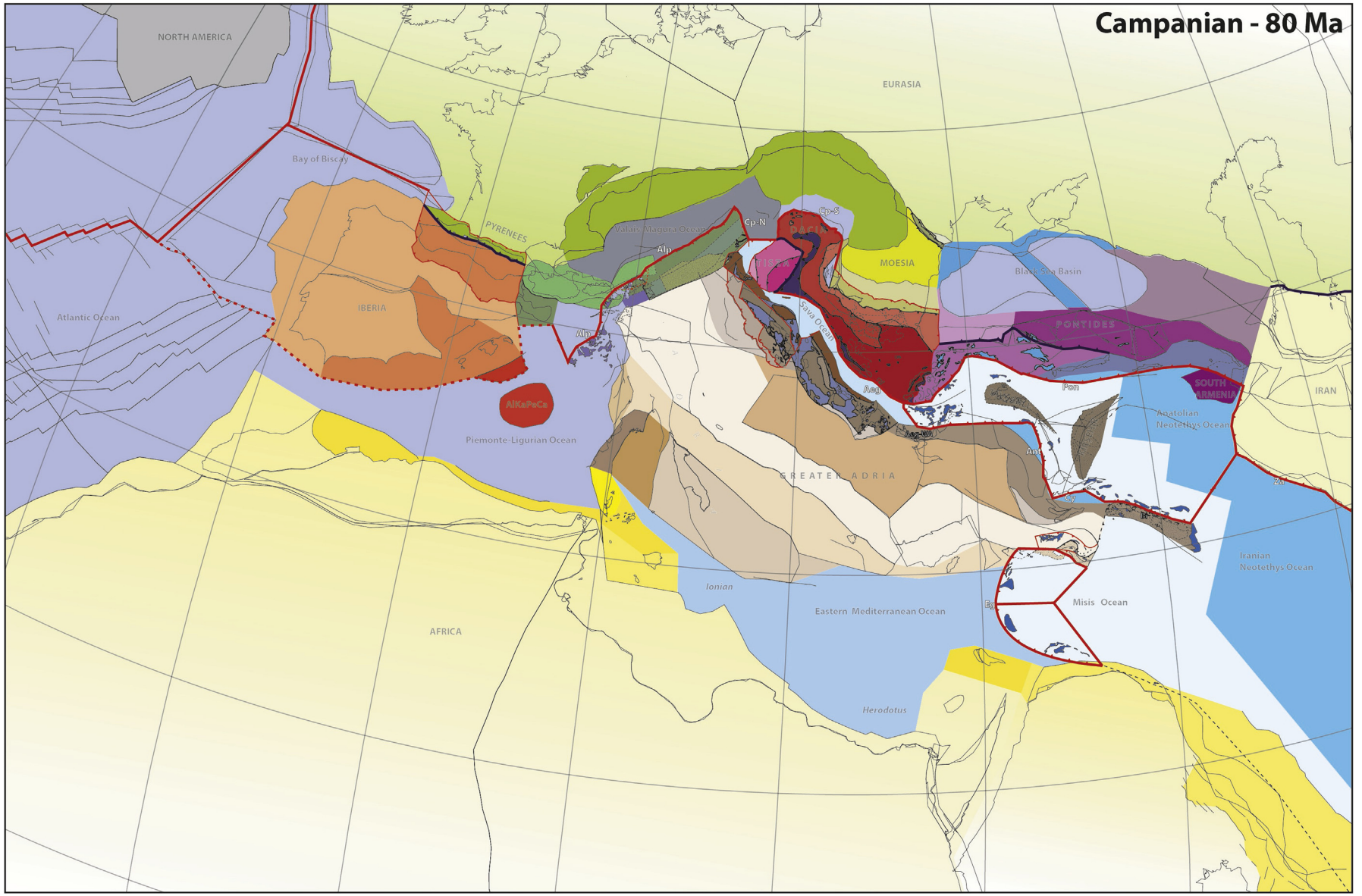

Fig. 39. Paleotectonic map of the Mediterranean region for the Campanian (80 Ma). Map is projected in a Europe-fixed reference frame. Latitudinal and longitudinal graticules in 10° intervals. See Supplementary Information 1 – map 6 for a larger version of the map that includes abbreviations of the detailed tectonic units. GPlates rotation files are provided in Supplementary Information 3. For key to tectonic units, see Fig. 5.

et al. (2010, 2015) and Stampfli and Hochard (2009) indicate a narrower Briançonnais-Valais domain, and a wide Piemonte-Ligurian Ocean, in their reconstructions. Schettino and Turco (2010) do not map a Briançonnais domain but infer that only the Valais-Magura Ocean subducted below Adria in the Alps.

Finally, there are first-order differences between previous reconstructions and ours concerning the width and area of the Austroalpine nappes. Stampfli and Hochard (2009) have a reconstruction largely similar to ours, with the Austroalpine nappes still located north of the Tisza Block at 60 Ma while being connected to Adria in the west. Schettino and Turco (2010) place the Austroalpine units north of Tisza, but disconnected from Adria separated by the Dinaridic trench that in their reconstruction continues to the western Alps. Handy et al. (2015), finally, place the Austroalpine units against northern Adria, entirely west of Tisza. This requires 300 km more extension in the northern Pannonian Basin than we reconstructed, for which there is no observational basis.

7.4.2. Eastern Mediterranean region

At 60 Ma, subduction of the Sava Ocean is in its terminal stages and is transitioning to collision with the Cretaceous Pelagonian orogen. Prior to 60 Ma, this orogen, which formed in Cretaceous time following ophiolite emplacement (Fig. 14) was part of the eastern margin of Greater Adria (Fig. 38, SI1 – map 5). This subduction zone connects eastward with the trench below the Bozkır unit of the Lycian Nappes of western Turkey where the Dilek nappe is starting to subduct and the Afyon Zone had accreted to the orogen a few million years prior and is at the onset of its extensional exhumation. At the eastern part of the Pelagonian orogen we restored the paleomagnetically documented rotation of Parnassos and Pelaginian units (Fig. 28) during 60–55 Ma oblique collision of the platform with western Anatolian units along the N-S trending trench segment (Fig. 38). In Northern Greece, we restored the Nestos thrust, placing the Pangain-Pirin nappe of the Rhodope (reconstructed as underpinnings of the Circum-Rhodope unit) south of the rest of the Rhodope nappe stack. We reconstructed the associated shortening also to the east, widening the Circum-Rhodope unit west of the West Black Sea Transform (Fig. 38, SI1 – map 5).

In Central Anatolia, we restored the Central Pontide orocline, which transfers all Central Anatolian units southward. The Kırşehir orocline is fully restored and the block is now a NNE-SSW trending lenticular window below the Bozkır unit and associated ophiolites. Extensional Paleogene exhumation of the Tavşanlı and Afyon zones is restored, and the two zones lie buried below the Bozkır unit. Subduction occurs along a kinked trench from the E-W trending Lycian nappes segment to the N-S trending Antalya segment – where at 60 Ma the Aladağ nappe had just accreted, and then towards the Gürün Curl in another E-W trending segment. The Geyikdağı unit is restored to its pre-accretionary width. The Alanya, Antalya, Binboğa, and Malatya nappes and associated ophiolites lie as passive riders on the southern Tauride margin. Across the Eastern Mediterranean Ocean, the Troodos, and Baer-Bassit and other Arabian ophiolites were also already emplaced and are being unconformably covered by sediments.

The subduction zone that now lies along the northern fringes of the Geyikdağı Platform in the Gürün Curl connects to the Bitlis subduction zone along the same right-lateral transform fault as shown in the 45 Ma time-slice (Fig. 38). Where in the Gürün Curl the trench is accreting upper continental crustal nappes, there is no accretion at the Bitlis trench. This trench is retreating southward relative to the upper plate, generating upper plate extension that will culminate in the Maden-Hakkari Basin. We provisionally restored this extension, of which no magnitude estimate was ever made, and the Bitlis-Easternmost Tauride domain is consequently narrower than at 45 Ma. Stratigraphic constraints, however, show that these metamorphics were at the surface, and that most of its exhumation occurred prior to 60 Ma (e.g. Kuşcu et al. (2010)). We connect the Bitlis trench with the Zagros trench along a right-lateral transform fault.

Finally, to the north of the eastern Taurides, the width of the oceanic lithosphere east of the Kırşehir Block is wider than at 45 Ma, as a result of the restored Central Pontide orocline. The Ecemiş Fault does not exist yet, and the eastern Taurides are contiguous with the Central Taurides. The Pontides trench connects instead westward to the Izmir-Ankara-Erzincan Suture Zone where collision of the Kırşehir Block with the Pontides is restored at 60 Ma.

Differences of our reconstruction with previous reconstructions now increase which show vastly different plate boundary configurations and paleogeographies around 60 Ma. Schettino and Turco (2010) indicate that subduction around 60 Ma occurred only along the Pontide margin with no thrusting in the Taurides. They infer a second north-dipping subduction zone between the Kırşehir Block and the rest of the Taurides in their 67 Ma time-slice. They also infer active oceanic spreading in the Eastern Mediterranean Ocean in the latest Cretaceous. The reconstruction of Barrier et al. (2018) is similar in that they also infer a single subduction zone at 60 Ma along the Pontide margin consuming oceanic lithosphere along most of it length, except for in Greece and Armenia. Sosson et al. (2016) also infer collision of a Tauride margin with overlying ophiolite with the Pontides around 60 Ma along a single Anatolian subduction zone, but instead interpret that these ophiolites were all Jurassic. This likely follows from their assumption that the South Armenian Block is a contiguous part of the Tauride Platform, and that the ophiolites overlying both are the same.

Moix et al. (2008) and Stampfli and Hochard (2009) map a subduction zone along the margin of the Dilek Basin, which they connect with the Eastern Mediterranean Ocean in Central Anatolia – their reconstruction does not contain continental platforms connected to Beydağları in the east. Instead, they place the eastern Taurides around 60–70 Ma north of a north-dipping trench that connects to the Aegean trench in the west. Moreover, they infer active westward invasion of the Eastern Mediterranean Ocean of the subduction zone that carries the Troodos Ophiolite in its forearc. This subduction zone emplaces the Alanya nappes on the eastern Beydağları margin. The reconstructions of Moix et al. (2008) and Stampfli and Hochard (2009) furthermore infer full continent-continent collision between the Pontides and Taurides across the rest of Turkey.

Menant et al. (2016) infers terminal oceanic subduction along the Izmir-Ankara-Erzincan Suture Zone, whereby the obduction-related orogen of the Tavşanlı, Afyon, and Kırşehir units and overlying Cretaceous ophiolites collide with the Pontides, similar to our reconstruction. They infer that Cretaceous ophiolites were also emplaced onto the eastern Pelagonian Zone of Greece.

7.5. Campanian – 80 Ma

7.5.1. Western and Central Mediterranean region

At 80 Ma, Africa-Eurasia motion in the westernmost Mediterranean region is almost entirely accommodated in the Pyrenees, which are in the early stages of their formation. Our reconstruction systematically only identifies the modern northern and southern thrust fronts of the Pyrenees, but in reality, the orogen is a foreland propagating set of thrust sheets, and the zone of active deformation was narrower than displayed on Fig. 39 and SI1 - map 6.

Iberia is separated from Corsica and the Stilo-Aspromonte-Peloritan Block by a right-lateral transform. Inherted from our previous reconstructions, we map a plate boundary along the latter block, connected to the Alpine, south-dipping intra-oceanic subduction zone below the Ligurian ophiolites by a transform fault. The

Briançonnais terrane lies on the downgoing Eurasian north of the active subduction zone, where the Piemonte-Ligurian units and the Sesia fragment are being buried in the subduction zone.

To the east of the Briançonnais terrane, the lower Austro-Alpine rocks are being accreted to the upper plate at 80 Ma. Prior to 80 Ma, as a result, these lower Austroalpine units restore as the eastward continuation of the Briançonnais terrane, which became incorporated in the orogen earlier as a result of the NE-ward motion of Adria prior to 80 Ma (see also SI 4 for a movie of the reconstruction). The 80 Ma time-slice thus defined the paleogeographic extent of the Magura Ocean, which occupies the space between the lower Austroalpine units and Eurasia (Fig. 39, SI1 – map 6).

The Magura Ocean connects to the southeast to the Ceahlau-Severin Ocean between the Dacia units and Eurasia, which at 80 Ma is subducting slowly below the Dacia units. Farther to the southwest, the South Carpathians part of the Ceahlau-Severin Ocean was already closed by 80 Ma (in the Severin suture) by the Dacia-derived Getic nappes reaching the Danubian promontory of the Moesian Platform.

In the Dinarides, multiple major thrusts are active at 80 Ma, emplacing Sava suture units onto the Jadar Kopaonik nappe, the Jadar-Kopaonik nappe onto the Drina-Ivanjica nappe, likely the East Bosnian-Durmitor on the Pre-Karst nappe, which in turn overthrusts the High Karst unit. Collectively, the Dinarides form a diffuse plate boundary from the Sava suture towards the Adriatic foreland. Because there is no evidence for this deformation in the Aegean-Albanian region, we infer that the motions on these thrusts are transferred to the Sava suture along a proto-Scutari-Pec Fault.

For the western Mediterranean region, an alternative reconstruction for Iberia assumes an Early to Late Cretaceous transform motion of Iberia relative to Eurasia. This assumption is based on interpretations of the geology of the Pyrenees, whereby Late Cretaceous high-temperature metamorphism, volcanism, and extensional basin formation in the North Pyrenean Zone is interpreted to be responsible for the exhumation of peridotite massifs. The inferred transform motion of Iberia relative to Eurasia predicts gradual and slow, ~20° counterclockwise rotation of Iberia relative to Eurasia throughout much of the Cretaceous (Jammes et al., 2009; Olivet, 1996) and several Mediterranean reconstructions adopted this view (Handy et al., 2010; Schettino and Turco, 2010; Stampfli and Hochard, 2009). Handy et al. (2010) therefore inferred that the Valais Ocean was still opening around 90 Ma, although their later rendition Handy et al. (2015) modified the view on the Iberian rotation and preferred the marine magnetic anomaly and paleomagnetic constraints that suggest an earlier, larger rotation, and a disconnection from Corsica-Sardinia (Figs. 18 and 21). A gradual eastward Iberian motion generates E-W convergence in the Mediterranean realm. Stampfli and Hochard (2009) therefore infer a subduction zone along the northern Iberian margin, the Pyrenees, and around the Briançonnais terrane with the latter terrane in the upper plate, consuming both Valais and Piemonte-Ligurian oceanic lithosphere. They infer that the north-dipping subduction zone below the Briançonnais terrane was consumed in the south-dipping Alpine subduction zone of the western Alps. Schettino and Turco (2010) infer a west-dipping subduction zone below Sardinia, Corsica, and within the Valais Ocean, connecting with a north-Iberian transform fault. Handy et al. (2010), and also Handy et al. (2015), infer a southeast-dipping, Alpine subduction zone along the Iberian margin, with the AlKaPeCa units in the upper plate, similar to their reconstructions for the Paleogene.

Csontos and Vörös (2004), finally, argue that a fully oceanic corridor existed from the Bay of Biscay to the Valais Ocean with no active plate boundary at 80 Ma. They reconstructed Africa-Europe convergence at a northwest-dipping subduction zone along the Iberian margin connected to the Alpine intra-oceanic subduction zone with a transform fault. This latter plate boundary is similar to our solution.

7.5.2. Eastern Mediterranean region

In the Aegean region, subduction at 80 Ma was north-directed along the southern and western Circum-Rhodopian margin and consumed Sava oceanic lithosphere. The Pelagonian orogen is inactive and is located on the Adriatic margin of the Sava Ocean in a downgoing plate position. In the upper plate, thrusting propagates forward and northward at 80 Ma from the thrust below the Sredna Gora nappe into the Balkanides. Restoration of the 80-60 Ma thrusting has restored overthrusted Moesian Platform that is equivalent to the Danubian Zone of the southern Carpathians (Fig. 39, SI1 – map 6). This thrusting is bounded to the east along the West Black-Sea transform, and its southern continuation which we infer is the (oblique) thrust between the Circum-Rhodope unit and the Sakarya terrane.

At the transition between the Aegean and Anatolian region, we infer a trench-trench-trench triple junction between the Sava and Izmir-Ankara-Erzincan trenches, and a third, intra-oceanic trench in the upper plate of which are the Cretaceous supra-subduction zone ophiolites that form the highest structural unit of the Central and Southern Anatolian orogen (Fig. 39, SI1 – map 6). The eastern two trenches form the boundaries of a plate that consists mainly (but not entirely, see below) of oceanic lithosphere and that was named the 'Anadolu Plate' by Gürer et al. (2016). The frontal part of this plate was underthrusted by continental crust of the Kırşehir and Tavşanlı blocks between ~95 and 85 Ma, and may be considered 'obducted', although we interpret subduction to have continued after accretion of these continental units as thick or thin-skinned nappes to the upper plate (see van Hinsbergen et al., 2016). The obducted parts of the Anadolu Plate and the underlying mélange was mapped in the younger time-slices as the Bozkır unit, but from 80 Ma and farther back in time, we map it as oceanic supra-subduction zone lithosphere that forms a coherent upper plate. The Kırşehir and Tavşanlı blocks are not exposed at 80 Ma and lie buried below this lithosphere.

The intra-oceanic subduction zone has a similar but more pronounced staircase pattern than at 60 Ma as a result of the restoration of exhumation of the lenticular Kırşehir Block. To the west of this massif, the trench is ~N-S trending, parallel to the magmatic arc that is intruding the Kırşehir Block at this time. The Afyon Zone is undergoing active sedimentation in a downgoing plate position, and of the lithosphere that subducted between the ~90-85 Ma accretion of the Kırşehir and Tavşanlı blocks and the ~70-65 Ma underthrusting and accretion of the Afyon Zone, there are no known geological relics other than deep-marine flysch in the Bozkır unit. We infer that this lithosphere was likely oceanic and map this as the intra-Tauride Basin *sensu* van Hinsbergen et al. (2016).

In eastern Turkey, we trace the subduction zone south of the Anadolu Plate north of the Gürün Curl where it is still in an intra-oceanic position. In the easternmost Taurides and Munzur Massif, however, the Tauride units are already metamorphosed by 80 Ma, and we infer that these massifs were being underthrusted below (or obducted by) the Anadolu Plate oceanic lithosphere. Our restoration at 80 Ma has restored extensional exhumation of the metamorphic massifs at 80 Ma, and because almost all Tauride units in eastern Turkey are metamorphic (Oberhänsli et al., 2014; Topuz et al., 2017), we infer a narrow strip of continental crust amidst ocean. This narrow strip of continent was at 80 Ma already obducted from the south and east, which buried and metamorphosed the Bitlis and Püturge Massifs by ~84 Ma. Fig. 40 displays two extra time-slices at 85 and 90 Ma, which illustrates our view on how a single, kinked subduction zone radially rolled back westwards, and emplaced ophiolites on all sides onto this narrow continental strip. This evolution bears resemblance to the evolution of the Bird's Head Peninsula in the Banda region of eastern

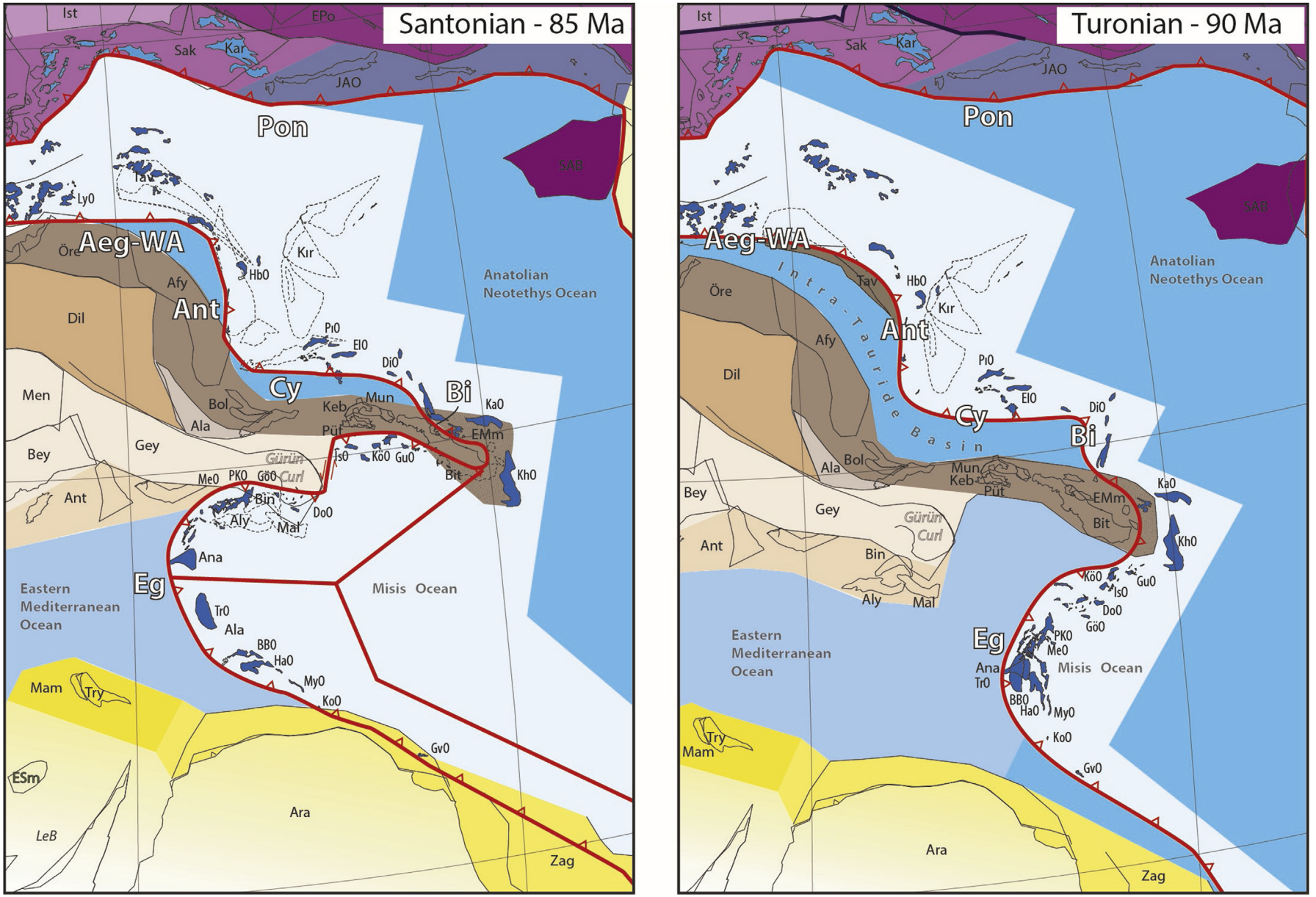

Fig. 40. Detailed paleotectonic map for the eastern Mediterranean region for the Santonain (85 Ma) and Turonian (90 Ma). Map is projected in a Europe-fixed reference frame. Latitudinal and longitudinal graticules in 10° intervals. GPlates rotation files are provided in Supplementary Information 3. For key to tectonic units, see Fig. 5.

Indonesia, and its accreted former western continuation – the Sula Spur (Pownall et al., 2014; Spakman and Hall, 2010). In our reconstruction, northward obduction onto the southern, Bitlis-Püturge and Keban blocks led to northward decreasing metamorphism and was followed by break-off of the eastern Egypt Slab identified in Hafkenscheid et al. (2006), van der Meer et al. (2010) and Gürer (2017). Subsequent incorporation of this nappe stack into the northern subduction branch, emplacing e.g. the Divriği Ophiolite onto the Munzur Massif, led to accretion of the orogen to the Anadolu Plate, the subduction of the lithospheric underpinnings, and places the orogen above the north-dipping subduction zone displayed in the later time-slices, which was responsible for the extensional exhumation and widespread Cretaceous to Eocene arc magmatism in eastern Anatolia. As in younger time-slices, we infer that the Bitlis subduction zone was connected to the Zagros trench by a transform fault (Fig. 39).

From 90 to 80 Ma, the westward roll-back of the Egypt Slab into the Eastern Mediterranean Ocean emplaced not only the ophiolites of the Bitlis and Püturge Massifs, but also those of northern Arabia, and the eastern and southern Gürün Curl and the Alanta and Antalya nappes. At 80 Ma, the ophiolites of the Antalya nappes, as well as the already metamorphosed Alanya nappes are restored southeastward to an amphitheater-shaped trench. We infer that a transform, much like the north African transform of the Miocene, accommodated the westward motion of the Antalya Ophiolites and Alanya nappes, and thus restore the Alanya nappes as the distal southern margin of the southeastern Geyikdağı Platform, adjacent by the more proximal and lower-grade metamorphic Malatya and Binboğa metamorphics. The thunneling of the subduction zone from the wider ocean between the Bitlis-Püturge margin and Arabia to the narrower margin between the Geyikdağı Platform and Arabia led to transpression at the southeastern Geyikdağı corner during westward roll-back, transpressionally emplacing the Malatya metamorphics and overlying ophiolites onto the Binboğa metamorphics and ophiolites. Tearing of the Egypt Slab along the southern Geyikdağı margin allowed for the rise of the Campanian plutons that intrude this thrusted sequence, similar to the Miocene granitoids that intrude the Kabylides following tearing.

The westward roll-back into the eastern Mediterranean Ocean fulfills with the opposite rotations of the southern Tauride and Arabian and Cyprus ophiolites constrained paleomagnetically (Maffione et al., 2017; Morris et al., 2017) (Fig. 34). It consumed the pre-existing Triassic and Carboniferous oceanic crust preserved farther west in the Ionian and Herodotus Basins, relics of which are found below e.g. the Mersin Ophiolite. The newly formed Misis oceanic crust formed in a supra-subduction zone, arc or back-arc environment explaining the finding of Turonian and Campanian arc rocks in accretionary prisms of the Misis Mélange and the western Bitlis Suture Zone. Spreading in the Misis Ocean must have continued until the final emplacement of the Antalya, Troodos, and NW Arabian ophiolites in the Maastrichtian. It must also have occurred at high angles to the southeastern Geyikdağı margin to explain why some of the SE Anatolian ophiolites are younger, ~87-85 Ma in the Kömürhan Ophiolite (Karaoğlan et al., 2012), than the bulk of Anatolian ophiolites where supra-subduction zone ridges were oriented parallel to the obduction front and only a short time span of supra-subduction zone spreading can be preserved in the narrow strip of oceanic crust that obducts and escapes subduction (Maffione et al., 2017). We reconstruct the metamorphic Trypa group of Northern Cyprus as the obducted north African margin, and the Mammonia complex as offscrapings from that margin, and from the Eastern Mediterranean oceanic lithosphere consumed by the Egypt Slab that subducted below the Troodos Ophiolite in the Cretaceous.

The Izmir-Ankara-Erzincan subduction zone at 80 Ma consumes Cretaceous supra-subduction zone oceanic crust in the west, but eastwards also Neotethyan crust that existed prior to the initiation of the subduction zone below the Anadolu Plate around 105 Ma. Subduction is northwards, and in the upper plate, the Black Sea is in the final stages of opening as a back-arc basin. In the far-east, the South Armenian Block is about to collide with Eurasia, and we restored the paleomagnetically documented clockwise rotation that occurred during collision (Fig. 33). The South Armenian Block is at 80 Ma underthrusting below the Jurassic ophiolites located in the forearc of the Pontides and the Transcaucasus ranges. This block is not overthrusted by the Cretaceous supra-subduction zone ophiolites that are at 80 Ma overthrusting the easternmost Taurides and our restoration identifies the South Armenian Block prior to 75 Ma collision as part of the Anadolu Plate, separated from the Taurides by ~600 km wide Neotethys Oceanic lithosphere (Fig. 39, Si1 – map 6) that became consumed in the Kağızman-Khoy suture between the 75 Ma accretion of the South Armenian Block to Eurasia and the Neogene.

Previous reconstructions are strongly variable for the late Cretaceous eastern Mediterranean region. Csontos and Vörös (2004) map the northernmost active thrust of the Balkanides as a south-dipping subduction zone active alongside an oblique northeast dipping subduction zone, in their reconstruction still located west of the Pelagonian Platform in the Pindos Basin. They continue these trenches into the Anatolian domain, but their reconstruction was primarily focused on the Carpathian realm. The reconstructions of Stampfli and Hochard (2009) and Moix et al. (2008) provide similar explanations for the emplacement of the Troodos, and Arabian ophiolites, and also their reconstruction of the easternmost Taurides with obduction around an E-W ribbon continent is similar to ours, although intra-oceanic subduction in their reconstruction starts already in the Early Cretaceous. Their reconstruction infers subduction/obduction along the northern Taurides margin in Anatolia, and a subduction zone along the Pontides and the northern Sava margin similar to ours, although they do not merge the trenches in a triple junction in western Turkey but end the southern subduction zone within-plate. Sosson et al. (2016) does infer a trench-trench-trench triple junction in western Turkey similar to our reconstruction, but infers that all Anatolian ophiolites, including the Jurassic ophiolites of the Izmir-Ankara-Erzincan suture zone and overlying the South Armenian Block, were derived from the same forearc and same plate, instead of from two as in our scenario. They reconstruct a continental connection between the South Armenian Block and the Taurides.

Such a continental connection also features in Barrier et al. (2018), but those authors infer as many as seven E-W trending late Cretaceous subduction zones in the eastern Mediterranean region, six north-dipping and one south-dipping. The northernmost is along the Pontides and connects along a N-S transform to the Zagros trench, similar to our reconstruction. They then infer subduction zones that initiated intra-oceanically north of the Kırşehir Block, one south of the Kırşehir Block in the intra-Tauride Basin, one that forms within an ocean (their Berit Ocean) that they reconstruct between the Geyikdağı unit and a block that contains the Alanya nappes, the Kyrenia ranges, the Malatya metamorphics and the Bitlis Massif, one to the south of this block and one along the northern Arabian-northwest African margin emplacing ophiolites. In addition, they infer an isolated, narrow, south-dipping subduction zone emplacing the Antalya nappes onto the Beydağları Platform. The latter subduction zones end within-plate in the west, whilst they infer a N-S trending transform fault between the Pelagonian orogen and the Anatolian subduction zones, which is similar to our reconstruction. Robertson et al. (2013c) present a similar scenario of six north-dipping subduction zones and one isolated east-dipping subduction zone below the western margin of the Kırşehir Block. Menant et al. (2016) restrict their 80 Ma reconstruction to the domain between

Pontides and Taurides, where they reconstruct two intra-oceanic subduction zones on either side of the Kırşehir Block that end within-plate. Okay and Nikishin (2015) map two subduction zones in the late Cretaceous in Anatolia, located in similar positions as ours and connected in the west through a transform fault. Reconstructions that identify arcs give an E-W trend for the arc of the Kırşehir Block, instead of N-S as in our reconstruction (Barrier et al., 2018; Menant et al., 2016; Okay and Nikishin, 2015). Schettino and Turco (2010), finally, reconstruct only one subduction zone in the Campanian of Anatolia, along the Pontide margin but two in Greece, along the Sava and Pindos margins, as well as a transform fault from the southeast Aegean realm to southern Iberia across Adria and the Piemonte-Ligurian Ocean. They infer active oceanic spreading in the eastern Mediterranean region in absence of subduction.

7.6. Albian – 100 Ma

7.6.1. Western and Central Mediterranean region

Iberia at 100 Ma has just undergone its counterclockwise rotation documented paleomagnetically (Fig. 18) and is in incipient collision with Eurasia. Extension and high-temperature metamorphism documented in the suture zone is interpreted as local responses to break-off of the Reggane Slab (Vissers et al. (2016). To the south, Iberia is separated with a transform fault from Africa, which we assume was parallel to the Iberian margin and along which subduction initiated in the late Cretaceous to Paleogene accommodating incipient Africa-Iberia convergence (see also van Hinsbergen et al., 2014a). As a result, we reconstruct the AlKaPeCa units as part of the African Plate at 100 Ma (Fig. 41, SI1 – map 7). Iberia and the Corsica-Sardinia Block are separated by a transform fault, as in later time-slices.

The Alpine subduction zone to the east is in a similar orientation as in the 80 Ma time-slice, but because Africa-Europe motion is almost parallel to this orientation between 100 and 80 Ma, this subduction zone is now highly oblique, and subduction is slow. The Upper Austroalpine units of the AlCaPa domain are restored towards the southwest along with Adria, and the Eo-Alpine high-pressure metamorphic units are being buried as part of the downgoing Eurasian Plate, on their way to their ~90 Ma climax metamorphic conditions. These units consequently restore immediately adjacent to the lower Austroalpine units. The Sesia fragment of the western Alps, which was being buried at 80 Ma, is now restored separated from Adria by oceanic lithosphere. However, in order for the Sesia fragment to be separated from both Adria and the Briançonnais terrane by oceanic lithosphere, as dictated by the geology of the western Alps, we restore Sesia prior to its underthrusting as part of the African/Adriatic Plate. This means that we interpret its underthrusting essentially as subduction erosion, whereby a thrust develops within Adria upon collision of the Sesia fragment with the Briançonnais terrane along which the oceanic lithosphere between Sesia and Adria is consumed before thrusting propagates downward into the crust of the Briançonnais terrane in the Cenozoic. Hence, prior to burial, the Sesia fragment is restored as contiguous with Adria in the upper plate of the subduction zone, rather than as part of the downgoing plate contiguous with Eurasia. Sesia would then restore as a western peninsula of the upper Austroalpine units (Fig. 41, SI1 – map 7).

Towards the east, the Alpine subduction zone wraps around the Tisza and Dacia domains and connects to the thrust below the Sredna Gora nappe, ending against the West Black Sea Transform (Fig. 41, SI1 – map 7). Convergence between Adria and Moesia, however, was widely distributed over major thrusts in the Dinarides, the Sava Suture, the Tisza, as well as within and at the exterior of the Dacia nappes. Our reconstruction infers a clockwise rotation of the Tisza Block between 100 and 80 Ma to avoid overlap with the northern Dinarides of the Medvednica and Bükk blocks, but there are no paleomagnetic data to test this. This rotation aligns the thrusts of the Tisza Block with those of the Dacia units and Dinarides (Fig. 41, SI1 – map 7).

Contrary to the 80 Ma thrust slice, the active thrusting in the Dinarides is now continuing into the Aegean domain, whereby thrusting of the Upper Pelagonian over the Lower Pelagonian nappe is active. In older time-slices, we interpret this thrusting as related to subduction (of the Algeria Slab, see below), but at 100 Ma, the thrusting within and at the exterior of the Dacia units south of the Moesian Platform and of the Pelagonian orogen accommodate Africa-Europe convergence and do not require (nor preclude) the presence of a slab. We infer that at 100 Ma, the subduction zone along the northern margin of the Sava Ocean is incipient. The Sava Ocean ends in the east against a transform fault (Fig. 41, SI1 – map 7).

Previous reconstructions infer contiguity between Corsica-Sardinia-Briançonnais with Iberia and assume transform motion between Iberia and Eurasia. Stampfli and Hochard (2009) reconstruct a pull-apart ocean opening between Iberia and Eurasia, whereby the plate boundary transitions into a south-dipping subduction zone within the Valais Ocean, connecting around the Briançonnais terrane with the subduction zone along the Austroalpine units. These are reconstructed to the northeast of Tisza, as part of the upper plate of Adria with a northeastward dipping subduction zone along the Sava suture between Tisza and the Dinarides. They define a narrow ribbon continent – narrower in N-S direction than the modern AlCaPa domain requiring post-100 Ma N-S extension – adjacent to a wide Sava Ocean that is bounded by a north-dipping subduction zone below the Rhodopian-Dacia units. Handy et al. (2010) continues the Bay of Biscay spreading towards the Valais Ocean and infers Alpine, south-dipping subduction between Iberia and their AlKaPeCa Block within the Piemonte-Ligurian Ocean. To the east, this subduction zone becomes intracontinental, as in our reconstruction, and buries continental rocks of the Eo-Alpine high-pressure units and the lower Austroalpine nappes. As in our reconstruction, they place the Sesia fragment in the upper plate of the Alpine subduction zone, moving together with Adria. Schettino and Turco (2010), finally, have a similar scenario at 100 Ma as at 80 Ma, with active oblique spreading in the Pyrenean domain bounded in the east by a west-dipping subduction zone around the Corsica-Sardinia and within the Valais Ocean, connected with a triple junction with the Alpine subduction zone that continues around Tisza and Dacia connecting with a northeast-dipping subduction zone below Eurasia. Their Tisza-Dacia unit is now a contiguous part of the Adriatic continent, and no ocean is reconstructed between Tisza and the Dinarides, or Dacia.

7.6.2. Eastern Mediterranean region

Around 100 Ma, the intra-oceanic subduction zone above which the Cretaceous supra-subduction zone forearc crust will form around 95 Ma, is in its incipient stages. Lu/Hf ages of garnet in metamorphic soles suggest that intra-oceanic thrusting was active by ~104 Ma (Peters et al., 2018; Pourteau et al., 2019), but supra-subduction zone spreading had not started yet. All oceanic lithosphere thus either belonged to the Neotethys Ocean or Eastern Mediterranean Ocean and the Misis oceanic lithosphere did not exist yet (Fig. 41, SI1 – map 7). The South Armenian Block is reconstructed as a microcontinent that is part of the otherwise entirely oceanic Anadolu Plate. There are no direct constraints on the motion of the Anadolu Plate relative to Africa and Eurasia other than that motion is convergent with both, and we partition convergence more or less equally over the two trenches surrounding Anadolu Plate for much of the 100-80 Ma interval. This restoration has some uncertainty, but the resulting paleolatitude curve for the South Armenian Block is consistent with

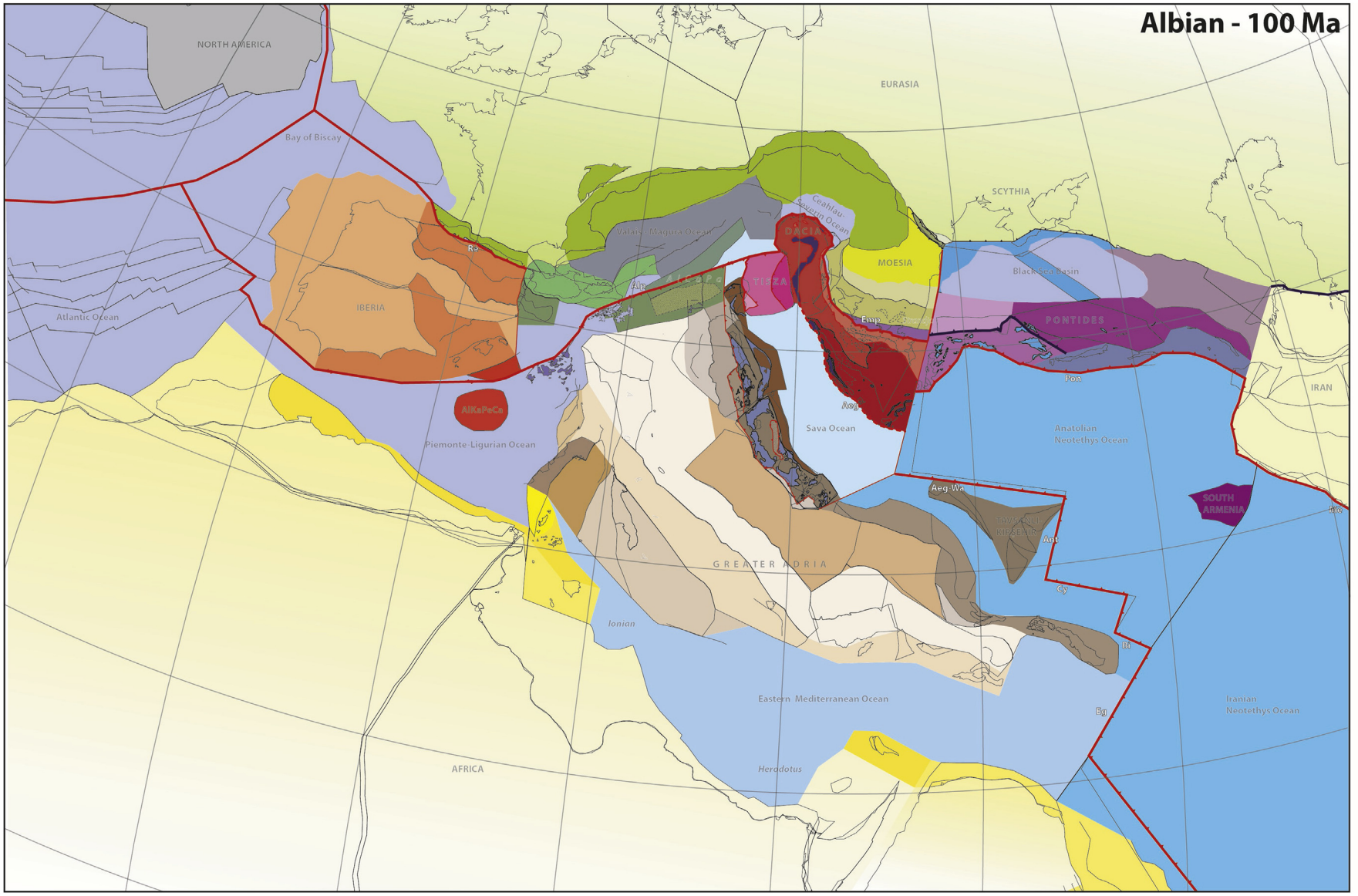

Fig. 41. Paleotectonic map of the Mediterranean region for the Albian (100 Ma). Map is projected in a Europe-fixed reference frame. Latitudinal and longitudinal graticules in 10° intervals. See Supplementary Information 1 – map 7 for a larger version of the map that includes abbreviations of the detailed tectonic units. GPlates rotation files are provided in Supplementary Information 3. For key to tectonic units, see Fig. 5.

paleomagnetic data (Fig. 33). To the north, the Pontide trench is accommodating northward Neotethys subduction, and the Black Sea Basin is opening as a back-arc basin.

Previous reconstructions either inferred only a single subduction zone along the Pontide margin (Menant et al., 2016; Schettino and Turco, 2010), or a second, intra-oceanic subduction zone similar to our reconstruction (Barrier et al., 2018; Moix et al., 2008; Sosson et al., 2016; Stampfli and Hochard, 2009). All these reconstructions, however, assume that this intra-oceanic subduction zone started well before 100 Ma, varying from ~180 to 140 Ma. It is noteworthy that Csontos and Vörös (2004) by 100 Ma restored the Tisza Block south of the Moesian Platform, instead of to the northwest as in our reconstruction. This requires a significant northward motion of Tisza relative to both Africa and Eurasia after 100 Ma. Schettino and Turco (2010) infer that the Eastern Mediterranean Ocean had not opened yet by 100 Ma and restore Greater Adriatic units against the African margin.

7.7. Aptian – 120 Ma

Iberia is at 120 Ma undergoing its ~40° ccw rotation phase relative to Eurasia that follows from marine magnetic anomalies as well as from paleomagnetic data (Fig. 18). This rotation occurs around a pole in the eastern Bay of Biscay, which is actively spreading, and is accommodated by northward subduction in the Pyrenees, consuming oceanic lithosphere of the Iberian Plate preserved in the modern Reggane lower mantle slab (Vissers et al., 2016). Iberian rotation is accommodated to the south by a right-lateral transform between Africa and Iberia – with opposite sense of shear as at 100 Ma given the higher Iberian rotation rate in the Aptian – and with a right-lateral transform from the Corsica-Sardinia Block (Fig. 42, SI1 – map 8).

The Alpine subduction zone is highly oblique and is slowly consuming Piemonte-Ligurian Ocean units. Towards the east, the Alpine subduction zone curves to a N-S orientation and accommodates the eastward thrusting of the East Vardar Ophiolites onto the Dacia Block, and farther south to the emplacement of the Circum-Rhodope units onto the Serbo-Macedonian and Sreda Gora units. The Dacia Block in the Carpathian realm is now fully separated from the Moesian Platform and Danubian promontory by the Ceahlau-Severin Ocean. The Tisza Block is restored to its pre-thrusting dimension and lies separated by Sava oceanic corridors from the Alpine units to the north, the Dacia units to the east and the Dinaridic units to the west (Fig. 42, SI1 – map 8).

Thrusting of the Rhodopian nappes is now almost entirely restored. As explained in section 5.10, we interpret the Rhodopian nappe stack to form below a decollement along which the Dacia nappes detached, and above a second, deeper decollement that stripped the nappes from their lower crustal and lithospheric mantle underpinnings. This way, we restore the Rhodope Lower Unit as underpinnings of the Danubian Zone (or Struma unit in Bulgaria), the Rhodope Lower Unit as underpinnings of the Sredna Gora unit, and the Rhodope Uppermost and Pangaion-Pirin units as the underpinnings of the Circum-Rhodope and Serbomacedonian units. The Middle Rhodope unit with evidence for Triassic and Jurassic high-pressure metamorphism, and both Permo-Triassic, but also middle Jurassic mafic magmatic protoliths finds no known equivalent in the Dacia nappe stack. We therefore restore it as a separate belt between the Danubian and Sredna Gora units, where it represents a Triassic suture zone. The Rhodope Middle Unit may represent a pre-Cretaceous suture zone of which no rocks were incorporated in the Cretaceous orogen. Given the middle-Jurassic mafic protolith ages that were also retrieved from the Rhodope Middle Unit (Froitzheim et al., 2014) it is possible that a the Rhodope Middle Unit formed in a subduction zone that following pre-middle Jurassic suturing became reactivated to form a lateral equivalent oceanic basin to the Ceahlau-Severin Ocean. This basin may then have been the host of the Trojan Flysch units found in the Balkanides. Although admittedly speculative and based on sparse information, our reconstruction follows this latter scenario and infers that the Rhodope Middle Unit (Fig. 42, see for tagged geological units SI1 – map 8) are located in a Jurassic extensional basin – but this choice does not dramatically change the reconstruction of older time-slices.

At 120 Ma, shortening may still accommodate part of the deformation observed below the East Bosnian-Durmitor nappe of the Dinarides and possibly is still accommodating the overlying contact with the Drina-Ivanjica unit initiated earlier in the Late Jurassic. At this time, deformation is still accommodated below the Upper Pelagonian Nappe of the Aegean nappe stack. Whether there is still an actively subducting slab at this time attached to the Pelagonian margin (which would be the Algerian Slab) or to the Dacia margin (the Emporios Slab) is possible, but not be required as thrusting could be driven by Africa-Europe convergence alone in absence of subduction. These slabs may thus also have broken off slightly before 120 Ma.

Both the Pelagonian and Circum-Rhodope thrusts are bounded to the southeast by a transform fault that separates the Sava Ocean from the Neotethys Ocean of the Anatolian domain. The Neotethys Ocean in the Anatolian segment is subducting northward in a single subduction zone below the Pontide margin. In the upper plate of the Pontide subduction zone, the Black Sea is in the early stages of opening. The Pontide trench connects with the subduction zone (where at this time the Mesopotamia Slab is subducting) along the Iranian Cimmerides with a N-S trending highly oblique transform fault at which the Khoy Mélange is accreting. To the south, Greater Adria is now surrounded by passive margins. So is the South Armenian Block, which is a microcontinent surrounded by Neotethyan oceanic lithosphere, bounded to the east and west by fracture zones (Fig. 42, SI1 - map 8), or an active transform to the east depending on the kinematic evolution of the Neotethys in between Iran and Arabia which is not restored in detail in this paper.

Previous reconstructions bear first-order similarities with our restoration. Differences pertain in the west to the assumption of Cretaceous extension in the Pyrenean domain requiring a smaller rotation of Iberia than in our restoration (Csontos and Vörös, 2004; Handy et al., 2010; Schettino and Turco, 2010; Stampfli and Hochard, 2009). As for previous time-slices, this reconstruction requires Iberia-Adria convergence, accommodated in the different reconstructions by subduction of or below the Iberian margin, or the Corsica-Sardinia margin that is assumed in these reconstructions to be part of the Iberian Plate.

In the Alpine realm, our reconstruction differs from previous restorations by restoring nappe stacking in the Austroalpine domain. Previous reconstructions indicate a schematic, narrow continental corridor (Stampfli and Hochard, 2009), or a continental promontory of northern Adria that is less than half the size of our reconstruction (Csontos and Vörös, 2004; Schettino and Turco, 2010) in which no active deformation is indicated in the Cretaceous. These reconstructions require several hundred kilometers of N-S and/or E-W extension in the eastern Alps on top of what we already reconstructed here for the late Cenozoic. As a result, these reconstructions show a much wider Piemonte-Ligurian Ocean north of Adria than in ours. Handy et al. (2010) explicitly restored shortening in the Austroalpine nappes and consequently show a much narrower Piemonte-Ligurian Ocean north of Adria.

The smaller paleogeographic area occupied by continental crust in the reconstruction of Csontos and Vörös (2004), and their reconstruction of Tisza to the South of Moesia led them to inferring a wide Ceahlau-Severin Ocean that connected the Magura Ocean towards the Neotethyan domain of Anatolia. Their reconstruction

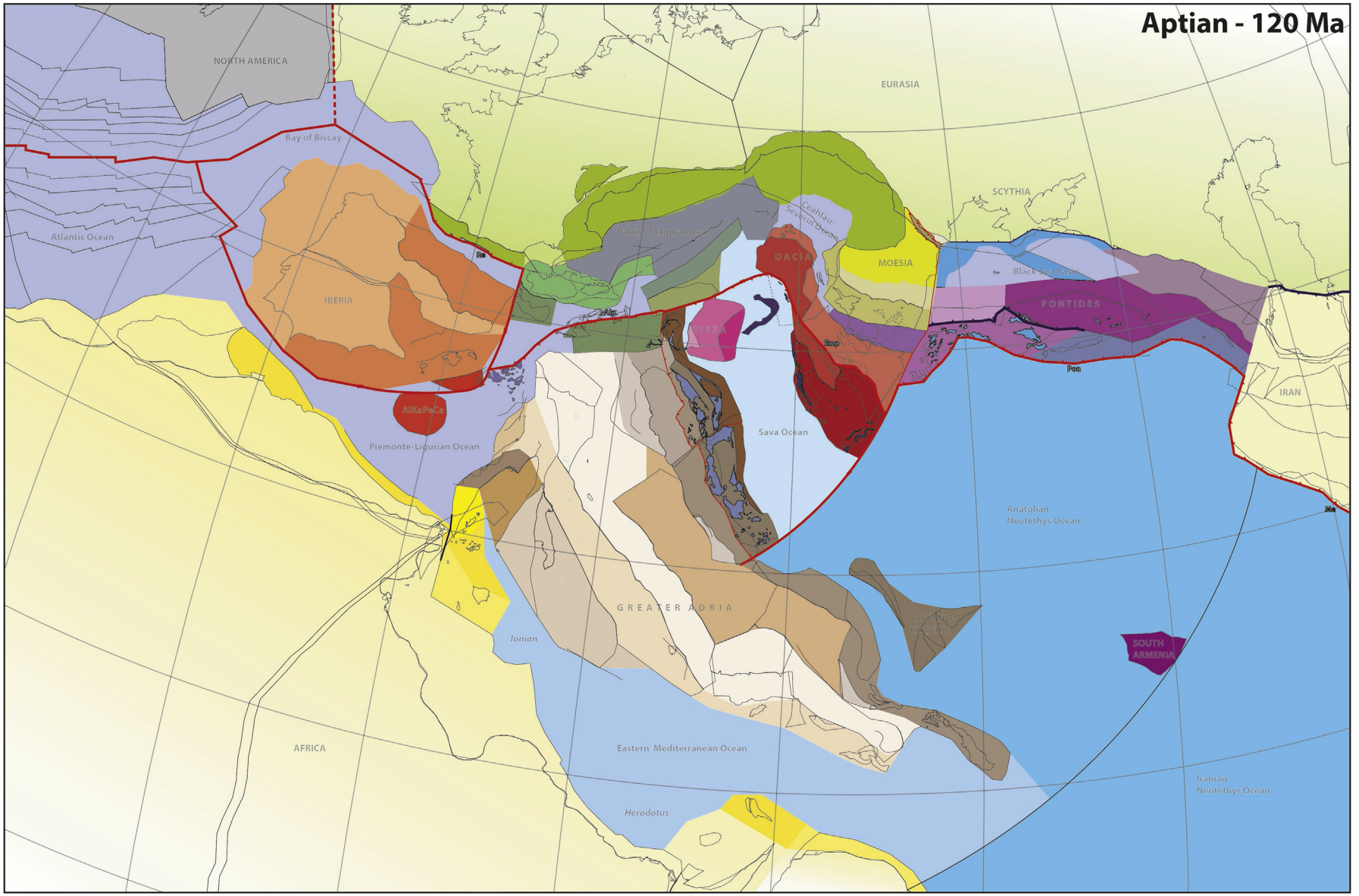

Fig. 42. Paleotectonic map of the Mediterranean region for the Aptian (120 Ma). Map is projected in a Europe-fixed reference frame. Latitudinal and longitudinal graticules in 10° intervals. See Supplementary Information 1 – map 8 for a larger version of the map that includes abbreviations of the detailed tectonic units. GPlates rotation files are provided in Supplementary Information 3. For key to tectonic units, see Fig. 5.

infers a major northwestward component of the Dacia and Tisza units relative to Eurasia and Africa and restored the Dacia units of the northern Aegean region to an Aptian position occupied in our reconstruction by the Pontides.

Stampfli and Hochard (2009) instead infer wide oceanic domain in the Aegean-Anatolian segments, dipping northwards below the Rhodope and Pontides. To the east, they connect this trench southward to the subduction zone along the southern Iranian margin but restore a wide oceanic domain within Iran. We note that our reconstruction of Iran is highly simplistic and does not take any pre-Miocene deformation of Iran – of which there is plenty (Moghadam and Stern, 2015) – into account. The reconstruction of Stampfli and Hochard (2009) as well as Moix et al. (2008) and Sosson et al. (2016) infer still two subduction zones within the Anatolian domain and show the intra-oceanic subduction zone above which the Cretaceous Anatolian Ophiolites formed in the Aptian to the north of the Greater Adriatic margin. Schettino and Turco (2010) infers that there was no northward subduction in the Anatolian region, but instead infer that Africa-Europe convergence was accommodated by northward subduction at an intra-oceanic trench emplacing ophiolites onto Greater Adria in both Greece (in Aptian time equivalent to the thrust below the Upper Pelagonian Nappe in our reconstruction) and Anatolia, which is not present in our reconstruction. They infer Early Cretaceous ophiolite emplacement onto the Kırşehir Block.

Finally, Le Pichon et al. (2019) recently proposed a different reconstruction whereby Adria moved with a major Jurassic to Cretaceous left-lateral transform fault along the North African margin opening the Eastern Mediterranean Ocean as a pull-apart basin. Their reconstruction suggests that Adria rotated ~50° clockwise relative to Africa after 120 Ma and converged 800 km with Eurasia. If correct, this would lead to a dramatically different restoration of the Mediterranean region than shown in our reconstruction.

7.8. Berriasian – 140 Ma

At 140 Ma, Iberia was surrounded by ridges and transforms that end in triple junctions in the Piemonte-Ligurian Ocean. Atlantic Ocean reconstructions between Africa and North America and Iberia and North America show that the ridge of the Piemonte-Ligurian Ocean must have been connected to the Central Atlantic ridge along a transform fault between Iberia and Africa at which oceanic crust may have accreted in pull-apart basins (e.g., Vissers et al., 2013), like in the Gulf of California in the Miocene (Stock and Hodges, 1989). Towards the northeast, the Piemonte-Ligurian ridge is reconstructed between the Briançonnais terrane and the lower Austroalpine and Eo-Alpine units, towards the Magura Ocean (Fig. 43, SI1 - map 9). We restore opening of the Valais Ocean in the Early Cretaceous, by a clockwise rotation of the Corsica-Sardinia-Briançonnais Block. We reconstruct the initiation of Alpine subduction around 125 Ma, as predicted by a change in Africa-Europe convergence dictated by the Atlantic Ocean reconstruction. We note, however, that this coincides with the onset of the Cretaceous Quiet Zone in the time scale we use Gradstein et al. (2012), which means that this onset may occur later and is poorly constrained (and see the discussion in e.g. Midtkandal et al. (2016) on the onset age of the Cretaceous Quiet Zone, which may also be younger, ~122-121 Ma). Early Cretaceous shortening, however, has been documented in the upper Austroalpine nappes (e.g., Handy et al., 2010) and references therein).

Around the Sava Ocean, two opposite facing orogens are forming at 140 Ma. On the Adriatic margin, the Dinarides and Pelagonian orogen are now fully restored and both are being obducted by the West Vardar Ophiolites. Among these, the Meliaticum Ophiolites on the eastern Austroalpine nappes restore west of the Bükk blocks and form the westernmost West Vardar Ophiolites. Simultaneously, the East Vardar Ophiolites are obducting onto the Dacia margin. To the south, the East Vardar Ophiolites are obducting the Dacia megaunit, including the Circum-Rhodope unit. We infer that at this stage, subduction is active at both sides of the Sava Ocean: the Algeria Slab subducted eastward below the West Vardar Ophiolites and the Emporios Slab below the East Vardar Ophiolites (see www.atlas-of-the-underworld.org and van der Meer et al. (2018)). Please note that the East Vardar ophiolites are now reconstructed in the middle of the Sava Ocean, particularly the South Apuseni Mountains segment adjacent to Tisza. It actually means the poorly known Western (presently northwestern) margin of Dacia (i.e. Biharia) must have been connected with a wider thinned continental margin, presently thrusted by Tisza in the narrow sector separating Tisza from Dacia. Furthermore, we reconstruct the West and East Vardar Ophiolites to the center of the ocean between Adria and Dacia at 170 Ma (see next section), which requires divergence between the two obduction fronts between 170 and final emplacement onto these margins at 130 Ma, by which time thrusting propagates into the passive margin. Given overall Adria-Dacia convergence reconstructed from the Atlantic Plate circuit, such extension necessitates roll-back and the presence of two slabs at 140 Ma. Lithosphere formed above these two slabs is displayed as Sava oceanic lithosphere, of Middle Jurassic to Early Cretaceous age, whilst lithosphere subducted below the Sava oceanic lithosphere is mapped as Neotethys Ocean, of Triassic to Middle Jurassic age. There is no evidence that the Tisza Block was ever obducted by ophiolites, and we therefore reconstruct it as a microcontinent within the Sava Ocean, in an upper plate position relative to both subduction zones. The two trenches on either side of the Sava Ocean end against a transform fault at the transition to the Anatolian segment.

There is no evidence that Jurassic ophiolites also obducted the Greater Adriatic margin of Turkey. All Jurassic ophiolites of Turkey are located in a structurally higher position than the Cretaceous ophiolites. This means that the Greater Adriatic margin was free from obducted ophiolites in the Cretaceous, and that the Jurassic Anatolian ophiolites were located in an upper plate position relative to the Cretaceous ophiolites. The simplest scenario is then to locate them in the Pontides forearc, adjacent to the Jurassic Pontides and Lesser Caucasus Arcs (Mederer et al., 2014; Okay et al., 2014). In the upper plate of this subduction zone are two Jurassic basins that have the same age as the Jurassic ophiolites of the Izmir-Ankara-Erzincan Suture Zone: The Intra-Pontide Ocean in the west and the Greater Caucasus Basin in the east. At 140 Ma, the Intra-Pontide Ocean is closing in the upper plate of the Neotethyan subduction zone. We infer full closure of the intra-Pontide suture by 130 Ma at which time the Black Sea Basin starts opening and the upper plate transitions from compression to extension.

At 140 Ma, there was likely still active mid-ocean ridge spreading in the Neotethys Ocean, whereby the ridge was approaching the Pontides. The subduction of this ridge may have triggered opening of the Black Sea back-arc basin. This ridge was located north of the South Armenian microcontinent in our reconstruction, but we infer that there was an active transform plate boundary between the Anatolian and Iranian segments of the Neotethys in the Late Jurassic-Early Cretaceous. Arc-type granodiorite intrusions of ~155 Ma in the South Armenian Block are interpreted to be related to subduction (Hässig et al., 2015), which we infer must then have occurred by oblique convergence at the transform fault to the east of the South Armenian Block, perhaps similar to the highly oblique subduction at the Arabia-India Plate boundary in the Paleocene (Gaina et al., 2015). We schematically indicate such an oblique subduction zone to the east of the South Armenian microcontinent in our 140 Ma reconstruction (Fig. 43, SI1 – map 9).

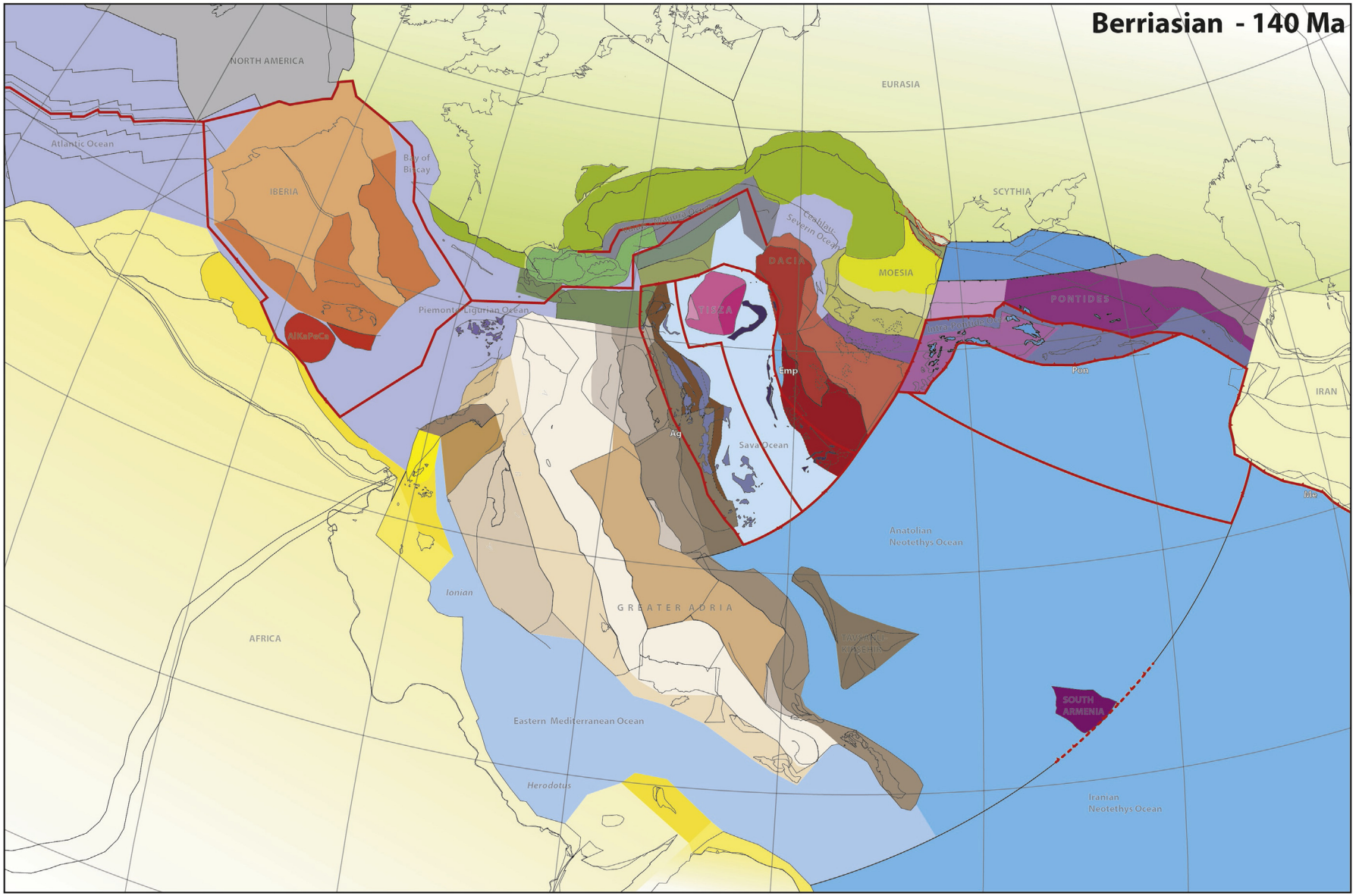

Fig. 43. Paleotectonic map of the Mediterranean region for the Berriasian (140 Ma). Map is projected in a Europe-fixed reference frame. Latitudinal and longitudinal graticules in 10° intervals. See Supplementary Information 1 – map 9 for a larger version of the map that includes abbreviations of the detailed tectonic units. GPlates rotation files are provided in Supplementary Information 3. For key to tectonic units, see Fig. 5.

Previous reconstructions all agree that at 140 Ma, the Piemonte-Ligurian Ocean was still spreading. Most reconstructions place Iberia against the North American and Armorican margin and infer initial break-up at or after 140 Ma (Csontos and Vörös, 2004; Handy et al., 2010; Schettino and Turco, 2010), and Stampfli and Hochard (2009) indicate pre-drift extension in the Central Atlantic and Bay of Biscay Basins. Because in these reconstructions Corsica-Sardinia-Briançonnais is assumed to be part of Iberia, they predict opening of the Valais Ocean after 140 Ma, whereas in our reconstruction we open the Valais Ocean during a phase of Adria-Europe divergence between ~155 and 145 Ma.

Most previous reconstructions infer an east-dipping subduction zone below Sava Oceanic lithosphere emplacing the West Vardar Ophiolites on the Greater Adriatic margin around 140 Ma (Barrier et al., 2018; Csontos and Vörös, 2004; Handy et al., 2010; Schettino and Turco, 2010; Stampfli and Hochard, 2009). On the eastern side of the Sava Ocean, reconstructions vary more. Stampfli and Hochard (2009) also reconstruct a south-west dipping subduction zone emplacing East Vardar Ophiolites. Where our reconstruction places Tisza in the upper plate and connects the two subduction zones with a transform between Tisza and the Eo- and lower Austroalpine units, Stampfli and Hochard (2009) and Moix et al. (2008) infer that the trench curved around and placed the Tisza Block in the obducted margin. They connect the East Vardar trench to a west-dipping intra-oceanic subduction zone with the Sava suture in the upper plate. Csontos and Vörös (2004) and Golonka (2004) reconstruct subduction zone below the Dacia and Tisza units in this time. Schettino and Turco (2010) reconstruct no subduction or deformation along the eastern Sava margin.

In the Anatolian segment, most reconstructions infer a north-dipping subduction zone along the Pontide margin around 140 Ma (Barrier et al., 2018; Golonka, 2004; Robertson et al., 2013c; Sosson et al., 2016). Barrier et al. (2018) restore some 500 km of Cretaceous extension in the eastern Black Sea and Greater Caucasus Basin and align the eastern Pontide trench with the thrust front of the North Dobrogea orogen. Stampfli and Hochard (2009) and Moix et al. (2008), however, reconstruct a passive margin between the Pontide units and the Neotethys around 140 Ma, and place the Sanandaj-Sirjan Zone, which is part of the Iranian Cimmerides, as the southern conjugate margin. This implies ~1500 km eastward motion of the Sandandaj-Sirjan Block in the Cretaceous. They infer that the Sanandaj-Sirjan Block and the Neotethys Ocean Basin to the north were subducting westwards below the Sava (their Vardar) Ocean. Stampfli and Hochard (2009) and Moix et al. (2008) infer that around 140 Ma the subduction zone that emplaces Cretaceous ophiolites onto Greater Adria, Arabia, and northern Africa, initiates close to the Sanandaj-Sirjan margin, opening a 'Semail' Ocean (similar to our Misis ocean, but referring to the Semail Massif of Oman) in the upper plate.

Robertson et al. (2013c) presents a reconstruction similar to ours with one subduction zone along the Pontides with the Jurassic ophiolites in the Pontide forearc. Greater Adria is in a downgoing plate position as part of the African Plate, as in our reconstruction, although they reconstructed a separate 'Berit' Ocean between the Geyikdağı unit and the Bitlis, Malatya, and Kyrenia blocks. This Berit Ocean also features in Barrier et al. (2018) who, moreover, infer that the West Vardar subduction continued into the Anatolian realm and from there all the way to the Indian Ocean. They infer that this subduction zone emplaced ophiolites onto the Pelagonian and Dinarides margin in the Early Cretaceous, and that this same subduction zone was responsible for the late Cretaceous obduction of northern Greater Adria in the Anatolian segment. Sosson et al. (2016) also infers that the Cretaceous ophiolites were obducted by a subduction zone that existed since at least middle Jurassic time, but ends this trench in a triple junction with north-dipping trenches below Dacia and the Pontides at the longitude of western Anatolia throughout the Jurassic and Cretaceous.

7.9. Bajocian – 170 Ma

At 170 Ma, Iberia was undergoing pre-drift extension in the Atlantic domain and the Piemonte-Ligurian Ocean is in the early stages of opening (Fig. 44, SI1 – map 10). The Piemonte-Ligurian Ocean opened as part of the Atlantic system: after 180 Ma, we connect Greater Adria to Africa and open the Piemonte-Ligurian Ocean by accommodating the deficit of Central Atlantic spreading to the north of the Newfoundland-Gibraltar Fracture Zone as Piemonte Ligurian Ocean spreading (Vissers et al., 2013; see also Frisch, 1979). Reconstructing the Piemonte-Ligurian Ocean brings the Northern margin of Adria, including the Southern Alps and the Ivrea body, adjacent to the southwestern European margin containing rocks of the North Pyrenean Zone. To the west, the Ivrea body of NW Adria lies against the Cap de Creus margin of the easternmost Axial Zone of the Pyrenees, which at 170 Ma is undergoing continental extension (Vissers et al., 2017). Because the Stilo-Aspromonte-Peloritan unit of Calabria has high-grade Variscan metamorphic rocks similar to those found in the Axial Zone of the Pyrenees and in NW Adria, but much higher grade than those of southwest Sardinia which instead contains low-grade metamorphic Variscan foreland units (see sections 5.4 and 5.5.2), we restore this part of Calabria adjacent to Sesia and the upper Austroalpine units against the North Pyrenean Zone. We infer that during oblique break-up of this margin, the Stilo-Aspromonte-Peloritan unit moved along a transform fault to Sardinia, after which it was left behind by a jump in the rift to the south. This jump was also responsible for opening oceanic lithosphere (or exhuming mantle) between the Sesia fragment and NW Adria. Following this extension, the oblique Alpine trench formed south of the Stilo-Aspromonte-Peloritan unit, but north of the Sesia fragment, leading to their separation. It was also at this margin that we infer the Pyrenean ultramafic bodies were exhumed, in the wake of the rifting Stilo-Aspromonte-Peloritan Block, in Middle Jurassic time. They were then during Early Cretaceous subduction accreted to the North Pyrenean Zone, and received a thermal pulse resetting their $^{40}Ar/^{39}Ar$ clocks following Albian slab break-off (see also Vissers et al., 2016).

The opening of the Piemonte-Ligurian Ocean generates E-W contraction between the Greater Adriatic margin and the Dacia domain, which is accommodated by subduction initiation within the Balkan Neotethys (Maffione and van Hinsbergen, 2018). There just prior to 170 Ma the mid-ocean ridge of the Neotethys, relics of which are preserved as a belt of MORB ophiolites in the West Vardar Ophiolite belt of the Albanides and Hellenides, subduction started, probably along oceanic detachment faults adjacent to the mid-Neotethys ridge (Maffione et al., 2015). Reactivation of the ridge in the upper plate led to the supra-subduction zone type crust found in the rest of the West Vardar Ophiolites. Subduction below the East Vardar Ophiolites must also have been active at 170 Ma. In this reconstruction, we infer that subduction below the East Vardar Ophiolites also initiated, perhaps on the eastern flank of the mid-Neotethys ridge. We will discuss alternatives in the discussion section.

The Sava ridge and adjacent trenches abut in the north and south against transform faults. The southern lies at the transition to the Anatolian segment, the northern along the Eo- and lower Austroalpine continental units that lie now restored against the south European margin (Fig. 44, SI1 – map 10). Restoring the Tisza Block is challenging, as direct kinematic constraints are lacking. Based on stratigraphic arguments, e.g. Haas and Péró (2004) suggested that the Tisza Block in Early Jurassic and earlier times was connected to the northeastern, Central European margin of the Tethys rather than the Adriatic margin. In absence of other

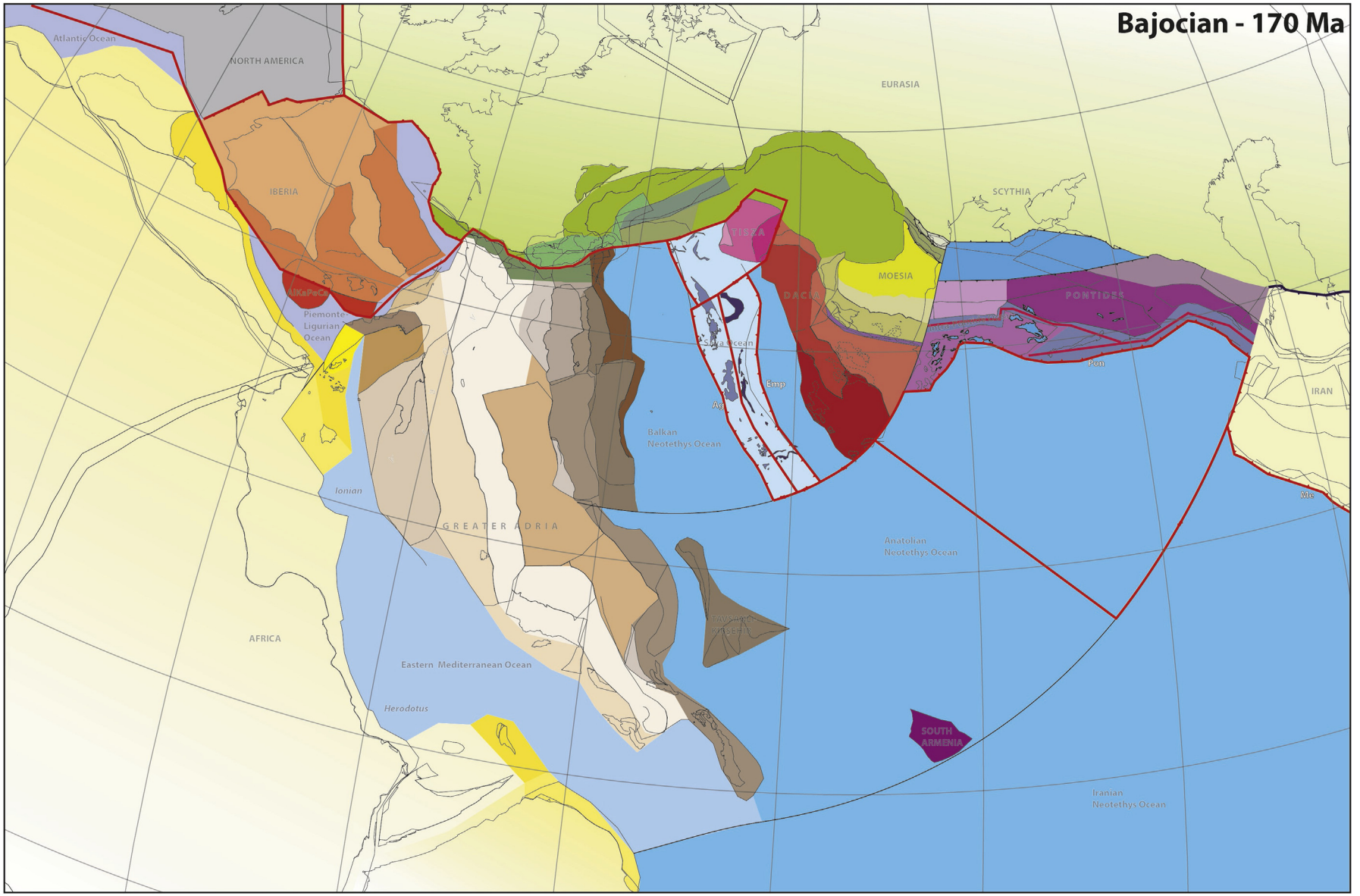

Fig. 44. Paleotectonic map of the Mediterranean region for the Bajocian (170 Ma). Map is projected in a Europe-fixed reference frame. Latitudinal and longitudinal graticules in 10° intervals. See Supplementary Information 1 – map 10 for a larger version of the map that includes abbreviations of the detailed tectonic units. GPlates rotation files are provided in Supplementary Information 3. For key to tectonic units, see Fig. 5.

constraints, we use this as argument to restore the Tisza Block to the northeast. We accommodate this by inferring that the East Vardar trench did not continue prior to 150 Ma between Tisza and Dacia, but that Tisza was connected to the west Sava Plate above the West Vardar subduction zone. We accommodate the roll-back of this subduction zone to the northeast of the Tisza Block, thereby restoring Tisza to the Central European margin, adjacent to, and to the north of Dacia. We accommodate the NE-SW opening of the Ceahlau-Severin Ocean at the East Vardar trench, and restore a speculative similar amount of extension decreasing the area occupied in the reconstruction by the Middle Rhodope Unit.

In the Anatolian segment, active Neotethys spreading is accommodated by transform faults between the Sava and Iranian Neotethys segments, and by northward subduction below the Pontide trench in the north. This trench was in its nascent stages and generated extension in the upper plate (Fig. 44, SI1 – map 10). This extension opened the Intra-Pontide Ocean in the west, generates the extension that forms the Jurassic south-Pontide and Armenian supra-subduction zone ophiolites, and in the east extension was partitioned over the forearc and the Greater Caucasus Basin in the back-arc. Arc magmatism on the Eastern Pontides and in the Transcaucasus ranges suggests that the oceanic forearc was narrow between a trench and a continental arc, as reconstructed elsewhere, e.g. in the Early Cretaceous of Tibet (Huang et al., 2015) or the Triassic of Baja California (Boschman et al., 2018).

Previous reconstructions follow similar logic for the opening of the Piemonte-Ligurian Ocean, which in all cases is closed going backwards in time by Early or Middle Jurassic time (Csontos and Vörös, 2004; Handy et al., 2010; Schettino and Turco, 2010; Stampfli and Hochard, 2009). Only Le Pichon et al. (2019) suggested that Adria did not form the conjugate margin of SE Iberia and instead restore the crust underlying the modern NW-SE trending Adriatic sea to parallel to the North African margin of Lybia and Egypt, and infer ~50° clockwise rotation of Adria relative to Africa accommodated along a transform, and some 800 km of convergence between northern Adria and Europe.

To the northeast of Adria, Stampfli and Hochard (2009) and Moix et al. (2008) reconstruct two NE-SW striking oceanic basins, Meliata and Maliac, separated by a 'Transdanubian' Block. These oceans strike orthogonal to the Balkan Neotethys and Sava Ocean in our reconstruction. They infer that these oceans were subducted eastward below oceanic lithosphere that emplaced the West Vardar Ophiolites on which in their reconstruction subduction started at or before 220 Ma. Csontos and Vörös (2004) link the opening of the Ceahlau-Severin Ocean as well as the Balkan Neotethys to the Magura Ocean and Piemonte-Ligurian system and suggest that this was accommodated by subduction in the North Dobrogea orogen. They reconstruct the emplacement of the West and East Vardar Ophiolites to result from a northwestward radially rolling back system similar in style to our Late Cretaceous scenario for the southeastern Mediterranean region (compare their Fig. 24 with our Fig. 40). Barrier et al. (2018) and Sosson et al. (2016) infer a similar subduction zone along the south Pontide margin as in our reconstruction but restore a second northeast dipping intra-oceanic subduction zone within the Anatolian Neotethys, that will eventually obduct the Cretaceous Anatolian ophiolites. Moreover, Barrier et al. (2018) infer that the Eastern Mediterranean Ocean was closed prior to 180 Ma and opened by NW-SE extension in the course of the Jurassic. They do not specify how the NW-SE convergence that this would have generated in the western Mediterranean region was accommodated.

7.10. Hettangian and Ladinian - 200 and 240 Ma

At 200 Ma, Adria is fixed relative to Eurasia in a somewhat tighter fit, but otherwise similar configuration as at 170 Ma (Fig. 45 and SI1 – map 11). Late Triassic to Early Jurassic (220-180 Ma) extension between Europe and North America reconstructed from the Norwegian and Greenland margins (Torsvik et al., 2012) is accommodated in our reconstruction in the Bay of Biscay region, in the western Piemonte-Ligurian Ocean, where it is mainly a transform motion, and from there towards the Eastern Mediterranean Ocean. The direction of extension is more or less parallel to the Tunisian and Levant margins, and the amount of extension is more or less equal to the width of the Eastern Mediterranean Ocean. Restoring this extension using the poles of Torsvik et al. (2012) leads to a tight fit of Greater Adria within the North African margin in the Early Triassic (Fig. 46 and SI1 – map 12). We infer that the Lago Negro Basin opened due to a small component of transtension and rotation of the Apenninic-Lazio-Abruzzo Platform. We note that our reconstruction accommodates all extension between northern Iberia and the Armorican margin. This simplification leads to a large overlap of the northern Iberian and South Pyrenean units and the Armorican margin yet leaves part of the southern Piemonte-Ligurian Ocean unrestored. Moreover, there is unequivocal evidence for Late Triassic to Early Jurassic extension in the Atlas rift and Iberia (Arche and López-Gómez, 1996; Frizon de Lamotte et al., 2008) and extension was likely much more widely distributed than modeled here. This, however, would require a more southwestward restoration of Iberia against North America than in the reconstruction of Sibuet et al. (2012) that we use as input.

We restore several hundreds of kilometers of pre-drift extension between the Apulian Platform and North Africa, restoring the Hyblean plateau closer to the African margin. In the eastern Mediterranean region, our reconstruction restores several hundreds of kilometers of Triassic pre-drift extension and latest Triassic oceanization, juxtaposing the Gürün Curl margin of the Geyikdağı Platform against the west Arabian margin. The Eratosthenes Seamount and the Trypa unit of Northern Cyprus are restored to closer to Africa and Arabia. The easternmost Taurides and Bitlis Massifs form the conjugate margin of NW Arabia (Figs. 45 and 46 and SI1 – maps 11 and 12). The resulting reconstruction restores the North African and Greater Adriatic conjugate margins and the Triassic to Early Jurassic portion of the Eastern Mediterranean Ocean by 'Atlantic' spreading, i.e. kinematically linked to predrift extension within the Atlantic realm. The reconstruction also leaves space for the Herodotus Ocean within the north Gondwana margin, which was already open in the Carboniferous (Granot, 2016). This ocean may be a relict back-arc basin from the Paleozoic but is in any case unrelated to the Atlantic or Neotethyan systems.

By closing the Piemonte-Ligurian and Eastern Mediterranean oceans, all extension induced by Atlantic break-up and oceanization is restored. The Central and Eastern Mediterranean region are contained between the Adriatic and Eurasian margins, which were either stationary (prior to 180 Ma), or converging after 180 Ma. The overwhelming evidence for Triassic and Jurassic extension and ocean spreading within the Neotethyan domain therefore unequivocally requires that all area gained by extension was balanced by area loss due to subduction, with little or no accretion. This observation has long been the basis for invoking that prior to the opening of the Neotethys, the area between Adria/Arabia and Eurasia was occupied by an earlier ocean, the Paleotethys (e.g., Şengör et al., 1980, 1984). Contrary to the closure history of the Neotethys Ocean, which has left spectacularly deformed orogens that are the focus of restoration of this paper, the geological record of the Paleotethys is extremely sparse and reconstructing the Paleotethys subduction zone, and identifying its suture, is particularly challenging. With little or no accretion Our reconstruction places the Paleotethys suture along the northeastern margin of the Dacia megaunit in the Balkan segment, and along the northern Pontides, north of the Istanbul, Eastern Pontides, and

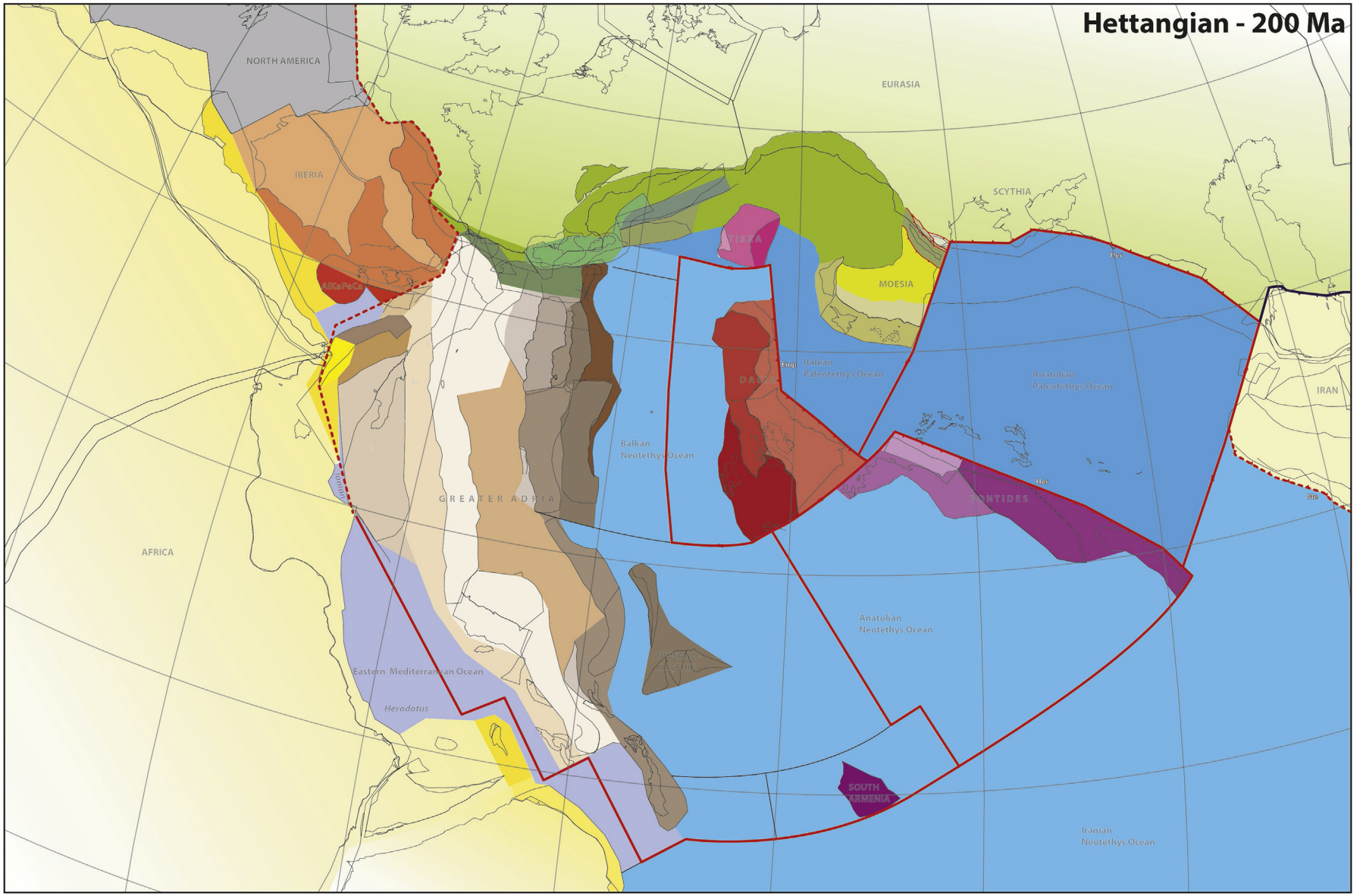

Fig. 45. Paleotectonic map of the Mediterranean region for the Hettangian (200 Ma). Map is projected in a Europe-fixed reference frame. Latitudinal and longitudinal graticules in 10° intervals. See Supplementary Information 1 – map 11 for a larger version of the map that includes abbreviations of the detailed tectonic units. GPlates rotation files are provided in Supplementary Information 3. For key to tectonic units, see Fig. 5.

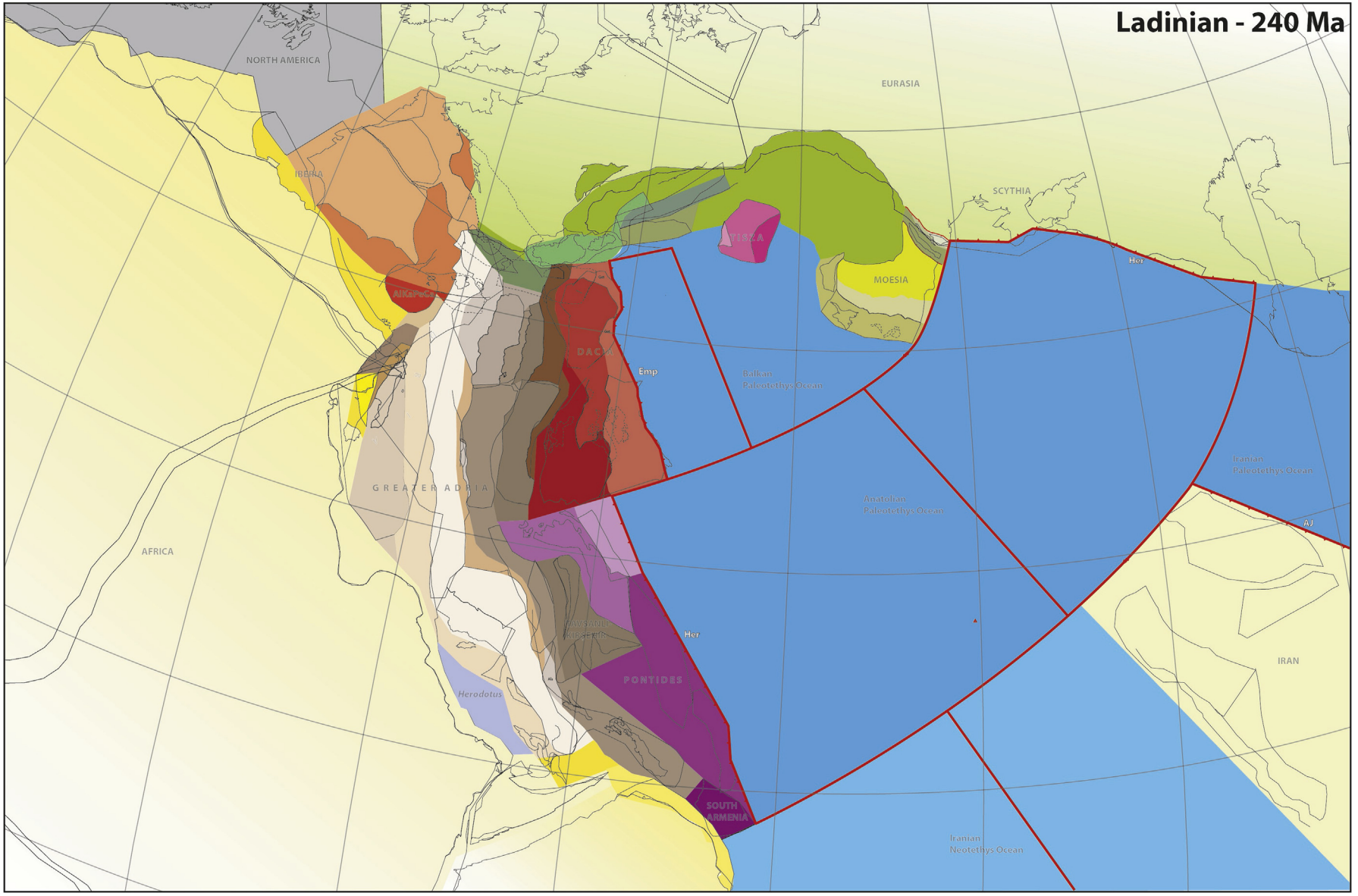

Fig. 46. Paleotectonic map of the Mediterranean region for the Ladinian (240 Ma). Map is projected in a Europe-fixed reference frame. Latitudinal and longitudinal graticules in 10° intervals. See Supplementary Information 1 — map 12 for a larger version of the map that includes abbreviations of the detailed tectonic units. GPlates rotation files are provided in Supplementary Information 3. For key to tectonic units, see Fig. 5.

Transcaucasus range in the Anatolian segment.

In the Balkan segment, extension of the Neotethys, documented in the nappes of the Dinarides and Hellenides, started around 240 Ma. Triassic basalts and pelagic sediments are also the oldest oceanic relic found in mélanges below the West Vardar Ophiolites (see section 5.11) confirming a Triassic onset of oceanization. MORB basalts preserved in the westernmost belt of the West Vardar Ophiolites demonstrate that oceanic Balkan Neotethys spreading continued until ~170 Ma. By inference, Paleotethys subduction must therefore have been active for at least 70 Ma, from 240 to 170 Ma in order to drive the ocean spreading of the Neotethys. Moreover, because the Pindos Basin contains Triassic basalts with a back-arc basin geochemistry (Pe-Piper and Piper, 1991), and there is evidence for Late Paleozoic arc volcanism in rocks of e.g. the Phyllite-Quartzite unit of Crete (lying tratigraphically below the Tripolitza Platform) (Zulauf et al., 2015, 2016), Paleotethys subduction must have been dipping below the northeastern Adriatic margin and opening of the Neotethys requires northeastward rollback of the Paleotethys slab.

Because seismic tomography reveals only one anomaly below the Aegean Slab that is a candidate to contain the subducted Paleotethys lithosphere – the Emporios Slab of van der Meer et al. (2018). Maffione and van Hinsbergen (2018) recently postulated that this anomaly must contain the lithosphere subducted below the East Vardar Ophiolites prior to inception of the Aegean subduction zone around 100 Ma (Fig. 41), as well as the lithosphere of the Paleotethys Ocean. They tentatively postulated that therefore the East Vardar Ophiolites formed above the subduction zone that had been consuming the Paleotethys lithosphere since the Triassic.

The problem with that suggestion – as admitted by Maffione and van Hinsbergen (2018) – is that there is no geological record of any pre-Triassic ocean-derived sediment, nor a pre-middle Jurassic metamorphic record in the mélanges below the East Vardar Ophiolites. The only record of Triassic to Early Jurassic subduction in the Balkan Peninsula is contained in the Middle Rhodopian Unit, also known as the Nestos Suture (Turpaud and Reischmann, 2010) and in the Balkanide units (Schmid et al., 2019). Because of the intense Cretaceous metamorphism in the Rhodope, the early history of the Nestos suture is notoriously difficult to constrain, but if the Triassic-Jurassic ages for high-pressure metamorphism in the Rhodope Middle Unit are correct. However, the constraints of our restoration make this Middle Rhope Units the underpinnings of a Jurassic suture zone contained in the Balkans (the Kotel flysch), recently interpreted, then this is the only record of Paleotethys subduction that we are aware of in the Balkan Peninsula. As described above, we restored top-to-the-north late Triassic-Jurassic thrusting with at least 50 km shortening in the North Dobrogea orogen inverting a (Permian?) - Early Triassic basin in North Dobrogea, but there is no evidence that there was ever a Triassic or Jurassic ocean or a subduction zone accommodating hundreds of kilometers of subduction there. To the east, North Dobrogea has been correlated with the Triassic – Lower Jurassic deep-water foredeep sedimentation and Middle - Late Jurassic arc magmatism in Crimea (e.g., Meijers et al., 2010a, 2010b, 2010c). Our restoration, however, suggests that Crimea and North Dobrogea were separated by a long-lived transform plate boundary, and the stratigraphy and structure of Crimea may not be representative for North Dobrogea.

Our reconstruction of the Rhodope Middle Unit – which is based on several first-order assumptions, including top-north thrusting of the Rhodopian nappe stack at depth below a decollement at the base of the Dacia units – would place the Nestos/Paleotethys suture between the Danubian/Struma Zone and the Sredna Gora/Getic Zone of Dacia. Laterally, this would mean that this suture was reactivated to open the Ceahlau-Severin Ocean, which may have destroyed much of the geological record of the suture. Assuming that the Nestos suture represents the Paleotethys suture, and that our reconstruction of the Rhodope Middle Unit is correct, we therefore reconstruct the Dacia megaunit as the Balkan 'Cimmerian' Block, and as conjugate margin of the Jadar Kopaonik margin of the Dinarides, Albanides, and Hellenides.

In Anatolia, unequivocal evidence for the location of a Paleotethys suture is also sparse. A prominent record of Triassic high-pressure metamorphic rocks is present in the form of the Karakaya complex found in windows below the Pontides (see section 5.12.1). The direction of underthrusting of the Karakaya rocks below the Pontides cannot be constrained with any certainty from the rocks themselves, however and other lines of evidence are required. Şengör and Yılmaz (1981) interpreted the Karakaya rocks to derive from a Permo-Triassic back-arc basin above the Paleotethys subduction zone, but the finding of Devonian cherts within the Karakaya complex makes a strong case that this unit represents a Paleotethys-derived subduction complex (Okay et al., 2011). Okay and Nikishin (2015) pointed at a Triassic volcanic arc buried on the southern Eurasian margin of Russia, north of the Black Sea and Caucasus and used this as argument for northward subduction. The location of the trench responsible for this arc must be south of the Greater Caucasus, where an ophiolitic suture zone between the Scythian Platform and Upper Paleozoic eclogites is unconformably covered by upper Paleozoic sediments (see section 5.12.4) and is thus too old to be a Paleotethys suture. Because the basement of the Transcaucasus and eastern Pontides also have Late Paleozoic ages and formed in an orogenic setting at this time, most authors infer that Paleotethys subduction occurred to the south of the Pontides. This would, however, imply an arc-trench distance of >500 km, which is unlikely. A closer trench could have been located along the south Crimean margin, accreting the deep-marine Triassic to lower Jurassic Tauric Flysch (Fig. 45, SI1 – maps 11 and 12). Towards the east, there is no geological record of a suture zone between the Greater Caucasus and Transcaucasus ranges that both contain an Upper Paleozoic crystalline basement. We note, however, that the Greater Caucasus Basin must have accommodated hundreds of kilometers of extension to come close to oceanization, and subsequently subducted some 300 km during formation of the Lesser Caucasus orocline, and the geological record of its basement, and any suture zone contained therein, has thus been lost during the post-Early Jurassic tectonic history.

There is also evidence for southward Paleotethys subduction. For instance, the Menderes Massif contains Permian and Triassic granitoids with an arc signature (Candan et al., 2016a) and Sayit et al. (2015a) reported lower Upper Triassic (Carnian) arc lavas intercalating with pelagic limestones and radiolarian cherts from the Lycian nappes. Our reconstruction therefore invokes two-sided subduction, and a suture zone below the modern Black Sea and lost in the opening and closure history of the Greater Caucasus Basin. A northward subduction zone accreted the Tauric Flysch of Crimea and formed the Triassic South Russian Arc. The southward subduction zone dipped below Sakarya, the Eastern Pontides, and the Transcaucasus range, and opened the Anatolian Neotethys Ocean in the Triassic. We restore the Pontides against the Greater Adriatic Margin in the Early Triassic (Fig. 46, SI1 – map 12). This is consistent with the recent conclusion of Ülgen et al. (2018) based on sediment provenance analysis that sediments derived from the Strandja Massif (Circum-Rhodope belt) were deposited in Triassic time on the Istanbul Zone, which in our reconstruction are adjacent (Fig. 46, SI1 – map 12).

We reconstruct the South Armenian Block first as part of the Transcaucasus range during initial opening of the Neotethys Ocean, which became an isolated microcontinent due to a ridge jump, a well-known mechanism of microcontinent formation in e.g. the Indian Ocean (Torsvik et al., 2013), at 210 Ma that left it in its reconstructed position that followed from restoring the Lesser

Caucasus Orocline, its 75 Ma collision and rotation, and its history as part of the Anadolu Plate. Our reconstruction follows previous reconstructions of Paleotethys closure for the Iranian segment (Barrier et al., 2018; Muttoni et al., 2009).

Our reconstruction follows for the Anatolian segment more or less the scenario long advocated for by Şengör and Yılmaz (1981). Those authors inferred that the Paleotethys closure occurred around a pivot in the Moesian Platform, a scenario that leaves the opening of the Balkan Neotethys unexplained. Most other authors infer a single, northward Paleotethys subduction zone below the Pontide-Transcaucasus margin, with Neotethys opening along the Paleotethys passive margin with Greater Adria (Barrier et al., 2018; Golonka, 2004; Okay and Nikishin, 2015; Robertson et al., 2013c). Csontos and Vörös (2004), however, infer that the Paleotethys subduction zone was located along the Apulian and Ionian-Geyikdağı margin, and consider the Eastern Mediterranean Ocean a remnant basin of the Paleotethys. Moix et al. (2008) and Stampfli and Hochard (2009) present a reconstruction that is a hybrid between the above scenarios. They infer a Paleotethys suture within the Dinarides, between the Tripolitza and Pindos units of Greece, and between Menderes and Geyikdağı and the Tavşanlı and Kırşehir blocks. Csontos and Vörös (2004), Moix et al. (2008) and Stampfli and Hochard (2009) infer that the extension of the Pindos Basin and the Balkan Neotethys occurred above a north-dipping Paleotethys subduction zone. Moix et al. (2008) and Stampfli and Hochard (2009) infer that to the east, Paleotethys subduction occurred northward rifting the Sanandaj-Sirjan Zone off the Pontides. Finally, Schettino and Turco (2010) reconstruct no subduction and no extension within the Balkan or Anatolian Neotethys in the Triassic.

8. Discussion

8.1. Artifacts, uncertainties, and alternatives

In the previous section, we described how the systematic reconstruction protocol we used (Table 2) and the data provided from the Atlantic ocean floor and Mediterranean orogens led to a kinematic reconstruction of tectonic units, and where this reconstruction differs from previous reconstructions. In this section, we will assess uncertainties in our reconstructions and which where patterns on our maps be artifacts of our reconstruction approach and choices. With these caveats in mind, we will then address the main differences with previous reconstructions and discuss to what extent these differences may concern viable alternative solutions.

As basis for our reconstruction, we used the tectonic map of the Mediterranean region of Schmid et al. (2019), expanded to the west and east to cover our entire study area. This map interprets modern outcrop patterns, which result from paleogeographic distribution, deformation, and erosion. We chose to propagate these outcrop patterns, for instance of nappe fronts, back in time in our reconstruction. The benefit of this approach is that these patterns provide users with a reference to track a particular modern location back in time, but the reader of our maps should bear in mind that the often detailed and complex shape of a thrust fault in our reconstructions is inherited from today's pattern and may not be representative for the presented time-slice.

Using present-day outcrop patterns in our reconstructions also prevented us from significantly changing the area of a tectonic unit in the reconstruction without evidence for deformation. For instance, many previous reconstructions map the Austroalpine units to cover a paleogeographic area that is much smaller than today's area, even when corrected for documented Miocene extension. That would require net extension despite the fact that these units are now a thrusted nappe stack. Our approach prevented us from letting our ideas on a paleotectonic configuration prevail over the systematic reconstruction hierarchy. It also defines the scale of tectonic problems in the past. For instance, the amount of pre-drift extension accommodated within Adria and Southern Europe prior to the opening of the Piemonte-Ligurian Ocean is unquantified and therefore not restored in any detail but may be estimated from the overlap between restored units the Adriatic and European margins (which is a few hundred kilometers, a common number for pre-drift extension (Torsvik et al., 2008). In places of reconstructed overlap, we have offered an interpretation of a paleotectonic configuration based on our reconstruction, but the GPlates reconstruction lines are visible on the map allowing a reader to see what we reconstructed, and what we interpreted based on that.

Artifact arise from the, often, regional character of research communities. For instance, the Dinarides and the Hellenides have each their own communities, definitions and logic, which led to two different interpretations of orogenic evolution. For both orogens, we applied more or less cylindrical deformation histories, projecting along-strike observations to a 2D evolution. Differences in interpreted history from such orogenic segments were reconstructed along known faults, in this case the Scutari-Pec Fault, but it is possible that some displacements, or jumps on the map between paleotectonic units across such faults are an artifact of this reconstruction approach. We believe that the major transform systems between the Iranian, Anatolian, Balkan, and Alps segments, as well as the Scutari-Pec Fault, that we infer were inherited from Paleozoic time (Fig. 46), were real structures, but in more detail, we may also culminate errors associated with assumptions on cylindricity on these structures.

Our reconstruction is consistent with marine magnetic anomaly reconstructions of the Atlantic Ocean and Bay of Biscay, available constraints on fault motions, and paleomagnetism, but all of these constraints come with uncertainties. Some of these may be quantified (Iaffaldano and Stein, 2017), for instance, uncertainties in ocean floor reconstructions are typically on the order of some tens of kilometers (Doubrovine and Tarduno, 2008), although uncertainty in plate motion changes during the Cretaceous Quiet Zone (~125-83 Ma according to Gradstein et al., 2012, or ~121-83 Ma according to Midtkandal et al. (2016)) are larger. Paleomagnetic data, particularly when compiled in APWPs may be associated with uncertainties of ~5°, but for individual poles, these uncertainties may be considerably larger. Finally, uncertainties in timing of deformation, and magnitude of displacement are often hard to quantify. To use reconstructions like ours for future quantitative input in physical modelling it is important that we develop approaches to quantify such uncertainties.

With these caveats in mind, we will now address the viability of alternative scenarios. Many differences of our reconstruction with previous renditions stem from data unavailable (or not compiled) at that time. In addition, our reconstruction is the first to systematically include paleomagnetic constraints. The most prominent differences with previous reconstructions identified in Section 7, however, stem from more philosophical choices and assumptions and will be addressed below.

8.2. Iberia rotation, Briançonnais-Corsica-Sardinia-Iberia contiguity, and Pyrenean evolution

Many previous reconstructions assume that Iberia moved gradually eastward along the southern Eurasian margin, causing transtensional opening of a Pyrenean Ocean throughout the Early Cretaceous. This reconstruction assumes that high-temperature metamorphism in the Pyrenees around 100 Ma was related to hyperextension and mantle exhumation and predicts a gradual counterclockwise rotation of Iberia of not more than ~20°. This would have caused Early Cretaceous E-W convergence between

Adria and Iberia. In addition, previous reconstructions also assume that Corsica-Sardinia and the Briançonnais terrane were a contiguous part of Iberia until the Paleogene. Combined, this reconstruction would require subduction between the Briançonnais, Corsica, and Sardinia throughout the Cretaceous (e.g., Schettino and Turco, 2010; Stampfli and Hochard, 2009).

First, recent paleomagnetic data (Advokaat et al., 2014b) (Fig. 21) demonstrate that Sardinia, and by inference Corsica and the Briançonnais terrane, did not experience the Cretaceous rotation of Iberia, and rotated independently from Iberia since the latest Cretaceous. These units were therefore not contiguous and invoking Early Cretaceous subduction in the Valais domain (e.g., Schettino and Turco, 2010; Stampfli and Hochard, 2009), for which there is no independent geological evidence, is no longer necessary.

Second, the transtensional scenario for Iberia motion is inconsistent with marine magnetic anomaly constraints, and mispredicts the Iberian declination by some 20° prior to ~120 Ma (van Hinsbergen et al., 2017; Vissers et al., 2016). To reconcile the assumption of Cretaceous instead of Jurassic hyperextension with these records, the M0 magnetic anomaly has alternatively been interpreted by post-spreading, passive margin-parallel volcanic belts (Nirrengarten et al., 2017). Furthermore, Barnett-Moore et al. (2017) suggested that ~90% of paleomagnetic data from Iberia are unreliable, except for the low-rotation outliers. Combined, this would allow Iberia to break off North America and Europe only in the Albian-Aptian during which time high-temperature metamorphism occurred in the Pyrenees. We note that even if this is correct, Iberia is still restored in Jurassic time in a similar, but less rotated, position as it is in our reconstruction. This means that also in that case, the Aquitanian (northern Pyrenean) margin restores adjacent to northern Adria, which then still rifts and drifts away during Central Atlantic opening, so in all cases was there Jurassic break-up and extension in the (northern) Pyrenees, allowing to explain the Jurassic ages derived from Pyrenean peridotite complexes. Our reconstruction does not speculate that the paleomagnetic and marine magnetic anomaly data are false for the Iberian case, and instead follows these data as it does everywhere else, which lead to a viable restoration in which orogenic structure, paleomagnetism, marine magnetic anomalies, seismic tomography, and orogenic evolution of the Alpine and Apenninic domain are straightforwardly reconciled.

For the thermal event that affected the Central Pyrenees after rotation, as well as the recently documented heating and uplift-related exhumation documented from low-T thermochronology (Rat et al., 2019; Ternois et al., 2019), shallow slab break-off as proposed by Vissers et al. (2016) may provide a solution. It is of course well possible that the explanation of Vissers et al. (2016) is incorrect. We stress, however, that the hypothesis of Vissers et al. (2016) is based on the kinematic reconstruction, whereas the alternative reconstructions assuming transtension in the Pyrenees (e.g., Jammes et al., 2009; Mouthereau et al., 2014) are based on the hypothesis of hyperextension derived from the Pyrenees: the reconstruction of long-term, Cretaceous transtension between Iberia and Europeis inconsistent with all independent lines of evidence. Falsifying Vissers et al. (2016)'s hypothesis for Cretaceous metamorphism in the Pyrenees does not falsify their kinematic reconstruction. If Cretaceous hyperextension is the cause of the high-temperature metamorphism and mantle exhumation in the Pyrenees as widely interpreted (e.g., Clerc and Lagabrielle, 2014; Mouthereau et al., 2014), kinematic constraints require that this extension occurred locally, after a phase of major rotation of Iberia and convergence in the Pyrenees.

8.3. Adria-Africa motion

Because we restore all Adria-derived nappe stacks of the Mediterranean that collectively define Greater Adria (e.g., Fig. 42) relative to, eventually, the Apulian Platform, different reconstructions of Adria versus Africa will have impact on a large part of the reconstruction, and the older the Adria-Africa motion, the larger the impact. Our reconstruction restores ~10° counterclockwise rotation of Adria versus Africa since 20 Ma (van Hinsbergen et al., 2014b), assumes that Adria was fixed relative to Africa between 180 and 20 Ma, and fixed relative to Eurasia before 180 Ma (see sections 7.9 and 7.10), which satisfies paleomagnetic constraints well (Fig. 19). Le Breton et al. (2017) recently suggested that the rotation was smaller, ~6°, based on reconstructions of the Dinarides, whereas Ustaszewski et al. (2008) arrived at ~20° based on reconstructions of the southern Alps. Whilst both reconstructions may be within the bounds of the spread in paleomagnetic data, such post-20 Ma rotations will only have limited impact for our paleogeography. Larger (smaller) rotations will call for a somewhat narrower (wider) Lago Negro Basin in the Southern Apennines, wider (narrower) Ionian Basin in the Hellenides, and more (less) extension in the Strait of Sicily, but because most Greater Adriatic nappes have decoupled from Adria prior to 20 Ma, their distribution will not change. Haldan et al. (2014), however, pointed out that these relatively minor rotations do have great impact on the use of paleomagnetic data from Adria in reconstructing Pangea: Assuming that Adria did not rotate relative to Africa leads to paleolatitudinal overlaps between Southern and Northern Pangea, which form the basis for Pangea B reconstructions that call for a major Permian shear zone with 1000's of kms displacement through the heart of Pangea (e.g. Muttoni et al., 2003). Because Africa rotated ~50° counterclockwise since the Permian, small Miocene vertical axis rotations of Adria translate into paleolatitudinal changes for Adria in times of Pangea, and restoring 10° Miocene counterclockwise rotation predicts significantly more southward Adria-derived paleolatitudes, decreasing the overlap and the Adria-based necessity for Pangea B.

Le Pichon et al. (2019) recently postulated that Adria has not been a rigid part of Africa at all, but instead underwent almost 1000 km of left-lateral strike slip motion since 170 Ma, opening the Eastern Mediterranean Ocean as pull-apart basin, and rotating Adria clockwise by ~50° relative to Africa. If correct, this would have major implications for our paleogeographic maps. The upper Austroalpine units, for instance, would become the conjugate margin of SE Iberia, and the Dinarides of Eurasia. The scenario of Le Pichon et al. (2019), however, is straightforwardly tested against paleomagnetic data. Their 50° clockwise Adria-Africa rotation since the Jurassic is not only inconsistent with data from Adria (Fig. 19), but also of Sicily (Fig. 21), the Northern Apennines (Fig. 23), the upper Austroalpine units (Fig. 26), the Dalmatian and High Karst zones of the Dinarides (Fig. 27), and the Tripolitza and Ionian zones of Albania and Greece (Fig. 28), which instead follow the African APWP prior to their orogenic rotations in the Late Cretaceous and Cenozoic. We therefore do not consider the scenario of Le Pichon et al. (2019) a viable alternative.

8.4. Western Mediterranean roll back and subduction polarity reversal

In the western Mediterranean region, a much studied and debated subduction polarity reversal occurred in the latest Eocene to early Oligocene (compare Figs. 36 and 37). This polarity reversal is unequivocal for Corsica and the Northern Apennines: the Ligurian Massifs overlie a Cretaceous to late Eocene subduction complex on Corsica, and an early Oligocene subduction complex in the Northern Apennines (Figs. 10 and 11). Along-strike to the southwest, however, unequivocal evidence for ‘Alpine’, southeast dipping subduction disappears and the nappe stack of Calabria and Alboran-Kabylides regions is straightforwardly explained by

northwest-dipping subduction (e.g., Lonergan and White, 1997; van Hinsbergen et al., 2014a, 2014b). Our reconstruction therefore assumes a transform between the Alpine and Calabrian trench prior to the polarity reversal (Fig. 37).

Handy et al. (2010) presented an alternative solution, whereby the Alpine subduction polarity continued along all of the Iberian margin prior to the Oligocene. Although we see no conclusive argument for it, this alternative is possible. Because pre-35 Ma Africa-Iberia convergence is less than 100 km, it would have little consequence for our reconstruction of AlKaPeCa, but it would place the Calabrian units as part of the African Plate instead of Eurasia prior to 35 Ma. Following the logic of Handy et al. (2010), Calabria would then restore adjacent to the Baleares margin in Pangea reconstructions, instead of against the North Pyrenean Zone. We note that the solution of Handy et al. (2010) would result in a zone of inherited lithosphere weakness between African and south-Iberia that is in contrast with the strong margin that was invoked to explain the present-day geometry and presence of the Rif-Gibraltar-Betic slab, particularly, under the Betic Cordillera (Chertova et al., 2014).

8.5. Aegean oroclinal bending and the role of trench-parallel extension

Our reconstruction of the Eocene and younger Aegean region follows van Hinsbergen and Schmid (2012) and restores Aegean extension by closing the triangular extensional complexes of the Rhodope, the Cyclades-Menderes, and South Aegean regions (Figs. 12, 35 and 36, see SI1 – maps 2 and 3). This reconstruction successfully predicts the paleomagnetically documented, opposite rotations of the Aegean and SW Anatolian regions (Figs. 28 and 29) and realigns the stretching lineations on both sides of the Mid-Cycladic Lineament to an original NNE-SSW extension direction (Pastor-Galán et al., 2017). As pointed out by van Hinsbergen and Schmid (2012), reconstructing oroclinal bending in the Aegean region in combination with an extensional upper plate requires a trenchward-increasing amount of trench-parallel extension. They argued that the Mid-Cycladic Lineament accommodated part of this trench-parallel extension and was an extensional fault instead of a strike-slip fault as originally inferred by Walcott and White (1998). Malandri et al. (2017) later studied the only location where the Mid-Cycladic Lineament is exposed, on the island of Paros, and showed that it is there a low-angle normal fault within crystalline Cycladic basement, and paleomagnetically confirmed that this fault accommodated the rotation difference that is proportional to the angle between stretching lineations.

The alternative hypothesis of Menant et al. (2016) and Brun et al. (2016) follows Jolivet et al. (2010) in assuming that the detachment faults recognized along the northern Cyclades (the North Cycladic Detachment System) was prior to extension also a laterally contiguous fault that was kinked during oroclinal bending, without trench-parallel extension. This alternative requires some 400 km of trench-parallel convergence during (mostly Miocene) oroclinal bending, either by westward motion of Anatolia or southeastward motion of western Greece and the Balkan. In this scenario, the region to the south of the North Cycladic Detachment System (including the Mid-Cycladic Lineament) must still undergo trench-parallel extension, albeit less than in our reconstruction, but the region to the north must experience northward increasing E-W shortening, up to 100's of kms in the Rhodope region.

There is no evidence for such major trench-parallel shortening in the Rhodope in the Miocene. There is also no evidence for 100's of km of Miocene extrusion of Anatolia, which would place Eastern Anatolia over Iran in the Early Miocene. The highest estimates for the magnitude of Anatolian extrusion is ~85 km, mostly if not all in the Pliocene after the bulk of Aegean oroclinal bending (e.g., Armijo et al., 1999). Similarly, there is no evidence for 100's of km of southeastward extrusion of the Balkan peninsula towards the Aegean region. For these regions, we conclude that the Aegean oroclinal bending was accommodated without major trench-parallel motions, requiring combined trench-normal and trench-parallel extension in the back-arc region.

8.6. Northern Mediterranean paleogeography

From our reconstruction follows a somewhat different paleogeography than widely perceived for the northern Mediterranean region. Our reconstruction suggests that continental rocks found in the Eo- and lower Austroalpine units of the AlCaPa megaunit formed essentially the eastern continuation of the Briançonnais terrane, with perhaps a narrow corridor connecting the Valais-Magura Ocean to the Piemonte Ligurian Ocean. Previous reconstructions instead either placed the AlCaPa units in a narrow corridor between Adria and Tisza or did not specify their paleogeographic location and thrusting history. The reconstruction closest to ours is that of Handy et al. (2010) who also reconstructed a continental domain to the northeast of Adria, and north of the Dinarides that became obliquely overthrusted by northern Adria during its northeastward Cretaceous motion relative to Eurasia. Theirreconstruction, however, has a narrower Valais Ocean and Briançonnais terrane leaving more space for a Piemonte-Ligurian Ocean.

Our reconstruction protocol is primarily based on structural constraints. If post-nappe emplacement extension is restored, the paleogeographic area covered by rocks now contained in a thrust nappe must be equal to, or larger than the modern area defined by the nappe, or klippen thereof, depending on the amount of erosion and the magnitude of within-nappe shortening. Particularly for the western Alps, extension is not thought to be of major importance. We have restored extension associated with western Alpine oroclinal bending and the westward retreat of the west Alpine thrust front, and subsequently placed superimposed nappes adjacent to each other and this defined the width of the Valais Ocean and Briançonnais terrane in our reconstruction. Assuming a narrower width of these paleogeographic domains requires invoking large-scale N-S extension during or after nappe stacking for which there is no evidence.

Our reconstruction then accretes much of the Piemonte-Ligurian oceanic units of the Alps during Cretaceous oblique subduction, restoring these units south of the Provence/Corsica-Sardinia margin. Whilst the Schistes Lustrés units of Corsica contain evidence for Late Cretaceous high-pressure metamorphism at ~84 Ma (Lahondère and Guerrot, 1997), most geochronological records give much younger, Cenozoic ages. Atlantic ocean floor reconstructions show that the minimum paleogeographic width of the Alpine nappe stack is much larger than the amount of Cenozoic Africa-Europe convergence between northern Adria and southern Germany. Moreover, the western Alpine nappe stacking must have occurred over a longer period of time than suggested by geochronological results from high-pressure rocks. A straightforward solution to this problem may be that the moment of decoupling of a nappe from a downgoing plate may not coincide with the end of burial and beginning of prograde metamorphism if the upper plate is under compression. In such cases, climax metamorphism may occur in several nappes simultaneously and not reflect their timing of underthrusting and incorporation in the orogen. Unless major Cenozoic extension in the western Alps becomes documented, we consider the narrower paleogeography of the Alpine units that

allow for a wider Piemonte-Ligurian Ocean as no viable alternative.

8.7. Cretaceous eastern Mediterranean subduction configuration and initiation

Our reconstruction differs significantly from previous reconstructions for the Cretaceous of the eastern Mediterranean region in either the timing of intra-oceanic subduction initiation that culminates in Massif emplacement onto Greater Adria, and/or the amount of subduction zones that formed. Our restoration is in our view the simplest solution, whereby all ophiolites of Anatolia (Jurassic and Cretaceous) are straightforwardly restored and explained by the evolution of only two subduction zones, one of which started in the Jurassic (~180 Ma) along the southern Pontide margin and one in the Late Cretaceous (~105 Ma), intra-oceanically but close to the Greater Adriatic margin. Previous proposals instead invoked the simultaneous initiation of up to six different subduction zones (e.g., in up to four ocean basins, with subduction initiation timing varying from the middle Jurassic to Late Cretaceous.

Recent work on metamorphic soles of Anatolian (and wider Tethyan) ophiolites now resolve the timing of subduction initiation. Metamorphic soles connected to the Cretaceous supra-subduction zone ophiolites (thus not isolated metamorphic blocks in sub-ophiolitic mélanges) exclusively give $^{40}Ar/^{39}Ar$ cooling ages and U/Pb zircon ages that are similar as the spreading ages retrieved from the crust of the overlying ophiolites: ~94-90 Ma for the Anatolian region (van Hinsbergen et al., 2016) and references therein) and 96-95 Ma for the ophiolites farther east in Oman (Guilmette et al., 2018; Rioux et al., 2016). Importantly, recent Lu/Hf ages on garnet from the high-pressure, high-temperature (10–15 kbar, ~800–900 °C) top parts of these soles from Anatolia as well as Oman show that prograde metamorphism preserved below all these ophiolites was simultaneous, ~104 Ma (Guilmette et al., 2018; Peters et al., 2018; Pourteau et al., 2019). This shows that subduction started slowly at or shortly before 104 Ma, and that upper plate extension, e.g., due to initiation of slab roll-back generating the supra-subduction zone forearc lithosphere followed 8–12 Ma later. This upper plate extension led to the exhumation of the underlying soles, explaining the synchronicity of sole climax metamorphic and cooling ages with ophiolite crust formation ages (Guilmette et al., 2018; van Hinsbergen et al., 2015). The Cretaceous Anatolian ophiolites thus formed at a 1000's of km long intra-oceanic subduction zone from Anatolia to Oman around 104 Ma, and there is no evidence from the ophiolites or the sub-ophiolitic mélanges that this subduction zone existed before this time.

The northern, Jurassic supra-subduction zone ophiolites along the Central and Eastern Pontides and overlying the South Armenian Block are viewed by Barrier et al. (2018) and Sosson et al. (2016) as derived from the same plate as the Cretaceous ophiolites. High-pressure garnet amphibolites in mélanges underlying these ophiolites, however, yielded Jurassic ages, again with similar ages as the crust of the overlying supra-subduction zone ophiolites, ~180-160 Ma (Çelik et al., 2013, 2016; Çörtük et al., 2016). This demonstrates that subduction below these ophiolites started at or before the middle Jurassic, well before the Cretaceous subduction zone to the south. Hässig et al. (2019) recently interpreted low-pressure (6–7 kbar, 600 °C) amphibolites with ~90 Ma $^{40}Ar/^{39}Ar$ cooling ages and rutile U/Pb ages found in the mélange below the Jurassic supra-subduction zone ophiolites on the South Armenian Block as metamorphic sole rocks and invoked that Cretaceous subduction formed within an older, Jurassic supra-subduction zone ocean basin. It is questionable, however, whether this isolated slice of amphibolite must have formed in a metamorphic sole. Within the same mélange, eclogites are found with the same cooling ages whereas also retrogression of eclogites through the amphibolite field is well-known from other subduction systems, e.g. on Cuba (Blanco-Quintero et al., 2011). This would require a relatively warm subduction zone perhaps due to the close proximity of a slab edge to the east (Figs. 39 and 40). In any case, these data show that the Jurassic and Cretaceous ophiolites did not form above the same subduction zone.

Our reconstruction for the Cretaceous, which is similar to those shown in van Hinsbergen et al. (2016); Gürer et al. (2016); Gürer and van Hinsbergen (2019) and McPhee and van Hinsbergen (2019), agrees in first order with Moix et al. (2008) and Stampfli and Hochard (2009) in explaining the complex distribution of ophiolites by the roll-back and rotation of originally N-S trending subduction systems. Our restoration invokes several of such segments reactivating fracture zones and ocean-continent transitions along the Adriatic margin, which is required to explain the short time in particular Central and Western Anatolia between subduction initiation and obduction – the reconstructions of Moix et al. (2008) and Stampfli and Hochard (2009) allowed several tens of millions of years for intra-oceanic subduction to arrive at the continental margin, instead of a few to 20 Myr that follows from the data summarized above, and in Figs. 16 and 17. Reconstructions invoking up to six simultaneously forming intra-oceanic subduction zones (e.g., Barrier et al., 2018; Menant et al., 2016; Robertson et al., 2013c) assume that (i) all subduction initiated along north-dipping subduction zones and (ii) along E-W trending axes. Paleomagnetic data from the ophiolites of Cyprus, NW Arabia, and from Anatolia on both sides of the Taurides, however, all demonstrate that these formed at ~N-S striking ridges, not E-W (Inwood et al., 2009b; Maffione et al., 2017; Morris and Anderson, 2002; Morris et al., 2017; van Hinsbergen et al., 2016) and underwent major rotations that are consistent with our reconstruction (e.g., Fig. 34). The modern obduction fronts are consequently restored to N-S striking paleo-trenches, not E-W. In addition, the arc that intruded the Kırşehir Block after its accretion to the upper oceanic plate of which the Central Anatolian Massifs are relics of, is restored to a N-S orientation (Lefebvre et al., 2013a), not E-W as often portrayed (Barrier et al., 2018; Menant et al., 2016). Paleomagnetic data thus support that the conceptual solution of Moix et al. (2008) and Stampfli and Hochard (2009) explaining the modern ophiolite distribution by the evolution of a single subduction zone with N-S striking segments comply with the most up-to-date time constraints and argue against only E-W striking segments. This removes the necessity of invoking simultaneous subduction in multiple basins, which would require a series of weakness zones with identical strength to turn into subduction, at distances away from each other that are only two or three times the thickness of the lithosphere, which we consider a rather unlikely scenario.

Considerable progress for especially the southeastern Anatolian orogen can be made by obtaining structural constraints on its modern architecture of especially the southeastern Anatolian orogen. Our attempt to retrieve this architecture (Fig. 17) is based on sparse structural data. Our reconstruction invokes major N-S extension in eastern Turkey to account for the exhumation of its widespread metamorphic basement but no structural constraints on extension directions during the Cretaceous to Paleocene exhumation, or even the very presence of extensional faults, are available. The effects of subsequent Eocene shortening are only poorly constrained. Our restoration of the SE Anatolian domain to north of the Gürün Curl (Figs. 39–41) complies with the 40 Myr time difference in deformation between these two regions but is conceptual and may require updates in the future.

8.8. The Mediterranean Paleotethys problem

Reconstructing the Paleotethys is the most challenging aspect of reconstructions of the Mediterranean back to the times of Pangea. For one, such reconstructions suffer from errors made in restoring

the complex deformation history of the Cretaceous and Cenozoic which unavoidably propagate back in time. But the most challenging and intriguing problem is that there are few geological records that demonstrate the location of a Paleotethys suture zone. This lack of record is particularly challenging for our reconstruction, because there are only few constraints useful for our reconstruction protocol available for constraining the location of the Paleotethys. In absence of an accretionary record, any major fault may have accommodated the closure of the Paleotethys, and there are numerous candidates (Csontos and Vörös, 2004; Moix et al., 2008; Okay and Nikishin, 2015; Şengör and Yılmaz, 1981), and Figs. 45 and 46, all of them inconclusive.

Candidates to host cryptic sutures have elsewhere been identified using paleomagnetic data that demonstrate a wide separation of now juxtaposed units (e.g. van Hinsbergen et al., 2012, 2019), or long time gaps between the accretion of nappes in a foreland propagating fold-and-thrust belt that may represent time intervals of wholesale underthrusting (McPhee et al., 2018b; van Hinsbergen et al., 2012). Because the width of the Paleotethys decreases westwards, obtaining sufficient paleomagnetic resolution to test Triassic positions of Dacia or the Pontides requires large paleomagnetic datasets from Triassic rocks. For Dacia there are currently no such data and paleomagnetic data from the Pontides are sparse for the Triassic, and highly scattered for the Jurassic and younger and require detailed future work. Moreover, because the Paleotethys closure left no major fold-and-thrust belt at all, identifying gaps in a propagating nappe system is not possible.

In this respect, the position of Dacia and Moesia evolution is critical for our choice on the location of the Paleotethys. Based on extensive thermochronological procenance studies, Balintoni et al. (2009) and Balintoni and Balica (2013) interpreted that the Dacia pre-Alpine terranes outcropping in the Romanian Carpathians originated from a North African Ordovician orogenic event that reworked older African crust. These authors speculated that a "Paleotethys" ocean opened in Devonian in the East Carpathians and Apuseni Mountains and closed in the late Paleozoic, where the lower plate may have been the Gondwana margin. The Danubian nappes derived from Moesia and now incorporated in the South Carpathians have also a Gondwana affinity but were most likely already sutured and accreted against Moesia during the Early Paleozoic (Iancu et al., 2005a, 2005b). The Moesian Platform itself also has a strong northern Gondwana affinity near the Silurian-Devonian transition (Vaida et al., 2005), but most of studies agree that Moesia was already aligned with the East-European Platform in the Late Paleozoic (and only moved relative to Eurasia by opening and closure of the relatively narrow North Dobrogea rift), as in our reconstruction.

Our reconstruction hinges on the interpretation that the Rhodope Middle Unit represents a Triassic-Jurassic subduction complex, and that the Rhodope Middle Unit restores between the Danubian/Struma and Dacia units. The latter reconstructions follows from the new interpretation that the Rhodope units form a top-to-the-south thrust belt that formed structurally below the Dacia thrust belt (Schmid et al., 2019), but both interpretations may be challenged in the future. Our reconstruction of the Karakaya complex as a Paleotethys subduction mélange, as opposed to a small marginal basin that closed somewhere in the upper plate of a Paleotethys subduction zone (Şengör and Yılmaz, 1981), hinges on the finding of Devonian ribbon cherts in the Triassic mélange (Okay et al., 2011). Otherwise, arguments for the location of trenches along the northern Pontide margin and southern Russian margin come from inferred volcanic arcs. But because we have not systematically incorporated arc magmatism, or absence thereof, in our reconstruction protocol (deliberately, to make our reconstruction useful as an independent platform to study relationships between magmatism, subduction, and orogenesis), the double subduction interpretation for the Anatolian Paleotethys (Figs. 45 and 46) is speculative at best. Others have used geochronological constraints from basement provinces as argument for reconstruction, assuming that 'Variscan' basement was exclusively present on the Eurasian margin (e.g., Kock et al., 2007; Zlatkin et al., 2018). Our reconstruction instead infers that Late Paleozoic subduction and metamorphism occurred on both margins, whereby the high-grade basement of the Pontides and Cyclades form the lateral continuation of the Variscan basement of the NW African Meseta. The Anatolian Neotethys then reactivated the Variscan orogenic front, like in the Atlas farther west, and separated the Variscan from the Pan-African basement provinces. Using basement age as argument for paleogeographic evolution requires an understanding of past plate boundary and orogenic processes, which we prefer to base on paleogeographic and -tectonic reconstruction instead. Our reconstruction of the Mediterranean Paleotethys is consistent with our reconstruction protocol and with our understanding of orogenic architecture but is much open for debate.

9. Summary and conclusions

In this paper we provide a kinematic restoration of Mediterranean tectonic evolution from the Present back to 240 million years ago. To this end, we review the architecture of the Mediterranean orogens from the Atlantic coast in the west to the Caucasus and the East Anatolian plateau in the east. We provide a comprehensive review of the architecture of Mediterranean orogens and basins and built a reconstruction based on Atlantic and Red Sea Ocean floor reconstructions and structural geological constraints on Mediterranean deformation. This reconstruction is tested against a paleomagnetic database of ~2300 published paleomagnetic sites from the Mediterranean region. We provide 12 (paleo-)tectonic maps of the region and isolate first-order differences between our reconstruction and previous propositions. All reconstruction files and paleomagnetic files, as well as A1 versions of the (paleo)tectonic maps and a movie of the reconstruction are provided as Supplementary Information to this paper.

Acknowledgements

DJJvH, MM, and DG acknowledge ERC Starting Grant number 306810 (SINK) to DJJvH. DJJvH acknowledges NWO VIDI grant 864.11.004 and NWO VICI grant 865.17.001. THT and WS acknowledge financial support from the Research Council of Norway through its Centres of Excellence funding scheme, project number 223272 (CEED). We thank two anonymous reviewers for their constructive comments. DJJvH started this Mediterranean reconstruction project in 2009 at the Norwegian Geological Survey (NGU, Trondheim) and Physics of Geological Processes (PGP) group at the University of Oslo, Norway and thanks his colleagues there for inspiration, opportunity, and discussion. DJJvH thanks Claudio Faccenna for an introduction into and discussion about the geology of the Apennines. DJJvH thanks Alexis Plunder, Peter McPhee, Kalijn Peters, Ayten Koç, Lydian Boschman, Cor Langereis, Jan-Willem Zachariasse, and Eldert Advokaat for discussions on Mediterranean tectonics, plate reconstructions, and paleomagnetism. Douwe van der Meer is thanked for years of discussions on correlations between Mediterranean orogenesis and mantle structure. Special thanks go to Mathijs Koymans for continuously developing tools on www.paleomagnetism.org to facilitate the development of the paleomagnetic databases and analyses presented in this paper.

Appendix A. Supplementary data

Supplementary data to this article can be found online at https://doi.org/10.1016/j.gr.2019.07.009.

References

Abdul Aziz, H., Hilgen, F., Krijgsman, W., Sanz, E., Calvo, J.P., 2000. Astronomical forcing of sedimentary cycles in the middle to late Miocene continental Calatayud Basin (NE Spain). Earth Planet. Sci. Lett. 177, 9–22.

Abdul Aziz, H., van Dam, J., Hilgen, F.J., Krijgsman, W., 2004. Astronomical forcing in upper Miocene continental sequences: implications for the geomagnetic polarity time scale. Earth Planet. Sci. Lett. 222, 243–258.

Abdul Aziz, H., Böhme, M., Rocholl, A., Zwing, A., Prieto, J., Wijbrans, J.R., Heissig, K., Bachtadse, V., 2007. Integrated stratigraphy and 40Ar/39Ar chronology of the early to middle Miocene upper freshwater Molasse in eastern Bavaria (Germany). Int. J. Earth Sci. 97, 115–134.

Abels, H.A., Abdul Aziz, H., Ventra, D., Hilgen, F.J., 2009. Orbital climate forcing in Mudflat to marginal lacustrine deposits in the Miocene Teruel Basin (Northeast Spain). J. Sediment. Res. 79, 831–847.

Abrahamsen, N., Schönharting, G., 1987. Palaeomagnetic timing of the rotation and translation of Cyprus. Earth Planet. Sci. Lett. 81, 409–418.

Acosta, J., Munoz, A., Herranz, P., Palomo, C., Ballesteros, M., Vaquero, M., Uchupi, E., 2001. Geodynamics of the Emile Baudot escarpment and the Balearic promontory, western Mediterranean. Mar. Pet. Geol. 18, 349–369.

Adamia, S.A., Chkhotua, T., Kekelia, M., Lordkipanidze, M., Shavishvili, I., Zakariadze, G., 1981. Tectonics of the Caucasus and adjoining regions: implications for the evolution of the Tethys ocean. J. Struct. Geol. 3, 437–447.

Adamia, S., Alania, V., Chabukiani, A., Kutelia, Z., Sadradze, N., 2011a. Great Caucasus (Cavcasioni): a long-lived north-Tethyan back-arc basin. Turk. J. Earth Sci. 20, 611–628.

Adamia, S., Zakariadze, G., Chkhotua, T., Sadradze, N., Tsereteli, N., Chabukiani, A., Gventsadze, A., 2011b. Geology of the Caucasus: a review. Turk. J. Earth Sci. 20, 489–544.

Adamia, S., Chkhotua, T., Gavtadze, T., Lebanidze, Z., Lursmanashvili, N., Sadradze, N., Zakaraia, D., Zakariadze, G., 2017. Tectonic setting of Georgia–eastern Black Sea: a review. Geol. Soc., Lond., Spec. Publ. 428, 11–40.

Advokaat, E.L., van Hinsbergen, D.J.J., Kaymakcı, N., Vissers, R.L.M., Hendriks, B.W.H., 2014a. Late cretaceous extension and Palaeogene rotation-related contraction in Central Anatolia recorded in the Ayhan-Büyükkışla basin. Int. Geol. Rev. 56, 1813–1836.

Advokaat, E.L., van Hinsbergen, D.J.J., Maffione, M., Langereis, C.G., Vissers, R.L.M., Cherchi, A., Schroeder, R., Madani, H., Columbu, S., 2014b. Eocene rotation of Sardinia, and the paleogeography of the western Mediterranean region. Earth Planet. Sci. Lett. 401, 183–195.

Affolter, T., 2004. Map view retrodeformation of an arcuate fold-and-thrust belt: the Jura case. J. Geophys. Res. 109.

Affolter, T., Faure, J.-L., Gratier, J.-P., Colletta, B., 2008. Kinematic models of deformation at the front of the Alps: new data from map-view restoration. Swiss J. Geosci. 101, 289–303.

Agirrezabala, L.M., Dinarès-Turell, J., 2013. Albian syndepositional block rotation and its geological consequences, Basque–Cantabrian Basin (western Pyrenees). Geol. Mag. 150, 986–1001.

Agnini, C., Muttoni, G., Kent, D.V., Rio, D., 2006. Eocene biostratigraphy and magnetic stratigraphy from Possagno, Italy: the calcareous nannofossil response to climate variability. Earth Planet. Sci. Lett. 241, 815–830.

Agnini, C., Fornaciari, E., Giusberti, L., Grandesso, P., Lanci, L., Luciani, V., Muttoni, G., Palike, H., Rio, D., Spofforth, D.J.A., Stefani, C., 2011. Integrated biomagnetostratigraphy of the Alano section (NE Italy): a proposal for defining the middle-late Eocene boundary. Geol. Soc. Am. Bull. 123, 841–872.

Aguilar, C., Liesa, M., Castiñeiras, P., Navidad, M., 2014. Late Variscan metamorphic and magmatic evolution in the eastern Pyrenees revealed by U–Pb age zircon dating. J. Geol. Soc. 171, 181–192.

Aiello, I.W., Hagstrum, J.T., 2001. Paleomagnetism and paleogeography of Jurassic radiolarian cherts from the Northern Apennines of Italy. Geol. Soc. Am. Bull. 113, 469–481.

Aiello, I.W., Hagstrum, J.T., Principi, G., 2008. Peri-equatorial paleolatitudes for Jurassic radiolarian cherts of Greece. Tectonophysics 448, 33–48.

Akbayram, K., Okay, A.I., Satır, M., 2013. Early cretaceous closure of the Intra-Pontide Ocean in western Pontides (northwestern Turkey). J. Geodyn. 65, 38–55.

Akbayram, K., Sorlien, C.C., Okay, A.I., 2016. Evidence for a minimum 52±1km of total offset along the northern branch of the North Anatolian Fault in northwest Turkey. Tectonophysics 668–669, 35–41.

Akdoğan, R., Okay, A., Dunkl, I., 2019. Striking variation in the provenance of the lower and upper cretaceous turbidites in the Central Pontides (Northern Turkey) related to the opening of the Black Sea. Tectonics 38, 1050–1069.

Akopyan, T.G., Minasyan, D.O., 1973. Paleomagnetic Directions and Pole Positions: Data for the USSR. Soviet Geophysical Committee, World Data Center-B, Moscow.

Aksu, A.E., Calon, T., Hall, J., Kurtboğan, B., Gürçay, S., Çifçi, G., 2014. Complex interactions fault fans developed in a strike-slip system: Kozan Fault Zone, Eastern Mediterranean Sea. Mar. Geol. 351, 91–107.

Aktaş, G., Robertson, A.H.F., 1984. The Maden Complex, SE Turkey: evolution of a Neotethyan active margin. Geol. Soc., Lond., Spec. Publ. 17, 375–402.

Aktaş, G., Robertson, A., 1990. Tectonic evolution of the Tethys suture zone in SE Turkey: evidence from the petrology and geochemistry of late cretaceous and middle Eocene extrusives, Ophiolites–Oceanic crustal analogues. In: Proceedings of the International Symposium Troodos, pp. 311–329.

Akıncı, A.C., Robertson, A.H.F., Ünlügenç, U.C., 2016. Late Cretaceous–Cenozoic subduction–collision history of the Southern Neotethys: new evidence from the Çağlayancerit area, SE Turkey. Int. J. Earth Sci. 105, 315–337.

Al-Riyami, K., Robertson, A., 2002. Mesozoic sedimentary and magmatic evolution of the Arabian continental margin, northern Syria: evidence from the Baer–Bassit Mélange. Geol. Mag. 139.

Al-Riyami, K., Robertson, A., Dixon, J., Xenophontos, C., 2002. Origin and emplacement of the late cretaceous Baer–Bassit ophiolite and its metamorphic sole in NW Syria. Lithos 65, 225–260.

Aldanmaz, E., van Hinsbergen, D.J.J., Yıldız-Yüksekol, Ö., Schmidt, M.W., McPhee, P.J., Meisel, T., Güçtekin, A., Mason, P.R.D., 2019. Depletion and Refertilization of Spinel-Peridotites During Supra-Subduction Zone Spreading: Evidence from Cretaceous Ophiolites in Southern Turkey and Northern Cyprus. Lithos submitted.

Alexandre, P., Chalot-Prat, F., Saintot, A., Wijbrans, J., Stephenson, R., Wilson, M., Kitchka, A., Stovba, S., 2004. The 40Ar/39Ar dating of magmatic activity in the Donbas fold belt and the Scythian platform (Eastern European Craton). Tectonics 23.

Alfonsi, L., 1997. Paleomagnetic and anisotropy of magnetic susceptibility (AMS) analyses of the Plio-Pleistocene extensional Todi Basin, central Italy. Ann. Geophys. 40.

Allerton, S., Vine, F., 1987. Spreading structure of the Troodos ophiolite, Cyprus: some paleomagnetic constraints. Geology 15, 593–597.

Allerton, S., Lonergan, L., Platt, J.P., Platzman, E.S., McClelland, E., 1993. Palaeomagnetic rotations in the eastern Betic Cordillera, southern Spain. Earth Planet. Sci. Lett. 119, 225–241.

Allerton, S., Reicherter, K., Platt, J.P., 1994. A structural and palaeomagnetic study of a section through the eastern Subbetic, Southern Spain. J. Geol. Soc. 151, 659–668.

Alparslan, G., Dilek, Y., 2017. Seafloor spreading structure, geochronology, and tectonic evolution of the Küre ophiolite, Turkey: a Jurassic continental backarc basin oceanic lithosphere in southern Eurasia. Lithosphere 10, 14–34.

Amaudric du Chaffaut, S., Saliot, P., 1979. La region de Corte; secteur cle pour la comprehension du metamorphisme alpin en Corse. Bull. Soc. Géol. France 7, 149–154.

Amodio Morelli, L., Bonardi, G., Colonna, V., Dietrich, D., Giunta, G., Ippolito, F., Liguori, V., Lorenzoni, S., Paglionico, A., Perrone, V., Piccarreta, G., Russo, M., Scandone, P., Zanettin Lorenzoni, E., Zuppetta, A., 1976. L'arco Calabro-Peloritano nell'orogene appenninico-maghrebide. Mem. Soc. Geol. Ital. 17, 1–60.

Andreani, L., Loget, N., Rangin, C., Le Pichon, X., 2010. New structural constraints on the southern Provence thrust belt (France): evidences for an Eocene shortening event linked to the Corsica-Sardinia subduction. Bull. Soc. Géol. France 181, 547–563.

Andreucci, B., Castelluccio, A., Jankowski, L., Mazzoli, S., Szaniawski, R., Zattin, M., 2013. Burial and exhumation history of the Polish Outer Carpathians: discriminating the role of thrusting and post-thrusting extension. Tectonophysics 608, 866–883.

Andrew, T., Robertson, A.H.F., 2002. The Beyşehir–Hoyran–Hadim Nappes: genesis and emplacement of Mesozoic marginal and oceanic units of the northern Neotethys in southern Turkey. J. Geol. Soc. London 159, 529–543.

Andrić, N., Sant, K., Mațenco, L., Mandic, O., Tomljenović, B., Pavelić, D., Hrvatović, H., Demir, V., Ooms, J., 2017. The link between tectonics and sedimentation in asymmetric extensional basins: inferences from the study of the Sarajevo-Zenica Basin. Mar. Pet. Geol. 83, 305–332.

Angelucci, A., Devoto, G., 1966. Geologia del Monte Caccume (Frosinone). Geologica Romana, pp. 177–196.

Angiolini, L., Carabelli, L., Nicora, A., Crasquin-Soleau, S., Marcoux, J., Rettori, R., 2007. Brachiopods and other fossils from the Permo–Triassic boundary beds of the Antalya Nappes (SW Taurus, Turkey). Geobios 40, 715–729.

Antić, M.D., Kounov, A., Trivić, B., Wetzel, A., Peytcheva, I., von Quadt, A., 2016. Alpine thermal events in the central Serbo-Macedonian Massif (southeastern Serbia). Int. J. Earth Sci. 105, 1485–1505.

Antić, M.D., Kounov, A., Trivić, B., Spikings, R., Wetzel, A., 2017. Evidence of Variscan and Alpine tectonics in the structural and thermochronological record of the central Serbo-Macedonian Massif (south-eastern Serbia). Int. J. Earth Sci. 106, 1665–1692.

Arche, A., López-Gómez, J., 1996. Origin of the Permian-Triassic Iberian basin, central-eastern Spain. Tectonophysics 266, 443–464.

Argand, E., 1924. Compte-Rendu du 13e Congres Géologique International, pp. 171–372. Brussels.

Argentieri, A., Mattei, M., Rossetti, F., Argnan, A., Salvini, F., Funiciello, R., 1998. Tectonic evolution of the Amantea Basin (Calabria, southern Italy): comparing in-land and off-shore data. Ann. Tect. 12, 79–96.

Argles, T.W., Prince, C.I., Foster, G.L., Vance, D., 1999. New garnets for old? Cautionary tales from young mountain belts. Earth Planet. Sci. Lett. 172, 301–309.

Argnani, A., 1987. The Gela Nappe: evidence of accretionary mélange in the Maghrebian foredeep of Sicily. Mem. Soc. Geol. Ital. 38, 419–428.

Argnani, A., 2000. The Southern Tyrrhenian subduction system: recent evolution and neotectonic implications. Ann. Geophys. 43.

Argnani, A., 2009. Evolution of the southern Tyrrhenian slab tear and active tectonics along the western edge of the Tyrrhenian subducted slab. Geol. Soc., Lond., Spec. Publ. 311, 193–212.

Argnani, A., 2012. Plate motion and the evolution of Alpine Corsica and Northern Apennines. Tectonophysics 579, 207–219.

Argnani, A., Lucchi, F.R., 2001. Tertiary Silicoclastic Turbidite Systems of the Northern Apennines, Anatomy of an Orogen: the Apennines and Adjacent Mediterranean Basins. Springer, pp. 327–349.

Argnani, A., Favalli, P., Frugoni, F., Gasperini, M., Ligi, M., Marani, M., Mattietti, G.,

Mele, G., 1993. Foreland deformational pattern in the Southern Adriatic Sea. Ann. Geophys. 36.
Armijo, R., Meyer, B., Hubert, A., Barka, A., 1999. Westward propagation of the North Anatolian fault into the northern Aegean: timing and kinematics. Geology 27, 267–270.
Arragoni, S., Maggi, M., Cianfarra, P., Salvini, F., 2016. The Cenozoic fold-and-thrust belt of Eastern Sardinia: evidences from the integration of field data with numerically balanced geological cross section. Tectonics 35, 1404–1422.
Arthaud, F., Laurent, P., 1995. Stress, deformation and displacement within the north-Pyrenean foreland of the Mediterranean Languedoc. Geodin. Acta 8, 142–157.
Asanidze, B., Adamiya, S.A., Tabagua, I., Odikadze, N.S., 2009. The territory of Georgia and surrounding countries in the Upper Cretaceous: paleomagnetic data. Izv., Phys. Solid Earth 45, 583–594.
Asatryan, G., Danelian, T., Seyler, M., Sahakyan, L., Galoyan, G., Sosson, M., Avagyan, A., Hubert, B., Person, A., Vantalon, S., 2012. Latest Jurassic–Early Cretaceous Radiolarian assemblages constrain episodes of submarine volcanic activity in the Tethyan oceanic realm of the Sevan ophiolites (Armenia). Bull. Soc. Géol. France 183, 319–330.
Atzemoglou, A., 1997. Paleomagnetic Results from Northern Greece and their Contribution to the Interpretation of the Geodynamic Evolution of the Area during the Tertiary. Doctorate Thesis. Aristotle Univ. of Thessaloniki.
Atzemoglou, A., Kondopoulou, D., Papamarinopoulos, S., Dimitriadis, S., 1994. Palaeomagnetic evidence for block rotations in the western Greek Rhodope. Geophys. J. Int. 118, 221–230.
Aubouin, J., Blanchet, R., Cadet, J.-P., Celet, P., Charvet, J., Chorowicz, J., Cousin, M., Rampnoux, J.-P., 1970. Essai sur la géologie des Dinarides. Bull. Soc. Géol. France 7, 1060–1095.
Avagyan, A., Shahidi, A., Sosson, M., Sahakyan, L., Galoyan, G., Muller, C., Vardanyan, S., Firouzi, K.B., Bosch, D., Danelian, T., 2017. New data on the tectonic evolution of the Khoy region, NW Iran. Geol. Soc., Lond., Spec. Publ. 428, 99–116.
Avdeev, B., Niemi, N.A., 2011. Rapid Pliocene exhumation of the Central Greater Caucasus constrained by low-temperature thermochronometry. Tectonics 30.
Avigad, D., Garfunkel, Z., Jolivet, L., Azañón, J.M., 1997. Back arc extension and denudation of Mediterranean eclogites. Tectonics 16, 924–941.
Avigad, D., Baer, G., Heimann, A., 1998. Block rotations and continental extension in the central Aegean Sea: palaeomagnetic and structural evidence from Tinos and Mykonos (Cyclades, Greece). Earth Planet. Sci. Lett. 157, 23–40.
Avşar, Ü., İşseven, T., 2009. Regional clockwise rotation of the Armutlu Peninsula, Western Turkey, resolved from palaeomagnetic study of Eocene volcanics. Tectonophysics 475, 415–422.
Awalt, M.B., Whitney, D.L., 2018. Petrogenesis of kyanite-and corundum-bearing mafic granulite in a meta-ophiolite, SE Turkey. J. Metamorph. Geol. 36, 881–904.
Bache, F., Olivet, J.L., Gorini, C., Aslanian, D., Labails, C., Rabineau, M., 2010. Evolution of rifted continental margins: the case of the Gulf of Lions (Western Mediterranean Basin). Earth Planet. Sci. Lett. 292, 345–356.
Badescu, D., 1997. Tectono-thermal regimes and lithosphere behaviour in the External Dacides in the Upper Triassic and Jurassic Tethyan opening (Romanian Carpathians). Tectonophysics 282, 167–188.
Baes, M., Govers, R., Wortel, R., 2011. Subduction initiation along the inherited weakness zone at the edge of a slab: insights from numerical models. Geophys. J. Int. 184, 991–1008.
Bailey, W.R., Holdsworth, R.E., Swarbrick, R.E., 2000. Kinematic history of a reactivated oceanic suture: the Mamonia Complex Suture Zone, SW Cyprus. J. Geol. Soc. 157, 1107–1126.
Balázs, A., Maţenco, L., Magyar, I., Horváth, F., Cloetingh, S., 2016. The link between tectonics and sedimentation in back-arc basins: new genetic constraints from the analysis of the Pannonian Basin. Tectonics 35, 1526–1559.
Balázs, A., Burov, E., Maţenco, L., Vogt, K., Francois, T., Cloetingh, S., 2017. Symmetry during the syn- and post-rift evolution of extensional back-arc basins: the role of inherited orogenic structures. Earth Planet. Sci. Lett. 462, 86–98.
Balázs, A., Maţenco, L., Vogt, K., Cloetingh, S., Gerya, T., 2018. Extensional Polarity Change in Continental Rifts: inferences From 3-D Numerical Modeling and Observations. J. Geophys. Res.: Solid Earth 123, 8073–8094.
Balestro, G., Festa, A., Dilek, Y., 2019. Structural architecture of the Western Alpine Ophiolites, and the Jurassic seafloor spreading tectonics of the Alpine Tethys. J. Geol. Soc. jgs2018-2099.
Balintoni, I., 1996. Transilvanidele Vestice, Comentarii Structurale. In: Studia Universitas Babeş-Bolyai Seria Geologia, vol. 41, pp. 95–100.
Balintoni, I., Balica, C., 2013. Carpathian peri-Gondwanan terranes in the East Carpathians (Romania): a testimony of an Ordovician, North-African orogeny. Gondwana Res. 23, 1053–1070.
Balintoni, I., Balica, C., Ducea, M.N., Chen, F.K., Hann, H.P., Sabliovschi, V., 2009. Late Cambrian-Early Ordovician Gondwanan terranes in the Romanian Carpathians: a zircon U-Pb provenance study. Gondwana Res. 16, 119–133.
Balintoni, I., Balica, C., Ducea, M.N., Stremţan, C., 2011. Peri-Amazonian, Avalonian-type and Ganderian-type terranes in the South Carpathians, Romania: the Danubian domain basement. Gondwana Res. 19, 945–957.
Balla, Z., 1986. Palaeotectonic reconstruction of the central Alpine-Mediterranean belt for the Neogene. Tectonophysics 127, 213–243.
Banks, C.J., Robinson, A.G., 1998. Mesozoic strike-slip back-arc basins of the western Black Sea region. Mem.-Am. Assoc. Pet. Geol. 53–62.
Banks, C.J., Robinson, A.G., Williams, M.P., 1998. Structure and regional tectonics of the Achara-Trialet fold belt and the adjacent Rioni and Kartli foreland basins, Republic of Georgia. Mem.-Am. Assoc. Pet. Geol. 331–346.
Barbera, X., Parés, J.M., Cabrera, L., Anadón, P., 1994. High-resolution magnetic stratigraphy across the Oligocene-Miocene boundary in an alluvial-lacustrine succession (Ebro Basin, northeast Spain). Phys. Earth Planet. Inter. 85, 181–193.
Barbera, X., Cabrera, L., Parés, J.M., 1997. Error de inclinación paleomagnética en materiales aluviales del Oligoceno superior del sector Suroriental de la Cuenca del Ebro (Region Surpirenaica, NE de España). Acta Geol. Hisp. 32 (3–4), 221–235, 1997.
Barchi, M.R., Alvarez, W., Shimabukuro, D.H., 2012. The Umbria-Marche Apennines as a double orogen: observations and hypotheses. Ital. J. Geosci. 131, 258–271.
Barnett-Moore, N., Font, E., Neres, M., 2017. A reply to the comment on "Assessing discrepancies between previous plate kinematic models of mesozoic Iberia and their constraints" by Barnett-Moore et al. Tectonics 36, 3286–3297.
Barrier, E., Vrielynck, B., 2008. MEBE Atlas of Paleotectonic Maps of the Middle East: Commission for the Geological Map of the World. Paris.
Barrier, E., Vrielynck, B., Bergerat, F., Brunet, M.-F., Mosar, J., Poisson, A., Sosson, M., 2008. Palaeotectonic Maps of the Middle East: Tectono-Sedimentary-Palinspastic Maps from Late Norian to Pliocene.
Barrier, E., Vrielynck, B., Brouillet, J., Brunet, M., 2018. Paleotectonic Reconstruction of the Central Tethyan Realm. Tectonono-Sedimentary-Palinspastic maps from Late Permian to Pliocene. In: CCGM/CGMW, Paris. CCGM/CGMW Paris: France.
Bassant, P., Van Buchem, F.S.P., Strasser, A., Görür, N., 2005. The stratigraphic architecture and evolution of the Burdigalian carbonate—siliciclastic sedimentary systems of the Mut Basin, Turkey. Sediment. Geol. 173, 187–232.
Bauer, C., Rubatto, D., Krenn, K., Proyer, A., Hoinkes, G., 2007. A zircon study from the Rhodope metamorphic complex, N-Greece: time record of a multistage evolution. Lithos 99, 207–228.
Baumgartner, P., 1985. Jurassic Sedimentary Evolution and Nappe Emplacement in the Argolis Peninsula (Peloponnesus, Greece). Mém. Soc. Helv. Sci. Nat 99, 1–111.
Baydemir, N., 1990. Palaeomagnetism of the Eocene volcanic rocks in the eastern Black Sea region. Istanb. Univ. Müh. Fak., Yerbilim. Derg. 7, 167–176.
Bazhenov, M.L., Burtman, V.S., 1986. Paleomagnetic directions and Pole Positions: Data for the USSR. Soviet Geophysical Committee, World Data Center-B, Moscow.
Bazhenov, M., Burtman, V., 1990. Structural Arcs of the Alpine Belt: Carpathians-Caucasus-Pamir. Academy of Sciences Press, Moscow (in Russian).
Bazhenov, M.L., Burtman, V.S., 2002. Eocene paleomagnetism of the Caucasus (southwest Georgia): oroclinal bending in the Arabian syntaxis. Tectonophysics 344, 247–259.
Bazhenov, M.L., Burtman, V.S., Levashova, N.L., 1996. Lower and Middle Jurassic paleomagnetic results from the south Lesser Caucasus and the evolution of the Mesozoic Tethys ocean. Earth Planet. Sci. Lett. 141, 79–89.
Bağcı, U., 2013. The geochemistry and petrology of the ophiolitic rocks from the Kahramanmaraş region, southern Turkey. Turk. J. Earth Sci. 22, 536–562.
Beauchamp, W., Allmendinger, R.W., Barazangi, M., Demnati, A., El Alji, M., Dahmani, M., 1999. Inversion tectonics and the evolution of the High Atlas Mountains, Morocco, based on a geological-geophysical transect. Tectonics 18, 163–184.
Beaumont, C., Muñoz, J.A., Hamilton, J., Fullsack, P., 2000. Factors controlling the Alpine evolution of the central Pyrenees inferred from a comparison of observations and geodynamical models. J. Geophys. Res.: Solid Earth 105, 8121–8145.
Beck, M.E., Burmester, R.F., Kondopoulou, D.P., Atzemoglou, A., 2001. The palaeomagnetism of Lesbos, NE Aegean, and the eastern Mediterranean inclination anomaly. Geophys. J. Int. 145, 233–245.
Bega, Z., 2015. Hydrocarbon exploration potential of Montenegro—a brief review. J. Pet. Geol. 38, 317–330.
Behr, W.M., Platt, J.P., 2012. Kinematic and thermal evolution during two-stage exhumation of a Mediterranean subduction complex. Tectonics 31.
Behrmann, J.H., Stiasny, S., Milicka, J., Pereszlenyi, M., 2000. Quantitative reconstruction of orogenic convergence in the northeast Carpathians. Tectonophysics 319, 111–127.
Beidinger, A., Decker, K., 2014. Quantifying early Miocene in-sequence and out-of-sequence thrusting at the Alpine-Carpathian junction. Tectonics 33, 222–252.
Bellahsen, N., Jolivet, L., Lacombe, O., Bellanger, M., Boutoux, A., Garcia, S., Mouthereau, F., Le Pourhiet, L., Gumiaux, C., 2012. Mechanisms of margin inversion in the external Western Alps: implications for crustal rheology. Tectonophysics 560, 62–83.
Beltrando, M., Lister, G.S., Rosenbaum, G., Richards, S., Forster, M.A., 2010. Recognizing episodic lithospheric thinning along a convergent plate margin: the example of the early Oligocene Alps. Earth-Sci. Rev. 103, 81–98.
Beltrando, M., Zibra, I., Montanini, A., Tribuzio, R., 2013. Crustal thinning and exhumation along a fossil magma-poor distal margin preserved in Corsica: a hot rift to drift transition? Lithos 168–169, 99–112.
Beltrando, M., Compagnoni, R., Ferrando, S., Mohn, G., Frasca, G., Odasso, N., Vukmanovič, Z., Masini, E., 2014. Crustal thinning and mantle exhumation in the Levone area (Southern Canavese Zone, Western Alps). A Field Guide Across the Margins of Alpine Tethys. J. Virtual Explor. Electronic Edition 48.
Benaouali-Mebarek, N., Frizon de Lamotte, D., Roca, E., Bracene, R., Faure, J.-L., Sassi, W., Roure, F., 2006. Post-Cretaceous kinematics of the Atlas and Tell systems in central Algeria: early foreland folding and subduction-related deformation. Compt. Rendus Geosci. 338, 115–125.
Benderev, A., Atanassova, R., Andreev, A., Hristov, V., Bojadgieva, K., Kolev, S., 2015. Hydrochemical Characteristics of Erma Reka Geothermal Reservoir (S. Bulgaria). In: Proceedings World Geothermal Congress Melbourne, Australia.
Bennett, R.A., Hreinsdóttir, S., Buble, G., Bašić, T., Bačić, e., Marjanović, M., Casale, G.,

Gendaszek, A., Cowan, D., 2008. Eocene to present subduction of southern Adria mantle lithosphere beneath the Dinarides. Geology 36.
Benzaggagh, M., Mokhtari, A., Rossi, P., Michard, A., El Maz, A., Chalouan, A., Saddiqi, O., Rjimati, E.-C., 2014. Oceanic units in the core of the External Rif (Morocco): intramargin hiatus or South-Tethyan remnants? J. Geodyn. 77, 4–21.
Berza, T., Iancu, V., 1994. Variscan events in the basement of the Danubian nappes (South Carpathians). Rom. J. Tectonics Reg. Geol. 75, 93–104.
Bergerat, F., Vangelov, D., Dimov, D., 2010. Brittle deformation, palaeostress field reconstruction and tectonic evolution of the Eastern Balkanides (Bulgaria) during Mesozoic and Cenozoic times. Geol. Soc., Lond., Spec. Publ. 340, 77–111.
Berndt, T., Ruiz-Martínez, V.C., Chalouan, A., 2015. New constraints on the evolution of the Gibraltar Arc from palaeomagnetic data of the Ceuta and Beni Bousera peridotites (Rif, northern Africa). J. Geodyn. 84, 19–39.
Bernoulli, D., 2001. Mesozoic-Tertiary Carbonate Platforms, Slopes and Basins of the External Apennines and Sicily, Anatomy of an orogen: the Apennines and Adjacent Mediterranean Basins. Springer, pp. 307–325.
Bernoulli, D., De Graciansky, P.C., Monod, O., 1974. The extension of the Lycian Nappes (SW Turkey) into the southeastern Aegean Islands. Eclogae Geol. Helv. 67, 39–90.
Berra, F., Lanfranchi, A., Jadoul, F., 2017. Comments on "The Cenozoic fold-and-thrust belt of Eastern Sardinia: evidences from the integration of field data with numerically balanced geological cross section" by Arragoni et al., 2016. Tectonics 36, 182–187.
Berza, T., Drăgănescu, A., 1988. The Cerna-Jiu fault system (South Carpathians, Romania), a major tertiary transcurrent lineament. DS Inst. Geol. Geofiz 72, 43–57.
Berza, T., Kräutner, H.G., Dimitrescu, R., 1983. Nappe structure of the Danubian window of the central South Carpathians. An. Inst. Geol. Geofiz 60, 31–34.
Besse, J., Courtillot, V., 2002. Apparent and true polar wander and the geometry of the geomagnetic field over the last 200 Myr. J. Geophys. Res.: Solid Earth 107. EPM 6-1-EPM 6-31.
Besse, J., Pozzi, J.-P., Mascle, G., Feinberg, H., 1984. Paleomagnetic study of Sicily: consequences for the deformation of Italian and African margins over the last 100 million years. Earth Planet. Sci. Lett. 67, 377–390.
Beyarslan, M., 2017. Supra-subduction zone magmatism of the Koçali ophiolite, SE Turkey. J. Afr. Earth Sci. 129, 390–402.
Beyarslan, M., Bingöl, A.F., 2000. Petrology of a supra-subduction zone ophiolite (Elazığ, Turkey). Can. J. Earth Sci. 37, 1411–1424.
Beyarslan, M., Lın, Y.-C., Bingöl, A.F., Chung, S.-L., 2016. Zircon U-Pb age and geochemical constraints on the origin and tectonic implication of Cadomian (Ediacaran-Early Cambrian) magmatism in SE Turkey. J. Asian Earth Sci. 130, 223–238.
Bezert, P., Caby, R., 1988. Sur l'age post-bartonien des evenements tectono-metamorphiques alpins en bordure orientale de la Corse cristalline (Nord de Corte). Bull. Soc. Géol. France 4, 965–971.
Bianco, C., Brogi, A., Caggianelli, A., Giorgetti, G., Liotta, D., Meccheri, M., 2015. HP-LT metamorphism in Elba Island: implications for the geodynamic evolution of the inner Northern Apennines (Italy). J. Geodyn. 91, 13–25.
Birkenmajer, K., 1985. Major Strike-Slip Faults of the Pieniny Klippen Belt and the Tertiary Rotation of the Carpathians. Publications of the Institute of Geophysics, pp. 101–115.
Bizon, G., 1967. Contribution à la Connaissance des Foraminifères Planctoniques d'Épire et des îles Ioniennes: (Grèce occidentale) Depuis le Paléogène Supérieur Jusqu'au Pliocène. Publication de l'Institute Français du Pétrole, pp. 1–44.
Blanco-Quintero, I.F., García-Casco, A., Gerya, T.V., 2011. Tectonic blocks in serpentinite mélange (eastern Cuba) reveal large-scale convective flow of the subduction channel. Geology 39, 79–82.
Blumenthal, M., 1947. Geologie der Taurusketten im Hinterland von Seydişehir und Beyşehir. Verlag nicht ermittelbar.
Bocin, A., Stephenson, R., Mocanu, V., Maţenco, L., 2009. Architecture of the south-eastern Carpathians nappes and Focsani Basin (Romania) from 2D ray tracing of densely-spaced refraction data. Tectonophysics 476, 512–527.
Bodinier, J.-L., Morten, L., Puga, E., Diaz de Federico, A., 1987. Geochemistry of metabasites from the Nevado-Filabride Complex, Betic Cordilleras, Spain: relics of a dismembered ophiolitic sequence. Lithos 20, 235–245.
Boiano, U., 1993. Le facies torbiditiche grossolane del Flysch di Gorgoglione (Miocene, Appennino lucano): caratteri deposizionali ed ipotesi sulla formazione degli strati amalgamati. G. Geol. 55, 179–187.
Boiano, U., 1997. Anatomy of a siliciclastic turbidite basin: the Gorgoglione Flysch, upper Miocene, southern Italy: physical stratigraphy, sedimentology and sequence-stratigraphic framework. Sediment. Geol. 107, 231–262.
Bokelmann, G., Rodler, F.-A., 2014. Nature of the Vrancea seismic zone (Eastern Carpathians) – New constraints from dispersion of first-arriving P-waves. Earth Planet. Sci. Lett. 390, 59–68.
Bol'shakov, A., Solodovnikov, G., 1981. On the Geomagnetic Field Intensity in the Late Cretaceous. Izv. Akad. Nauk SSSR, Ser. Fiz. Zemli, pp. 58–68.
Bonardi, G., 2003. Oligocene-to-early Miocene depositional and structural evolution of the Calabria–Peloritani Arc southern terrane (Italy) and geodynamic correlations with the Spain Betics and Morocco Rif. Geodin. Acta 16, 149–169.
Bonardi, G., Compagnoni, R., Perrone, V., 1984. Riequilibrazioni metamorfiche di probabile età alpina nell'Unità dell'Aspromonte. Rendiconti Soc. Ital. Mineral. Petrol. 39, 613–628.
Boncheva, I., Lakova, I., Sachanski, V., Koenigshof, P., 2010. Devonian stratigraphy, correlations and basin development in the Balkan Terrane, western Bulgaria. Gondwana Res. 17, 573–582.
Bonev, N., Stampfli, G., 2008. Petrology, geochemistry and geodynamic implications of Jurassic island arc magmatism as revealed by mafic volcanic rocks in the Mesozoic low-grade sequence, eastern Rhodope, Bulgaria. Lithos 100, 210–233.
Bonev, N., Dilek, Y., Hanchar, J.M., Bogdanov, K., Klain, L., 2011. Nd–Sr–Pb isotopic composition and mantle sources of Triassic rift units in the Serbo-Macedonian and the western Rhodope massifs (Bulgaria–Greece). Geol. Mag. 149, 146–152.
Bonev, N., Spikings, R., Moritz, R., Marchev, P., Collings, D., 2013. 40Ar/39Ar age constraints on the timing of Tertiary crustal extension and its temporal relation to ore-forming and magmatic processes in the Eastern Rhodope Massif, Bulgaria. Lithos 180–181, 264–278.
Bonev, N., Marchev, P., Moritz, R., Collings, D., 2015. Jurassic subduction zone tectonics of the Rhodope Massif in the Thrace region (NE Greece) as revealed by new U–Pb and 40Ar/39Ar geochronology of the Evros ophiolite and high-grade basement rocks. Gondwana Res. 27, 760–775.
Booth-Rea, G., Ranero, C.R., Martínez-Martínez, J.M., Grevemeyer, I., 2007. Crustal types and Tertiary tectonic evolution of the Alborán sea, western Mediterranean. Geochem. Geophys. Geosyst. 8.
Booth-Rea, G., Jabaloy-Sánchez, A., Azdimousa, A., Asebriy, L., Vílchez, M.V., Martínez-Martínez, J.M., 2012. Upper-crustal extension during oblique collision: the Temsamane extensional detachment (eastern Rif, Morocco). Terra Nova 24, 505–512.
Bornovas, J., Perry, L.J., Temple, P.G., Mirkou, R.M., Keraudren, B., 1980. Geologic Map of Greece. Zakynthos Island.
Borojević Šoštarić, S., Palinkaš, A.L., Neubauer, F., Cvetković, V., Bernroider, M., Genser, J., 2014. The origin and age of the metamorphic sole from the Rogozna Mts., Western Vardar Belt: new evidence for the one-ocean model for the Balkan ophiolites. Lithos 192–195, 39–55.
Bortolotti, V., Marroni, M., Pandolfi, L., Principi, G.t., Saccani, E., 2002. Interaction between mid-ocean ridge and subduction magmatism in Albanian ophiolites. J. Geol. 110, 561–576.
Bortolotti, V., Marroni, M., Pandolfi, L., Principi, G., 2005. Mesozoic to Tertiary tectonic history of the Mirdita ophiolites, northern Albania. Isl. Arc 14, 471–493.
Boschman, L.M., van Hinsbergen, D.J.J., Torsvik, T.H., Spakman, W., Pindell, J.L., 2014. Kinematic reconstruction of the Caribbean region since the Early Jurassic. Earth-Sci. Rev. 138, 102–136.
Boschman, L.M., van Hinsbergen, D.J.J., Kimbrough, D.L., Langereis, C.G., Spakman, W., 2018. 220 Myr of Farallon Plate subduction below Mexico. Geochem. Geophys. Geosyst. 19, 4649–4672.
Bosellini, F.R., 2006. Biotic changes and their control on Oligocene-Miocene reefs: a case study from the Apulia Platform margin (southern Italy). Palaeogeogr. Palaeoclimatol. Palaeoecol. 241, 393–409.
Bosellini, A., Morsilli, M., Neri, C., 1999. Long-term event stratigraphy of the Apulia Platform margin (Upper Jurassic to Eocene, Gargano, southern Italy). J. Sediment. Res. 69, 1241–1252.
Boulton, S.J., Robertson, A.H., 2007. The Miocene of the Hatay area, S Turkey: transition from the Arabian passive margin to an underfilled foreland basin related to closure of the Southern Neotethys Ocean. Sediment. Geol. 198, 93–124.
Boulton, S.J., Robertson, A.H., Ellam, R.M., Şafak, Ü., Ünlügenç, U.C., 2007. Strontium isotopic and micropalaeontological dating used to help redefine the stratigraphy of the neotectonic Hatay Graben, southern Turkey. Turk. J. Earth Sci. 16, 141–179.
Boullin, J.P., Durand-Delga, M., Olivier, P., 1986. Betic Rifian and Tyrrhenian Arc: Distinctive features, genesis and development stages. In: Wezel, F. (Ed.), The Origin of Arcs. Elsevier, New York, pp. 281–304.
Boyden, J.A., Müller, R.D., Gurnis, M., Torsvik, T.H., Clark, J.A., Turner, M., Ivey-Law, H., Watson, R.J., Cannon, J.S., 2011. Next-Generation Plate-Tectonic Reconstructions using GPlates, Geoinformatics: Cyberinfrastructure for the Solid Earth Sciences. Cambridge University Press, Cambridge, pp. 95–113.
Bozkurt, E., Winchester, J.A., Yiğitbaş, E., Ottley, C.J., 2008. Proterozoic ophiolites and mafic–ultramafic complexes marginal to the İstanbul Block: an exotic terrane of Avalonian affinity in NW Turkey. Tectonophysics 461, 240–251.
Bozkurt, E., Satır, M., Buğdaycıoğlu, Ç., 2011. Surprisingly young Rb/Sr ages from the Simav extensional detachment fault zone, northern Menderes Massif, Turkey. J. Geodyn. 52, 406–431.
Božović, M., Prelević, D., Romer, R.L., Barth, M., Van Den Bogaard, P., Boev, B., 2013. The Demir Kapija Ophiolite, Macedonia (FYROM): a Snapshot of Subduction Initiation within a Back-arc. J. Petrol. 54, 1427–1453.
Boztuğ, D., Harlavan, Y., Arehart, G., Avci, N., 2005. K–Ar age, whole-rock and isotope geochemistry of A-type granitoids in the Divriği–Sivas region, eastern-central Anatolia, Turkey. Lithos.
Boztuğ, D., Jonckheere, R.C., Heizler, M., Ratschbacher, L., Harlavan, Y., Tichomirova, M., 2009. Timing of post-obduction granitoids from intrusion through cooling to exhumation in central Anatolia, Turkey. Tectonophysics 473, 223–233.
Bradley, K.E., Vassilakis, E., Hosa, A., Weiss, B.P., 2013. Segmentation of the Hellenides recorded by Pliocene initiation of clockwise block rotation in Central Greece. Earth Planet. Sci. Lett. 362, 6–19.
Bragin, N.Y., Bragina, L.G., Djerić, N., Toljić, M., 2011. Triassic and Jurassic radiolarians from sedimentary blocks of ophiolite mélange in the Avala Gora area (Belgrade surroundings, Serbia). Stratigr. Geol. Correl. 19, 631–640.
Brede, R., 1992. Structural aspects of the Middle and the High Atlas (Morocco) phenomena and causalities. Geol. Rundsch. 81, 171–184.
Broadley, L., Platzman, E., Platt, J., Papanikolaou, M., Matthews, S., 2006. Paleomagnetism and the Tectonic Evolution of the Ionian Zone, Northwestern Greece, Special Paper 409: Postcollisional Tectonics and Magmatism in the Mediterranean Region and Asia, pp. 137–155.

Bröcker, M., Pidgeon, R.T., 2007. Protolith ages of meta-igneous and metatuffaceous rocks from the Cycladic blueschist unit, Greece: results of a reconnaissance U-Pb zircon study. J. Geol. 115, 83–98.
Bronner, A., Sauter, D., Manatschal, G., Péron-Pinvidic, G., Munschy, M., 2011. Magmatic breakup as an explanation for magnetic anomalies at magma-poor rifted margins. Nat. Geosci. 4, 549–553.
Brown, S.A.M., Robertson, A.H.F., 2003. Sedimentary geology as a key to understanding the tectonic evolution of the Mesozoic–Early Tertiary Paikon Massif, Vardar suture zone, N Greece. Sediment. Geol. 160, 179–212.
Brown, S.A.M., Robertson, A.H.F., 2004. Evidence for Neotethys rooted within the Vardar suture zone from the Voras Massif, northernmost Greece. Tectonophysics 381, 143–173.
Brun, J.-P., Sokoutis, D., 2007. Kinematics of the Southern Rhodope Core Complex (North Greece). Int. J. Earth Sci. 96, 1079–1099.
Brun, J.P., Sokoutis, D., 2010. 45 m.y. of Aegean crust and mantle flow driven by trench retreat. Geology 38, 815–818.
Brun, J.P., Sokoutis, D., 2018. Core complex segmentation in North Aegean, a dynamic view. Tectonics 37, 1797–1830.
Brun, J.-P., Faccenna, C., Gueydan, F., Sokoutis, D., Philippon, M., Kydonakis, K., Gorini, C., 2016. The two-stage Aegean extension, from localized to distributed, a result of slab rollback acceleration. Can. J. Earth Sci. 53, 1142–1157.
Brunet, M.F., 1997. Subsidence along the ECORS Bay of Biscay deep seismic profile. Mém. Soc. Géol. France 171, 167–176.
Brunet, C., Monié, P., Jolivet, L., Cadet, J.P., 2000. Migration of compression and extension in the Tyrrhenian Sea, insights from 40Ar/39Ar ages on micas along a transect from Corsica to Tuscany. Tectonophysics 321, 127–155.
Brunet, M.-F., Korotaev, M.V., Ershov, A.V., Nikishin, A.M., 2003. The South Caspian Basin: a review of its evolution from subsidence modelling. Sediment. Geol. 156, 119–148.
Bucher, S., Ulardic, C., Bousquet, R., Ceriani, S., Fügenschuh, B., Gouffon, Y., Schmid, S.M., 2004. Tectonic evolution of the Briançonnais units along a transect (ECORS-CROP) through the Italian-French Western Alps. Eclogae Geol. Helv. 97, 321–345.
Burchfiel, B.C., Bleahu, M., 1976. Geology of Romania. Geological Society of America.
Burchfiel, B.C., Nakov, R., 2015. The multiply deformed foreland fold-and-thrust belt of the Balkan orogen, northern Bulgaria. Geosphere 11, 463–490.
Burchfiel, B.C., Nakov, R., Dumurdzanov, N., Papanikolaou, D., Tzankov, T., Serafimovski, T., King, R.W., Kotzev, V., Todosov, A., Nurce, B., 2008. Evolution and dynamics of the Cenozoic tectonics of the South Balkan extensional system. Geosphere 4.
Burg, J.-P., 2012. Rhodope: from Mesozoic convergence to Cenozoic extension: review of petro-structural data in the geochronological frame. J. Virtual Explor. 42, 1.
Burrus, J., 1984. Contribution to a geodynamic synthesis of the Provencal Basin (north-western Mediterranean). Mar. Geol. 55, 247–269.
Butler, R.W.H., Grasso, M., La Manna, F., 1992. Origin and deformation of the Neogene–Recent Maghrebian foredeep at the Gela Nappe, SE Sicily. J. Geol. Soc. 149, 547–556.
Butler, R.W.H., Corrado, S., Mazzoli, S., De Donatis, M., Di Bucci, D., Naso, G., Scrocca, D., Nicolai, C., Zucconi, V., 2000. Variabilità spazio-temporale degli stili tettonici nella catena a pieghe e sovrascorrimenti appenninica. Rendiconti Lincei 11, 5–39.
Caccavari, A., Calvo-Rathert, M., Goguitchaichvili, A., Huaiyu, H., Vashakidze, G., Vegas, N., 2014. Palaeomagnetism and 40Ar/39Ar age of a Pliocene lava flow sequence in the Lesser Caucasus: record of a clockwise rotation and analysis of palaeosecular variation. Geophys. J. Int. 197, 1354–1370.
Cadet, J.-P., 1970. Esquisse géologique de la Bosnie-Herzégovine méridionale et du Monténégro occidental. Bull. Soc. Géol. France 7, 973–985.
Čadjenović, D., Kilibarda, Z., Radulović, N., 2008. Late Triassic to Late Jurassic evolution of the Adriatic carbonate platform and Budva Basin, southern Montenegro. Sediment. Geol. 204, 1–17.
Calamita, F., Cello, G., Deiana, G., Paltrinieri, W., 1994. Structural styles, chronology rates of deformation, and time-space relationships in the Umbria-Marche thrust system (Central Apennines, Italy). Tectonics 13, 873–881.
Calamita, F., Satolli, S., Scisciani, V., Esestime, P., Pace, P., 2011. Contrasting styles of fault reactivation in curved orogenic belts: examples from the Central Apennines (Italy). Bulletin 123, 1097–1111.
Calamita, F., Satolli, S., Turtù, A., 2012. Analysis of thrust shear zones in curve-shaped belts: deformation mode and timing of the Olevano-Antrodoco-Sibillini thrust (Central/Northern Apennines of Italy). J. Struct. Geol. 44, 179–187.
Calvo, M., Osete, M.L., Vegas, R., 1994. Palaeomagnetic rotations in opposite senses in southeastern Spain. Geophys. Res. Lett. 21, 761–764.
Calvo, M., Vegas, R., Osete, M.L., 1997. Palaeomagnetic results from upper Miocene and Pliocene rocks from the Internal Zone of the eastern Betic Cordilleras (southern Spain). Tectonophysics 277, 271–283.
Calvo, M., Cuevas, J., Tubıa, J.M., 2001. Preliminary palaeomagnetic results on Oligocene–early Miocene mafic dykes from southern Spain. Tectonophysics 332, 333–345.
Calvo-Rathert, M., Cuevas, J., Tubía, J.M., Bógalo, M.F., Gogichaishvili, A., 2007. A paleomagnetic study of the Basque Arc (Basque-Cantabrian Basin, Western Pyrenees). Int. J. Earth Sci. 96, 1163–1178.
Calvo-Rathert, M., Goguitchaichvili, A., Bógalo, M.-F., Vegas-Tubía, N., Carrancho, Á., Sologashvili, J., 2011. A paleomagnetic and paleointensity study on Pleistocene and Pliocene basaltic flows from the Djavakheti Highland (Southern Georgia, Caucasus). Phys. Earth Planet. Inter. 187, 212–224.
Calvo-Rathert, M., Bógalo, M.F., Gogichaishvili, A., Sologashvili, J., Vashakidze, G., 2013. New paleomagnetic and paleointensity data from Pliocene lava flows from the Lesser Caucasus. J. Asian Earth Sci. 73, 347–361.
Candan, O., Çetinkaplan, M., Oberhänsli, R., Rimmelé, G., Akal, C., 2005. Alpine high-P/low-T metamorphism of the Afyon Zone and implications for the metamorphic evolution of Western Anatolia, Turkey. Lithos 84, 102–124.
Candan, O., Akal, C., Koralay, O., Okay, A., Oberhänsli, R., Prelević, D., Mertz-Kraus, R., 2016a. Carboniferous granites on the northern margin of Gondwana, Anatolide-Tauride Block, Turkey–Evidence for southward subduction of Paleotethys. Tectonophysics 683, 349–366.
Candan, O., Koralay, O.E., Topuz, G., Oberhänsli, R., Fritz, H., Collins, A.S., Chen, F., 2016b. Late Neoproterozoic gabbro emplacement followed by early Cambrian eclogite-facies metamorphism in the Menderes Massif (W. Turkey): implications on the final assembly of Gondwana. Gondwana Res. 34, 158–173.
Cao, S., Neubauer, F., Bernroider, M., Liu, J., 2013. The lateral boundary of a metamorphic core complex: the Moutsounas shear zone on Naxos, Cyclades, Greece. J. Struct. Geol. 54, 103–128.
Capella, W., Maţenco, L., Dmitrieva, E., Roest, W.M.J., Hessels, S., Hssain, M., Chakor-Alami, A., Sierro, F.J., Krijgsman, W., 2017. Thick-skinned tectonics closing the Rifian Corridor. Tectonophysics 710–711, 249–265.
Capitanio, F.A., Goes, S., 2006. Mesozoic spreading kinematics: consequences for Cenozoic Central and Western Mediterranean subduction. Geophys. J. Int. 165, 804–816.
Capitanio, F.A., Faccenna, C., Funiciello, R., Salvini, F., 2011. Recent tectonics of Tripolitania, Libya: an intraplate record of Mediterranean subduction. Geol. Soc., Lond., Spec. Publ. 357, 319–328.
Carey, S.W., 1955. The orocline concept in geotectonics-Part I. Pap. Proc. Royal Soc. Tasmania 89, 255–288.
Caricchi, C., Cifelli, F., Sagnotti, L., Sani, F., Speranza, F., Mattei, M., 2014. Paleomagnetic evidence for a post-Eocene 90° CCW rotation of internal Apennine units: a linkage with Corsica-Sardinia rotation? Tectonics 33, 374–392.
Carmignani, L., Kligfield, R., 1990. Crustal extension in the Northern Apennines: the transition from compression to extension in the Alpi Apuane core complex. Tectonics 9, 1275–1303.
Carmignani, L., Carosi, R., Di Pisa, A., Gattiglio, M., Musumeci, G., Oggiano, G., Carlo Pertusati, P., 1994. The hercynian chain in Sardinia (Italy). Geodin. Acta 7, 31–47.
Carrapa, B., Bertotti, G., Krijgsman, W., 2003. Subsidence, stress regime and rotation (s) of a tectonically active sedimentary basin within the western Alpine Orogen: the Tertiary Piedmont Basin (Alpine domain, NW Italy). Geol. Soc., Lond., Spec. Publ. 208, 205–227.
Carrigan, C.W., Mukasa, S.B., Haydoutov, I., Kolcheva, K., 2003. Ion microprobe U-Pb zircon ages of pre-Alpine rocks in the Balkan, Sredna Gora, and Rhodope terranes of Bulgaria: constraints on Neoproterozoic and Variscan tectonic evolution. J. Czech Geol. Soc. 48, 1–2.
Carrigan, C.W., Mukasa, S.B., Haydoutov, I., Kolcheva, K., 2005. Age of Variscan magmatism from the Balkan sector of the orogen, central Bulgaria. Lithos 82, 125–147.
Casati, P., Bertozzi, P., Cita, M.B., Longinelli, A., Damiani, V., 1976. Stratigraphy and paleoenvironment of the Messinian “Colombacci” formation in the Periadriatic Trough. A pilot study. Mem. Soc. Geol. Ital 16, 173–195.
Casero, P., Roure, F., Endignoux, L., Moretti, I., Muller, C., Sage, L., Vially, R., 1988. Neogene geodynamic evolution of the Southern Apennines. Mem. Soc. Geol. Ital. 41, 109–120.
Casini, L., Funedda, A., Oggiano, G., 2010. A balanced foreland-hinterland deformation model for the Southern Variscan belt of Sardinia, Italy. Geol. J. 45, 634–649.
Casini, L., Cuccuru, S., Maino, M., Oggiano, G., Tiepolo, M., 2012. Emplacement of the Arzachena Pluton (Corsica–Sardinia Batholith) and the geodynamics of incoming Pangaea. Tectonophysics 544–545, 31–49.
Castellarin, A., Cantelli, L., Fesce, A.M., Mercier, J.L., Picotti, V., Pini, G.A., Prosser, G., Selli, L., 1992. Alpine compressional tectonics in the Southern Alps. Relationships with the N-Apennines. Ann. Tect. 6, 62–94.
Castelluccio, A., Andreucci, B., Zattin, M., Ketcham, R.A., Jankowski, L., Mazzoli, S., Szaniawski, R., 2015. Coupling sequential restoration of balanced cross sections and low-temperature thermochronometry: the case study of the Western Carpathians. Lithosphere 7, 367–378.
Catalano, R., d'Argenio, B., Gregor, C.B., Nairn, A.E.M., Nardi, G., Renda, P., 1984. Mesozoic volcanics of western sicily. Geol. Rundsch. 73, 577–598.
Catalano, S., Monaco, C., Tortorici, L., Tansi, C., 1993. Pleistocene strike-slip tectonics in the Lucanian Apennine (southern Italy). Tectonics 12, 656–665.
Catalano, R., Di Stefano, P., Sulli, A., Vitale, F.P., 1996. Paleogeography and structure of the central Mediterranean: sicily and its offshore area. Tectonophysics 260, 291–324.
Catalano, R., Doglioni, C., Merlini, S., 2001. On the mesozoic Ionian basin. Geophys. J. Int. 144, 49–64.
Catalano, R., Valenti, V., Albanese, C., Accaino, F., Sulli, A., Tinivella, U., Gasparo Morticelli, M., Zanolla, C., Giustiniani, M., 2013. Sicily's fold–thrust belt and slab roll-back: the SI.RI.PRO. seismic crustal transect. J. Geol. Soc. 170, 451–464.
Cavazza, W., 1989. Detrital modes and provenances of the Stilo-Capo d'Orlando Formation (Miocene), southern Italy. Sedimentology 36, 1077–1090.
Cavazza, W., Barone, M., 2010. Large-scale sedimentary recycling of tectonic mélange in a forearc setting: the Ionian basin (Oligocene-Quaternary, southern Italy). Geol. Soc. Am. Bull. 122, 1932–1949.
Cavazza, W., Zattin, M., Ventura, B., Zuffa, G.G., 2001. Apatite fission-track analysis of Neogene exhumation in northern Corsica (France). Terra Nova 13, 51–57.
Cavazza, W., Cattò, S., Zattin, M., Okay, A.I., Reiners, P., 2018. Thermochronology of

the Miocene Arabia-Eurasia collision zone of southeastern Turkey. Geosphere 14, 2277–2293.
Cavinato, G.P., DeCelles, P.G., 1999. Extensional basins in the tectonically bimodal Central Apennines fold-and-thrust belt, Italy: response to corner flow above a subducting slab in retrograde motion. Geology 27.
Cazzini, F., Zotto, O.D., Fantoni, R., Ghielmi, M., Ronchi, P., Scotti, P., 2015. Oil and gas in the Adriatic foreland, Italy. J. Pet. Geol. 38, 255–279.
Çelik, Ö.F., Delaloye, M., Feraud, G., 2006. Precise 40 Ar–39 Ar ages from the metamorphic sole rocks of the Tauride Belt Ophiolites, southern Turkey: implications for the rapid cooling history. Geol. Mag. 143, 213–227.
Çelik, Ö.F., Marzoli, A., Marschik, R., Chiaradia, M., Neubauer, F., Öz, İ., 2011. Early–Middle Jurassic intra-oceanic subduction in the İzmir-Ankara-Erzincan Ocean, Northern Turkey. Tectonophysics 509, 120–134.
Çelik, Ö.F., Chiaradia, M., Marzoli, A., Billor, Z., Marschik, R., 2013. The Eldivan ophiolite and volcanic rocks in the İzmir–Ankara–Erzincan suture zone, Northern Turkey: geochronology, whole-rock geochemical and Nd–Sr–Pb isotope characteristics. Lithos 172–173, 31–46.
Çelik, Ö.F., Chiaradia, M., Marzoli, A., Özkan, M., Billor, Z., Topuz, G., 2016. Jurassic metabasic rocks in the Kızılırmak accretionary complex (Kargı region, Central Pontides, Northern Turkey). Tectonophysics 672–673, 34–49.
Cello, G., Mazzoli, S., 1998. Apennine tectonics in southern Italy: a review. J. Geodyn. 27, 191–211.
Cello, G., Tortorici, L., Martini, N., Paltrinieri, W., 1989. Structural styles in the frontal zones of the Southern Apennines, Italy: an example from the Molise District. Tectonics 8, 753–768.
Cemen, I., Göncüoğlu, M.C., Dirik, K., 1999. Structural evolution of the Tuzgölü basin in Central Anatolia, Turkey. J. Geol. 107, 693–706.
Cerrina Feroni, A., Martelli, L., Martinelli, P., Ottria, G., Catanzariti, R., 2002. Carta Geologico-Strutturale dell'Appennino Emiliano-Romagnolo in Scala 1: 250.000. Regione Emilia-Romagna—CNR, Pisa. S. EL. CA, Firenze.
Çetinkaplan, M., Pourteau, A., Candan, O., Koralay, O.E., Oberhänsli, R., Okay, A.I., Chen, F., Kozlu, H., Şengün, F., 2016. P–T–t evolution of eclogite/blueschist facies metamorphism in Alanya Massif: time and space relations with HP event in Bitlis Massif, Turkey. Int. J. Earth Sci. 105, 247–281.
Chalouan, A., Michard, A., 1990. The Ghomarides nappes, Rif coastal range, Morocco: a variscan chip in the Alpine belt. Tectonics 9, 1565–1583.
Chalouan, A., Michard, A., Feinberg, H., Montigny, R., Saddiqi, O., 2001. The Rif mountain building (Morocco); a new tectonic scenario. Bull. Soc. Géol. France 172, 603–616.
Chalouan, A., El Mrihi, A., El Kadiri, K., Bahmad, A., Salhi, F., Hlila, R., 2006. Maureta nian flysch nappe in the northwestern Rif Cordillera (Morocco): deformation chronology and evidence for a complex nappe emplacement. Geol. Soc., Lond., Spec. Publ. 262, 161–175.
Chalouan, A., Michard, A., El Kadiri, K., Negro, F., de Lamotte, D.F., Soto, J.I., Saddiqi, O., 2008. The Rif Belt, Continental Evolution: the Geology of Morocco. Springer, pp. 203–302.
Chamot-Rooke, N., Rangin, C., Le Pichon, X., group, D.w., 2005. Deep Offshore Tectonics of the Eastern Mediterranean: a Synthesis of Deep Marine Data in the Eastern Mediterranean: the Ionian Basin and Margins, the Calabria Wedge and the Mediterranean Ridge. Mem. Soc. Geol. France 64.
Chan, G.H.-N., Malpas, J., Xenophontos, C., Lo, C.-H., 2007. Timing of subduction zone metamorphism during the formation and emplacement of Troodos and Baer–Bassit ophiolites: insights from 40Ar–39Ar geochronology. Geol. Mag. 144.
Channell, J.E.T., 1977. Palaeomagnetism of limestones from the Gargano Peninsula (Italy), and the implication of these data. Geophys. J. Int. 51, 605–616.
Channell, J.E.T., 1992. Paleomagnetic data from Umbria (Italy): implications for the rotation of Adria and Mesozoic apparent polar wander paths. Tectonophysics 216, 365–378.
Channell, J.E.T., Doglioni, C., 1994. Early Triassic paleomagnetic data from the Dolomites (Italy). Tectonics 13, 157–166.
Channell, J.E.T., Erba, E., 1992. Early Cretaceous polarity chrons CM0 to CM11 recorded in northern Italian land sections near Brescia. Earth Planet. Sci. Lett. 108, 161–179.
Channell, J.E.T., Tarling, D.H., 1975. Palaeomagnetism and the rotation of Italy. Earth Planet. Sci. Lett. 25, 177–188.
Channell, J.E.T., Catalano, R., D'Argenio, B., 1980. Palaeomagnetism and deformation of the Mesozoic continental margin in Sicily. Tectonophysics 61, 391–407.
Channell, J.E.T., Lowrie, W., Pialli, P., Venturi, F., 1984. Jurassic magnetic stratigraphy from Umbrian (Italian) land sections. Earth Planet. Sci. Lett. 68, 309–325.
Channell, J.E.T., Oldow, J.S., Catalano, R., d'Argenio, B., 1990. Paleomagnetically determined rotations in the western Sicilian fold and thrust belt. Tectonics 9, 641–660.
Channell, J.E.T., Doglioni, C., Stoner, J.S., 1992. Jurassic and Cretaceous paleomagnetic data from the Southern Alps (Italy). Tectonics 11, 811–822.
Channell, J.E.T., Tüysüz, O., Bektas, O., Şengör, A.M.C., 1996. Jurassic-Cretaceous paleomagnetism and paleogeography of the Pontides (Turkey). Tectonics 15, 201–212.
Chatzaras, V., Xypolias, P., Doutsos, T., 2006. Exhumation of high-pressure rocks under continuous compression: a working hypothesis for the southern Hellenides (central Crete, Greece). Geol. Mag. 143.
Chen, F., Siebel, W., Satir, M., Terzioğlu, M., Saka, K., 2002. Geochronology of the Karadere basement (NW Turkey) and implications for the geological evolution of the Istanbul zone. Int. J. Earth Sci. 91, 469–481.
Chernyaev, V.Y., 1986. Paleomagnetic Directions and Pole Positions: Data for the USSR. Soviet Geophysical Committee, World Data Center-B, Moscow.
Chertova, M.V., Spakman, W., Geenen, T., van den Berg, A.P., van Hinsbergen, D.J.J., 2014. Underpinning tectonic reconstructions of the western Mediterranean region with dynamic slab evolution from 3-D numerical modeling. J. Geophys. Res.: Solid Earth 119, 5876–5902.
Chiari, M., Marcucci, M., Prela, M., 2002. New species of Jurassic radiolarians in the sedimentary cover of ophiolites in the Mirdita area, Albania. Micropaleontology 61–87.
Chiari, M., Bortolotti, V., Marcucci, M., Photiades, A., Principi, G., 2003. The Middle Jurassic siliceous sedimentary cover at the top of the Vourinos ophiolite (Greece). Ofioliti 28, 95–103.
Chiari, M., Marcucci, M., Prela, M., 2004. Radiolarian assemblages from the Jurassic cherts of Albania: new data. Ofioliti 29, 95–105.
Chiari, M., Djerić, N., Garfagnoli, F., Hrvatović, H., Krstić, M., Levi, N., Malasoma, A., Marroni, M., Menna, F., Nirta, G., 2011. The geology of the Zlatibor-Maljen area (western Serbia): a geotraverse across the ophiolites of the Dinaric-Hellenic collisional belt. Ofioliti 36, 139–166.
Choukroune, P., 1976. A Discussion on natural strain and geological structure-Strain patterns in the Pyrenean Chain. Philos. Trans. Royal Soc. Lond. A 283, 271–280.
Cifelli, F., Rossetti, F., Mattei, M., Hirt, A.M., Funiciello, R., Tortorici, L., 2004. An AMS, structural and paleomagnetic study of quaternary deformation in eastern Sicily. J. Struct. Geol. 26, 29–46.
Cifelli, F., Mattei, M., Rossetti, F., 2007. Tectonic evolution of arcuate mountain belts on top of a retreating subduction slab: the example of the Calabrian Arc. J. Geophys. Res. 112.
Cifelli, F., Mattei, M., Della Seta, M., 2008a. Calabrian Arc oroclinal bending: the role of subduction. Tectonics 27.
Cifelli, F., Mattei, M., Porreca, M., 2008b. New paleomagnetic data from Oligocene–upper Miocene sediments in the Rif chain (northern Morocco): insights on the Neogene tectonic evolution of the Gibraltar arc. J. Geophys. Res. 113.
Çinku, M.C., 2011. Paleogeographic evidence on the Jurassic tectonic history of the Pontides: new paleomagnetic data from the Sakarya continent and Eastern Pontides. Int. J. Earth Sci. 100, 1633–1645.
Çinku, M.C., 2017. Paleomagnetic results from Northeast Anatolia: remagnetization in Late Cretaceous sandstones and tectonic rotation at the Eastern extension of the Izmir–Ankara–Erzincan suture zone. Acta Geophysica 65, 1095–1109.
Çinku, M.C., Ustaömer, T., Hirt, A.M., Hisarlı, Z.M., Heller, F., Orbay, N., 2010. Southward migration of arc magmatism during latest Cretaceous associated with slab steepening, East Pontides, N Turkey: new paleomagnetic data from the Amasya region. Phys. Earth Planet. Inter. 182, 18–29.
Çinku, M.C., Hisarlı, Z.M., Heller, F., Orbay, N., Ustaömer, T., 2011. Middle Eocene paleomagnetic data from the eastern Sakarya Zone and the central Pontides: implications for the tectonic evolution of north central Anatolia. Tectonics 30.
Çinku, M.C., Hisarli, Z.M., Yılmaz, Y., Ülker, B., Kaya, N., Öksüm, E., Orbay, N., Özbey, Z.Ü., 2016. The tectonic history of the Niğde-Kırşehir Massif and the Taurides since the Late Mesozoic: paleomagnetic evidence for two-phase orogenic curvature in Central Anatolia. Tectonics 35, 772–811.
Çinku, M.C., Heller, F., Ustaömer, T., 2017. New paleomagnetic results from Upper Cretaceous arc-type rocks from the northern and southern branches of the Neotethys ocean in Anatolia. Int. J. Earth Sci. 106, 2575–2592.
Cipollari, P., Cosentino, D., 1995. Miocene unconformities in the Central Apennines: geodynamic significance and sedimentary basin evolution. Tectonophysics 252, 375–389.
Cirilli, S., Márton, P., Vigli, L., 1984. Implications of a combined biostratigraphic and palaeomagnetic study of the Umbrian Maiolica Formation. Earth Planet. Sci. Lett. 69, 203–214.
Cirrincione, R., Ortolano, G., Pezzino, A., Punturo, R., 2008. Poly-orogenic multistage metamorphic evolution inferred via P–T pseudosections: an example from Aspromonte Massif basement rocks (Southern Calabria, Italy). Lithos 103, 466–502.
Cirrincione, R., Fazio, E., Ortolano, G., Pezzino, A., Punturo, R., 2012. Fault-related rocks: deciphering the structural–metamorphic evolution of an accretionary wedge in a collisional belt, NE Sicily. Int. Geol. Rev. 54, 940–956.
Cirrincione, R., Fazio, E., Fiannacca, P., Ortolano, G., Pezzino, A., Punturo, R., Romano, V., Sacco, V., 2013. The Alpine evolution of the Aspromonte Massif: constraints for geodynamic reconstruction of the Calabria–Peloritani Orogen. Geol. Field Trips 5, 1–73.
Ciulavu, M., Mählmann, R.F., Schmid, S.M., Hofmann, H., Seghedi, A., Frey, M., 2008. Metamorphic evolution of a very low- to low-grade metamorphic core complex (Danubian window) in the South Carpathians. Geol. Soc., Lond., Spec. Publ. 298, 281–315.
Civile, D., Lodolo, E., Tortorici, L., Lanzafame, G., Brancolini, G., 2008. Relationships between magmatism and tectonics in a continental rift: the Pantelleria Island region (Sicily Channel, Italy). Mar. Geol. 251, 32–46.
Clark, M., Robertson, A., 2002. The role of the Early Tertiary Ulukisla Basin, southern Turkey, in suturing of the Mesozoic Tethys ocean. J. Geol. Soc. 159, 673–690.
Clark, M., Robertson, A., 2005. Uppermost Cretaceous–Lower Tertiary Ulukışla Basin, south-central Turkey: sedimentary evolution of part of a unified basin complex within an evolving Neotethyan suture zone. Sediment. Geol. 173, 15–51.
Clerc, C., Lagabrielle, Y., 2014. Thermal control on the modes of crustal thinning leading to mantle exhumation: insights from the Cretaceous Pyrenean hot paleomargins. Tectonics 33, 1340–1359.
Clerc, C., Lahfid, A., Monié, P., Lagabrielle, Y., Chopin, C., Poujol, M., Boulvais, P., Ringenbach, J.C., Masini, E., de St Blanquat, M., 2015. High-temperature metamorphism during extreme thinning of the continental crust: a reappraisal of

the North Pyrenean passive paleomargin. Solid Earth 6, 643–668.
Clube, T.M.M., 1985. The Palaerotation of the Troodos Microplate. University of Edinburgh.
Clube, T.M.M., Robertson, A.H.F., 1986. The palaeorotation of the Troodos Microplate, Cyprus, in the late Mesozoic-early Cenozoic plate tectonic framework of the eastern Mediterranean. Surv. Geophys. 8, 375–437.
Clube, T.M.M., Creer, K.M., Robertson, A.H.F., 1985. Palaeorotation of the Troodos microplate, Cyprus. Nature 317, 522.
Çolakoğlu, A.R., Günay, K., Göncüoğlu, M.C., Oyan, V., Erdoğan, K., 2014. Geochemical evaluation of the Late Maastrichtian subduction-related volcanism in the Southern Neotethys in Van area, and a correlation across the Turkish–Iranian border. Ofioliti 39, 51–65.
Collins, A.S., Robertson, A.H.F., 1997. Lycian mélange, southwestern Turkey: an emplaced Late Cretaceous accretionary complex. Geology 25, 255–258.
Collins, A.S., Robertson, A.H.F., 1999. Evolution of the Lycian Allochthon, western Turkey, as a north-facing Late Palaeozoic to Mesozoic rift and passive continental margin. Geol. J. 34, 107–138.
Collins, A.S., Robertson, A.H.F., 2003. Kinematic evidence for Late Mesozoic-Miocene emplacement of the Lycian Allochthon over the Western Anatolide Belt, SW Turkey. Geol. J. 38, 295–310.
Collombet, M., Thomas, J.C., Chauvin, A., Tricart, P., Bouillin, J.P., Gratier, J.P., 2002. Counterclockwise rotation of the western Alps since the Oligocene: new insights from paleomagnetic data. Tectonics 21, 14-11–14-15.
Comas, M., Platt, J.P., Soto, J., Watts, A., 1999. The origin and Tectonic History of the Alboran Basin: insights from Leg 161 Results. In: Proceedings of the Ocean Drilling Program, Scientific Results, vol. 161. Ocean Drilling Program, pp. 555–580.
Corrado, S., Di Bucci, D., Naso, G., Butler, R.W.H., 1997. Thrusting and strike-slip tectonics in the Alto Molise region (Italy): implications for the Neogene-Quaternary evolution of the Central Apennine orogenic system. J. Geol. Soc. 154, 679–688.
Çörtük, R.M., Çelik, Ö.F., Özkan, M., Sherlock, S.C., Marzoli, A., Altıntaş, İ.E., Topuz, G., 2016. Origin and geodynamic environments of the metamorphic sole rocks from the İzmir–Ankara–Erzincan suture zone (Tokat, northern Turkey). Int. Geol. Rev. 58, 1839–1855.
Cosentino, D., Cipollari, P., Marsili, P., Scrocca, D., 2010. Geology of the Central Apennines: a regional review. J. Virtual Explor. 36, 1–37.
Costa, E., Garcés, M., López-Blanco, M., Serra-Kiel, J., Bernaola, G., Cabrera, L., Beamud, E., 2013. The Bartonian-Priabonian marine record of the eastern South Pyrenean foreland basin (NE Spain): a new calibration of the larger foraminifers and calcareous nannofossil biozonation. Geologica Acta 11, 177–193.
Coulon, C., Megartsi, M.h., Fourcade, S., Maury, R.C., Bellon, H., Louni-Hacini, A., Cotten, J., Coutelle, A., Hermitte, D., 2002. Post-collisional transition from calc-alkaline to alkaline volcanism during the Neogene in Oranie (Algeria): magmatic expression of a slab breakoff. Lithos 62, 87–110.
Cowgill, E., Forte, A.M., Niemi, N., Avdeev, B., Tye, A., Trexler, C., Javakhishvili, Z., Elashvili, M., Godoladze, T., 2016. Relict basin closure and crustal shortening budgets during continental collision: an example from Caucasus sediment provenance. Tectonics 35, 2918–2947.
Cox, A., Hart, R.B., 1986. Plate Tectonics: How it Works. John Wiley & Sons.
Crespo-Blanc, A., 2007. Superimposed folding and oblique structures in the palaeomargin-derived units of the Central Betics (SW Spain). J. Geol. Soc. 164, 621–636.
Crespo-Blanc, A., Campos, J., 2001. Structure and kinematics of the South Iberian paleomargin and its relationship with the Flysch Trough units: extensional tectonics within the Gibraltar Arc fold-and-thrust belt (western Betics). J. Struct. Geol. 23, 1615–1630.
Crispini, L., Capponi, G., 2001. Tectonic evolution of the Voltri Group and Sestri Voltaggio Zone (southern limit of the NW Alps): a review. Ofioliti 26, 161–164.
Črne, A.E., Weissert, H., Goričan, Š., Bernasconi, S.M., 2011. A biocalcification crisis at the Triassic-Jurassic boundary recorded in the Budva Basin (Dinarides, Montenegro). Bulletin 123, 40–50.
Crouzet, C., Ménard, G., Rochette, P., 1996. Post-middle Miocene rotations recorded in the Bourg d'Oisans area (Western Alps, France) by paleomagnetism. Tectonophysics 263, 137–148.
Csontos, L., 1995. Tertiary tectonic evolution of the Intra-Carpathian area: a review. Acta Vulcan 7, 1–13.
Csontos, L., Nagymarosy, A., 1998. The Mid-Hungarian line: a zone of repeated tectonic inversions. Tectonophysics 297, 51–71.
Csontos, L., Vörös, A., 2004. Mesozoic plate tectonic reconstruction of the Carpathian region. Palaeogeogr. Palaeoclimatol. Palaeoecol. 210, 1–56.
Culshaw, N., Mosonyi, E., Reynolds, P., 2011. New 40Ar/39Ar laser single-grain ages of muscovites from mylonitic schists in the Rodna Mountains, Eastern Carpathians, Romania: correlations with microstructure. Int. J. Earth Sci. 101, 291–306.
D'Agostino, N., Giuliani, R., Mattone, M., Bonci, L., 2001. Active crustal extension in the Central Apennines (Italy) inferred from GPS measurements in the interval 1994–1999. Geophys. Res. Lett. 28, 2121–2124.
D'Agostino, N., Avallone, A., Cheloni, D., D'Anastasio, E., Mantenuto, S., Selvaggi, G., 2008. Active tectonics of the Adriatic region from GPS and earthquake slip vectors. J. Geophys. Res. 113.
Dallanave, E., Agnini, C., Muttoni, G., Rio, D., 2009. Magneto-biostratigraphy of the Cicogna section (Italy): implications for the late Paleocene–early Eocene time scale. Earth Planet. Sci. Lett. 285, 39–51.
Dallanave, E., Agnini, C., Muttoni, G., Rio, D., 2012. Paleocene magneto-biostratigraphy and climate-controlled rock magnetism from the Belluno Basin, Tethys Ocean, Italy. Palaeogeogr. Palaeoclimatol. Palaeoecol. 337–338, 130–142.
Dallanave, E., Kirscher, U., Hauck, J., Hesse, R., Bachtadse, V., Wortmann, U.G., 2018. Palaeomagnetic time and space constraints of the Early Cretaceous Rhenodanubian Flysch zone (Eastern Alps). Geophys. J. Int. 213, 1804–1817.
Danelian, T., Robertson, A.H.F., Collins, A.S., Poisson, A., 2006. Biochronology of Jurassic and Early Cretaceous radiolarites from the Lycian Mélange (SW Turkey) and implications for the evolution of the Northern Neotethyan ocean. Geol. Soc., Lond., Spec. Publ. 260, 229–236.
Danelian, T., Asatryan, G., Sahakyan, L., Galoyan, G.H., Sosson, M., Avagyan, A., 2010. New and revised radiolarian biochronology for the sedimentary cover of ophiolites in the Lesser Caucasus (Armenia). Geol. Soc., Lond., Spec. Publ. 340, 383–391.
Danelian, T., Zambetakis-Lekkas, A., Galoyan, G., Sosson, M., Asatryan, G., Hubert, B., Grigoryan, A., 2014. Reconstructing Upper Cretaceous (Cenomanian) paleoenvironments in Armenia based on Radiolaria and benthic Foraminifera; implications for the geodynamic evolution of the Tethyan realm in the Lesser Caucasus. Palaeogeogr. Palaeoclimatol. Palaeoecol. 413, 123–132.
Danelian, T., Asatryan, G., Galoyan, G., Sahakyan, L., Stepanyan, J., 2015. Late Jurassic–Early Cretaceous radiolarian age constraints from the sedimentary cover of the Amasia ophiolite (NW Armenia), at the junction between the Izmir–Ankara–Erzinçan and Sevan–Hakari suture zones. Int. J. Earth Sci. 105, 67–80.
Darin, M., Umhoefer, P.J., Thomson, S., 2018. Rapid late Eocene Exhumation of the Sivas Basin (Central Anatolia) Driven by Initial Arabia-Eurasia Collision. Tectonics.
Davis, P.B., Whitney, D.L., 2006. Petrogenesis of lawsonite and epidote eclogite and blueschist, Sivrihisar Massif, Turkey. J. Metamorph. Geol. 24, 823–849.
De Broucker, G., Mellin, A., Duindam, P., 1998. Tectonostratigraphic Evolution of the Transylvanian Basin, Pre-salt Sequence, Romania. Geological and Hydrocarbon Potential of the Romanian areas, Bucharest Geosciences Forum 1, pp. 36–70.
de Graciansky, P.C., 1972. Recherches Géologiques Dans le Taurus Lycien Occidental. Université Paris, Sud (Orsay).
de Leeuw, A., Mandic, O., Krijgsman, W., Kuiper, K., Hrvatovic, H., 2012. Paleomagnetic and geochronologic constraints on the geodynamic evolution of the Central Dinarides. Tectonophysics 530–531, 286–298.
de Leeuw, A., Filipescu, S., Maţenco, L., Krijgsman, W., Kuiper, K., Stoica, M., 2013. Paleomagnetic and chronostratigraphic constraints on the Middle to late Miocene evolution of the Transylvanian Basin (Romania): implications for Central Paratethys stratigraphy and emplacement of the Tisza–Dacia plate. Glob. Planet. Change 103, 82–98.
de Mulder, E.F.J., 1975. Microfauna and sedimentary-tectonic history of the Oligo-Miocene of the Ionian Islands and Western Epirus (Greece). Utrecht Micropaleontol. Bull. 13, 1–139.
De Saint Blanquat, M., Bajolet, F., Grand'Homme, A., Proietti, A., Zanti, M., Boutin, A., Clerc, C., Lagabrielle, Y., Labaume, P., 2016. Cretaceous mantle exhumation in the central Pyrenees: new constraints from the peridotites in eastern Ariège (North Pyrenean zone, France). Compt. Rendus Geosci. 348, 268–278.
de Vicente, G., Vegas, R., Muñoz Martín, A., Silva, P.G., Andriessen, P., Cloetingh, S., González Casado, J.M., Van Wees, J.D., Álvarez, J., Carbó, A., Olaiz, A., 2007. Cenozoic thick-skinned deformation and topography evolution of the Spanish Central System. Glob. Planet. Change 58, 335–381.
Decandia, F.A., 1972. La zona ofiolitiferadel Bracco nel settore compreso fra Levanto e la Val Graveglia (App. Ligure). Mem. Soc. Geol. Ital. 11, 503–530.
Decker, K., Peresson, H., 1996. Tertiary Kinematics in the Alpine-Carpathian-Pannonian System: Links between Thrusting, Transform Faulting and Crustal Extension. Special Publication - European Association of Petroleum Geoscientists, pp. 69–80.
Deenen, M.H.L., Langereis, C.G., van Hinsbergen, D.J.J., Biggin, A.J., 2011. Geomagnetic secular variation and the statistics of palaeomagnetic directions. Geophys. J. Int. 186, 509–520.
Degnan, P.J., Robertson, A.H.F., 1998. Mesozoic-early Tertiary passive margin evolution of the Pindos ocean (NW Peloponnese, Greece). Sediment. Geol. 117, 33–70.
Deino, A., Gattacceca, J., Rizzo, R., Montanari, A., 2001. 40Ar/39Ar dating and paleomagnetism of the Miocene volcanic succession of Monte Furru (Western Sardinia): implications for the rotation history of the Corsica-Sardinia Microplate. Geophys. Res. Lett. 28, 3373–3376.
Del Moro, A., Fornelli, A., Piccarreta, G., 2000. Tectonothermal history of the Hercynian continental crust of the Serre (southern Calabria, Italy) monitored by Rb–Sr biotite resetting. Terra Nova 12, 239–244.
DeMets, C., Iaffaldano, G., Merkouriev, S., 2015a. High-resolution Neogene and Quaternary estimates of Nubia-Eurasia-North America Plate motion. Geophys. J. Int. 203, 416–427.
DeMets, C., Merkouriev, S., Sauter, D., 2015b. High-resolution estimates of Southwest Indian Ridge plate motions, 20 Ma to present. Geophys. J. Int. 203, 1495–1527.
Demirtaşlı, E., Turhan, N., Bilgin, A.Z., Selim, M., 1984. Geology of the Bolkar mountains, Geology of the Taurus Belt, p. 141.
Dercourt, J., , et al.Zonenshain, L.P., Ricou, L.E., Kazmin, V.G., Le Pichon, X., Knipper, A.L., Grandjacquet, C., Sbortshikov, I.M., Geyssant, J., Lepvrier, C., 1986. Geological evolution of the Tethys belt from the Atlantic to the Pamirs since the Lias. Tectonophysics 123, 241–315.
Dercourt, J., Gaetani, M., Vrielynck, B., 2000. Atlas Peri-Tethys Palaeogeographical Maps. CCGM.
Derman, A.S., Gürbüz, K., 2007. Nature, provenance and relationships of early

Miocene palaeovalley fills, northern Adana Basin, Turkey: their significance for sediment-bypassing on a carbonate shelf. Turk. J. Earth Sci. 16, 181–209.
Dermitzakis, M.D., 1978. Stratigraphy and sedimentary history of the Miocene of Zakynthos (Ionian Islands, Greece). Annulaire Geol. Pays Hell. 29, 47–186.
Dewey, J.F., Helman, M.L., Knott, S.D., Turco, E., Hutton, D.H.W., 1989. Kinematics of the western Mediterranean. Geol. Soc., Lond., Spec. Publ. 45, 265–283.
Di Staso, A., Perrone, V., Perrotta, S., Zaghloul, M.N., Durand-Delga, M., 2010. Stratigraphy, age and petrography of the Beni Issef successions (External Rif; Morocco): insights for the evolution of the Maghrebian Chain. Compt. Rendus Geosci. 342, 718–730.
Di Stefano, A., Baldassini, N., Maniscalco, R., Speranza, F., Maffione, M., Cascella, A., Foresi, L.M., 2015. New bio-magnetostratigraphic data on the Miocene Moria section (Northern Apennines, Italy): connections between the Mediterranean region and the North Atlantic Ocean. Newslett. Stratigr. 48, 135–152.
Díaz de Neira, J.A., Gil-Gil, J., 2013. Ascription of the island of Ibiza to the Prebetic of Alicante (Betic Range, Spain) after correlation of Lower Cretaceous sedimentary successions. Cretac. Res. 41, 194–209.
Dilek, Y., 2006. Collision tectonics of the Mediterranean region: causes and consequences. Spec. Pap. - Geol. Soc. Am. 409, 1.
Dilek, Y., Furnes, H., 2011. Ophiolite genesis and global tectonics: geochemical and tectonic fingerprinting of ancient oceanic lithosphere. Geol. Soc. Am. Bull. 123, 387–411.
Dilek, Y., Furnes, H., Shallo, M., 2008. Geochemistry of the Jurassic Mirdita Ophiolite (Albania) and the MORB to SSZ evolution of a marginal basin oceanic crust. Lithos 100, 174–209.
Dilek, Y., Imamverdiyev, N., Altunkaynak, Ş., 2010. Geochemistry and tectonics of Cenozoic volcanism in the Lesser Caucasus (Azerbaijan) and the peri-Arabian region: collision-induced mantle dynamics and its magmatic fingerprint. Int. Geol. Rev. 52, 536–578.
Dimitrijević, M.D., Mijović-Pilić, D., 1997. Geology of Yugoslavia. Geoinstitute, Belgrade.
Dimo-Lahitte, A., Monié, P., Vergély, P., 2001. Metamorphic soles from the Albanian ophiolites: petrology,40Ar/39Ar geochronology, and geodynamic evolution. Tectonics 20, 78–96.
Dinarès-Turell, J., Sprovieri, R., Caruso, A., Di Stefano, E., Gomis-Coll, E., Pueyo, J.J., Rouchy, J.M., Taberner, C., 1997. Premilinary integrated magnetostratigrafía and biostratigraphic correlation in the Miocene Lorca basin,(Murcia, SE Spain). Acta Geol. Hisp. 32, 161–170.
Dinarès-Turell, J., Ortí, F., Playa, E., Rosell, L., 1999. Palaeomagnetic chronology of the evaporitic sedimentation in the Neogene Fortuna Basin (SE Spain): early restriction preceding the Messinian Salinity Crisis. Palaeogeogr. Palaeoclimatol. Palaeoecol. 154, 161–178.
Dinarès-Turell, J., Diez, J.B., Rey, D., Arnal, I., 2005. “Buntsandstein” magnetostratigraphy and biostratigraphic reappraisal from eastern Iberia: early and Middle Triassic stage boundary definitions through correlation to Tethyan sections. Palaeogeogr. Palaeoclimatol. Palaeoecol. 229, 158–177.
Dinter, D.A., Royden, L., 1993. Late Cenozoic extension in northeastern Greece: strymon Valley detachment system and Rhodope metamorphic core complex. Geology 21, 45–48.
Dinu, C., Wong, H.K., Tambrea, D., Maţenco, L., 2005. Stratigraphic and structural characteristics of the Romanian Black Sea shelf. Tectonophysics 410, 417–435.
Dirik, K., Göncüoğlu, M.C., Kozlu, H., 1999. Stratigraphy and pre-Miocene tectonic evolution of the southwestern part of the Sivas Basin, Central Anatolia, Turkey. Geol. J. 34, 303–319.
Djoković, I., 1985. The use of structural analysis in determining the fabric of Palaeozoic formations in the Drina-Ivanjica region. Geol. Anal. Balk. Poluos. 49, 11–160.
Do Couto, D., Gorini, C., Jolivet, L., Lebret, N., Augier, R., Gumiaux, C., d'Acremont, E., Ammar, A., Jabour, H., Auxietre, J.-L., 2016. Tectonic and stratigraphic evolution of the Western Alboran Sea Basin in the last 25 Myrs. Tectonophysics 677, 280–311.
Doglioni, C., 1991. A proposal for the kinematic modelling of W-dipping subductions-possible applications to the Tyrrhenian-Apennines system. Terra Nova 3, 423–434.
Doglioni, C., Harabaglia, P., Merlini, S., Mongelli, F., Peccerillo, A.t., Piromallo, C., 1999. Orogens and slabs vs. their direction of subduction. Earth-Sci. Rev. 45, 167–208.
Dokuz, A., Aydınçakır, E., Kandemir, R., Karslı, O., Siebel, W., Derman, A.S., Turan, M., 2017. Late Jurassic Magmatism and Stratigraphy in the Eastern Sakarya Zone, Turkey: evidence for the Slab Breakoff of Paleotethyan Oceanic Lithosphere. J. Geol. 125, 1–31.
Doubrovine, P.V., Tarduno, J.A., 2008. Linking the Late Cretaceous to Paleogene Pacific plate and the Atlantic bordering continents using plate circuits and paleomagnetic data. J. Geophys. Res. 113.
Doubrovine, P.V., Steinberger, B., Torsvik, T.H., 2012. Absolute plate motions in a reference frame defined by moving hot spots in the Pacific, Atlantic, and Indian oceans. J. Geophys. Res.: Solid Earth 117.
Drinia, H., Antonarakou, A., 2012. Palaeoceanography of the Miocene (Tortonian) deposits of the Pre-Apulian zone, western Greece, as recorded by foraminifer and stable isotope records. Int. J. Earth Sci. 101, 521–534.
Druguet, E., Castro, A., Chichorro, M., Pereira, M.F., Fernández, C., 2014. Zircon geochronology of intrusive rocks from Cap de Creus, Eastern Pyrenees. Geol. Mag. 151, 1095–1114.
Duchesne, J.-C., Liegeois, J.-P., Iancu, V., Berza, T., Matukov, D.I., Tatu, M., Sergeev, S.A., 2008. Post-collisional melting of crustal sources: constraints from geochronology, petrology and Sr, Nd isotope geochemistry of the Variscan Sichevita and Poniasca granitoid plutons (South Carpathians, Romania). Int. J. Earth Sci. 97, 705–723.
Duermeijer, C.E., Langereis, C.G., 1998. Astronomical dating of a tectonic rotation on Sicily and consequences for the timing and extent of a middle Pliocene deformation phase. Tectonophysics 298, 243–258.
Duermeijer, C.E., Krijgsman, W., Langereis, C.G., Ten Veen, J.H., 1998a. Post-early Messinian counterclockwise rotations on Crete: implications for late Miocene to Recent kinematics of the southern Hellenic arc. Tectonophysics 298, 177–189.
Duermeijer, C.E., Van Vugt, N., Langereis, C.G., Meulenkamp, J.E., Zachariasse, W.J., 1998b. A major late Tortonian rotation phase in the Crotone basin using AMS as tectonic tilt correction and timing of the opening of the Tyrrhenian basin. Tectonophysics 287, 233–249.
Duermeijer, C.E., Krijgsman, W., Langereis, C.G., Meulenkamp, J.E., Triantaphyllou, M.V., Zachariasse, W.J., 1999. A Late Pleistocene clockwise rotation phase of Zakynthos (Greece) and implications for the evolution of the western Aegean arc. Earth Planet. Sci. Lett. 173, 315–331.
Duermeijer, C.E., Nyst, M., Meijer, P.T., Langereis, C.G., Spakman, W., 2000. Neogene evolution of the Aegean arc: paleomagnetic and geodetic evidence for a rapid and young rotation phase. Earth Planet. Sci. Lett. 176, 509–525.
Duman, T.Y., Emre, Ö., 2013. The East Anatolian Fault: geometry, segmentation and jog characteristics. Geol. Soc., Lond., Spec. Publ. 372, 314. SP372.
Dunn, A.M., Reynolds, P.H., Clarke, D.B., Ugidos, J.M., 1998. A comparison of the age and composition of the Shelburne dyke, Nova Scotia, and the Messejana dyke, Spain. Can. J. Earth Sci. 35, 1110–1115.
Dupont-Nivet, G., Vasiliev, I., Langereis, C.G., Krijgsman, W., Panaiotu, C., 2005. Neogene tectonic evolution of the southern and eastern Carpathians constrained by paleomagnetism. Earth Planet. Sci. Lett. 236, 374–387.
Durand-Delga, M., Rossi, P., Olivier, P., Puglisi, D., 2000. Situation Structurale et Nature Ophiolitique de Roches Basiques Jurassiques Associées aux Flyschs Maghrébins du Rif (Maroc) et de Sicile (Italie). In: Comptes Rendus de l'Académie des Sciences-Series IIA-Earth and Planetary Science, vol. 331, pp. 29–38.
Durmishi, C., 2014. Geodynamic Evolution, Petroleum Geology, Potential Source Rocks, reservoirs, Seals Carbonate Sedimentary Systems, Ionian and Sazani Zones, Albania. Bul. Shk. Gjeol. 5, 1–57.
Ebner, F., Vozárová, A., Kovács, S., 2007. Die variszische Orogenese im Circum-Pannonischen Raum–reflektiert an Devon–Karbon-Sedimenten. Jb. Geol. B.-A. 147, 315–329.
Edel, J.B., Dubois, D., Marchant, R., Hernandez, J., Cosca, M., 2001. La rotation miocene inferieur du bloc corso-sarde; nouvelles contraintes paleomagnetiques sur la fin du mouvement. Bull. Soc. Geol. France 172, 275–283.
Edwards, M.A., Grasemann, B., 2009. Mediterranean snapshots of accelerated slab retreat: subduction instability in stalled continental collision. Geol. Soc., Lond., Spec. Publ. 311, 155–192.
Egal, E., 1992. Structures and tectonic evolution of the external zone of Alpine Corsica. J. Struct. Geol. 14, 1215–1228.
El Atrassi, F., Brunet, F., Bouybaouene, M., Chopin, C., Chazot, G., 2011. Melting textures and microdiamonds preserved in graphite pseudomorphs from the Beni Bousera peridotite massif, Morocco. Eur. J. Mineral. 23, 157–168.
El Kadiri, K., Hlila, R., Sanz de Galdeano, C., López-Garrido, A.C., Chalouan, A., Serrano, F., Bahmad, A., Guerra-Merchán, A., Liemlahi, H., 2006. Regional correlations across the Internides-Externides front (northwestern Rif Belt, Morocco) during the Late Cretaceous-Early Burdigalian times: palaeogeographical and palaeotectonic implications. Geol. Soc., Lond., Spec. Publ. 262, 193–215.
Elbra, T., Bubík, M., Reháková, D., Schnabl, P., Čížková, K., Pruner, P., Kdýr, Š., Svobodová, A., Švábenická, L., 2018. Magneto-and biostratigraphy across the Jurassic-Cretaceous boundary in the Kurovice section, Western Carpathians, Czech Republic. Cretac. Res. 89, 211–223.
Ellouz, N., Roure, F., Săndulescu, M., Badescu, D., 1994. Balanced cross sections in the eastern Carpathians (Romania): a tool to quantify Neogene dynamics. Geodyn. Evolut. Sediment. Basins 305–325.
Elmas, A., Yılmaz, Y., 2003. Development of an oblique subduction zone—tectonic evolution of the Tethys suture zone in southeast Turkey. Int. Geol. Rev. 45, 827–840.
Elter, P., Pertusati, P.C., 1973. Considerazioni sul limite Alpi-Appennino e sulle sue relazioni con l'arco delle Alpi Occidentali. Mem. Soc. Geol. Ital. 12, 359–375.
Elter, G., Elter, P., Sturani, C., Weidmann, M., 1966. Sur la prolongation du domaine ligure de l'Apennin dans le Monferrat et les Alpes et sur l'origine de la Nappe de la Simme sl des Préalpes romandes et chablaisiennes. Arch. Sci. 19, 279–377.
Elter, P., Grasso, M., Parotto, M., Vezzani, L., 2003. Structural setting of the Apennine-Maghrebian thrust belt. Episodes 26, 205–211.
Elter, F.M., Elter, P., Eva, C., Eva, E., Kraus, R.K., Padovano, M., Solarino, S., 2012. An alternative model for the recent evolution of the Northern–Central Apennines (Italy). J. Geodyn. 54, 55–63.
Erak, D., Maţenco, L., Toljić, M., Stojadinovic, U., Andriessen, P.A.M., Willingshofer, E., Ducea, M.N., 2017. From nappe stacking to extensional detachments at the contact between the Carpathians and Dinarides – the Jastrebac Mountains of Central Serbia. Tectonophysics 710, 162–183.
Erdem, E., Bingöl, A., 1995. Pütürge (Malatya) metamorfitlerinin petrografik özellikleri. FÜ Fen ve Müh. Bilimleri Dergisi 7, 73–85.
Erduran, M., Endrun, B., Meier, T., 2008. Continental vs. oceanic lithosphere beneath the eastern Mediterranean Sea—implications from Rayleigh wave dispersion measurements. Tectonophysics 457, 42–52.
Ershov, A.V., Brunet, M.F., Nikishin, A.M., Bolotov, S.N., Nazarevich, B.P., Korotaev, M.V., 2003. Northern Caucasus basin: thermal history and synthesis

of subsidence models. Sediment. Geol. 156, 95–118.
Espurt, N., Hippolyte, J.-C., Saillard, M., Bellier, O., 2012a. Geometry and kinematic evolution of a long-living foreland structure inferred from field data and cross section balancing, the Sainte-Victoire System, Provence, France. Tectonics 31.
Espurt, N., Hippolyte, J.C., Saillard, M., Bellier, O., 2012b. Geometry and kinematic evolution of a long-living foreland structure inferred from field data and cross section balancing, the Sainte-Victoire System, Provence, France. Tectonics 31.
Espurt, N., Hippolyte, J.C., Kaymakcı, N., Sangu, E., 2014. Lithospheric structural control on inversion of the southern margin of the Black Sea Basin, Central Pontides, Turkey. Lithosphere 6, 26–34.
Esteban, J.J., Cuevas, J., Tubía, J.M., Sergeev, S., Larionov, A., 2011. A revised Aquitanian age for the emplacement of the Ronda peridotites (Betic Cordilleras, southern Spain). Geol. Mag. 148, 183–187.
Etheve, N., Frizon de Lamotte, D., Mohn, G., Martos, R., Roca, E., Blanpied, C., 2016. Extensional vs contractional Cenozoic deformation in Ibiza (Balearic Promontory, Spain): integration in the West Mediterranean back-arc setting. Tectonophysics 682, 35–55.
Evans, I., Hall, S.A., 1990. Paleomagnetic constraints on the tectonic evolution of the Sakarya Continent, northwestern Anatolia. Tectonophysics 182, 357–372.
Eyuboglu, Y., Dudas, F.O., Santosh, M., Xiao, Y., Yi, K., Chatterjee, N., Wu, F.-Y., Bektaş, O., 2016. Where are the remnants of a Jurassic ocean in the eastern Mediterranean region? Gondwana Res. 33, 63–91.
Eyuboglu, Y., Dudas, F.O., Chatterjee, N., Santosh, M., Billor, M.Z., Yuva, S., 2018. Petrology, geochronology and tectonic setting of early Triassic alkaline metagabbros from the Eastern Pontide Orogenic Belt (NE Turkey): implications for the geodynamic evolution of Gondwana's early Mesozoic northern margin. Tectonics 37, 3174–3206.
Eyuboğlu, Y., Santosh, M., Yi, K., Bektaş, O., Kwon, S., 2012. Discovery of Miocene adakitic dacite from the Eastern Pontides Belt (NE Turkey) and a revised geodynamic model for the late Cenozoic evolution of the Eastern Mediterranean region. Lithos 146–147, 218–232.
Eyuboğlu, Y., Dudas, F.O., Santosh, M., Yi, K., Kwon, S., Akaryali, E., 2013. Petrogenesis and U–Pb zircon chronology of adakitic porphyries within the Kop ultramafic massif (Eastern Pontides Orogenic Belt, NE Turkey). Gondwana Res. 24, 742–766.
Faccenna, C., Becker, T.W., 2010. Shaping mobile belts by small-scale convection. Nature 465, 602–605.
Faccenna, C., Mattei, M., Funiciello, R., Jolivet, L., 1997. Styles of back-arc extension in the central Mediterranean. Terra Nova 9, 126–130.
Faccenna, C., Becker, T.W., Lucente, F.P., Jolivet, L., Rossetti, F., 2001a. History of subduction and back arc extension in the Central Mediterranean. Geophys. J. Int. 145, 809–820.
Faccenna, C., Funiciello, F., Giardini, D., Lucente, P., 2001b. Episodic back-arc extension during restricted mantle convection in the Central Mediterranean. Earth Planet. Sci. Lett. 187, 105–116.
Faccenna, C., Jolivet, L., Piromallo, C., Morelli, A., 2003. Subduction and the depth of convection in the Mediterranean mantle. J. Geophys. Res.: Solid Earth 108.
Faccenna, C., Piromallo, C., Crespo-Blanc, A., Jolivet, L., Rossetti, F., 2004. Lateral slab deformation and the origin of the western Mediterranean arcs. Tectonics 23.
Faccenna, C., Becker, T.W., Auer, L., Billi, A., Boschi, L., Brun, J.P., Capitanio, F.A., Funiciello, F., Horvàth, F., Jolivet, L., 2014. Mantle dynamics in the Mediterranean. Rev. Geophys. 52, 283–332.
Farinacci, A., Köylüoğlu, M., 1982. Evolution of the Jurassic-Cretaceous Taurus Shelf (southern Turkey). Boll. Soc. Paleontol. Ital. 21, 267–276.
Faryad, S.W., Henjes-Kunst, F., 1997. Petrological and KAr and40Ar39Ar age constraints for the tectonothermal evolution of the high-pressure Meliata unit, Western Carpathians (Slovakia). Tectonophysics 280, 141–156.
Faupl, P., Pavlopoulos, A., Klotzli, U., Petrakakis, K., 2006. On the provenance of mid-Cretaceous turbidites of the Pindos zone (Greece): implications from heavy mineral distribution, detrital zircon ages and chrome spinel chemistry. Geol. Mag. 143, 329–342.
Faure, M., Rossi, P., Gaché, J., Melleton, J., Frei, D., Li, X., Lin, W., 2014. Variscan orogeny in Corsica: new structural and geochronological insights, and its place in the Variscan geodynamic framework. Int. J. Earth Sci. 103, 1533–1551.
Favali, P., Funiciello, R., Mattietti, G., Mele, G., Salvini, F., 1993. An active margin across the Adriatic Sea (central Mediterranean Sea). Tectonophysics.
Fazio, E., Cirrincione, R., Pezzino, A., 2015. Tectono-metamorphic map of the southwestern flank of the Aspromonte Massif (southern Calabria-Italy). J. Maps 11, 85–100.
Fazzuoli, M., Pandeli, E., Sani, F., 1994. Considerations on the sedimentary and structural evolution of the Tuscan Domain since Early Liassic to Tortonian. Mem. Soc. Geol. Ital. 48, 31–50.
Feinberg, H., Saddiqi, O., Michard, A., 1996. New constraints on the bending of the Gibraltar Arc from palaeomagnetism of the Ronda peridotites (Betic Cordilleras, Spain). Geol. Soc., Lond., Spec. Publ. 105, 43–52.
Fellin, M.G., Reiners, P.W., Brandon, M.T., Wüthrich, E., Balestrieri, M.L., Molli, G., 2007. Thermochronologic evidence for the exhumational history of the Alpi Apuane metamorphic core complex, Northern Apennines, Italy. Tectonics 26.
Fernandez, O., 2019. The Jurassic evolution of the Africa-Iberia conjugate margin and its implications on the evolution of the Atlantic-Tethys triple junction. Tectonophysics 750, 379–393.
Fernández-Blanco, D., 2014. Evolution of Orogenic Plateaus at Subduction Zones: Sinking and raising the Southern Margin of the Central Anatolian Plateau. Vrije Universiteit, Amsterdam.
Fernández-Blanco, D., Bertotti, G., Çiner, A., 2013. Cenozoic tectonics of the Tuz Gölü Basin (Central Anatolian Plateau, Turkey). Turk. J. Earth Sci. 22, 715–738.
Fernández-Blanco, D., Bertotti, G., Aksu, A., Hall, J., 2019. Monoclinal flexure of an orogenic plateau margin during subduction, south Turkey. Basin Res. https://doi.org/10.1111/bre.12341.
Ferrandini, J., Ferrandini, M., Rossi, P., Savary-Sismondini, B., 2010. Définition et datation de la Formation de Venaco (Corse) : dépôt d'origine gravitaire d'âge Priabonien. Compt. Rendus Geosci. 342, 921–929.
Ferrando, S., Bernoulli, D., Compagnoni, R., 2004. The Canavese zone (internal Western Alps): a distal margin of Adria. Schweiz. Mineral. Petrogr. Mittl. 84, 237–256.
Ferrer, O., Roca, E., Benjumea, B., Muñoz, J.A., Ellouz, N., Marconi, T., 2008. The deep seismic reflection MARCONI-3 profile: role of extensional Mesozoic structure during the Pyrenean contractional deformation at the eastern part of the Bay of Biscay. Mar. Pet. Geol. 25, 714–730.
Ferriere, J., Stais, A., 1995. Nouvelle interprétation de la suture téthysienne vardarienne d'après l'analyse des séries de Péonias (Vardar oriental, Hellénides internes). Bull. Soc. Géol. France 166, 327–339.
Ferrière, J., Bonneau, M., Caridroit, M., Bellier, J.-P., Gorican, S., Kollmann, H., 2001. Les Nappes Tertiaires du Païkon (Zone du Vardar, Macédoine, Grèce): Arguments Stratigraphiques Pour une Nouvelle Interprétation Structurale. In: Comptes Rendus de l'Académie des Sciences-Series IIA-Earth and Planetary Science, vol. 332, pp. 695–702.
Festa, A., Balestro, G., Dilek, Y., Tartarotti, P., 2015. A Jurassic oceanic core complex in the high-pressure Monviso ophiolite (western Alps, NW Italy). Lithosphere 7, 646–652.
Filipović, I., Jovanović, D., Sudar, M., Pelikán, P., Kovács, S., Less, G., Hips, K., 2003. Comparison of the Variscan–Early Alpine evolution of the Jadar Block (NW Serbia) and "Bükkium"(NE Hungary) terranes; some paleogeographic implications. Slovak Geol. Mag 9, 3–21.
Finetti, I., 1982. Structure, stratigraphy and evolution of central Mediterranean. Boll. Geofis. Teor. Appl. 24, 247–312.
Finetti, I., 1985. Structure and Evolution of the Central Mediterranean (Pelagian and Ionian Seas), Geological Evolution of the Mediterranean Basin. Springer, pp. 215–230.
Finetti, I.R., Boccaletti, M., Bonini, M., Del Ben, A., Geletti, R., Pipan, M., Sani, F., 2001. Crustal section based on CROP seismic data across the North Tyrrhenian–Northern Apennines–Adriatic Sea. Tectonophysics 343, 135–163.
Fisher, R.A., 1953. Dispersion on a sphere. Proc. R. Soc. Lond. A 217, 295–305.
Flecker, R., Poisson, A., Robertson, A.H.F., 2005. Facies and palaeogeographic evidence for the Miocene evolution of the Isparta Angle in its regional eastern Mediterranean context. Sediment. Geol. 173, 277–314.
Fleury, J.J., 1975. La premier flysch de Pinde témoin de ensemble des événements orogéniques mésozoiques antecretacé supérieureavant affecte les H'llenides internes. CR Acad. Sci 281, 1459.
Fleury, J.J., Godfriaux, I., 1974. Arguments pour l'attribution de la série de la fenêtre de l'Olympe (Grece)a la zone de Gavrovo Tripolitza: présence de fossiles du Maastrichtien et de l'Eocene inférieur (et moyen?). Ann. Soc. Géol. Nord 94, 149–156.
Floyd, P.A., Göncüoğlu, M.C., Winchester, J.A., Yaliniz, M.K., 2000. Geochemical Character and Tectonic Environment of Neotethyan Ophiolitic Fragments and Metabasites in the Central Anatolian Crystalline Complex, Turkey. Geol. Soc., Lond., Spec. Publ. 173, 183–202.
Fodor, L., Jelen, B., Márton, E., Skaberne, D., Čar, J., Vrabec, M., 1998. Miocene-Pliocene tectonic evolution of the Slovenian Periadriatic fault: implications for Alpine-Carpathian extrusion models. Tectonics 17, 690–709.
Fodor, L., Bada, G., Csillag, G., Horváth, E., Ruszkiczay-Rüdiger, Z., Palotás, K., Síkhegyi, F., Timár, G., Cloetingh, S., Horváth, F., 2005. An outline of neotectonic structures and morphotectonics of the western and central Pannonian Basin. Tectonophysics 410, 15–41.
Font, E., Fernandes, S., Neres, M., Carvallo, C., Martins, L., Madeira, J., Youbi, N., 2015. Paleomagnetism of the Central Atlantic Magmatic Province in the Algarve basin, Portugal: first insights. Tectonophysics 663, 364–377.
Forte, A.M., Cowgill, E., Murtuzayev, I., Kangarli, T., Stoica, M., 2013. Structural geometries and magnitude of shortening in the eastern Kura fold-thrust belt, Azerbaijan: implications for the development of the Greater Caucasus Mountains. Tectonics 32, 688–717.
Frisch, W., 1979. Tectonic progradation and plate tectonic evolution of the Alps. Tectonophysics 60, 121–139.
Frisch, W., Kuhlemann, J., Dunkl, I., Brügel, A., 1998. Palinspastic reconstruction and topographic evolution of the Eastern Alps during late Tertiary tectonic extrusion. Tectonophysics 297, 1–15.
Frisch, W., Dunkl, I., Kuhlemann, J., 2000. Post-collisional orogen-parallel large-scale extension in the Eastern Alps. Tectonophysics 327, 239–265.
Frizon de Lamotte, D., Saint Bezar, B., Bracène, R., Mercier, E., 2000. The two main steps of the Atlas building and geodynamics of the western Mediterranean. Tectonics 19, 740–761.
Frizon de Lamotte, D., Zizi, M., Missenard, Y., Hafid, M., El Azzouzi, M., Maury, R.C., Charrière, A., Taki, Z., Benammi, M., Michard, A., 2008. The Atlas System, Continental Evolution: the Geology of Morocco. Springer, pp. 133–202.
Frizon de Lamotte, D., Raulin, C., Mouchot, N., Wrobel-Daveau, J.-C., Blanpied, C., Ringenbach, J.-C., 2011. The southernmost margin of the Tethys realm during the Mesozoic and Cenozoic: initial geometry and timing of the inversion processes. Tectonics 30.
Froitzheim, N., Schmid, S.M., Frey, M., 1996. Mesozoic paleogeography and the timing of eclogite-facies metamorphism in the Alps: a working hypothesis. Eclogae Geol. Helv. 89, 81.
Froitzheim, N., Conti, P.t., Van Daalen, M., 1997. Late Cretaceous, synorogenic, low-

angle normal faulting along the Schlinig fault (Switzerland, Italy, Austria) and its significance for the tectonics of the Eastern Alps. Tectonophysics 280, 267–293.
Froitzheim, N., Jahn-Awe, S., Frei, D., Wainwright, A.N., Maas, R., Georgiev, N., Nagel, T.J., Pleuger, J., 2014. Age and composition of meta-ophiolite from the Rhodope Middle Allochthon (Satovcha, Bulgaria): a test for the maximum-allochthony hypothesis of the Hellenides. Tectonics 33, 1477–1500.
Fügenschuh, B., Schmid, S.M., 2005. Age and significance of core complex formation in a very curved orogen: evidence from fission track studies in the South Carpathians (Romania). Tectonophysics 404, 33–53.
Fügenschuh, B., Mancktelow, N.S., Seward, D., 2000. Cretaceous to Neogene cooling and exhumation history of the Oetztal-Stubai basement complex, eastern Alps: a structural and fission track study. Tectonics 19, 905–918.
Funedda, A., Meloni, M.A., Loi, A., 2015. Geology of the Variscan basement of the Laconi-Asuni area (central Sardinia, Italy): the core of a regional antiform refolding a tectonic nappe stack. J. Maps 11, 146–156.
Gaina, C., Roest, W.R., Müller, R.D., 2002. Late Cretaceous–Cenozoic deformation of northeast Asia. Earth Planet. Sci. Lett. 197, 273–286.
Gaina, C., Torsvik, T.H., van Hinsbergen, D.J.J., Medvedev, S., Werner, S.C., Labails, C., 2013. The African Plate: a history of oceanic crust accretion and subduction since the Jurassic. Tectonophysics 604, 4–25.
Gaina, C., van Hinsbergen, D.J.J., Spakman, W., 2015. Tectonic interactions between India and Arabia since the Jurassic reconstructed from marine geophysics, ophiolite geology, and seismic tomography. Tectonics 34, 875–906.
Gallais, F., Gutscher, M.-A., Graindorge, D., Chamot-Rooke, N., Klaeschen, D., 2011. A Miocene tectonic inversion in the Ionian Sea (central Mediterranean): evidence from multichannel seismic data. J. Geophys. Res. 116.
Gallet, Y., Besse, J., Krystyn, L., Théveniaut, H., Marcoux, J., 1993. Magnetostratigraphy of the Kavur Tepe section (southwestern Turkey): a magnetic polarity time scale for the Norian. Earth Planet. Sci. Lett. 117, 443–456.
Gallet, Y., Besse, J., Krystyn, L., Théveniaut, H., Marcoux, J., 1994. Magnetostratigraphy of the Mayerling section (Austria) and Erenkolu Mezarlik (Turkey) section: improvement of the Carnian (late Triassic) magnetic polarity time scale. Earth Planet. Sci. Lett. 125, 173–191.
Gallet, Y., Krystyn, L., Besse, J., Saidi, A., Ricou, L.-E., 2000. New constraints on the Upper Permian and Lower Triassic geomagnetic polarity timescale from the Abadeh section (central Iran). J. Geophys. Res.: Solid Earth 105, 2805–2815.
Gallet, Y., Krystyn, L., Marcoux, J., Besse, J., 2007. New constraints on the End-Triassic (Upper Norian–Rhaetian) magnetostratigraphy. Earth Planet. Sci. Lett. 255, 458–470.
Gallhofer, D., Quadt, A.v., Peytcheva, I., Schmid, S.M., Heinrich, C.A., 2015. Tectonic, magmatic, and metallogenic evolution of the Late Cretaceous arc in the Carpathian-Balkan orogen. Tectonics 34, 1813–1836.
Gallhofer, D., von Quadt, A., Schmid, S.M., Guillong, M., Peytcheva, I., Seghedi, I., 2017. Magmatic and tectonic history of Jurassic ophiolites and associated granitoids from the South Apuseni Mountains (Romania). Swiss J. Geosci. 110, 699–719.
Galoyan, G., Rolland, Y., Sosson, M., Corsini, M., Melkonyan, R., 2007. Evidence for superposed MORB, oceanic plateau and volcanic arc series in the Lesser Caucasus (Stepanavan, Armenia). Compt. Rendus Geosci. 339, 482–492.
Galoyan, G., Rolland, Y., Sosson, M., Corsini, M., Billo, S., Verati, C., Melkonyan, R., 2009. Geology, geochemistry and 40Ar/39Ar dating of Sevan ophiolites (Lesser Caucasus, Armenia): evidence for Jurassic Back-arc opening and hot spot event between the South Armenian Block and Eurasia. J. Asian Earth Sci. 34, 135–153.
Gamkrelidze, I., 1986. Geodynamic evolution of the Caucasus and adjacent areas in Alpine time. Tectonophysics 127, 261–277.
Garcés, M., Agustí, J., Cabrera, L., Parés, J.M., 1996. Magnetostratigraphy of the Vallesian (late Miocene) in the Vallès-Penedès basin (northeast Spain). Earth Planet. Sci. Lett. 142, 381–396.
Garcés, M., Krijgsman, W., Calvo, J.P., Alcalá, L., Alonso-Zarza, A.M., Darn, J.v., 1997. late Miocene alluvial sediments from the Teruel area: magnetostratigraphy, magnetic susceptibility, and facies organization. Acta Geol. Hisp. 32, 171–184.
Gardosh, M.A., Garfunkel, Z., Druckman, Y., Buchbinder, B., 2010. Tethyan rifting in the Levant Region and its role in Early Mesozoic crustal evolution. Geol. Soc., Lond., Spec. Publ. 341, 9–36.
Gasanov, A.Z., 1979. Paleomagnetic Directions and Pole Positions: Data for the USSR. Soviet Geophysical Committee, World Data Center-B, Moscow.
Gattacceca, J., Speranza, F., 2002. Paleomagnetism of Jurassic to Miocene sediments from the Apenninic carbonate platform (Southern Apennines, Italy): evidence for a 60 counterclockwise Miocene rotation. Earth Planet. Sci. Lett. 201, 19–34.
Gattacceca, J., Deino, A., Rizzo, R., Jones, D.S., Henry, B., Beaudoin, B., Vadeboin, F., 2007. Miocene rotation of Sardinia: new paleomagnetic and geochronological constraints and geodynamic implications. Earth Planet. Sci. Lett. 258, 359–377.
Gautier, P., Brun, J.-P., Moriceau, R., Sokoutis, D., Martinod, J., Jolivet, L., 1999. Timing, kinematics and cause of Aegean extension: a scenario based on a comparison with simple analogue experiments. Tectonophysics 315, 31–72.
Gautier, P., Bozkurt, E., Hallot, E., Dirik, K., 2002. Dating the exhumation of a metamorphic dome: geological evidence for pre-Eocene unroofing of the Nigde Massif (Central Anatolia, Turkey). Geol. Mag. 139.
Gautier, P., Bozkurt, E., Bosse, V., Hallot, E., Dirik, K., 2008. Coeval extensional shearing and lateral underflow during Late Cretaceous core complex development in the Niğde Massif, Central Anatolia, Turkey. Tectonics 27.
Gautier, P., Bosse, V., Cherneva, Z., Didier, A., Gerdjikov, I., Tiepolo, M., 2017. Polycyclic alpine orogeny in the Rhodope metamorphic complex: the record in migmatites from the Nestos shear zone (N. Greece). Bull. Soc. Géol. France 188, 36.
Gawlick, H.-J., Sudar, M., Suzuki, H., Derić, N., Missoni, S., Lein, R., Jovanović, D., 2009. Upper Triassic and Middle Jurassic radiolarians from the ophiolitic mélange of the Dinaridic Ophiolite Belt, SW Serbia. Neues Jahrb. Geol. Paläontol. - Abh. 253, 293–311.
Gawlick, H.J., Sudar, M.N., Missoni, S., Suzuki, H., Lein, R., Jovanovic, D., 2017. Triassic—Jurassic geodynamic history of the Dinaric Ophiolite Belt (Inner Dinarides, SW Serbia). J. Alp. Geol. 55, 1–167.
Gealey, W., 1988. Plate tectonic evolution of the Mediterranean-Middle East region. Tectonophysics 155, 285–306.
Gehring, A.U., Keller, P., Heller, F., 1991. Paleomagnetism and tectonics of the Jura arcuate mountain belt in France and Switzerland. Tectonophysics 186, 269–278.
Gelabert, B., Sabat, F., Rodríguez-Perea, A., 1992. A structural outline of the Serra de Tramuntana of Mallorca (Balearic Islands). Tectonophysics 203, 167–183.
Gelati, R., Gnaccolini, M., Falletti, P., Catrullo, D., 1992. Stratigrafia sequenziale della successione oligo-miocenica delle Langhe, Bacino Terziario Ligure-Piemontese. Riv. Ital. Paleontol. Stratigrafia. (Res. Paleontol. Stratigr.) 98.
Georgiev, G., Dabovski, C., Stanisheva-Vassileva, G., 2001. East Srednogorie-Balkan Rift Zone, vol. 6. Peri-Tethys Memoir, pp. 259–293.
Georgiev, N., Henry, B., Jordanova, N., Froitzheim, N., Jordanova, D., Ivanov, Z., Dimov, D., 2009. The emplacement mode of Upper Cretaceous plutons from the southwestern part of the Sredna Gora Zone (Bulgaria): structural and AMS study. Geol. Carpathica 60, 15–33.
Georgiev, N., Pleuger, J., Froitzheim, N., Sarov, S., Jahn-Awe, S., Nagel, T.J., 2010. Separate Eocene–early Oligocene and Miocene stages of extension and core complex formation in the Western Rhodopes, Mesta Basin, and Pirin Mountains (Bulgaria). Tectonophysics 487, 59–84.
Gerdjikov, I., 2005. Alpine metamorphism and granitoid magmatism in the Strandja zone: new data from the Sakar unit, SE Bulgaria. Turk. J. Earth Sci. 14, 167–183.
Gerzina, N., Csontos, L., 2003. Deformation sequence in the Vardar zone: surroundings of Jadar block; Serbia. Ann. Univ. Sci. Budapestinensis, Sect. Geol. 35, 139–140.
Gessner, K., Piazolo, S., Güngör, T., Ring, U., Kröner, A., Passchier, C., 2001a. Tectonic significance of deformation patterns in granitoid rocks of the Menderes nappes, Anatolide belt, southwest Turkey. Int. J. Earth Sci. 89, 766–780.
Gessner, K., Ring, U., Passchier, C.W., GÜNgÖR, T., 2001b. How to resist subduction: evidence for large-scale out-of-sequence thrusting during Eocene collision in western Turkey. J. Geol. Soc. 158, 769–784.
Gessner, K., Gallardo, L.A., Markwitz, V., Ring, U., Thomson, S.N., 2013. What caused the denudation of the Menderes Massif: review of crustal evolution, lithosphere structure, and dynamic topography in southwest Turkey. Gondwana Res. 24, 243–274.
Ghisetti, F., Barchi, M., Bally, A.W., Moretti, I., Vezzani, L., 1993. Conflicting Balanced Structural Sections across the Central Apennines (Italy): Problems and Implications, Generation, Accumulation and Production of Europe's Hydrocarbons III. Springer, pp. 219–231.
Giacomini, F., Bomparola, R.M., Ghezzo, C., Guldbransen, H., 2006. The geodynamic evolution of the Southern European Variscides: constraints from the U/Pb geochronology and geochemistry of the lower Palaeozoic magmatic-sedimentary sequences of Sardinia (Italy). Contrib. Mineralo. Petrol. 152, 19.
Giunta, G., Nigro, F., Renda, P., 2000. Extensional tectonics during Maghrebides chain building since late Miocene: examples from Northern Sicily. Ann. Soc. Geol. Pol. 70, 81–98.
Glavatovic, B., 2007. Seismogenic Model for Montenegro: Overview of Relevant Data. First Workshop for the Nato Science for Peace Project, 983054 ed, pp. 7–9.
Gobarenko, V., Yegorova, T., Stephenson, R., 2017. Local tomography model of the northeastern Black Sea: intra-plate crustal underthrusting. Geol. Soc., Lond., Spec. Publ. 428, 221–239.
Goffé, B., Michard, A., Garcia-Duenas, V., Gonzalez-Lodeiro, F., Monie, P., Campos, J., Galindo-Zaldivar, J., Jabaloy, A., Martinez-Martinez, J.M., Simancas, J.F., 1989. First evidence of high-pressure, low-temperature metamorphism in the Alpujarride nappes, Betic Cordilleras (SE Spain). Eur. J. Miner. 139–142.
Goguitchaichvili, A., Valdivia, L.A., Morales, J., Caballero, C., González, J.A., 2000. New contributions to the Early Pliocene geomagnetic field strength: case study of southern Caucasus volcanics. Geofís. Int. 39, 277–284.
Goguitchaichvili, A., Cervantes, M.A., Rathert, M.C., Camps, P., Sologashvili, J., Maissuradze, G., 2009. Gilbert-Gauss geomagnetic reversal recorded in Pliocene volcanic sequences from Georgia (Lesser Caucasus): revisited. Earth, Planets Space 61, 71–81.
Gökten, E., Floyd, P.A., 2007. Stratigraphy and geochemistry of pillow basalts within the ophiolitic mélange of the İzmir–Ankara–Erzincan suture zone: implications for the geotectonic character of the northern branch of Neotethys. Int. J. Earth Sci. 96, 725–741.
Golonka, J., 2004. Plate tectonic evolution of the southern margin of Eurasia in the Mesozoic and Cenozoic. Tectonophysics 381, 235–273.
Gómez-Pugnaire, M.T., Rubatto, D., Fernández-Soler, J.M., Jabaloy, A., López-Sánchez-Vizcaíno, V., González-Lodeiro, F., Galindo-Zaldívar, J., Padrón-Navarta, J.A., 2012. Late Variscan magmatism in the Nevado-Filábride Complex: U-Pb geochronologic evidence for the pre-Mesozoic nature of the deepest Betic complex (SE Spain). Lithos 146–147, 93–111.
Gomis, E., Parés, J.M., Cabrera, L., 1999. Nuevos datos magnetoestratigráficos del tránsito Oligoceno-Mioceno en el sector SE de la Cuenca del Ebro (provincias de Lleida, Zaragoza y Huesca, NE de España). Acta Geol. Hisp. 32 (3–4), 185–200, 1999.
Göncüoğlu, M.C., Türeli, K., 1993. Petrology and geodynamic interpretation of plagiogranites from central Anatolian ophiolites (Aksaray-Turkey). Turk. J. Earth

Sci. 2, 195–203.
Göncüoğlu, M., Turhan, N., 1984. Geology of the Bitlis metamorphic belt. In: International Symposium on Geology of the Taurus Belt. Proceedings of the Mineral Research and Exploration Institute of Turkey, p. 244. Ankara.
Göncüoğlu, C., Özcan, A., Turhan, N., Isik, A., 1992. Stratigraphy of Kütahya Region. ISGB-92 Guide Book, Ankara.
Göncüoğlu, M.C., Erler, A., Toprak, V., Yaliniz, K.M., Kuşcu, I., Köksal, S., Dirik, K., 1993. Orta Anadolu Masifin batı bölümünün jeolojisi. Bolum 3, 3313.
Göncüoğlu, M.C., Marroni, M., Pandolfi, L., Ellero, A., Ottria, G., Catanzariti, R., Tekin, U.K., Sayit, K., 2014. The Arkot Dağ Mélange in Araç area, central Turkey: evidence of its origin within the geodynamic evolution of the Intra-Pontide suture zone. J. Asian Earth Sci. 85, 117–139.
Gong, Z., Langereis, C.G., Mullender, T.A.T., 2008. The rotation of Iberia during the Aptian and the opening of the Bay of Biscay. Earth Planet. Sci. Lett. 273, 80–93.
Goričan, Š., 1994. Jurassic and Cretaceous radiolarian biostratigraphy and sedimentary evolution of the Budva Zone (Dinarides, Montenegro). Mém. Géol. 18, 1–177.
Goričan, Š., Košir, A., Rožič, B., Šmuc, A., Gale, L., Kukoč, D., Celarc, B., Črne, A.E., Kolar-Jurkovšek, T., Placer, L., 2012. Mesozoic deep-water basins of the eastern Southern Alps (NW Slovenia). In: 29th IAS Meeting of Sedimentology.
Gorini, C., Le Marrec, A., Mauffret, A., 1993. Contribution to the structural and sedimentary history of the Gulf of Lions (western Mediterranean) from the ECORS profiles, industrial seismic profiles and well data. Bull. Soc. Géol. France 164, 353–363.
Görür, N., Oktay, F.Y., Seymen, I., Şengör, A.M.C., 1984. Palaeotectonic evolution of the Tuzgölü basin complex, Central Turkey: sedimentary record of a Neo-Tethyan closure. Geol. Soc., Lond., Spec. Publ. 17, 467–482.
Görür, N., Tüysüz, O., Celal Şengör, A.M., 1998. Tectonic evolution of the central Anatolian basins. Int. Geol. Rev. 40, 831–850.
Grabowski, J., 2005. New Berriasian palaeopole from the Central West Carpathians (Tatra Mountains, southern Poland): does it look Apulian? Geophys. J. Int. 161, 65–80.
Grabowski, J., Nemčok, M., 1999. Summary of paleomagnetic data from the Central West Carpathians of Poland and Slovakia: evidence for the late cretaceous-early tertiary transpression. Phys. Chem. Earth, Part A: Solid Earth Geodesy 24, 681–685.
Gradstein, F.M., Ogg, J.G., Schmitz, M., Ogg, G., 2012. The Geologic Time Scale 2012. Elsevier.
Graessner, T., Schenk, V., Bröcker, M., Mezger, K., 2000. Geochronological constraints on the timing of granitoid magmatism, metamorphism and post-metamorphic cooling in the Hercynian crustal cross-section of Calabria. J. Metamorph. Geol. 18, 409–421.
Grandic, S., Biancone, M., Samarzija, J., 2001. Geophysical and stratigraphic evidence of the Triassic rift structuration in the Adriatic offshore area. Nafta 52, 383–396.
Grange, M., Scharer, U., Merle, R., Girardeau, J., Cornen, G., 2010. Plume-Lithosphere Interaction during Migration of Cretaceous Alkaline Magmatism in SW Portugal: evidence from U-Pb Ages and Pb-Sr-Hf Isotopes. J. Petrol. 51, 1143–1170.
Granot, R., 2016. Palaeozoic oceanic crust preserved beneath the eastern Mediterranean. Nat. Geosci. 9, 701–705.
Granot, R., Abelson, M., Ron, H., Agnon, A., 2006. The oceanic crust in 3D: paleomagnetic reconstruction in the Troodos ophiolite gabbro. Earth Planet. Sci. Lett. 251, 280–292.
Graziano, R., 2013. Sedimentology, biostratigraphy and event stratigraphy of the Early Aptian Oceanic Anoxic Event (OAE1A) in the Apulia Carbonate Platform Margin – Ionian Basin System (Gargano Promontory, southern Italy). Cretac. Res. 39, 78–111.
Grenerczy, G., Sella, G., Stein, S., Kenyeres, A., 2005. Tectonic implications of the GPS velocity field in the northern Adriatic region. Geophys. Res. Lett. 32 https://doi.org/10.1029/2005GL022947.
Gröger, H.R., Tischler, M., Fügenschuh, B., Schmid, S.M., 2013. Thermal history of the Maramureş area (Northern Romania) constrained by zircon fission track analysis: cretaceous metamorphism and Late Cretaceous to Paleocene exhumation. Geol. Carpathica 64, 383–398.
Grădinaru, E., 1988. Jurassic sedimentary rocks and bimodal volcanics of the Carjelari-Camena outcrop belt: evidence for a transtensile regime of the Peceneaga-Camena Fault. St. Cerc. Geol. Geofiz. Geogr.(Geol.) 33, 97–121.
Grădinaru, E., 1995. Mesozoic rocks in North Dobrogea: an overview. IGCP Project 1–4.
Guellec, S., Mugnier, J.-L., Tardy, M., Roure, F., 1990. Neogene evolution of the western Alpine foreland in the light of ECORS data and balanced cross-section. Mém. Soc. Géol. France 156, 165–184.
Guilmette, C., Smit, M.A., van Hinsbergen, D.J.J., Gürer, D., Corfu, F., Savard, D., 2018. Forced subduction initiation revealed by crust-sole couple geochronology of the Semail ophiolite of Oman. Nat. Geosci. 11, 688–695.
Gül, M., 2007. Effects of antecedent topography on reefal carbonate deposition: early-middle Miocene of the Adana Basin, S Turkey. J. Asian Earth Sci. 31, 18–34.
Gülyüz, E., Kaymakcı, N., Meijers, M.J.M., van Hinsbergen, D.J.J., Lefebvre, C., Vissers, R.L.M., Hendriks, B.W.H., Peynircioğlu, A.A., 2013. late Eocene evolution of the Çiçekdağı Basin (central Turkey): syn-sedimentary compression during microcontinent–continent collision in central Anatolia. Tectonophysics 602, 286–299.
Güngör, T., Erdoğan, B., 2002. Tectonic significance of mafic volcanic rocks in a Mesozoic sequence of the Menderes Massif, West Turkey. Int. J. Earth Sci. 91, 386–397.
Gürer, M.D., 2017. Subduction Evolution in the Anatolian region: the Rise, Demise, and Fate of the Anadolu Plate. University, Utrecht, p. 239.
Gürer, D., van Hinsbergen, D.J.J., 2019. Diachronous demise of the Neotethys Ocean as a driver for non-cylindrical orogenesis in Anatolia. Tectonophysics 760, 96–106.
Gürer, D., van Hinsbergen, D.J.J., Maţenco, L., Corfu, F., Cascella, A., 2016. Kinematics of a former oceanic plate of the Neotethys revealed by deformation in the Ulukışla basin (Turkey). Tectonics 35, 2385–2416.
Gürer, D., Plunder, A., Kirst, F., Corfu, F., Schmid, S.M., van Hinsbergen, D.J.J., 2018a. A long-lived Late Cretaceous–early Eocene extensional province in Anatolia? Structural evidence from the Ivriz Detachment, southern central Turkey. Earth Planet. Sci. Lett. 481, 111–124.
Gürer, D., van Hinsbergen, D.J.J., Özkaptan, M., Creton, I., Koymans, M.R., Cascella, A., Langereis, C.G., 2018b. Paleomagnetic constraints on the timing and distribution of Cenozoic rotations in Central and Eastern Anatolia. Solid Earth 9, 295–322.
Gurnis, M., Turner, M., Zahirovic, S., DiCaprio, L., Spasojevic, S., Müller, R.D., Boyden, J., Seton, M., Manea, V.C., Bower, D.J., 2012. Plate tectonic reconstructions with continuously closing plates. Comput. Geosci. 38, 35–42.
Gürsoy, H., Piper, J.D.A., Tatar, O., Temiz, H., 1997. A palaeomagnetic study of the Sivas Basin, central Turkey: crustal deformation during lateral extrusion of the Anatolian Block. Tectonophysics 271, 89–105.
Gürsoy, H., Piper, J.D.A., Tatar, O., Mesci, L., 1998. Palaeomagnetic study of the Karaman and Karapinar volcanic complexes, central Turkey: neotectonic rotation in the south-central sector of the Anatolian Block. Tectonophysics 299, 191–211.
Gürsoy, H.I., Piper, J.D.A., Tatar, O., 1999. Palaeomagnetic study of the Galatean Volcanic Province, north-central Turkey: neogene deformation at the northern border of the Anatolian Block. Geol. J. 34, 7–23.
Gürsoy, H., Piper, J.D.A., Tatar, O., 2003. Neotectonic deformation in the western sector of tectonic escape in Anatolia: palaeomagnetic study of the Afyon region, central Turkey. Tectonophysics 374, 57–79.
Gürsoy, H., Tatar, O., Piper, J.D.A., Koçbulut, F., Akpınar, Z., Huang, B., Roberts, A.P., Mesci, B.L., 2011. Palaeomagnetic study of the Kepezdağ and Yamadağ volcanic complexes, central Turkey: neogene tectonic escape and block definition in the central-east Anatolides. J. Geodyn. 51, 308–326.
Guseynov, A.N., Gajiev, E.M., Isaeva, M.I., 1989. Paleomagnetic Directions and Pole Positions: Data for the USSR. Soviet Geophysical Committee, World Data Center-B, Moscow.
Gutnic, M., 1979. Géologie des taurides occidentales (Turquie). Mém. Soc. Géol. France.
Gągała, Ł., Vergés, J., Saura, E., Malata, T., Ringenbach, J.-C., Werner, P., Krzywiec, P., 2012. Architecture and orogenic evolution of the northeastern Outer Carpathians from cross-section balancing and forward modeling. Tectonophysics 532–535, 223–241.
Haas, J., Péró, C., 2004. Mesozoic evolution of the Tisza Mega-unit. Int. J. Earth Sci. 93, 297–313.
Hafkenscheid, E., Wortel, M.J.R., Spakman, W., 2006. Subduction history of the Tethyan region derived from seismic tomography and tectonic reconstructions. J. Geophys. Res. 111 (B8), B08401. https://doi.org/10.1029/2005JB003791.
Haldan, M.M., Meijers, M.J.M., Langereis, C.G., Larsen, B.T., Heyer, H., 2014. New palaeomagnetic results from the Oslo Graben, a Permian Superchron lava province. Geophys. J. Int. 199, 1554–1571.
Hamai, L., Petit, C., Le Pourhiet, L., Yelles-Chaouche, A., Déverchère, J., Beslier, M.-O., Abtout, A., 2018. Towards subduction inception along the inverted North African margin of Algeria? Insights from thermo-mechanical models. Earth Planet. Sci. Lett. 501, 13–23.
Hámor, G., 1985. Geology of the Nógrád-Cserhát area. Geol. Hung. 22, 1–307.
Handy, M.R., Franz, L., Heller, F., Janott, B., Zurbriggen, R., 1999. Multistage accretion and exhumation of the continental crust (Ivrea crustal section, Italy and Switzerland). Tectonics 18, 1154–1177.
Handy, M.R., Schmid, S.M., Bousquet, R., Kissling, E., Bernoulli, D., 2010. Reconciling plate-tectonic reconstructions of Alpine Tethys with the geological–geophysical record of spreading and subduction in the Alps. Earth-Sci. Rev. 102, 121–158.
Handy, M.R., Ustaszewski, K., Kissling, E., 2015. Reconstructing the Alps–Carpathians–Dinarides as a key to understanding switches in subduction polarity, slab gaps and surface motion. Int. J. Earth Sci. 104, 1–26.
Harrison, R.W., Tsiolakis, E., Stone, B.D., Lord, A., McGeehin, J.P., Mahan, S.A., Chirico, P., 2013. Late Pleistocene and Holocene uplift history of Cyprus: implications for active tectonics along the southern margin of the Anatolian microplate. Geol. Soc., Lond., Spec. Publ. 372, 561–584.
Hässig, M., Rolland, Y., Sosson, M., Galoyan, G., Müller, C., Avagyan, A., Sahakyan, L., 2013a. New structural and petrological data on the Amasia ophiolites (NW Sevan–Akera suture zone, Lesser Caucasus): insights for a large-scale obduction in Armenia and NE Turkey. Tectonophysics 588, 135–153.
Hässig, M., Rolland, Y., Sosson, M., Galoyan, G., Sahakyan, L., Topuz, G., Çelik, Ö.F., Avagyan, A., Müller, C., 2013b. Linking the NE Anatolian and Lesser Caucasus ophiolites: evidence for large-scale obduction of oceanic crust and implications for the formation of the Lesser Caucasus-Pontides Arc. Geodin. Acta 26, 311–330.
Hässig, M., Rolland, Y., Sahakyan, L., Sosson, M., Galoyan, G., Avagyan, A., Bosch, D., Müller, C., 2015. Multi-stage metamorphism in the South Armenian Block during the Late Jurassic to Early Cretaceous: tectonics over south-dipping subduction of northern branch of Neotethys. J. Asian Earth Sci. 102, 4–23.
Hässig, M., Rolland, Y., Sosson, M., 2017. From seafloor spreading to obduction: Jurassic–Cretaceous evolution of the northern branch of the Neotethys in the Northeastern Anatolian and Lesser Caucasus regions. Geol. Soc., Lond., Spec. Publ. 428, 41–60.

Hässig, M., Rolland, Y., Melis, R., Sosson, M., Galoyan, G., Bruguier, O., 2019. PTT history of the Amasia and Stepanavan sub-ophiolitic metamorphic units (NW Armenia, Lesser Caucasus): implications for metamorphic sole development and for the obduction process. Ofioliti 44, 43–70.
Haubold, H., Scholger, R., Frisch, W., Summesberger, H., Mauritsch, H.J., 1999. Reconstruction of the geodynamic evolution of the Northern Calcareous Alps by means of paleomagnetism. Phys. Chem. Earth, Part A: Solid Earth Geod. 24, 697–703.
Hayward, A.B., 1984. Sedimentation and basin formation related to ophiolite nappe emplacement, Miocene, SW Turkey. Sediment. Geol. 40, 105–129.
Helvaci, C., Griffin, W.L., 1984. Rb-Sr geochronology of the Bitlis Massif, Avnik (Bingöl) area, SE Turkey. Geol. Soc., Lond., Spec. Publ. 17, 403–413.
Hempton, M.R., 1985. Structure and deformation history of the Bitlis suture near Lake Hazar, southeastern Turkey. Geol. Soc. Am. Bull. 96, 233–243.
Henry, B., 1992. Structural implications of paleomagnetic data from Pelvoux-Belledonne area (French Alps). Tectonophysics 216, 327–338.
Henry, P., Azambre, B., Montigny, R., Rossy, M., Stevenson, R.K., 1998. Late mantle evolution of the Pyrenean sub-continental lithosphericmantle in the light of new 40Ar–39Ar and Sm–Nd ages on pyroxenites and peridotites (Pyrenees, France). Tectonophysics 296, 103–123.
Herwartz, D., Nagel, T.J., Münker, C., Scherer, E.E., Froitzheim, N., 2011. Tracing two orogenic cycles in one eclogite sample by Lu–Hf garnet chronometry. Nat. Geosci. 4, 178–183.
Heymes, T., Bouillin, J.P., Pêcher, A., Monié, P., Compagnoni, R., 2008. Middle Oligocene extension in the Mediterranean Calabro-Peloritan belt (southern Italy): insights from the Aspromonte nappes pile. Tectonics 27.
Heymes, T., Monié, P., Arnaud, N., Pêcher, A., Bouillin, J.-P., Compagnoni, R., 2010. Alpine tectonics in the Calabrian–Peloritan belt (southern Italy): new 40Ar/39Ar data in the Aspromonte Massif area. Lithos 114, 451–472.
Hieke, W., Cita, M.B., Forcella, F., Mueller, C., 2006. Geology of the Victor Hensen Seahill (Ionian Sea, eastern Mediterranean); insights from the study of cored sediment sequences. Boll. Soc. Geol. Ital. 125, 245–257.
Higgins, M., Schoenbohm, L.M., Brocard, G., Kaymakcı, N., Gosse, J.C., Cosca, M.A., 2015. New kinematic and geochronologic evidence for the Quaternary evolution of the Central Anatolian fault zone (CAFZ). Tectonics 34, 2118–2141.
Hippolyte, J.C., 2002. Geodynamics of Dobrogea (Romania): new constraints on the evolution of the Tornquist–Teisseyre Line, the Black Sea and the Carpathians. Tectonophysics 357, 33–53.
Hippolyte, J.C., Müller, C., Kaymakcı, N., Sangu, E., 2010. Dating of the Black Sea Basin: new nannoplankton ages from its inverted margin in the Central Pontides (Turkey). Geol. Soc., Lond., Spec. Publ. 340, 113–136.
Hirt, A.M., Lowrie, W., 1988. Paleomagnetism of the Umbrian-Marches orogenic belt. Tectonophysics 146, 91–103.
Hisarlı, Z.M., 2011. New paleomagnetic constraints on the late Cretaceous and early Cenozoic tectonic history of the Eastern Pontides. J. Geodyn. 52, 114–128.
Hisarlı, Z.M., Çinku, M.C., Ustaömer, T., Keskin, M., Orbay, N., 2016. Neotectonic deformation in the Eurasia–Arabia collision zone, the East Anatolian Plateau, E Turkey: evidence from palaeomagnetic study of Neogene–Quaternary volcanic rocks. Int. J. Earth Sci. 105, 139–165.
Hoeck, V., Ionescu, C., Balintoni, I., Koller, F., 2009. The Eastern Carpathians "ophiolites" (Romania): remnants of a Triassic ocean. Lithos 108, 151–171.
Hoogerduijn Strating, E.H., 1994. Extensional faulting in an intraoceanic subduction complex—Working hypothesis for the Palaeogene of the Alps-Apennine system. Tectonophysics 238, 255–273.
Hoogerduijn Strating, E.H., Van Wamel, W.A., Vissers, R.L.M., 1991. Some constraints on the kinematics of the Tertiary Piemonte Basin (northwest Italy). Tectonophysics 198, 47–51.
Horner, F., Freeman, R., 1983. Palaeomagnetic evidence from pelagic limestones for clockwise rotation of the Ionian zone, western Greece. Tectonophysics 98, 11–27.
Horner, F., Heller, F., 1983. Lower Jurassic magnetostratigraphy at the Breggia Gorge (Ticino, Switzerland) and Alpe Turati (Como, Italy). Geophys. J. Royal Astron. Soc. 73, 705–718.
Horner, F., Lowrie, W., 1981. Paleomagnetic evidence from Mesozoic carbonate rocks for the rotation of Sardinia. J. Geophys. - Z. Geophys. 49, 11–19.
Horváth, F., Bada, G., Szafián, P., Tari, G., Ádám, A., Cloetingh, S., 2006. Formation and deformation of the Pannonian Basin: constraints from observational data. Geol. Soc., Lon., Mem. 32, 191–206.
Horváth, F., Musitz, B., Balázs, A., Végh, A., Uhrin, A., Nádor, A., Koroknai, B., Pap, N., Tóth, T., Wórum, G., 2015. Evolution of the Pannonian basin and its geothermal resources. Geothermics 53, 328–352.
Hosseinpour, M., Williams, S., Seton, M., Barnett-Moore, N., Müller, R.D., 2016. Tectonic evolution of Western Tethys from Jurassic to present day: coupling geological and geophysical data with seismic tomography models. Int. Geol. Rev. 58, 1616–1645.
Houša, V., Krs, M., Man, O., Pruner, P., Venhodová, D., Cecca, F., Nardi, G., Piscitello, M., 2004. Combined magnetostratigraphic, palaeomagnetic and calpionellid investigations across Jurassic/Cretaceous boundary strata in the Bosso Valley, Umbria, central Italy. Cretac. Res. 25, 771–785.
Hrvatović, H., 2006. Geological guidebook through Bosnia and Herzegovina. Geol. Sur. Feder. Bosnia Herzegovina, Sarajevo 172.
Hrvatović, H., Pamić, J., 2005. Principal thrust-nappe structures of the Dinarides. Acta Geol. Hungarica 48, 133–151.
Huang, W., van Hinsbergen, D.J.J., Maffione, M., Orme, D.A., Dupont-Nivet, G., Guilmette, C., Ding, L., Guo, Z., Kapp, P., 2015. Lower Cretaceous Xigaze ophiolites formed in the Gangdese forearc: evidence from paleomagnetism, sediment provenance, and stratigraphy. Earth Planet. Sci. Lett. 415, 142–153.
Hubert-Ferrari, A., Armijo, R., King, G., Meyer, B., Barka, A., 2002. Morphology, displacement, and slip rates along the North Anatolian Fault, Turkey. J. Geophys. Res.: Solid Earth 107. ETG-9.
Hurst, S.D., Verosub, K.L., Moores, E.M., 1992. Paleomagnetic constraints on the formation of the Solea Graben, Troodos Ophiolite, Cyprus. Tectonophysics 208, 431–445.
Hüsing, S.K., Hilgen, F.J., Abdul Aziz, H., Krijgsman, W., 2007. Completing the Neogene geological time scale between 8.5 and 12.5 Ma. Earth Planet. Sci. Lett. 253, 340–358.
Hüsing, S.K., Kuiper, K.F., Link, W., Hilgen, F.J., Krijgsman, W., 2009a. The upper Tortonian–lower Messinian at Monte dei Corvi (Northern Apennines, Italy): completing a Mediterranean reference section for the Tortonian Stage. Earth Planet. Sci. Lett. 282, 140–157.
Hüsing, S.K., Zachariasse, W.-J., van Hinsbergen, D.J.J., Krijgsman, W., Inceöz, M., Harzhauser, M., Mandic, O., Kroh, A., 2009b. Oligocene–Miocene basin evolution in SE Anatolia, Turkey: constraints on the closure of the eastern Tethys gateway. Geol. Soc., Lond., Spec. Publ. 311, 107–132.
Hüsing, S.K., Cascella, A., Hilgen, F.J., Krijgsman, W., Kuiper, K.F., Turco, E., Wilson, D., 2010. Astrochronology of the Mediterranean Langhian between 15.29 and 14.17Ma. Earth Planet. Sci. Lett. 290, 254–269.
Huvaz, O., 2009. Comparative petroleum systems analysis of the interior basins of Turkey: implications for petroleum potential. Mar. Pet. Geol. 26, 1656–1676.
Iaffaldano, G., Stein, S., 2017. Impact of uncertain reference-frame motions in plate kinematic reconstructions: a theoretical appraisal. Earth Planet. Sci. Lett. 458, 349–356.
Iancu, V., Maruntiu, M., Johan, V., Ledru, P., 1998. High-grade metamorphic rocks in the pre-Alpine nappe stack of the Getic-Supragetic basement (Median Dacides, South Carpathians, Romania). Miner. Petrol. 63, 173–198.
Iancu, V., Berza, T., Seghedi, A., Gheuca, I., Hann, H.-P., 2005a. Alpine polyphase tectono-metamorphic evolution of the South Carpathians: a new overview. Tectonophysics 410, 337–365.
Iancu, V., Berza, T., Seghedi, A., Marunţiu, M., 2005b. Palaeozoic rock assemblages incorporated in the South Carpathian Alpine thrust belt (Romania and Serbia): a review. Geol. Belg.
Iannace, A., Vitale, S., D'Errico, M., Mazzoli, S., Di Staso, A., Macaione, E., Messina, A., Reddy, S.M., Somma, R., Zamparelli, V., Zattin, M., Bonardi, G., 2007. The carbonate tectonic units of northern Calabria (Italy): a record of Apulian palaeomargin evolution and Miocene convergence, continental crust subduction, and exhumation of HP LT rocks. J. Geol. Soc. 164, 1165–1186.
IGRS-IFP, 1966. Étude Géologique de l'Epire (Grèce Nord-Occidentale). Technip Paris.
Ilić, A., Neubauer, F., 2005. Tertiary to recent oblique convergence and wrenching of the Central Dinarides: constraints from a palaeostress study. Tectonophysics 410, 465–484.
Ilić, A., Neubauer, F., Handler, R., 2005. Late Paleozoic–Mesozoic tectonics of the Dinarides revisited: implications from 40Ar/39Ar dating of detrital white micas. Geology 33, 233–236.
Inwood, J., Anderson, M.W., Morris, A., Robertson, A.H.F., 2009a. Successive structural events in the Hatay ophiolite of southeast Turkey: distinguishing oceanic, emplacement and post-emplacement phases of faulting. Tectonophysics 473, 208–222.
Inwood, J., Morris, A., Anderson, M.W., Robertson, A.H.F., 2009b. Neotethyan intraoceanic microplate rotation and variations in spreading axis orientation: palaeomagnetic evidence from the Hatay ophiolite (southern Turkey). Earth Planet. Sci. Lett. 280, 105–117.
Ionescu, C., Hoeck, V., Tomek, C., Koller, F., Balintoni, I., Beşuţiu, L., 2009. New insights into the basement of the Transylvanian Depression (Romania). Lithos 108, 172–191.
Iorio, M., Nardi, G., Pierattini, D., Tarling, D.H., 1996. Palaeomagnetic evidence of block rotations in the Matese Mountains, Southern Apennines, Italy. Geol. Soc., Lond., Spec. Publ. 105, 133–139.
Iribarren, L., Vergés, J., Camurri, F., Fullea, J., Fernàndez, M., 2007. The structure of the Atlantic–Mediterranean transition zone from the Alboran Sea to the Horseshoe Abyssal Plain (Iberia–Africa plate boundary). Mar. Geol. 243, 97–119.
Isik, V., 2009. The ductile shear zone in granitoid of the Central Anatolian Crystalline Complex, Turkey: implications for the origins of the Tuzgölü basin during the Late Cretaceous extensional deformation. J. Asian Earth Sci. 34, 507–521.
Isik, V., Tekeli, O., Seyitoğlu, G., 2004. The 40Ar/39Ar age of extensional ductile deformation and granitoid intrusion in the northern Menderes core complex: implications for the initiation of extensional tectonics in western Turkey. J. Asian Earth Sci. 23, 555–566.
Isik, V., Lo, C.-H., Göncüoğlu, C., Demirel, S., 2008. 39Ar/40Ar Ages from the Yozgat Batholith: preliminary Data on the Timing of Late Cretaceous Extension in the Central Anatolian Crystalline Complex, Turkey. J. Geol. 116, 510–526.
Isik, V., Uysal, I.T., Caglayan, A., Seyitoğlu, G., 2014. The evolution of intraplate fault systems in central Turkey: structural evidence and Ar-Ar and Rb-Sr age constraints for the Savcılı Fault Zone. Tectonics 33, 1875–1899.
Ismail-Zadeh, A., Maţenco, L., Radulian, M., Cloetingh, S., Panza, G., 2012. Geodynamics and intermediate-depth seismicity in Vrancea (the south-eastern Carpathians): current state-of-the art. Tectonophysics 530–531, 50–79.
Ivanov, R., 1981. The deep-seated Central-Rhodope Nappe and the interference tectonics of the Rhodope crystalline basement. Geol. Balc. 11, 47–66.
Ivanov, Z., 1988. Aperçu général sur l'évolution géologique et structurale du massif

des Rhodopes dans le cadre des Balkanides. Bull. Soc. Géol. France 4, 227–240.
İmer, A., Richards, J.P., Creaser, R.A., 2013. Age and tectonomagmatic setting of the Eocene Çöpler–Kabataş magmatic complex and porphyry-epithermal Au deposit, East Central Anatolia, Turkey. Miner. Depos. 48, 557–583.
İşseven, T., Tüysüz, O., 2006. Palaeomagnetically defined rotations of fault-bounded continental blocks in the North Anatolian Shear Zone, North Central Anatolia. J. Asian Earth Sci. 28, 469–479.
Jackson, K.C., 1990. A palaeomagnetic study of Apennine thrusts, Italy: Monte Maiella and Monte Raparo. Tectonophysics 178, 231–240.
Jacobshagen, V., 1987. Geologie von Griechenland. Schweizerbart'sche Verlagsbuchhandlung.
Jaffey, N., Robertson, A., 2005. Non-marine sedimentation associated with Oligocene-Recent exhumation and uplift of the Central Taurus Mountains, S Turkey. Sediment. Geol. 173, 53–89.
Jahn-Awe, S., Froitzheim, N., Nagel, T.J., Frei, D., Georgiev, N., Pleuger, J., 2010. Structural and geochronological evidence for Paleogene thrusting in the western Rhodopes, SW Bulgaria: elements for a new tectonic model of the Rhodope Metamorphic Province. Tectonics 29.
Jaillard, E., 1999. The late Cretaceous-Eocene sedimentation in the internal Briançonnais units of Vanoise (French Alps): witnesses of early alpine movements. Eclogae Geol. Helv. 92, 211–220.
Jammes, S., Manatschal, G., Lavier, L., Masini, E., 2009. Tectonosedimentary evolution related to extreme crustal thinning ahead of a propagating ocean: example of the western Pyrenees. Tectonics 28.
Janák, M., Froitzheim, N., Lupták, B., Vrabec, M., Ravna, E.J.K., 2004. First evidence for ultrahigh-pressure metamorphism of eclogites in Pohorje, Slovenia: tracing deep continental subduction in the Eastern Alps. Tectonics 23.
Janák, M., Froitzheim, N., Yoshida, K., Sasinková, V., Nosko, M., Kobayashi, T., Hirajima, T., Vrabec, M., 2015. Diamond in metasedimentary crustal rocks from Pohorje, Eastern Alps: a window to deep continental subduction. J. Metamorph. Geol. 33, 495–512.
Jenkins, D.A.L., 1972. Structural development of western Greece. AAPG Bull. 56, 128–149.
Jeřábek, P., Lexa, O., Schulmann, K., Plašienka, D., 2012. Inverse ductile thinning via lower crustal flow and fold-induced doming in the West Carpathian Eo-Alpine collisional wedge. Tectonics 31.
Joffe, S., Garfunkel, Z., 1987. Plate kinematics of the circum Red Sea—a re-evaluation. Tectonophysics 141, 5–22.
Johnson, R.J.E., Van der Voo, R., Lowrie, W., 1984. Paleomagnetism and late diagenesis of Jurassic carbonates from the Jura Mountains, Switzerland and France. Geol. Soc. Am. Bull. 95, 478–488.
Johnson, C.L., Constable, C.G., Tauxe, L., Barendregt, R., Brown, L.L., Coe, R.S., Layer, P., Mejia, V., Opdyke, N.D., Singer, B.S., Staudigel, H., Stone, D.B., 2008. Recent investigations of the 0-5 Ma geomagnetic field recorded by lava flows. Geochem. Geophys. Geosyst. 9.
Jolivet, L., Brun, J.-P., 2010. Cenozoic geodynamic evolution of the Aegean. Int. J. Earth Sci. 99, 109–138.
Jolivet, L., Dubois, R., Fournier, M., Goffé, B., Michard, A., Jourdan, C., 1990. Ductile extension in alpine Corsica. Geology 18.
Jolivet, L., Goffé, B., Monié, P., Truffert-Luxey, C., Patriat, M., Bonneau, M., 1996. Miocene detachment in Crete and exhumation P-T-t paths of high-pressure metamorphic rocks. Tectonics 15, 1129–1153.
Jolivet, L., Faccenna, C., Goffé, B., Mattei, M., Rossetti, F., Brunet, C., Storti, F., Funiciello, R., Cadet, J.P., d'Agostino, N., Parra, T., 1998. Midcrustal shear zones in postorogenic extension: example from the northern Tyrrhenian Sea. J. Geophys. Res.: Solid Earth 103, 12123–12160.
Jolivet, L., Faccenna, C., Goffé, B., Burov, E., Agard, P., 2003. Subduction tectonics and exhumation of high-pressure metamorphic rocks in the Mediterranean orogens. Am. J. Sci. 303, 353–409.
Jolivet, L., Faccenna, C., Piromallo, C., 2009. From mantle to crust: stretching the Mediterranean. Earth Planet. Sci. Lett. 285, 198–209.
Jolivet, L., Lecomte, E., Huet, B., Denèle, Y., Lacombe, O., Labrousse, L., Le Pourhiet, L., Mehl, C., 2010. The North Cycladic Detachment System. Earth Planet. Sci. Lett. 289, 87–104.
Jolivet, L., Gorini, C., Smit, J., Leroy, S., 2015a. Continental breakup and the dynamics of rifting in back-arc basins: the Gulf of Lion margin. Tectonics 34, 662–679.
Jolivet, L., Menant, A., Sternai, P., Rabillard, A., Arbaret, L., Augier, R., Laurent, V., Beaudoin, A., Grasemann, B., Huet, B., 2015b. The geological signature of a slab tear below the Aegean. Tectonophysics 659, 166–182.
Jordan, G., Meijninger, B.M.L., van Hinsbergen, D.J.J., Meulenkamp, J.E., Dijk, P.M.v., 2005. Extraction of morphotectonic features from DEMs: development and applications for study areas in Hungary and NW Greece. Int. J. Appl. Earth Observ. Geoinf. 7, 163–182.
Jovane, L., Savian, J.F., Coccioni, R., Frontalini, F., Bancalà, G., Catanzariti, R., Luciani, V., Bohaty, S.M., Wilson, P.A., Florindo, F., 2013. Integrated magnetobiostratigraphy of the middle Eocene–lower Oligocene interval from the Monte Cagnero section, central Italy. Geol. Soc., Lond., Spec. Publ. 373, 79–95.
Juárez, M.T., Osete, M.L., Meléndez, G., Langereis, C.G., Zijderveld, J.D.A., 1994. Oxfordian magnetostratigraphy of the Aguilón and Tosos sections (Iberian Range, Spain) and evidence of a pre-Oligocene overprint. Phys. Earth Planet. Inter. 85, 195–211.
Juárez, M.T., Osete, M.L., Meléndez, G., Lowrie, W., 1995. Oxfordian magnetostratigraphy in the Iberian Range. Geophys. Res. Lett. 22, 2889–2892.
Juárez, M.T., Osete, M.L., Vegas, R., Langereis, C.G., Meléndez, G., 1996. Palaeomagnetic study of Jurassic limestones from the Iberian Range (Spain): tectonic implications. Geol. Soc., Lond., Spec. Publ. 105, 83–90.
Juárez, M.T., Lowrie, W., Osete, M.L., Meléndez, G., 1998. Evidence of widespread Cretaceous remagnetisation in the Iberian Range and its relation with the rotation of Iberia. Earth Planet. Sci. Lett. 160, 729–743.
Kamberis, E., Sotiropoulos, S., Aximniotou, O., Tsaila-Monopoli, S., Ioakim, C., 2000. Late Cenozoic deformation of the Gavrovo and Ionian zones in NW Peloponnesos (western Greece). Ann. Geophys. 43.
Karakhanyan, A.K., 1986. Paleomagnetic Directions and Pole Positions: Data for the USSR. Soviet Geophysical Committee, World Data Center-B, Moscow.
Karamata, S., 2006. The geological development of the Balkan Peninsula related to the approach, collision and compression of Gondwanan and Eurasian units. Geol. Soc., Lond., Spec. Publ. 260, 155–178.
Karamata, S., Krstić, B., Dimitrijević, M.D., Knežević, V., Dimitrijević, M.N., Filipović, I., 1994. Terranes between the Adriatic and the Carpatho-Balkan Arc. In: Bulletin CVIII de l'Acad. Serbe des Sciences et des Arts, Classe des Sciences Naturelles et Mathematiques, vol. 35, pp. 47–68.
Karaoğlan, F., Parlak, O., Klötzli, U., Thöni, M., Koller, F., 2012. U–Pb and Sm–Nd geochronology of the ophiolites from the SE Turkey: implications for the Neotethyan evolution. Geodin. Acta 25, 146–161.
Karaoğlan, F., Parlak, O., Klötzli, U., Koller, F., Rızaoğlu, T., 2013a. Age and duration of intra-oceanic arc volcanism built on a supra-subduction zone type oceanic crust in southern Neotethys, SE Anatolia. Geosci. Front. 4, 399–408.
Karaoğlan, F., Parlak, O., Robertson, A., Thöni, M., Klötzli, U., Koller, F., Okay, A.İ., 2013b. Evidence of Eocene high-temperature/high-pressure metamorphism of ophiolitic rocks and granitoid intrusion related to Neotethyan subduction processes (Doğanşehir area, SE Anatolia). Geol. Soc., Lond., Spec. Publ. 372, 321. SP372.
Karaoğlu, Ö., Selçuk, A.S., Gudmundsson, A., 2017. Tectonic controls on the Karlıova triple junction (Turkey): implications for tectonic inversion and the initiation of volcanism. Tectonophysics 694, 368–384.
Karapetian, S., Jrbashian, R., Mnatsakanian, A.K., 2001. Late collision rhyolitic volcanism in the north-eastern part of the Armenian Highland. J. Volcanol. Geotherm. Res. 112, 189–220.
Karkoshkin, A.I., 1979. Paleomagnetic Directions and Pole Positions: Data for the USSR. Soviet Geophysical Committee, World Data Center-B, Moscow.
Karkoshkin, A.I., 1982. Paleomagnetic directions and pole positions: Data for the USSR. Soviet Geophysical Committee, World Data Center-B, Moscow.
Kastelic, V., Vannoli, P., Burrato, P., Fracassi, U., Tiberti, M.M., Valensise, G., 2013. Seismogenic sources in the Adriatic Domain. Mar. Pet. Geol. 42, 191–213.
Kastens, K.A., 1991. Rate of outward growth of the Mediterranean Ridge accretionary complex. Tectonophysics 199, 25–50.
Kavak, K.Ş., Parlak, O., Temiz, H., 2017. Geochemical characteristics of ophiolitic rocks from the southern margin of the Sivas basin and their implications for the Inner Tauride Ocean, Central-Eastern Turkey. Geodin. Acta 29, 160–180.
Kaygusuz, A., Arslan, M., Siebel, W., Sipahi, F., Ilbeyli, N., 2012. Geochronological evidence and tectonic significance of Carboniferous magmatism in the southwest Trabzon area, eastern Pontides, Turkey. Int. Geol. Rev. 54, 1776–1800.
Kaymakcı, N., Duermeijer, C.E., Langereis, C.O.R., White, S.H., Van Dijk, P.M., 2003. Palaeomagnetic evolution of the Cankırı Basin (central Anatolia, Turkey): implications for oroclinal bending due to indentation. Geol. Mag. 140, 343–355.
Kaymakcı, N., Özçelik, Y., White, S.H., Van Dijk, P.M., 2009. Tectono-stratigraphy of the Çankırı Basin: late Cretaceous to early Miocene evolution of the Neotethyan Suture Zone in Turkey. Geol. Soc., Lond., Spec. Publ. 311, 67–106.
Kaymakcı, N., Inceöz, M., Ertepinar, P., Koç, A., 2010. Late Cretaceous to Recent kinematics of SE Anatolia (Turkey). Geol. Soc., Lond., Spec. Publ. 340, 409–435.
Kaymakcı, N., Langereis, C., Özkaptan, M., Özacar, A.A., Gülyüz, E., Üzel, B., Sözbilir, H., 2018. Paleomagnetic evidence for upper plate response to a STEP fault, SW Anatolia. Earth Planet. Sci. Lett. 498, 101–115.
Kazmin, V., Schreider, A., Bulychev, A., 2000. Early stages of evolution of the Black Sea. Geol. Soc., Lond., Spec. Publ. 173, 235–249.
Keay, S., Lister, G., 2002. African provenance for the metasediments and metaigneous rocks of the Cyclades, Aegean Sea, Greece. Geology 30, 235–238.
Keller, P., Lowrie, W., Gehring, A.U., 1994. Palaeomagnetic evidence for post-thrusting tectonic rotation in the Southeast Pyrenees, Spain. Tectonophysics 239, 29–42.
Kelley, S.P., Platt, J.P., 1999. 22. Ar-Ar dating of biotite and muscovite from Alboran basement samples, site 976. Proc. Ocean Drill. Program, Sci. Results 161, 301.
Kempf, O., Pfiffner, A.O., 2004. Early Tertiary evolution of the North Alpine Foreland Basin of the Swiss Alps and adjoining areas. Basin Res. 16, 549–567.
Kempf, O., Schlunegger, F., Strunck, P., Matter, A., 1998. Palaeomagnetic evidence for late Miocene rotation of the Swiss Alps: results from the north Alpine foreland basin. Terra Nova 10, 6–10.
Kempler, D., 1998. Eratoshenes seamount: the possible spearhead of incipient continental collision in the eastern Mediterranean. Proc. Ocean Drill. Program, Sci. Results 160, 709–721.
Keskin, M., Pearce, J.A., Mitchell, J., 1998. Volcano-stratigraphy and geochemistry of collision-related volcanism on the Erzurum–Kars Plateau, northeastern Turkey. J. Volcanol. Geotherm. Res. 85, 355–404.
Ketin, I., 1948. Über die tektonisch-mechanischen Folgerungen aus den grossen anatolischen Erdbeben des letzten Dezenniums. Geol. Rundsch. 36, 77–83.
Khaburzaniya, I.A., 1982. Paleomagnetic Directions and Pole Positions: Data for the USSR. Soviet Geophysical Committee, World Data Center-B, Moscow.
Khalafov, A.A., 1986. Paleomagnetic Directions and Pole Positions: Data for the USSR. Soviet Geophysical Committee, World Data Center-B, Moscow.
Khalatbari-Jafari, M., Juteau, T., Bellon, H., Emami, H., 2003. Discovery of two ophiolite complexes of different ages in the Khoy area (NW Iran). Compt. Rendus Geosci. 335, 917–929.

Khalatbari-Jafari, M., Juteau, T., Bellon, H., Whitechurch, H., Cotten, J., Emami, H., 2004. New geological, geochronological and geochemical investigations on the Khoy ophiolites and related formations, NW Iran. J. Asian Earth Sci. 23, 507–535.
Khramov, A., 1973. Paleomagnetic Directions and Pole Positions: Data for the USSR. Soviet Geophysical Committee, World Data Center-B, Moscow.
Khramov, A., 1975. Paleomagnetic Directions and Pole Positions: Data for the USSR. Soviet Geophysical Committee, World Data Center-B, Moscow.
Khramov, A., 1979. Paleomagnetic Directions and Pole Positions: Data for the USSR. Soviet Geophysical Committee, World Data Center-B, Moscow.
Khramov, A., 1982. Paleomagnetic Directions and Pole Positions: Data for the USSR. Soviet Geophysical Committee, World Data Center-B, Moscow.
Khriachtchevskaia, O., Stovba, S., Stephenson, R., 2010. Cretaceous–Neogene tectonic evolution of the northern margin of the Black Sea from seismic reflection data and tectonic subsidence analysis. Geol. Soc., Lond., Spec. Publ. 340, 137–157.
Kie, T.H., 1988. Magnetotectonics in the Piemont Tertiary basin. Phys. Earth Planet. Inter. 52, 308–319.
Kilias, A., Frisch, W., Avgerinas, A., Dunkl, I., Falalakis, G., Gawlick, H.-J., 2010. Alpine architecture and kinematics of deformation of the northern Pelagonian nappe pile in the Hellenides. Austrian J. Earth Sci. 103, 4–28.
Kilzi, M.A., Grégoire, M., Bosse, V., Benoît, M., Driouch, Y., de Saint Blanquat, M., Debat, P., 2016. Geochemistry and zircon U–Pb geochronology of the ultramafic and mafic rocks emplaced within the anatectic series of the Variscan Pyrenees: the example of the Gavarnie–Heas dome (France). Compt. Rendus Geosci. 348, 107–115.
Kinnaird, T.C., Robertson, A.H.F., Morris, A., 2011. Timing of uplift of the Troodos Massif (Cyprus) constrained by sedimentary and magnetic polarity evidence. J. Geol. Soc. 168, 457–470.
Kirchner, K.L., Behr, W.M., Loewy, S., Stockli, D.F., 2016. early Miocene subduction in the western Mediterranean: constraints from Rb-Sr multimineral isochron geochronology. Geochem. Geophys. Geosyst. 17, 1842–1860.
Kirscher, U., Aubele, K., Muttoni, G., Ronchi, A., Bachtadse, V., 2011. Paleomagnetism of Jurassic carbonate rocks from Sardinia: no indication of post-Jurassic internal block rotations. J. Geophys. Res. 116.
Kirscher, U., Oms, O., Bruch, A., Shatilova, I., Chochishvili, G., Bachtadse, V., 2017. The Calabrian in the Western Transcaucasian basin (Georgia): paleomagnetic constraints from the Gurian regional stage. Quat. Sci. Rev. 160, 96–107.
Kirschvink, J.L., 1980. The least-squares line and plane and the analysis of palaeomagnetic data. Geophys. J. Royal Astron. Soc. 62, 699–718.
Kisch, H.J., 1981. Burial diagenesis in Tertiary "flysch" of the external zones of the Hellenides in central Greece and the Olympos region, and its tectonic significance. Eclogae Geol. Helv. 74, 603–624.
Kissel, C., Laj, C., 1988. The Tertiary geodynamical evolution of the Aegean arc: a paleomagnetic reconstruction. Tectonophysics 146, 183–201.
Kissel, C., Poisson, A., 1986. Etude paléomagnétique préliminaire des formations néogènes du bassin d'Antalya (Taurides occidentales-Turquie). In: Comptes rendus de l'Académie des sciences. Série 2, Mécanique, Physique, Chimie, Sciences de l'univers, Sciences de la Terre, vol. 302, pp. 711–716.
Kissel, C., Poisson, A., 1987. Étude paléomagnetique préliminaire des formations cénozoïques des Beydağları (Taurides occidentales, Turquie). In: Comptes rendus de l'Académie des sciences. Série 2, Mécanique, Physique, Chimie, Sciences de l'univers, Sciences de la Terre, vol. 304, pp. 343–348.
Kissel, C., Laj, C., Müller, C., 1985. Tertiary geodynamical evolution of northwestern Greece: paleomagnetic results. Earth Planet. Sci. Lett. 72, 190–204.
Kissel, C., Kondopoulou, D., Laj, C., Papadopoulos, P., 1986a. New paleomagnetic data from Oligocene formations of northern Aegea. Geophys. Res. Lett. 13, 1039–1042.
Kissel, C., Laj, C., Poisson, A., Savaşçin, Y., Simeakis, K., Mercier, J.L., 1986b. Paleomagnetic evidence for Neogene rotational deformations in the Aegean domain. Tectonics 5, 783–795.
Kissel, C., Laj, C., Poisson, A., Simeakis, K., 1989. A Pattern of Block Rotations in Central Aegea, Paleomagnetic Rotations and Continental Deformation. Springer, pp. 115–129.
Kissel, C., Speranza, F., Milicevic, V., 1995. Paleomagnetism of external southern and central Dinarides and northern Albanides: implications for the Cenozoic activity of the Scutari-Pec Transverse Zone. J. Geophys. Res.: Solid Earth 100, 14999–15007.
Kissel, C., Laj, C., Poisson, A., Görür, N., 2003. Paleomagnetic reconstruction of the Cenozoic evolution of the Eastern Mediterranean. Tectonophysics 362, 199–217.
Kligfield, R., Hunziker, J., Dallmeyer, R.D., Schamel, S., 1986. Dating of deformation phases using K-Ar and 40Ar/39Ar techniques: results from the Northern Apennines. J. Struct. Geol. 8, 781–798.
Klitgord, K., Schouten, H., 1986. Plate kinematics of the central Atlantic. In: Vogt, P.R., Tucholke, B.E. (Eds.), The Western North Atlantic Region. Geological Society of America, pp. 351–378.
Klötzli, U.S., Buda, G., Skiöld, T., 2004. Zircon typology, geochronology and whole rock Sr–Nd isotope systematics of the Mecsek Mountain granitoids in the Tisia Terrane (Hungary). Miner. Petrol. 81, 113–134.
Knipper, A., Khain, E., 1980. Structural position of ophiolites of the Caucasus. Ofioliti 2, 297–314.
Knott, S.D., Turco, E., 1991. Late Cenozoic kinematics of the Calabrian arc, Southern Italy. Tectonics 10, 1164–1172.
Kocak, K., Leake, B.E., 1994. The petrology of the Ortakoy district and its ophiolite at the western edge of the Middle Anatolian Massif, Turkey. J. Afr. Earth Sci. 18, 163–174.
Kock, S., Martini, R., Reischmann, T., Stampfli, G.M., 2007. Detrital zircon and micropalaeontological ages as new constraints for the lowermost tectonic unit (Talea Ori unit) of Crete, Greece. Palaeogeogr. Palaeoclimatol. Palaeoecol. 243, 307–321.
Kockel, F., 1977. Erläuterungen zur Geologischen Karte der Chalkidhiki und angrenzender Gebiete 1: 100 000 (Nord-Griechenland). Bundesanstalt für Geowissenschaften und Rohstoffe.
Kockel, F., 1986. Die Vardar-(Axios) Zone. Geologie von Griechenland, pp. 150–168.
Koepke, J., Seidel, E., Kreuzer, H., 2002. Ophiolites on the Southern Aegean islands Crete, Karpathos and Rhodes: composition, geochronology and position within the ophiolite belts of the Eastern Mediterranean. Lithos 65, 183–203.
Koglin, N., Kostopoulos, D., Reischmann, T., 2009. Geochemistry, petrogenesis and tectonic setting of the Samothraki mafic suite, NE Greece: trace-element, isotopic and zircon age constraints. Tectonophysics 473, 53–68.
Kondopoulou, D., Lauer, J.P., 1984. Palaeomagnetic data from Tertiary units of the north Aegean zone. Geol. Soc., Lond., Spec. Publ. 17, 681–686.
Kondopoulou, D., Westphal, M., 1986. Paleomagnetism of the Tertiary intrusives from Chalkidiki (northern Greece). J. Geophys.-Z. Geophys. 59, 62–66.
Kondopoulou, D., Sen, S., Aidona, E., van Hinsbergen, D.J.J., Koufos, G., 2011. Rotation history of Chios Island, Greece since the middle Miocene. J. Geodyn. 51, 327–338.
Korbar, T., 2009. Orogenic evolution of the External Dinarides in the NE Adriatic region: a model constrained by tectonostratigraphy of Upper Cretaceous to Paleogene carbonates. Earth-Sci. Rev. 96, 296–312.
Kotlyar, G.V., Baud, A., Pronina, G.P., Zakharov, Y.D., Vuks, V.Y., Nestell, M.K., Belyaeva, G.V., Marcoux, J., 1999. Permian and Triassic exotic limestone blocks of the Crimea. Geodiversitas 21, 299–323.
Kounov, A., Schmid, S.M., 2012. Fission-track constraints on the thermal and tectonic evolution of the Apuseni Mountains (Romania). Int. J. Earth Sci. 102, 207–233.
Kounov, A., Seward, D., Bernoulli, D., Burg, J.P., Ivanov, Z., 2004. Thermotectonic evolution of an extensional dome: the Cenozoic Osogovo-Lisets core complex (Kraishte zone, western Bulgaria). Int. J. Earth Sci. 93, 1008–1024.
Kounov, A., Seward, D., Burg, J.-P., Bernoulli, D., Ivanov, Z., Handler, R., 2010. Geochronological and structural constraints on the Cretaceous thermotectonic evolution of the Kraishte zone, western Bulgaria. Tectonics 29.
Kounov, A., Wüthrich, E., Seward, D., Burg, J.-P., Stockli, D., 2015. Low-temperature constraints on the Cenozoic thermal evolution of the Southern Rhodope Core Complex (Northern Greece). Int. J. Earth Sci. 104, 1337–1352.
Kováč, M., Plašienka, D., Soták, J., Vojtko, R., Oszczypko, N., Less, G., Ćosović, V., Fügenschuh, B., Králiková, S., 2016. Paleogene palaeogeography and basin evolution of the Western Carpathians, Northern Pannonian domain and adjoining areas. Glob. Planet. Change 140, 9–27.
Kowalczyk, G., Zügel, P., 1997. Die Vatia-Schichten-Flysch der Plattenkalk-Serie des Peloponnes. Cour. Forsch. Inst. Senckenberg 201, 259–275.
Koymans, M.R., Langereis, C.G., Pastor-Galán, D., van Hinsbergen, D.J.J., 2016. Paleomagnetism.org: an online multi-platform open source environment for paleomagnetic data analysis. Comput. Geosci. 127–137.
Koç, A., Kaymakcı, N., 2013. Kinematics of Sürgü Fault Zone (Malatya, Turkey): a remote sensing study. J. Geodyn. 65, 292–307.
Koç, A., van Hinsbergen, D.J.J., Kaymakcı, N., Langereis, C.G., 2016. Late Neogene oroclinal bending in the central Taurides: a record of terminal eastward subduction in southern Turkey? Earth Planet. Sci. Lett. 434, 75–90.
Koç, A., Kaymakcı, N., Van Hinsbergen, D.J.J., Kuiper, K.F., 2017. Miocene tectonic history of the Central Tauride intramontane basins, and the paleogeographic evolution of the Central Anatolian Plateau. Glob. Planet. Change 158, 83–102.
Koç, A., van Hinsbergen, D.J., Langereis, C.G., 2018. Rotations of normal fault blocks quantify extension in the Central Tauride intramontane basins, SW Turkey. Tectonics 37, 2307–2327.
Koçbulut, F., Akpınar, Z., Tatar, O., Piper, J.D.A., Roberts, A.P., 2013. Palaeomagnetic study of the Karacadağ Volcanic Complex, SE Turkey: monitoring Neogene anticlockwise rotation of the Arabian Plate. Tectonophysics 608, 1007–1024.
Koçyiğit, A., 1991. An example of an accretionary forearc basin from northern Central Anatolia and its implications for the history of subduction of Neo-Tethys in Turkey. Geol. Soc. Am. Bull. 103, 22–36.
Krahl, J., Kauffmann, G., Kozur, H., Richter, D., Förster, O., Heinritzi, F., 1983. Neue Daten zur biostratigraphie und zur tektonischen lagerung der Phyllit-Gruppe und der Trypali-Gruppe auf der Insel Kreta (Griechenland). Geol. Rundsch. 72, 1147–1166.
Krahl, J., Kauffmann, G., Richter, D., Kozur, H., Möller, I., Förster, O., Heinritzi, F., Dornsiepen, U., 1986. Neue Fossilfunde in der Phyllit-Gruppe Ostkretas (Griechenland). Z. Deutsch. Geol. Ges. 523–536.
Kräutner, H.G., Bindea, G., 2002. Structural units in the pre-Alpine basement of the eastern Carpathians. Geol. Carpathia 53.
Kräutner, H.G., Krstić, B., 2002. Alpine and Pre-Alpine structural units within the Southern Carpathians and the Eastern Balkanides. In: Proceedings of XVII. Congress of Carpathian-Balkan Geological Association Bratislava.
Kreemer, C., Holt, W.E., Haines, A.J., 2003. An integrated global model of present-day plate motions and plate boundary deformation. Geophys. J. Int. 154, 8–34.
Krenn, K., Bauer, C., Proyer, A., Mposkos, E., Hoinkes, G., 2008. Fluid entrapment and reequilibration during subduction and exhumation: a case study from the high-grade Nestos shear zone, Central Rhodope, Greece. Lithos 104, 33–53.
Krenn, K., Bauer, C., Proyer, A., Klötzli, U., Hoinkes, G., 2010. Tectonometamorphic evolution of the Rhodope orogen. Tectonics 29.
Kreuzer, H., Harre, W., Lenz, H., Wendt, I., Henjes-Kunst, F., Okrusch, M., 1978. K/Ar- und Rb/Sr-Daten von Mineralen aus dem polymetamorphen Kristallin der

Kykladen-Insel Ios (Griechenland). Fortschritte der Mineralogie 56, 69–70.
Krézsek, C., Bally, A.W., 2006. The Transylvanian Basin (Romania) and its relation to the Carpathian fold and thrust belt: insights in gravitational salt tectonics. Mar. Pet. Geol. 23, 405–442.
Krézsek, C., Filipescu, S., Silye, L., Maţenco, L., Doust, H., 2010. Miocene facies associations and sedimentary evolution of the Southern Transylvanian Basin (Romania): implications for hydrocarbon exploration. Mar. Pet. Geol. 27, 191–214.
Krézsek, C., Lăpădat, A., Maţenco, L., Arnberger, K., Barbu, V., Olaru, R., 2013. Strain partitioning at orogenic contacts during rotation, strike–slip and oblique convergence: paleogene–early Miocene evolution of the contact between the South Carpathians and Moesia. Glob. Planet. Change 103, 63–81.
Krijgsman, W., Duermeijer, C.E., Langereis, C.G., de Bruijn, H., Saraç, G., Andriessen, P.A.M., 1996. Magnetic polarity stratigraphy of late Oligocene to middle Miocene mammal-bearing continental deposits in central Anatolia (Turkey). Newslett. Stratigr. 13–29.
Krijgsman, W., Blanc-Valleron, M.-M., Flecker, R., Hilgen, F., Kouwenhoven, T., Merle, D., Orszag-Sperber, F., Rouchy, J.-M., 2002. The onset of the Messinian salinity crisis in the Eastern Mediterranean (Pissouri Basin, Cyprus). Earth Planet. Sci. Lett. 194, 299–310.
Krohe, A., 1987. Kinematics of Cretaceous nappe tectonics in the Austroalpine basement of the Koralpe region (eastern Austria). Tectonophysics 136, 171–196.
Krs, M., Krsová, M., Pruner, P., 1996. Palaeomagnetism and palaeogeography of the Western Carpathians from the Permian to the Neogene. Geol. Soc., Lond., Spec. Publ. 105, 175–184.
Krzywiec, P., 2001. Contrasting tectonic and sedimentary history of the central and eastern parts of the Polish Carpathian foredeep basin—results of seismic data interpretation. Mar. Pet. Geol. 18, 13–38.
Kukoč, D., Goričan, Š., Košir, A., Belak, M., Halamić, J., Hrvatović, H., 2015. Middle Jurassic age of basalts and the post-obduction sedimentary sequence in the Guevgueli Ophiolite Complex (Republic of Macedonia). Int. J. Earth Sci. 104, 435–447.
Kurz, W., Handler, R., Bertoldi, C., 2008. Tracing the exhumation of the Eclogite Zone (Tauern Window, Eastern Alps) by 40Ar/39Ar dating of white mica in eclogites. Swiss J. Geosci. 101, 191–206.
Kuşcu, İ., Gencalioğlu Kuşcu, G., Tosdal, R.M., Ulrich, T.D., Friedman, R., 2010. Magmatism in the southeastern Anatolian orogenic belt: transition from arc to post-collisional setting in an evolving orogen. Geol. Soc., Lond., Spec. Publ. 340, 437–460.
Kuşcu, İ., Tosdal, R.M., Gencalioğlu-Kuşcu, G., Friedman, R., Ullrich, T.D., 2013. Late Cretaceous to middle Eocene magmatism and metallogeny of a portion of the Southeastern Anatolian orogenic belt, East-Central Turkey. Econ. Geol. 108, 641–666.
Kydonakis, K., Gallagher, K., Brun, J.-P., Jolivet, M., Gueydan, F., Kostopoulos, D., 2014. Upper Cretaceous exhumation of the western Rhodope Metamorphic Province (Chalkidiki Peninsula, northern Greece). Tectonics 33, 1113–1132.
Kydonakis, K., Brun, J.-P., Poujol, M., Monié, P., Chatzitheodoridis, E., 2016. Inferences on the Mesozoic evolution of the North Aegean from the isotopic record of the Chalkidiki block. Tectonophysics 682, 65–84.
Labails, C., 2007. La Marge Sud-Marocaine et les Premières Phases D'ouverture de l'océan Atlantique Central. Géosciences Marines. Université de Bretagne Occidentale, p. 280.
Labails, C., Olivet, J.-L., Aslanian, D., Roest, W.R., 2010. An alternative early opening scenario for the Central Atlantic Ocean. Earth Planet. Sci. Lett. 297, 355–368.
Lacombe, O., Jolivet, L., 2005. Structural and kinematic relationships between Corsica and the Pyrenees-Provence domain at the time of the Pyrenean orogeny. Tectonics 24.
Lagabrielle, Y., Labaume, P., de Saint Blanquat, M., 2010. Mantle exhumation, crustal denudation, and gravity tectonics during Cretaceous rifting in the Pyrenean realm (SW Europe): insights from the geological setting of the lherzolite bodies. Tectonics 29.
Lagabrielle, Y., Vitale Brovarone, A., Ildefonse, B., 2015. Fossil oceanic core complexes recognized in the blueschist metaophiolites of Western Alps and Corsica. Earth-Sci. Rev. 141, 1–26.
Lahondère, D., Guerrot, C., 1997. Datation Sm–Nd du métamorphisme éclogitique en Corse alpine: un argument pour l'existence au Crétacé supérieur d'une zone de subduction active localisée sous le bloc corso-sarde. Géol. France 3, 3–11.
Laj, C., Jamet, M., Sorel, D., Valente, J.P., 1982. First paleomagnetic results from Mio-Pliocene series of the Hellenic sedimentary arc. Tectonophysics 86, 45–67.
Lalomov, A.V., 2007. Reconstruction of paleohydrodynamic conditions during the formation of Upper Jurassic conglomerates of the Crimean Peninsula. Lithol. Miner. Resour. 42, 268–280.
Lampert, S.A., Lowrie, W., Hirt, A.M., Bernoulli, D., Mutti, M., 1997. Magnetic and sequence stratigraphy of redeposited Upper Cretaceous limestones in the Montagna della Maiella, Abruzzi, Italy. Earth Planet. Sci. Lett. 150, 79–93.
Lanari, P., Rolland, Y., Schwartz, S., Vidal, O., Guillot, S., Tricart, P., Dumont, T., 2014. P-T-testimation of deformation in low-grade quartz-feldspar-bearing rocks using thermodynamic modelling and40Ar/39Ar dating techniques: example of the Plan-de-Phasy shear zone unit (Briançonnais Zone, Western Alps). Terra Nova 26, 130–138.
Lanci, L., Lowrie, W., Montanari, A., 1998. Stratigrafia magnetica ad alta risoluzione del limite Eocene-Oligocene nella successione Umbro-Marchigiana. Rendiconti Lincei 9, 103–123.
Langone, A., Gueguen, E., Prosser, G., Caggianelli, A., Rottura, A., 2006. The Curinga-Girifalco fault zone (northern Serre, Calabria) and its significance within the Alpine tectonic evolution of the western Mediterranean. J. Geodyn. 42, 140–158.
Larrasoaña, J., Parés, J., del Valle, J.n., Millán Garrido, H., 2003a. Triassic paleomagnetism from the Western Pyrenees revisited: implications for the Iberian–Eurasian Mesozoic plate boundary. Tectonophysics 362, 161–182.
Larrasoaña, J.C., Parés, J.M., Millán, H., del Valle, J., Pueyo, E.L., 2003b. Paleomagnetic, structural, and stratigraphic constraints on transverse fault kinematics during basin inversion: the Pamplona Fault (Pyrenees, north Spain). Tectonics 22.
Latal, C., Scholger, R., Preisinger, A., 2000. Paleomagnetic investigations imply rotations within the cretaceous-tertiary transition section at Cerbara (Italy). Phys. Chem. Earth, Part A: Solid Earth Geod. 25, 499–503.
Le Breton, E., Handy, M.R., Molli, G., Ustaszewski, K., 2017. Post-20 Ma Motion of the Adriatic Plate: new Constraints From Surrounding Orogens and Implications for Crust-Mantle Decoupling. Tectonics 36, 3135–3154.
Le Pichon, X., Şengör, C., İmren, C., 2019. A new approach to the opening of the Eastern Mediterranean Sea and the origin of the Hellenic Subduction Zone Part 1: the Eastern Mediterranean Sea. Can. J. Earth Sci. (in press).
Leever, K.A., Maţenco, L., Bertotti, G., Cloetingh, S., Drijkoningen, G.G., 2006. Late orogenic vertical movements in the Carpathian Bend Zone - seismic constraints on the transition zone from orogen to foredeep. Basin Res. 18, 521–545.
Lefebvre, C., 2011. The Tectonics of the Central Anatolian Crystalline Complex: a Structural, Metamorphic and Paleomagnetic Study (PhD thesis).
Lefebvre, C., Barnhoorn, A., van Hinsbergen, D.J.J., Kaymakcı, N., Vissers, R.L.M., 2011. Late Cretaceous extensional denudation along a marble detachment fault zone in the Kırşehir massif near Kaman, central Turkey. J. Struct. Geol. 33, 1220–1236.
Lefebvre, C., Meijers, M.J.M., Kaymakcı, N., Peynircioğlu, A., Langereis, C.G., van Hinsbergen, D.J.J., 2013a. Reconstructing the geometry of central Anatolia during the late Cretaceous: large-scale Cenozoic rotations and deformation between the Pontides and Taurides. Earth Planet. Sci. Lett. 366, 83–98.
Lefebvre, C., Umhoefer, P., Kaymakcı, N., Meijers, M., Teyssier, C., Whitney, D., Reid, M., Gencalioğlu Kuşcu, G., Cosca, M., Brocard, G., 2013b. The Gürün Curl, SE Turkey: a Potential Link from Crustal Tectonics to Mantle Dynamics in the Arabia-Eurasia Collision-Escape Zone. AGU Fall Meeting Abstracts.
Lefebvre, C., Peters, M.K., Wehrens, P.C., Brouwer, F.M., van Roermund, H.L.M., 2015. Thermal history and extensional exhumation of a high-temperature crystalline complex (Hırkadağ Massif, Central Anatolia). Lithos 238, 156–173.
Legeay, E., Pichat, A., Kergaravat, C., Ribes, C., Callot, J.-P., Ringenbach, J.-C., Bonnel, C., Hoareau, G., Poisson, A., Mohn, G., 2018. Geology of the Central Sivas Basin (Turkey). J. Maps 1–12.
Lenkey, L., 1999. Geothermics of the Pannonian Basin and its Bearing on the Tectonics of Basin Evolution. Vrije Universiteit, Amsterdam.
Lenoir, X., Garrido, C.J., Bodinier, J.-L., Dautria, J.-M., Gervilla, F., 2001. The Recrystallization Front of the Ronda Peridotite: evidence for Melting and Thermal Erosion of Subcontinental Lithospheric Mantle beneath the Alboran Basin. J. Petrol. 42, 141–158.
Lentini, F., Carbone, S., Di Stefano, A., Guarnieri, P., 2002. Stratigraphical and structural constraints in the Lucanian Apennines (southern Italy): tools for reconstructing the geological evolution. J. Geodyn. 34, 141–158.
Lesić, V., Márton, E., Cvetkov, V., 2007. Paleomagnetic detection of Tertiary rotations in the Southern Pannonian Basin (Fruška Gora). Geol. Carpathica 58, 185–193.
Lesić, V., Márton, E., Gajić, V., Jovanović, D., Cvetkov, V., 2017. Clockwise vertical-axis rotation in the West Vardar zone of Serbia: tectonic implications. Swiss J. Geosci. 1–17.
Letouzey, J., Biju-Duval, B., Dorkel, A., Gonnard, R., Kristchev, K., Montadert, L., Sungurlu, O., 1977. The Black Sea: a marginal basin; geophysical and geological data. Technip, Paris. In: International Symposium on the Structural History of the Mediterranean Basins, pp. 363–376.
Li, X.-H., Faure, M., Lin, W., Manatschal, G., 2013. New isotopic constraints on age and magma genesis of an embryonic oceanic crust: the Chenaillet Ophiolite in the Western Alps. Lithos 160–161, 283–291.
Li, S., Advokaat, E.L., van Hinsbergen, D.J.J., Koymans, M., Deng, C., Zhu, R., 2017. Paleomagnetic constraints on the Mesozoic-Cenozoic paleolatitudinal and rotational history of Indochina and South China: review and updated kinematic reconstruction. Earth-Sci. Rev. 171, 58–77.
Liati, A., Gebauer, D., Fanning, C.M., 2004. The age of ophiolitic rocks of the Hellenides (Vourinos, Pindos, Crete): first U–Pb ion microprobe (SHRIMP) zircon ages. Chem. Geol. 207, 171–188.
Liati, A., Froitzheim, N., Fanning, C.M., 2005. Jurassic ophiolites within the Valais domain of the Western and Central Alps: geochronological evidence for re-rifting of oceanic crust. Contrib. Miner. Petrol. 149, 446–461.
Liati, A., Gebauer, D., Fanning, C.M., 2011. Geochronology of the Alpine UHP Rhodope Zone: a Review of Isotopic Ages and Constraints on the Geodynamic Evolution. In: Dobrzhinetskaya, L.F., Faryad, S.W., Wallis, S., Cuthbert, S. (Eds.), Ultrahigh-Pressure Metamorphism. Elsevier, London, pp. 295–324.
Liati, A., Theye, T., Fanning, C.M., Gebauer, D., Rayner, N., 2016. Multiple subduction cycles in the Alpine orogeny, as recorded in single zircon crystals (Rhodope zone, Greece). Gondwana Res. 29, 199–207.
Licht, A., Coster, P., Ocakoğlu, F., Campbell, C., Métais, G., Mulch, A., Taylor, M., Kappelman, J., Beard, K.C., 2017. Tectono-stratigraphy of the Orhaniye Basin, Turkey: implications for collision chronology and Paleogene biogeography of central Anatolia. J. Asian Earth Sci. 143, 45–58.
Lippert, P.C., van Hinsbergen, D.J.J., Dupont-Nivet, G., 2014. Early Cretaceous to present latitude of the central proto-Tibetan Plateau: a paleomagnetic synthesis with implications for Cenozoic tectonics, paleogeography, and climate of Asia. Geol. Soc. Am. Spec. Pap. 507, 1–21.
Lips, A.L.W., Cassard, D., Sözbilir, H., Yılmaz, H., Wijbrans, J.R., 2001. Multistage

exhumation of the Menderes Massif, western Anatolia (Turkey). Int. J. Earth Sci. 89, 781–792.
Lonergan, L., 1993. Timing and kinematics of deformation in the Malaguide Complex, internal zone of the Betic Cordillera, southeast Spain. Tectonics 12, 460–476.
Lonergan, L., Mange-Rajetzky, M.A., 1994. Evidence for Internal Zone unroofing from foreland basin sediments, Betic Cordillera, SE Spain. J. Geol. Soc. 151, 515–529.
Lonergan, L., White, N., 1997. Origin of the Betic-Rif mountain belt. Tectonics 16, 504–522.
Loprieno, A., 2001. A Combined Structural and Sedimentological Approach to Decipher the Evolution of the Valais Domain in Savoy: (Western Alps), p. 285. PhD Thesis, Universität Basel.
Loprieno, A., Bousquet, R., Bucher, S., Ceriani, S., Dalla Torre, F.H., Fügenschuh, B., Schmid, S.M., 2010. The Valais units in Savoy (France): a key area for understanding the palaeogeography and the tectonic evolution of the Western Alps. Int. J. Earth Sci. 100, 963–992.
Lordkipanidze, M., Meliksetian, B., Djarbashian, R., 1989. Mesozoic–Cenozoic magmatic evolution of the Pontian–Crimean–Caucasian region. IGCP Project 198, 103–124.
Løvlie, R., Støle, G., Spjeldnæs, N., 1989. Magnetic polarity stratigraphy of Pliocene-Pleistocene marine sediments from Rhodos, eastern Mediterranean. Phys. Earth Planet. Inter. 54, 340–352.
Löwen, K., Bröcker, M., Berndt, J., 2014. Depositional ages of clastic metasediments from Samos and Syros, Greece: results of a detrital zircon study. Int. J. Earth Sci. 104, 205–220.
Lowrie, W., Alvarez, W., 1984. Lower Cretaceous magnetic stratigraphy in Umbrian pelagic limestone sections. Earth Planet. Sci. Lett. 71, 315–328.
Lowrie, W., Lanci, L., 1994. Magnetostratigraphy of Eocene-Oligocene boundary sections in Italy: no evidence for short subchrons within chrons 12R and 13R. Earth Planet. Sci. Lett. 126, 247–258.
Lucifora, S., Cifelli, F., Mattei, M., Sagnotti, L., Cosentino, D., Roberts, A.P., 2012. Inconsistent magnetic polarities in magnetite- and greigite-bearing sediments: understanding complex magnetizations in the late Messinian in the Adana Basin (southern Turkey). Geochem. Geophys. Geosyst. 13.
Lucifora, S., Cifelli, F., Rojay, F.B., Mattei, M., 2013. Paleomagnetic rotations in the late Miocene sequence from the Çankırı Basin (Central Anatolia, Turkey): the role of strike-slip tectonics. Turk. J. Earth Sci. 22, 778–792.
Lyberis, N., Yurur, T., Chorowicz, J., Kasapoğlu, E., Gundogdu, N., 1992. The East Anatolian Fault: an oblique collisional belt. Tectonophysics 204, 1–15.
Macchiavelli, C., Vergés, J., Schettino, A., Fernàndez, M., Turco, E., Casciello, E., Torne, M., Pierantoni, P.P., Tunini, L., 2017. A new southern North Atlantic isochron map: insights into the drift of the Iberian plate since the Late Cretaceous. J. Geophys. Res.: Solid Earth 122, 9603–9626.
Mackintosh, P.W., Robertson, A.H., 2013. Sedimentary and structural evidence for two-phase Upper Cretaceous and Eocene emplacement of the Tauride thrust sheets in central southern Turkey. Geol. Soc., Lond., Spec. Publ. 372, 299–322.
Maddy, D., Schreve, D., Demir, T., Veldkamp, A., Wijbrans, J.R., van Gorp, W., van Hinsbergen, D.J.J., Dekkers, M.J., Scaife, R., Schoorl, J.M., Stemerdink, C., van der Schriek, T., 2015. The earliest securely-dated hominin artefact in Anatolia? Quat. Sci. Rev. 109, 68–75.
Maddy, D., Veldkamp, A., Demir, T., van Gorp, W., Wijbrans, J.R., van Hinsbergen, D.J.J., Dekkers, M.J., Schreve, D., Schoorl, J.M., Scaife, R., Stemerdink, C., van der Schriek, T., Bridgland, D.R., Aytaç, A.S., 2017. The Gediz River fluvial archive: a benchmark for Quaternary research in Western Anatolia. Quat. Sci. Rev. 166, 289–306.
Maffione, M., van Hinsbergen, D.J.J., 2018. Reconstructing plate boundaries in the Jurassic Neo-Tethys from the East and West Vardar Ophiolites (Greece, Serbia). Tectonics 37, 858–887.
Maffione, M., Speranza, F., Faccenna, C., Cascella, A., Vignaroli, G., Sagnotti, L., 2008. A synchronous Alpine and Corsica-Sardinia rotation. J. Geophys. Res. 113.
Maffione, M., Morris, A., Anderson, M.W., 2013a. Recognizing detachment-mode seafloor spreading in the deep geological past. Sci. Rep. 3, 2336.
Maffione, M., Speranza, F., Cascella, A., Longhitano, S.G., Chiarella, D., 2013b. A ~125° post-early Serravallian counterclockwise rotation of the Gorgoglione Formation (Southern Apennines, Italy): new constraints for the formation of the Calabrian Arc. Tectonophysics 590, 24–37.
Maffione, M., Thieulot, C., van Hinsbergen, D.J.J., Morris, A., Plümper, O., Spakman, W., 2015. Dynamics of intraoceanic subduction initiation: 1. Oceanic detachment fault inversion and the formation of supra-subduction zone ophiolites. Geochem. Geophys. Geosyst. 16, 1753–1770.
Maffione, M., Hinsbergen, D.J.J., Gelder, G.I.N.O., Goes, F.C., Morris, A., 2017. Kinematics of Late Cretaceous subduction initiation in the Neo-Tethys Ocean reconstructed from ophiolites of Turkey, Cyprus, and Syria. J. Geophys. Res.: Solid Earth 122, 3953–3976, 701.
Maggi, M., Rossetti, F., Corfu, F., Theye, T., Andersen, T.B., Faccenna, C., 2012. Clinopyroxene-rutile phyllonites from the East Tenda Shear Zone (Alpine Corsica, France): pressure-temperature-time constraints to the Alpine reworking of Variscan Corsica. J. Geol. Soc. 169, 723–732.
Mahdjoub, Y., Choukroune, P., Kienast, J.P., 1997. Kinematics of a complex Alpine segment; superimposed tectonic and metamorphic events in the Petite Kabylie Massif (northern Algeria). Bull. Soc. Géol. France 168, 649–661.
Maillard, A., Mauffret, A., Watts, A.B., Torné, M., Pascal, G., Buhl, P., Pinet, B., 1992. Tertiary sedimentary history and structure of the Valencia trough (western Mediterranean). Tectonophysics 203, 57–75.
Malandri, C., Soukis, K., Maffione, M., Özkaptan, M., Vassilakis, E., Lozios, S., van Hinsbergen, D.J.J., 2017. Vertical-axis rotations accommodated along the Mid-Cycladic lineament on Paros Island in the extensional heart of the Aegean orocline (Greece). Lithosphere 9, 78–99.
Malasoma, A., Marroni, M., Musumeci, G., Pandolfi, L., 2006. High-pressure mineral assemblage in granitic rocks from continental units, Alpine Corsica, France. Geol. J. 41, 49–59.
Malinverno, A., Ryan, W.B.F., 1986. Extension in the Tyrrhenian Sea and shortening in the Apennines as result of arc migration driven by sinking of the lithosphere. Tectonics 5, 227–245.
Manatschal, G., Sauter, D., Karpoff, A.M., Masini, E., Mohn, G., Lagabrielle, Y., 2011. The Chenaillet Ophiolite in the French/Italian Alps: an ancient analogue for an Oceanic Core Complex? Lithos 124, 169–184.
Mancktelow, N.S., 1992. Neogene lateral extension during convergence in the Central Alps: evidence from interrelated faulting and backfolding around the Simplonpass (Switzerland). Tectonophysics 215, 295–317.
Mandic, O., Sant, K., Kallanxhi, M.-E., Ćorić, S., Theobalt, D., Grunert, P., de Leeuw, A., Krijgsman, W., 2018. Integrated bio-magnetostratigraphy of the Badenian reference section Ugljevik in southern Pannonian Basin-implications for the Paratethys history (middle Miocene, Central Europe). Glob. Planet. Change.
Manzotti, P., Ballèvre, M., Zucali, M., Robyr, M., Engi, M., 2014. The tectonometamorphic evolution of the Sesia–Dent Blanche nappes (internal Western Alps): review and synthesis. Swiss J. Geosci. 107, 309–336.
Marcucci, M., 1996. The Lumi i zi (Puke) section of the Kalur cherts: radiolarian assemblages and comparison with other sections in northern Albania. Ofioliti 21, 71–76.
Marcucci, M., Kodra, A., Pirdeni, A., Gjata, T., 1994. Radiolarian assemblage in the Triassic and Jurassic cherts of Albania. Ofioliti 19, 105–114.
Maron, M., Muttoni, G., Dekkers, M.J., Mazza, M., Roghi, G., Breda, A., Krijgsman, W., Rigo, M., 2017. Contribution to the magnetostratigraphy of the Carnian: new magneto-biostratigraphic constraints from Pignola-2 and Dibona marine sections. Italy. Newslett. Stratigr. 50, 187–203.
Marovic, M., Djokovic, I., Toljic, M., Spahic, D., Milivojevic, J., 2007. Extensional unroofing of the Veliki Jastrebac dome (Serbia). Geoloski Anali Balk. Poluostrva 21–27.
Marroni, M., Pandolfi, L., 1996. The deformation history of an accreted ophiolite sequence: the Internal Liguride units (Northern Apennines, Italy). Geodin. Acta 9, 13–29.
Marroni, M., Pandolfi, L., 2003. Deformation history of the ophiolite sequence from the Balagne Nappe, northern Corsica: insights in the tectonic evolution of Alpine Corsica. Geol. J. 38, 67–83.
Marroni, M., Pandolfi, L., 2007. The architecture of an incipient oceanic basin: a tentative reconstruction of the Jurassic Liguria-Piemonte basin along the Northern Apennines–Alpine Corsica transect. Int. J. Earth Sci. 96, 1059–1078.
Marroni, M., Treves, B., 1998. Hidden Terranes in the Northern Apennines, Italy: a Record of Late Cretaceous- Oligocene Transpressional Tectonics. J. Geol. 106, 149–162.
Marroni, M., Della Croce, G., Meccheri, M., 1988. Structural evolution of the M. Gottero Unit in the M. Zatta/M. Ghiffi sector, Ligurian-Emilian Apennines, Italy. Ofioliti 13, 29–42.
Marroni, M., Molli, G., Ottria, G., Pandolfi, L., 2001. Tectono-sedimentary evolution of the External Liguride units (Northern Apennines, Italy): insights in the pre-collisional history of a fossil ocean-continent transition zone. Geodin. Acta 14, 307–320.
Marroni, M., Pandolfi, L., Ribecai, C., 2004. Palynological dating of the Alturaia Arkose (Balagne, northern Corsica): geological implications. Comptes Rendus Palevol 3, 643–651.
Marroni, M., Meneghini, F., Pandolfi, L., 2010. Anatomy of the Ligure-Piemontese subduction system: evidence from Late Cretaceous–middle Eocene convergent margin deposits in the Northern Apennines, Italy. Int. Geol. Rev. 52, 1160–1192.
Marsellos, A.E., Kidd, W.S.F., Garver, J.I., 2010. Extension and exhumation of the HP/LT rocks in the Hellenic forearc ridge. Am. J. Sci. 310, 1–36.
Marsellos, A., Foster, D.A., Kamenov, G., Kyriakopoulos, K., 2012. Detrital zircon U-Pb data from the Hellenic south Aegean belts: constraints on the age and source of the South Aegean basement. J. Virtual Explor. 42, 1–12.
Martin, M., Wenzel, F., 2006. High-resolution teleseismic body wave tomography beneath SE-Romania - II. Imaging of a slab detachment scenario. Geophys. J. Int. 164, 579–595.
Martin, L.A.J., Rubatto, D., Vitale Brovarone, A., Hermann, J., 2011. late Eocene lawsonite-eclogite facies metasomatism of a granulite sliver associated to ophiolites in Alpine Corsica. Lithos 125, 620–640.
Martin-Rojas, I., Somma, R., Delgado, F., EsteVez, A., Iannace, A., Perrone, V., Zamparelli, V., 2009. Triassic continental rifting of Pangaea: direct evidence from the Alpujarride carbonates, Betic Cordillera, SE Spain. J. Geol. Soc. 166, 447–458.
Martínez-García, P., Comas, M., Soto, J.I., Lonergan, L., Watts, A.B., 2013. Strike-slip tectonics and basin inversion in the Western Mediterranean: the Post-Messinian evolution of the Alboran Sea. Basin Res. 25, 361–387.
Márton, E., 2002. The bending model of the Transdanubian Central Range (Hungary) in the light of Triassic palaeomagnetic data. Geophys. J. Int. 134, 625–633.
Márton, P., D'Andrea, M., 1992. Palaeomagnetically inferred tectonic rotations of the Abruzzi and northwestern Umbria. Tectonophysics 202, 43–53.
Márton, E., Fodor, L., 2003. Tertiary paleomagnetic results and structural analysis from the Transdanubian Range (Hungary): rotational disintegration of the Alcapa unit. Tectonophysics 363, 201–224.

Márton, E., Márton, P., 1996. Large scale rotations in North Hungary during the Neogene as indicated by palaeomagnetic data. Geol. Soc., Lond., Spec. Publ. 105, 153–173.
Márton, E., Moro, A., 2009. New paleomagnetic results from imbricated Adria: Ist Island and related areas. Geologia Croatica 62, 107–114.
Márton, E., Nardi, G., 1994. Cretaceous palaeomagnetic results from Murge (Apulia, southern Italy): tectonic implications. Geophys. J. Int. 119, 842–856.
Márton, E., Veljovic, D., 1983. Paleomagnetism of the Istria peninsula, Yugoslavia. Tectonophysics 91, 73–87.
Márton, E., Milicevic, V., Veljovic, D., 1990a. Paleomagnetism of the Kvarner islands, Yugoslavia. Phys. Earth Planet. Inter. 62, 70–81.
Márton, E., Papanikolaou, D.J., Lekkas, E., 1990b. Paleomagnetic results from the Pindos, Paxos, and Ionian zones of Greece. Phys. Earth Planet. Inter. 62, 60–69.
Márton, E., Pagac, P., Túnyi, I., 1992. Paleomagnetic investigations on Late Cretaceous-Cenozoic sediments from the NW part of the Pannonian Basin. Geol. Carpathica 43, 363–368.
Márton, E., Vass, D., Túnyi, I., 1996. Rotation of the South Slovak Paleogene and lower Miocene rocks indicated by paleomagnetic data. Geol. Carpathica 47, 31–41.
Márton, E., Mastella, L., Tokarski, A.K., 1999. Large counterclockwise rotation of the Inner West Carpathian Paleogene Flysch—Evidence from paleomagnetic investigations of the Podhale Flysch (Poland). Phys. Chem. Earth, Part A: Solid Earth Geod. 24, 645–649.
Márton, E., Kuhlemann, J., Frisch, W., Dunkl, I., 2000a. Miocene rotations in the Eastern Alps — palaeomagnetic results from intramontane basin sediments. Tectonophysics 323, 163–182.
Márton, E., Vass, D., Túnyi, I., 2000b. Counterclockwise rotations of the Neogene rocks in the East Slovak Basin. Geol. Carpathica 51, 159–168.
Márton, E., Fodor, L., Jelen, B., Márton, P., Rifelj, H., Kevrić, R., 2002a. Miocene to Quaternary deformation in NE Slovenia: complex paleomagnetic and structural study. J. Geodyn. 34, 627–651.
Márton, E., Pavelić, D., Tomljenović, B., Avanić, R., Pamić, J., Márton, P., 2002b. In the wake of a counterclockwise rotating Adriatic microplate: neogene paleomagnetic results from northern Croatia. Int. J. Earth Sci. 91, 514–523.
Márton, E., Drobne, K., Ćosović, V., Moro, A., 2003. Palaeomagnetic evidence for Tertiary counterclockwise rotation of Adria. Tectonophysics 377, 143–156.
Márton, E., Abranches, M.C., Pais, J., 2004. Iberia in the Cretaceous: new paleomagnetic results from Portugal. J. Geodyn. 38, 209–221.
Márton, E., Jelen, B., Tomljenović, B., Pavelić, D., poljak, M., Avanić, R., pamić, J., 2006. Late Neogene counterclockwise rotation in the SW part of the Pannonian Basin. Geol. Carpathica 57, 41–46.
Márton, E., Ćosović, V., Moro, A., Zvocak, S., 2008. The motion of Adria during the Late Jurassic and Cretaceous: new paleomagnetic results from stable Istria. Tectonophysics 454, 44–53.
Márton, E., Jelenska, M., Tokarski, A.K., Soták, J., Kovác, M., Spišiak, J., 2009a. Current-independent paleomagnetic declinations in flysch basins: a case study from the Inner Carpathians. Geodin. Acta 22, 73–82.
Márton, E., Rauch, M., Krejčí, O., Tokarski, A., Bubík, M., 2009b. An integrated palaeomagnetic and AMS study of the Tertiary flysh from the Outer Western Carpathians. Geophys. J. Int. 177, 925–940.
Márton, E., Rauch-Włodarska, M., Krejčí, O., Tokarski, A.K., Bubík, M., 2009c. An integrated palaeomagnetic and AMS study of the Tertiary flysch from the Outer Western Carpathians. Geophys. J. Int. 177, 925–940.
Márton, E., Ćosović, V., Bucković, D., Moro, A., 2010a. The tectonic development of the Northern Adriatic region constrained by Jurassic and Cretaceous paleomagnetic results. Tectonophysics 490, 93–102.
Márton, E., Zampieri, D., Grandesso, P., Ćosović, V., Moro, A., 2010b. New Cretaceous paleomagnetic results from the foreland of the Southern Alps and the refined apparent polar wander path for stable Adria. Tectonophysics 480, 57–72.
Márton, E., Tokarski, A.K., Krejčí, O., Rauch, M., Olszewska, B., Petrová, P.T., Wójcik, A., 2011a. 'Non-European' Palaeomagnetic Directions from the Carpathian Foredeep at the Southern Margin of the European Plate. Terra Nova no-no.
Márton, E., Zampieri, D., Kázmér, M., Dunkl, I., Frisch, W., 2011b. New Paleocene–Eocene paleomagnetic results from the foreland of the Southern Alps confirm decoupling of stable Adria from the African plate. Tectonophysics 504, 89–99.
Márton, E., Grabowski, J., Plašienka, D., Túnyi, I., Krobicki, M., Haas, J., Pethe, M., 2013. New paleomagnetic results from the Upper Cretaceous red marls of the Pieniny Klippen Belt, Western Carpathians: evidence for general CCW rotation and implications for the origin of the structural arc formation. Tectonophysics 592, 1–13.
Márton, E., Ćosović, V., Moro, A., 2014. New stepping stones, Dugi otok and Vis islands, in the systematic paleomagnetic study of the Adriatic region and their significance in evaluations of existing tectonic models. Tectonophysics 611, 141–154.
Márton, E., Pavelić, D., Vranjković, A., Ćosović, V., 2016. Reappraisal of the palaeomagnetism of the Miocene intramontane Pag and Drniš–Sinj basins, External Dinarides (Croatia). Tectonophysics 676, 125–134.
Márton, E., Zampieri, D., Ćosović, V., Moro, A., Drobne, K., 2017. Apparent polar wander path for Adria extended by new Jurassic paleomagnetic results from its stable core: tectonic implications. Tectonophysics 700–701, 1–18.
Măruntiu, M., Ménot, R.P., Tapardel, C., 1997. Cryptic variation and geochemistry of cumulate pile from Tisovita-Iuți ophiolite : preliminary approach of magma chamber evolution and tectonic setting. In: Geology of the Danube Gorges, International Symposium, Milanovac - Orsova. Institute of Geology, Belgrade.
Maţenco, L., Bertotti, G., Dinu, C., Cloetingh, S., 1997. Tertiary tectonic evolution of the external South Carpathians and the adjacent Moesian platform (Romania). Tectonics 16 (6), 896–911.
Mattei, M., Funiciello, R., Kissel, C., 1995. Paleomagnetic and structural evidence for Neogene block rotations in the Central Apennines, Italy. J. Geophys. Res.: Solid Earth 100, 17863–17883.
Mattei, M., Kissel, C., Funiciello, R., 1996. No tectonic rotation of the Tuscan Tyrrhenian margin (Italy) since Late Messinian. J. Geophys. Res.: Solid Earth 101, 2835–2845.
Mattei, M., Cipollari, P., Cosentino, D., Argentieri, A., Rossetti, F., Speranza, F., Di Bella, L., 2002. The Miocene tectono-sedimentary evolution of the southern Tyrrhenian Sea: stratigraphy, structural and palaeomagnetic data from the on-shore Amantea basin (Calabrian Arc, Italy). Basin Res. 14, 147–168.
Mattei, M., D'Agostino, N., Zananiri, I., Kondopoulou, D., Pavlides, S., Spatharas, V., 2004. Tectonic evolution of fault-bounded continental blocks: comparison of paleomagnetic and GPS data in the Corinth and Megara basins (Greece). J. Geophys. Res.: Solid Earth 109.
Mattei, M., Cifelli, F., Rojas, I.M., Crespo Blanc, A., Comas, M., Faccenna, C., Porreca, M., 2006. Neogene tectonic evolution of the Gibraltar Arc: new paleomagnetic constraints from the Betic chain. Earth Planet. Sci. Lett. 250, 522–540.
Mauffret, A., Maldonado, A., Campillo, A.C., 1992. Tectonic framework of the eastern Alboran and western Algerian Basins, Western Mediterranean. Geo-Mar. Lett. 12, 104–110.
Mauffret, A., Frizon de Lamotte, D., Lallemant, S., Gorini, C., Maillard, A., 2004. E-W opening of the Algerian Basin (Western Mediterranean). Terra Nova 16, 257–264.
Mauritsch, H.J., Scholger, R., Bushati, S.L., Ramiz, H., 1995. Palaeomagnetic results from southern Albania and their significance for the geodynamic evolution of the Dinarides, Albanides and Hellenides. Tectonophysics 242, 5–18.
Mauritsch, H., Scholger, R., Bushati, S., Xhomo, A., 1996. Palaeomagnetic investigations in Northern Albania and their significance for the geodynamic evolution of the Adriatic-Aegean realm. Geol. Soc., Lon., Spec. Publ. 105, 265–275.
Maury, R.C., Fourcade, S., Coulon, C., El Azzouzi, M.h., Bellon, H., Coutelle, A., Ouabadi, A., Semroud, B., Megartsi, M.h., Cotten, J., Belanteur, O., Louni-Hacini, A., Piqué, A., Capdevila, R., Hernandez, J., Réhault, J.-P., 2000. Post-collisional Neogene Magmatism of the Mediterranean Maghreb Margin: a Consequence of Slab Breakoff. In: Comptes Rendus de l'Académie des Sciences - Series IIA - Earth and Planetary Science, vol. 331, pp. 159–173.
Mazzoli, S., Barkham, S., Cello, G., Gambini, R., Mattioni, L., Shiner, P., Tondi, E., 2001a. Reconstruction of continental margin architecture deformed by the contraction of the Lagonegro Basin, Southern Apennines, Italy. J. Geol. Soc. 158, 309–319.
Mazzoli, S., Lanci, L., De Donatis, M., 2001b. Paleomagnetic rotations in thrust belts: a case-study from the Marche–Romagna area (Northern Apennines, Italy). J. Geodyn. 32, 373–393.
Mazzoli, S., D'Errico, M., Aldega, L., Corrado, S., Invernizzi, C., Shiner, P., Zattin, M., 2008. Tectonic burial and "young" (<10 Ma) exhumation in the Southern Apennines fold-and-thrust belt (Italy). Geology 36.
Maţenco, L., 2017. Tectonics and Exhumation of Romanian Carpathians: Inferences from Kinematic and Thermochronological Studies, Landform Dynamics and Evolution in Romania. Springer, pp. 15–56.
Maţenco, L., Radivojević, D., 2012. On the formation and evolution of the Pannonian Basin: constraints derived from the structure of the junction area between the Carpathians and Dinarides. Tectonics 31.
Maţenco, L., Schmid, S., 1999. Exhumation of the Danubian nappes system (South Carpathians) during the Early Tertiary: inferences from kinematic and paleostress analysis at the Getic/Danubian nappes contact. Tectonophysics 314, 401–422.
Maţenco, L., Bertotti, G., Leever, K., Cloetingh, S., Schmid, S.M., Tărăpoancă, M., Dinu, C., 2007. Large-scale deformation in a locked collisional boundary: interplay between subsidence and uplift, intraplate stress, and inherited lithospheric structure in the late stage of the SE Carpathians evolution. Tectonics 26.
Maţenco, L., Krézsek, C., Merten, S., Schmid, S., Cloetingh, S., Andriessen, P., 2010. Characteristics of collisional orogens with low topographic build-up: an example from the Carpathians. Terra Nova 22, 155–165.
Maţenco, L., Munteanu, I., ter Borgh, M., Stanica, A., Tilita, M., Lericolais, G., Dinu, C., Oaie, G., 2016. The interplay between tectonics, sediment dynamics and gateways evolution in the Danube system from the Pannonian Basin to the western Black Sea. Sci. Total Environ. 543, 807–827.
McCann, T., Chalot-Prat, F., Saintot, A., 2010. The Early Mesozoic evolution of the Western Greater Caucasus (Russia): triassic–Jurassic sedimentary and magmatic history. Geol. Soc., Lond., Spec. Publ. 340, 181.
McCay, G.A., Robertson, A.H.F., 2012. late Eocene–Neogene sedimentary geology of the Girne (Kyrenia) Range, Northern Cyprus: a case history of sedimentation related to progressive and diachronous continental collision. Sediment. Geol. 265–266, 30–55.
McKenzie, D.P., Parker, R.L., 1967. The North Pacific: an example of tectonics on a sphere. Nature 216, 1276–1280.
McPhee, P.J., van Hinsbergen, D.J.J., 2019. Tectonic reconstruction of Cyprus reveals late Miocene continental collision between Africa and Anatolia. Gondwana Res. 68, 158–173.
McPhee, P.J., Altıner, D., van Hinsbergen, D.J.J., 2018a. First Balanced Cross Section Across the Taurides Fold-Thrust Belt: geological Constraints on the Subduction History of the Antalya Slab in Southern Anatolia. Tectonics 37, 3738–3759.

McPhee, P.J., van Hinsbergen, D.J.J., Maffione, M., Altiner, D., 2018b. Palinspastic reconstruction versus cross-section balancing: how complete is the Central Taurides fold-thrust belt (Turkey)? Tectonics 37, 4535–4566.
McPhee, P.J., van Hinsbergen, D.J.J., Thomson, S., 2019. Denudation and Submergence of the Taurides Fold-and-Thrust Belt Preceding the Rise of the Central Anatolian Plateau. Geology 15, 1927–1942.
McQuarrie, N., van Hinsbergen, D.J.J., 2013. Retrodeforming the Arabia-Eurasia collision zone: age of collision versus magnitude of continental subduction. Geology 41, 315–318.
Medaris, G., Ducea, M., Ghent, E., Iancu, V., 2003. Conditions and timing of high-pressure Variscan metamorphism in the South Carpathians, Romania. Lithos 70, 141–161.
Mederer, J., Moritz, R., Ulianov, A., Chiaradia, M., 2013. Middle Jurassic to Cenozoic evolution of arc magmatism during Neotethys subduction and arc-continent collision in the Kapan Zone, southern Armenia. Lithos 177, 61–78.
Mederer, J., Moritz, R., Zohrabyan, S., Vardanyan, A., Melkonyan, R., Ulianov, A., 2014. Base and precious metal mineralization in Middle Jurassic rocks of the Lesser Caucasus: a review of geology and metallogeny and new data from the Kapan, Alaverdi and Mehmana districts. Ore Geol. Rev. 58, 185–207.
Medialdea, T., Vegas, R., Somoza, L., Vázquez, J.T., Maldonado, A., Díaz-del-Río, V., Maestro, A., Córdoba, D., Fernández-Puga, M.C., 2004. Structure and evolution of the "Olistostrome" complex of the Gibraltar Arc in the Gulf of Cádiz (eastern Central Atlantic): evidence from two long seismic cross-sections. Mar. Geol. 209, 173–198.
Meijers, M.J.M., Kaymakcı, N., van Hinsbergen, D.J.J., Langereis, C.G., Stephenson, R.A., Hippolyte, J.-C., 2010a. Late Cretaceous to Paleocene oroclinal bending in the central Pontides (Turkey). Tectonics 29, TC4016. https://doi.org/10.1029/2009TC00262.
Meijers, M.J.M., Langereis, C.G., van Hinsbergen, D.J.J., Kaymakcı, N., Stephenson, R.A., Altıner, D., 2010b. Jurassic–Cretaceous low paleolatitudes from the circum-Black Sea region (Crimea and Pontides) due to True Polar Wander. Earth Planet. Sci. Lett. 296, 210–226.
Meijers, M.J.M., Vrouwe, B., van Hinsbergen, D.J.J., Kuiper, K.F., Wijbrans, J., Davies, G.R., Stephenson, R.A., Kaymakcı, N., Maţenco, L., Saintot, A., 2010c. Jurassic arc volcanism on Crimea (Ukraine): implications for the paleo-subduction zone configuration of the Black Sea region. Lithos 119, 412–426.
Meijers, M.J.M., van Hinsbergen, D.J.J., Dekkers, M.J., Altıner, D., Kaymakcı, N., Langereis, C.G., 2011. Pervasive Palaeogene remagnetization of the central Taurides fold-and-thrust belt (southern Turkey) and implications for rotations in the Isparta Angle. Geophys. J. Int. 184, 1090–1112.
Meijers, M.J., Smith, B., Kirscher, U., Mensink, M., Sosson, M., Rolland, Y., Grigoryan, A., Sahakyan, L., Avagyan, A., Langereis, C., 2015a. A paleolatitude reconstruction of the South Armenian Block (Lesser Caucasus) for the Late Cretaceous: constraints on the Tethyan realm. Tectonophysics 644, 197–219.
Meijers, M.J.M., Smith, B., Kirscher, U., Mensink, M., Sosson, M., Rolland, Y., Grigoryan, A., Sahakyan, L., Avagyan, A., Langereis, C., Müller, C., 2015b. A paleolatitude reconstruction of the South Armenian Block (Lesser Caucasus) for the Late Cretaceous: constraints on the Tethyan realm. Tectonophysics 644–645, 197–219.
Meijers, M.J.M., Strauss, B.E., Özkaptan, M., Feinberg, J.M., Mulch, A., Whitney, D.L., Kaymakçı, N., 2016. Age and paleoenvironmental reconstruction of partially remagnetized lacustrine sedimentary rocks (Oligocene Aktoprak basin, central Anatolia, Turkey). Geochem. Geophys. Geosyst. 17, 914–939.
Meijers, M.J.M., Smith, B., Pastor-Galán, D., Degenaar, R., Sadradze, N., Adamia, S., Sahakyan, L., Avagyan, A., Sosson, M., Rolland, Y., Langereis, C.G., Müller, C., 2017. Progressive orocline formation in the Eastern Pontides–Lesser Caucasus. Geol. Soc., Lond., Spec. Publ. 428, 117–143.
Meijninger, B.M.L., Vissers, R.L.M., 2007. Thrust-related extension in the Prebetic (Southern Spain) and closure of the North Betic Strait. Rev. Soc. Geol. España 20, 153–171.
Meinhold, G., Kostopoulos, D.K., 2013. The Circum-Rhodope Belt, northern Greece: age, provenance, and tectonic setting. Tectonophysics 595–596, 55–68.
Menant, A., Jolivet, L., Vrielynck, B., 2016. Kinematic reconstructions and magmatic evolution illuminating crustal and mantle dynamics of the eastern Mediterranean region since the late Cretaceous. Tectonophysics 675, 103–140.
Merten, S., 2011. Thermo-Tectonic Evolution of a Convergent Orogen with Low Topographic Build-up: Exhumation and Kinematic Patterns in the Romanian Carpathians Derived from Thermochronology. Vrije Universiteit Amsterdam.
Merten, S., Maţenco, L., Foeken, J.P.T., Stuart, F.M., Andriessen, P.A.M., 2010. From nappe stacking to out-of-sequence postcollisional deformations: cretaceous to Quaternary exhumation history of the SE Carpathians assessed by low-temperature thermochronology. Tectonics 29.
Merten, S., Maţenco, L., Foeken, J.P.T., Andriessen, P.A.M., 2011. Toward understanding the post-collisional evolution of an orogen influenced by convergence at adjacent plate margins: late Cretaceous-Tertiary thermotectonic history of the Apuseni Mountains. Tectonics 30.
Messina, A., Somma, R., Macaione, E., Carbone, G., Careri, G., 2004. Peloritani Continental Crust composition (Southern Italy): geological and petrochemical evidence. Boll. Soc. Geol. Ital., Vol. Spec. 123, 405–441.
Métois, M., D'Agostino, N., Avallone, A., Chamot-Rooke, N., Rabaute, A., Duni, L., Kuka, N., Koci, R., Georgiev, I., 2015. Insights on continental collisional processes from GPS data: dynamics of the peri-Adriatic belts. J. Geophys. Res.: Solid Earth 120, 8701–8719.
Meulenkamp, J.E., Sissingh, W., 2003. Tertiary palaeogeography and tectonostratigraphic evolution of the Northern and Southern Peri-Tethys platforms and the intermediate domains of the African–Eurasian convergent plate boundary zone. Palaeogeogr. Palaeoclimatol. Palaeoecol. 196, 209–228.
Michard, A., Whitechurch, H., Ricou, L.E., Montigny, R., Yazgan, E., 1984. Tauric subduction (Malatya-Elazığ provinces) and its bearing on tectonics of the Tethyan realm in Turkey. Geol. Soc., Lond., Spec. Publ. 17, 361–373.
Michard, A., Feinberg, H., El-Azzab, D., Bouybaouene, M., Saddiqi, O., 1992. A serpentinite ridge in a collisional paleomargin setting: the Beni Malek massif, External Rif, Morocco. Earth Planet. Sci. Lett. 113, 435–442.
Michard, A., Goffé, B., Liati, A., Mountrakis, D., 1994. Découverte du Faciès Schiste Bleu Dans les Nappes du Circum-Rhodope: Un Élément d'une Ceinture HP-BT Éohellénique en Grèce Septentrionale? Comptes Rendus de l'Académie des Sciences. In: Série 2. Sciences de la terre et des planètes, vol. 318, pp. 1535–1542.
Michard, A., Negro, F., Saddiqi, O., Bouybaouene, M.L., Chalouan, A., Montigny, R., Goffé, B., 2006. Pressure–temperature–time constraints on the Maghrebide mountain building: evidence from the Rif–Betic transect (Morocco, Spain), Algerian correlations, and geodynamic implications. Compt. Rendus Geosci. 338, 92–114.
Michard, A., Soulaimani, A., Hoepffner, C., Ouanaimi, H., Baidder, L., Rjimati, E., Saddiqi, O., 2010. The south-western branch of the Variscan Belt: evidence from Morocco. Tectonophysics 492, 1–24.
Michel, G.W., Waldhör, M., Neugebauer, J., Appel, E., 1995. Sequential rotation of stretching axes, and block rotations: a structural and paleomagnetic study along the North Anatolian Fault. Tectonophysics 243, 97–118.
Micheletti, F., Fornelli, A., Piccarreta, G., Barbey, P., Tiepolo, M., 2008. The basement of Calabria (southern Italy) within the context of the Southern European Variscides: LA-ICPMS and SIMS U–Pb zircon study. Lithos 104, 1–11.
Micheletti, F., Fornelli, A., Piccarreta, G., Tiepolo, M., 2009. U–Pb zircon data of Variscan meta-igneous and igneous acidic rocks from an Alpine shear zone in Calabria (southern Italy). Int. J. Earth Sci. 100, 139–155.
Midtkandal, I., Svensen, H.H., Planke, S., Corfu, F., Polteau, S., Torsvik, T.H., Faleide, J.I., Grundvåg, S.-A., Selnes, H., Kürschner, W., 2016. The Aptian (Early Cretaceous) oceanic anoxic event (OAE1a) in Svalbard, Barents Sea, and the absolute age of the Barremian-Aptian boundary. Palaeogeogr. Palaeoclimatol. Palaeoecol. 463, 126–135.
Mikes, T., Christ, D., Petri, R., Dunkl, I., Frei, D., Báldi-Beke, M., Reitner, J., Wemmer, K., Hrvatović, H., von Eynatten, H., 2008. Provenance of the Bosnian Flysch. Swiss J. Geosci. 101, 31–54.
Mikhailov, V.O., Panina, L.V., Polino, R., Koronovsky, N.V., Kiseleva, E.A., Klavdieva, N.V., Smolyaninova, E.I., 1999. Evolution of the North Caucasus foredeep: constraints based on the analysis of subsidence curves. Tectonophysics 307, 361–379.
Miladinova, I., Froitzheim, N., Nagel, T.J., Janák, M., Georgiev, N., Fonseca, R.O., Sandmann, S., Münker, C., 2018. Late Cretaceous eclogite in the Eastern Rhodopes (Bulgaria): evidence for subduction under the Sredna Gora magmatic arc. Int. J. Earth Sci. 1–17.
Miletto, M., Polino, R., 1992. A gravity model of the crust beneath the Tertiary Piemonte basin (northwestern Italy). Tectonophysics 212, 243–256.
Milia, A., Torrente, M.M., 2014. Early-stage rifting of the Southern Tyrrhenian region: the Calabria–Sardinia breakup. J. Geodyn. 81, 17–29.
Minasyan, D.O., Karakhanyan, A.K., 1982. Paleomagnetic Directions and Pole Positions: Data for the USSR. Soviet Geophysical Committee, World Data Center-B, Moscow.
Minasyan, D.O., Karakhanyan, A.K., 1986. Geomagnitnoe Pole v Armenii b Kaynozoe. Acad. Sci. Armenia SSR, Erevan.
Minasyan, D.O., Karakhanyan, A.K., 1989. Paleomagnetic Directions and Pole Positions: Data for the USSR. Soviet Geophysical Committee, World Data Center-B, Moscow.
Minasyan, D.O., Karakhanyan, A.K., 1991. O paleomagnetisme granitsi eotsena I oligotsena na primere razresa u s.Landzhar Y.Armenii. IV All-Union Congress on Geomagnetism. Vladimir-Suzdal 2, 80–81.
Minelli, L., Faccenna, C., 2010. Evolution of the Calabrian accretionary wedge (central Mediterranean). Tectonics 29.
Mirăuţă, E., 1982. Biostratigraphy of the Triassic deposits in the Somova-Sarica Hill zone (North Dobrogea) with special regard of the eruption age. In: Dări de seamă ale şedinţelor Institutului de Geologie şi Geofizică, vol. 64, pp. 63–78.
Mirăuţă, O., Mirăuţă, E., 1964. Prezenţa Devonianului mediu în zona colinelor Mahmudiei (Dobrogea de Nord). In: Dari de Seama ale Institutului de Geologie si Geofizica, vol. 52, pp. 275–289.
Moghadam, H.S., Stern, R.J., 2015. Ophiolites of Iran: keys to understanding the tectonic evolution of SW Asia:(II) Mesozoic ophiolites. J. Asian Earth Sci. 100, 31–59.
Moghadam, H.S., Corfu, F., Stern, R.J., Lotfibakhsh, A., 2019. The Eastern Khoy Metamorphic Complex of NW Iran: a Jurassic ophiolite or continuation of the Sanandaj-Sirjan Zone? J. Geol. Soc. (in press).
Moix, P., Goričan, Š., 2014. Jurassic and Cretaceous radiolarian assemblages from the Bornova mélange in northern Karaburun Peninsula (western Turkey) and its connection to the İzmir–Ankara mélanges. Geodin. Acta 26, 56–67.
Moix, P., Beccaletto, L., Kozur, H.W., Hochard, C., Rosselet, F., Stampfli, G.M., 2008. A new classification of the Turkish terranes and sutures and its implication for the paleotectonic history of the region. Tectonophysics 451, 7–39.
Moix, P., Beccaletto, L., Masset, O., Kozur, H., Dumitrica, P., Vachard, D., Martini, R., Stampfli, G., 2011. Geology and Correlation of the Mersin Mélanges, Southern Turkey. Turk. J. Earth Sci. 20, 57–98.
Molli, G., 2008. Northern Apennine–Corsica orogenic system: an updated overview. Geol. Soc., Lond., Spec. Publ. 298, 413–442.
Molli, G., Malavieille, J., 2010. Orogenic processes and the Corsica/Apennines

geodynamic evolution: insights from Taiwan. Int. J. Earth Sci. 100, 1207–1224.
Molli, G., Giorgetti, G., Meccheri, M., 2001. Structural and petrological constraints on the tectono-metamorphic evolution of the Massa Unit (Alpi Apuane, NW Tuscany, Italy). Geol. J. 35, 251–264.
Molli, G., Tribuzio, R., Marquer, D., 2006. Deformation and metamorphism at the eastern border of the Tenda Massif (NE Corsica): a record of subduction and exhumation of continental crust. J. Struct. Geol. 28, 1748–1766.
Molli, G., Crispini, L., Malusà, M., Mosca, P., Piana, F., Federico, L., 2010. Geology of the Western Alps-Northern Apennine junction area: a regional review. Eds.) Marco Beltrando, Angelo Peccerillo, Massimo Mattei, Sandro Conticelli, and Carlo Doglioni. J. Virtual Explor. 36, 3.
Monaco, C., Tortorici, L., 1995. Tectonic role of ophiolite-bearing terranes in the development of the Southern Apennines orogenic belt. Terra Nova 7, 153–160.
Monaco, C., Tortorici, L., Paltrinieri, W., 1998. Structural evolution of the Lucanian Apennines, southern Italy. J. Struct. Geol. 20, 617–638.
Monaco, C., Tortorici, L., Catalano, S., Paltrinieri, W., Steel, N., 2001. The role of Pleistocene strike-slip tectonics in the Neogene-Quaternary evolution of the southern Apennine orogenic belt: implications for oil trap development. J. Pet. Geol. 24, 339–359.
Monié, P., Torres-Roldán, R.L., García-Casco, A., 1994. Cooling and exhumation of the Western Betic Cordilleras, 40Ar/39Ar thermochronological constraints on a collapsed terrane. Tectonophysics 238, 353–379.
Monsef, I., Rahgoshay, M., Mohajjel, M., Moghadam, H.S., 2010. Peridotites from the Khoy Ophiolitic Complex, NW Iran: evidence of mantle dynamics in a supra-subduction-zone context. J. Asian Earth Sci. 38, 105–120.
Montadert, L., Roberts, D.G., de Charpal, O., Guennoc, P., 1979. Rifting and Subsidence of the Northern Continental Margin of the Bay of Biscay.
Moreau, M.G., Berthou, J.Y., Malod, J.-A., 1997. New paleomagnetic Mesozoic data from the Algarve (Portugal): fast rotation of Iberia between the Hauterivian and the Aptian. Earth Planet. Sci. Lett. 146, 689–701.
Moritz, R., Rezeau, H., Ovtcharova, M., Tayan, R., Melkonyan, R., Hovakimyan, S., Ramazanov, V., Selby, D., Ulianov, A., Chiaradia, M., 2016. Long-lived, stationary magmatism and pulsed porphyry systems during Tethyan subduction to post-collision evolution in the southernmost Lesser Caucasus, Armenia and Nakhitchevan. Gondwana Res. 37, 465–503.
Morley, C.K., 1988. Out-of-sequence thrusts. Tectonics 7, 539–561.
Morley, C.K., 1996. Models for relative motion of crustal blocks within the Carpathian region, based on restorations of the outer Carpathian thrust sheets. Tectonics 15, 885–904.
Morris, A., 1995. Rotational deformation during Palaeogene thrusting and basin closure in eastern central Greece: palaeomagnetic evidence from Mesozoic carbonates. Geophys. J. Int. 121, 827–847.
Morris, A., Anderson, M., 1996. First palaeomagnetic results from the Cycladic Massif, Greece, and their implications for Miocene extension directions and tectonic models in the Aegean. Earth Planet. Sci. Lett. 142, 397–408.
Morris, A., Anderson, M.W., 2002. Palaeomagnetic results from the Baër-Bassit ophiolite of northern Syria and their implication for fold tests in sheeted dyke terrains. Phys. Chem. Earth, Parts A/B/C 27, 1215–1222.
Morris, A., Maffione, M., 2016. Is the Troodos ophiolite (Cyprus) a complete, transform fault–bounded Neotethyan ridge segment? Geology 44, 199–202.
Morris, A., Robertson, A.H.F., 1993. Miocene remagnetisation of carbonate platform and Antalya Complex units within the Isparta angle, SW Turkey. Tectonophysics 220, 243–266.
Morris, A., Creer, K.M., Robertson, A.H.F., 1990. Palaeomagnetic evidence for clockwise rotations related to dextral shear along the Southern Troodos Transform Fault, Cyprus. Earth Planet. Sci. Lett. 99, 250–262.
Morris, A., Anderson, M.W., Robertson, A.H., 1998. Multiple tectonic rotations and transform tectonism in an intraoceanic suture zone, SW Cyprus. Tectonophysics 299, 229–253.
Morris, A., Anderson, M.W., Robertson, A.H., Al-Riyami, K., 2002. Extreme tectonic rotations within an eastern Mediterranean ophiolite (Baër–Bassit, Syria). Earth Planet. Sci. Lett. 202, 247–261.
Morris, A., Anderson, M.W., Inwood, J., Robertson, A.H.F., 2006. Palaeomagnetic insights into the evolution of Neotethyan oceanic crust in the eastern Mediterranean. Geol. Soc., Lond., Spec. Publ. 260, 351–372.
Morris, A., Robertson, A.H., Anderson, M.W., Hodgson, E., 2016. Did the Kyrenia Range of Northern Cyprus rotate with the Troodos–Hatay microplate during the tectonic evolution of the eastern Mediterranean? Int. J. Earth Sci. 105, 399–415.
Morris, A., Anderson, M.W., Omer, A., Maffione, M., van Hinsbergen, D.J.J., 2017. Rapid fore-arc extension and detachment-mode spreading following subduction initiation. Earth Planet. Sci. Lett. 478, 76–88.
Mosar, J., Kangarli, T., Bochud, M., Glasmacher, U.A., Rast, A., Brunet, M.-F., Sosson, M., 2010. Cenozoic-Recent tectonics and uplift in the Greater Caucasus: a perspective from Azerbaijan. Geol. Soc., Lond., Spec. Publ. 340, 261–280.
Mosca, P., Polino, R., Rogledi, S., Rossi, M., 2009. New data for the kinematic interpretation of the Alps–Apennines junction (Northwestern Italy). Int. J. Earth Sci. 99, 833–849.
Most, T., 2003. Geodynamic Evolution of the Eastern Pelagonian Zone in Northwestern Greece and the Republic of Macedonia, Implications from U/Pb, Rb/Sr, K/Ar, Ar/Ar, Geochronology and Fission Track Thermochronology. University of Tubingen, Phd, Germany, pp. 1–170.
Mostardini, F., Merlini, S., 1986. Appennino Centro Meridionale: Sezione Geologiche e Proposta di Modello Strutturale, vol. 73. Congresso Società Geologica Italiana.
Mourik, A.A., Bijkerk, J.F., Cascella, A., Hüsing, S.K., Hilgen, F.J., Lourens, L.J., Turco, E., 2010. Astronomical tuning of the La Vedova High Cliff section (Ancona, Italy)—Implications of the middle Miocene Climate Transition for Mediterranean sapropel formation. Earth Planet. Sci. Lett. 297, 249–261.
Mouthereau, F., 2011. Timing of uplift in the Zagros belt/Iranian plateau and accommodation of late Cenozoic Arabia–Eurasia convergence. Geol. Mag. 148, 726–738.
Mouthereau, F., Filleaudeau, P.-Y., Vacherat, A., Pik, R., Lacombe, O., Fellin, M.G., Castelltort, S., Christophoul, F., Masini, E., 2014. Placing limits to shortening evolution in the Pyrenees: role of margin architecture and implications for the Iberia/Europe convergence. Tectonics 33, 2283–2314.
Moyà-Solà, S., Köhler, M., Alba, D.M., Casanovas-Vilar, I., Galindo, J., Robles, J.M., Cabrera, L., Garcés, M., Almécija, S., Beamud, E., 2009. First partial face and upper dentition of the middle Miocene hominoid Dryopithecus fontani from Abocador de Can Mata (Vallès-Penedès Basin, Catalonia, NE Spain): taxonomic and phylogenetic implications. Am. J. Phys. Anthropol.: Off. Publ. Am. Assoc. Phys. Anthropol. 139, 126–145.
Muceku, B., van der Beek, P., Bernet, M., Reiners, P., Mascle, G., Tashko, A., 2008. Thermochronological evidence for Mio-Pliocene late orogenic extension in the north-eastern Albanides (Albania). Terra Nova 20, 180–187.
Mugnier, J.L., Guellec, S., Ménard, G., Roure, F., Tardy, M., Vialon, P., 1990. A crustal scale balanced cross-section through the external Alps deduced from the ECORS profile. Mém. Soc. Géol. France Geol. 170, 203–216.
Mukasa, S.B., Ludden, J.N., 1987. Uranium-lead isotopic ages of plagiogranites from the Troodos ophiolite, Cyprus, and their tectonic significance. Geology 15, 825–828.
Mulcahy, S.R., Vervoort, J.D., Renne, P.R., 2014. Dating subduction-zone metamorphism with combined garnet and lawsonite Lu–Hf geochronology. J. Metamorph. Geol. 32, 515–533.
Müller, D., Royer, J.-Y., Cande, S., Roest, W.R., Maschenkov, S., 1999. New constraints on the Late Cretaceous/Tertiary plate tectonic evolution of the Caribbean. Sediment. Basins World 33–59.
Müller, R.D., Sdrolias, M., Gaina, C., Roest, W.R., 2008. Age, spreading rates, and spreading asymmetry of the world's ocean crust. Geochem. Geophys. Geosyst. 9.
Muñoz, J.A., 1992. Evolution of a continental collision belt: ECORS-Pyrenees crustal balanced cross-section. In: McClay, K.R. (Ed.), Thrust Tectonics. Springer Netherlands, Dordrecht, pp. 235–246.
Munteanu, I., Matenco, L., Dinu, C., Cloetingh, S., 2011. Kinematics of back-arc inversion of the Western Black Sea Basin. Tectonics 30.
Muratov, M.V., Arkhipov, I.V., Uspenskaya, Y.A., 1984. Structural evolution of the Crimean mountains and comparison with the western Caucasus and the eastern Balkan ranges. Int. Geol. Rev. 26, 1259–1266.
Muttoni, G., Kent, D.V., 1994. Paleomagnetism of latest Anisian (Middle Triassic) sections of the Prezzo Limestone and the Buchenstein Formation, Southern Alps, Italy. Earth Planet. Sci. Lett. 122, 1–18.
Muttoni, G., Kent, D.V., Channell, J.E.T., 1996. Evolution of Pangea: paleomagnetic constraints from the Southern Alps, Italy. Earth Planet. Sci. Lett. 140, 97–112.
Muttoni, G., Argnani, A., Kent, D.V., Abrahamsen, N., Cibin, U., 1998. Paleomagnetic evidence for Neogene tectonic rotations in the Northern Apennines, Italy. Earth Planet. Sci. Lett. 154, 25–40.
Muttoni, G., Lanci, L., Argnani, A., Hirt, A.M., Cibin, U., Abrahamsen, N., Lowrie, W., 2000. Paleomagnetic evidence for a Neogene two-phase counterclockwise tectonic rotation in the Northern Apennines (Italy). Tectonophysics 326, 241–253.
Muttoni, G., Garzanti, E., Alfonsi, L., Cirilli, S., Germani, D., Lowrie, W., 2001. Motion of Africa and Adria since the Permian: paleomagnetic and paleoclimatic constraints from northern Libya. Earth Planet. Sci. Lett. 192, 159–174.
Muttoni, G., Kent, D.V., Garzanti, E., Brack, P., Abrahamsen, N., Gaetani, M., 2003. Early Permian Pangea 'B'to Late Permian Pangea 'A'. Earth Planet. Sci. Lett. 215, 379–394.
Muttoni, G., Kent, D.V., Olsen, P.E., Stefano, P.D., Lowrie, W., Bernasconi, S.M., Hernández, F.M., 2004. Tethyan magnetostratigraphy from Pizzo Mondello (Sicily) and correlation to the Late Triassic Newark astrochronological polarity time scale. GSA Bull. 116, 1043–1058.
Muttoni, G., Mattei, M., Balini, M., Zanchi, A., Gaetani, M., Berra, F., 2009. The drift history of Iran from the Ordovician to the Triassic. Geol. Soc., Lond., Spec. Publ. 312, 7–29.
Muttoni, G., Dallanave, E., Channell, J.E.T., 2013. The drift history of Adria and Africa from 280Ma to Present, Jurassic true polar wander, and zonal climate control on Tethyan sedimentary facies. Palaeogeogr. Palaeoclimatol. Palaeoecol. 386, 415–435.
Nagel, T.J., Schmidt, S., Janák, M., Froitzheim, N., Jahn-Awe, S., Georgiev, N., 2011. The exposed base of a collapsing wedge: the Nestos shear zone (Rhodope Metamorphic Province, Greece). Tectonics 30.
Nairn, S.P., Robertson, A.H.F., Ünlügenç, U.C., Tasli, K., İnan, N., 2013. Tectonostratigraphic evolution of the Upper Cretaceous–Cenozoic central Anatolian basins: an integrated study of diachronous ocean basin closure and continental collision. Geol. Soc., Lond., Spec. Publ. 372, 343–384.
Natal'in, B.A., Şengör, A.M.C., 2005. Late Palaeozoic to Triassic evolution of the Turan and Scythian platforms: the pre-history of the Palaeo-Tethyan closure. Tectonophysics 404, 175–202.
Natal'in, B.A., Sunal, G., Gün, E., Wang, B., Zhiqing, Y., 2016. Precambrian to Early Cretaceous rocks of the Strandja Massif (northwestern Turkey): evolution of a long lasting magmatic arc. Can. J. Earth Sci. 53, 1312–1335.
Naydenov, K., Peytcheva, I., von Quadt, A., Sarov, S., Kolcheva, K., Dimov, D., 2013. The Maritsa strike-slip shear zone between Kostenets and Krichim towns, South Bulgaria — Structural, petrographic and isotope geochronology study.

Tectonophysics 595–596, 69–89.
Negro, F., Beyssac, O., Goffé, B., Saddiqi, O., Bouybaouene, M.L., 2006. Thermal structure of the Alboran Domain in the Rif (northern Morocco) and the Western Betics (southern Spain). Constraints from Raman spectroscopy of carbonaceous material. J. Metamorph. Geol. 24, 309–327.
Negro, F., Agard, P., Goffé, B., Saddiqi, O., 2007. Tectonic and metamorphic evolution of the Temsamane units, External Rif (northern Morocco): implications for the evolution of the Rif and the Betic–Rif arc. J. Geol. Soc. 164, 829–842.
Neill, I., Meliksetian, K., Allen, M., Navarsardyan, G., Karapetyan, S., 2013. Pliocene–Quaternary volcanic rocks of NW Armenia: magmatism and lithospheric dynamics within an active orogenic plateau. Lithos 180, 200–215.
Neill, I., Meliksetian, K., Allen, M.B., Navasardyan, G., Kuiper, K., 2015. Petrogenesis of mafic collision zone magmatism: the Armenian sector of the Turkish–Iranian Plateau. Chem. Geol. 403, 24–41.
Nemčok, M., Nemčok, J., Wojtaszek, M., Ludhova, L., Klecker, R.A., Sercombe, W.J., Coward, M.P., Keith, J.F., 2000. Results of 2D balancing along 20 and 21 30'longitude and pseudo-3D in the Smilno Tectonic Window: implications for shortening mechanisms of the West Carpathian accretionary wedge. Geol. Carpathica 51.
Nemčok, M., Krzywiec, P., Wojtaszek, M., Ludhová, L., Klecker, R.A., Sercombe, W.J., Coward, M.P., 2006. Tertiary development of the Polish and eastern Slovak parts of the Carpathian accretionary wedge: insights from balanced cross-sections. Geol. Carpathica 57, 355–370.
Neres, M., Font, E., Miranda, J.M., Camps, P., Terrinha, P., Mirão, J., 2012. Reconciling Cretaceous paleomagnetic and marine magnetic data for Iberia: new Iberian paleomagnetic poles. J. Geophys. Res.: Solid Earth 117.
Neubauer, F., Genser, J., Handler, R., 1999. The Eastern Alps: result of a two-stage collision process. Mitt. Österreichischen Geol. Ges. 92, 117–134.
Nicolae, I., Saccani, E., 2003. Petrology and geochemistry of the Late Jurassic calc-alkaline series associated to Middle Jurassic ophiolites in the South Apuseni Mountains (Romania). Swiss Bull. Miner. Petrol. 83, 81–96.
Nicolosi, I., Speranza, F., Chiappini, M., 2006. Ultrafast oceanic spreading of the Marsili Basin, southern Tyrrhenian Sea: evidence from magnetic anomaly analysis. Geology 34, 717–720.
Nievergelt, P., Liniger, M., Froitzheim, N., Mählmann, R.F., 1996. Early to mid Tertiary crustal extension in the Central Alps: the Turba mylonite zone (eastern Switzerland). Tectonics 15, 329–340.
Nikishin, A., Ziegler, P.A., Panov, D.I., Nazarevich, B.P., Brunet, M.-F., Stephenson, R., Bolotov, S., Tikhomirov, P., 2001. Mesozoic and Cainozoic Evolution of the Scythian Platform-Black Sea-Caucasus Domain. Mémoires du Muséum National d'Histoire Naturelle, pp. 295–346.
Nikishin, A., Ershov, A., Nikishin, V.A., 2010. Geological history of Western Caucasus and adjacent foredeeps based on analysis of the regional balanced section. Dokl. Earth Sci. 430, 155–157.
Nikishin, A.M., Okay, A., Tüysüz, O., Demirer, A., Wannier, M., Amelin, N., Petrov, E., 2015a. The Black Sea basins structure and history: new model based on new deep penetration regional seismic data. Part 2: tectonic history and paleogeography. Mar. Pet. Geol. 59, 656–670.
Nikishin, A.M., Okay, A.I., Tüysüz, O., Demirer, A., Amelin, N., Petrov, E., 2015b. The Black Sea basins structure and history: new model based on new deep penetration regional seismic data. Part 1: basins structure and fill. Mar. Pet. Geol. 59, 638–655.
Nikishin, A.M., Wannier, M., Alekseev, A.S., Almendinger, O.A., Fokin, P.A., Gabdullin, R.R., Khudoley, A.K., Kopaevich, L.F., Mityukov, A.V., Petrov, E.I., Rubtsova, E.V., 2015c. Mesozoic to Recent Geological History of Southern Crimea and the Eastern Black Sea region. Geological Society, London. Special Publications 428.
Nikogosian, I.K., Bracco Gartner, A.J.J., van Bergen, M.J., Mason, P.R.D., van Hinsbergen, D.J.J., 2018. Mantle sources of recent Anatolian intraplate magmatism: a regional plume or local tectonic origin? Tectonics 37, 4535–4566.
Nirrengarten, M., Manatschal, G., Tugend, J., Kusznir, N.J., Sauter, D., 2017. Nature and origin of the J-magnetic anomaly offshore Iberia-Newfoundland: implications for plate reconstructions. Terra Nova 29, 20–28.
Noguera, A.M., Rea, G., 2000. Deep structure of the Campanian–Lucanian Arc (Southern Apennine, Italy). Tectonophysics 324, 239–265.
Nurlu, N., Parlak, O., Robertson, A., von Quadt, A., 2016. Implications of Late Cretaceous U–Pb zircon ages of granitic intrusions cutting ophiolitic and volcanogenic rocks for the assembly of the Tauride allochthon in SE Anatolia (Helete area, Kahramanmaraş Region, SE Turkey). Int. J. Earth Sci. 105, 283–314.
Oaie, G., Seghedi, A., Radan, S., Vaida, M., 2005. Sedimentology and source area composition for the Neoproterozoic-Eocambrian turbidites from East Moesia. Geol. Bel. 84, 78–105.
Oberhänsli, R., Candan, O., Bousquet, R., Rimmele, G., Okay, A., Goff, J., 2010a. Alpine high pressure evolution of the eastern Bitlis complex, SE Turkey. Geol. Soc., Lond., Spec. Publ. 340, 461.
Oberhänsli, R., Candan, O., Wilke, F., 2010b. Geochronological Evidence of Pan-African Eclogites from the Central Menderes Massif, Turkey. Turk. J. Earth Sci. 19, 431–447.
Oberhänsli, R., Candan, O., Koralay, E., Bousquet, R., Okay, A., 2012. Dating Subduction Events in East Anatolia, Turkey. Turkish J Earth Sci 21, 1–17.
Oberhänsli, R., Koralay, E., Candan, O., Pourteau, A., Bousquet, R., 2014. Late Cretaceous eclogitic high-pressure relics in the Bitlis Massif. Geodin. Acta 26, 175–190.
Ogniben, L., 1960. Nota illustrativa dello schema geologico della Sicilia nord-orientale. Riv. Min. Sic 64, 183–212.
Ogniben, L., 1969. Schema introduttivo alla geologia del confine calabro-lucano. Mem. Soc. Geol. Ital. 8, 453–763.
Okay, A.I., 1981. Lawsonite zone blueschists and a sodic amphibole producing reaction in the Tavşanlı Region, Northwest Turkey. Contrib. Miner. Petrol. 75, 179–186.
Okay, A., 1984. Distribution and characteristics of the north-west Turkish blueschists. Geol. Soc., Lond., Spec. Publ. 17, 455–466.
Okay, A., 1989. Geology of the Menderes Massif and the Lycian Nappes south of Denizli, western Taurides. Miner. Resour. Explor. Bull. 109, 37–51.
Okay, A., Altıner, D., 2007. A condensed Mesozoic section in the Bornova Flysch Zone: a fragment of the Anatolide-Tauride carbonate platform. Turk. J. Earth Sci. 16, 257–279.
Okay, A., Göncüoğlu, M.C., 2004. The Karakaya complex: a review of data and concepts. Turk. J. Earth Sci. 13, 77–95.
Okay, A.I., Monié, P., 1997. Early Mesozoic subduction in the Eastern Mediterranean: evidence from Triassic eclogite in northwest Turkey. Geology 25, 595–598.
Okay, A.I., Nikishin, A.M., 2015. Tectonic evolution of the southern margin of Laurasia in the Black Sea region. Int. Geol. Rev. 57, 1051–1076.
Okay, A.I., Özgül, N., 1984. HP/LT metamorphism and the structure of the Alanya Massif, Southern Turkey: an allochthonous composite tectonic sheet. Geol. Soc., Lond., Spec. Publ. 17, 429–439.
Okay, A.I., Whitney, D.L., 2010. Blueschists, eclogites, ophiolites and suture zones in northwest Turkey: a review and a field excursion guide. Ofioliti 35, 131–172.
Okay, A.I., Celal Şengör, A.M., Görür, N., 1994. Kinematic history of the opening of the Black Sea and its effect on the surrounding regions. Geology 22, 267–270.
Okay, A.I., Satir, M., Maluski, H., Siyako, M., Monie, P., Metzger, R., Akyüz, S., 1996. Paleo-and Neo-Tethyan events in northwestern Turkey: geologic and geochronologic constraints. World Reg. Geol. 420–441.
Okay, A., Satır, M., Tüysüz, O., Akyüz, S., Chen, F., 2001a. The tectonics of the Strandja Massif: late-Variscan and mid-Mesozoic deformation and metamorphism in the northern Aegean. Int. J. Earth Sci. 90, 217–233.
Okay, A.I., Tansel, İ., Tüysüz, O., 2001b. Obduction, subduction and collision as reflected in the Upper Cretaceous–lower Eocene sedimentary record of western Turkey. Geol. Mag. 138, 117–142.
Okay, A.I., Monod, O., Monié, P., 2002. Triassic blueschists and eclogites from northwest Turkey: vestiges of the Paleo-Tethyan subduction. Lithos 64, 155–178.
Okay, A.I., Satir, M., Siebel, W., 2006a. Pre-Alpide Palaeozoic and Mesozoic orogenic events in the Eastern Mediterranean region. Geol. Soc., Lon., Mem. 32, 389.
Okay, A.I., Tuysuz, O., Satir, M., Ozkan-Altiner, S., Altiner, D., Sherlock, S., Eren, R.H., 2006b. Cretaceous and Triassic subduction-accretion, high-pressure-low-temperature metamorphism, and continental growth in the Central Pontides, Turkey. Geol. Soc. Am. Bull. 118, 1247–1269.
Okay, A.I., Bozkurt, E., Satır, M., Yiğitbaş, E., Crowley, Q.G., Shang, C.K., 2008a. Defining the southern margin of Avalonia in the Pontides: geochronological data from the Late Proterozoic and Ordovician granitoids from NW Turkey. Tectonophysics 461, 252–264.
Okay, A.I., Satir, M., Zattin, M., Cavazza, W., Topuz, G., 2008b. An Oligocene ductile strike-slip shear zone: the Uludag Massif, northwest Turkey-Implications for the westward translation of Anatolia. Geol. Soc. Am. Bull. 120, 893–911.
Okay, A.I., Zattin, M., Cavazza, W., 2010. Apatite fission-track data for the Miocene Arabia-Eurasia collision. Geology 38, 35–38.
Okay, A.I., Noble, P.J., Tekin, U.K., 2011. Devonian radiolarian ribbon cherts from the Karakaya Complex, Northwest Turkey: implications for the Paleo-Tethyan evolution. Compt. Rendus Palevol 10, 1–10.
Okay, A.I., İşintek, İ., Altıner, D., Özkan-Altıner, S., Okay, N., 2012. An olistostrome–mélange belt formed along a suture: Bornova Flysch zone, western Turkey. Tectonophysics 568–569, 282–295.
Okay, A.I., Sunal, G., Sherlock, S., Alt, ner, D., Tüysüz, O., Kylander-Clark, A.R.C., Aygül, M., 2013. Early Cretaceous sedimentation and orogeny on the active margin of Eurasia: Southern Central Pontides, Turkey. Tectonics 32, 1247–1271.
Okay, A.I., Sunal, G., Tüysüz, O., Sherlock, S., Keskin, M., Kylander-Clark, A.R.C., 2014. Low-pressure-high-temperature metamorphism during extension in a Jurassic magmatic arc, Central Pontides, Turkey. J. Metamorph. Geol. 32, 49–69.
Oktay, F.Y., 1981. Savcılıbüyükoba (Kaman) Çevresinde Orta Anadolu Masifi Tortul Örtüsünün Jeolojisi ve Sedimentolojisi.
Okuyucu, C., Tekin, U.K., Noble, P.J., Bedi, Y., Saydam-Demiray, D.G., Sayit, K., 2018. Foraminifera, Radiolaria and Conodont assemblages from the Early Mississipian (late Tournaisian)/Early Pennsylvanian (early Bashkirian) blocks within the Mersin Mélange, southern Turkey: biochronological and paleogeographical implications. Palaeoworld 27, 438–457.
Olivet, J., 1996. Kinematics of the Iberian Plate. In: Bulletin des Centres de Recherches Exploration-Production Elf Aquitaine, vol. 20, pp. 131–195.
Oms, O., Dinarès-Turell, J., Remacha, E., 2003. Magnetic Stratigraphy from Deep Clastic Turbidites: an Example from the Eocene Hecho Group (Southern Pyrenees). Studia Geophys. Geod. 47, 275–288.
Önal, M., Kaya, M., 2007. Stratigraphy and tectono-sedimentary evolution of the Upper Cretaceous–Tertiary sequence in the southern part of the Malatya Basin, East Anatolia, Turkey. J. Asian Earth Sci. 29, 878–890.
Orbay, N., Bayburdi, A., 1979. Palaeomagnetism of dykes and tuffs from the Mesudiye region and rotation of Turkey. Geophys. J. Royal Astron. Soc. 59, 437–444.
Ortner, H., Stingl, V., 2001. Facies and Basin Development of the Oligocene in the Lower Inn Valley, Tyrol/Bavaria. Verlag der Österreichischen Akademie der Wissenschaften, Wien, pp. 153–196.
Ortolano, G., Cirrincione, R., Pezzino, A., 2005. P-T evolution of Alpine metamorphism in the southern Aspromonte Massif (Calabria - Italy). Schweiz. Mineral. Petrogr. Mittl. 85, 31–56.

Osete, M.L., Rey, D., Villalaín, J.J., Juárez, M.T., 1997. Geol. Mijnb. (Geology and Mining) 76, 105–119.
Osete, M.-L., Gialanella, P.-R., Gómez, J.J., Villalaín, J.J., Goy, A., Heller, F., 2007. Magnetostratigraphy of Early–Middle Toarcian expanded sections from the Iberian Range (central Spain). Earth Planet. Sci. Lett. 259, 319–332.
Oszczypko, N., 2006. Late Jurassic-Miocene evolution of the Outer Carpathian fold-and-thrust belt and its foredeep basin (Western Carpathians, Poland). Geol. Q. 50, 169–194.
Oszczypko, N., Ślączka, A., Bubniak, I., Olszewska, B., Garecka, M., 2017. The position and age of flysch deposits in the Crimean Mountains (Southern Ukraine). Geol. Q. 61, 697–722. https://doi.org/10.7306/gq.1359.
Oudet, J., Münch, P., Verati, C., Ferrandini, M., Melinte-Dobrinescu, M., Gattacceca, J., Cornée, J.J., Oggiano, G., Quillévéré, F., Borgomano, J., Ferrandini, J., 2010. Integrated chronostratigraphy of an intra-arc basin: 40Ar/39Ar datings, micro-palaeontology and magnetostratigraphy of the early Miocene Castelsardo basin (northern Sardinia, Italy). Palaeogeogr. Palaeoclimatol. Palaeoecol. 295, 293–306.
Özdamar, Ş., Roden, M.F., Esenli, F., Uz, B., Wampler, J.M., 2012. Geochemical features and K-Ar age data from metadetrital rocks and high-K metasomatized meta-rhyolites in the Afyon- Bolkardağ Zone (Ilgin-Konya), SW Turkey. Neues Jahrbuch für Mineralogie - Abhandlungen: J. Mineral. Geochem. 189, 155–176.
Özdamar, Ş., Billor, M.Z., Sunal, G., Esenli, F., Roden, M.F., 2013. First U–Pb SHRIMP zircon and 40Ar/39Ar ages of metarhyolites from the Afyon–Bolkardag Zone, SW Turkey: implications for the rifting and closure of the Neo-Tethys. Gondwana Res. 24, 377–391.
Özer, S., 1998. Rudist bearing Upper Cretaceousmetamorphic sequences of the Menderes Massif (Western Turkey). Geobios 31, 235–249.
Özer, S., 2005. Two new species of canaliculate rudists (Dictyoptychidae) from southeastern Turkey. Geobios 38, 235–245.
Özer, S., Sözbilir, H., 2003. Presence and tectonic significance of Cretaceous rudist species in the so-called Permo-Carboniferous Göktepe Formation, central Menderes metamorphic massif, western Turkey. Int. J. Earth Sci. 92, 397–404.
Özgül, N., 1976. Some geological aspects of the Taurus orogenic belt (Turkey). Bull. Geol. Soc. Turkey 19, 65–78.
Özgül, N., 1984. Stratigraphy and tectonic evolution of the Central Taurides. In: Geology of the Taurus Belt, pp. 77–90.
Özgül, N., Turkuca, A., Ozyardimci, N., Bingol, I., Senol, M., Uysal, S., 1981. Munzurların Temel Jeoloji Ozellikleri. MTA Report 6995.
Özkaptan, M., Gulyuz, E., Kaymakcı, N., Langereis, C.G., 2016. Paleomagnetic Reconstruction of the Neotethyan Suture in Central Anatolia (Turkey). AGU Fall Meeting Abstracts.
Palamakumbura, R.N., Robertson, A.H.F., Kinnaird, T.C., Sanderson, D.C.W., 2015. Sedimentary development and correlation of Late Quaternary terraces in the Kyrenia Range, Northern Cyprus, using a combination of sedimentology and optical luminescence data. Int. J. Earth Sci. 105, 439–462.
Palamakumbura, R.N., Robertson, A.H.F., Kinnaird, T.C., van Calsteren, P., Kroon, D., Tait, J.A., 2016. Quantitative dating of Pleistocene deposits of the Kyrenia Range, Northern Cyprus: implications for timing, rates of uplift and driving mechanisms. J. Geol. Soc. 173, 933–948.
Palencia Ortas, A., Osete, M.L., Vegas, R., Silva, P., 2006. Paleomagnetic study of the Messejana Plasencia dyke (Portugal and Spain): a lower Jurassic paleopole for the Iberian plate. Tectonophysics 420, 455–472.
Pálfy, J., Mundil, R., Renne, P.R., Bernor, R.L., Kordos, L., Gasparik, M., 2007. U–Pb and 40Ar/39Ar dating of the Miocene fossil track site at Ipolytarnóc (Hungary) and its implications. Earth Planet. Sci. Lett. 258, 160–174.
Pamić, J.J., 1984. Triassic magmatism of the Dinarides in Yugoslavia. Tectonophysics 109, 273–307.
Pamić, J., Tomljenović, B., Balen, D., 2002. Geodynamic and petrogenetic evolution of Alpine ophiolites from the central and NW Dinarides: an overview. Lithos 65, 113–142.
Pamić, J., Balogh, K., Hrvatović, H., Balen, D., Jurković, I., Palinkaš, L., 2004. K–Ar and Ar–Ar dating of the Palaeozoic metamorphic complex from the Mid-Bosnian Schist Mts., Central Dinarides, Bosnia and Hercegovina. Miner. Petrol. 82, 65–79.
Panaiotu, C., 1998. Paleomagnetic constraints on the geodynamic history of Romania. Monograph of Southern Carpathians. Rep. Geodesy 7, 205–216.
Panaiotu, C., 1999. Paleomagnetic Studies in Romania: Tectonophysic Implications. Unpublished PhD thesis University Bucharest.
Panaiotu, C.G., Panaiotu, C.E., 2010. Palaeomagnetism of the Upper Cretaceous Sânpetru Formation (Haţeg Basin, South Carpathians). Palaeogeogr. Palaeoclimatol. Palaeoecol. 293, 343–352.
Panaiotu, C.G., Pécskay, Z., Hambach, U., Seghedi, I., Panaiotu, C.E., Itaya, C.E.T., Orleanu, M., Szakács, A., 2004. Short-lived Quaternary volcanism in the Persani Mountains (Romania) revealed by combined K–Ar and paleomagnetic data. Geol. Carpathica 55, 333–339.
Panaiotu, C.G., Vişan, M., Ţugui, A., Seghedi, I., Panaiotu, A.G., 2012. Palaeomagnetism of the South Harghita volcanic rocks of the East Carpathians: implications for tectonic rotations and palaeosecular variation in the past 5 Ma. Geophys. J. Int. 189, 369–382.
Paraschiv, D., 1979. Platforma Moesică şi Zăcămintele ei de Hidrocarburi. Editura Academiei Republicii Socialiste România.
Paraschiv, D., 1983. Stages in the Moesian Platform history. An. Inst. Geol., Geofiz 60, 178–198.
Paraschiv, D., 1997. The pre-Paratethys buried denudational surface in Romanian territory. Rev. Roum. Géogr. 41, 21–32.
Parés, J., Dinarès-Turell, J., 1994. Iberian Triassic paleomagnetism revisited: intraplate block rotations versus polar wandering. Geophys. Res. Lett. 21, 2155–2158.
Parés, J.M., Roca, E., 1996. The significance of tectonic-related tertiary remagnetization along the margins of the Valencia trough. J. Geodyn. 22, 207–227.
Parés, J.M., Freeman, R., Roca, E., 1992. Neogene structural development in the Valencia trough margins from palaeomagnetic data. Tectonophysics 203, 111–124.
Parés, J.M., Voo, R., Stamatakos, J., 1996. Palaeomagnetism of Permian and Triassic red beds of NW Spain and implications for the tectonic evolution of the Asturian—Cantabrian Arc. Geophys. J. Int. 126, 893–901.
Parlak, O., 2006. Geodynamic significance of granitoid magmatism in the southeast Anatolian orogen: geochemical and geochronogical evidence from Goksun–Afsin (Kahramanmaras, Turkey) region. Int. J. Earth Sci. 95, 609–627.
Parlak, O., 2016. The tauride ophiolites of Anatolia (Turkey): a review. J. Earth Sci. 27, 901–934.
Parlak, O., Delaloye, M., 1999. Precise 40Ar/39Ar ages from the metamorphic sole of the Mersin ophiolite (southern Turkey). Tectonophysics 301, 145–158.
Parlak, O., Bozkurt, E., Delaloye, M., 1996. The Obduction Direction of the Mersin Ophiolite: structural Evidence from Subophiolitic Metamorphics in the Central Tauride Belt, Southern Turkey. Int. Geol. Rev. 38, 778–786.
Parlak, O., HÖCk, V., Kozlu, H., Delaloye, M., 2004. Oceanic crust generation in an island arc tectonic setting, SE Anatolian orogenic belt (Turkey). Geol. Mag. 141, 583–603.
Parlak, O., Yılmaz, H., Boztuğ, D., 2006. Origin and tectonic significance of the metamorphic sole and isolated dykes of the Divriği ophiolite (Sivas, Turkey): evidence for slab break-off prior to ophiolite emplacement. Turk. J. Earth Sci. 15, 25–45.
Parlak, O., Karaoğlan, F., Rızaoğlu, T., Klötzli, U., Koller, F., Billor, Z., 2013a. U–Pb and 40Ar–39Ar geochronology of the ophiolites and granitoids from the Tauride belt: implications for the evolution of the Inner Tauride suture. J. Geodyn. 65, 22–37.
Parlak, O., Karaoğlan, F., Rizaoğlu, T., Nurlu, N., Bağcı, U., Höck, V., Önal, A.Ö., Kürüm, S., Topak, Y., 2013b. Petrology of the İspendere (Malatya) ophiolite from the Southeast Anatolia: implications for the Late Mesozoic evolution of the southern Neotethyan ocean. Geol. Soc., Lond., Spec. Publ. 372, 219–247.
Pascual, J.O., Parés, J.M., Langereis, C.G., Zijderveld, J.D.A., 1992. Magnetostratigraphy and rock magnetism of the Ilerdian stratotype at Tremp, Spain. Phys. Earth Planet. Inter. 74, 139–157.
Pasquale, V., Verdoya, M., Chiozzi, P., 2005. Thermal Structure of the Ionian Slab. Pure Appl. Geophys. 162, 967–986.
Pastor-Galán, D., Mulchrone, K.F., Koymans, M.R., van Hinsbergen, D.J.J., Langereis, C.G., 2017. Bootstrapped total least squares orocline test: a robust method to quantify vertical-axis rotation patterns in orogens, with examples from the Cantabrian and Aegean oroclines. Lithosphere 9, 499–511.
Patacca, E., Scandone, P., 2007. Geology of the Southern Apennines. Boll. Soc. Geol. Ital. 7, 75–119.
Patacca, E., R, S., Scandone, P., 1990. Tyrrhenian Basin and Apenninic Arcs: kinematic relations since late Tortonian times. Mem. Soc. Geol. Ital. 45, 425–451.
Patacca, E., Scandone, P., Di Luzio, E., Cavinato, G.P., Parotto, M., 2008. Structural architecture of the Central Apennines: interpretation of the CROP 11 seismic profile from the Adriatic coast to the orographic divide. Tectonics 27.
Patriat, P., Achache, J., 1984. India-Eurasia collision chronology has implications for crustal shortening and driving mechanism of plates. Nature 311, 615–621.
Pe-Piper, G., 1978. The Cenozoic Volcanic Rocks of Lesbos Island. Unpub. MSc Thesis. University of Patras.
Pe-Piper, G., 1982. Geochemistry, tectonic setting and metamorphism of mid-triassic volcanic rocks of Greece. Tectonophysics 85, 253–272.
Pe-Piper, G., Piper, D.J.W., 1991. Early Mesozoic oceanic subduction-related volcanic rocks, Pindos Basin, Greece. Tectonophysics 192, 273–292.
Pearce, J.A., Robinson, P.T., 2010. The Troodos ophiolitic complex probably formed in a subduction initiation, slab edge setting. Gondwana Res. 18, 60–81.
Pearson, D.G., Davies, G.R., Nixon, P.H., Milledge, H.J., 1989. Graphitized diamonds from a peridotite massif in Morocco and implications for anomalous diamond occurrences. Nature 338, 60.
Pechersky, D.M., Nguyen, T.K.T., 1979. Paleomagnetic Directions and Pole Positions: Data for the USSR. Soviet Geophysical Committee, World Data Center-B, Moscow.
Peeters, Hoek, Brinkhuis, Wilpshaar, Boer, D., Krijgsman, Meulenkamp, 1998. Differentiating glacio-eustacy and tectonics; a case study involving dinoflagellate cysts from the Eocene–Oligocene transition of the Pindos Foreland Basin (NW Greece). Terra Nova 10, 245–249.
Pellegrino, A.G., Maniscalco, R., Speranza, F., Hernandez-Moreno, C., Sturiale, G., 2016. Paleomagnetism of the Hyblean Plateau, Sicily: a review of the existing data set and new evidence for lack of block rotation from the Scicli-Ragusa Fault System. Ital. J. Geosci. 135, 300–307.
Pepe, F., Sulli, A., Bertotti, G., Catalano, R., 2005. Structural highs formation and their relationship to sedimentary basins in the north Sicily continental margin (southern Tyrrhenian Sea): implication for the Drepano Thrust. Front. Tectonophysics 409, 1–18.
Peral, M., Király, Á., Zlotnik, S., Funiciello, F., Fernàndez, M., Faccenna, C., Vergés, J., 2018. Opposite subduction polarity in adjacent plate segments. Tectonics 37, 3285–3302.
Perchuk, A., Philippot, P., 1997. Rapid cooling and exhumation of eclogitic rocks from the Great Caucasus, Russia. J. Metamorph. Geol. 15, 299–310.
Pérez-Rodríguez, I., Lees, J.A., Larrasoaña, J.C., Arz, J.A., Arenillas, I., 2012. Planktonic foraminiferal and calcareous nannofossil biostratigraphy and

magnetostratigraphy of the uppermost Campanian and Maastrichtian at Zumaia, northern Spain. Cretac. Res. 37, 100–126.
Perincek, D., Kozlu, H., 1984. Stratigraphical and structural relations of the units in the Afsin-Elbistan- Doganshehir region (Eastern Taurus). In: Tekeli, O., Göncüoğlu, C. (Eds.), Geology of the Taurus Belt. Proceedings of International Symposium. MTA, Ankara, pp. 181–198.
Pertusati, P.C., Horrenberger, J.C., 1975. Studio strutturale degli Scisti di Val Lavagna (Unita del Monte Gottero, Appennino ligure). Ital. J. Geosci. 94, 1375–1436.
Pescatore, T., Renda, P., Schiattarella, M., Tramutoli, M., 1999. Stratigraphic and structural relationships between Meso-Cenozoic Lagonegro basin and coeval carbonate platforms in Southern Apennines, Italy. Tectonophysics 315, 269–286.
Peters, K., van Hinsbergen, D., Smit, M., van Roermund, H., Brouwer, F., Plunder, A., Guilmette, C., 2018. Magnitude and Meaning of Time Lags between the Formation and Cooling of Neotethyan Metamorphic Soles from Multi-Chronology. EGU General Assembly Conference Abstracts, p. 11957.
Petrík, I., Janák, M., Froitzheim, N., Georgiev, N., Yoshida, K., Sasinková, V., Konečný, P., Milovská, S., 2016. Triassic to Early Jurassic (c. 200 Ma) UHP metamorphism in the Central Rhodopes: evidence from U-Pb-Th dating of monazite in diamond-bearing gneiss from Chepelare (Bulgaria). J. Metamorph. Geol. 34, 265–291.
Pfiffner, O.A., 1986. Evolution of the north Alpine foreland basin in the Central Alps. Spec. Publ. Int. Assoc. Sedimentol. 8, 219–228.
Philippon, M., Brun, J.-P., Gueydan, F., 2011. Tectonics of the Syros blueschists (Cyclades, Greece): from subduction to Aegean extension. Tectonics 30.
Philippon, M., Brun, J.-P., Gueydan, F., 2012. Deciphering subduction from exhumation in the segmented Cycladic Blueschist Unit (Central Aegean, Greece). Tectonophysics 524–525, 116–134.
Philippon, M., Brun, J.-P., Gueydan, F., Sokoutis, D., 2014. The interaction between Aegean back-arc extension and Anatolia escape since middle Miocene. Tectonophysics 631, 176–188.
Piana, F., 2000. Structural Setting of Western Monferrato (Alps-Apennines Junction Zone, NW Italy). Tectonics 19, 943–960.
Picotti, V., Pazzaglia, F.J., 2008. A new active tectonic model for the construction of the Northern Apennines mountain front near Bologna (Italy). J. Geophys. Res.: Solid Earth 113.
Pierre, F.D., Ghisetti, F., Lanza, R., Vezzani, L., 1992. Palaeomagnetic and structural evidence of Neogene tectonic rotation of the Gran Sasso range (Central Apennines, Italy). Tectonophysics 215, 335–348.
Piguet, B., McNeill, D., Kindler, P., 2000. Tectonic rotation and diverse remanence carriers revealed by the paleomagnetism of Eo-Oligocene turbidites from two Ultrahelvetic units (Western Alps, Haute-Savoie, France). Tectonophysics 321, 359–375.
Piper, J.D.A., Gürsoy, H., Tatar, O., 2002a. Palaeomagnetism and magnetic properties of the Cappadocian ignimbrite succession, central Turkey and Neogene tectonics of the Anatolian collage. J. Volcanol. Geotherm. Res. 117, 237–262.
Piper, J.D.A., Gürsoy, H.I., Tatar, O., İşseven, T., Koçyiğit, A., 2002b. Palaeomagnetic evidence for the Gondwanian origin of the Taurides and rotation of the Isparta Angle, southern Turkey. Geol. J. 37, 317–336.
Piper, J.D.A., Tatar, O., Gursoy, H., Koçbulut, F., Mesci, B.L., 2006. Paleomagnetic analysis of neotectonic deformation in the Anatolian accretionary collage, Turkey. In: Dilek, Y., Pavlides, S. (Eds.), Postcollisional Tectonics and Magmatism in the Mediterranean Region and Asia. Geological Society of America.
Piper, J.D.A., Gürsoy, H., Tatar, O., Beck, M.E., Rao, A., Koçbulut, F., Mesci, B.L., 2010. Distributed neotectonic deformation in the Anatolides of Turkey: a palaeomagnetic analysis. Tectonophysics 488, 31–50.
Piper, J.D.A., Koçbulut, F., Gürsoy, H., Tatar, O., Viereck, L., Lepetit, P., Roberts, A.P., Akpınar, Z., 2013. Palaeomagnetism of the Cappadocian Volcanic Succession, Central Turkey: major ignimbrite emplacement during two short (Miocene) episodes and Neogene tectonics of the Anatolian collage. J. Volcanol. Geotherm. Res. 262, 47–67.
Placer, L., 1998. Contribution to the macrotectonic subdivision of the border region between Southern Alps and External Dinarides. Geologija 41, 223–255.
Plašienka, D., 1997. Cretaceous tectonochronology of the Central Western Carpathians, Slovakia. Geol. Carpathica 48, 99–111.
Plašienka, D., 2003. Development of basement-involved fold and thrust structures exemplified by the Tatric–Fatric–Veporic nappe system of the Western Carpathians (Slovakia). Geodin. Acta 16, 21–38.
Plašienka, D., 2012. Early stages of structural evolution of the Carpathian Klippen Belt (Slovakian Pieniny sector). Miner. Slovaca 44, 1–16.
Plašienka, D., 2018. Continuity and Episodicity in the Early Alpine Tectonic Evolution of the Western Carpathians: how Large-Scale Processes Are Expressed by the Orogenic Architecture and Rock Record Data. Tectonics 37, 2029–2079.
Platt, J.P., Compagnoni, R., 1990. Alpine ductile deformation and metamorphism in a calabrian base- ment nappe (Aspromonte, south Italy). Eclogae Geol. Helv. 83, 41–58.
Platt, J.P., Vissers, R.L.M., 1989. Extensional collapse of thickened continental lithosphere: a working hypothesis for the Alboran Sea and Gibraltar arc. Geology 17, 540–543.
Platt, J.P., Whitehouse, M.J., 1999. early Miocene high-temperature metamorphism and rapid exhumation in the Betic Cordillera (Spain): evidence from U–Pb zircon ages. Earth Planet. Sci. Lett. 171, 591–605.
Platt, J., Allerton, S., Kirker, A., Platzman, E., 1995. Origin of the western Subbetic arc (South Spain): palaeomagnetic and structural evidence. J. Struct. Geol. 17, 765–775.
Platt, J.P., Allerton, S., Kirker, A., Mandeville, C., Mayfield, A., Platzman, E.S., Rimi, A., 2003. The ultimate arc: differential displacement, oroclinal bending, and vertical axis rotation in the External Betic-Rif arc. Tectonics 22.
Platt, J.P., Kelley, S.P., Carter, A., Orozco, M., 2005. Timing of tectonic events in the Alpujarride Complex, Betic Cordillera, southern Spain. J. Geol. Soc. 162, 451–462.
Platt, J.P., Anczkiewicz, R., Soto, J.I., Kelley, S.P., Thirlwall, M., 2006. early Miocene continental subduction and rapid exhumation in the western Mediterranean. Geology 34, 981–984.
Platt, J.P., Behr, W.M., Johanesen, K., Williams, J.R., 2013. The betic-rif arc and its Orogenic Hinterland: a review. Ann. Rev. Earth Planet. Sci. 41, 313–357.
Platzman, E.S., 1994. East-west thrusting and anomalous magnetic declinations in the Sierra Gorda, Betic Cordillera, southern Spain. J. Struct. Geol. 16, 11–20.
Platzman, E., Lowrie, W., 1992. Paleomagnetic evidence for rotation of the Iberian Peninsula and the external Betic Cordillera, Southern Spain. Earth Planet. Sci. Lett. 108, 45–60.
Platzman, E., Platt, J.P., 2004. Kinematics of a twisted core complex: oblique axis rotation in an extended terrane (Betic Cordillera, southern Spain). Tectonics 23.
Platzman, E.S., Platt, J.P., Tapirdamaz, C., Sanver, M., Rundle, C.C., 1994. Why are there no clockwise rotations along the North Anatolian Fault Zone? J. Geophys. Res.: Solid Earth 99, 21705–21715.
Platzman, E.S., Tapirdamaz, C., Sanver, M., 1998. Neogene anticlockwise rotation of central Anatolia (Turkey): preliminary palaeomagnetic and geochronological results. Tectonophysics 299, 175–189.
Platzman, E., Platt, J.P., Kelley, S.P., Allerton, S., 2000. Large clockwise rotations in an extensional allochthon, Alboran Domain (southern Spain). J. Geol. Soc. 157, 1187.
Plesi, G., Galli, M., Daniele, G., 2002. The Monti Rognosi Ophiolitic Unit (cfr. Calvana Unit Auct.) paleogeographic position in the External Ligurian Domain, relationships with the tectonicunits derived from the Adriatic margin. Boll. Soc. Geol. Ital. 121, 273–284.
Plunder, A., Agard, P., Chopin, C., Okay, A.I., 2013. Geodynamics of the Tavşanlı zone, western Turkey: insights into subduction/obduction processes. Tectonophysics 608, 884–903.
Plunder, A., Agard, P., Chopin, C., Pourteau, A., Okay, A.I., 2015. Accretion, underplating and exhumation along a subduction interface: from subduction initiation to continental subduction (Tavşanlı zone, W. Turkey). Lithos 226, 233–254.
Plunder, A., Agard, P., Chopin, C., Soret, M., Okay, A.I., Whitechurch, H., 2016. Metamorphic sole formation, emplacement and blueschist facies overprint: early subduction dynamics witnessed by western Turkey ophiolites. Terra Nova 28, 329–339.
Poisson, A., 1967. Données nouvelles sur le Crétacé superieur et le Tertiaire du Taurus au NW d'Antalya (Turquie). Compt. Rendus Acad. Sci. Paris 264, 2443–2446.
Poisson, A., 1977. Recherches Géologiques dans les Taurides Occidentales (Turquie). Universite de Paris-Sud (Centre D'orsay).
Poisson, A., Guezou, J.C., Ozturk, A., Inan, S., Temiz, H., Gürsöy, H., Kavak, K.S., ÖZden, S., 1996. Tectonic Setting and Evolution of the Sivas Basin, Central Anatolia, Turkey. Int. Geol. Rev. 38, 838–853.
Poisson, A., Yağmurlu, F., Bozcu, M., Şentürk, M., 2003. New insights on the tectonic setting and evolution around the apex of the Isparta Angle (SW Turkey). Geol. J. 38, 257–282.
Polat, A., Casey, J.F., 1995. A structural record of the emplacement of the Pozanti-Karsanti ophiolite onto the Menderes-Taurus block in the late Cretaceous, eastern Taurides, Turkey. J. Struct. Geol. 17, 1673–1688.
Porkoláb, K., Kövér, S., Benkó, Z., Héja, G.H., Fialowski, M., Soós, B., Spajić, N.G., Đerić, N., Fodor, L., 2019. Structural and geochronological constraints from the Drina-Ivanjica thrust sheet (Western Serbia): implications for the Cretaceous–Paleogene tectonics of the Internal Dinarides. Swiss J. Geosci. 112, 217–234.
Porreca, M., Mattei, M., 2010. Tectonic and environmental evolution of Quaternary intramontane basins in Southern Apennines (Italy): insights from palaeomagnetic and rock magnetic investigations. Geophys. J. Int. 182, 682–698.
Pourteau, A., Candan, O., Oberhänsli, R., 2010. High-pressure metasediments in central Turkey: constraints on the Neotethyan closure history. Tectonics 29.
Pourteau, A., Sudo, M., Candan, O., Lanari, P., Vidal, O., Oberhänsli, R., 2013. Neotethys closure history of Anatolia: insights from 40Ar-39Ar geochronology andP-Testimation in high-pressure metasedimentary rocks. J. Metamorph. Geol. 31, 585–606.
Pourteau, A., Bousquet, R., Vidal, O., Plunder, A., Duesterhoeft, E., Candan, O., Oberhänsli, R., 2014. Multistage growth of Fe–Mg–carpholite and Fe–Mg–-chloritoid, from field evidence to thermodynamic modelling. Contrib. Miner. Petrol. 168.
Pourteau, A., Scherer, E.E., Schorn, S., Bast, R., Schmidt, A., Ebert, L., 2019. Thermal evolution of an ancient subduction interface revealed by Lu–Hf garnet geochronology, Halilbağı Complex (Anatolia). Geosci. Front. 10, 127–148.
Pownall, J.M., Hall, R., Armstrong, R.A., Forster, M.A., 2014. Earth's youngest known ultrahigh-temperature granulites discovered on Seram, eastern Indonesia. Geology 42, 279–282.
Précigout, J., Gueydan, F., Garrido, C.J., Cogné, N., Booth-Rea, G., 2013. Deformation and exhumation of the Ronda peridotite (Spain). Tectonics.
Prelević, D., Wehrheim, S., Reutter, M., Romer, R.L., Boev, B., Božović, M., van den Bogaard, P., Cvetković, V., Schmid, S.M., 2017. The Late Cretaceous Klepa basalts in Macedonia (FYROM)-Constraints on the final stage of Tethys closure in the Balkans. Terra Nova 29, 145–153.
Pruner, P., Houša, V., Olóriz, F., Košťák, M., Krs, M., Man, O., Schnabl, P., Venhodová, D., Tavera, J.M., Mazuch, M., 2010. High-resolution magnetostratigraphy and biostratigraphic zonation of the Jurassic/Cretaceous boundary

strata in the Puerto Escaño section (southern Spain). Cretac. Res. 31, 192–206.
Pueyo Anchuela, Ó., Pueyo, E.L., Pocoví Juan, A., Gil Imaz, A., 2012. Vertical axis rotations in fold and thrust belts: comparison of AMS and paleomagnetic data in the Western External Sierras (Southern Pyrenees). Tectonophysics 532–535, 119–133.
Pueyo, E.L., Millán, H., Pocoví, A., 2002. Rotation velocity of a thrust: a paleomagnetic study in the External Sierras (Southern Pyrenees). Sediment. Geol. 146, 191–208.
Pueyo, E.L., Mauritsch, H.J., Gawlick, H.J., Scholger, R., Frisch, W., 2007. New evidence for block and thrust sheet rotations in the central northern Calcareous Alps deduced from two pervasive remagnetization events. Tectonics 26.
Puga, E., Diaz de Federico, A., Fediukova, E., Bondi, M., Morten, L., 1989. Petrology, geochemistry and metamorphic evolution of the ophiolitic eclogites and related rocks from the Sierra Nevada (Betic Cordilleras, Southeastern Spain). Schweiz. Mineral. Petrogr. Mittl. 69, 435–455.
Puga, E., Fanning, M., Díaz de Federico, A., Nieto, J.M., Beccaluva, L., Bianchini, G., Díaz Puga, M.A., 2011. Petrology, geochemistry and U–Pb geochronology of the Betic Ophiolites: inferences for Pangaea break-up and birth of the westernmost Tethys Ocean. Lithos 124, 255–272.
Putiš, M., Gawlick, H.-J., Frisch, W., Sulák, M., 2007. Cretaceous transformation from passive to active continental margin in the Western Carpathians as indicated by the sedimentary record in the Infratatric unit. Int. J. Earth Sci. 97, 799.
Pătrașcu, Ș., 1993. Palaeomagnetic study of some Neogene magmatic rocks from the Oaș-Igniș-Văratec-Tibleș Mountains (Romania). Geophys. J. Int. 113, 215–224.
Pătrașcu, S., Bleahu, M., Panaiotu, C., 1992. The paleomagnetism of the Upper Cretaceous magmatic rocks in the Banat area of South Carpathians: tectonic implications. Tectonophysics 213, 341–352.
Pătrașcu, S., Bleahu, M., Panaiotu, C., 1990. Tectonic implications of paleomagnetic research into Upper Cretaceous magmatic rocks in the Apuseni Mountains, Romania. Tectonophysics 180, 309–322.
Pătrașcu, S., Panaiotu, C., Seclăman, M., Panaiotu, C.E., 1994. Timing of rotational motion of Apuseni Mountains (Romania): paleomagnetic data from Tertiary magmatic rocks. Tectonophysics 233, 163–176.
Rabinowitz, P.D., 1974. The Boundary Between Oceanic and Continental Crust in the Western North Atlantic, the geology of Continental Margins. Springer, pp. 67–84.
Radeff, G., Schildgen, T.F., Cosentino, D., Strecker, M.R., Cipollari, P., Darbaş, G., Gürbüz, K., 2017. Sedimentary evidence for late Messinian uplift of the SE margin of the Central Anatolian Plateau: Adana Basin, southern Turkey. Basin Res. 29, 488–514.
Radwany, M., Whitney, D.L., Brocard, G., Umhoefer, P.J., Teyssier, C., 2017. Ophiolite gabbro from source to sink: a record of tectonic and surface processes in Central Anatolia. Geosphere 13, 1329–1358.
Rahl, J., Anderson, K., Brandon, M., Fassoulas, C., 2005. Raman spectroscopic carbonaceous material thermometry of low-grade metamorphic rocks: calibration and application to tectonic exhumation in Crete, Greece. Earth Planet. Sci. Lett. 240, 339–354.
Rampone, E., Hofmann, A.W., Raczek, I., 2009. Isotopic equilibrium between mantle peridotite and melt: evidence from the Corsica ophiolite. Earth Planet. Sci. Lett. 288, 601–610.
Rat, J., Mouthereau, F., Brichau, S., Crémades, A., Bernet, M., Balvay, M., Ganne, J., Lahfid, A., Gautheron, C., 2019. Tectono-thermal evolution of the Cameros basin: implications for Tectonics of North Iberia. Tectonics 38. https://doi.org/10.1029/2018TC005294.
Ratschbacher, L., Frisch, W., Hans-Gert, L., Merle, O., 1991. Lateral extrusion in the eastern Alps, PArt 2: structural analysis. Tectonics 10, 257–271.
Ratschbacher, L., Linzer, H.-G., Moser, F., Strusievicz, R.-O., Bedelean, H., Har, N., Mogoș, P.-A., 1993. Cretaceous to Miocene thrusting and wrenching along the central south Carpathians due to a corner effect during collision and orocline formation. Tectonics 12, 855–873.
Ratschbacher, L., Dingeldey, C., Miller, C., Hacker, B.R., McWilliams, M.O., 2004. Formation, subduction, and exhumation of Penninic oceanic crust in the Eastern Alps: time constraints from 40Ar/39Ar geochronology. Tectonophysics 394, 155–170.
Reiser, M.K., Schuster, R., Spikings, R., Tropper, P., Fugenschuh, B., 2017. From nappe stacking to exhumation: cretaceous tectonics in the Apuseni Mountains (Romania). Int. J. Earth Sci. 106, 659–685.
Resimić-Šarić, K., Cvetković, V., Balogh, K., 2005. Radiometric K/ag data as evidence of the geodynamic evolution of the Ždraljica ophiolitic complex, central Serbia. Geoloski Anal. Balk. Poluos. 73–79.
Rey, D., Turner, P., Ramos, A., 1996. Palaeomagnetism and magnetostratigraphy of the Middle Triassic in the Iberian Ranges (Central Spain). Geol. Soc., Lond., Spec. Publ. 105, 59–82.
Rezaii, L., Moazzen, M., 2014. Mineral chemistry of the ophiolitic peridotites and gabbros from the Serow area: implications for tectonic setting and locating the Neotethys suture in NW Iran. Central Eur. Geol. 57, 385–402.
Rezeau, H., Moritz, R., Wotzlaw, J.-F., Tayan, R., Melkonyan, R., Ulianov, A., Selby, D., d'Abzac, F.-X., Stern, R.A., 2016. Temporal and genetic link between incremental pluton assembly and pulsed porphyry Cu-Mo formation in accretionary orogens. Geology 44, 627–630.
Rezeau, H., Moritz, R., Leuthold, J., Hovakimyan, S., Tayan, R., Chiaradia, M., 2017. 30 Myr of Cenozoic magmatism along the Tethyan margin during Arabia–Eurasia accretionary orogenesis (Meghri–Ordubad pluton, southernmost Lesser Caucasus). Lithos 288, 108–124.
Ribeiro, P., Silva, P.F., Moita, P., Kratinova, Z., Marques, F.O., Henry, B., 2013. Palaeomagnetism in the Sines massif (SW Iberia) revisited: evidences for Late Cretaceous hydrothermal alteration and associated partial remagnetization. Geophys. J. Int. 195, 176–191.
Ricchetti, G., Ciaranfi, N., Luperto Sinni, E., Mongelli, F., Pieri, P., 1988. Geodinamica ed evoluzione sedimentaria e tettonica dell'avampaese apulo. Mem. Soc. Geol. It 41, 57–82.
Ricou, L.E., Marcoux, J., Whitechurch, H., 1984. The Mesozoic organization of the Taurides: one or several ocean basins? Geol. Soc., Lond., Spec. Publ. 17, 349–359.
Ricou, L.E., Burg, J.P., Godfriaux, I., Ivanov, Z., 1998. Rhodope and Vardar: the metamorphic and the olistostromic paired belts related to the Cretaceous subduction under Europe. Geodin. Acta 11, 285–309.
Rimmelé, G., Jolivet, L., Oberhänsli, R., Goffé, B., 2003a. Deformation history of the high-pressure Lycian Nappes and implications for tectonic evolution of SW Turkey. Tectonics 22.
Rimmelé, G., Oberhänsli, R., Goffé, B., Jolivet, L., Candan, O., Çetinkaplan, M., 2003b. First evidence of high-pressure metamorphism in the "Cover Series" of the southern Menderes Massif. Tectonic and metamorphic implications for the evolution of SW Turkey. Lithos 71, 19–46.
Rimmelé, G., Parra, T., Goffé, B., Oberhänsli, R., Jolivet, L., Candan, O., 2005. Exhumation Paths of High-Pressure–Low-Temperature Metamorphic Rocks from the Lycian Nappes and the Menderes Massif (SW Turkey): a Multi-Equilibrium Approach. J. Petrol. 46, 641–669.
Ring, U., Yngwe, F., 2018. "To Be, or Not to Be, That Is the Question"—The Cretan Extensional Detachment, Greece. Tectonics 37, 3069–3084.
Ring, U., Layer, P.W., Reischmann, T., 2001. Miocene high-pressure metamorphism in the Cyclades and Crete, Aegean Sea, Greece: evidence for large-magnitude displacement on the Cretan detachment. Geology 29, 395–398.
Ring, U., Johnson, C., Hetzel, R., Gessner, K., 2003. Tectonic denudation of a Late Cretaceous-Tertiary collisional belt: regionally symmetric cooling patterns and their relation to extensional faults in the Anatolide belt of western Turkey. Geol. Mag. 140, 421–441.
Ring, U., Will, T., Glodny, J., Kumerics, C., Gessner, K., Thomson, S., Güngör, T., Monié, P., Okrusch, M., Drüppel, K., 2007. Early exhumation of high-pressure rocks in extrusion wedges: cycladic blueschist unit in the eastern Aegean, Greece, and Turkey. Tectonics 26.
Ring, U., Glodny, J., Will, T., Thomson, S., 2010. The Hellenic Subduction System: high-Pressure Metamorphism, Exhumation, Normal Faulting, and Large-Scale Extension. Ann. Rev. Earth Planet. Sci. 38, 45–76.
Rioux, M., Garber, J., Bauer, A., Bowring, S., Searle, M., Kelemen, P., Hacker, B., 2016. Synchronous formation of the metamorphic sole and igneous crust of the Semail ophiolite: new constraints on the tectonic evolution during ophiolite formation from high-precision U–Pb zircon geochronology. Earth Planet. Sci. Lett. 451, 185–195.
Rizeli, M.E., Beyarslan, M., Wang, K.-L., Bingöl, A.F., 2016. Mineral chemistry and petrology of mantle peridotites from the Guleman ophiolite (SE Anatolia, Turkey): evidence of a forearc setting. J. Afr. Earth Sci. 123, 392–402.
Robertson, A.H.F., 1998. Tectonic significance of the Eratosthenes Seamount: a continental fragment in the process of collision with a subduction zone in the eastern Mediterranean (Ocean Drilling Program Leg 160). Tectonophysics 298, 63–82.
Robertson, A.H.F., 2002. Overview of the genesis and emplacement of Mesozoic ophiolites in the Eastern Mediterranean Tethyan region. Lithos 65, 1–67.
Robertson, A., 2004. Development of concepts concerning the genesis and emplacement of Tethyan ophiolites in the Eastern Mediterranean and Oman regions. Earth-Sci. Rev. 66, 331–387.
Robertson, A.H.F., Kinnaird, T.C., 2015. Structural development of the central Kyrenia Range (north Cyprus) in its regional setting in the eastern Mediterranean region. Int. J. Earth Sci. 105, 417–437.
Robertson, A., Shallo, M., 2000. Mesozoic–Tertiary tectonic evolution of Albania in its regional Eastern Mediterranean context. Tectonophysics 316, 197–254.
Robertson, A.H.F., Ustaömer, T., 2004. Tectonic evolution of the Intra-Pontide suture zone in the Armutlu Peninsula, NW Turkey. Tectonophysics 381, 175–209.
Robertson, A.H.F., Woodcock, N.H., 1981. Alakir çay Group, antalya complex, SW Turkey: a deformed Mesozoic carbonate margin. Sediment. Geol. 30, 95–131.
Robertson, A.H.F., Clift, P.D., Degnan, P.J., Jones, G., 1991. Palaeogeographic and palaeotectonic evolution of the Eastern Mediterranean Neotethys. Palaeogeogr. Palaeoclimatol. Palaeoecol. 87, 289–343.
Robertson, A.H.F., Kidd, R.B., Ivanov, M.K., Limonov, A.F., Woodside, J.M., Galindo-Zaldivar, J., Nieto, L., 1995. Eratosthenes Seamount: collisional processes in the easternmost Mediterranean in relation to the Plio-Quaternary uplift of southern Cyprus. Terra Nova 7, 254–264.
Robertson, A., Unlügenç, Ü.C., İnan, N., Taşlı, K., 2004a. The Misis–Andırın Complex: a Mid-Tertiary mélange related to late-stage subduction of the Southern Neotethys in S Turkey. J. Asian Earth Sci. 22, 413–453.
Robertson, A.H.F., Ustaomer, T., Pickett, E.A., Collins, A.S., Andrew, T., Dixon, J.E., 2004b. Testing models of Late Palaeozoic-Early Mesozoic orogeny in Western Turkey: support for an evolving open-Tethys model. J. Geol. Soc. 161, 501–511.
Robertson, A.H.F., Ustaömer, T., Parlak, O., Ünlügenç, U.C., Taşlı, K., İnan, N., 2006. The Berit transect of the Tauride thrust belt, S Turkey: late Cretaceous–Early Cenozoic accretionary/collisional processes related to closure of the Southern Neotethys. J. Asian Earth Sci. 27, 108–145.
Robertson, A., Parlak, O., Rizaoğlu, T., Ünlügenç, Ü., İnan, N., Tasli, K., Ustaömer, T., 2007. Tectonic evolution of the South Tethyan ocean: evidence from the Eastern Taurus Mountains (Elaziğ region, SE Turkey). Geol. Soc., Lond., Spec. Publ. 272, 231–270.
Robertson, A.H.F., Tasli, K., İNan, N., 2011. Evidence from the Kyrenia Range, Cyprus, of the northerly active margin of the Southern Neotethys during Late

Cretaceous–Early Cenozoic time. Geol. Mag. 149, 264–290.
Robertson, A.H.F., Parlak, O., Ustaomer, T., 2012. Overview of the Palaeozoic-Neogene evolution of Neotethys in the Eastern Mediterranean region (southern Turkey, Cyprus, Syria). Pet. Geosci. 18, 381–404.
Robertson, A., Parlak, O., Metin, Y., Vergili, Ö., Tasli, K., İnan, N., Soycan, H., 2013a. Late Palaeozoic–Cenozoic tectonic development of carbonate platform, margin and oceanic units in the Eastern Taurides, Turkey. Geol. Soc., Lond., Spec. Publ. 372, 316. SP372.
Robertson, A.H.F., McCay, G.A., Tasli, K., Yildiz, A., 2013b. Eocene development of the northerly active continental margin of the Southern Neotethys in the Kyrenia Range, north Cyprus. Geol. Mag. 151, 692–731.
Robertson, A.H.F., Parlak, O., Ustaömer, T., 2013c. Late Palaeozoic–Early Cenozoic tectonic development of Southern Turkey and the easternmost Mediterranean region: evidence from the inter-relations of continental and oceanic units. Geol. Soc., Lond., Spec. Publ. 372, 9–48.
Robertson, A., Boulton, S.J., Taslı, K., Yıldırım, N., İnan, N., Yıldız, A., Parlak, O., 2016. Late Cretaceous–Miocene sedimentary development of the Arabian continental margin in SE Turkey (Adıyaman Region): implications for regional palaeogeography and the closure history of Southern Neotethys. J. Asian Earth Sci. 115, 571–616.
Robinson, A.G., 1997. Regional and Petroleum Geology of the Black Sea and Surrounding Region. AAPG.
Robinson, A.G., Banks, C.J., Rutherford, M.M., Hirst, J.P.P., 1995. Stratigraphic and structural development of the Eastern Pontides, Turkey. J. Geol. Soc. 152, 861.
Robinson, A.G., Rudat, J.H., Banks, C.J., Wiles, R.L.F., 1996. Petroleum geology of the Black Sea. Mar. Pet. Geol. 13, 195–223.
Roest, R.W., Srivastava, P.S., 1991. Kinematics of the plate boundaries between Eurasia, Iberia, and Africa in the North Atlantic from the Late Cretaceous to the present. Geology 19, 613.
Rojay, B., 1995. Post-Triassic evolution of central Pontides; evidence from Amasya region, northern Anatolia. Geol. Romana 31, 329–350.
Rolland, Y., Billo, S., Corsini, M., Sosson, M., Galoyan, G., 2009a. Blueschists of the Amassia-Stepanavan suture zone (Armenia): linking Tethys subduction history from E-Turkey to W-Iran. Int. J. Earth Sci. 98, 533–550.
Rolland, Y., Galoyan, G., Bosch, D., Sosson, M., Corsini, M., Fornari, M., Verati, C., 2009b. Jurassic back-arc and Cretaceous hot-spot series In the Armenian ophiolites — Implications for the obduction process. Lithos 112, 163–187.
Rolland, Y., Galoyan, G., Sosson, M., Melkonyan, R., Avagyan, A., 2010. The Armenian Ophiolite: insights for Jurassic back-arc formation, Lower Cretaceous hot spot magmatism and Upper Cretaceous obduction over the South Armenian Block. Geol. Soc., Lond., Spec. Publ. 340, 353–382.
Rolland, Y., Sosson, M., Adamia, S., Sadradze, N., 2011. Prolonged Variscan to Alpine history of an active Eurasian margin (Georgia, Armenia) revealed by 40Ar/39Ar dating. Gondwana Res. 20, 798–815.
Rolland, Y., Perincek, D., Kaymakcı, N., Sosson, M., Barrier, E., Avagyan, A., 2012. Evidence for ~80–75 Ma subduction jump during Anatolide–Tauride–Armenian block accretion and ~48 Ma Arabia–Eurasia collision in Lesser Caucasus–East Anatolia. J. Geodyn. 56–57, 76–85.
Rolland, Y., Hässig, M., Bosch, D., Meijers, M.J.M., Sosson, M., Bruguier, O., Adamia, S., Sadradze, N., 2016. A review of the plate convergence history of the East Anatolia-Transcaucasus region during the Variscan: insights from the Georgian basement and its connection to the Eastern Pontides. J. Geodyn. 96, 131–145.
Romano, S.S., Dörr, W., Zulauf, G., 2004. Cambrian granitoids in pre-Alpine basement of Crete (Greece): evidence from U-Pb dating of zircon. Int. J. Earth Sci. 93, 844–859.
Rosenbaum, G., Lister, G.S., 2004a. Formation of Arcuate Orogenic Belts in the Western Mediterranean Region, Special Paper 383: Orogenic Curvature: Integrating Paleomagnetic and Structural Analyses, pp. 41–56.
Rosenbaum, G., Lister, G.S., 2004b. Neogene and Quaternary rollback evolution of the Tyrrhenian Sea, the Apennines, and the Sicilian Maghrebides. Tectonics 23.
Rosenbaum, G., Lister, G.S., 2005. The Western Alps from the Jurassic to Oligocene: spatio-temporal constraints and evolutionary reconstructions. Earth-Sci. Rev. 69, 281–306.
Rosenbaum, G., Lister, G.S., Duboz, C., 2002a. Reconstruction of the tectonic evolution of the western Mediterranean since the Oligocene. J. Virtual Explor. 8, 107–130.
Rosenbaum, G., Lister, G.S., Duboz, C., 2002b. Relative motions of Africa, Iberia and Europe during Alpine orogeny. Tectonophysics 359, 117–129.
Rosenbaum, G., Lister, G.S., Duboz, C., 2004. The Mesozoic and Cenozoic motion of Adria (central Mediterranean): a review of constraints and limitations. Geodin. Acta 17, 125–139.
Rosenbaum, G., Regenauer-Lieb, K., Weinberg, R., 2005. Continental extension: from core complexes to rigid block faulting. Geology 33.
Rosenbaum, G., Gasparon, M., Lucente, F.P., Peccerillo, A., Miller, M.S., 2008. Kinematics of slab tear faults during subduction segmentation and implications for Italian magmatism. Tectonics 27.
Rossetti, F., Faccenna, C., Goffé, B., Monié, P., Argentieri, A., Funiciello, R., Mattei, M., 2001. Alpine structural and metamorphic signature of the Sila Piccola Massif nappe stack (Calabria, Italy): insights for the tectonic evolution of the Calabrian Arc. Tectonics 20, 112–133.
Rossetti, F., Faccenna, C., Jolivet, L., Goffé, B., Funiciello, R., 2002. Structural signature and exhumation PTt paths of the blueschist units exposed in the interior of the Northern Apennine chain, tectonic implications. Boll. Soc. Geol. Ital. 121, 829–842.
Rossetti, F., Goffé, B., Monié, P., Faccenna, C., Vignaroli, G., 2004. Alpine orogenic P-T-t-deformation history of the Catena Costiera area and surrounding regions (Calabrian Arc, southern Italy): the nappe edifice of north Calabria revised with insights on the Tyrrhenian-Apennine system formation. Tectonics 23.
Rossetti, F., Glodny, J., Theye, T., Maggi, M., 2015. Pressure–temperature–deformation–time of the ductile Alpine shearing in Corsica: from orogenic construction to collapse. Lithos 218–219, 99–116.
Rossi, P., Cocherie, A., Fanning, C.M., Deloule, É., 2006. Variscan to eo-Alpine events recorded in European lower-crust zircons sampled from the French Massif Central and Corsica, France. Lithos 87, 235–260.
Roşu, E., Seghedi, I., Downes, H., Alderton, D.H.M., Szakács, A., Pécskay, Z., Panaiotu, C., Panaiotu, C.E., Nedelcu, L., 2004. Extension-related Miocene calc-alkaline magmatism in the Apuseni Mountains, Romania: origin of magmas. Swiss Bull. Miner. Petrol. 84, 153–172.
Roure, F., Choukroune, P., Berasteguy, X., Muñoz, J., Villien, A., Matheron, P., Bareyt, M., Segurat, M., Camara, P., Deramond, J., 1989. ECORS Deep seismic data and balanced cross-section; geometric constraints on the evolution of the Pyrenees. Tectonics 8, 41–50.
Roure, F., Roca, E., Sassi, W., 1993. The Neogene evolution of the outer Carpathian flysch units (Poland, Ukraine and Romania): kinematics of a foreland/fold-and-thrust belt system. Sediment. Geol. 86, 177–201.
Roure, F., Nazaj, S., Mushka, K., Fili, I., Cadet, J.-P., Bonneau, M., 2004. Kinematic evolution and petroleum systemsAn appraisal of the outer Albanides. Mem. Am. Assoc. Pet. Geol. 82, 474–493.
Royden, L.H., 1993. The tectonic expression slab pull at continental convergent boundaries. Tectonics 12, 303–325.
Royden, L., Burchfiel, B.C., 1989. Are systematic variations in thrust belt style related to plate boundary processes?(the Western Alps versus the Carpathians). Tectonics 8, 51–61.
Royden, L., Faccenna, C., 2018. Subduction orogeny and the Late Cenozoic evolution of the mediterranean arcs. Ann. Rev. Earth Planet. Sci. 46, 261–289.
Ruiz-Martínez, V.C., Torsvik, T.H., van Hinsbergen, D.J.J., Gaina, C., 2012. Earth at 200Ma: global palaeogeography refined from CAMP palaeomagnetic data. Earth Planet. Sci. Lett. 331–332, 67–79.
Răbăgia, T., Tărăpoancă, M., 1999. Tectonic evolution of the Romanian part of the Moesian platform: an integrated model. Rom. J. Tecton. Reg. Geol 77, 58.
Răbăgia, T., Maţenco, L., Cloetingh, S., 2011. The interplay between eustacy, tectonics and surface processes during the growth of a fault-related structure as derived from sequence stratigraphy: the Govora–Ocnele Mari antiform, South Carpathians. Tectonophysics 502, 196–220.
Rădulescu, D.P., Cornea, I., Săndulescu, M., Constantinescu, P., Rădulescu, F., Pompilian, A., 1976. Structure de la crôute terrestre en Roumanie. Essai d'interprétation des études séismiques profondes. An. Inst. Geol. Geofiz 50, 5–36.
Rızaoğlu, T., Parlak, O., Höck, V., Koller, F., Hames, W.E., Billor, Z., 2009. Andean-type active margin formation in the eastern Taurides: geochemical and geochronogical evidence from the Baskil granitoid (Elazığ, SE Turkey). Tectonophysics 473, 188–207.
Saadallah, A., Caby, R., 1996. Alpine extensional detachment tectonics in the Grande Kabylie metamorphic core complex of the Maghrebides (northern Algeria). Tectonophysics 267, 257–273.
Sàbat, F., Gelabert, B., Rodríguez-Perea, A., Giménez, J., 2011. Geological structure and evolution of Majorca: implications for the origin of the Western Mediterranean. Tectonophysics 510, 217–238.
Saccani, E., Photiades, A., 2004. Mid-ocean ridge and supra-subduction affinities in the Pindos ophiolites (Greece): implications for magma genesis in a forearc setting. Lithos 73, 229–253.
Saccani, E., Seghedi, A., Nicolae, I., 2004. Evidence of rift magmatism from preliminary petrological data on Lower Triassic mafic rocks from the North Dobrogea orogen (Romania). Ofioliti 29, 231–241.
Saccani, E., Bortolotti, V., Marroni, M., Pandolfi, L., Photiades, A., Principi, G., 2008a. The Jurassic association of backarc basin ophiolites and calc-alkaline volcanics in the Guevgueli Complex (Northern Greece): implication for the evolution of the Vardar Zone. Ofioliti 33, 209–227.
Saccani, E., Principi, G., Garfagnoli, F., Menna, F., 2008b. Corsica ophiolites: geochemistry and petrogenesis of basaltic and metabasaltic rocks. Ofioliti 33, e207.
Saddiqi, O., Feinberg, H., El Azzab, D., Michard, A., 1995. Paleomagnetisme des Peridotites des Beni Bousera (Rif interne, Maroc): Consequences Pour l'evolution Miocene de l'Arc de Gibraltar (Palaeomagnetism of the Beni Bousera Peridotites (Internal Rif, Morocco): Consequences for the Miocene Evolution of the Gibraltar Arc). In: Comptes Rendus-Academie des Sciences, Serie II: Sciences de la Terre et des Planetes, vol. 321, pp. 361–368.
Sagnotti, L., 1992. Paleomagnetic evidence for a Pleistocene counterclockwise rotation of the Sant'Arcangelo Basin, southern Italy. Geophys. Res. Lett. 19, 135–138.
Sagnotti, L., Mattei, M., Faccenna, C., Funiciello, R., 1994. Paleomagnetic evidence for no tectonic rotation of the central Italy Tyrrhenian margin since upper Pliocene. Geophys. Res. Lett. 21, 481–484.
Sagnotti, L., Winkler, A., Alfonsi, L., Fabio, F., Marra, F., 2000. Paleomagnetic constraints on the Plio-Pleistocene geodynamic evolution of the external central-Northern Apennines (Italy). Earth Planet. Sci. Lett. 180, 243–257.
Sahabi, M., Aslanian, D., Olivet, J.-L., 2004. Un nouveau point de départ pour l'histoire de l'Atlantique central. Compt. Rendus Geosci. 336, 1041–1052.
Saintot, A., Angelier, J., 2002. Tectonic paleostress fields and structural evolution of the NW-Caucasus fold-and-thrust belt from Late Cretaceous to Quaternary. Tectonophysics 357, 1–31.
Saintot, A., Brunet, M.-F., Yakovlev, F., Sébrier, M., Stephenson, R., Ershov, A., Chalot-

Prat, F., McCann, T., 2006a. The Mesozoic-Cenozoic tectonic evolution of the Greater Caucasus. Geol. Soc., Lond., Mem. 32, 277–289.
Saintot, A., Stephenson, R.A., Stovba, S., Brunet, M.-F., Yegorova, T., Starostenko, V., 2006b. The evolution of the southern margin of Eastern Europe (Eastern European and Scythian platforms) from the latest Precambrian-Early Palaeozoic to the Early Cretaceous. Geol. Soc., Lond., Mem. 32, 481–505.
Sánchez Rodríguez, L., 1998. Pre-Alpine and Alpine Evolution of the Ronda Ultramafic Complex and its Country-Rocks (Betic chain, southern Spain): U-Pb SHRIMP Zircon and Fission-Track Dating. ETH Zurich.
Sánchez-Rodríguez, L., Gebauer, D., 2000. Mesozoic formation of pyroxenites and gabbros in the Ronda area (southern Spain), followed by early Miocene subduction metamorphism and emplacement into the middle crust: U–Pb sensitive high-resolution ion microprobe dating of zircon. Tectonophysics 316, 19–44.
Sanfilippo, A., Tribuzio, R., 2012. Building of the deepest crust at a fossil slow-spreading centre (Pineto gabbroic sequence, Alpine Jurassic ophiolites). Contrib. Miner. Petrol. 165, 705–721.
Sani, F., Del Ventisette, C., Montanari, D., Bendkik, A., Chenakeb, M., 2007. Structural evolution of the Rides Prerifaines (Morocco): structural and seismic interpretation and analogue modelling experiments. Int. J. Earth Sci. 96, 685–706.
Sant, K., Andrić, N., Mandic, O., Demir, V., Pavelić, D., Rundić, L., Hrvatović, H., Maţenco, L., Krijgsman, W., 2018a. Magneto-biostratigraphy and paleoenvironments of the Miocene freshwater sediments of the Sarajevo-Zenica Basin. Palaeogeogr. Palaeoclimatol. Palaeoecol. 506, 48–69.
Sant, K., Mandic, O., Rundić, L., Kuiper, K.F., Krijgsman, W., 2018b. Age and evolution of the Serbian Lake System: integrated results from middle Miocene Lake Popovac. Newslett. Stratigr. 51, 117–143.
Santantonio, M., Carminati, E., 2010. Jurassic rifting evolution of the Apennines and Southern Alps (Italy): parallels and differences. Geol. Soc. Am. Bull. 123, 468–484.
Santantonio, M., Scrocca, D., Lipparini, L., 2013. The Ombrina-Rospo Plateau (Apulian Platform): evolution of a Carbonate Platform and its Margins during the Jurassic and Cretaceous. Mar. Pet. Geol. 42, 4–29.
Sanver, M., Ponat, E., 1981. Paleomagnetic results from Kirzehi and surrounding area-rotation of the Kirzehir Massif. Istanbul Earth Sci. Rev. 1, 231–238.
Sanz de Galdeano, C., Andreo, B., García-Tortosa, F.J., López-Garrido, A.C., 2001. The Triassic palaeogeographic transition between the Alpujarride and Malaguide complexes. Betic–Rif Internal Zone (S Spain, N Morocco). Palaeogeogr. Palaeoclimatol. Palaeoecol.
Sari, B., 2002. Upper Cretaceous Stratigraphy of the Bey Dağlar Carbonate Platform, Korkuteli Area (Western Taurides, Turkey). Turkish J. Earth Sci. 11, 39–59.
Saribudak, M., 1989. New results and a palaeomagnetic overview of the Pontides in northern Turkey. Geophys. J. Int. 99, 521–531.
Satolli, S., Calamita, F., 2008. Differences and similarities between the central and the Southern Apennines (Italy): examining the Gran Sasso versus the Matese-Frosolone salients using paleomagnetic, geological, and structural data. J. Geophys. Res. 113.
Satolli, S., Speranza, F., Calamita, F., 2005. Paleomagnetism of the Gran Sasso range salient (Central Apennines, Italy): pattern of orogenic rotations due to translation of a massive carbonate indenter. Tectonics 24.
Satolli, S., Besse, J., Speranza, F., Calamita, F., 2007. The 125–150 Ma high-resolution Apparent Polar Wander Path for Adria from magnetostratigraphic sections in Umbria–Marche (Northern Apennines, Italy): timing and duration of the global Jurassic–Cretaceous hairpin turn. Earth Planet. Sci. Lett. 257, 329–342.
Satolli, S., Besse, J., Calamita, F., 2008. Paleomagnetism of Aptian–Albian sections from the Northern Apennines (Italy): implications for the 150–100 Ma apparent polar wander of Adria and Africa. Earth Planet. Sci. Lett. 276, 115–128.
Sayit, K., Tekin, U.K., Göncüoğlu, M.C., 2011. Early-middle Carnian radiolarian cherts within the Eymir Unit, Central Turkey: constraints for the age of the Palaeotethyan Karakaya Complex. J. Asian Earth Sci. 42, 398–407.
Sayit, K., Göncüoğlu, M.C., Tekin, U.K., 2015a. Middle Carnian Arc-Type Basalts from the Lycian Nappes, Southwestern Anatolia: early Late Triassic Subduction in the Northern Branch of Neotethys. J. Geol. 123, 561–579.
Sayit, K., Marroni, M., Göncüoğlu, M.C., Pandolfi, L., Ellero, A., Ottria, G., Frassi, C., 2015b. Geological setting and geochemical signatures of the mafic rocks from the Intra-Pontide Suture Zone: implications for the geodynamic reconstruction of the Mesozoic Neotethys. Int. J. Earth Sci. 105, 39–64.
Sayit, K., Bedi, Y., Tekin, U.K., Göncüoğlu, M.C., Okuyucu, C., 2017. Middle Triassic back-arc basalts from the blocks in the Mersin Mélange, southern Turkey: implications for the geodynamic evolution of the Northern Neotethys. Lithos 268–271, 102–113.
Sayıt, K., Göncüoğlu, M.C., 2013. Geodynamic evolution of the Karakaya Mélange Complex, Turkey: a review of geological and petrological constraints. J. Geodyn. 65, 56–65.
Scharf, A., Handy, M.R., Favaro, S., Schmid, S.M., Bertrand, A., 2013. Modes of orogen-parallel stretching and extensional exhumation in response to microplate indentation and roll-back subduction (Tauern Window, Eastern Alps). Int. J. Earth Sci. 102, 1627–1654.
Schattner, U., 2010. What triggered the early-to-mid Pleistocene tectonic transition across the entire eastern Mediterranean? Earth Planet. Sci. Lett. 289, 539–548.
Schattner, U., Ben-Avraham, Z., 2007. Transform margin of the northern Levant, eastern Mediterranean: from formation to reactivation. Tectonics 26.
Scheepers, P., 1992. No tectonic rotation for the Apulia-Gargano foreland in the Pleistocene. Geophys. Res. Lett. 19, 2275–2278.
Scheepers, P.J.J., Langereis, C.G., 1993. Analysis of NRM directions from the Rossello composite: implications for tectonic rotations of the Caltanissetta basin, Sicily. Earth Planet. Sci. Lett. 119, 243–258.
Scheepers, P.J.J., Langereis, C.G., Hilgen, F.J., 1993. Counter-clockwise rotations in the Southern Apennines during the Pleistocene: paleomagnetic evidence from the Matera area. Tectonophysics 225, 379–410.
Scheepers, P.J.J., Langereis, C.G., Zijderveld, J.D.A., Hilgen, F.J., 1994. Paleomagnetic evidence for a Pleistocene clockwise rotation of the Calabro-Peloritan block (southern Italy). Tectonophysics 230, 19–48.
Schefer, S., Egli, D., Missoni, S., Bernoulli, D., Fügenschuh, B., Gawlick, H.-J., Jovanovic, D., Krystyn, L., Lein, R., Schmid, S., Sudar, M., 2010. Triassic metasediments in the internal Dinarides (Kopaonik area, southern Serbia): stratigraphy, paleogeographic and tectonic significance. Geol. Carpathica 61, 89–109.
Schefer, S., Cvetković, V., Fügenschuh, B., Kounov, A., Ovtcharova, M., Schaltegger, U., Schmid, S., 2011. Cenozoic granitoids in the Dinarides of southern Serbia: age of intrusion, isotope geochemistry, exhumation history and significance for the geodynamic evolution of the Balkan Peninsula. Int. J. Earth Sci. 100, 1181–1206.
Schenk, V., 1990. The Exposed Crustal Cross Section of Southern Calabria, Italy: structure and Evolution of a Segment of Hercynian Crust. In: Salisbury, M.H., Fountain, D.M. (Eds.), Exposed Cross-Sections of the Continental Crust. Springer Netherlands, Dordrecht, pp. 21–42.
Schenker, F.L., Fellin, M.G., Burg, J.P., 2014. Polyphase evolution of Pelagonia (northern Greece) revealed by geological and fission-track data. Solid Earth Discuss. 6, 3075–3109.
Schepers, G., van Hinsbergen, D.J.J., Spakman, W., Kosters, M.E., Boschman, L.M., McQuarrie, N., 2017. South-American plate advance and forced Andean trench retreat as drivers for transient flat subduction episodes. Nat. Commun. 8, 15249.
Scherreiks, R., Meléndez, G., BouDagher-Fadel, M., Fermeli, G., Bosence, D., 2014. Stratigraphy and tectonics of a time-transgressive ophiolite obduction onto the eastern margin of the Pelagonian platform from Late Bathonian until Valanginian time, exemplified in northern Evvoia, Greece. Int. J. Earth Sci. 103, 2191–2216.
Schettino, A., Turco, E., 2006. Plate kinematics of the Western Mediterranean region during the Oligocene and early Miocene. Geophys. J. Int. 166, 1398–1423.
Schettino, A., Turco, E., 2010. Tectonic history of the western Tethys since the Late Triassic. Geol. Soc. Am. Bull. 123, 89–105.
Schildgen, T.F., Cosentino, D., Caruso, A., Buchwaldt, R., Yıldırım, C., Bowring, S.A., Rojay, B., Echtler, H., Strecker, M.R., 2012. Surface expression of eastern Mediterranean slab dynamics: neogene topographic and structural evolution of the southwest margin of the Central Anatolian Plateau, Turkey. Tectonics 31.
Schirmer, W., Weber, J., Bachtadse, V., BouDagher-Fadel, M., Heller, F., Lehmkuhl, F., Panayides, I., Schirmer, U., 2010. Fluvial stacking due to plate collision and uplift during the Early Pleistocene in Cyprus. Central Eur. J. Geosci. 2.
Schleiffarth, W., Darin, M., Reid, M., Umhoefer, P.J., 2018. Dynamics of episodic Late Cretaceous–Cenozoic magmatism across Central to Eastern Anatolia: new insights from an extensive geochronology compilation. Geosphere 14, 1990–2008.
Schmid, S., Kissling, E., 2000. The arc of the western Alps in the light of geophysical data on deep crustal structure. Tectonics 19, 62–85.
Schmid, S., Aebli, H., Heller, F., Zingg, A., 1989. The role of the Periadriatic Line in the tectonic evolution of the Alps. Geol. Soc., Lond., Spec. Publ. 45, 153–171.
Schmid, S.M., Pfiffner, O.A., Froitzheim, N., Schönborn, G., Kissling, E., 1996. Geophysical-geological transect and tectonic evolution of the Swiss-Italian Alps. Tectonics 15, 1036–1064.
Schmid, S.M., Berza, T., Diaconescu, V., Froitzheim, N., Fügenschuh, B., 1998. Orogen-parallel extension in the Southern Carpathians. Tectonophysics 297, 209–228.
Schmid, S.M., Fügenschuh, B., Kisseling, E., Schuster, R., 2004a. TRANSMED Transects IV, V and VI: Three lithospheric Transects across the Alps and their Forelands, The TRANSMED Atlas: the Mediterranean Region from Crust to Mantle. Springer Verlag.
Schmid, S.M., FÜgenschuh, B., Kissling, E., Schuster, R., 2004b. Tectonic map and overall architecture of the Alpine orogen. Eclogae Geol. Helv. 97, 93–117.
Schmid, S.M., Bernoulli, D., Fügenschuh, B., Maţenco, L., Schefer, S., Schuster, R., Tischler, M., Ustaszewski, K., 2008. The Alpine-Carpathian-Dinaridic orogenic system: correlation and evolution of tectonic units. Swiss J. Geosci. 101, 139–183.
Schmid, S.M., Bernoulli, D., Fügenschuh, B., Schefer, S., Oberhänsli, R., Ustaszewski, K., 2011. Tracing the closure of Neotethys from the Alps to Western Turkey II: similarities and differences between Dinarides, Hellenides and Anatolides-Taurides. Geophys. Res. Abstr. 13.
Schmid, S.M., Scharf, A., Handy, M.R., Rosenberg, C.L., 2013. The Tauern Window (Eastern Alps, Austria): a new tectonic map, with cross-sections and a tectonometamorphic synthesis. Swiss J. Geosci. 106, 1–32.
Schmid, S.M., Kissling, E., Diehl, T., van Hinsbergen, D.J.J., Molli, G., 2017. Ivrea mantle wedge, arc of the Western Alps, and kinematic evolution of the Alps–Apennines orogenic system. Swiss J. Geosci. 110, 581–612.
Schmid, S.M., Bernoulli, D., Fügenschuh, B., Georgiev, N., Kounov, A., Maţenco, L., Oberhänsli, R., Pleuger, J., Schefer, S., Schuster, R., Tomljenović, B., Ustaszewski, K., van Hinsbergen, D.J.J., 2019. Tectonic Units of the Alpine Collision Zone between Eastern Alps and Western Turkey. Gondwana Res.
Schmidt, A., Pourteau, A., Candan, O., Oberhänsli, R., 2015. Lu–Hf geochronology on cm-sized garnets using microsampling: new constraints on garnet growth rates and duration of metamorphism during continental collision (Menderes Massif, Turkey). Earth Planet. Sci. Lett. 432, 24–35.
Scholger, R., Stingl, K., 2004. New paleomagnetic results from the middle Miocene (Karpatian and Badenian) in Northern Austria. Geol. Carpathica-Bratisl. 55, 199–206.
Scholger, R., Mauritsch, H.J., Brandner, R., 2000. Permian–Triassic boundary

magnetostratigraphy from the Southern Alps (Italy). Earth Planet. Sci. Lett. 176, 495–508.
Schönborn, G., 1999. Balancing cross sections with kinematic constraints: the Dolomites (northern Italy). Tectonics 18, 527–545.
Schott, J.J., Peres, A., 1987a. Paleomagnetism of Permo-Triassic Redbeds from the Asturias and Cantabric Chain (northern Spain): evidence for strong lower Tertiary remagnetizations. Tectonophysics 140, 179–191.
Schott, J.J., Peres, A., 1987b. Paleomagnetism of the Lower Cretaceous redbeds from northern Spain: evidence for a multistage acquisition of magnetization. Tectonophysics 139, 239–253.
Schott, J.J., Peres, A., 1988. Paleomagnetism of Permo-Triassic red beds in the western Pyrenees: evidence for strong clockwise rotations of the Paleozoic units. Tectonophysics 156, 75–88.
Schott, J.-J., Montigny, R., Thuizat, R., 1981. Paleomagnetism and potassium-argon age of the Messejana dike (Portugal and Spain): angular limitation to the rotation of the Iberian Peninsula since the Middle Jurassic. Earth Planet. Sci. Lett. 53, 457–470.
Schuster, R., 2015. Zur Geologie der Ostalpen. Abh. Geol. Bundesanst. 64, 143–165.
Scisciani, V., Calamita, F., 2009. Active intraplate deformation within Adria: examples from the Adriatic region. Tectonophysics 476, 57–72.
Scotese, C.R., 2001. Atlas of Earth History. University of Texas at Arlington. Department of Geology. PALEOMAP Project.
Scrocca, D., 2006. Thrust front segmentation induced by differential slab retreat in the Apennines (Italy). Terra Nova 18, 154–161.
Scrocca, D., Carminati, E., Doglioni, C., 2005. Deep structure of the Southern Apennines, Italy: thin-skinned or thick-skinned? Tectonics 24.
Seaton, N.C.A., Teyssier, C., Whitney, D.L., Heizler, M.T., 2014. Quartz and calcite microfabric transitions in a pressure and temperature gradient, Sivrihisar, Turkey. Geodin. Acta 26, 191–206.
Seghedi, A., 2001. The North Dobrogea orogenic belt (Romania): a review. Mém. Muséum Natl. d'histoire Nat. 186, 237–257.
Seghedi, A., 2012. Palaeozoic Formations from Dobrogea and Pre-Dobrogea–An Overview. Turk. J. Earth Sci. 21.
Seghedi, A., Berza, T., Iancu, V., Maruntiu, M., Oaie, G., 2005a. Neoproterozoic terranes in the Moesian basement and in the Alpine Danubian nappes of the South Carpathians. Geol. Belg. 8, 4–19.
Seghedi, A., Vaida, M., Iordan, M., Verniers, J., 2005b. Paleozoic evolution of the Romanian part of the Moesian Platform: an overview. Geol. Belg. 8, 99–120.
Sen, S., Seyitoğlu, G., 2009. Magnetostratigraphy of early–middle Miocene deposits from east–west trending Alaşehir and Büyük Menderes grabens in western Turkey, and its tectonic implications. Geol. Soc., Lond., Spec. Publ. 311, 321–342.
Şenel, M., 2002. Geological Map of Turkey in 1/500.000 Scale: Konya Sheet. Publication of Mineral Research and Exploration Directorate of Turkey (MTA), Ankara.
Şengör, A.C., 1984. The Cimmeride orogenic system and the tectonics of Eurasia. Geol. Soc. Am. Spec. Pap. 195, 82.
Şengör, A.M.C., 1987. Tectonics of the tethysides: orogenic collage development in a collisional setting. Ann. Rev. Earth Planet. Sci. 15, 213–244.
Şengör, A.M.C., Yılmaz, Y., 1981. Tethyan evolution of Turkey: a plate tectonic approach. Tectonophysics 75, 181–241.
Şengör, A.M.C., Yılmaz, Y., Ketin, I., 1980. Remnants of a pre–Late Jurassic ocean in northern Turkey: fragments of Permian-Triassic Paleo-Tethys? Geol. Soc. Am. Bull. 91.
Şengör, A.M.C., Yılmaz, Y., Sungurlu, O., 1984. Tectonics of the Mediterranean Cimmerides: nature and evolution of the western termination of Palaeo-Tethys. Geol. Soc., Lond., Spec. Publ. 17, 77–112.
Şengör, A.M.C., Tüysüz, O., İmren, C., Sakınç, M., Eyidoğan, H., Görür, N., Le Pichon, X., Rangin, C., 2005. The North Anatolian Fault: a new look. Ann. Rev. Earth Planet. Sci. 33, 37–112.
Şengör, A.M.C., Özeren, M.S., Keskin, M., Sakınç, M., Özbakır, A.D., Kayan, İ., 2008. Eastern Turkish high plateau as a small Turkic-type orogen: implications for post-collisional crust-forming processes in Turkic-type orogens. Earth-Sci. Rev. 90, 1–48.
Şengün, F., Koralay, O.E., 2016. Early Variscan magmatism along the southern margin of Laurasia: geochemical and geochronological evidence from the Biga Peninsula, NW Turkey. Int. J. Earth Sci. 106, 811–826.
Séranne, M., 1999. The Gulf of Lion continental margin (NW Mediterranean) revisited by IBS: an overview. Geol. Soc., Lond., Spec. Publ. 156, 15–36.
Seton, M., Müller, R.D., Zahirovic, S., Gaina, C., Torsvik, T., Shephard, G., Talsma, A., Gurnis, M., Turner, M., Maus, S., Chandler, M., 2012. Global continental and ocean basin reconstructions since 200Ma. Earth-Sci. Rev. 113, 212–270.
Seyitoğlu, G., Isik, V., Gürbüz, E., Gürbüz, A., 2017. The discovery of a low-angle normal fault in the Taurus Mountains: the İvriz detachment and implications concerning the Cenozoic geology of southern Turkey*. Turk. J. Earth Sci. 26, 189–205.
Seymen, I., 1984. Geological evolution of the metamorphic rocks in the Kırs ehir Massif. In: Ketin Simpozyumu, pp. 133–148.
Sheremet, Y., Sosson, M., Muller, C., Gintov, O., Murovskaya, A., Yegorova, T., 2016a. Key problems of stratigraphy in the Eastern Crimea Peninsula: some insights from new dating and structural data. Geol. Soc., Lond., Spec. Publ. 428.
Sheremet, Y., Sosson, M., Ratzov, G., Sydorenko, G., Voitsitskiy, Z., Yegorova, T., Gintov, O., Murovskaya, A., 2016b. An offshore-onland transect across the north-eastern Black Sea basin (Crimean margin): evidence of Paleocene to Pliocene two-stage compression. Tectonophysics 688, 84–100.
Sherlock, S., Kelley, S., Inger, S., Harris, N., Okay, A., 1999. 40Ar-39Ar and Rb-Sr geochronology of high-pressure metamorphism and exhumation history of the Tavşanlı Zone, NW Turkey. Contrib. Miner. Petrol. 137, 46–58.
Shnyukov, E., Shcherbakov, I., Shnyukova, E., 1997. Palaeo-Island Arc in the Northern Black Sea. Chornobylinterinform, Kiev (in Russian).
Shreider, A.A., 2005. Opening of the deep-water basin of the Black Sea. Oceanology 45, 560–571.
Sibuet, J.-C., Srivastava, S.P., Spakman, W., 2004. Pyrenean orogeny and plate kinematics. J. Geophys. Res.: Solid Earth 109.
Sibuet, J.-C., Rouzo, S., Srivastava, S., 2012. Plate tectonic reconstructions and paleogeographic maps of the central and North Atlantic oceans. Can. J. Earth Sci. 49, 1395–1415.
Simon-Labric, T., Rolland, Y., Dumont, T., Heymes, T., Authemayou, C., Corsini, M., Fornari, M., 2009. 40Ar/39Ar dating of Penninic Front tectonic displacement (W Alps) during the lower Oligocene (31-34 Ma). Terra Nova 21, 127–136.
Sinclair, H.D., Juranov, S.G., Georgiev, G., Byrne, P., Mountney, N.P., 1998. The Balkan thrust wedge and foreland basin of eastern Bulgaria: structural and stratigraphic development. Mem.-Am. Assoc. Pet. Geol. 91–114.
Sirna, M., 1988. Elementi di tettonica transpressiva lungo la linea di Atina (Lazio Meridionale). Mem. Soc. Geol. Ital. 41, 1179–1190.
Skourlis, K., Doutsos, T., 2003. The Pindos Fold-and-thrust belt (Greece): inversion kinematics of a passive continental margin. Int. J. Earth Sci. 92, 891–903.
Soffel, H., 1972. Anticlockwise rotation of Italy between the Eocene and Miocene: palaeomagnetic evidence from the Colli Euganei, Italy. Earth Planet. Sci. Lett. 17, 207–210.
Sokhadze, G., Floyd, M., Godoladze, T., King, R., Cowgill, E., Javakhishvili, Z., Hahubia, G., Reilinger, R., 2018. Active convergence between the Lesser and Greater Caucasus in Georgia: constraints on the tectonic evolution of the Lesser–Greater Caucasus continental collision. Earth Planet. Sci. Lett. 481, 154–161.
Sokoutis, D., Brun, J.P., Van Den Driessche, J., Pavlides, S., 1993. A major Oligo-Miocene detachment in southern Rhodope controlling north Aegean extension. J. Geol. Soc. 150, 243–246.
Sokół, K., Halama, R., Meliksetian, K., Savov, I.P., Navasardyan, G., Sudo, M., 2018. Alkaline magmas in zones of continental convergence: the Tezhsar volcano-intrusive ring complex, Armenia. Lithos 320, 172–191.
Somin, M.L., 2011. Pre-Jurassic basement of the Greater Caucasus: brief overview. Turk. J. Earth Sci. 20, 545–610.
Somma, R., Messina, A., Mazzoli, S., 2005. Syn-orogenic extension in the Peloritani Alpine Thrust Belt (NE Sicily, Italy): evidence from the Alì Unit. Compt. Rendus Geosci. 337, 861–871.
Sonnette, L., Humbert, F., Aubourg, C., Gattacceca, J., Lee, J.-C., Angelier, J., 2014. Significant rotations related to cover–substratum decoupling: example of the Dôme de Barrôt (Southwestern Alps, France). Tectonophysics 629, 275–289.
Sosson, M., Rolland, Y., Müller, C., Danelian, T., Melkonyan, R., Kekelia, S., Adamia, S., Babazadeh, V., Kangarli, T., Avagyan, A., 2010. Subductions, obduction and collision in the Lesser Caucasus (Armenia, Azerbaijan, Georgia), new insights. Geol. Soc., Lond., Spec. Publ. 340, 329–352.
Sosson, M., Stephenson, R., Sheremet, Y., Rolland, Y., Adamia, S., Melkonian, R., Kangarli, T., Yegorova, T., Avagyan, A., Galoyan, G., Danelian, T., Hässig, M., Meijers, M., Müller, C., Sahakyan, L., Sadradze, N., Alania, V., Enukidze, O., Mosar, J., 2016. The eastern Black Sea-Caucasus region during the Cretaceous: new evidence to constrain its tectonic evolution. Compt. Rendus Geosci. 348, 23–32.
Sotiropoulos, S., Kamberis, E., Triantaphyllou, M.V., Doutsos, T., 2003. Thrust sequences in the central part of the External Hellenides. Geol. Mag. 140, 661–668.
Spakman, W., Hall, R., 2010. Surface deformation and slab–mantle interaction during Banda arc subduction rollback. Nat. Geosci. 3, 562–566.
Spakman, W., Wortel, R., 2004. A Tomographic View on Western Mediterranean Geodynamics. In: Cavazza, W., Roure, F., Spakman, W., Stampfli, G.M., Ziegler, P.A. (Eds.), The TRANSMED Atlas. The Mediterranean Region from Crust to Mantle: Geological and Geophysical Framework of the Mediterranean and the Surrounding Areas. Springer Berlin Heidelberg, Berlin, Heidelberg, pp. 31–52.
Spakman, W., Chertova, M.V., van den Berg, A., van Hinsbergen, D.J.J., 2018. Puzzling features of western Mediterranean tectonics explained by slab dragging. Nat. Geosci. 11, 211–216.
Spalluto, L., Caffau, M., 2010. Stratigraphy of the mid-Cretaceous shallow-water limestones of the Apulia Carbonate Platform (Murge, Apulia, southern Italy). Ital. J. Geosci. 129, 335–352.
Spalluto, L., Pieri, P., 2008. Geologic map of the Mesozoic-Cenozoic carbonate units cropping out in the south-western Gargano Promontory (southern Italy): new stratigraphic constraints for the tectonic evolution of the area. Development of Geological Knowledge on the Apulian-Campanian and Tuscan-Umbrian-Marchean Apennines. Mem. Descr. Carta Geol. Ital. 77, 147–176.
Speranza, F., 2003. Genesis and evolution of a curved mountain front: paleomagnetic and geological evidence from the Gran Sasso range (Central Apennines, Italy). Tectonophysics 362, 183–197.
Speranza, F., Parisi, G., 2007. High-resolution magnetic stratigraphy at Bosso Stirpeto (Marche, Italy): anomalous geomagnetic field behaviour during early Pliensbachian (early Jurassic) times? Earth Planet. Sci. Lett. 256, 344–359.
Speranza, F., Kissel, C., Islami, I., Hyseni, A., Laj, C., 1992. First paleomagnetic evidence for rotation of the Ionian Zone of Albania. Geophys. Res. Lett. 19, 697–700.
Speranza, F., Islami, I., Kissel, C., Hyseni, A., 1995. Paleomagnetic evidence for Cenozoic clockwise rotation of the external Albanides. Earth Planet. Sci. Lett. 129, 121–134.
Speranza, F., Sagnotti, L., Mattei, M., 1997. Tectonics of the Umbria-Marche-Romagna

Arc (central Northern Apennines, Italy): new paleomagnetic constraints. J. Geophys. Res.: Solid Earth 102, 3153–3166.
Speranza, F., Mattei, M., Naso, G., Di Bucci, D., Corrado, S., 1998. Neogene–Quaternary evolution of the central Apennine orogenic system (Italy): a structural and palaeomagnetic approach in the Molise region. Tectonophysics 299, 143–157.
Speranza, F., Maniscalco, R., Mattei, M., Di Stefano, A., Butler, R.W.H., Funiciello, R., 1999. Timing and magnitude of rotations in the frontal thrust systems of southwestern Sicily. Tectonics 18, 1178–1197.
Speranza, F., Mattei, M., Sagnotti, L., Grasso, F., 2000. Rotational differences between the northern and southern Tyrrhenian domains: palaeomagnetic constraints from the Amantea basin (Calabria, Italy). J. Geol. Soc. 157, 327.
Speranza, F., Villa, I.M., Sagnotti, L., Florindo, F., Cosentino, D., Cipollari, P., Mattei, M., 2002. Age of the Corsica–Sardinia rotation and Liguro–Provençal Basin spreading: new paleomagnetic and Ar/Ar evidence. Tectonophysics 347, 231–251.
Speranza, F., Maniscalco, R., Grasso, M., 2003. Pattern of orogenic rotations in central-eastern Sicily: implications for the timing of spreading in the Tyrrhenian Sea. J. Geol. Soc. 160, 183–195.
Speranza, F., Macrì, P., Rio, D., Fornaciari, E., Consolaro, C., 2011. Paleomagnetic evidence for a post-1.2 Ma disruption of the Calabria terrane: consequences of slab breakoff on orogenic wedge tectonics. Geol. Soc. Am. Bull. 123, 925–933.
Speranza, F., Minelli, L., Pignatelli, A., Chiappini, M., 2012. The Ionian Sea: the oldest in situ ocean fragment of the world? J. Geophys. Res.: Solid Earth 117.
Speranza, F., Hernandez-Moreno, C., Avellone, G., Gasparo Morticelli, M., Agate, M., Sulli, A., Di Stefano, E., 2018. Understanding Paleomagnetic Rotations in Sicily: thrust Versus Strike-Slip Tectonics. Tectonics 37, 1138–1158.
Spray, J.G., Roddick, J.C., 1980. Petrology and 40Ar/39Ar geochronology of some hellenic sub-ophiolite metamorphic rocks. Contrib. Miner. Petrol. 72, 43–55.
Spray, J.G., Bébien, J., Rex, D.C., Roddick, J.C., 1984. Age constraints on the igneous and metamorphic evolution of the Hellenic-Dinaric ophiolites. Geol. Soc., Lond., Spec. Publ. 17, 619–627.
Srivastava, S.P., Roest, W.R., 1996. Porcupine plate hypothesis-Comment. Mar. Geophys. Res. 18, 589–593.
Srivastava, S.P., Tapscott, C.R., 1986. Plate kinematics of the North Atlantic. Geol. North Am. 1000, 379–404.
Srivastava, S.P., Verhoef, J., 1992. Evolution of Mesozoic sedimentary basins around the North Central Atlantic: a preliminary plate kinematic solution. Geol. Soc., Lond., Spec. Publ. 62, 397.
Srivastava, S.P., Roest, W.R., Kovacs, L.C., Oakey, G., Lévesque, S., Verhoef, J., Macnab, R., 1990a. Motion of Iberia since the Late Jurassic: results from detailed aeromagnetic measurements in the Newfoundland Basin. Tectonophysics 184, 229–260.
Srivastava, S.P., Schouten, H., Roest, W.R., Klitgord, K.D., Kovacs, L.C., Verhoef, J., Macnab, R., 1990b. Iberian plate kinematics: a jumping plate boundary between Eurasia and Africa. Nature 344, 756.
Stampfli, G.M., 1993. Le Briançonnais, terrain exotique dans les Alpes? Eclogae Geol. Helv. 86, 1–45.
Stampfli, G.M., Borel, G., 2002. A plate tectonic model for the Paleozoic and Mesozoic constrained by dynamic plate boundaries and restored synthetic oceanic isochrons. Earth Planet. Sci. Lett. 196, 17–33.
Stampfli, G.M., Hochard, C., 2009. Plate tectonics of the Alpine realm. Geol. Soc., Lond., Spec. Publ. 327, 89–111.
Stampfli, G.M., Kozur, H.W., 2006. Europe from the Variscan to the Alpine cycles. Mem.-Geol. Soc. Lond. 32, 57.
Stampfli, G., Marcoux, J., Baud, A., 1991. Tethyan margins in space and time. Palaeogeogr. Palaeoclimatol. Palaeoecol. 87, 373–409.
Stankevitch, E.K., Sholpo, L.E., 1971. Paleomagnetic Directions and Pole Positions: Data for the USSR. Soviet Geophysical Committee, World Data Center-B, Moscow.
Stefanescu, M., 1983. General remarks on the Eastern Carpathian flysch and its depositional environment. Rev. Roum. G6ol. Gdophys. Gdogr 27, 59–64.
Stephenson, R., 2004. EUROPROBE GeoRift, volume 3: Intraplate Tectonics and Basin Dynamics - the lithosphere of the southern Eastern European Craton and its Margin - Preface. Tectonophysics 381, 1–4.
Stephenson, R., Schellart, W.P., 2010. The Black Sea back-arc basin: insights to its origin from geodynamic models of modern analogues. Geol. Soc., Lond., Spec. Publ. 340, 11–21.
Stephenson, R.A., Yegorova, T., Brunet, M.F., Stovba, S., Wilson, M., Starostenko, V., Saintot, A., Kusznir, N., 2006. Late Palaeozoic intra- and pericratonic basins on the East European Craton and its margins. Geol. Soc., Lond., Mem. 32, 463.
Stich, D., Serpelloni, E., de Lis Mancilla, F., Morales, J., 2006. Kinematics of the Iberia–Maghreb plate contact from seismic moment tensors and GPS observations. Tectonophysics 426, 295–317.
Stock, J., Hodges, K., 1989. Pre-Pliocene extension around the Gulf of California and the transfer of Baja California to the Pacific plate. Tectonics 8, 99–115.
Stock, J.M., Molnar, P., 1983. Some geometrical aspects of uncertainties in combined plate reconstructions. Geology 11, 697–701.
Stoica, A.M., Ducea, M.N., Roban, R.D., Jianu, D., 2015. Origin and evolution of the South Carpathians basement (Romania): a zircon and monazite geochronologic study of its Alpine sedimentary cover. Int. Geol. Rev. 58, 510–524.
Stojadinovic, U., Matenco, L., Andriessen, P.A.M., Toljić, M., Foeken, J.P.T., 2013. The balance between orogenic building and subsequent extension during the Tertiary evolution of the NE Dinarides: constraints from low-temperature thermochronology. Glob. Planet. Change 103, 19–38.
Stojadinovic, U., Matenco, L., Andriessen, P., Toljić, M., Rundić, L., Ducea, M.N., 2017. Structure and provenance of Late Cretaceous–Miocene sediments located near the NE Dinarides margin: inferences from kinematics of orogenic building and subsequent extensional collapse. Tectonophysics 710–711, 184–204.
Storetvedt, K.M., Mogstad, H., Abranches, M.C., Mitchell, J.G., Serralheiro, A., 1987. Palaeomagnetism and isotopic age data from Upper Cretaceous igneous rocks of W. Portugal; geological correlation and plate tectonic aspects. Geophys. J. Royal Astron. Soc. 88, 241–263.
Storetvedt, K., Mitchell, J.G., Abranches, M.C., Oftedahl, S., 1990. A new kinematic model for Iberia; further palaeomagnetic and isotopic age evidence. Phys. Earth Planet. Inter. 62, 109–125.
Sunal, G., Satir, M., Natal'in, B.A., Topuz, G., Vonderschmidt, O., 2011. Metamorphism and diachronous cooling in a contractional orogen: the Strandja Massif, NW Turkey. Geol. Mag. 148, 580–596.
Sussman, A.J., Butler, R.F., Dinarès-Turell, J., Vergés, J., 2004. Vertical-axis rotation of a foreland fold and implications for orogenic curvature: an example from the Southern Pyrenees, Spain. Earth Planet. Sci. Lett. 218, 435–449.
Swarbrick, R.E., Naylor, M.A., 1980. The Kathikas mélange, SW Cyprus: late Cretaceous submarine debris flows. Sedimentology 27, 63–78.
Săndulescu, M., 1975. Essai de Synthese Structurale des Carpathes.
Săndulescu, M., 1980. Analyse Géotectonique des Chaînes Alpines Situées Autour de la Mer Noire Occidentale, vol. 56. Anuarul Institutului de Geologie si Geofizica, Bucharest, pp. 5–54.
Săndulescu, M., 1984. Geotectonica României (Geotectonics of Romania). Ed. Tehnică, Bucharest.
Săndulescu, M., 1988. Cenozoic tectonic history of the Carpathians. The Pannonian Basin-A Study in Basin Evolution. Am. Assoc. Petrol. Geol. Mem. 45, 17–25.
Săndulescu, M., 1994. Overview on Romanian geology. Rom. J. Tecton. Reg. Geol., Suppl. 2 75, 3–15.
Săndulescu, M., Visarion, M., 1978. Considerations sur la structure tectonique du soubassement de la depression de Transylvanie. DS Inst. Geol. Geofiz 64, 153–173.
Săndulescu, M., Visarion, M., 1988. La structure des plate-formes situées dans l'avant-pays et au-dessous des nappes du flysch des Carpathes orientales. St. Tehn. Econ., Geofiz 15, 62–67.
Taberner, C., Dinarés-Turell, J., Giménez, J., Docherty, C., 1999. Basin infill architecture and evolution from magnetostratigraphic cross-basin correlations in the southeastern Pyrenean foreland basin. GSA Bull. 111, 1155–1174.
Tari, V., 2002. Evolution of the Northern and Western Dinarides: a Tectonostratigraphic Approach, Continental Collision and the Tectono-Sedimentary Evolution of Forelands. Copernicus.
Tari, G., 2005. The divergent continental margins of the Jurassic proto-Pannonian Basin: implications for the petroleum systems of the Vienna Basin and the Moesian Platform. In: Transactions GCSSEPM Foundation Th Annual Res. Conf. SEPM, pp. 955–986.
Tari, G., Horváth, F., Rumpler, J., 1992. Styles of extension in the Pannonian Basin. Tectonophysics 208, 203–219.
Tari, G., Dicea, O., Faulkerson, I., Georgiev, G., Popov, S., Stefanescu, M., Weir, G., 1998. Cimmerian and Alpine stratigraphy and structural evolution of the Moesian Platform (Romania/Bulgaria). Mem.-Am. Assoc. Pet. Geol. 63–90.
Tari, G., Dövényi, P., Dunkl, I., Horváth, F., Lenkey, L., Stefanescu, M., Szafián, P., Tóth, T., 1999. Lithospheric structure of the Pannonian basin derived from seismic, gravity and geothermal data. Geol. Soc., Lond., Spec. Publ. 156, 215.
Tatar, O., Piper, J.D.A., Park, R.G., Gürsoy, H., 1995. Palaeomagnetic study of block rotations in the Niksar overlap region of the North Anatolian Fault Zone, central Turkey. Tectonophysics 244, 251–266.
Tatar, O., Piper, J.D.A., Gürsoy, H., Temiz, H., 1996. Regional Significance of Neotectonic Counterclockwise Rotation in Central Turkey. Int. Geol. Rev. 38, 692–700.
Tatar, O., Piper, J.D.A., Gürsoy, H., 2000. Palaeomagnetic study of the Erciyes sector of the Ecemiş Fault Zone: neotectonic deformation in the Southeastern part of the Anatolian Block. Geol. Soc., Lond., Spec. Publ. 173, 423.
Tatar, O., Gürsoy, H., Piper, J.D.A., 2002. Differential neotectonic rotations in Anatolia and the Tauride Arc: palaeomagnetic investigation of the Erenlerdağ Volcanic Complex and Isparta volcanic district, south–central Turkey. J. Geol. Soc. 159, 281.
Teixell, A., 1996. The Ansó transect of the southern Pyrenees: basement and cover thrust geometries. J. Geol. Soc. 153, 301.
Teixell, A., 1998. Crustal structure and orogenic material budget in the west central Pyrenees. Tectonics 17, 395–406.
Teixell, A., Arboleya, M.-L., Julivert, M., Charroud, M., 2003. Tectonic shortening and topography in the central High Atlas (Morocco). Tectonics 22.
Tekin, U.K., Göncüoğlu, M.C., 2007. Discovery of the oldest (Upper Ladinian to Middle Carnian) radiolarian assemblages from the Bornova flysch zone in western Turkey: implications for the evolution of the Neotethyan Izmir-Ankara ocean. Ofioliti 32, 131–150.
Tekin, U.K., Göncüoğlu, M.C., Turhan, N., 2002. First evidence of Late Carnian radiolarians from the Izmir–Ankara suture complex, central Sakarya, Turkey: implications for the opening age of the Izmir–Ankara branch of Neo-Tethys. Geobios 35, 127–135.
Tekin, U.K., Ural, M., Göncüoğlu, M.C., Arslan, M., Kürüm, S., 2015. Upper Cretaceous Radiolarian ages from an arc–back-arc within the Yüksekova Complex in the southern Neotethys mélange, SE Turkey. Compt. Rendus Palevol 14, 73–84.
Tekin, U.K., Bedi, Y., Okuyucu, C., Göncüoğlu, M.C., Sayit, K., 2016. Radiolarian biochronology of upper Anisian to upper Ladinian (Middle Triassic) blocks and tectonic slices of volcano-sedimentary successions in the Mersin Mélange, southern Turkey: new insights for the evolution of Neotethys. J. Afr. Earth Sci.

124, 409–426.
Tempier, C., 1987. Modele nouveau de mise en place des structures provencales. Bull. Soc. Géol. France III, 533–540.
ten Veen, J.H., Kleinspehn, K.L., 2002. Geodynamics along an increasingly curved convergent plate margin: late Miocene-Pleistocene Rhodes, Greece. Tectonics 21, 8-1-8-21.
ten Veen, J.H., Kleinspehn, K.L., 2003. Incipient continental collision and plate-boundary curvature: late Pliocene–Holocene transtensional Hellenic forearc, Crete, Greece. J. Geol. Soc. 160, 161–181.
ten Veen, J.H., Woodside, J.M., Zitter, T.A.C., Dumont, J.F., Mascle, J., Volkonskaia, A., 2004. Neotectonic evolution of the Anaximander Mountains at the junction of the Hellenic and Cyprus arcs. Tectonophysics 391, 35–65.
ten Veen, J.H., 2004. Extension of Hellenic forearc shear zones in SW Turkey: the Pliocene–Quaternary deformation of the Eşen Çay Basin. J. Geodyn. 37, 181–204.
Ternois, S., Odlum, M., Ford, M., Pik, R., Stockli, D., Tibari, B., Vacherat, A., Bernard, V., 2019. Thermochronological evidence of early orogenesis, eastern Pyrenees, France. Tectonics 28. https://doi.org/10.1029/2018TC005254.
Thiébault, F., 1979. Stratigraphie de la série des calcschistes et merbres (“Plattenkalk”) en fenêtre dans les massifs du Taygete et du Paron (Péloponnese-Grece). In: Proceedings of the VI Colloqium of the Geology of the Aegean Region. Institute of Geology and Mining Exploration, Athens, pp. 691–701.
Thiébault, F., Fleury, J.J., Clément, B., Dégardin, J.M., 1994. Paleogeographic and paleotectonic implications of clay mineral distribution in late Jurassic-early Cretaceous sediments of the Pindos-Olonos and Beotian Basins, Greece. Palaeogeogr. Palaeoclimatol. Palaeoecol. 108, 23–40.
Thomas, J.C., Claudel, M.E., Collombet, M., Tricart, P., Chauvin, A., Dumont, T., 1999. First paleomagnetic data from the sedimentary cover of the French Penninic Alps: evidence for Tertiary counterclockwise rotations in the Western Alps. Earth Planet. Sci. Lett. 171, 561–574.
Thomson, S.N., Stöckhert, B., Brix, M.R., 1998. Thermochronology of the high-pressure metamorphic rocks of Crete, Greece: implications for the speed of tectonic processes. Geology 26.
Thön, i, M., Miller, C., Blichert-Toft, J., Whitehouse, M.J., Konzett, J., Zanetti, A., 2008. Timing of high-pressure metamorphism and exhumation of the eclogite type-locality (Kupplerbrunn–Prickler Halt, Saualpe, south-eastern Austria): constraints from correlations of the Sm–Nd, Lu–Hf, U–Pb and Rb–Sr isotopic systems. J. Metamorph. Geol. 26, 561–581.
Thöny, W., Ortner, H., Scholger, R., 2006. Paleomagnetic evidence for large en-bloc rotations in the Eastern Alps during Neogene orogeny. Tectonophysics 414, 169–189.
Tikhomirov, P.L., Chalot-Prat, F., Nazarevich, B.P., 2004. Triassic volcanism in the Eastern Fore-Caucasus: evolution and geodynamic interpretation. Tectonophysics 381, 119–142.
Tiliță, M., Maţenco, L., Dinu, C., Ionescu, L., Cloetingh, S., 2013. Understanding the kinematic evolution and genesis of a back-arc continental “sag” basin: the Neogene evolution of the Transylvanian Basin. Tectonophysics 602, 237–258.
Tischler, M., Gröger, H.R., Fügenschuh, B., Schmid, S.M., 2006. Miocene tectonics of the Maramures area (Northern Romania): implications for the Mid-Hungarian fault zone. Int. J. Earth Sci. 96, 473–496.
Toljić, M., Maţenco, L., Ducea, M.N., Stojadinović, U., Milivojević, J., Đerić, N., 2013. The evolution of a key segment in the Europe–Adria collision: the Fruška Gora of northern Serbia. Glob. Planet. Change 103, 39–62.
Toljić, M., Maţenco, L., Stojadinović, U., Willingshofer, E., Ljubović-Obradović, D., 2018. Understanding fossil fore-arc basins: inferences from the Cretaceous Adria-Europe convergence in the NE Dinarides. Glob. Planet. Change 171, 167–184.
Tomaschek, F., Keiter, M., Kennedy, A.K., Ballhaus, C., 2008. Pre-Alpine basement within the Northern Cycladic Blueschist Unit on Syros Island, Greece [Präalpines Grundgebirge in der Nördlichen Kykladischen Blauschiefereinheit auf der Insel Syros, Griechenland.]. Z. Dtsch. Ges. Geowiss. 159, 521–531.
Tomljenović, B., Csontos, L., 2001. Neogene–Quaternary structures in the border zone between Alps, Dinarides and Pannonian Basin (Hrvatsko zagorje and Karlovac Basins, Croatia). Int. J. Earth Sci. 90, 560–578.
Tomljenović, B., Csontos, L., Márton, E., Márton, P., 2008. Tectonic evolution of the northwestern Internal Dinarides as constrained by structures and rotation of Medvednica Mountains, North Croatia. Geol. Soc., Lond., Spec. Publ. 298, 145–167.
Topchishvili, M., 1996. Stratigraphy of the Lower Jurassic formations of Georgia. In: Proceedings of the Geological Institute of Academy of Sciences of Georgia, p. 216. New Series 108.
Topuz, G., 2004. Aluminous granulites from the Pulur complex, NE Turkey: a case of partial melting, efficient melt extraction and crystallisation. Lithos 72, 183–207.
Topuz, G., Altherr, R., Schwarz, W.H., Dokuz, A., Meyer, H.-P., 2006. Variscan amphibolite-facies rocks from the Kurtoğlu metamorphic complex (Gümüşhane area, Eastern Pontides, Turkey). Int. J. Earth Sci. 96, 861–873.
Topuz, G., Altherr, R., Siebel, W., Schwarz, W.H., Zack, T., Hasözbek, A., Barth, M., Satır, M., Şen, C., 2010. Carboniferous high-potassium I-type granitoid magmatism in the Eastern Pontides: the Gümüşhane pluton (NE Turkey). Lithos 116, 92–110.
Topuz, G., Göçmengil, G., Rolland, Y., Çelik, Ö.F., Zack, T., Schmitt, A.K., 2013. Jurassic accretionary complex and ophiolite from northeast Turkey: no evidence for the Cimmerian continental ribbon. Geology 41, 255–258.
Topuz, G., Çelik, O.F., Şengör, A.M.C., Altintas, I.E., Zack, T., Rolland, Y., Barth, M., 2014a. Jurassic ophiolite formation and emplacement as backstop to a subduction-accretion complex in northeast Turkey, the Refahiye ophiolite, and relation to the Balkan ophiolites. Am. J. Sci. 313, 1054–1087.
Topuz, G., Okay, A.I., Altherr, R., Schwarz, W.H., Sunal, G., Altınkaynak, L., 2014b. Triassic warm subduction in northeast Turkey: evidence from the Ağvanis metamorphic rocks. Isl. Arc 23, 181–205.
Topuz, G., Candan, O., Zack, T., Yılmaz, A., 2017. East Anatolian plateau constructed over a continental basement: no evidence for the East Anatolian accretionary complex. Geology 45, 791–794.
Torsvik, T.H., Cocks, L.R.M., 2017. Earth History and Palaeogeography. Cambridge University Press, p. 312.
Torsvik, T.H., Müller, R.D., Van der Voo, R., Steinberger, B., Gaina, C., 2008. Global plate motion frames: toward a unified model. Rev. Geophys. 46.
Torsvik, T.H., Steinberger, B., Gurnis, M., Gaina, C., 2010. Plate tectonics and net lithosphere rotation over the past 150My. Earth Planet. Sci. Lett. 291, 106–112.
Torsvik, T.H., Van der Voo, R., Preeden, U., Mac Niocaill, C., Steinberger, B., Doubrovine, P.V., van Hinsbergen, D.J.J., Domeier, M., Gaina, C., Tohver, E., Meert, J.G., McCausland, P.J.A., Cocks, L.R.M., 2012. Phanerozoic polar wander, palaeogeography and dynamics. Earth-Sci. Rev. 114, 325–368.
Torsvik, T.H., Amundsen, H., Hartz, E.H., Corfu, F., Kusznir, N., Gaina, C., Doubrovine, P.V., Steinberger, B., Ashwal, L.D., Jamtveit, B., 2013. A Precambrian microcontinent in the Indian Ocean. Nat. Geosci. 6, 223–227.
Tozzi, M., Kissel, C., Funiciello, R., Laj, C., Parotto, M., 1988. A clockwise rotation of southern Apulia? Geophys. Res. Lett. 15, 681–684.
Tremblay, A., Meshi, A., Deschamps, T., Goulet, F., Goulet, N., 2015. The Vardar zone as a suture for the Mirdita ophiolites, Albania: constraints from the structural analysis of the Korabi-Pelagonia zone. Tectonics 34, 352–375.
Tretyak, A.N., 1979. Paleomagnetic Directions and Pole Positions: Data for the USSR. Soviet Geophysical Committee, World Data Center-B, Moscow.
Tropeano, M., Spalluto, L., Moretti, M., Pieri, P., Sabato, L., 2004. Depositi carbonatici infrapleistocenici di tipo foramol in sistemi di scarpata (Salento–Italia meridionale). Il Quat. 17, 537–546.
Tubía, J.M., Cuevas, J., Esteban, J.J., Gil Ibarguchi, J.I., 2009. Remnants of a Mesozoic Rift in a Subducted Terrane of the Alpujarride Complex (Betic Cordilleras, Southern Spain). J. Geol. 117, 71–87.
Túnyi, I., Márton, E., 1996. Indications for large Tertiary rotation in the Carpathian-northern Pannonian region outside the North Hungarian Paleogene Basin. Geol. Carpathica 47, 43–49.
Túnyi, I., Janocko, J., Jacko, S., 2008. Paleomagnetic investigations of the basal Borove Formation in the Liptov Depression (Central-Carpathian Paleogene basin). Geol. Carpathica-Bratisl. 59, 237.
Turpaud, P., Reischmann, T., 2010. Characterisation of igneous terranes by zircon dating: implications for UHP occurrences and suture identification in the Central Rhodope, northern Greece. Int. J. Earth Sci. 99, 567–591.
Tüysüz, O., Dellaloğlu, A.A., Terzioğlu, N., 1995. A magmatic belt within the Neo-Tethyan suture zone and its role in the tectonic evolution of northern Turkey. Tectonophysics 243, 173–191.
Tărăpoancă, M., Bertotti, G., Maţenco, L., Dinu, C., Cloetingh, S.A.P.L., 2003. Architecture of the Focşani Depression: a 13 km deep basin in the Carpathians bend zone (Romania). Tectonics 22.
Ubide, T., Wijbrans, J.R., Galé, C., Arranz, E., Lago, M., Larrea, P., 2014. Age of the Cretaceous alkaline magmatism in northeast Iberia: implications for the Alpine cycle in the Pyrenees. Tectonics 33, 1444–1460.
Ülgen, S.C., Lom, N., Sunal, G., Gerdes, A., Şengör, A.M.C., 2018. The Strandja Massif and the İstanbul Zone were once parts of the same palaeotectonic unit: new data from Triassic detrital zircons. Geodin. Acta 30, 212–224.
Underhill, J.R., 1988. Triassic evaporites and Plio-Quaternary diapirism in western Greece. J. Geol. Soc. 145, 269–282.
Underhill, J.R., 1989. Late Cenozoic deformation of the Hellenide foreland, western Greece. Geol. Soc. Am. Bull. 101, 613–634.
Ünlügenç, U.C., Akıncı, A.C., 2015. Sedimentary development of the Oligocene Karsantı Basin, southern Turkey, in its regional tectonic setting. J. Asian Earth Sci. 105, 173–191.
Ustaömer, T., Robertson, A.H.F., 2000. Geochemical evidence used to test alternative plate tectonic models for pre-Upper Jurassic (Palaeotethyan) units in the Central Pontides, N Turkey. Geol. J. 34, 25–53.
Ustaömer, T.m., Robertson, A.H.F., 2010. Late Palaeozoic-Early Cenozoic tectonic development of the Eastern Pontides (Artvin area), Turkey: stages of closure of Tethys along the southern margin of Eurasia. Geol. Soc., Lond., Spec. Publ. 340, 281–327.
Ustaömer, P.A., Ustaömer, T., Gerdes, A., Robertson, A.H.F., Collins, A.S., 2012. Evidence of Precambrian sedimentation/magmatism and Cambrian metamorphism in the Bitlis Massif, SE Turkey utilising whole-rock geochemistry and U–Pb LA-ICP-MS zircon dating. Gondwana Res. 21, 1001–1018.
Ustaszewski, K., Schmid, S.M., Fügenschuh, B., Tischler, M., Kissling, E., Spakman, W., 2008. A map-view restoration of the Alpine-Carpathian-Dinaridic system for the early Miocene. Swiss J. Geosci. 101, 273–294.
Ustaszewski, K., Schmid, S.M., Lugović, B., Schuster, R., Schaltegger, U., Bernoulli, D., Hottinger, L., Kounov, A., Fügenschuh, B., Schefer, S., 2009. Late Cretaceous intra-oceanic magmatism in the internal Dinarides (northern Bosnia and Herzegovina): implications for the collision of the Adriatic and European plates. Lithos 108, 106–125.
Ustaszewski, K., Kounov, A., Schmid, S.M., Schaltegger, U., Krenn, E., Frank, W., Fügenschuh, B., 2010. Evolution of the Adria-Europe plate boundary in the northern Dinarides: from continent-continent collision to back-arc extension. Tectonics 29.
Üzel, B., Langereis, C.G., Kaymakcı, N., Sözbilir, H., Özkaymak, Ç., Özkaptan, M., 2015. Paleomagnetic evidence for an inverse rotation history of Western Anatolia

during the exhumation of Menderes core complex. Earth Planet. Sci. Lett. 414, 108–125.
Üzel, B., Sümer, Ö., Özkaptan, M., Özkaymak, Ç., Kuiper, K., Sözbilir, H., Kaymakcı, N., İnci, U., Langereis, C.G., 2017. Palaeomagnetic and geochronological evidence for a major middle Miocene unconformity in Söke Basin (western Anatolia) and its tectonic implications for the Aegean region. J. Geol. Soc. 174, 721–740.
Vaes, B., van Hinsbergen, D.J.J., Boschman, L.M., 2019. Reconstruction of subduction and back-arc spreading in the NW Pacific and Aleutian Basin: clues to causes of Cretaceous and Eocene plate reorganizations. Tectonics 38, 1367–1413.
Vaida, M., Seghedi, A., Verniers, J., 2005. Northern Gondwanan affinity of the East Moesian Terrane based on chitinozoans. Tectonophysics 410, 379–387.
Valcárcel, M., Soto, R., Beamud, E., Oliva-Urcia, B., Muñoz, J.A., Biete, C., 2016. Integration of palaeomagnetic data, basement-cover relationships and theoretical calculations to characterize the obliquity of the Altomira–Loranca structures (central Spain). Geol. Soc., Lond., Spec. Publ. 425, 169–188.
Valente, J.P., Laj, C., Sorel, D., Roy, S., Valet, J.P., 1982. Paleomagnetic results from Mio-Pliocene marine sedimentary series in Crete. Earth Planet. Sci. Lett. 57, 159–172.
van de Lagemaat, S.H., van Hinsbergen, D.J.J., Boschman, L.M., Kamp, P.J., Spakman, W., 2018. Southwest Pacific Absolute Plate Kinematic Reconstruction Reveals Major Cenozoic Tonga-Kermadec Slab Dragging. Tectonics 37, 2647–2674.
van der Boon, A., van Hinsbergen, D.J.J., Rezaeian, M., Gürer, D., Honarmand, M., Pastor-Galán, D., Krijgsman, W., Langereis, C.G., 2018. Quantifying Arabia–Eurasia convergence accommodated in the Greater Caucasus by paleomagnetic reconstruction. Earth Planet. Sci. Lett. 482, 454–469.
van der Kaaden, G., 1966. The significance and distribution of glaucophane rocks in Turkey. Bull. Miner. Res. Explor. Inst. Turk. 67, 37–67.
van der Meer, D.G., Spakman, W., van Hinsbergen, D.J.J., Amaru, M.L., Torsvik, T.H., 2010. Towards absolute plate motions constrained by lower-mantle slab remnants. Nat. Geosci. 3, 36–40.
van der Meer, D.G., van Hinsbergen, D.J.J., Spakman, W., 2018. Atlas of the underworld: slab remnants in the mantle, their sinking history, and a new outlook on lower mantle viscosity. Tectonophysics 723, 309–448.
van der Voo, R., 1968. Paleomagnetism and the Alpine tectonics of Eurasia IV: Jurassic, Cretaceous and Eocene pole positions from northeastern Turkey. Tectonophysics 6, 251–269.
van der Voo, R., 1969. Paleomagnetic evidence for the rotation of the Iberian Peninsula. Tectonophysics 7, 5–56.
Van Der Voo, R., Zijderveld, J.D.A., 1971. Renewed paleomagnetic study of the Lisbon volcanics and implications for the rotation of the Iberian Peninsula. J. Geophys. Res. 76, 3913–3921.
van Gelder, I.E., Maţenco, L., Willingshofer, E., Tomljenović, B., Andriessen, P.A.M., Ducea, M.N., Beniest, A., Gruić, A., 2015. The tectonic evolution of a critical segment of the Dinarides-Alps connection: kinematic and geochronological inferences from the Medvednica Mountains, NE Croatia. Tectonics 34, 1952–1978.
van Hinsbergen, D.J.J., 2010. A key extensional metamorphic complex reviewed and restored: the Menderes Massif of western Turkey. Earth-Sci. Rev. 102, 60–76.
van Hinsbergen, D.J.J., Schmid, S.M., 2012. Map view restoration of Aegean-West Anatolian accretion and extension since the Eocene. Tectonics 31. https://doi.org/10.1029/2012tc003132.
van Hinsbergen, D.J.J., Hafkenscheid, E., Spakman, W., Meulenkamp, J.E., Wortel, R., 2005a. Nappe stacking resulting from subduction of oceanic and continental lithosphere below Greece. Geology 33.
van Hinsbergen, D.J.J., Langereis, C.G., Meulenkamp, J.E., 2005b. Revision of the timing, magnitude and distribution of Neogene rotations in the western Aegean region. Tectonophysics 396, 1–34.
van Hinsbergen, D.J.J., Zachariasse, W.J., Wortel, M.J.R., Meulenkamp, J.E., 2005c. Underthrusting and exhumation: a comparison between the External Hellenides and the "hot" Cycladic and "cold" South Aegean core complexes (Greece). Tectonics 24. https://doi.org/10.1029/2004tc001692.
van Hinsbergen, D.J.J., van der Meer, D.G., Zachariasse, W.J., Meulenkamp, J.E., 2006. Deformation of western Greece during Neogene clockwise rotation and collision with Apulia. Int. J. Earth Sci. 95, 463–490.
van Hinsbergen, D.J.J., Krijgsman, W., Langereis, C.G., Cornée, J.J., Duermeijer, C.E., van Vugt, N., 2007. Discrete Plio-Pleistocene phases of tilting and counter-clockwise rotation in the southeastern Aegean arc (Rhodos, Greece): early Pliocene formation of the south Aegean left-lateral strike-slip system. J. Geol. Soc. 164, 1133–1144.
van Hinsbergen, D.J.J., Dupont-Nivet, G., Nakov, R., Oud, K., Panaiotu, C., 2008. No significant post-Eocene rotation of the Moesian Platform and Rhodope (Bulgaria): implications for the kinematic evolution of the Carpathian and Aegean arcs. Earth Planet. Sci. Lett. 273, 345–358.
van Hinsbergen, D.J.J., Dekkers, M.J., Bozkurt, E., Koopman, M., 2010a. Exhumation with a twist: paleomagnetic constraints on the evolution of the Menderes metamorphic core complex, western Turkey. Tectonics 29.
van Hinsbergen, D.J.J., Dekkers, M.J., Koc, A., 2010b. Testing Miocene remagnetization of Beydağları: timing and amount of Neogene rotations in SW Turkey. Turk. J. Earth Sci. 19, 123–156.
van Hinsbergen, D.J.J., Kaymakcı, N., Spakman, W., Torsvik, T.H., 2010c. Reconciling the geological history of western Turkey with plate circuits and mantle tomography. Earth Planet. Sci. Lett. 297, 674–686.
van Hinsbergen, D.J.J., Kapp, P., Dupont-Nivet, G., Lippert, P.C., DeCelles, P.G., Torsvik, T.H., 2011. Restoration of Cenozoic deformation in Asia and the size of Greater India. Tectonics 30. https://doi.org/10.1029/2011tc002908.
van Hinsbergen, D.J.J., Lippert, P.C., Dupont-Nivet, G., McQuarrie, N., Doubrovine, P.V., Spakman, W., Torsvik, T.H., 2012. Greater India Basin hypothesis and a two-stage Cenozoic collision between India and Asia. Proc. Natl. Acad. Sci. U. S. A. 109, 7659–7664.
van Hinsbergen, D.J.J., Vissers, R.L., Spakman, W., 2014a. Origin and consequences of western Mediterranean subduction, rollback, and slab segmentation. Tectonics 33, 393–419.
van Hinsbergen, D.J.J., Mensink, M., Langereis, C.G., Maffione, M., Spalluto, L., Tropeano, M., Sabato, L., 2014b. Did Adria rotate relative to Africa? Solid Earth 5, 611–629.
van Hinsbergen, D.J.J., Peters, K., Maffione, M., Spakman, W., Guilmette, C., Thieulot, C., Plümper, O., Gürer, D., Brouwer, F.M., Aldanmaz, E., Kaymakcı, N., 2015. Dynamics of intraoceanic subduction initiation: 2. Supra-subduction zone ophiolite formation and metamorphic sole exhumation in context of absolute plate motions. Geochem. Geophys. Geosyst. 16, 1771–1785.
van Hinsbergen, D.J.J., Maffione, M., Plunder, A., Kaymakcı, N., Ganerød, M., Hendriks, B.W.H., Corfu, F., Gürer, D., de Gelder, G.I.N.O., Peters, K., McPhee, P.J., Brouwer, F.M., Advokaat, E.L., Vissers, R.L.M., 2016. Tectonic evolution and paleogeography of the Kırşehir Block and the Central Anatolian Ophiolites, Turkey. Tectonics 35, 983–1014.
van Hinsbergen, D.J.J., Spakman, W., Vissers, R.L.M., Meer, D.G., 2017. Comment on "Assessing Discrepancies Between Previous Plate Kinematic Models of Mesozoic Iberia and Their Constraints" by Barnett-Moore Et Al. Tectonics 36, 3277–3285.
van Hinsbergen, D.J.J., Lippert, P.C., Li, S., Huang, W., Advokaat, E.L., Spakman, W., 2019. Reconstructing Greater India: paleogeographic, kinematic, and geodynamic perspectives. Tectonophysics 760, 69–94.
Van Hoof, A.A.M., Langereis, C.G., 1992. The upper and lower Thvera sedimentary geomagnetic reversal records from southern Sicily. Earth Planet. Sci. Lett. 114, 59–75.
Van Hoof, A.A.M., Van Os, B.J.H., Langereis, C.G., 1993. The upper and lower Nunivak sedimentary geomagnetic transitional records from southern Sicily. Phys. Earth Planet. Inter. 77, 297–313.
van Unen, M., Maţenco, L., Nader, F.H., Darnault, R., Mandic, O., Demir, V., 2019. Kinematics of foreland-vergent crustal accretion: inferences from the Dinarides evolution. Tectonics.
Vandenberg, J., 1983. Reappraisal of paleomagnetic data from Gargano (South Italy). Tectonophysics 98, 29–41.
Vandenberg, J., Wonders, A.A.H., 1976. Paleomagnetic evidence of large fault displacement around the PO-basin. Tectonophysics 33, 301–320.
VandenBerg, J., Wonders, A.A.H., 1980. Paleomagnetism of Late Mesozoic pelagic limestones from the southern Alps. J. Geophys. Res.: Solid Earth 85, 3623–3627.
Varga, R.J., Gee, J.S., Bettison-Varga, L., Anderson, R.S., Johnson, C.L., 1999. Early establishment of seafloor hydrothermal systems during structural extension: paleomagnetic evidence from the Troodos ophiolite, Cyprus. Earth Planet. Sci. Lett. 171, 221–235.
Varol, E., Bedi, Y., Tekin, U.K., Uzuncimen, S., 2011. Geochemical and petrological characteristics of late Triassic basic volcanic rocks from the Kocali complex, SE Turkey: implications for the Triassic evolution of southern Tethys. Ofioliti 36, 101–115.
Varol, B., Şen, Ş., Ayyıldız, T., Sözeri, K., Karakaş, Z., Métais, G., 2016. Sedimentology and stratigraphy of Cenozoic deposits in the Kağızman-Tuzluca Basin, northeastern Turkey. Int. J. Earth Sci. 105, 107–137.
Vekua, L.V., 1971. Paleomagnetic Directions and Pole Positions: Data for the USSR. Soviet Geophysical Committee, World Data Center-B, Moscow.
Vergés, J., Fernàndez, M., 2012. Tethys–Atlantic interaction along the Iberia–Africa plate boundary: the Betic–Rif orogenic system. Tectonophysics 579, 144–172.
Vergés, J., García-Senz, J., 2001. Mesozoic evolution and Cainozoic inversion of the Pyrenean rift. Mém. Muséum Natl. d'histoire Nat. 186, 187–212.
Vergés, J., Sàbat, F., 1999. Constraints on the Neogene Mediterranean kinematic evolution along a 1000 km transect from Iberia to Africa. Geol. Soc., Lond., Spec. Publ. 156, 63–80.
Vergés, J., Millán, H., Roca, E., Muñoz, J.A., Marzo, M., Cirés, J., Bezemer, T.D., Zoetemeijer, R., Cloetingh, S., 1995. Eastern Pyrenees and related foreland basins: pre-, syn- and post-collisional crustal-scale cross-sections. Mar. Pet. Geol. 12, 903–915.
Vezzani, L., Festa, A., Ghisetti, F.C., 2010. Geology and Tectonic Evolution of the Central-Southern Apennines, Italy, Geology and Tectonic Evolution of the Central-Southern Apennines, pp. 1–58. Italy.
Vigliotti, L., Alvarez, W., McWilliams, M., 1990. No relative rotation detected between Corsica and Sardinia. Earth Planet. Sci. Lett. 98, 313–318.
Vignaroli, G., Rossetti, F., Rubatto, D., Theye, T., Lisker, F., Phillips, D., 2010. Pressure-temperature-deformation-time (P-T-d-t) exhumation history of the Voltri Massif HP complex, Ligurian Alps, Italy. Tectonics 29.
Villa, I.M., Bucher, S., Bousquet, R., Kleinhanns, I.C., Schmid, S.M., 2014. Dating Polygenetic Metamorphic Assemblages along a Transect across the Western Alps. J. Petrol. 55, 803–830.
Villasante-Marcos, V., Osete, M.L., Gervilla, F., García-Dueñas, V., 2003. Palaeomagnetic study of the Ronda peridotites (Betic Cordillera, southern Spain). Tectonophysics 377, 119–141.
Vincent, S.J., Allen, M.B., Ismail-Zadeh, A.D., Flecker, R., Foland, K.A., Simmons, M.D., 2005. Insights from the Talysh of Azerbaijan into the Paleogene evolution of the South Caspian region. Geol. Soc. Am. Bull. 117.
Vincent, S.J., Morton, A.C., Carter, A., Gibbs, S., Barabadze, T.G., 2007. Oligocene uplift of the Western Greater Caucasus: an effect of initial Arabia?Eurasia collision. Terra Nova 19, 160–166.

Vincent, S.J., Carter, A., Lavrishchev, V.A., Rice, S.P., Barabadze, T.G., Hovius, N., 2011. The exhumation of the western Greater Caucasus: a thermochronometric study. Geol. Mag. 148, 1–21.
Vincent, S.J., Braham, W., Lavrishchev, V.A., Maynard, J.R., Harland, M., 2016. The formation and inversion of the western Greater Caucasus Basin and the uplift of the western Greater Caucasus: implications for the wider Black Sea region. Tectonics 35, 2948–2962.
Visarion, M., Săndulescu, M., Stanica, D., Veliciu, S., 1988. Contributions a la Connaissance de la Structure Profonde de la Plateforme Moesienne en Roumanie. In: St. Tehn. Econ., Ser. Geogiz., D, vol. 15, pp. 211–222.
Vishnevskaya, V.S., Djeric, N., Zakariadze, G.S., 2009. New data on Mesozoic Radiolaria of Serbia and Bosnia, and implications for the age and evolution of oceanic volcanic rocks in the Central and Northern Balkans. Lithos 108, 72–105.
Vissers, R.L.M., 2012. Extension in a convergent tectonic setting; a lithospheric view on the Alboran system of SW Europe. Geol. Belg. 15, 53.
Vissers, R.L.M., Meijer, P.T., 2012a. Iberian plate kinematics and Alpine collision in the Pyrenees. Earth-Sci. Rev. 114, 61–83.
Vissers, R.L.M., Meijer, P.T., 2012b. Mesozoic rotation of Iberia: subduction in the Pyrenees? Earth-Sci. Rev. 110, 93–110.
Vissers, R.L.M., Platt, J.P., Wal, D., 1995. Late orogenic extension of the Betic Cordillera and the Alboran Domain: a lithospheric view. Tectonics 14, 786–803.
Vissers, R.L.M., van Hinsbergen, D.J.J., Meijer, P.T., Piccardo, G.B., 2013. Kinematics of Jurassic ultra-slow spreading in the Piemonte Ligurian ocean. Earth Planet. Sci. Lett. 380, 138–150.
Vissers, R.L.M., van Hinsbergen, D.J.J., van der Meer, D.G., Spakman, W., 2016. Cretaceous slab break-off in the Pyrenees: Iberian plate kinematics in paleomagnetic and mantle reference frames. Gondwana Res. 34, 49–59.
Vissers, R.L.M., van Hinsbergen, D.J.J., Wilkinson, C.M., Ganerød, M., 2017. Middle Jurassic shear zones at Cap de Creus (eastern Pyrenees, Spain): a record of predrift extension of the Piemonte–Ligurian Ocean? J. Geol. Soc. 174, 289–300.
Vitale, S., Ciarcia, S., 2013. Tectono-stratigraphic and kinematic evolution of the Southern Apennines/Calabria–Peloritani Terrane system (Italy). Tectonophysics 583, 164–182.
Vitale Brovarone, A., Herwartz, D., 2013. Timing of HP metamorphism in the Schistes Lustrés of Alpine Corsica: new Lu–Hf garnet and lawsonite ages. Lithos 172–173, 175–191.
Vitale Brovarone, A., Beltrando, M., Malavieille, J., Giuntoli, F., Tondella, E., Groppo, C., Beyssac, O., Compagnoni, R., 2011. Inherited Ocean–Continent Transition zones in deeply subducted terranes: insights from Alpine Corsica. Lithos 124, 273–290.
Vitale Brovarone, A., Beyssac, O., Malavieille, J., Molli, G., Beltrando, M., Compagnoni, R., 2013. Stacking and metamorphism of continuous segments of subducted lithosphere in a high-pressure wedge: the example of Alpine Corsica (France). Earth-Sci. Rev. 116, 35–56.
Vitale, S., Ciarcia, S., Tramparulo, F.D.A., 2013. Deformation and stratigraphic evolution of the Ligurian Accretionary Complex in the Southern Apennines (Italy). J. Geodyn. 66, 120–133.
Vlahović, I., Tišljar, J., Velić, I., Matičec, D., 2005. Evolution of the Adriatic Carbonate Platform: palaeogeography, main events and depositional dynamics. Palaeogeogr. Palaeoclimatol. Palaeoecol. 220, 333–360.
Vojtko, R., Králiková, S., Jeřábek, P., Schuster, R., Danišík, M., Fügenschuh, B., Minár, J., Madarás, J., 2016. Geochronological evidence for the Alpine tectonothermal evolution of the Veporic Unit (Western Carpathians, Slovakia). Tectonophysics 666, 48–65.
von Quadt, A., Moritz, R., Peytcheva, I., Heinrich, C.A., 2005. 3: geochronology and geodynamics of Late Cretaceous magmatism and Cu–Au mineralization in the Panagyurishte region of the Apuseni–Banat–Timok–Srednogorie belt, Bulgaria. Ore Geol. Rev. 27, 95–126.
Vörös, A., 1977. Provinciality of the Mediterranean lower Jurassic brachiopod fauna: causes and plate-tectonic implications. Palaeogeogr. Palaeoclimatol. Palaeoecol. 21, 1–16.
Vozárová, A., Ebner, F., Kovács, S., Kräutner, H.G., Szederkenyi, T., Krstić, B., Sremac, J., Aljinovič, D., Novak, M., Skaberne, D., 2009. Late Variscan (Carboniferous to Permian) environments in the Circum Pannonian Region. Geol. Carpathica 60, 71–104.
Vrabec, M., Fodor, L., 2006. Late Cenozoic tectonics of Slovenia: structural styles at the northeastern corner of the Adriatic microplate. In: Pinter, N., Gyula, G., Weber, J., Stein, S., Medak, D. (Eds.), The Adria Microplate: GPS Geodesy, Tectonics and Hazards. Springer Netherlands, Dordrecht, pp. 151–168.
Wagreich, M., Decker, K., 2001. Sedimentary tectonics and subsidence modelling of the type Upper Cretaceous Gosau basin (Northern Calcareous Alps, Austria). Int. J. Earth Sci. 90, 714–726.
Wagreich, M., Faupl, P., 1994. Palaeogeography and geodynamic evolution of the Gosau Group of the Northern Calcareous Alps (Late Cretaceous, Eastern Alps, Austria). Palaeogeogr. Palaeoclimatol. Palaeoecol. 110, 235–254.
Walcott, C., White, S., 1998. Constraints on the kinematics of post-orogenic extension imposed by stretching lineations in the Aegean region. Tectonophysics 298, 155–175.
Weber, S., Bucher, K., 2015. An eclogite-bearing continental tectonic slice in the Zermatt–Saas high-pressure ophiolites at Trockener Steg (Zermatt, Swiss Western Alps). Lithos 232, 336–359.
Weltje, G.J., 1992. Oligocene to early Miocene sedi- mentation and tectonics in the southern part of the Calabrian-Peloritani Arc (Aspromonte, southern Italy): a record of mixed-mode piggy-back basin evolution. Basin Res. 4, 37–68.
Westaway, R., Arger, J., 2001. Kinematics of the Malatya–Ovacik fault zone. Geodin. Acta 14, 103–131.
Whitney, D.L., Bozkurt, E., 2002. Metamorphic history of the southern Menderes massif, western Turkey. GSA Bull. 114, 829–838.
Whitney, D.L., Dilek, Y., 1998. Metamorphism during Alpine Crustal Thickening and Extension in Central Anatolia, Turkey: the Niğde Metamorphic Core Complex. J. Petrol. 39, 1385–1403.
Whitney, D.L., Hamilton, M.A., 2004. Timing of high-grade metamorphism in central Turkey and the assembly of Anatolia. J. Geol. Soc. 161, 823–828.
Whitney, D.L., Teyssier, C., Dilek, Y., Fayon, A.K., 2001. Metamorphism of the Central Anatolian Crystalline Complex, Turkey: influence of orogen-normal collision vs. wrench-dominated tectonics on P–T–t paths. J. Metamorph. Geol. 19, 411–432.
Whitney, D.L., Teyssier, C., Fayon, A.K., Hamilton, M.A., Heizler, M., 2003. Tectonic controls on metamorphism, partial melting, and intrusion: timing and duration of regional metamorphism and magmatism in the Niğde Massif, Turkey. Tectonophysics 376, 37–60.
Wiederkehr, M., Sudo, M., Bousquet, R., Berger, A., Schmid, S.M., 2009. Alpine orogenic evolution from subduction to collisional thermal overprint: the 40Ar/39Ar age constraints from the Valaisan Ocean, central Alps. Tectonics 28.
Willingshofer, E., Neubauer, F., Cloetingh, S., 1999. The significance of Gosau-type basins for the late cretaceous tectonic history of the Alpine-Carpathian belt. Phys. Chem. Earth, Part A: Solid Earth Geod. 24, 687–695.
Wölfler, A., Kurz, W., Fritz, H., Stüwe, K., 2011. Lateral extrusion in the Eastern Alps revisited: refining the model by thermochronological, sedimentary, and seismic data. Tectonics 30.
Wortel, M.J.R., Spakman, W., 2000. Subduction and slab detachment in the Mediterranean-Carpathian region. Science 290, 1910–1917.
Xypolias, P., Dorr, W., Zulauf, G., 2006. Late Carboniferous plutonism within the pre-Alpine basement of the External Hellenides (Kithira, Greece): evidence from U-Pb zircon dating. J. Geol. Soc. 163, 539–547.
Yakovlev, F., 2005. Prognosis of structure of the main baundaries for the Earth's crust based on data of deformations estimations in a folded Alpine sedimentary cover, the example of the Great Caucasus. Geophys. Res. Abstr. 7160.
Yaliniz, M.K., Floyd, P.A., Göncüoğlu, M.C., 1996. Supra-subduction zone ophiolites of Central Anatolia: geochemical evidence from the Sarikaraman Ophiolite, Aksaray, Turkey. Mineral. Mag. 697.
Yaliniz, K.M., Floyd, P.A., Göncüoğlu, M.C., 2000. Geochemistry of Volcanic Rocks from the Çiçekdağ, Ophiolite, Central Anatolia, Turkey, and Their Inferred Tectonic Setting within the Northern Branch of the Neotethyan Ocean. Geol. Soc., Lond., Spec. Publ. 173, 203–218.
Yanev, S., 2000. Palaeozoic terranes of the Balkan Peninsula in the framework of Pangea assembly. Palaeogeogr. Palaeoclimatol. Palaeoecol. 161, 151–177.
Yiğitbaş, E., Yılmaz, Y., 1996. New evidence and solution to the Maden complex controversy of the Southeast Anatolian orogenic belt (Turkey). Geol. Rundsch. 85, 250–263.
Yiğitbaş, E., Kerrich, R., Yılmaz, Y., Elmas, A., Xie, Q., 2004. Characteristics and geochemistry of Precambrian ophiolites and related volcanics from the Istanbul–Zonguldak Unit, Northwestern Anatolia, Turkey: following the missing chain of the Precambrian South European suture zone to the east. Precambrian Res. 132, 179–206.
Yıldırım, E., 2015. Geochemistry, petrography and tectonic significance of the ophiolitic rocks, felsic intrusions and Eocene volcanic rocks of an imbrication zone (Helete area, Southeast Turkey). J. Afr. Earth Sci. 107, 89–107.
Yılmaz, A., 1985. Basic geological characteristics and structural evolution of the region between Upper Kelkit stream and Munzur Mountains. Bull. Geol. Soc. Turk 28, 79–92.
Yılmaz, Y.C., 1993. New evidence and model on the evolution of the southeast Anatolian orogen. Geol. Soc. Am. Bull. 105, 251–271.
Yılmaz, C., 1994. Evolution of the Munzur Carbonate Platform during the Mesozoic, Middle-Eastern Anatolia (Turkey). Géol. Méditerranéenne 21, 195–196.
Yılmaz, O., Michel, R., Vialette, Y., Bonhomme, M., 1981. Réinterprétation des données isotopiques Rb-Sr obtenues sur les métamorphites de la partie méridionale du massif de Bitlis (Turquie). Sci. Géol., Bull. Mém. 34, 59–73.
Yılmaz, Y., Şaroğlu, F., Güner, Y., 1987. Initiation of the neomagmatism in East Anatolia. Tectonophysics 134, 177–199.
Yılmaz, Y., Tüysüz, O., Yigitbas, E., Can Genç, S., Şengör, A.M.C., 1998. Geology and tectonic evolution of the Pontides. Mem.-Am. Assoc. Pet. Geol. 183–226.
Yılmaz, A., Adamia, S., Chabukiani, A., Chkhotua, T., ErdoĞan, K., Tuzcu, S., KarabiyikoĞlu, M., 2000. Structural correlation of the southern Transcaucasus (Georgia)-eastern Pontides (Turkey). Geol. Soc., Lond., Spec. Publ. 173, 171–182.
Yılmaz, A., Yılmaz, H., Kaya, C., Boztug, D., 2010. The nature of the crustal structure of the Eastern Anatolian Plateau, Turkey. Geodin. Acta 23, 167–183.
Yılmaz, A., Adamia, S., Yılmaz, H., 2014. Comparisons of the suture zones along a geotraverse from the Scythian Platform to the Arabian Platform. Geosci. Front. 5, 855–875.
Zachariasse, W.J., van Hinsbergen, D.J.J., Fortuin, A.R., 2011. Formation and fragmentation of a late Miocene supradetachment basin in central Crete: implications for exhumation mechanisms of high-pressure rocks in the Aegean forearc. Basin Res. 23, 678–701.
Zaghloul, M.N., Critelli, S., Perri, F., Mongelli, G., Perrone, V., Sonnino, M., Tucker, M., Aiello, M., Ventimiglia, C., 2010. Depositional systems, composition and geochemistry of Triassic rifted-continental margin redbeds of the Internal Rif Chain, Morocco. Sedimentology 57, 312–350.
Zananiri, I., Kondopoulou, D., Dimitriadis, S., Kilias, A., 2013. Insights into the geotectonic evolution of the southern Rhodope as inferred from a combined AMS, microtextural and paleomagnetic study of the Tertiary Symvolon and Vrondou plutons. Tectonophysics 595–596, 106–124.
Zanella, E., 1998. Paleomagnetism of Pleistocene volcanic rocks from Pantelleria

Island (Sicily Channel), Italy. Phys. Earth Planet. Inter. 108, 291–303.
Zarki-Jakni, B., van der Beek, P., Poupeau, G., Sosson, M., Labrin, E., Rossi, P., Ferrandini, J., 2004. Cenozoic denudation of Corsica in response to Ligurian and Tyrrhenian extension: results from apatite fission track thermochronology. Tectonics 23.
Zattin, M., Cavazza, W., Okay, A.I., Federici, I., Fellin, M.G., Pignalosa, A., Reiners, P., 2010. A precursor of the North Anatolian Fault in the Marmara Sea region. J. Asian Earth Sci. 39, 97–108.
Zibret, L., Vrabec, M., 2016. Palaeostress and kinematic evolution of the orogen-parallel nw-se striking faults in the nw external dinarides of Slovenia unraveled by mesoscale fault-slip data analysis. Geol. Croatica 69, 295–305.
Ziegler, P.A., 1990. Geological Atlas of Western and Central Europe. Geological Society of London.
Zimmerman, A., Stein, H.J., Hannah, J.L., Koželj, D., Bogdanov, K., Berza, T., 2007. Tectonic configuration of the Apuseni–Banat—Timok–Srednogorie belt, Balkans-South Carpathians, constrained by high precision Re–Os molybdenite ages. Miner. Depos. 43, 1–21.
Zitter, T.A.C., Woodside, J.M., Mascle, J., 2003. The Anaximander Mountains: a clue to the tectonics of southwest Anatolia. Geol. J. 38, 375–394.
Zlatkin, O., Avigad, D., Gerdes, A., 2018. New detrital zircon geochronology from the Cycladic Basement (Greece): implications for the Paleozoic accretion of peri-Gondwanan terranes to Laurussia. Tectonics.
Zonenshain, L.P., Le Pichon, X., 1986. Deep basins of the Black Sea and Caspian Sea as remnants of Mesozoic back-arc basins. Tectonophysics 123, 181–211.
Zulauf, G., Dörr, W., Fisher-Spurlock, S.C., Gerdes, A., Chatzaras, V., Xypolias, P., 2015. Closure of the Paleotethys in the External Hellenides: constraints from U–Pb ages of magmatic and detrital zircons (Crete). Gondwana Res. 28, 642–667.
Zulauf, G., Dörr, W., Krahl, J., Lahaye, Y., Chatzaras, V., Xypolias, P., 2016. U–Pb zircon and biostratigraphic data of high-pressure/low-temperature metamorphic rocks of the Talea Ori: tracking the Paleotethys suture in central Crete, Greece. Int. J. Earth Sci. 105, 1901–1922.
Zwart, H.J., 1979. The Geology of the Central Pyrenees. Geologisch en mineralogisch Instituut der Rijksuniversiteit, Leiden.

Douwe van Hinsbergen (PhD, Utrecht University, 2004) is Professor of Global Tectonics and Paleogeography at Utrecht University, the Netherlands, where he has taught since 2012. Van Hinsbergen studies global plate tectonics, orogenesis, and paleogeography across the globe, and closely collaborates with modelers of geodynamics and paleoclimate to advance understanding in the physics driving geological processes particularly related to plate tectonics. His research was sponsored by an ERC Starting Grant, and by Veni, Vidi, and Vici grants of the Netherlands Organization for Scientific Research (NWO). Van Hinsbergen is author or co-author of over 160 articles in peer-reviewed international journals. His Mediterranean work started in 1998 with a Miocene conglomerate on Crete, Greece, and expanded from there. In 2009, he started a 3-year post-doctoral research project at the Norwegian Geological Survey at Trondheim, and subsequently at the Physics of Geological Processes group of Oslo University, Norway, focused on building a kinematic restoration of the Mediterranean region. The region turned out to be slightly more complex than anticipated then.

Trond Torsvik is a professor of geodynamics at the University of Oslo (Norway), with particular interests in palaeomagnetism, plate reconstructions and mantle dynamics. He is the Founding Director of the Center for Earth Evolution and Dynamics (CEED), and is a Fellow of the American Geophysical Union, Member of the Norwegian Academy and was awarded the Arthur Holmes Medal (European Union of Geosciences) in 2016, among various other awards and prizes. He has published around 250 scientific publications and one book (Earth History and Paleogeography, Cambridge University Press) which received the PROSE Award 2018.

Stefan Martin Schmid, professor emeritus, is a geologist currently working at the Institute of Geophysics, ETH Zurich where he does research in Tectonics and Geodynamics in close collaboration with his colleague Eduard Kissling who is an expert in seismology. During the last 10 years after retirement in 2008, he became focused on projects regarding the correlation of tectonic units from the Apennines over the Alps into Dinarides and Carpathians, into the Hellenides and finally to Western Turkey. He started this new focus on larger scale correlation and compilation work in 2008–2010 as a guest professor at FU Berlin (Alexander von Humboldt Forschungspreis) in close cooperation with Mark Handy. He is currently involved in projects such as "Kinematic reconstruction of the Mediterranean region since the Triassic" and "Lithosphere structure and Tectonics of the Alps". His former carrier, first at ANU Canberra in the group of Mervyn Paterson focused on experimental rock deformation. Subsequently he joined ETH Zürich and the group of John Ramsay working on microfabric analysis and structural geology. In 1989–2008 he was professor and head of department at Basel University, concentrating on larger scale tectonics, primarily on the geodynamics of the Alps but since 1994 also gradually moving into the Carpathians and Dinarides.

Liviu Matenco (PhD VU University Amsterdam 1997) is Professor of Tectonics and Sedimentary Basins at Utrecht University, The Netherlands. Liviu is a member of Academia Europaea and is leading the International Lithosphere Program Task Force on Sedimentary Basins. Liviu's research directions include processes that control the multi-scale formation and evolution of coupled orogens and sedimentary basins systems through an integration of multi-disciplinary field studies, analytical techniques and numerical/analogue modelling. His research aims to develop and validate novel concepts of sedimentary basin evolution and topography building by incorporating geological/geophysical datasets and modelling methodologies.

Marco Maffione is Lecturer of Tectonics and Structural Geology at the University of Birmingham (UK). His research focuses on large-scale tectonic processes, including detachment faulting at mid-ocean ridges, subduction initiation mechanisms, and the origin of ophiolites and the methods he uses are paleomagnetic, magnetic fabric, and structural geological analysis. He has worked extensively in the Mediterranean region, including Italy, Turkey, Serbia, Albania, Greece, and Cyprus, but also in Oman, the Andes, and Tibet, and has recently been involved in two International Ocean Discovery Program (IODP) expeditions.

Reinoud Vissers is emeritus professor in the field of mountain building processes at Utrecht University, the Netherlands, where he was appointed in 1978 as assistant professor in the Structural Geology and Tectonics group of Henk Zwart, became associate professor in 1986, and obtained the chair of orogeny and lithosphere extension in 1997. His dominantly field-oriented research has been focussed on the Betics in southern Spain, the Pyrenees, the Ligurian and central Alps, the Hellenides of the Greek mainland, and central Anatolia. Part of that research was focussed on exposures of mantle peridotites, but also on crustal processes and basin development in an orogenic context. He is author or coauthor of over 75 articles in peer-reviewed international journals.

Derya Gürer is a lecturer at the University of Queensland, Australia. She holds a PhD in Geology from Utrecht University, the Netherlands (2017) and an MSc. of Physics of Geological Processes from the University of Oslo, Norway (2012). Her background is in tectonics and geodynamics with core research interests spanning from field-based structural geology to isotope geochemistry, which she uses to constrain the kinematics and timescales of tectonic processes deforming the Earth's lithosphere at convergent margins in the Tethyan, and recently also in the SW Pacific realm. Her PhD research focused on reconstructing subduction, accretion and exhumation in the Mesozoic and Cenozoic Tethyan realm from forearc basins and underlying ophiolites and accretionary complexes in Anatolia.

Wim Spakman is professor of Geophysics at the Department of Earth Sciences at Utrecht University (The Netherlands). His research focusses on the relation between mantle structure & processes and tectonic evolution. In the past decade, he has ventured into 4-D thermo-mechanical modelling of geodynamic evolution of subduction. He published ~110 papers and several book chapters. In 1994, he received the AKZO-Nobel price in Earth Sciences for his pioneering work in seismic tomography. In 2016 he was elected member of the Norwegian Academy of Science and Letters